frontiers | Research Topics

Diabetic kidney disease: Routes to drug development, pharmacology and underlying molecular mechanisms.

Edited by
Swayam Prakash Srivastava and Divya Bhatia

Published in
Frontiers in Pharmacology

ISSN 1664-8714
ISBN 978-2-8325-2721-4
DOI 10.3389/978-2-8325-2721-4

About Frontiers

Frontiers is more than just an open access publisher of scholarly articles: it is a pioneering approach to the world of academia, radically improving the way scholarly research is managed. The grand vision of Frontiers is a world where all people have an equal opportunity to seek, share and generate knowledge. Frontiers provides immediate and permanent online open access to all its publications, but this alone is not enough to realize our grand goals.

Frontiers journal series

The Frontiers journal series is a multi-tier and interdisciplinary set of open-access, online journals, promising a paradigm shift from the current review, selection and dissemination processes in academic publishing. All Frontiers journals are driven by researchers for researchers; therefore, they constitute a service to the scholarly community. At the same time, the *Frontiers journal series* operates on a revolutionary invention, the tiered publishing system, initially addressing specific communities of scholars, and gradually climbing up to broader public understanding, thus serving the interests of the lay society, too.

Dedication to quality

Each Frontiers article is a landmark of the highest quality, thanks to genuinely collaborative interactions between authors and review editors, who include some of the world's best academicians. Research must be certified by peers before entering a stream of knowledge that may eventually reach the public - and shape society; therefore, Frontiers only applies the most rigorous and unbiased reviews. Frontiers revolutionizes research publishing by freely delivering the most outstanding research, evaluated with no bias from both the academic and social point of view. By applying the most advanced information technologies, Frontiers is catapulting scholarly publishing into a new generation.

What are Frontiers Research Topics?

Frontiers Research Topics are very popular trademarks of the *Frontiers journals series*: they are collections of at least ten articles, all centered on a particular subject. With their unique mix of varied contributions from Original Research to Review Articles, Frontiers Research Topics unify the most influential researchers, the latest key findings and historical advances in a hot research area.

Find out more on how to host your own Frontiers Research Topic or contribute to one as an author by contacting the Frontiers editorial office: frontiersin.org/about/contact

Diabetic kidney disease: Routes to drug development, pharmacology and underlying molecular mechanisms.

Topic editors

Swayam Prakash Srivastava — Weill Cornell Medical Center, NewYork-Presbyterian, United States

Divya Bhatia — Weill Cornell Medical Center, NewYork-Presbyterian, United States

Citation

Srivastava, S. P., Bhatia, D., eds. (2023). *Diabetic kidney disease: Routes to drug development, pharmacology and underlying molecular mechanisms.* Lausanne: Frontiers Media SA. doi: 10.3389/978-2-8325-2721-4

Table of contents

frontiers | Frontiers in Pharmacology

TYPE Editorial
PUBLISHED 08 August 2023
DOI 10.3389/fphar.2023.1252315

OPEN ACCESS

EDITED AND REVIEWED BY
Giuseppe Remuzzi,
Istituto di Ricerche Farmacologiche Mario Negri IRCCS, Italy

*CORRESPONDENCE
Swayam Prakash Srivastava,
swayam.cdri@gmail.com,
sps4004@med.cornell.edu

RECEIVED 03 July 2023
ACCEPTED 03 August 2023
PUBLISHED 08 August 2023

CITATION
Bhatia D and Srivastava SP (2023), Editorial: Diabetic kidney disease: routes to drug development, pharmacology and underlying molecular mechanisms. *Front. Pharmacol.* 14:1252315. doi: 10.3389/fphar.2023.1252315

Editorial: Diabetic kidney disease: routes to drug development, pharmacology and underlying molecular mechanisms

Divya Bhatia[1,2] and Swayam Prakash Srivastava[3]*

[1]Division of Nephrology and Hypertension, Joan and Sanford I. Weill Department of Medicine, New York, NY, United States, [2]NewYork-Presbyterian Hospital, Weill Cornell Medicine, New York, NY, United States, [3]Division of Regenerative Medicine, Department of Medicine, Hartman Institute of Therapeutic Organ Regeneration, Weill Cornell Medicine, New York, NY, United States

KEYWORDS

diabetic kidney disease, sodium-glucose cotransporter-2 (SGLT2) inhibitors, dipeptidyl peptidase-4 (DPP4 or CD26) inhibitors, N-acetyl-seryl-aspartyl-lysyl-proline (Ac-SDKP), sirtuin (SIRT)3, mitoquinone (MitoQ), kidney fibrosis, mitophagy

Editorial on the Research Topic
Diabetic kidney disease: routes to drug development, pharmacology and underlying molecular mechanisms

Introduction

Diabetic kidney disease (DKD) is one of the leading causes of kidney failure, which leads to end-stage renal disease (ESRD) and affects almost one-third of the total diabetic patients worldwide (Cooper and Warren, 2019; Tuttle et al., 2022). DKD is also one of the significant long-term complications, which not only imposes healthcare costs on patients with diabetes but substantially increases the rates of morbidity and mortality. A wide knowledge gap exists between biology and drug development which contributes to the suboptimal treatment options against DKD. An increased understanding of DKD is urgently needed for the development of novel therapeutics, which will help in targeting the changes that occur during the early stages of the disease. Several attempts have also been made to hybridize the process of biomarker discovery and drug development to arrest and reverse the inevitable events, which occur during the progression of DKD. However, currently approved therapeutic regimens such as angiotensin-converting enzyme (ACE) inhibitors, angiotensin II receptor blockers (ARBs), and statins, etc. can simply delay, but do not prevent the decline in kidney function and progression of ESRD (Gentile et al., 2014; Srivastava et al., 2020a; Hartman et al., 2020). Although these therapeutic agents help in reducing albuminuria in patients with DKD, they expose patients to multiple adverse reactions and drug intolerance. Thus, to improve kidney function in diabetic patients, there is an unmet need for new therapeutic strategies.

A variety of pharmacological agents are currently in clinical trials such as sodium glucose transporter-2 (SGLT-2) inhibitors and in preclinical settings including dipeptidase transferase-4 (DPP-4) inhibitors, mineralocorticoid receptor antagonists, N-acetyl-seryl-

aspartyl-lysyl-proline (Ac-SDKP), and endothelin receptor antagonists (ERAs) (Kanasaki et al., 2014; Li et al., 2020b; Srivastava et al., 2020b). These molecules have been shown to exhibit protective effects against increases in inflammatory and fibrotic responses in the kidney and worsening of kidney function in preclinical settings.

In this Research Topic, we provided a deeper insight into the recent advances in the pathophysiologic pathways, which can be modulated to prevent the worsening of diverse phenotypes of DKD. We also addressed the molecular mediators, which can be targeted to attenuate the progression of kidney fibrosis during DKD. Understanding these critical pathways and potential mediators will guide the discovery process of future therapeutic approaches against DKD.

Broadly we categorized this editorial into two major sections.

New molecular mechanisms in DKD

In recent years, we have worked on identifying new cellular and molecular mechanisms causative or protective in DKD. Defective central metabolism, i.e., reduced fatty acid oxidation (FAO) and induced abnormal glycolysis, accelerates the mesenchymal switching, and finally fibrogenesis (Kang et al., 2015; Srivastava et al., 2018). Dichloroacetate, 2-deoxyglucose, and C75 by correcting defective metabolism via promoting FAO levels in tubules, help in abolishing the fibrotic phenotype and improving kidney structure and functions (Kang et al., 2015). Sirtuin (SIRT)3 is the key regulator of central metabolism. SIRT3 induction provides protection to both tubules and kidney vasculature. SIRT3 abrogates abnormal glycolysis and improves lipid metabolism by transconversion of pyruvate kinase isozymes M1/M2 (PKM2) dimer to tetramer. SIRT3 also reduces the accumulation of hypoxia-inducible factor (HIF)-1α in the kidney tubules and endothelium (Srivastava et al., 2018; Srivastava et al., 2021b).

In this Research Topic, Li et al. described that Yin and Yang (YY)1 is involved in the upregulation LncRNA-ARAP1-AS2, which by promoting aberrant glycolysis caused fibrosis. The impaired glycolysis was associated with the activation of epidermal growth factor receptor (EGFR)/PKM2/HIF1α pathway. Their results highlight the role of YY1 in promoting glycolysis during DKD and suggest it as a potential therapeutic strategy for consideration.

Other molecules, i.e., endothelium glucocorticoid receptors (GR) and podocyte glucocorticoid receptors are critical in restoring cellular antifibrotic mechanisms, abolishing the mesenchymal metabolic shift and, associated kidney inflammation and fibrosis in diabetes (Srivastava et al., 2021c; Srivastava et al., 2021d). Glucocorticoid receptor negatively targets canonical Wnt signaling pathway, inflammation, and improves tubular and endothelial health (Srivastava et al., 2021d). Kidney endothelium-specific deficiency of SIRT3, GR, or fibroblast growth factor receptor (FGFR)1 accelerates the endothelial-to-mesenchymal transition (EndMT) by disrupting neighboring cell homeostasis and promoting epithelial–mesenchymal transition (EMT) in tubular cells during diabetes (Li et al., 2020a; Srivastava et al., 2021b; Srivastava et al., 2021d). This EndMT-mediated activation of partial EMT is caused due to systemic inflammation, accompanied by elevating levels of pro-mesenchymal and fibrotic cytokines, and reducing levels of anti-mesenchymal cytokines. Cumulative effects of systemic inflammation, defective central metabolism, and upregulated mesenchymal transcription factors, finally contribute to severe fibrosis in diabetic kidneys. Another article in this Research Topic described the role of nucleotide-binding oligomerization domain (NOD)-like receptors (NLPR3)-mediated pyroptosis in diabetic nephropathy (Wan et al.). This study demonstrated that the canonical NLRP3 inflammasome pathway, which involves the formation of membrane pores, and promotes inflammation, can also induce pyroptosis in the kidneys during DKD. This study suggests that targeting pyroptosis-associated proteins has therapeutic potential in the management of diabetes and related kidney disease.

Another study in this Research Topic by Cen et al. reported the protective effects of tetramethylpyrazine nitrone (TBN) in improving renal anemia, by maintaining iron homeostasis through activating the HIF via 5′ adenosine monophosphate-activated protein kinase (AMPK)/mammalian target of rapamycin (mTOR)/4E-binding protein 1 (4E-BP1) pathway. TBN, a nitrone derivative of tetramethylpyrazine also acts as a free radical scavenger against hydroxyl, superoxide, and peroxynitrite. Recently, we reported the therapeutic benefits of repleting the labile iron pool (LIP) of kidney macrophages in improving their antioxidant response and attenuating inflammation, and fibrosis during chronic kidney disease (CKD) (Patino et al., 2023). We also observed that the expression of superoxide dismutase-2 (SOD-2), an antioxidant enzyme decreased in the kidney during CKD, which was associated with an increase in mROS production by kidney macrophages (Bhatia et al., 2022). Therefore, it is critical to further investigate the therapeutic benefits of TBN as reported by Cen et al. against increases in oxidative stress, inflammation, and CKD-associated anemia.

New molecules against DKD

The discovery of SGLT-2 inhibitors has influential effects in the treatment of diabetes and associated kidney disease. The data from preclinical settings suggest that SGLT-2 inhibitors not only reduced worsening of kidney function and fibrosis, but, improved the overall structural impairments in the kidney of patients with DKD. The data from EMPA-REG OUTCOME clinical trials demonstrated that the use of SGLT-2 inhibitor, empagliflozin is safe and effective in reducing renal-related complications in patients with type 2 diabetes, suggesting the remarkable discovery in the treatment of DKD (Mayer et al., 2019). The SGLT-2 inhibitors provide protection against DKD through promoting the excretion of blood glucose in the urine and reducing intraglomerular pressure. However, the data from the diabetic mouse models have shown that the empagliflozin did not cause any change in blood pressure and blood glucose levels. These data from experimental models suggested that empagliflozin was able to reduce the aberrant glycolysis and induce the FAO in the tubules (Li et al., 2020b). Increased aberrant glycolysis and diminished FAO promote mesenchymal metabolic shift, which contributes to the deterioration of kidney function, structural abnormalities, and kidney fibrosis (Srivastava et al., 2018).

In this Research Topic, Hu et al. performed a systematic review to understand the efficacy and safety of SGLT-2 inhibitors in patients stratified in different groups based on their estimated glomerular filtration rate (eGFR). Based on the search using four databases, they reported that the SGLT2 inhibitors decreased the glycated hemoglobin (HbA1c) levels and body weight, which were in parallel with the baseline eGFR levels. However, SGLT2 inhibitor-mediated reductions in blood pressure levels were independent of the baseline eGFR in patients. Other reported potential therapeutic mediators, which have also shown to be effective against DKD include DPP-4 inhibitors and incretins analogs. Among different classes of DPP-4 inhibitors, linagliptin has been reported to be most effective in combating diabetes and associated kidney disease (Kanasaki et al., 2014). Linagliptin intake increased the levels of Ac-SDKP tetrapeptide and exhibited renal protection by delaying the progression of kidney disease.

Plant-derived synthetic compounds such as ursolic acid, paeoniflorin, and saponins are found to be effective against DKD. Interestingly ursolic acid improved the renal structural impairments and function through elevating FGFR1 and SIRT3 levels and reducing the expression of DPP-4 (Liu et al.). DPP-4 is known to exhibit profibrotic functions in the tubules. FGFR1 activation is related to the upregulation of microRNAs (miRNAs), such as miR-let-7s and miR-29s, these miRNAs exert antifibrotic effects (Srivastava et al., 2016). In addition, induction of SIRT3 also exhibits protective effects by abolishing the mesenchymal metabolism shift. Ac-SDKP mediates renal protection by binding with FGFR1 and elevating SIRT3 levels (Li et al., 2017; Srivastava et al., 2020b). Therefore, this tetrapeptide has great potential as a future therapeutic option for combating diabetes and related kidney disease (Srivastava et al., 2021a). The author Fang et al. reported that the Niaoduqing molecules mitigate high-glucose-induced podocyte injury by regulating advanced glycation endproducts/receptor for AGE (AGE/RAGE) signaling pathway.

The activation of SIRT3 is also known to attenuate NLRP3-mediated inflammation, apoptosis, and kidney fibrosis during DKD by inducing mitophagic activities (Feng et al., 2018). Mitochondrial-targeted approaches have also shown great efficacy against DKD in experimental models and patients (Bhatia et al., 2020). Mitoquinone (MitoQ), a mitochondrial-targeted coenzyme Q has been reported to mitigate albuminuria, glomerular hypertrophy, mesangial matrix expansion, and kidney fibrosis by restoring the expression of mitophagy regulators, including mitofusin (MFN)-2 and reducing mitochondrial fragmentation (Xiao et al., 2017). We have also observed the myeloid lineage-specific protective functions of MFN2 against increases in kidney macrophage-derived inflammatory and fibrotic responses during CKD (Bhatia et al., 2022). The efficacy of MitoQ was also investigated as part of a Phase IV controlled, double-blind clinical trial in stage 3–5 patients with CKD (ClinicalTrials.gov, Identifier number: NCT02364648). Szeto-Schiller-31 peptide (H-D-Arg-Dmt-Lys-Phe-NH2) (SS-31), a mitochondrial antioxidant also reduced macrophage recruitment, glomerulosclerosis, podocyte and endothelial cell death in the experimental model of DKD (Szeto et al., 2016).

In this Research Topic, a study by Wang et al. reported that sappanone A (SA), a plant-derived homoisoflavanone, prevented the worsening of kidney function in uninephrectomized and streptozotocin-induced DKD, by restoring the expression of nuclear factor kappa B (NF-κB) inhibitor alpha (IκBα). Their findings highlighted the protective effects of SA against increases in pro-inflammatory (interleukin-1β and tumor necrosis factor-α) and pro-fibrotic (transforming growth factor-β1 and collagen-IV) responses in the kidney during DKD. Restoration of IκBα is also critical in averting mitochondrial fragmentation and cytochrome (Cyt C)-mediated apoptotic cell death (Laforge et al., 2016). We also observed increases in circulating and urinary levels of Cyt C in experimental and human kidney fibrosis (Bhatia et al., 2022). The increased levels of Cyt C were associated with macrophage-mediated inflammatory and fibrotic events in the kidney (Bhatia et al., 2022). Therefore, the study by Wang et al. is important in confirming, that the SA-dependent protective effects against increases in inflammation and cell death during DKD are exerted via suppression of NF-κB pathway.

Another study by Chen et al. reviewed the therapeutic benefits of Chinese herbal medicines in suppressing oxidative stress, inflammation, and mitochondrial dysfunction. They highlighted that combining these herbal medicines with conventional therapies may further delay the progression of DKD effectively. These herbal medicines have been shown to modulate various pathways, including, i) Glucagon-like Peptide-1 (GLP)-receptor, ii) SGLT2, iii) SIRT1/AMPK, iv) AGE/RAGE, v) NF-κB, vi) nuclear factor erythroid 2–related factor 2 (Nrf2), vii) NLRP3, viii) Peroxisome proliferator-activated receptor-gamma coactivator (PGC)-1α, and ix) PINK1/Parkin-mediated mitophagy. We also reported that PINK1/Parkin-mediated mitophagy is downregulated in experimental and human kidney fibrosis (Bhatia et al., 2019). The expression of PGC-1α, which is a chief regulator of mitochondrial biogenesis has also been found to be suppressed in the kidney during fibrosis (Bhatia et al., 2022). Fenofibrate has been reported to promote mitochondrial fatty acid β-oxidation and regulate kidney function in patients with DKD by activating PGC-1α (Davis et al., 2011). Considering that kidneys are the second richest organ after the heart in mitochondrial content, it is anticipated and widely reported that mitochondrial dysfunction exaggerates the worsening of kidney diseases including DKD (Forbes and Thorburn, 2018; Bhatia and Choi, 2019; Bhatia et al., 2020). Mitophagy helps in the recycling of damaged mitochondrial components, which can act as mitochondrial damaged-associated molecular patterns (mtDAMPs) and promote inflammatory events in the kidney during DKD (Bhatia and Choi, 2023). These mtDAMPs, which include mitochondrial-derived reactive oxygen species (mROS), Cyt C, and cell-free or intracellular naked mitochondrial DNA (mtDNA) can exaggerate inflammation and fibrosis via activating NF-κB by toll-like receptor (TLR)-mediated signaling pathway. The mechanism of action of Chinese herbal medicines against the progression of DKD warrants further investigation.

Conclusion

Diabetic kidney disease is the chief cause of kidney failure and ESRD, which also increases cardiovascular events and mortality in the suffering patient population globally. It is important to understand the underlying mechanisms of diabetic milieu-induced kidney damage and progression of DKD. In this Research Topic, we have discussed potent therapeutic regimens for the management of DKD, tissue/cell/mitochondrial-specific novel biological mechanistic approaches, functions of regulatory

non-coding RNAs, and clinical data sets. We speculate that this Research Topic will provide basic essential information, that could be used in the design of potential therapeutic agents and help in the management of patients with DKD.

Author contributions

SS and DB wrote and edited the draft. All authors contributed to the article and approved the submitted version.

Funding

DB is supported by the 2T32HL134629-06A1 grant.

Conflict of interest

The authors declare that the research was conducted in the absence of any commercial or financial relationships that could be construed as a potential conflict of interest.

Publisher's note

All claims expressed in this article are solely those of the authors and do not necessarily represent those of their affiliated organizations, or those of the publisher, the editors and the reviewers. Any product that may be evaluated in this article, or claim that may be made by its manufacturer, is not guaranteed or endorsed by the publisher.

References

Bhatia, D., and Choi, M. E. (2019). The emerging role of mitophagy in kidney diseases. *J. Life Sci. (Westlake Village)* 3, 13–22. doi:10.36069/jols/20191203

Bhatia, D., and Choi, M. E. (2023). Autophagy and mitophagy: physiological implications in kidney inflammation and diseases. *Am. J. Physiol. Ren. Physiol.* 325, F1–F21. doi:10.1152/ajprenal.00012.2023

Bhatia, D., Chung, K. P., Nakahira, K., Patino, E., Rice, M. C., Torres, L. K., et al. (2019). Mitophagy-dependent macrophage reprogramming protects against kidney fibrosis. *JCI Insight* 4, e132826. doi:10.1172/jci.insight.132826

Bhatia, D., Capili, A., and Choi, M. E. (2020). Mitochondrial dysfunction in kidney injury, inflammation, and disease: potential therapeutic approaches. *Kidney Res. Clin. Pract.* 39, 244–258. doi:10.23876/j.krcp.20.082

Bhatia, D., Capili, A., Nakahira, K., Muthukumar, T., Torres, L. K., Choi, A. M. K., et al. (2022). Conditional deletion of myeloid-specific mitofusin 2 but not mitofusin 1 promotes kidney fibrosis. *Kidney Int.* 101, 963–986. doi:10.1016/j.kint.2022.01.030

Cooper, M., and Warren, A. M. (2019). A promising outlook for diabetic kidney disease. *Nat. Rev. Nephrol.* 15, 68–70. doi:10.1038/s41581-018-0092-5

Davis, T. M., Ting, R., Best, J. D., Donoghoe, M. W., Drury, P. L., Sullivan, D. R., et al. (2011). Effects of fenofibrate on renal function in patients with type 2 diabetes mellitus: the fenofibrate intervention and event lowering in diabetes (FIELD) study. *Diabetologia* 54, 280–290. doi:10.1007/s00125-010-1951-1

Feng, J., Lu, C., Dai, Q., Sheng, J., and Xu, M. (2018). SIRT3 facilitates amniotic fluid stem cells to repair diabetic nephropathy through protecting mitochondrial homeostasis by modulation of mitophagy. *Cell. Physiol. Biochem.* 46, 1508–1524. doi:10.1159/000489194

Forbes, J. M., and Thorburn, D. R. (2018). Mitochondrial dysfunction in diabetic kidney disease. *Nat. Rev. Nephrol.* 14, 291–312. doi:10.1038/nrneph.2018.9

Gentile, G., Mastroluca, D., Ruggenenti, P., and Remuzzi, G. (2014). Novel effective drugs for diabetic kidney disease? Or not? *Expert Opin. Emerg. Drugs* 19, 571–601. doi:10.1517/14728214.2014.979151

Hartman, R. E., Rao, P. S. S., Churchwell, M. D., and Lewis, S. J. (2020). Novel therapeutic agents for the treatment of diabetic kidney disease. *Expert Opin. Investig. Drugs* 29, 1277–1293. doi:10.1080/13543784.2020.1811231

Kanasaki, K., Shi, S., Kanasaki, M., He, J., Nagai, T., Nakamura, Y., et al. (2014). Linagliptin-mediated DPP-4 inhibition ameliorates kidney fibrosis in streptozotocin-induced diabetic mice by inhibiting endothelial-to-mesenchymal transition in a therapeutic regimen. *Diabetes* 63, 2120–2131. doi:10.2337/db13-1029

Kang, H. M., Ahn, S. H., Choi, P., Ko, Y. A., Han, S. H., Chinga, F., et al. (2015). Defective fatty acid oxidation in renal tubular epithelial cells has a key role in kidney fibrosis development. *Nat. Med.* 21, 37–46. doi:10.1038/nm.3762

Laforge, M., Rodrigues, V., Silvestre, R., Gautier, C., Weil, R., Corti, O., et al. (2016). NF-κB pathway controls mitochondrial dynamics. *Cell. Death Differ.* 23, 89–98. doi:10.1038/cdd.2015.42

Li, J., Shi, S., Srivastava, S. P., Kitada, M., Nagai, T., Nitta, K., et al. (2017). FGFR1 is critical for the anti-endothelial mesenchymal transition effect of N-acetyl-seryl-aspartyl-lysyl-proline via induction of the MAP4K4 pathway. *Cell. Death Dis.* 8, e2965. doi:10.1038/cddis.2017.353

Li, J., Liu, H., Srivastava, S. P., Hu, Q., Gao, R., Li, S., et al. (2020a). Endothelial FGFR1 (fibroblast growth factor receptor 1) deficiency contributes differential fibrogenic effects in kidney and heart of diabetic mice. *Hypertension* 76, 1935–1944. doi:10.1161/HYPERTENSIONAHA.120.15587

Li, J., Liu, H., Takagi, S., Nitta, K., Kitada, M., Srivastava, S. P., et al. (2020b). Renal protective effects of empagliflozin via inhibition of EMT and aberrant glycolysis in proximal tubules. *JCI Insight* 5, e129034. doi:10.1172/jci.insight.129034

Mayer, G. J., Wanner, C., Weir, M. R., Inzucchi, S. E., Koitka-Weber, A., Hantel, S., et al. (2019). Analysis from the EMPA-REG OUTCOME® trial indicates empagliflozin may assist in preventing the progression of chronic kidney disease in patients with type 2 diabetes irrespective of medications that alter intrarenal hemodynamics. *Kidney Int.* 96, 489–504. doi:10.1016/j.kint.2019.02.033

Patino, E., Bhatia, D., Vance, S. Z., Antypiuk, A., Uni, R., Campbell, C., et al. (2023). Iron therapy mitigates chronic kidney disease progression by regulating intracellular iron status of kidney macrophages. *JCI Insight* 8, e159235. doi:10.1172/jci.insight.159235

Srivastava, S. P., Shi, S., Kanasaki, M., Nagai, T., Kitada, M., He, J., et al. (2016). Effect of antifibrotic MicroRNAs crosstalk on the action of N-acetyl-seryl-aspartyl-lysyl-proline in diabetes-related kidney fibrosis. *Sci. Rep.* 6, 29884. doi:10.1038/srep29884

Srivastava, S. P., Li, J., Kitada, M., Fujita, H., Yamada, Y., Goodwin, J. E., et al. (2018). SIRT3 deficiency leads to induction of abnormal glycolysis in diabetic kidney with fibrosis. *Cell. Death Dis.* 9, 997. doi:10.1038/s41419-018-1057-0

Srivastava, S. P., Goodwin, J. E., Kanasaki, K., and Koya, D. (2020a). Inhibition of angiotensin-converting enzyme ameliorates renal fibrosis by mitigating DPP-4 level and restoring antifibrotic MicroRNAs. *Genes. (Basel)* 11, 211. doi:10.3390/genes11020211

Srivastava, S. P., Goodwin, J. E., Kanasaki, K., and Koya, D. (2020b). Metabolic reprogramming by N-acetyl-seryl-aspartyl-lysyl-proline protects against diabetic kidney disease. *Br. J. Pharmacol.* 177, 3691–3711. doi:10.1111/bph.15087

Srivastava, S. P., Kanasaki, K., and Goodwin, J. E. (2021a). Editorial: combating diabetes and diabetic kidney disease. *Front. Pharmacol.* 12, 716029. doi:10.3389/fphar.2021.716029

Srivastava, S. P., Li, J., Takagaki, Y., Kitada, M., Goodwin, J. E., Kanasaki, K., et al. (2021b). Endothelial SIRT3 regulates myofibroblast metabolic shifts in diabetic kidneys. *iScience* 24, 102390. doi:10.1016/j.isci.2021.102390

Srivastava, S. P., Zhou, H., Setia, O., Dardik, A., Fernandez-Hernando, C., and Goodwin, J. (2021c). Podocyte glucocorticoid receptors are essential for glomerular endothelial cell homeostasis in diabetes mellitus. *J. Am. Heart Assoc.* 10, e019437. doi:10.1161/JAHA.120.019437

Srivastava, S. P., Zhou, H., Setia, O., Liu, B., Kanasaki, K., Koya, D., et al. (2021d). Loss of endothelial glucocorticoid receptor accelerates diabetic nephropathy. *Nat. Commun.* 12, 2368. doi:10.1038/s41467-021-22617-y

Szeto, H. H., Liu, S., Soong, Y., Alam, N., Prusky, G. T., and Seshan, S. V. (2016). Protection of mitochondria prevents high-fat diet-induced glomerulopathy and proximal tubular injury. *Kidney Int.* 90, 997–1011. doi:10.1016/j.kint.2016.06.013

Tuttle, K. R., Agarwal, R., Alpers, C. E., Bakris, G. L., Brosius, F. C., Kolkhof, P., et al. (2022). Molecular mechanisms and therapeutic targets for diabetic kidney disease. *Kidney Int.* 102, 248–260. doi:10.1016/j.kint.2022.05.012

Xiao, L., Xu, X., Zhang, F., Wang, M., Xu, Y., Tang, D., et al. (2017). The mitochondria-targeted antioxidant MitoQ ameliorated tubular injury mediated by mitophagy in diabetic kidney disease via Nrf2/PINK1. *Redox Biol.* 11, 297–311. doi:10.1016/j.redox.2016.12.022

frontiers | Frontiers in Pharmacology

TYPE Original Research
PUBLISHED 16 August 2022
DOI 10.3389/fphar.2022.966786

OPEN ACCESS

EDITED BY
Swayam Prakash Srivastava,
Yale University, United States

REVIEWED BY
Lining Miao,
Second Hospital of Jilin University, China
Aditya Yashwant Sarode,
Columbia University, United States

*CORRESPONDENCE
Yongli Zhan,
zhanyongli88@sina.com

†These authors have contributed equally to this work

SPECIALTY SECTION
This article was submitted to Renal Pharmacology, a section of the journal Frontiers in Pharmacology

RECEIVED 11 June 2022
ACCEPTED 25 July 2022
PUBLISHED 16 August 2022

CITATION
Liu T, Mu S, Yang L, Mao H, Ma F, Wang Y and Zhan Y (2022), Comprehensive bibliometric analysis of sirtuins: Focus on sirt1 and kidney disease.
Front. Pharmacol. 13:966786.
doi: 10.3389/fphar.2022.966786

Comprehensive bibliometric analysis of sirtuins: Focus on sirt1 and kidney disease

Tongtong Liu[1†], Shujuan Mu[2†], Liping Yang[1], Huimin Mao[1], Fang Ma[1], Yuyang Wang[1] and Yongli Zhan[1*]

[1]Guang'anmen Hospital, China Academy of Chinese Medical Sciences, Beijing, China, [2]South District of Guang'anmen Hospital, China Academy of Chinese Medical Sciences, Beijing, China

Sirtuins, as regulators of metabolism and energy, have been found to play an important role in health and disease. Sirt1, the most widely studied member of the sirtuin family, can ameliorate oxidative stress, immune inflammation, autophagy, and mitochondrial homeostasis by deacetylating regulatory histone and nonhistone proteins. Notably, sirt1 has gradually gained attention in kidney disease research. Therefore, an evaluation of the overall distribution of publications concerning sirt1 based on bibliometric analysis methods to understand the thematic evolution and emerging research trends is necessary to discover topics with potential implications for kidney disease research. We conducted a bibliometric analysis of publications derived from the Web of Science Core Collection and found that publications concerning sirt1 have grown dramatically over the past 2 decades, especially in the past 5 years. Among these, the proportion of publications regarding kidney diseases have increased annually. China and the United States are major contributors to the study of sirt1, and Japanese researchers have made important contributions to the study of sirt1 in kidney disease. Obesity, and Alzheimer's disease are hotspots diseases for the study of sirt1, while diabetic nephropathy is regarded as a research hotspot in the study of sirt1 in kidney disease. NAD^+, oxidative stress, and p53 are the focus of the sirt1 research field. Autophagy and NLRP3 inflammasome are emerging research trends have gradually attracted the interest of scholars in sirt1, as well as in kidney disease. Notably, we also identified several potential research topics that may link sirt1 and kidney disease, which require further study, including immune function, metabolic reprogramming, and fecal microbiota.

KEYWORDS

bibliometric analysis, SIRT1, kidney disease, NAD, oxidative stress, autophagy

Introduction

Sirtuins belong to a highly evolutionarily conserved histone deacetylase (HDACs) family that is dependent on nicotinamide adenine dinucleotide (NAD^+) (Wang and Lin, 2021). Silent information regulator 2 (Sir2) was originally identified in yeast and named in 1987 (Ivy et al., 1986). Subsequently, Sir2 was found to be involved in regulating the

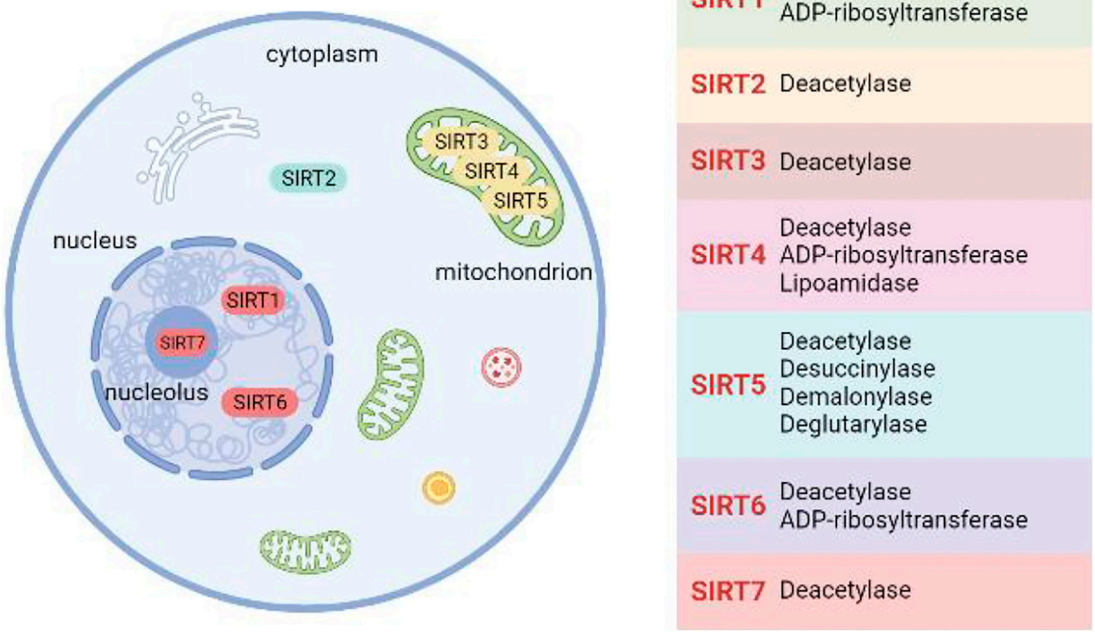

FIGURE 1
The role of sirtuins in kidney disease.

replicative lifespan of yeast, increasing the dose of Sir2 increased yeast lifespan by 30% (Kaeberlein et al., 1999). Sirtuins are homologous mammalian enzymes of Sir2 and consist of seven isoforms (sirt1-sirt7). The intracellular localization of Sirtuins is closely related to its function. Sirt1, sirt6, and sirt7 are mainly located in the nucleus, and primarily responsible for transcriptional regulation, repair of DNA and regulation of the cell cycle. Sirt3-sirt5 exist in mitochondria, and plays an important role in regulating cell energy metabolism. Sirt2 is the only directly available family member in the cytoplasm, and mainly functions in mitosis (Zhao et al., 2020). All members of the Sirtuins family have deacetylation properties, sirt1, sirt4, and sirt6 have been found to possess ADP-ribosyltransferase activity, sirt5 and sirt7 have also been reported to be a desuccinylase (Srivastava et al., 2020b; Gupta et al., 2022). Notably, sirt5 also has two unique properties of demalonylation and deglutarylation (Kumar and Lombard, 2018). Sirt4 has been reported to possess unique lipoamidase activity (Mathias et al., 2014) (Figure 1). Sirtuins, as a regulator of metabolism and energy, are closely associated with many aging-related diseases, including cardiovascular diseases (Soni et al., 2021), cancer (Aventaggiato et al., 2021), and neurodegenerative disorders (Leite et al., 2022). Accumulating evidence suggests that sirtuins play important roles in transcriptional regulation, cell survival, cell stress resistance, DNA damage and repair, and cell cycle regulation (Haigis and Sinclair, 2010). Interestingly, sirtuins were found to be central players in health improvement associated with calorie restriction and exercise training. In addition, some natural compounds (such as resveratrol, astragaloside IV, and honokiol) and small molecules (such as SRT1720, SRT1460, and SRT3025) have also been found to ameliorate diseases by activating sirtuins, which has made scholars realize the importance of sirtuins as potential pharmacological targets for many diseases (Dai et al., 2018).

Sirt1 is phylogenetically similar to yeast Sir2 and is the most extensively studied member of the sirtuin family. Sirt1 can regulate energy metabolism, immune inflammation, oxidative stress, mitochondrial homeostasis, autophagy, and apoptosis, and in turn ameliorates disease progression and aging by deacetylating regulatory histones and nonhistone proteins, such as peroxisome proliferator-activated receptor alpha (PPARα), PPAR gamma coactivator-1alpha (PGC-1α), and fork-head box protein (FOXO) (Zhao et al., 2020). The kidney is one of the major organs that are prone to aging-related diseases, especially in diabetes mellitus conditions. Multiple stresses lead to accelerated renal aging, including accumulation of advanced glycation end products, inflammation, autophagic damage, and oxidative stress (Guo et al., 2020). The study of sirt1 in kidney disease, especially in diabetic nephropathy (DN), has gradually gained the attention of researchers. On the one hand, sirt1 can improve renal resident cell injury and apoptosis by

directly regulating oxidative stress, mitochondrial homeostasis, and autophagy. On the other hand, sirt1 can modulate ectopic lipid accumulation in the kidney, ameliorate fibrosis, and prevent the progression of renal disease. In addition, sirt1 has also been found to ameliorate vascular endothelial injury and reduce complications of kidney disease, thereby improving the vulnerability of the kidney to aging (Morigi et al., 2018). Studies have found that the knockout of renal sirt1 can lead to the aggravation of inflammation, proteinuria, and fibrosis (He et al., 2010; Liu et al., 2014), and these phenotypes of renal injury may be significantly ameliorated by using resveratrol (RSV) (Kitada et al., 2011), NMN (Yasuda et al., 2021), or SRT1720 (Funk et al., 2010) to activate sirt1. Thus, sirt1 plays an irreplaceable role in the initiation and progression of kidney diseases.

Bibliometric analysis is an effective way to assess overall trends in a field. It not only helps researchers and clinicians understand core countries, institutions, and authors of a given research area and the most influential nodal publications, but also identifies thematic changes, emerging research trends, and research gaps in this area (Sabe et al., 2022). In recent years, there has been an explosion of research on the role of sirtuins in health and disease. However, studies evaluating the overall trends of sirtuins are scarce. To our knowledge, only one bibliometric analysis has evaluated sirt6 (Lu et al., 2018). Therefore, in this study, we evaluated the overall distribution of studies on sirtuins over the past 2 decades using the bibliometric analysis method, and with a particular focus on sirt1 and kidney disease. Through an analysis of the main research areas and emerging research trends in the field of sirt1 research, we hope to shed new light and ideas on the study of sirt1 in kidney disease.

Methods

Search strategy

The Web of Science Core Collection (WoSCC), the most comprehensive database for bibliometric analysis, was used to conduct a comprehensive search of publications related to sirtuins. We used topic subject (TS) as our search strategy, and the retrieval formula was set as TS = ("sirt" OR "sirtuin" OR "sirtuins" OR "SIRT1" OR "sirtuin1" OR "SIRT2" OR "sirtuin2" OR "SIRT3" OR "sirtuin3" OR "SIRT4" OR "sirtuin4" OR "SIRT5" OR "sirtuin5" OR "SIRT6" OR "sirtuin6" OR "SIRT7" OR "sirtuin7"). Publication type was restricted to "article" and "review". In addition, we performed additional analyses of sirtuin family members (sirt1-sirt7) separately, with a focus on the analysis of sirt1 and sirt1 in kidney disease. The retrieval formula is shown in Supplementary Table S1. The above process was completed in 1 day on 25 April 2022, to avoid bias from data updates.

Data analysis

Citespace (version 6.1.R1), VOSviewer (version 1.6.16), Bibliometrix 4.1.0 package (https://www.bibliometrix.org), and the Arrowsmith project (http://arrowsmith.psych.uic.edu) were used to analyze the collected data, including the overall distribution of publications, leading countries and institutions, core journals, active authors, co-citation references, and keyword analysis. The Journal Citation Reports (JCR) and Hirsch index (H-index) have also been used to assist in assessing the academic impact of journals and authors.

Citespace (Chen, 2004) was used to perform cluster analysis and burst analysis of co-references and keywords to understand the main research areas and emerging research trends of sirt1, and automated labelling for cluster interpretation. We defined modularity $Q > 0.3$ and mean silhouette >0.5 as indicators that the clustering results were sufficiently stable and reliable. Bibliometrix, based on the R project (Aria and Cuccurullo, 2017), was used to construct the thematic evolution of keywords, and the time cutting points were set as 2018 and 2020, respectively (recent five and 3 years). Next, VOSviewer (van Eck and Waltman, 2010) was used to extract and visualize the keywords for sirt1 in kidney disease research. Finally, the Arrowsmith project (Smalheiser et al., 2009) was used to construct an association between sirt1 and kidney disease. The retrieval formula of A-query (sirt1) was set as [sirt1 (MeSH Terms)] OR [sirtuin1 (MeSH Terms]), and the retrieval formula of C-query (kidney disease) was set as [kidney disease (MeSH Terms)] OR [renal disease (MeSH Terms)] OR [nephropathy (MeSH Terms)]. Using the keywords obtained from the Arrowsmith Project as the prediction group and the keywords extracted from VOSviewer was used as the confirmation group, and a Venn diagram of the two groups was drawn to obtain the potential links between sirt1 research and kidney disease. String (https://cn.string-db.org) was used to construct protein-protein interaction (PPI) networks for the target proteins.

Results

Overall distribution and publication trends of sirtuins

A total of 18225 publications from 1994 to 2022 were retrieved from the WoSCC. Through curve fitting analysis, we found that the publications about sirtuins showed a sharp growth trend with an annual growth rate of 13.10% in the last 5 years ($R^2 = 0.8386$, Figure 2A). From 1994 to 2004, studies on sirtuins were in their infancy, with no more than 50 articles published annually. Since 2005, the number of publications on sirtuins has increased dramatically at an average rate of 100 per year. Even from 2013, the growth rate of publications on sirtuins reached an average of 200 publications per year,

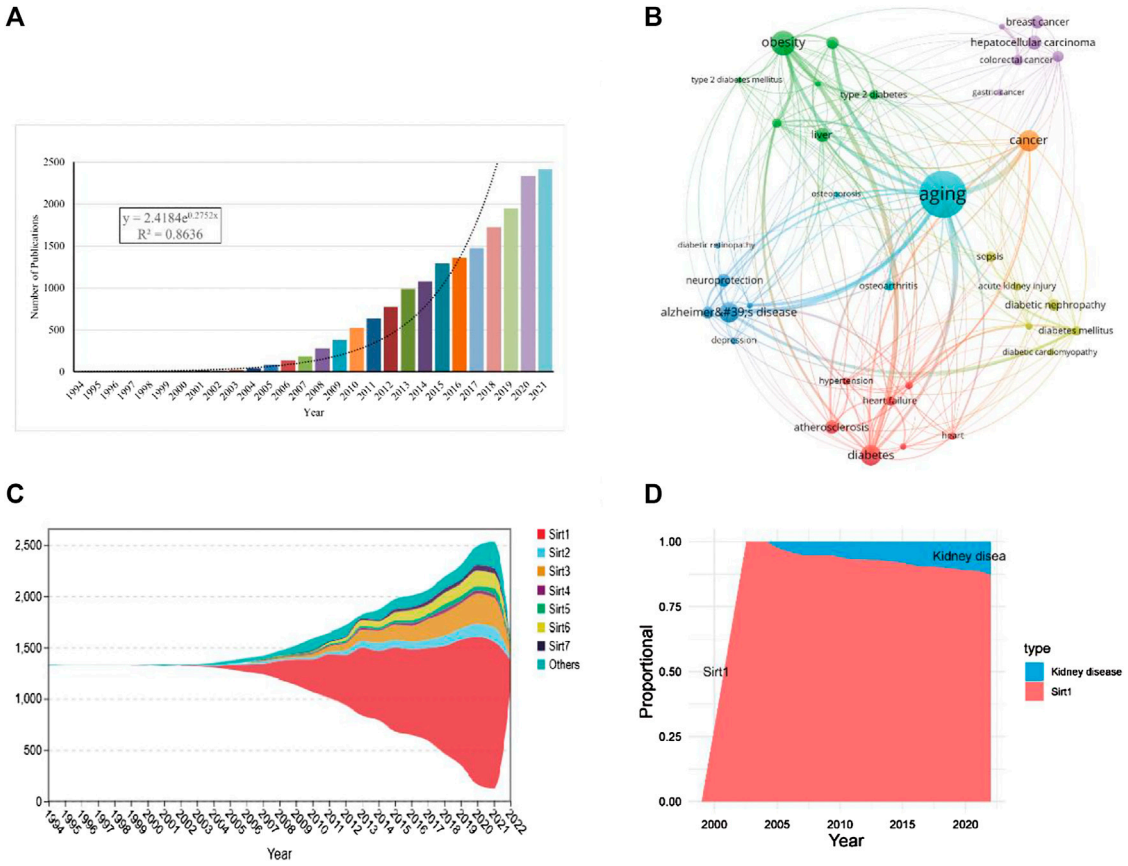

FIGURE 2
Overall distribution of sirtuins study. **(A)**. Global annual production trends in studies on sirtuins. **(B)**. Key diseases in sirtuins related research. **(C)**. Stream plots of annual production trends for the sirtuins family. **(D)**. The annual proportion of kidney disease in studies on sirt1.

TABLE 1 Top ten diseases most significantly associated with sirtuins in publications.

Rank	Disease	Occurrences
1	Aging	822
2	Obesity	340
3	Cancer	273
4	Diabetes	266
5	Alzheimer's disease	259
6	Liver	163
7	Hepatocellular Carcinoma	161
8	Atherosclerosis	154
9	Neuroprotection	144
10	Breast cancer	142

illustrating that research on sirtuins has gradually emerged in numerous fields.

Through co-occurrence analysis of the keywords of the retrieved publications, it was found that the diseases related to sirtuins research are mainly concentrated in aging, obesity, neurodegenerative diseases, cancer, and cardiovascular diseases (Figure 2B; Table 1). Publications about sirt1, growing rapidly ($R^2 = 0.9733$), were the most studied ($n = 11265$, 61.81%) and had the highest h-index (250) (Figure 2C; Table 2). There were 744 articles focusing on kidney disease, and the proportion of research investigating kidney disease and sirt1 increased annually (Figure 2D), suggesting that an increasing number of scholars have focused on the potential role of sirt1 in kidney disease. Next, we present an in-depth analysis of publications on sirt1, with a particular focus on the field of kidney disease.

TABLE 2 Overall distribution of publications in sirtuin family.

Sirtuins	Enzyme activity	Number of publications	Total times cited	Average citation frequency	Growth factor (R^2,2011–2021)	Annual growth rate (2017–2021)	H (%)-index
Sirtuins		18225	710588	38.98974	0.9852	13.10	304
Sirt1	Deacetylase, ADP-ribosyltransferase	11265 (61.81%)	454744	40.36787	0.9733	12.29	250
Sirt2	Deacetylase	1061 (5.82%)	42078	39.65881	0.9074	12.80	97
Sirt3	Deacetylase	2049 (11.24%)	80064	39.07467	0.9528	10.06	126
Sirt4	Deacetylase, ADP-ribosyltransferase, Lipoamidase	289 (1.58%)	16779	58.05882	0.6897	10.23	54
Sirt5	Deacetylase, desuccinylase, demalonylase, deglutarylase	390 (2.14%)	19871	50.95128	0.8766	24.56	64
Sirt6	Deacetylase, ADP-ribosyltransferase	1039 (5.70%)	42127	40.54572	0.8867	11.27	98
Sirt7	Deacetylase	363 (1.99%)	19500	53.71901	0.8454	8.68	64

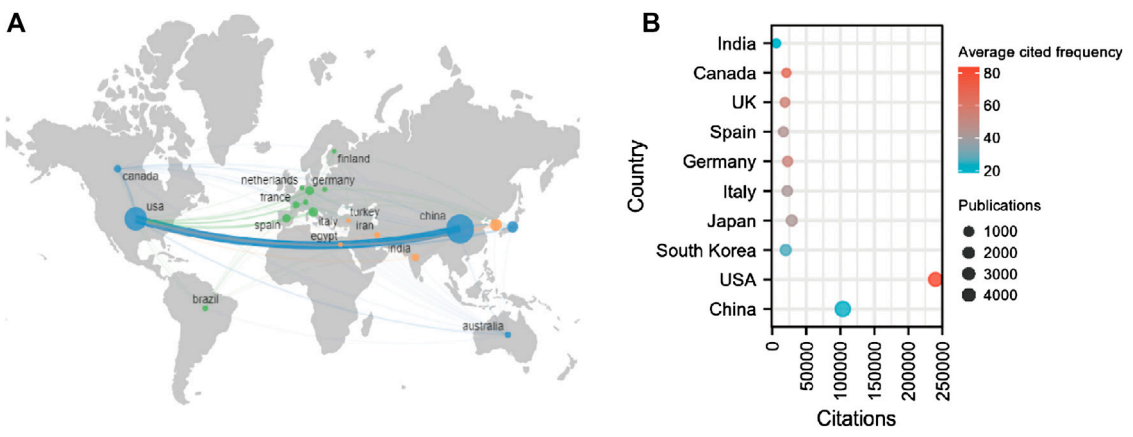

FIGURE 3
National contributions of the sirt1 study. **(A)** Global geographic distribution and collaboration regarding the study of sirt1. **(B)** The top ten highest productive countries for the study of sirt1.

Country, institution, and author analysis

In total, 6941 institutions from 92 countries contributed to publications related to sirt1. The United States is a central player in international collaboration and has partnered with many countries, most notably with China (Figure 3A).75.68% of publications were represented by the top ten countries with the largest number of publications (Table 3). China and the United States are far ahead of other countries in terms of the number of publications and total citations. In terms of average citation frequency, the United States (average cited 83.60 times) continues to rank first, followed by Canada (average cited 67.18 times) and the United Kingdom (average cited 53.94 times) (Figure 3B). Furthermore, seven of the ten most cited institutions worldwide are from the United States, which explains why the United States is far ahead of the world in terms of the total and average number of citations. In the field of kidney disease, China and the United States are still far ahead in terms of the number of publications and citations. However, Japan ranked first in terms of average citation frequency, followed by Italy and the United States (Supplemental Table S2). Kanazawa Medical University (cited 1799 times) and Shiga University of Medical Science (cited 1495 times) from Japan and Fudan University (cited 958 times) from China are the most influential institutions in the field of sirt1 in kidney diseases.

TABLE 3 The top 10 highest productive countries for the study of sirt1.

Rank	Country	Number of publications	Total times cited	Average citation frequency	H-index
1	China	4904 (43.53%)	103654	21.14	106
2	United States	2870 (25.48%)	239938	83.60	222
3	South Korea	762 (6.76%)	19723	25.88	66
4	Japan	673 (5.97%)	28504	42.35	86
5	Italy	524 (4.65%)	22025	42.03	74
6	Germany	424 (3.76%)	22516	53.10	75
7	Spain	377 (3.35%)	16498	43.76	65
8	United Kingdom	345 (3.06%)	18608	53.94	70
9	Canada	309 (2.74%)	20758	67.18	70
10	India	309 (2.74%)	5788	18.73	40

TABLE 4 The top five most cited authors for the study of sirt1.

Rank	Author	Institution	Country	Number of publications	Total times cited	Average citation frequency	H-index
1	Sinclair DA	Harvard Medical School	United States	66	20460	310.00	48
2	Guarente L	Massachusetts Institute of Technology	United States	63	18758	297.75	52
3	Auwerx J	Ecole Polytechnique Fédérale de Lausanne	Switzerland	50	16415	328.30	39
4	Puigserver P	Harvard Medical School	United States	17	12031	707.71	17
5	Mostoslavsky R	Harvard Medical School	United States	21	11734	558.76	20

A total of 39208 authors contributed to the study of sirt1. Frye RA from the University of Pittsburgh was the first scholar to publish publications on sirt1 in 1999 (Frye, 1999). Sinclair DA (cited 20460 times) from Harvard Medical School and Guarente L (cited 18758 times) from Massachusetts Institute of Technology (MIT), with the highest number of citations, were the most influential authors in terms of sirt1 research (Table 4). In the field of kidney disease, 3789 authors have been involved in the study of sirt1. Koya D from Kanazawa Medical University (cited 1799 times) and Kume S from Shiga University of Medical Science (cited 1446 times), as the most cited authors, were the most influential scholars (Supplemental Table S3). Koya D and Kume S were also the first to publish that sirt1 plays a key role in kidney disease.

Journal analysis

A total of 1665 journals published publications on Sirt1. According to the JCR, 582 (34.96%) journals appeared in JCR quartile 1 (Q1) and 444 (26.67%) journals were ranked in Q2 (Figure 4A), revealing the enormous academic impact of sirt1 research. Furthermore, a total of 5153 publications were published in these Q1 journals and 3690 in Q2 journals (Figure 4B), with mean impact factors of 8.55 and 4.18, respectively (Figure 4C). The Journal of Biological Chemistry, Cell, and Nature, as the journals with the highest academic impact in this field, are the three most cited journals, and eight of the ten most cited journals belong to the Q1, where Science, Nature, and Cell were the most frequently cited journals on average (Table 5). However, only three of the ten highest-volume journals appeared among the highly cited journals (Table 5). The dual-map overlay shows a total of three main citation paths in publications related to sirt1, where the publications performing citations were focused on the molecular, biology, immunology and medicine, medical, clinical field and the cited references were focused on the molecular, biology, genencs and health, nursing, medicine field (Figure 4D). In the field of kidney disease, 321 journals published relevant publications, 130 (40.5%) of which belonged to Q1, and 90 (28.04%) appeared in Q2 (Figure 4E), with mean impact factors of 18.91 and 10.18, respectively, which were better than all the publications on sirt1 (Figures 4F,G), illustrating the potential

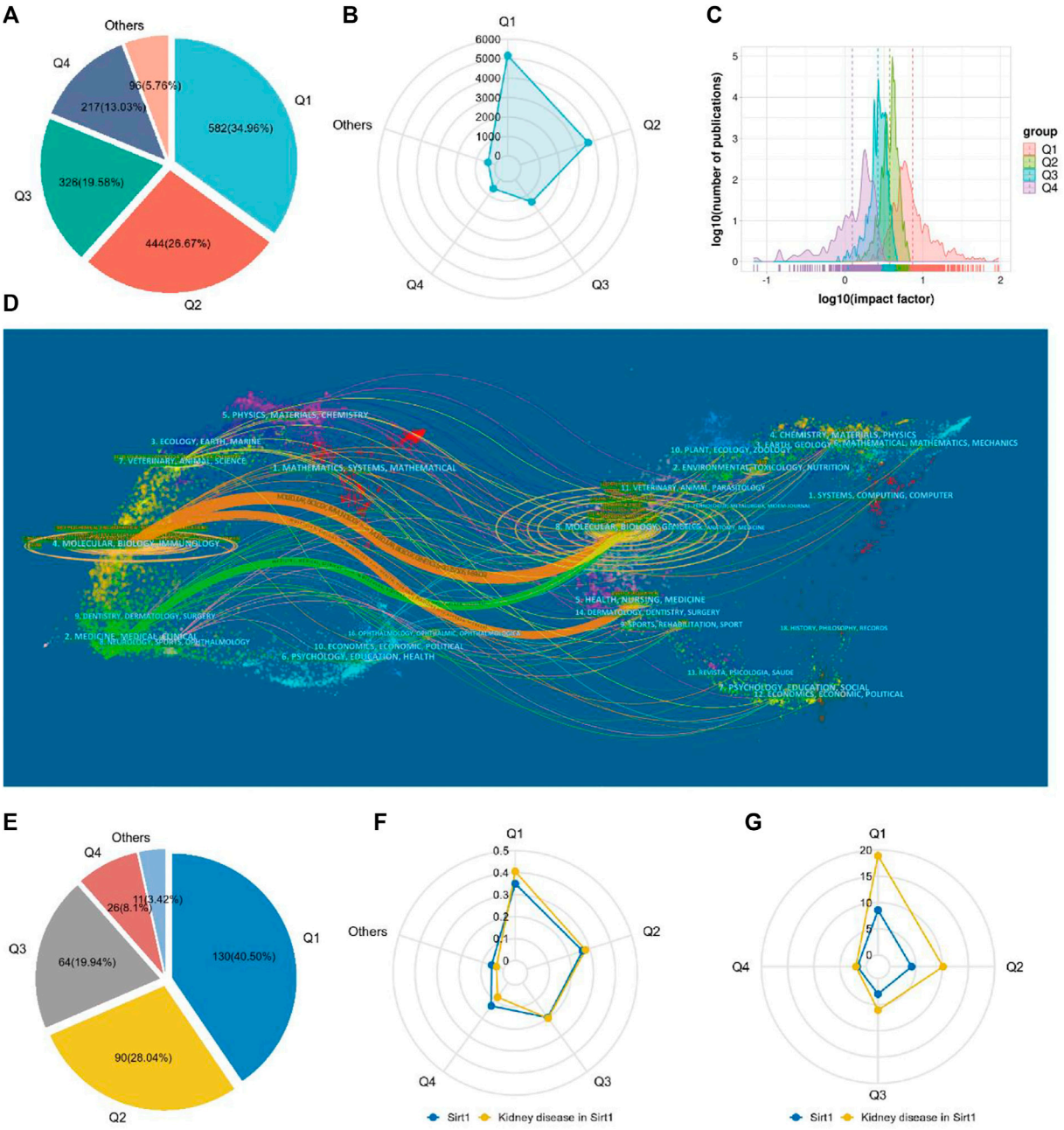

FIGURE 4
Characteristics of the core journals involved in the study of sirt1. **(A)** The quartile ranking of journals concerned with sirt1. **(B)** Radar plot of publication volume of sirt1 for journals in different quartile rankings. **(C)** Impact factor distribution of journals in different quartile rankings. **(D)** The dual-map overlay of the publications concerning sirt1. **(E)** The quartile ranking of journals concerned with sirt1 in kidney disease. **(F)** Radar plot of the proportion of different quartile rankings with respect to the number of publications of sirt1 and sirt1 in kidney disease. **(G)** Radar plot of Impact factor distribution of journals in different quartile rankings of sirt1 and sirt1 in kidney disease.

promise of sirt1 in kidney disease research. Journal of Clinical Investigation, Journal of the American Society of Nephrology (JASN), Aging Cell, and Kidney International (KI), as the most cited journals, were identified as the most influential journals (Supplemental Table S4).

Co-cited references analysis

In the top 10 most cited publications, a paper published by Lagouge et al. (2006) in Cell in 2006 was the most co-cited, with 3029 citations. This research reported that RSV, as an activator of

TABLE 5 Top ten journals with the largest number of publications and the most cited related to sirt1.

Rank	Journal	Number of publications	Total times cited	Average citation frequency	Journal (cited)	Number of publications	Total times cited	Average citation frequency
1	Plos one	309	14008	45.33	Journal of biological chemistry	181	20464	113.06
2	Biochemical and Biophysical Research Communications	211	8527	40.41	Cell	30	17476	582.53
3	Scientific reports	192	5254	27.36	Nature	21	17023	810.62
4	International Journal of Molecular Sciences	189	3051	16.14	Plos one	309	14008	45.33
5	Journal of biological chemistry	181	20464	113.06	Cell metabolism	47	13207	281.00
6	Oxidative Medicine and Cellular Longevity	136	3282	24.13	PNAS	56	10756	192.07
7	Frontiers in pharmacology	130	1715	13.19	Science	13	9496	730.46
8	Aging-us	125	3363	26.90	Biochemical and biophysical research communications	211	8527	40.41
9	Molecular medicine reports	123	1926	15.66	Molecular cell	31	6574	212.06
10	Oncotarget	115	3340	29.04	Embo journal	17	5699	335.24

sirt1, can promote energy and metabolic homeostasis and improve aerobic capacity. The article published in Nature by Howitz et al. (2003) was cited 2833 times and ranked second. They similarly reported that small molecules, such as RSV, can activate sirt1 and extend the lifespan of *Saccharomyces cerevisiae*. This underscores the importance of investigating sirt1 activating compounds (STACs). In addition, we analyzed the top ten most-cited publications in the last 5 years. The most cited article was written by Das et al. (2018) in 2018 and published in Cell. They reported that endothelial sirt1 deficiency is a reversible cause of vascular aging, and the NAD precursor NMN can reverse this change through sirt1. The second ranked article by citation number was published in the Journal of Neuroinflammation by Chen et al. (2018) in 2018, which showed that ω-3 polyunsaturated fatty acid supplementation can regulate HMGB1/NF-κB pathways through sirt1-mediated deacetylation to attenuate inflammatory responses. In terms of kidney disease, the most cited articles reported that RSV attenuates proteinuria, renal immunoglobulin deposition, and glomerulonephritis in lupus nephritis mice (Wang et al., 2014). In the last 5 years, the most cited articles were published by Ren et al. (2020), who reported that metformin, a classic hypoglycemic agent, produced renoprotective effects against diabetes *via* the AMPK/SIRT1-FoxO1 pathway. The second most focused article was a review published by Ralto et al.(2020), who reported that NAD^+ homeostasis plays an important role in kidney disease and health.

Next, we performed a cluster analysis of the co-cited references, resulting in seven clusters with a modularity Q of 0.646 and a mean silhouette value of 0.8156 (Figure 5A). The top five clusters were enriched for diseases associated with sirt1, including diabetes, skeletal muscle, cancer, and cognitive deficit. It is important to note that nicotinamide mononucleotides (NAD) appear to be a hotspot that gains considerable interest. When focusing on kidney disease, five clusters were extracted, with a modularity Q of 0.4116 and a mean silhouette value of 0.6787 (Figure 5B). We found that NAD^+ has also been the focus of research regarding sirt1 in kidney disease.

In addition, we performed an analysis of burst and obtained 778 burst references (Figure 5C). The reference with the strongest beginning of citation burst was published in Cell by Vaziri et al. (2001) in 2001. They described that sirt1 can deacetylate regulated p53, thus improving growth arrest or apoptosis. Similarly, the references with the second strongest beginning of citation burst were published by Luo et al. (2001) in Cell in 2001 and reported similar results. This illustrates that the regulation of deacetylation of p53 by sirt1 is a major discovery in sirt1 research. When focusing on the last 3 years, the reference with the strongest beginning of citation burst was published by Alves-fernandes D et al. and Zhang W et al., and they jointly focused on the important crosstalk role of sirt1 and oxidative stress in different diseases (Zhang et al., 2017; Alves-Fernandes and Jasiulionis, 2019). In terms of kidney disease, 49 burst references were found (Figure 5D), the publication by Brunet A et al. in Science in 2004 had the strongest beginning of citation burst, followed by Rodgers J et al., published in Nature in 2005, indicating that the regulation of FOXO and PGC-1α by sirt1 has received much attention from scholars in the field of kidney disease (Brunet et al., 2004; Rodgers et al., 2005). In the past 5 years, the publication by Liu R et al. in Diabetes in 2014 showed the strongest beginning of citation burst and found that transcription factors, such as p65 and STAT3, acetylation plays an important role in DN (Liu et al., 2014), followed by an article in JASN published by Morigi M et al. in 2018, who reviewed the central role of sirt1 in kidney health and disease (Morigi et al., 2018).

A

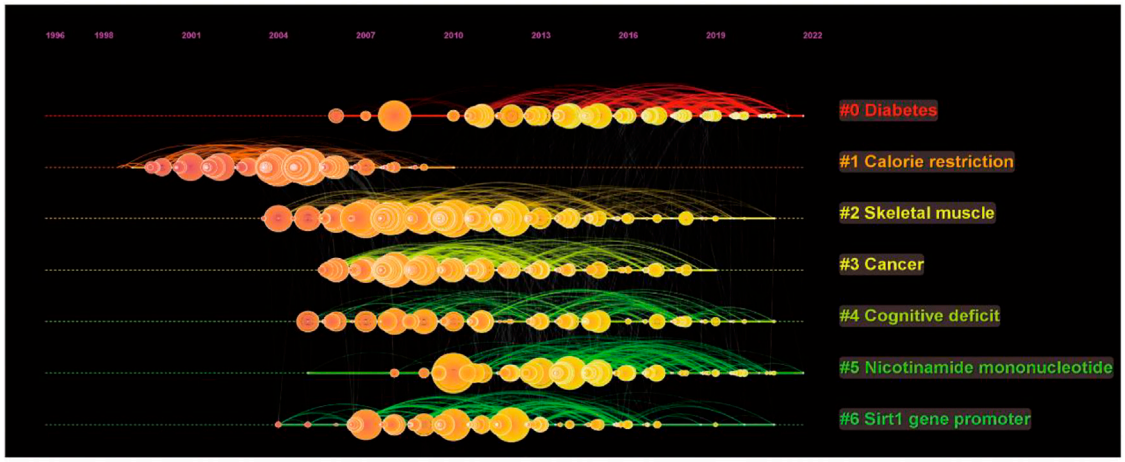

B

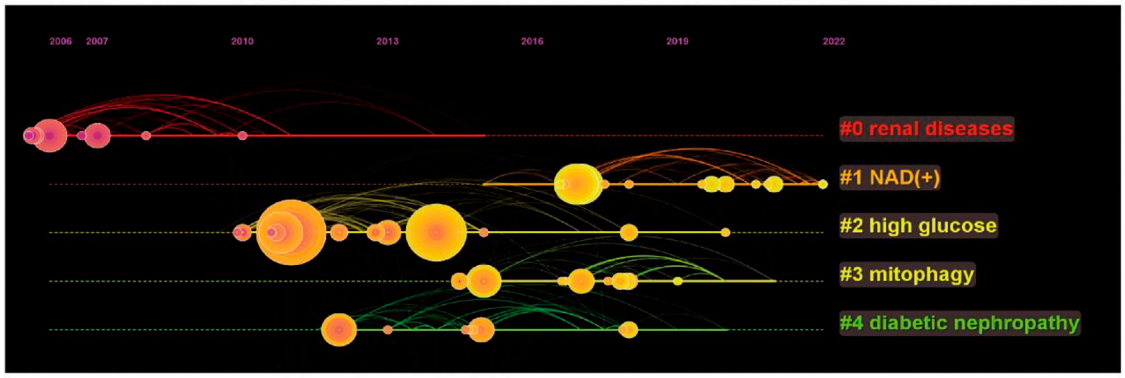

C

References	Year	Strength	Begin	End	1996 - 2022
Vaziri H, 2001, Cell	2001	117.78	2002	2009	
Luo J, 2001, Cell	2001	116.06	2001	2009	
Brunet A, 2004, Science	2004	114.03	2004	2012	
Alves-fernandes D, 2019, Int J Mol Sci	2019	24.3	2020	2022	
Zhang W, 2017, Oxid Med Cell Longev	2017	23.15	2020	2022	
Lee S, 2019, Bmb Rep	2019	21.99	2020	2022	

D

References	Year	Strength	Begin	End	2006 - 2022
Brunet A, 2004, Science	2004	9.17	2006	2012	
Rodgers J, 2005, Nature	2005	7.39	2007	2013	
Li J, 2010, Am J Pathol	2010	7.1	2014	2018	
Liu R, 2014, Diabetes	2014	5.45	2019	2020	
Morigi M, 2018, J Am Soc Nephrol	2018	5.06	2020	2022	
Hong Q, 2018, Kidney Int	2018	4.1	2019	2022	

FIGURE 5
Co-cited references analysis. **(A)** Timeline plot of clustering concerning sirt1. **(B)** Timeline plot of clustering concerning sirt1 in kidney disease. **(C)** Burst analysis concerning sirt1. **(D)** Burst analysis concerning sirt1 in kidney disease.

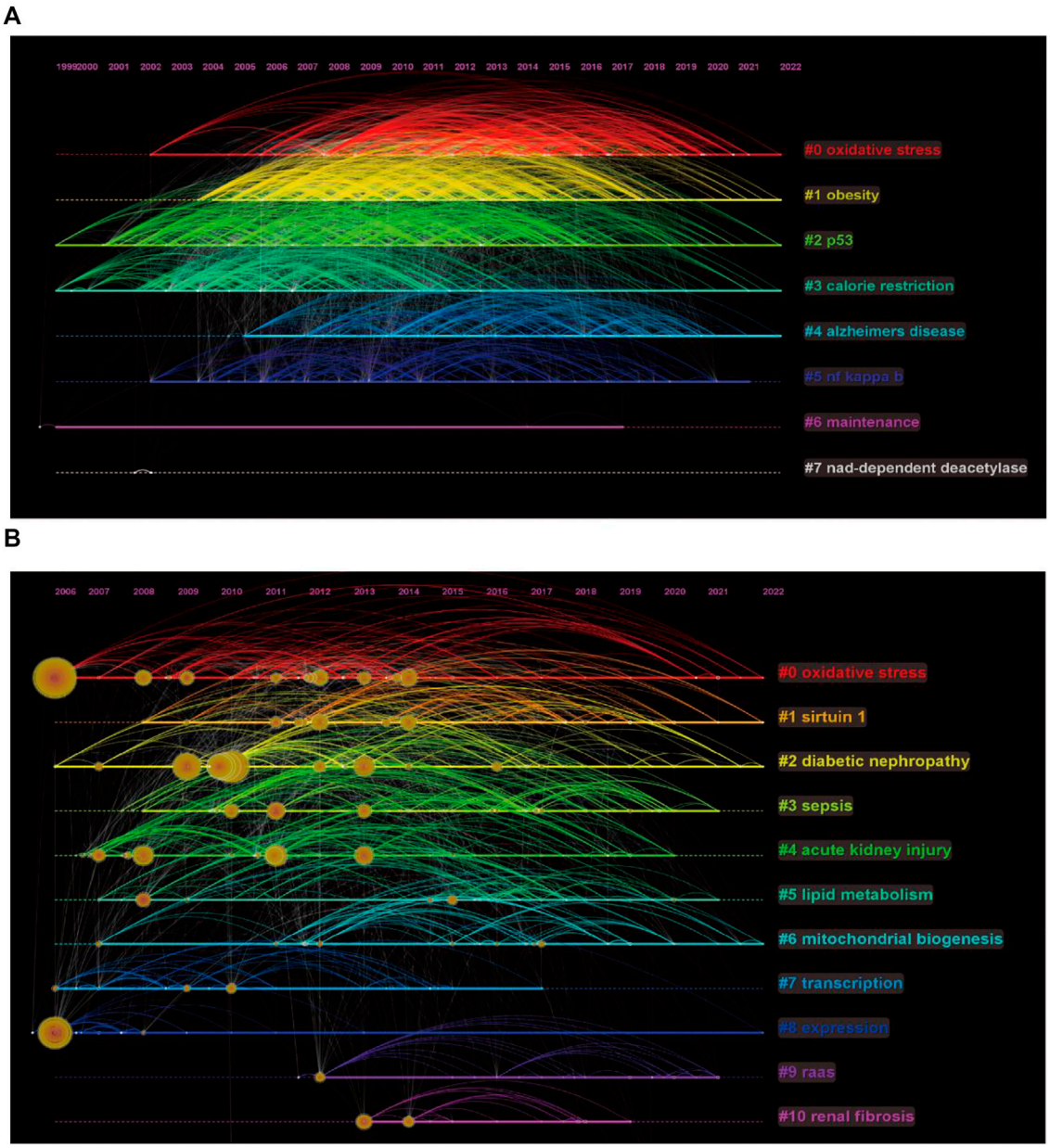

FIGURE 6
Keywords timeline of clustering. **(A)** Keywords timeline of clustering of sirt1. **(B)** Keywords timeline of clustering of sirt1 in kidney disease.

Keyword analysis

We performed clustering analysis on the extracted 24819 keywords and obtained eight clusters (Figure 6A). Obesity and Alzheimer's disease appear to be continuing hotspots for comparative attention among scholars investigating sirt1. In addition, regulation of oxidative stress and p53 by sirt1 appears to be a hotspot of ongoing interest in mechanistic studies. In terms of kidney disease, DN is a disease of considerable interest, and oxidative stress and mitochondrial biogenesis are mechanistic studies that have received continued attention (Figure 6B).

A total of 331 keywords were retrieved from the burst analysis (Figure 7A). "Calorie restriction," "life span," and "saccharomyces cerevisiae," as the keywords with the strongest citation bursts, indicate major areas in the study of sirt1. In the past 5 years, "autophagy," "injury," and "NLRP3 inflammasome" represent emerging areas in the study of sirt1. In addition, we found that the research theme of sirt1 changed over time (Figure 7B), in the last 3 years, "AMPK," "diabetic

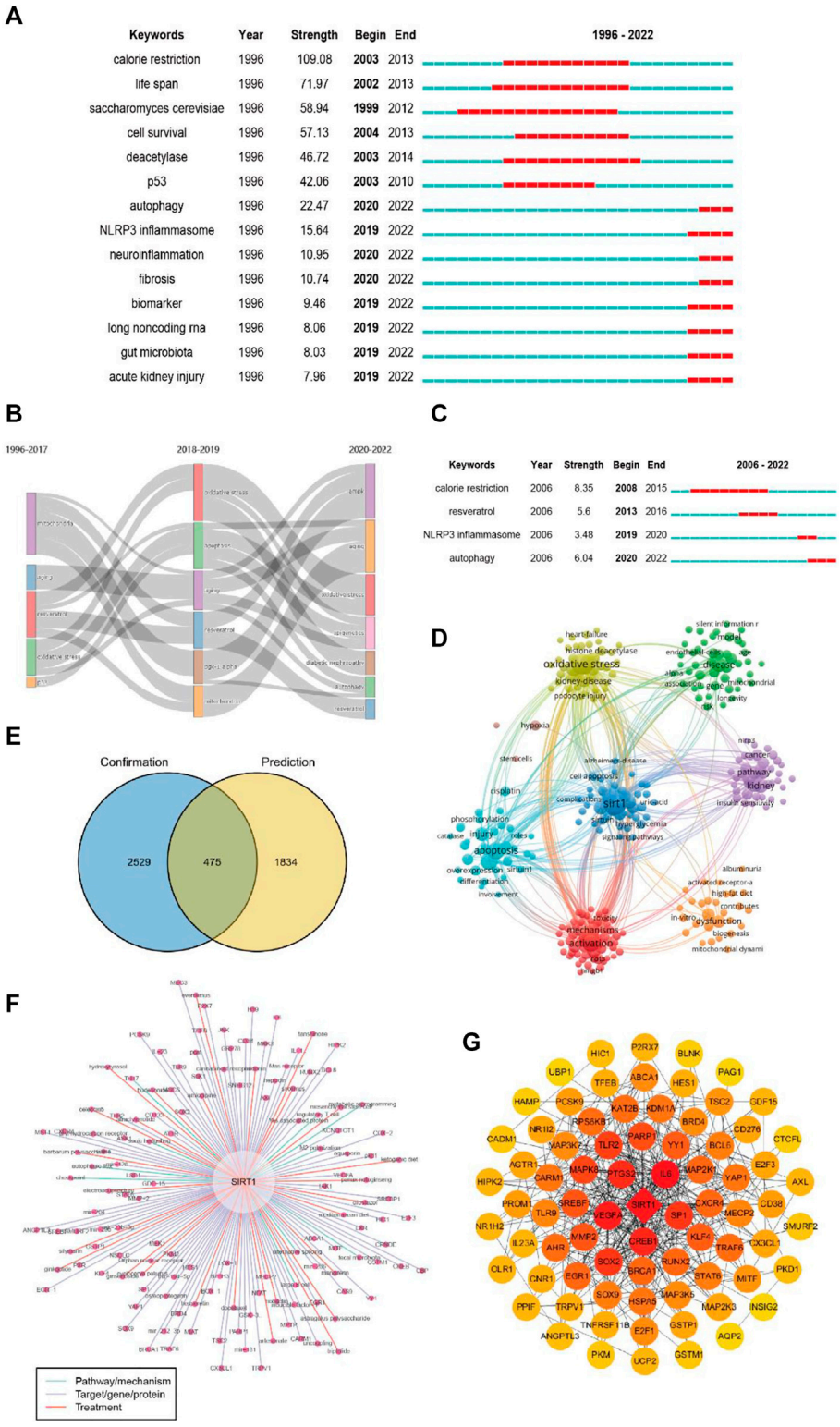

FIGURE 7
Keyword analysis. **(A)** Burst analysis concerning sirt1. **(B)** The thematic evolution of keywords. **(C)** Burst analysis concerning sirt1 in kidney disease. **(D)** Clustering of keywords related to sirt1 in kidney disease. **(E)** Venn diagram for the keywords linking sirt1 and kidney diseases. **(F)** Potential research topics linking sirt1 and kidney diseases. **(G)** PPI network for the targets related to sirt1 in kidney diseases.

TABLE 6 Potential links between Sirt1 and kidney disease.

Rank	Correlation probabilities	Target/gene/protein	Pathway/mechanism	Treatment
1	0.99	Hepcidin, CD38, PARP1, PCSK9, CD133	Ferroptosis, immune	Hydroxytyrosol, sirolimus
2	0.98	RUNX2, LSD1, COX-2, SOX9, CXCR4, E2F1, TLR2, TSC2, BRCA1, MMP-2, osteoprotegerin, TRPV1, B7-H3, HES1, CREB, EGR1, NSCLC, TFEB, inducible factor-1, LXR, IL6, HIPK2, H19, MEK1, cannabinoid receptor, aryl hydrocarbon receptor, VEGFA, KLF4, GSK-3β, MITF, HIC1, KCNQ1OT1, GDF-15, SREBP1, PXR, TRAF6, MEG3, YAP1	alternative splicing, regulatory T cell, sonic hedgehog, Th17, large B cell, metabolic reprogramming, autophagic flux	Docetaxel, mesenchymal stem cell, cilostazol, barbarum polysaccharide, ginsenoside, everolimus, panax notoginseng, oridonin
3	0.97	mir-204, MPTP, CAS9, JNK, PCAF, mir-181, IL-23, MSCS, STAT6, BOX-1, PKM2, aquaporin, uncoupling, mir-126, mir-29b, MST1, BCL6, ABCA1, CRNDE, IL-1β, AT1R, E2F3, SNHG12, S6K1, GSTM1, CBP, SOX2, PKD1	fecal microbiota, M2 polarization, checkpoint	Budesonide, ketogenic diet, astragalus polysaccharide, triptolide, hesperetin
4	0.96	mir-206, mir-194-5p, mir-23b-3p, mir-212-3p, Mas receptor, AXL, ASK1, Yes associated protein, GRP78, CARM1, Orphan nuclear receptor, BRD4, CX3CL1, SP1, MIAT, MECP2, P2X7, GSTP1, YY1, NFAT, ANGPTL3, SMURF2	—	mediterranean diet, mangiferin, amlodipine, tanshinone
5	0.95	TAK1, SREBP, LOX-1, EGR-1, TLR9, MKK3	—	silymarin, cyclocarya paliurus, ginkgolide, nobiletin, electroacupuncture, artesunate, celecoxib, atractylenolide

nephropathy" and "autophagy" have been the themes of greatest interest. In terms of kidney disease (Figure 7C), 13 keywords were retrieved from burst analysis. "Calorie restriction," "autophagy," and "acetylation," as the keywords with the strongest citation bursts, indicate major areas in the study of sirt1 in kidney disease, and "autophagy" and "NLRP3 inflammasome" also represent emerging areas in the past 5 years in the study of sirt1 in kidney disease.

In addition, we extracted and clustered the keywords of publications based on sirt1 studies involving kidney disease using VOSviewer. A total of 3004 keywords appeared more than five times, and these keywords formed eight clusters (Figure 7D), including sirt1-associated kidney disease (green clusters), mechanisms (purple, blue, yellow, and aquamarine clusters), and treatment options (red clusters).

Next, we explored possible connections between sirt1 and kidney disease based on the Arrowsmith project. After removing duplicates and synonyms, a total of 2309 keywords with correlations greater than 0.5 were obtained. We defined the keywords obtained from the Arrowsmith project as the "prediction" group and the keywords extracted from VOSviewer as the "confirmation" group. We constructed a Venn diagram for these two groups of keywords in the hope of discovering the keywords revealing kidney disease (Figure 7E). A total of 1834 keywords were found to serve as potential research topics linking sirt1 and kidney diseases, and the keywords with a correlation greater than 0.95 are shown in Table 6 and Figure 7F. We further constructed a PPI network for these targets and found that IL6, SP1, CREB1, VEGFA, and PTGS2 were the targets most closely related to sirt1 in kidney diseases (Figure 7G).

Discussion

General trends of sirtuins and kidney diseases

In this study, we conducted a holistic evaluation of sirtuin-related research over nearly 2 decades. We found that since 2013, research on sirtuins has exploded in various fields, likely because the crucial role of sirtuins in health and disease has gradually gained the attention of researchers and clinicians. We reviewed the retrieved publications by timeline and identified a few landmark publications, such as Frye, RA, in 1999, which reported five sirtuin (SIRT1-SIRT5) homologs to yeast sir2 and found that these proteins can metabolize NAD (Frye, 1999). NAD^+ has also received widespread attention as a fuel for sirtuins. In the last 3 years, two of the most cited articles have reported the important role of NAD^+ homeostasis in disease and health, and elevated NAD^+ levels have shown beneficial effects in various diseases (Katsyuba et al., 2020; Covarrubias et al., 2021). Cardiovascular diseases and neurodegenerative disorders are the main forces of sirtuin research. A recent highly cited article

reported that NAD^+ supplementation can reverse vascular aging by activating sirt1, and this effect could be further enhanced by hydrogen sulfide supplementation (another dietary restriction mimetic) (Das et al., 2018). Similarly, in another highly cited paper, NAD^+ supplementation was found to ameliorate neuroinflammation, DNA damage, and synaptic dysfunction in Alzheimer's disease (Hou et al., 2018). These results illustrate that NAD^+, an important branch in the study of sirtuins, has received extensive attention, which also provides inspiration for the study of sirtuins in kidney diseases. Notably, in this study, we found that sirt3 is the most widely studied member of sirtuins family after sirt1. Deficiency of sirt3 was shown to result in HIF1α accumulation and PKM2 dimer formation, and subsequently leads to aberrant glycolysis and mesenchymal transformations, ultimately promoting fibrosis in DN (Srivastava et al., 2018). Recently, sirt3 was reported to contribute to the improvement of metabolic reprogramming and endothelial-to-mesenchymal transition (EndMT) in endothelial cells of DN, leading to the amelioration of fibrosis (Srivastava et al., 2021a). Interestingly, deficiency of Fibroblast Growth Factor Receptor 1 (FGFR1) has been reported to mediate the EndMT in DN and aggravate fibrosis (Li et al., 2020). N-acetyl-seryl-aspartyl-lysyl-proline (AcSDKP) restores the expression of sirt3 and ameliorates fibrosis in DN (Srivastava et al., 2020a), an effect that was found to be partially dependent on FGFR1 (Li et al., 2020).

General trends of sirt1

Sirt1 is the most extensively studied member of the sirtuin family, with more than half of the sirtuin studies focused on sirt1. The United States and China were central participants in sirt1 studies. Harvard Medical School in the United States was a major contributor to sirt1 studies, and Sinclair DA's team was the representative. They previously reported that RSV acts as a sirt1 activator to mimic calorie restriction, improve the DNA stability of yeast, and prolong its lifespan by 70% (Howitz et al., 2003). Recently, Sinclair DA et al. focused on the significance of NAD^+ metabolism in disease and health. They found that activating sirt1 or increasing NAD^+ levels improved the health of patients with cardiovascular and metabolic diseases (Das et al., 2018; Kane and Sinclair, 2018). In addition, they also found that NAD^+ supplementation maintains telomere length and inhibits DNA damage, thus improving fibrotic disorders and premature aging (Amano et al., 2019). MIT in the United States is another important contributor to sirt1 research, and Guarente L's team is the leader. They found early that sirt1 can deacetylate and regulate p53 to improve cell aging and apoptosis (Vaziri et al., 2001), and a recent study found that NAD^+ supplementation rejuvenates stem cells in the aging intestine (Igarashi et al., 2019).

More than one-third of the publications were published in Q1 journals, showing the high academic influence of the research on sirt1, and with Cell, Nature, and Science being the most representative journals. Recently, an article published in Cell reported that the deacetylation of sirt1 produces an important protective effect against non-aging-related brain injury (Shin et al., 2021). Nature has recently reported dynamic changes in miR-34a targeting sirt1 (Baronti et al., 2020). In addition, based on co-cited references and keyword clusters and burst analysis, we found that diabetes, skeletal muscle, cancer, and cognitive deficit are hotspots diseases for the study of sirt1, and NAD^+, oxidative stress, and deacetylation regulation of p53 are hotspots in the research field of sirt1. In addition, we also found that autophagy, NLRP3 inflammasome, AMPK pathway have received much attention from researchers as emerging research trends in recent years. Both autophagy and sirt1 have been recognized as important players in the aging process, and the connection between them has attracted much interest. Cui et al. (2006) suggested that blockade of autophagy is accompanied by a decrease in sirt1 expression. The most cited articles reported that sirt1, as an important regulator of autophagy, can regulate protein expression *via* deacetylation of autophagy-related genes (*Atg*), such as *Atg5*, *Atg7*, and *Atg8*, while sirt1 deficiency resulted in impaired autophagy activation (Lee et al., 2008). A recent study identified sirt1 as a novel and selective substrate of nuclear autophagy and an important regulator of sirt1 protein homeostasis (Xu et al., 2020), while inhibition of autophagy could promote sirt1-mediated health benefits (Wang et al., 2021). NLRP3 inflammasome are reportedly involved in sirt1. Fu et al. (2013) showed that RSV, as a sirt1 activator, inhibits NLRP3 inflammasome activation, while sirt1 inhibition can significantly enhance the expression of inflammatory factors. The latest findings that the sirt1 agonist SRT1720 reduces NLRP3 inflammasome activation and pyroptosis in an Akt signaling-dependent manner (Han et al., 2020) and that NLRP3 knockout leads to increased NAD^+ levels and increased sirt1 expression, illustrate that the NLRP3 inflammasome appears to be involved in sirt1-associated-aging.

Sirt1 and kidney diseases

We found that kidney disease has gained increasing attention in recent years in the study of sirt1. China maintained its leading position both in terms of total publications and total citations, followed by researchers at the United States. Fudan University from China have been working on sirt1, and Hao CM's team is the main representative among these researchers. They found that sirt1 may serve as a potential pharmacological target for kidney injury (Guan et al., 2017), and that sirt1 activation effectively improves renal fibrosis (Huang et al., 2014), which may be related to the improvement of renal oxidative stress (He et al., 2010). In addition, it is worth mentioning that Japan has made an important contribution to research investigating sirt1 in kidney disease due to the high citation frequency. Koya D from Kanazawa Medical University and Kume S from Shiga University of Medical

Science are the main representatives of this group of researchers. Koya D and Kume S were early scholars in the field of kidney disease who focused on sirt1. As early as 2006, they reported that sirt1 deacetylates and regulates p53, and reduces mesangial cell apoptosis (Kume et al., 2006). The most influential article reported that calorie restriction enhances the adaptability of cells in aging kidneys to hypoxia through sirt1-dependent mitochondrial autophagy (Kume et al., 2010). Recently, a review by Koya D et al. discussed the relationship between sirt1 and oxidative stress in nephropathy, emphasizing that sirt1 activation in the kidney may represent a novel therapeutic strategy (Ogura et al., 2021). Furthermore, JASN, PLOS One, and KI are the most influential journals for sirt1 research in kidney disease. A recent publication in JASN reported that short-term treatment with NMN ameliorated the renal injury phenotype and survival of diabetic nephropathy by upregulating SIRT1 expression (Yasuda et al., 2021). Similarly, a recent article published in KI also reported that BF175 may reduce podocyte loss and renal dysfunction in diabetic nephropathy by activating sirt1 (Feng et al., 2021).

Oxidative stress and mitochondrial biogenesis were the main mechanisms involved in kidney disease. "Autophagy," "acetylation," and "NLRP3 inflammasome" have received much attention in the field of kidney disease as emerging research trends. It is widely accepted that sirt1 acts as a major driver of autophagy in kidney disease; however, the exact mechanism remains to be explored. As sirt1 is a novel substrate of autophagy, crosstalk between autophagy and sirt1 deserves significant attention in kidney disease (Xu et al., 2020; Wang et al., 2021). In addition, a recent study reported that the AMPK pathway maintains a high basal level of autophagy in podocytes independent of the mTOR pathway (Bork et al., 2020), this appears to provide important evidence for a link between autophagy and sirt1 in kidney disease. Notably, recent studies have shown that acetylation has emerged as an important regulatory mechanism of autophagy, and that acetylation not only regulates autophagy-related proteins but also affects autophagic function through the regulation of histones and transcription factors, indicating that deacetylation of sirt1 plays an important role in kidney disease, especially in autophagy (Xu and Wan, 2022). Crosstalk between sirt1 and the NLRP3 inflammasome plays an important role in kidney disease. Jiang et al. (2021) found that sirt1 knockout aggravated NLRP3 inflammasome activation in a mouse model of aldosterone infusion, and a recent report also found that sirt1 blunted NLRP3 inflammasome activation *via* autophagy to ameliorate IgA nephropathy (Wu et al., 2020). However, the complex connection between sirt1 and the NLRP3 inflammasome in kidney disease is poorly understood.

In addition, some neglected areas of kidney disease deserve attention as potential emerging hotspots in the study of Sirt1, such as immune, metabolic reprogramming and fecal microbiota. Immunity is a major cause of kidney diseases, including membranous nephropathy, lupus nephritis, and IgA nephropathy (Liu et al., 2020). Innate and adaptive immunity are involved in the initiation and maintenance of kidney injury (Dellepiane et al., 2020). Sirt1 has recently been found to act as an important regulator of immune cells and immune responses (Shen et al., 2021), which deserves the attention of researchers studying kidney diseases. In addition, metabolic reprogramming has been an emerging hotspot of kidney disease research in recent years, and changes in fatty acid metabolism and glucose metabolism have been found to be closely related to renal fibrosis (Zhu et al., 2021). Sirt1 plays an important role in energy and metabolic regulation (Ong and Ramasamy, 2018), and therefore, sirt1 may mediate metabolic reprogramming and play an important role in renal diseases. In addition, gut microbes and their derived metabolites were found to promote the progression of kidney disease and the development of severe complications, especially cardiovascular diseases (Mahmoodpoor et al., 2017; Feng et al., 2019). Recent studies have reported that deletion of sirt1 causes alterations in the gut microbiota, and sirt1 may be an important mediator of the interaction between the host and gut microbes (Wellman et al., 2017), which may provide important inspiration for the study of the gut-kidney axis. Notably, some natural ingredients, such as barbarum polysaccharides, Panax notoginseng, oridonin, triptolide, and hesperetin, deserve attention as potential therapeutic agents influencing sirt1 in kidney diseases.

Implication of sirt1 in diabetic kidney disease research

Cluster and burst analyses showed that DN was a primary focus in sirt1 research. Sirt1 plays an important role in the epigenetic regulations of renal tubules and podocytes in DN. Sirt1 can deacetylate regulated STAT3, p53, FOXO4 and PGC1-α to maintain podocyte function (Nakatani and Inagi, 2016), and activation of sirt1 promotes the expression of PGC1-α in podocytes, thereby ameliorating podocyte injury and proteinuria in DN (Hong et al., 2018). Similarly, sirt1 could also deacetylate regulated Beclin1 and p53 to improve tubular autophagy (Deng et al., 2021; Sun et al., 2021) and attenuate high glucose induced tubular injury and apoptosis (Wang et al., 2016). Interestingly, renal tubular sirt1 was found to regulate the expression of Claudin-1 to mediate crosstalk with podocytes to ameliorate proteinuria in DN (Hasegawa et al., 2013). In addition, recent studies have found that glucocorticoid receptor (GR) plays an important role in DN. Deficiency of GR of endothelial accelerates renal fibrosis in DN mice (Srivastava et al., 2021c), and the same results were found in DN mice with podocyte GR loss (Srivastava et al., 2021b). Importantly, sirt1 was found to be a transcriptional enhancer of GR and is independent of its deacetylase activity role (Suzuki et al., 2018). Interestingly, some emerging drugs also hold promise for improving DN through sirt1, such as glycolysis inhibitors (Lv

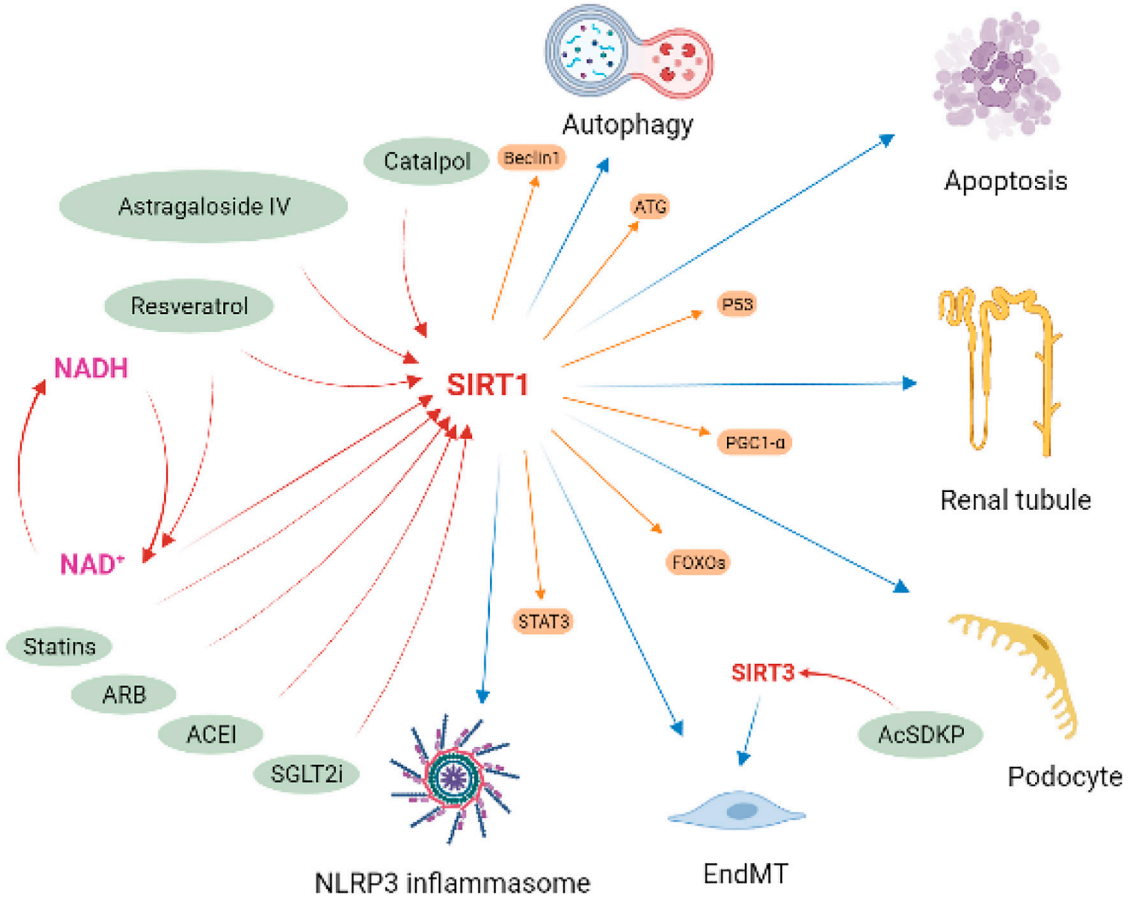

FIGURE 8
Implication of sirt1 in diabetic kidney disease. Sirt1 attenuated podocyte and tubule injury and apoptosis, improve endothelial-to-mesenchymal transition (EndMT), and regulated autophagy and NLRP3 inflammasome activation in DKD by deacetylating regulatory ATG, Beclin1, STAT3, p53, FOXOs and PGC1-α. Several drugs available in kidney disease have been shown to be partially contribute to the activation of the sirt1, including SGLT2i, ACEI, ARB, and statins. Some natural compounds have also been found to have the same effect, such as resveratrol, catalpol and astragaloside IV.

et al., 2018), DPP-4 inhibitors (linagliptin) (Elbaz et al., 2018), JAK/STA3 inhibitors (Wang et al., 2018), mineralocorticoid receptor agonists (Moore et al., 2012) and N-acetyl-seryl-aspartyl-lysyl-proline (Srivastava et al., 2020a).

Pharmacological prospect of sirt1 in kidney disease

In summary, sirt1 plays an important role in the regulation of inflammation, autophagy, oxidative stress, and mitochondrial homeostasis in kidney disease, especially in DN. *In vivo* and *in vitro* evidence shows that Sirt1 can serve as an important potential pharmacological target in kidney disease (Figure 8). Several drugs available in kidney disease have also been shown to be partially contribute to the activation of the sirt1, such as sodium glucose co-transporter two inhibitors (Packer, 2020), angiotensin-converting enzyme inhibitor (enalapril) (Veitch et al., 2021), angiotensin II receptor blocker (olmesartan) (Gu et al., 2016), and statins (Khayatan et al., 2022). In addition, some small molecule compounds, especially some natural compounds, targeting sirt1 may also serve as potentially promising candidates for the treatment of kidney diseases, like RSV, Catalpol and Astragaloside IV.

Limitation

Compared with the traditional review, bibliometrics is more tend to objective sort out a research field as a whole, which is suitable for the beginning of a research, to find the mainstream direction and emerging hot spots, so as to make more meaningful research. This study suggests our sirt1 as highly promising in the study of kidney diseases, especially in DN, and the relationship between Sirt1 and

immune, metabolic reprogramming and fecal microbiota in kidney diseases deserves significant attention. However, this study has some limitations that need to be considered. First, we developed a search formula in as much detail as possible; however, that is difficult to avoid some studies were not included in our analysis. Second, we selected as many landmark articles as possible; however, it is possible that some important publications and research directions were missed due to differences in the evaluation indicators on which we focused. Finally, we combined various bibliometric analysis methods in order to obtain more useful and instructive results, but due to the limitations of the algorithm, some newer views may not be presented.

Conclusion

Based on bibliometric analysis, we found that publications regarding sirt1 have increased dramatically in the last 2 decades, especially in the last 5 years, in which studies on kidney diseases have gained increasing attention. China and the United States are major contributors to sirt1 studies, and Japanese scholars have also made important contributions to studies about sirt1 in kidney disease. NAD^+, oxidative stress, and p53 are the main focus of scholars studying sirt1. Autophagy and NLRP3 inflammasome are emerging research trends that have gradually attracted the interest of researchers, especially regarding kidney diseases. In addition, some neglected potential research topics deserve further attention and in-depth studies.

Data availability statement

The original contributions presented in the study are included in the article/Supplementary Material, further inquiries can be directed to the corresponding author.

Author contributions

TL, SM, and YZ designed the study. FM and YW collected the data. TL, LY, and HM analyzed the data and drafted the manuscript. All authors contributed to the article and approved the final version of the manuscript.

Funding

This work was supported by grants from National Nature Science Foundation of China (82074393).

Conflict of interest

The authors declare that the research was conducted in the absence of any commercial or financial relationships that could be construed as a potential conflict of interest.

Publisher's note

All claims expressed in this article are solely those of the authors and do not necessarily represent those of their affiliated organizations, or those of the publisher, the editors and the reviewers. Any product that may be evaluated in this article, or claim that may be made by its manufacturer, is not guaranteed or endorsed by the publisher.

Supplementary material

The Supplementary Material for this article can be found online at: https://www.frontiersin.org/articles/10.3389/fphar.2022.966786/full#supplementary-material

References

Alves-Fernandes, D. K., and Jasiulionis, M. G. (2019). The role of SIRT1 on DNA damage response and epigenetic alterations in cancer. *Int. J. Mol. Sci.* 20 (13), E3153. doi:10.3390/ijms20133153

Amano, H., Chaudhury, A., Rodriguez-Aguayo, C., Lu, L., Akhanov, V., Catic, A., et al. (2019). Telomere dysfunction induces sirtuin repression that drives telomere-dependent disease. *Cell Metab.* 29 (6), 1274–1290. e1279. doi:10.1016/j.cmet.2019.03.001

Aria, M., and Cuccurullo, C. (2017). Bibliometrix : an R-tool for comprehensive science mapping analysis. *J. Inf.* 11 (4), 959–975. doi:10.1016/j.joi.2017.08.007

Aventaggiato, M., Vernucci, E., Barreca, F., Russo, M. A., and Tafani, M. (2021). Sirtuins' control of autophagy and mitophagy in cancer. *Pharmacol. Ther.* 221, 107748. doi:10.1016/j.pharmthera.2020.107748

Baronti, L., Guzzetti, I., Ebrahimi, P., Friebe Sandoz, S., Steiner, E., Schlagnitweit, J., et al. (2020). Base-pair conformational switch modulates miR-34a targeting of Sirt1 mRNA. *Nature* 583 (7814), 139–144. doi:10.1038/s41586-020-2336-3

Bork, T., Liang, W., Yamahara, K., Lee, P., Tian, Z., Liu, S., et al. (2020). Podocytes maintain high basal levels of autophagy independent of mtor signaling. *Autophagy* 16 (11), 1932–1948. doi:10.1080/15548627.2019.1705007

Brunet, A., Sweeney, L. B., Sturgill, J. F., Chua, K. F., Greer, P. L., Lin, Y., et al. (2004). Stress-dependent regulation of FOXO transcription factors by the SIRT1 deacetylase. *Science* 303 (5666), 2011–2015. doi:10.1126/science.1094637

Chen, C. (2004). Searching for intellectual turning points: progressive knowledge domain visualization. *Proc. Natl. Acad. Sci. U. S. A.* 101 (1), 5303–5310. doi:10.1073/pnas.0307513100

Chen, X., Chen, C., Fan, S., Wu, S., Yang, F., Fang, Z., et al. (2018). Omega-3 polyunsaturated fatty acid attenuates the inflammatory response by modulating microglia polarization through SIRT1-mediated deacetylation of the HMGB1/NF-κB pathway following experimental traumatic brain injury. *J. Neuroinflammation* 15 (1), 116. doi:10.1186/s12974-018-1151-3

Covarrubias, A. J., Perrone, R., Grozio, A., and Verdin, E. (2021). NAD(+) metabolism and its roles in cellular processes during ageing. *Nat. Rev. Mol. Cell Biol.* 22 (2), 119–141. doi:10.1038/s41580-020-00313-x

Cui, Q., Tashiro, S., Onodera, S., and Ikejima, T. (2006). Augmentation of oridonin-induced apoptosis observed with reduced autophagy. *J. Pharmacol. Sci.* 101 (3), 230–239. doi:10.1254/jphs.fpj06003x

Dai, H., Sinclair, D. A., Ellis, J. L., and Steegborn, C. (2018). Sirtuin activators and inhibitors: promises, achievements, and challenges. *Pharmacol. Ther.* 188, 140–154. doi:10.1016/j.pharmthera.2018.03.004

Das, A., Huang, G. X., Bonkowski, M. S., Longchamp, A., Li, C., Schultz, M. B., et al. (2018). Impairment of an endothelial NAD(+)-H(2)S signaling network is a reversible cause of vascular aging. *Cell* 173 (1), 74–89. e20. doi:10.1016/j.cell.2018.02.008

Dellepiane, S., Leventhal, J. S., and Cravedi, P. (2020). T cells and acute kidney injury: a two-way relationship. *Front. Immunol.* 11, 1546. doi:10.3389/fimmu.2020.01546

Deng, Z., Sun, M., Wu, J., Fang, H., Cai, S., An, S., et al. (2021). SIRT1 attenuates sepsis-induced acute kidney injury via Beclin1 deacetylation-mediated autophagy activation. *Cell Death Dis.* 12 (2), 217. doi:10.1038/s41419-021-03508-y

Elbaz, E. M., Senousy, M. A., El-Tanbouly, D. M., and Sayed, R. H. (2018). Neuroprotective effect of linagliptin against cuprizone-induced demyelination and behavioural dysfunction in mice: a pivotal role of AMPK/SIRT1 and JAK2/STAT3/NF-κB signalling pathway modulation. *Toxicol. Appl. Pharmacol.* 352, 153–161. doi:10.1016/j.taap.2018.05.035

Feng, J., Bao, L., Wang, X., Li, H., Chen, Y., Xiao, W., et al. (2021). Low expression of HIV genes in podocytes accelerates the progression of diabetic kidney disease in mice. *Kidney Int.* 99 (4), 914–925. doi:10.1016/j.kint.2020.12.012

Feng, Y. L., Cao, G., Chen, D. Q., Vaziri, N. D., Chen, L., Zhang, J., et al. (2019). Microbiome-metabolomics reveals gut microbiota associated with glycine-conjugated metabolites and polyamine metabolism in chronic kidney disease. *Cell. Mol. Life Sci.* 76 (24), 4961–4978. doi:10.1007/s00018-019-03155-9

Frye, R. A. (1999). Characterization of five human cDNAs with homology to the yeast SIR2 gene: Sir2-like proteins (sirtuins) metabolize NAD and may have protein ADP-ribosyltransferase activity. *Biochem. Biophys. Res. Commun.* 260 (1), 273–279. doi:10.1006/bbrc.1999.0897

Fu, Y., Wang, Y., Du, L., Xu, C., Cao, J., Fan, T., et al. (2013). Resveratrol inhibits ionising irradiation-induced inflammation in MSCs by activating SIRT1 and limiting NLRP-3 inflammasome activation. *Int. J. Mol. Sci.* 14 (7), 14105–14118. doi:10.3390/ijms140714105

Funk, J. A., Odejinmi, S., and Schnellmann, R. G. (2010). SRT1720 induces mitochondrial biogenesis and rescues mitochondrial function after oxidant injury in renal proximal tubule cells. *J. Pharmacol. Exp. Ther.* 333 (2), 593–601. doi:10.1124/jpet.109.161992

Gu, J., Yang, M., Qi, N., Mei, S., Chen, J., Song, S., et al. (2016). Olmesartan prevents microalbuminuria in db/db diabetic mice through inhibition of angiotensin II/p38/SIRT1-Induced podocyte apoptosis. *Kidney Blood Press. Res.* 41 (6), 848–864. doi:10.1159/000452588

Guan, Y., Wang, S. R., Huang, X. Z., Xie, Q. H., Xu, Y. Y., Shang, D., et al. (2017). Nicotinamide mononucleotide, an NAD(+) precursor, rescues age-associated susceptibility to AKI in a sirtuin 1-dependent manner. *J. Am. Soc. Nephrol.* 28 (8), 2337–2352. doi:10.1681/asn.2016040385

Guo, J., Zheng, H. J., Zhang, W., Lou, W., Xia, C., Han, X. T., et al. (2020). Accelerated kidney aging in diabetes mellitus. *Oxid. Med. Cell. Longev.* 2020, 1234059. doi:10.1155/2020/1234059

Gupta, R., Ambasta, R. K., and Kumar, P. (2022). Multifaced role of protein deacetylase sirtuins in neurodegenerative disease. *Neurosci. Biobehav. Rev.* 132, 976–997. doi:10.1016/j.neubiorev.2021.10.047

Haigis, M. C., and Sinclair, D. A. (2010). Mammalian sirtuins: biological insights and disease relevance. *Annu. Rev. Pathol.* 5, 253–295. doi:10.1146/annurev.pathol.4.110807.092250

Han, Y., Sun, W., Ren, D., Zhang, J., He, Z., Fedorova, J., et al. (2020). SIRT1 agonism modulates cardiac NLRP3 inflammasome through pyruvate dehydrogenase during ischemia and reperfusion. *Redox Biol.* 34, 101538. doi:10.1016/j.redox.2020.101538

Hasegawa, K., Wakino, S., Simic, P., Sakamaki, Y., Minakuchi, H., Fujimura, K., et al. (2013). Renal tubular Sirt1 attenuates diabetic albuminuria by epigenetically suppressing Claudin-1 overexpression in podocytes. *Nat. Med.* 19 (11), 1496–1504. doi:10.1038/nm.3363

He, W., Wang, Y., Zhang, M. Z., You, L., Davis, L. S., Fan, H., et al. (2010). Sirt1 activation protects the mouse renal medulla from oxidative injury. *J. Clin. Invest.* 120 (4), 1056–1068. doi:10.1172/jci41563

Hong, Q., Zhang, L., Das, B., Li, Z., Liu, B., Cai, G., et al. (2018). Increased podocyte Sirtuin-1 function attenuates diabetic kidney injury. *Kidney Int.* 93 (6), 1330–1343. doi:10.1016/j.kint.2017.12.008

Hou, Y., Lautrup, S., Cordonnier, S., Wang, Y., Croteau, D. L., Zavala, E., et al. (2018). NAD(+) supplementation normalizes key Alzheimer's features and DNA damage responses in a new AD mouse model with introduced DNA repair deficiency. *Proc. Natl. Acad. Sci. U. S. A.* 115 (8), E1876–e1885. doi:10.1073/pnas.1718819115

Howitz, K. T., Bitterman, K. J., Cohen, H. Y., Lamming, D. W., Lavu, S., Wood, J. G., et al. (2003). Small molecule activators of sirtuins extend *Saccharomyces cerevisiae* lifespan. *Nature* 425 (6954), 191–196. doi:10.1038/nature01960

Huang, X. Z., Wen, D., Zhang, M., Xie, Q., Ma, L., Guan, Y., et al. (2014). Sirt1 activation ameliorates renal fibrosis by inhibiting the TGF-β/Smad3 pathway. *J. Cell. Biochem.* 115 (5), 996–1005. doi:10.1002/jcb.24748

Igarashi, M., Miura, M., Williams, E., Jaksch, F., Kadowaki, T., Yamauchi, T., et al. (2019). NAD(+) supplementation rejuvenates aged gut adult stem cells. *Aging Cell* 18 (3), e12935. doi:10.1111/acel.12935

Ivy, J. M., Klar, A. J., and Hicks, J. B. (1986). Cloning and characterization of four SIR genes of *Saccharomyces cerevisiae*. *Mol. Cell. Biol.* 6 (2), 688–702. doi:10.1128/mcb.6.2.688

Jiang, M., Zhao, M., Bai, M., Lei, J., Yuan, Y., Huang, S., et al. (2021). SIRT1 alleviates aldosterone-induced podocyte injury by suppressing mitochondrial dysfunction and NLRP3 inflammasome activation. *Kidney Dis.* 7 (4), 293–305. doi:10.1159/000513884

Kaeberlein, M., McVey, M., and Guarente, L. (1999). The SIR2/3/4 complex and SIR2 alone promote longevity in *Saccharomyces cerevisiae* by two different mechanisms. *Genes Dev.* 13 (19), 2570–2580. doi:10.1101/gad.13.19.2570

Kane, A. E., and Sinclair, D. A. (2018). Sirtuins and NAD(+) in the development and treatment of metabolic and cardiovascular diseases. *Circ. Res.* 123 (7), 868–885. doi:10.1161/circresaha.118.312498

Katsyuba, E., Romani, M., Hofer, D., and Auwerx, J. (2020). NAD(+) homeostasis in health and disease. *Nat. Metab.* 2 (1), 9–31. doi:10.1038/s42255-019-0161-5

Khayatan, D., Razavi, S. M., Arab, Z. N., Khanahmadi, M., Momtaz, S., Butler, A. E., et al. (2022). Regulatory effects of statins on SIRT1 and other sirtuins in cardiovascular diseases. *Life (Basel)* 12 (5), 760. doi:10.3390/life12050760

Kitada, M., Kume, S., Imaizumi, N., and Koya, D. (2011). Resveratrol improves oxidative stress and protects against diabetic nephropathy through normalization of Mn-SOD dysfunction in AMPK/SIRT1-independent pathway. *Diabetes* 60 (2), 634–643. doi:10.2337/db10-0386

Kumar, S., and Lombard, D. B. (2018). Functions of the sirtuin deacylase SIRT5 in normal physiology and pathobiology. *Crit. Rev. Biochem. Mol. Biol.* 53 (3), 311–334. doi:10.1080/10409238.2018.1458071

Kume, S., Haneda, M., Kanasaki, K., Sugimoto, T., Araki, S., Isono, M., et al. (2006). Silent information regulator 2 (SIRT1) attenuates oxidative stress-induced mesangial cell apoptosis via p53 deacetylation. *Free Radic. Biol. Med.* 40 (12), 2175–2182. doi:10.1016/j.freeradbiomed.2006.02.014

Kume, S., Uzu, T., Horiike, K., Chin-Kanasaki, M., Isshiki, K., Araki, S., et al. (2010). Calorie restriction enhances cell adaptation to hypoxia through Sirt1-dependent mitochondrial autophagy in mouse aged kidney. *J. Clin. Invest.* 120 (4), 1043–1055. doi:10.1172/jci41376

Lagouge, M., Argmann, C., Gerhart-Hines, Z., Meziane, H., Lerin, C., Daussin, F., et al. (2006). Resveratrol improves mitochondrial function and protects against metabolic disease by activating SIRT1 and PGC-1alpha. *Cell* 127 (6), 1109–1122. doi:10.1016/j.cell.2006.11.013

Lee, I. H., Cao, L., Mostoslavsky, R., Lombard, D. B., Liu, J., Bruns, N. E., et al. (2008). A role for the NAD-dependent deacetylase Sirt1 in the regulation of autophagy. *Proc. Natl. Acad. Sci. U. S. A.* 105 (9), 3374–3379. doi:10.1073/pnas.0712145105

Leite, J. A., Ghirotto, B., Targhetta, V. P., de Lima, J., and Câmara, N. O. S. (2022). Sirtuins as pharmacological targets in neurodegenerative and neuropsychiatric disorders. *Br. J. Pharmacol.* 179 (8), 1496–1511. doi:10.1111/bph.15570

Li, J., Liu, H., Srivastava, S. P., Hu, Q., Gao, R., Li, S., et al. (2020). Endothelial FGFR1 (Fibroblast growth factor receptor 1) deficiency contributes differential fibrogenic effects in kidney and heart of diabetic mice. *Hypertension* 76 (6), 1935–1944. doi:10.1161/hypertensionaha.120.15587

Liu, R., Zhong, Y., Li, X., Chen, H., Jim, B., Zhou, M. M., et al. (2014). Role of transcription factor acetylation in diabetic kidney disease. *Diabetes* 63 (7), 2440–2453. doi:10.2337/db13-1810

Liu, W., Gao, C., Liu, Z., Dai, H., Feng, Z., Dong, Z., et al. (2020). Idiopathic membranous nephropathy: Glomerular pathological pattern caused by extrarenal immunity activity. *Front. Immunol.* 11, 1846. doi:10.3389/fimmu.2020.01846

Lu, K., Yu, S., Sun, D., Xing, H., An, J., Kong, C., et al. (2018). Scientometric analysis of SIRT6 studies. *Med. Sci. Monit.* 24, 8357–8371. doi:10.12659/msm.913644

Luo, J., Nikolaev, A. Y., Imai, S., Chen, D., Su, F., Shiloh, A., et al. (2001). Negative control of p53 by Sir2alpha promotes cell survival under stress. *Cell* 107 (2), 137–148. doi:10.1016/s0092-8674(01)00524-4

Lv, Q., Wang, K., Qiao, S., Yang, L., Xin, Y., Dai, Y., et al. (2018). Norisoboldine, a natural AhR agonist, promotes Treg differentiation and attenuates colitis via targeting glycolysis and subsequent NAD(+)/SIRT1/SUV39H1/H3K9me3 signaling pathway. *Cell Death Dis.* 9 (3), 258. doi:10.1038/s41419-018-0297-3

Mahmoodpoor, F., Rahbar Saadat, Y., Barzegari, A., Ardalan, M., and Zununi Vahed, S. (2017). The impact of gut microbiota on kidney function and pathogenesis. *Biomed. Pharmacother.* 93, 412–419. doi:10.1016/j.biopha.2017.06.066

Mathias, R. A., Greco, T. M., Oberstein, A., Budayeva, H. G., Chakrabarti, R., Rowland, E. A., et al. (2014). Sirtuin 4 is a lipoamidase regulating pyruvate dehydrogenase complex activity. *Cell* 159 (7), 1615–1625. doi:10.1016/j.cell.2014.11.046

Moore, R. L., Dai, Y., and Faller, D. V. (2012). Sirtuin 1 (SIRT1) and steroid hormone receptor activity in cancer. *J. Endocrinol.* 213 (1), 37–48. doi:10.1530/joe-11-0217

Morigi, M., Perico, L., and Benigni, A. (2018). Sirtuins in renal health and disease. *J. Am. Soc. Nephrol.* 29 (7), 1799–1809. doi:10.1681/asn.2017111218

Nakatani, Y., and Inagi, R. (2016). Epigenetic regulation through SIRT1 in podocytes. *Curr. Hypertens. Rev.* 12 (2), 89–94. doi:10.2174/1573402112666160302102515

Ogura, Y., Kitada, M., and Koya, D. (2021). Sirtuins and renal oxidative stress. *Antioxidants (Basel)* 10 (8), 1198. doi:10.3390/antiox10081198

Ong, A. L. C., and Ramasamy, T. S. (2018). Role of Sirtuin1-p53 regulatory axis in aging, cancer and cellular reprogramming. *Ageing Res. Rev.* 43, 64–80. doi:10.1016/j.arr.2018.02.004

Packer, M. (2020). Interplay of adenosine monophosphate-activated protein kinase/sirtuin-1 activation and sodium influx inhibition mediates the renal benefits of sodium-glucose co-transporter-2 inhibitors in type 2 diabetes: a novel conceptual framework. *Diabetes Obes. Metab.* 22 (5), 734–742. doi:10.1111/dom.13961

Ralto, K. M., Rhee, E. P., and Parikh, S. M. (2020). NAD(+) homeostasis in renal health and disease. *Nat. Rev. Nephrol.* 16 (2), 99–111. doi:10.1038/s41581-019-0216-6

Ren, H., Shao, Y., Wu, C., Ma, X., Lv, C., and Wang, Q. (2020). Metformin alleviates oxidative stress and enhances autophagy in diabetic kidney disease via AMPK/SIRT1-FoxO1 pathway. *Mol. Cell. Endocrinol.* 500, 110628. doi:10.1016/j.mce.2019.110628

Rodgers, J. T., Lerin, C., Haas, W., Gygi, S. P., Spiegelman, B. M., and Puigserver, P. (2005). Nutrient control of glucose homeostasis through a complex of PGC-1alpha and SIRT1. *Nature* 434 (7029), 113–118. doi:10.1038/nature03354

Sabe, M., Pillinger, T., Kaiser, S., Chen, C., Taipale, H., Tanskanen, A., et al. (2022). Half a century of research on antipsychotics and schizophrenia: a scientometric study of hotspots, nodes, bursts, and trends. *Neurosci. Biobehav. Rev.* 136, 104608. doi:10.1016/j.neubiorev.2022.104608

Shen, P., Deng, X., Chen, Z., Ba, X., Qin, K., Huang, Y., et al. (2021). SIRT1: a potential therapeutic target in autoimmune diseases. *Front. Immunol.* 12, 779177. doi:10.3389/fimmu.2021.779177

Shin, M. K., Vázquez-Rosa, E., Koh, Y., Dhar, M., Chaubey, K., Cintrón-Pérez, C. J., et al. (2021). Reducing acetylated tau is neuroprotective in brain injury. *Cell* 184 (10), 2715–2732. e2723. doi:10.1016/j.cell.2021.03.032

Smalheiser, N. R., Torvik, V. I., and Zhou, W. (2009). Arrowsmith two-node search interface: a tutorial on finding meaningful links between two disparate sets of articles in MEDLINE. *Comput. Methods Programs Biomed.* 94 (2), 190–197. doi:10.1016/j.cmpb.2008.12.006

Soni, S. K., Basu, P., Singaravel, M., Sharma, R., Pandi-Perumal, S. R., Cardinali, D. P., et al. (2021). Sirtuins and the circadian clock interplay in cardioprotection: focus on sirtuin 1. *Cell. Mol. Life Sci.* 78 (6), 2503–2515. doi:10.1007/s00018-020-03713-6

Srivastava, S. P., Goodwin, J. E., Kanasaki, K., and Koya, D. (2020a). Metabolic reprogramming by N-acetyl-seryl-aspartyl-lysyl-proline protects against diabetic kidney disease. *Br. J. Pharmacol.* 177 (16), 3691–3711. doi:10.1111/bph.15087

Srivastava, S. P., Kanasaki, K., and Goodwin, J. E. (2020b). Loss of mitochondrial control impacts renal health. *Front. Pharmacol.* 11, 543973. doi:10.3389/fphar.2020.543973

Srivastava, S. P., Li, J., Kitada, M., Fujita, H., Yamada, Y., Goodwin, J. E., et al. (2018). SIRT3 deficiency leads to induction of abnormal glycolysis in diabetic kidney with fibrosis. *Cell Death Dis.* 9 (10), 997. doi:10.1038/s41419-018-1057-0

Srivastava, S. P., Li, J., Takagaki, Y., Kitada, M., Goodwin, J. E., Kanasaki, K., et al. (2021a). Endothelial SIRT3 regulates myofibroblast metabolic shifts in diabetic kidneys. *iScience* 24 (5), 102390. doi:10.1016/j.isci.2021.102390

Srivastava, S. P., Zhou, H., Setia, O., Dardik, A., Fernandez-Hernando, C., and Goodwin, J. (2021b). Podocyte glucocorticoid receptors are essential for glomerular endothelial cell homeostasis in diabetes mellitus. *J. Am. Heart Assoc.* 10 (15), e019437. doi:10.1161/jaha.120.019437

Srivastava, S. P., Zhou, H., Setia, O., Liu, B., Kanasaki, K., Koya, D., et al. (2021c). Loss of endothelial glucocorticoid receptor accelerates diabetic nephropathy. *Nat. Commun.* 12 (1), 2368. doi:10.1038/s41467-021-22617-y

Sun, M., Li, J., Mao, L., Wu, J., Deng, Z., He, M., et al. (2021). p53 deacetylation alleviates sepsis-induced acute kidney injury by promoting autophagy. *Front. Immunol.* 12, 685523. doi:10.3389/fimmu.2021.685523

Suzuki, S., Iben, J. R., Coon, S. L., and Kino, T. (2018). SIRT1 is a transcriptional enhancer of the glucocorticoid receptor acting independently to its deacetylase activity. *Mol. Cell. Endocrinol.* 461, 178–187. doi:10.1016/j.mce.2017.09.012

van Eck, N. J., and Waltman, L. (2010). Software survey: VOSviewer, a computer program for bibliometric mapping. *Scientometrics* 84 (2), 523–538. doi:10.1007/s11192-009-0146-3

Vaziri, H., Dessain, S. K., Ng Eaton, E., Imai, S. I., Frye, R. A., Pandita, T. K., et al. (2001). hSIR2(SIRT1) functions as an NAD-dependent p53 deacetylase. *Cell* 107 (2), 149–159. doi:10.1016/s0092-8674(01)00527-x

Veitch, M. R., Thai, K., Zhang, Y., Desjardins, J. F., Kabir, G., Connelly, K. A., et al. (2021). Late intervention in the remnant kidney model attenuates proteinuria but not glomerular filtration rate decline. *Nephrol. Carlt.* 26 (3), 270–279. doi:10.1111/nep.13828

Wang, L., Xu, C., Johansen, T., Berger, S. L., and Dou, Z. (2021). SIRT1 - a new mammalian substrate of nuclear autophagy. *Autophagy* 17 (2), 593–595. doi:10.1080/15548627.2020.1860541

Wang, M., and Lin, H. (2021). Understanding the function of mammalian sirtuins and protein lysine acylation. *Annu. Rev. Biochem.* 90, 245–285. doi:10.1146/annurev-biochem-082520-125411

Wang, W., Li, F., Xu, Y., Wei, J., Zhang, Y., Yang, H., et al. (2018). JAK1-mediated Sirt1 phosphorylation functions as a negative feedback of the JAK1-STAT3 pathway. *J. Biol. Chem.* 293 (28), 11067–11075. doi:10.1074/jbc.RA117.001387

Wang, X. L., Wu, L. Y., Zhao, L., Sun, L. N., Liu, H. Y., Liu, G., et al. (2016). SIRT1 activator ameliorates the renal tubular injury induced by hyperglycemia *in vivo* and *in vitro* via inhibiting apoptosis. *Biomed. Pharmacother.* 83, 41–50. doi:10.1016/j.biopha.2016.06.009

Wang, Z. L., Luo, X. F., Li, M. T., Xu, D., Zhou, S., Chen, H. Z., et al. (2014). Resveratrol possesses protective effects in a pristane-induced lupus mouse model. *PLoS One* 9 (12), e114792. doi:10.1371/journal.pone.0114792

Wellman, A. S., Metukuri, M. R., Kazgan, N., Xu, X., Xu, Q., Ren, N. S. X., et al. (2017). Intestinal epithelial sirtuin 1 regulates intestinal inflammation during aging in mice by altering the intestinal microbiota. *Gastroenterology* 153 (3), 772–786. doi:10.1053/j.gastro.2017.05.022

Wu, C. Y., Hua, K. F., Yang, S. R., Tsai, Y. S., Yang, S. M., Hsieh, C. Y., et al. (2020). Tris DBA ameliorates IgA nephropathy by blunting the activating signal of NLRP3 inflammasome through SIRT1- and SIRT3-mediated autophagy induction. *J. Cell. Mol. Med.* 24 (23), 13609–13622. doi:10.1111/jcmm.15663

Xu, C., Wang, L., Fozouni, P., Evjen, G., Chandra, V., Jiang, J., et al. (2020). SIRT1 is downregulated by autophagy in senescence and ageing. *Nat. Cell Biol.* 22 (10), 1170–1179. doi:10.1038/s41556-020-00579-5

Xu, Y., and Wan, W. (2022). Acetylation in the regulation of autophagy. *Autophagy*, 1–9. doi:10.1080/15548627.2022.2062112

Yasuda, I., Hasegawa, K., Sakamaki, Y., Muraoka, H., Kawaguchi, T., Kusahana, E., et al. (2021). Pre-emptive short-term nicotinamide mononucleotide treatment in a mouse model of diabetic nephropathy. *J. Am. Soc. Nephrol.* 32 (6), 1355–1370. doi:10.1681/asn.2020081188

Zhang, W., Huang, Q., Zeng, Z., Wu, J., Zhang, Y., and Chen, Z. (2017). Sirt1 inhibits oxidative stress in vascular endothelial cells. *Oxid. Med. Cell. Longev.* 2017, 7543973. doi:10.1155/2017/7543973

Zhao, L., Cao, J., Hu, K., He, X., Yun, D., Tong, T., et al. (2020). Sirtuins and their biological relevance in aging and age-related diseases. *Aging Dis.* 11 (4), 927–945. doi:10.14336/ad.2019.0820

Zhu, X., Jiang, L., Long, M., Wei, X., Hou, Y., and Du, Y. (2021). Metabolic reprogramming and renal fibrosis. *Front. Med.* 8, 746920. doi:10.3389/fmed.2021.746920

frontiers | Frontiers in Pharmacology

TYPE Original Research
PUBLISHED 16 August 2022
DOI 10.3389/fphar.2022.953004

OPEN ACCESS

EDITED BY
Divya Bhatia,
Cornell University, United States

REVIEWED BY
Tapas C. Nag,
All India Institute of Medical Sciences, India
Raja Gopal Reddy Mooli,
University of Pittsburgh, United States

*CORRESPONDENCE
Chao Zheng,
chao_zheng@zju.edu.cn

‡These authors have contributed equally to this work and share first authorship

SPECIALTY SECTION
This article was submitted to Renal Pharmacology, a section of the journal Frontiers in Pharmacology

RECEIVED 25 May 2022
ACCEPTED 01 July 2022
PUBLISHED 16 August 2022

CITATION
Wang Z, Chen Z, Wang X, Hu Y, Kong J, Lai J, Li T, Hu B, Zhang Y, Zheng X, Liu X, Wang S, Ye S, Zhou Q and Zheng C (2022), Sappanone a prevents diabetic kidney disease by inhibiting kidney inflammation and fibrosis via the NF-κB signaling pathway.
Front. Pharmacol. 13:953004.
doi: 10.3389/fphar.2022.953004

Sappanone a prevents diabetic kidney disease by inhibiting kidney inflammation and fibrosis *via* the NF-κB signaling pathway

Zhe Wang[1‡], Zhida Chen[2‡], Xinyi Wang[3], Yepeng Hu[1], Jing Kong[1], Jiabin Lai[4], Tiekun Li[5], Bibi Hu[2], Yikai Zhang[1], Xianan Zheng[1], Xiaoxian Liu[2], Shengyao Wang[1,3], Shu Ye[1], Qiao Zhou[1] and Chao Zheng[1,3*]

[1]Department of Endocrinology, The Second Affiliated Hospital, School of Medicine, Zhejiang University, Hangzhou, China, [2]Department of Nephrology, The Second Affiliated Hospital, School of Medicine, Zhejiang University, Hangzhou, China, [3]Department of Endocrinology, The Second Affiliated Hospital and Yuying Children's Hospital of Wenzhou Medical University, Wenzhou, China, [4]Department of Pathology, The Second Affiliated Hospital, School of Medicine, Zhejiang University, Hangzhou, China, [5]Nanjing Kingmed Center for Clinical Laboratory Co., Ltd., Nanjing, China

Background: Low grade of sterile inflammation plays detrimental roles in the progression of diabetic kidney disease (DKD). Sappanone A (SA), a kind of homoisoflavanone isolated from the heartwood of *Caesalpinia sappan*, exerts anti-inflammatory effects in acute kidney injury. However, whether SA has beneficial effects on diabetic kidney disease remains further exploration.

Methods and Results: In the present study, uninephrectomized male mice were treated with Streptozotocin (STZ, 50 mg/kg) for five consecutive days to induce diabetes. Next, the diabetic mice were administered orally with SA (10, 20, or 30 mg/kg) or vehicle once per day. Our results showed that STZ treatment significantly enhanced damage in the kidney, as indicated by an increased ratio of kidney weight/body weight, elevated serum creatinine and blood urea nitrogen (BUN), as well as increased 24-h urinary protein excretion, whereas SA-treated mice exhibited a markedly amelioration in these kidney damages. Furthermore, SA attenuated the pathological changes, alleviated fibrotic molecules transforming growth factor-β1 (TGF-β1) and Collagen-IV (Col-IV) production, decreased inflammatory cytokines interleukin-1β (IL-1β) and tumor necrosis factor-α (TNF-α) expression in STZ-treated mice. Similarly, in glomerular mesangial cells, SA pretreatment decreased high glucose (HG)-induced proliferation, inflammatory cytokines excretion, and fibrotic molecules expression. Mechanistically, SA

Abbreviations: BUN, blood urea nitrogen; CCK-8, cell counting kit-8; Col-IV, collagen IV; Col-I, collagen I; DAPI, 4,6-diamino-2-phenyl indole; DKD, diabetic kidney disease; DMEM, Dulbecco's Modified Eagle's Medium; ECM, extracellular matrix; EdU, 5-ethynyl-2-deoxyuridine; ELISA, enzyme-linked immunosorbent assay; FBS, fetal bovine serum; GAPDH, glyceraldehyde-3-phosphate dehydrogenase; GBM, glomerular basement membrane; GDI, glomerular damage index; H&E, hematoxylin and eosin; HG, high glucose; IL-1β, interleukin-1β; IκBα, NF-κB inhibitor alpha; NF-κB, nuclear factor kappa B; NG, normal glucose; PAS, periodic acid-Schiff; PDTC, ammonium pyrrolidine dithiocarbamate; qPCR, quantitative real-time PCR; SA, Sappanone A; STZ, streptozotocin; TGF-β1, transforming growth factor-β1; TNF-α, tumor necrosis factor-α.

decreased the expression of nuclear factor kappa B (NF-κB) and restored the expression of total NF-κB inhibitor alpha (IκBα) both *in vivo* and *in vitro*.

Conclusion: Our data suggest that SA may prevent diabetes-induced kidney inflammation and fibrosis by inhibiting the NF-κB pathway. Hence, SA can be potential and specific therapeutic value in DKD.

KEYWORDS

NF-κB, nuclear factor kappa B, SA, sappanone A, diabetic kidney disease, glomerular mesangial cells, inflammation

Introduction

Diabetic kidney disease (DKD), a kind of diabetic microvascular complication, represents the most leading cause of end-stage kidney disease worldwide (Lu et al., 2020). DKD is characterized by glomerular hypertrophy, glomerular basement membrane (GBM) thickening, tubulointerstitial fibrosis, and extracellular matrix (ECM) expansion (Kanwar et al., 2011; Lim, 2014). As the major components of the glomerulus, glomerular mesangial cells play a critical role in regulating glomerular structure and function (Schlondorff and Banas, 2009). Owing to the consistent stimulation of high glucose (HG), the glomerular mesangial cells exhibit inappropriate proliferation, excessive inflammatory cytokines and fibrotic molecules excretion, which exacerbate ECM accumulation and the glomerular sclerosis (Schena and Gesualdo, 2005). Although extensive researches have been done in clarifying the inflammatory and fibrotic processes, the existing classic anti-inflammatory therapy could not efficiently prevent or reverse the development of DKD (Alicic et al., 2018; Tuleta and Frangogiannis, 2021). Hence, there is an urgent need to develop novel and effective therapeutic strategies for DKD.

Accumulating evidence indicates that consistent low grade of sterile inflammation is pivotal in the pathophysiology of DKD, including proinflammatory cytokines excretion, the chemokines and adhesive molecules recruitment, as well as nuclear factor κB (NF-κB) activation (Alicic et al., 2017; Rayego-Mateos et al., 2020; Liu et al., 2021). Among which, NF-κB activation is defined as an "inflammatory signature" which triggers kidney inflammation during the progression of DKD (Navarro-Gonzalez and Mora-Fernandez, 2008; Sanz et al., 2010; Navarro-Gonzalez et al., 2011). Under normal conditions, NF-κB remains inactive in the cytoplasm by interacting with the IκB proteins (inhibitors of NF-κB). Activation of NF-κB is initiated by degradation of IκB proteins in response to extracellular signals. After IκB proteins degradation, NF-κB enters the nucleus to induce the transcription of inflammatory genes (Navarro-Gonzalez et al., 2011). Ultimately, NF-κB activation regulates the expression of adhesion molecules, pro-inflammatory cytokines and chemokines that are associated with chronic kidney inflammation in DKD (Kim and Park, 2016). Besides, it is noteworthy that activation of NF-κB pathway is also involved in the development of kidney fibrosis. For instance, suppression of NF-κB pathway significantly attenuated kidney fibrosis in DKD (Liang et al., 2018; Sun et al., 2021).

Sappanone A (SA), a kind of homoisoflavanone isolated from the heartwood of *Caesalpinia sappan*, has been reported to exhibit anti-inflammatory effects (Lee et al., 2015). The classic inflammatory processes are associated with the action and recruitment of inflammatory cells like macrophages and T cells, and the corresponding cytokines excretion. In RAW264.7 cells, a murine macrophage cell line, SA treatment inhibited LPS-induced IL-6 expression (Chu et al., 2013). Recently, SA has been shown to play a critical role in various disease such as myocardial ischemia-reperfusion injury, cerebral ischemia-reperfusion injury and acute kidney injury (Kang et al., 2016; Shi et al., 2021; Wang et al., 2021). However, there is still no direct evidence to demonstrate whether SA has beneficial effects on DKD, and the potential mechanism remains unknown.

In the present study, we first detected the reno-protective effects of SA in Streptozotocin (STZ)-treated mice. Next, we performed *in vitro* experiments to further explore the underlying mechanisms of SA in HG-treated glomerular mesangial cells. Our research indicates that SA may prevent diabetes-induced kidney inflammation and fibrosis by inhibiting the NF-κB pathway.

Materials and methods

Animal models and treatment protocols

All experiments were approved by the Animal Care Committee of Zhejiang University, and the animal work was carried out at Zhejiang University. Six-eight weeks old C57BL/6J mice (20–23 g bodyweight) were purchased from Silaike Company (Shanghai, China). All mice were allowed free access to food and water, under controlled temperature (22–25°C), humidity (60%), and light (alternating 12-hour light/dark cycle) conditions. Because mice with a C57BL/6 background did not develop lesions of DKD readily after the induction of diabetes by STZ, uninephrectomy was performed to hasten the development of DKD (Zhou et al.,

2019). After a week of adaptive feeding, mice were fully anesthetized with their kidney exposed *via* a back incision, the left kidney was removed after ligaturing the kidney pedicle with a 4/0 surgical suture (Ahmad et al., 2019) and randomly divided into five groups (n = 5 per group): Control group, STZ group, STZ + SA 10 mg/kg group, STZ + SA 20 mg/kg group, and STZ + SA 30 mg/kg group. After a one-week recovery period from unilateral nephrectomy (Unx), mice rendered diabetic were induced by intraperitoneal (I.P) injection with STZ [50 mg/kg body weight dissolved in 100 mM citrate buffer (pH 4.5)] for five consecutive days. Meanwhile, mice in the Control group received the same volume of citrate buffer. At day 7, mice with a fasting-blood glucose >12 mmol/L were considered diabetes and were used for the further study (Zheng et al., 2019). Next, the diabetic mice in STZ + SA 10 mg/kg group, STZ + SA 20 mg/kg group, and STZ + SA 30 mg/kg group were orally treated with SA dissolved in 0.5% carboxymethyl cellulose at a dose of 10, 20, or 30 mg/kg SA every day, respectively. Meanwhile, mice in the Control group and STZ group were gavaged with the same volume of 0.5% carboxymethyl cellulose. The fasting blood glucose and body weight were measured every week for 12 weeks.

At the end of the experiment, mice were placed in individual metabolic cages for 24 h urine collection. The animals were then sacrificed and blood was collected from the right ventricle of the heart using a heparin-free syringe with a needle at the time of death. Blood urea nitrogen, serum creatinine, and daily urinary albumin excretion were measured using an automatic biochemical analyzer (Hitachi, Tokyo, and Japan). Kidney cortex was snap-frozen in liquid nitrogen for gene and protein expression analyses, and/or embedded in 4% paraformaldehyde for histological analyses.

Histological analysis and immunohistochemistry staining

The kidney was cut longitudinally along the long axis, fixed with 4% paraformaldehyde, embedded in paraffin, and cut into 5-μm-thick slices in a row. To determine the degree of pathological damage and fibrosis of kidney tissues, sections were stained with hematoxylin and eosin (H&E) and periodic acid-Schiff (PAS), and then the morphological changes of the kidneys were observed under a light microscope.

As previous described (Abais et al., 2014), glomerular morphology was observed and assessed semi-quantitatively. Briefly, 40 glomeruli per slide were counted and scored each as 0, 1, 2, 3 or 4. These values were respectively assigned according to the severity of sclerotic changes (0: 0%; 1: <25%; 2: 25–50%; 3: 51–75% or 4: >75% sclerosis of the glomerulus). The Glomerular Damage Index (GDI) comprised the average of these scores and was calculated according to the following formula: $[(N_1 \times 1) + (N_2 \times 2) + (N_3 \times 3) + (N_4 \times 4)]/n$, where N_1, N_2, N_3, and N_4 represent the numbers of glomeruli with scores of 1, 2, 3, 4, and n represents total glomeruli.

Enzyme-linked immunosorbent assay

The levels of IL-1β and TNF-α in kidney tissues and serum were assessed by Enzyme-linked immunosorbent assay (ELISA) according to manufacturer's instructions (MLBio, China).

Cell culture and treatment

Mouse glomerular mesangial cells SV40-MES-13 were purchased from ATCC and cultured in Dulbecco's Modified Eagle's Medium (DMEM, Gibco) in low glucose (5.5 mM of glucose) supplemented with 10% fetal bovine serum (FBS, Gibco) with 1% antibiotics (100 IU/ml penicillin-streptomycin), and then grown at 37°C with an atmosphere of 5% CO_2. Next, cells were treated with SA (10, 20, and 30 μM) dissolved in 0.1% dimethyl sulfoxide for 1 h before high glucose (30 mM, Sigma) treatment. After 24 h of culture, the supernatant and cells were collected for further analysis. To further explore the mechanism, mesangial cells were pretreated with ammonium pyrrolidine dithiocarbamate (PDTC, 50 μM, Sigma), a NF-κB inhibitor, along with SA prior to stimulating with HG for 24 h.

Cell proliferation assay

Cell proliferation was assessed using Cell Counting Kit-8 (CCK-8) (Dojindo, Japan) and a 5-ethynyl-2-deoxyuridine (EdU) labeling/detection kit (BeyoClick™ EdU Cell Proliferation Kit with Alexa Fluor 555, Beyotime, China). For CCK-8 assay, mesangial cells were seeded in a 96-well plate exposed to high glucose (30 mM) with or without pretreatment of different concentrations of SA for 24 h. Next, 10 μl CCK-8 reagent was added to each well containing 100 μl DMEM medium and the plate was incubated for 2 h at 37°C. Finally, a microplate reader (BioTek, United States) was used to detect the absorbance at 450 nm.

For EdU assay, cells were cultured in a 12-well plate and incubated with EdU for 2 h. Trypsin was added into the microcentrifuge tube to digest the cells, which were then fixed with 4% paraformaldehyde for 15 min and permeated with 0.3% Triton X-100 for another 15 min. Next, cells were incubated with the Click Reaction Mixture for 30 min at room temperature in a dark place following the manufacturer's instructions. Finally, cells were re-suspended in phosphate buffered saline (PBS) for flow cytometric analysis on the Beckman Coulter CytoFLEX LX (Beckman Coulter, United States). Data were analyzed using FlowJo software version 10 (Treestar).

RNA isolation and quantitative real-time PCR

Total RNA was extracted using TRIzol reagent (Invitrogen), followed by cDNA synthesis (1,000–2,000 ng total RNA samples) using a reverse transcription kit (Yeasen, China). Quantitative real-time PCR was performed using a SYBR Green qPCR kit (Yeasen, China), and the primers were designed and synthesized by Tsingke Biotech Com (Shanghai, China). Relative mRNA expression was normalized to GAPDH mRNA and then calculated using the $2^{-\triangle\triangle CT}$ method. The primer sets used are shown in Supplementary Table S1.

Western blot analysis

Total protein of both cultured cells and kidney cortex were extracted in RIPA lysis buffer (Beyotime) supplemented with phenylmethylsulfonyl fluoride (PMSF, Beyotime) and protein phosphatase inhibitor (Solarbio). Notably, the extraction and isolation of nuclear and cytoplasmic protein were performed according to the Nuclear and Cytoplasmic Protein Extraction Kit (Beyotime) protocol to confirm the activation of NF-kB by detecting the expression of nuclear NF-κB p65, cytosol NF-κB p65, and Lamin B. The concentration was then determined by the BCA protein assay reagent kit (Fdbio science) and the samples were homogenized in 5× SDS-sample buffer at a final concentration of 1×. Next, samples were denatured, resolved using 12% SurePAGE™ Bis–Tris Protein Gels (GenScript), and then transferred onto polyvinylidene difluoride (PVDF) membranes. After nonspecific binding was blocked with 5% nonfat dry milk in Tris-buffered saline for 1 h, membranes were incubated overnight with primary antibodies including TGF-β1 (1:1000, Abcam), Col-IV (1:1000, Proteintech), NF-κB p65 (1:1000, CST), IκBα (1:1000, CST), Lamin B (1:1000, CST), and Actin (1:2000, Abcam), at 4°C. On the next day, membranes were washed with Tris-buffered saline, incubated with horseradish peroxidase-conjugated secondary antibody (1: 5000, Yeasen) at 37°C for 1 h, and visualized using Amersham Image Quant 800 imaging system (GE Healthcare). Whole cell protein expression was normalized to Actin, whereas nuclear protein expression was normalized to Lamin B.

Assay of cellular NF-κB p65 translocation.

Cells were immunofluorescence-labeled using a Cellular NF-κB Translocation Kit (Beyotime) according to the manufacturer's instructions. After different treatments, cells were fixed with 4% paraformaldehyde and permeabilized with 0.3% Triton X-100 for 10 min. Next, cells were washed twice with PBS containing 0.5% Tween, and incubated with a blocking buffer for 1 h at room temperature. Cells were then incubated with primary NF-κB p65 antibody overnight at 4°C, followed by a Cy3-conjugated secondary antibody for 1 h at room temperature. Finally, cells were counterstained with DAPI for 5 min and then viewed under a fluorescence microscope (400×, Leica DMi8, Germany).

Statistical analysis

All statistical analyses were performed using GraphPad Prism v6.0 Software (United States). Data obtained are expressed as the means ± SEM. Each experiment was performed with three biological replicates. All experiments were performed at least three times. Two groups were examed *via* using two-tailed Student's *t*-test, while multiple groups were compared using ANOVA followed by a Student-Newman-Keuls test, differences were considered to be significant at $p < 0.05$.

Results

SA ameliorated kidney injury in STZ-induced diabetic mice

As shown in Figures 1A,B, STZ treatment in uninephrectomized mice caused a considerable increase of fasting blood glucose levels and a significant decrease in body weight, however, there was no difference among the STZ-treated mice with or without SA treatment. We subsequently examined a series of indices of kidney injury to assess the beneficial effects of SA. First, mice in STZ group induced greater kidney hypertrophy indicated by an increased ratio of kidney weight/body weight, which was significantly blunted by SA administration (Figure 1C). Consistently, serum creatinine and blood urea nitrogen (BUN) were markedly elevated after STZ treatment, in contrast, the elevation of serum creatinine and BUN were significantly attenuated by SA administration (Figures 1D,E). Moreover, 24 h urinary protein was markedly increased in STZ induced mice while the level was significantly decreased after SA treatment (Figure 1F). Collectively, above results suggest that SA administration ameliorates kidney injury in STZ-induced diabetic mice.

SA ameliorated pathological changes in the kidney and fibrosis in STZ-induced diabetic mice

H&E and PAS staining were performed to determine morphological changes in the kidney. As shown in Figure 2A, STZ-treated mice had remarkable glomerular sclerotic damage as indicated by glomerular mesangial expansion with hypercellularity, capillary collapse, and matrix deposition in glomeruli whereas these histopathological changes were markedly improved in SA-

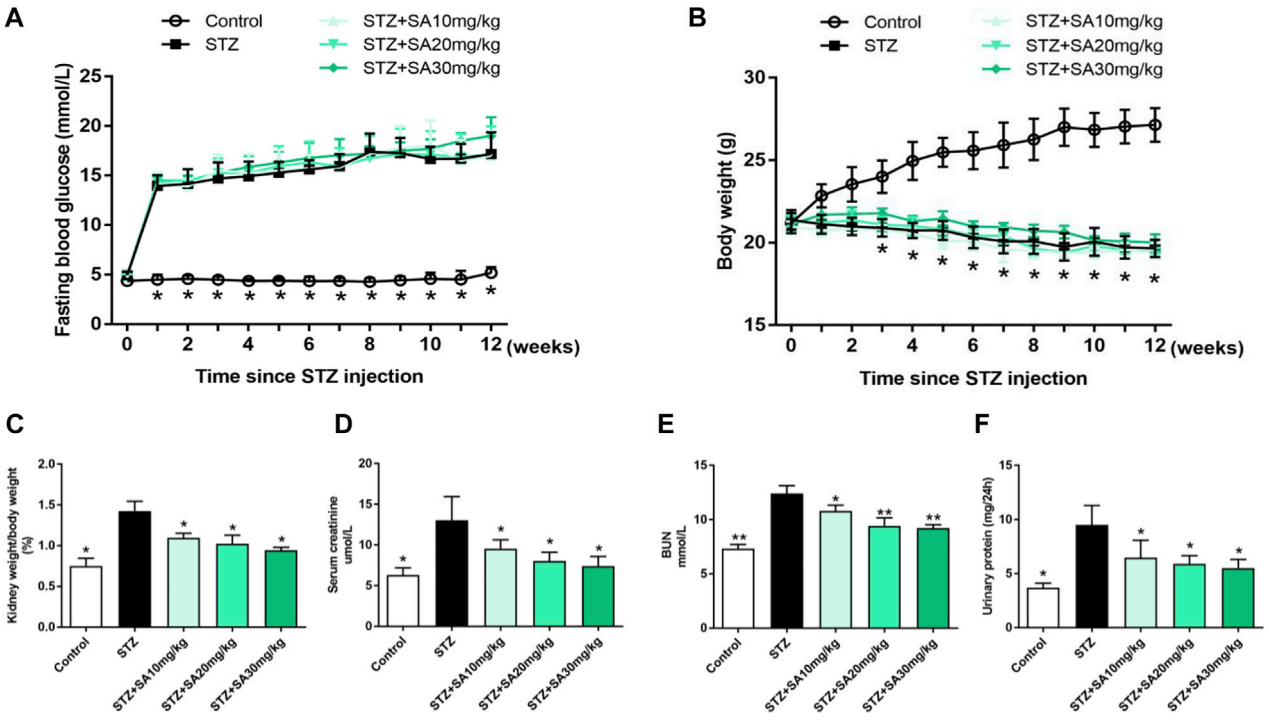

FIGURE 1
Effects of SA on metabolic and biochemical parameters in STZ-induced diabetic mice. **(A)** Fasting blood glucose levels. **(B)** Body weight. **(C)** Ratio of kidney weight to body weight. **(D,E)** The levels of serum creatinine and BUN. **(F)** 24-hour urinary protein. *N* = 5 per group. All data are shown as the mean ± SEM; **p* < 0.05 and ***p* < 0.01 versus STZ group. SA, Sappanone A; STZ, streptozotocin; BUN, blood urea nitrogen.

treated mice. Similar pattern of the morphological changes was observed by PAS staining (Figure 2B). The glomerular damage index is summarized in Figure 2C.

We further determine the effects of SA on kidney fibrosis under hyperglycemia. As shown in Figures 2D–F, the mRNA expression levels of the profibrotic molecules *Tgf-β1*, *Col-IV*, and *Col-I* were significantly increased in the kidney cortex of STZ-treated mice compared with control mice, in contrast, the expression of these fibrotic markers were blunted after SA administration. Similar pattern was observed on protein expression levels of TGF-β1 and Col-IV (Figures 2G,H). Taken together, the suppression of kidney fibrosis supports the possibility that SA has a beneficial effect against DKD, and the most obvious effects of SA on renoprotection is at a dosage of 30 mg/kg/d.

SA attenuated the systemic and kidney cortical inflammatory response in STZ-induced diabetic mice

It is well established that inflammation triggers the pathogenesis of DKD (Navarro-Gonzalez and Mora-Fernandez, 2008; Tang and Yiu, 2020). The present study detected increased circulating IL-1β and TNF-α levels during DKD. As shown in Figure 3A,B, different doses of SA administration alleviated IL-1β and TNF-α excretion in STZ treated mice. Consistently, SA treatment significantly inhibited the IL-1β and TNF-α production in kidney cortex (Figures 3C,D). In parallel with immunoblotting results, the mRNA levels of *IL-1β* and *TNF-α* were enhanced in kidney cortex of diabetic mice, however, SA effectively reversed above abnormalities (Figures 3E,F). As a master regulator of inflammation, the transcription factor NF-κB triggers numerous proinflammatory genes expression and plays a fundamental role in low grade sterile inflammation during hyperglycemia (Karin and Greten, 2005). Hence, we measured the protein expressions of IκBα and nuclear NF-κB p65. In STZ-treated mice, IκBα was significantly reduced while nuclear NF-κB p65 was increased in the kidney cortex compared with the normal control. In contrast, SA administration effectively reversed the pathological process (Figures 3G–I). Above results demonstrated that all three doses of SA exerted an anti-inflammatory action in STZ-treated mice.

SA decreased HG-induced proliferation and fibrosis in glomerular mesangial cells

In order to assess the toxicity of SA in glomerular mesangial cells, the cell viability was tested at different

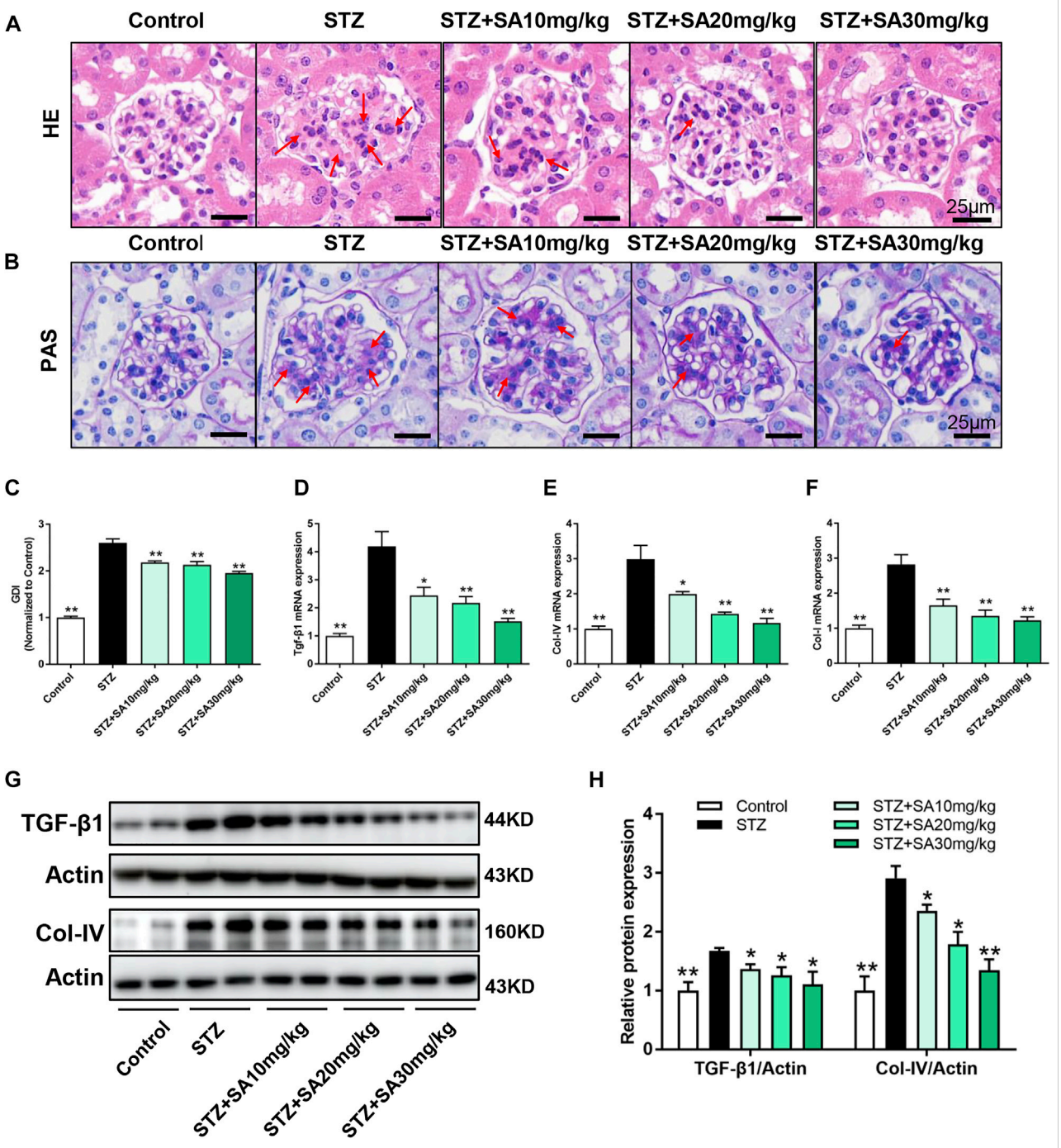

FIGURE 2
SA attenuates diabetes induced glomerular morphological changes and fibrotic process *in vivo*. **(A)** Representative photomicrographs showing glomerular structures (hematoxylin–eosin staining, 400×). Scale bar, 25 μm. **(B)** Representatives photomicrographs showing glomerular structures (PAS staining, 400×). Scale bar, 25 μm. **(C)** Summarized glomerular damage index in different groups. **(D–F)** The mRNA levels of *Tgf-β1*, *Col-IV*, and *Col-I* in kidney cortex. **(G–H)** Immunoblot and quantification for TGF-β1 and Col-IV expression. $N = 5$ per group. All data are shown as the mean ± SEM; $^{*}p < 0.05$ and $^{**}p < 0.01$ versus STZ group. HE, hematoxylin–eosin; PAS, Periodic Acid-Schiff; GDI, glomerular damage index; TGF-β1, transforming growth factor-β1; Col-IV, collagen-IV; Col-I, collagen-I.

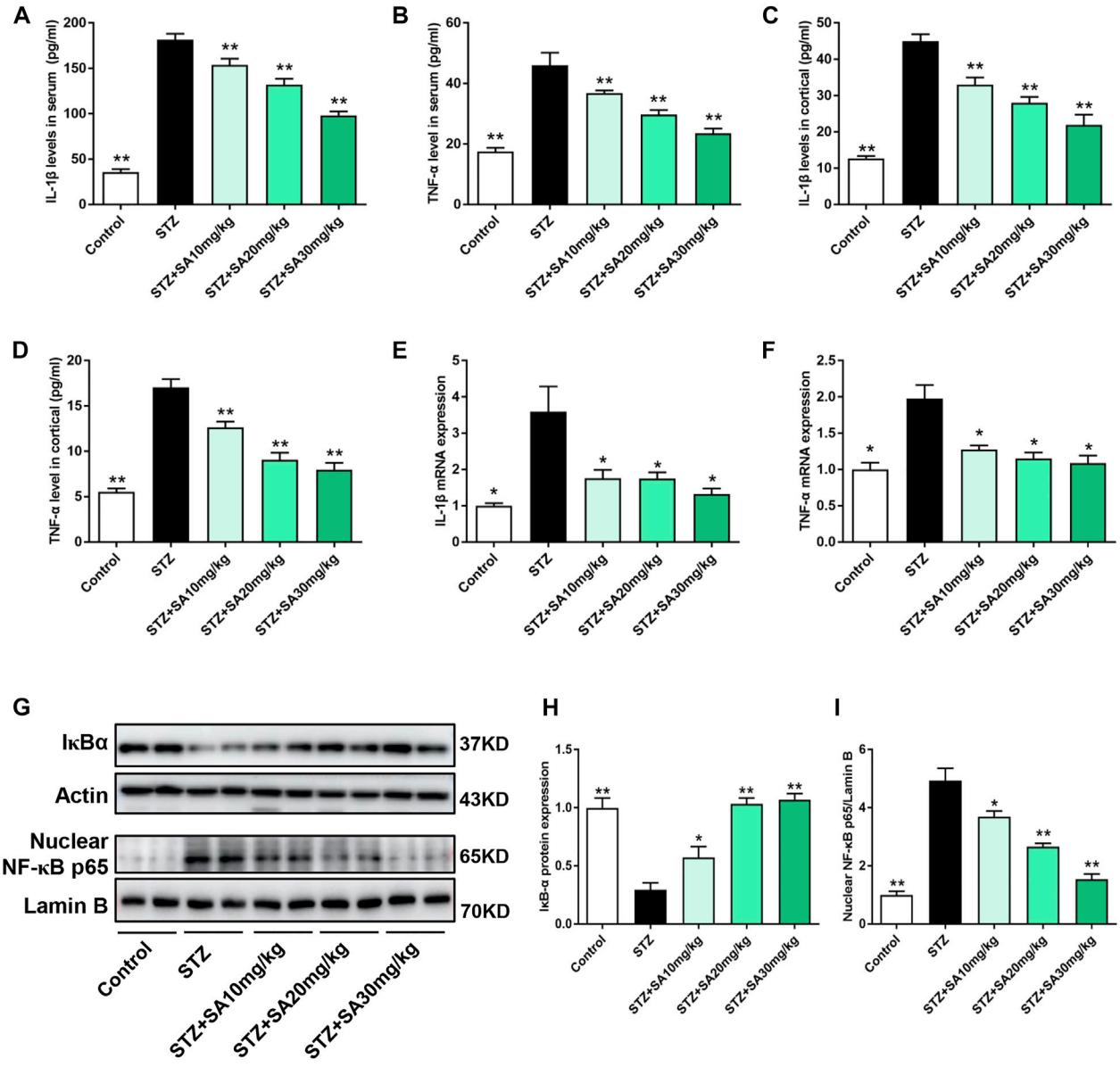

FIGURE 3
SA inhibited IL-1β and TNF-α expression as well as NF-κB activation in diabetic mice. **(A,B)** IL-1β and TNF-α excretions in serum. **(C,D)** IL-1β and TNF-α production in kidney cortex. **(E,F)** The mRNA levels of *IL-1β* and *TNF-α* in kidney cortex. **(G–I)** Western blot analysis and quantitative data for total IκBα and NF-κB p65 expression in different groups. $N = 5$ per group. All data are shown as the mean ± SEM; $^{*}p < 0.05$ and $^{**}p < 0.01$ versus STZ group. IL-1β, interleukin-1β; TNF-α, tumor necrosis factor-α; NF-κB, nuclear factor kappa B; IκBα, NF-κB inhibitor alpha.

concentrations. Results showed that there was no significant inhibition of cell viability when glomerular mesangial cells were stimulated by SA at concentrations less than 32 μM for 24 h (Figure 4A). Thus, the dose of SA for *in vitro* experiments were optimized to 10, 20, and 30 μM. Furthermore, HG promoted proliferation of glomerular mesangial cells, which was suppressed by SA in a dose-dependent manner (Figure 4B). In addition, EdU labeling and flow cytometry were performed to determine the proportion of proliferating cells (Figures 4C,D). Western blot results demonstrated that TGF-β1 and Col-IV expression in glomerular mesangial cells increased after HG stimulation, which were significantly inhibited by SA (Figures 4E,F). Consistently, SA treatment prevented HG-induced *Tgf-β1*, *Col-IV*, and *Col-I* mRNA expressions (Figures 4G–I). Taken together, it was evident that SA could inhibit the proliferation and fibrotic processes of mesangial cells in a dose-dependent manner.

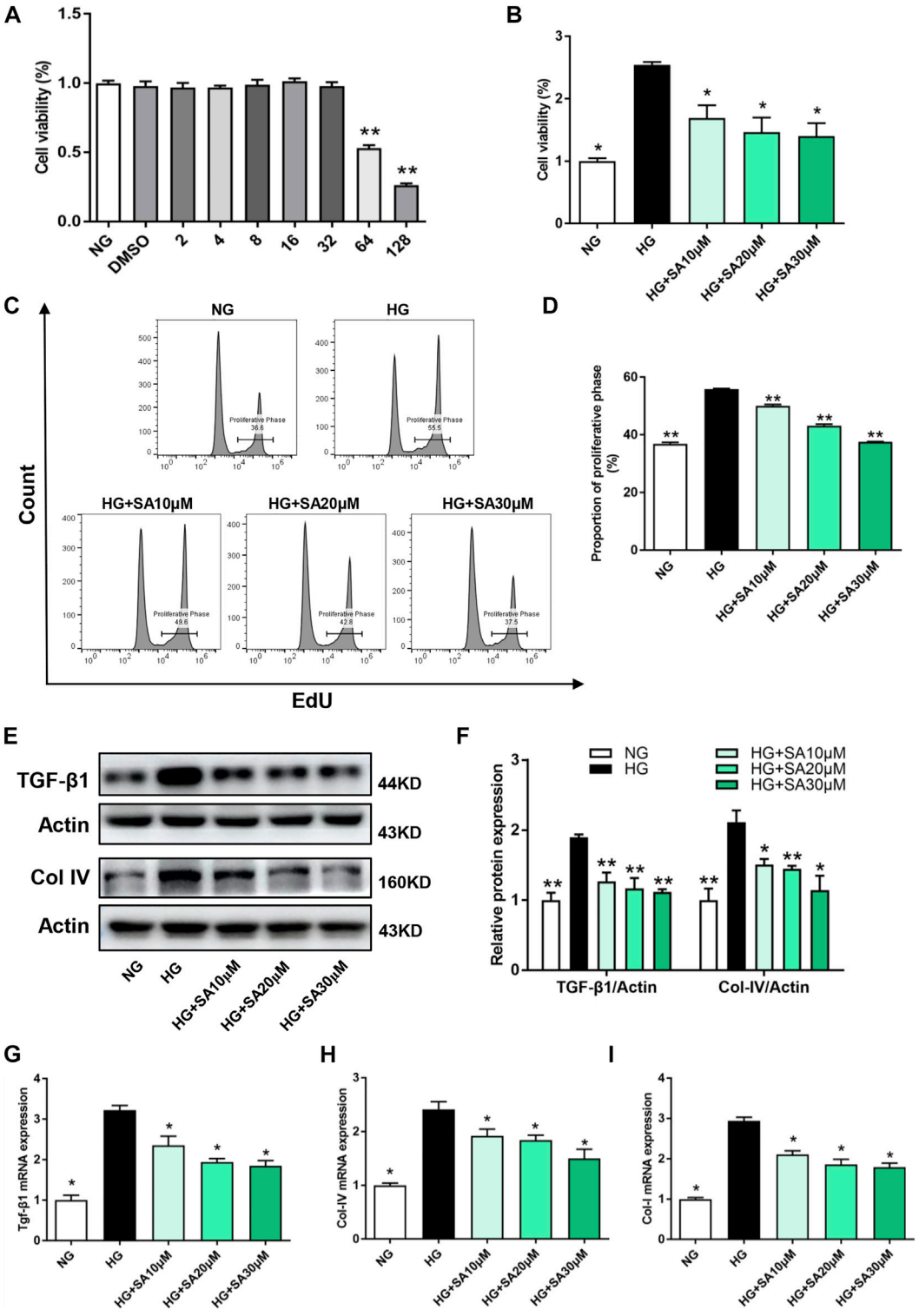

FIGURE 4
SA inhibits HG-induced proliferation and fibrosis in glomerular mesangial cells *in vitro*. **(A)** Cell viability of glomerular mesangial cells in different concentrations of SA (N = 4). $^{**}p < 0.01$ vs. NG group. **(B)** Cell viability in HG group with or without different dose of SA treatment (*N* = 4). **(C)** Flow cytometric analysis of mesangial cells stained with EdU. **(D)** Percentage of proliferative rates (*N* = 3). **(E–F)** Western blot analysis and quantitative data of TGF-β1 and Col-IV expression (*N* = 4). The mRNA levels of *Tgf-β1* **(G)**, *Col-IV* **(H)**, and *Col-I* **(I)** in glomerular mesangial cells (*N* = 3). All data are shown as the mean ± SEM; $^{*}p < 0.05$ and $^{**}p < 0.01$ versus HG group. NG, normal glucose; HG, high glucose; EdU, 5-ethynyl-2-deoxyuridine.

10.3389/fphar.2022.953004

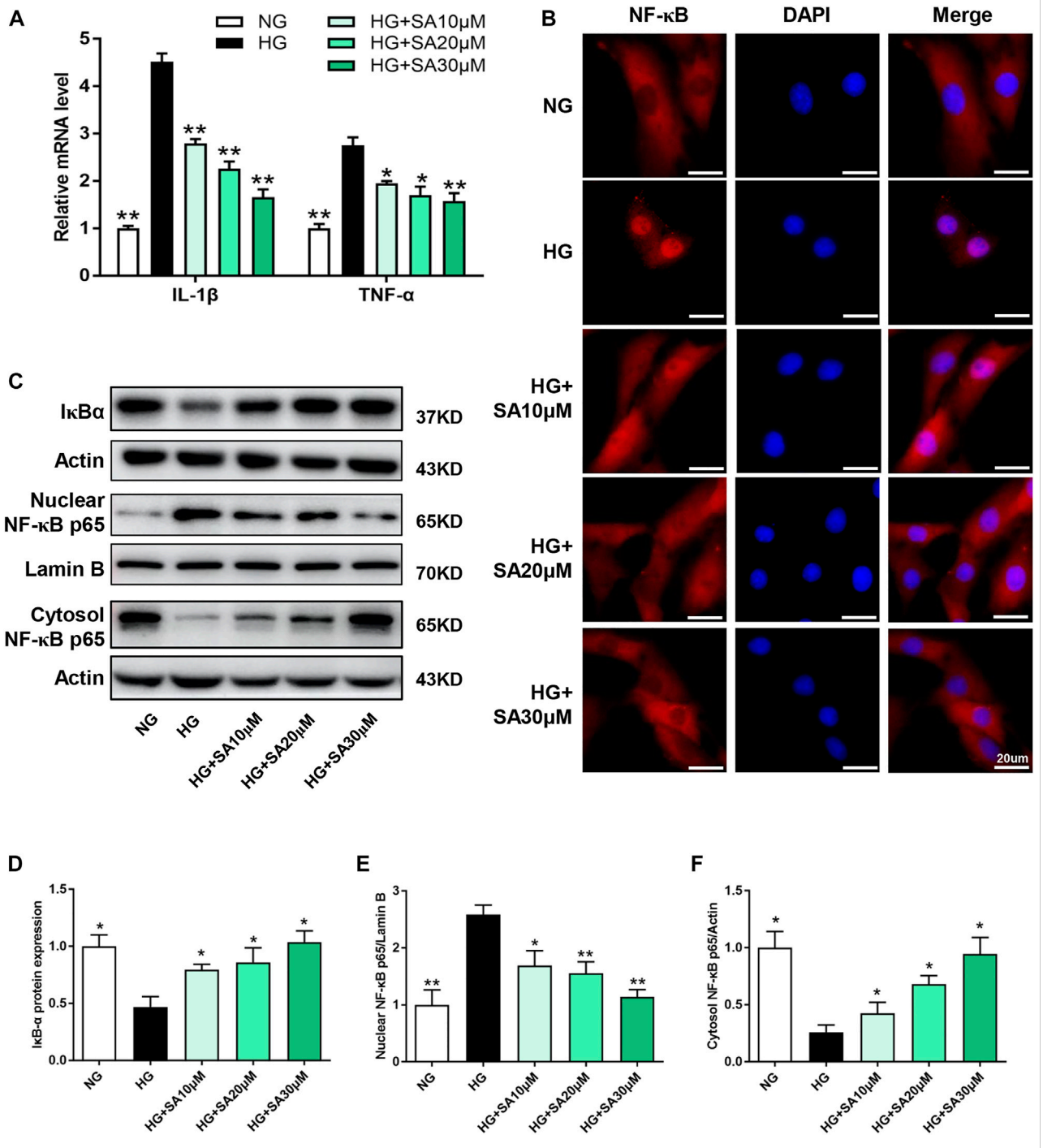

FIGURE 5
SA prevents HG-induced inflammatory responses *via* inhibiting IL-1β and TNF-α expression as well as NF-κB activation *in vitro*. **(A)** The mRNA level of proinflammatory cytokines *IL-1β* and *TNF-α* determined by reverse transcriptase polymerase chain reaction ($N = 3$). **(B)** Immunofluorescence localization of NF-κB p65 subunit (red) in mesangial cells, nuclei stained with fluorescent DAPI (blue). The images were acquired with a 40× magnification objective. Scale bar, 20 μm. **(C–F)** Immunoblot and quantification for total cell lysis IκBα, nuclear NF-κB p65 and cytoplasmic NF-κB p65 expression. ($N = 4$). All data are shown as the mean ± SEM; $^{*}p < 0.05$ and $^{**}p < 0.01$ versus HG group. DAPI, 4,6-diamino-2-phenyl indole.

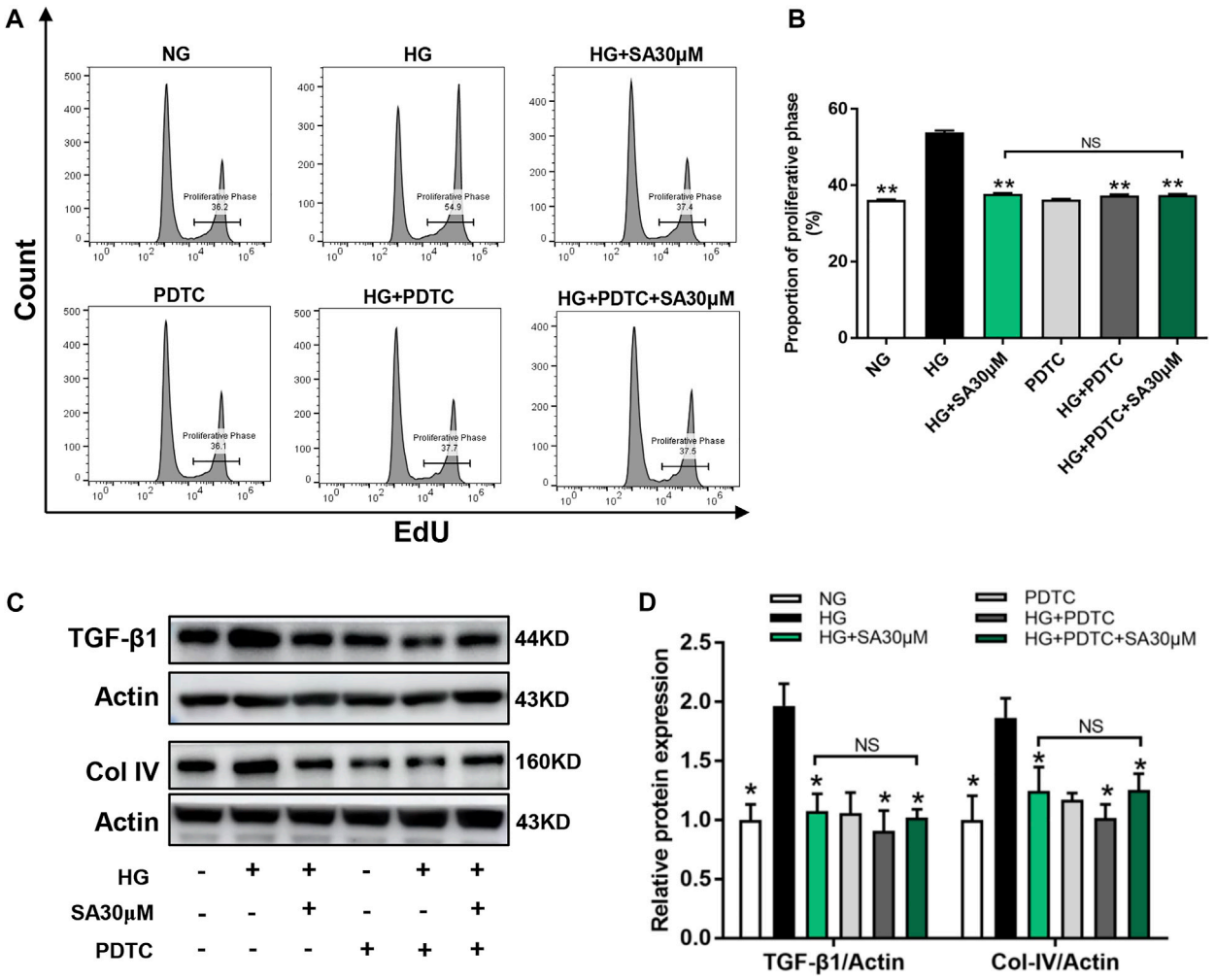

FIGURE 6
SA prevented HG-induced proliferation and fibrosis *via* inhibiting NF-κB pathway *in vitro*. Cells were pretreated with or without 50 μM PDTC, along with 30 μM SA for 1 h prior to stimulating with 30 mM HG. **(A)** Flow cytometric analysis of mesangial cells stained with EdU. **(B)** Percentage of proliferative rates ($N = 3$). **(C,D)** Western blot analysis and quantitative data of TGF-β1and Col-IV expression in treated mesangial cells ($N = 4$). All data are shown as the mean ± SEM; $^{*}p < 0.05$ and $^{**}p < 0.01$ versus HG group, NS: not significant. PDTC, ammonium pyrrolidine dithiocarbamate.

SA inhibited HG-induced inflammatory response in glomerular mesangial cells by blocking NF-κB pathway

To further investigate the effects of SA on inflammatory response *in vitro*, glomerular mesangial cells were pretreated with SA (10, 20, or 30 μM) for 1 h, followed by HG (30 mM) stimulation for an additional 24 h. *IL-1β*, and *TNF-α* mRNA expression increased significantly after HG stimulation, while SA pretreatment prevented HG-induced increase of the inflammatory cytokines in a dose-dependent manner (Figure 5A). Moreover, immunofluorescent microscopy indicated that SA prevented HG-induced nuclear translocation of p65 subunit (Figure 5B). In addition, we also assessed the effects of SA on IκBα degradation and p65 translocation in cultured glomerular mesangial cells. Our results showed that pretreatment with SA dose-dependently reversed the HG-induced degradation of IκBα, reduced HG-induced increase of nuclear NF-κB p65 levels and concomitant decrease of cytosolic NF-κB p65 levels (Figures 5C–F).

Next, we performed NF-κB inhibitor PDTC to further confirm that the effects of SA on HG-induced inflammatory response was mediated by the NF-κB pathway in glomerular mesangial cells. Mesangial cells were pretreated with or without 50 μM PDTC along with 30 μM SA for 1 h prior to HG stimulation. Although, both SA and PDTC prevented the increased proportion of cell proliferation induced by HG, there were no significant differences between the HG + SA group and the HG + SA + PDTC group (Figures 6A,B). Western blot analyses demonstrated that both SA and PDTC

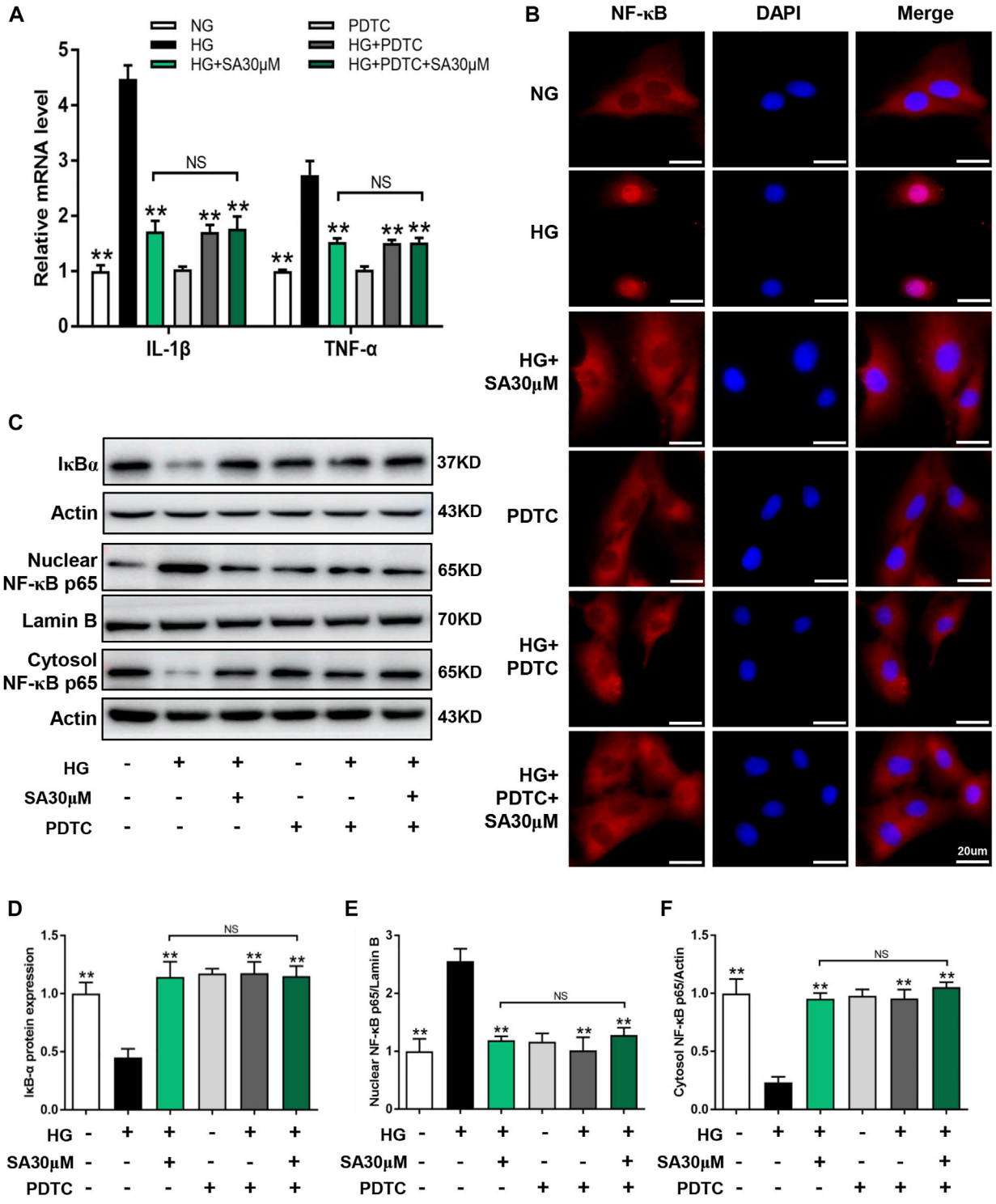

FIGURE 7
SA prevented HG-induced inflammatory process *via* inhibiting NF-κB pathway *in vitro*. Glomerular mesangial cells were pretreated with or without 50 μM PDTC, along with 30 μM SA for 1 h prior to stimulating with 30 mM HG. **(A)** The mRNA amounts of *IL-1β* and *TNF-α* in glomerular mesangial cells ($N = 3$). **(B)** Immunofluorescence localization of NF-κB p65 subunit (red) in glomerular mesangial cells, nuclei stained with fluorescent DAPI (blue). The images were acquired with a 40× magnification objective. Scale bar, 20 μm. **(C–F)** Immunoblot and quantification for nuclear NF-κB p65, cytoplasmic NF-κB p65, and total cell lysis IκBα expressions ($N = 4$). All data are shown as the mean ± SEM. $^{*}p < 0.05$ and $^{**}p < 0.01$ versus HG group, NS: not significant.

reduced the increased TGF-β1 and Col-IV protein levels induced by HG in mesangial cells, whereas SA combined with PDTC did not further improve the fibrosis (Figures 6C,D). Furthermore, SA and PDTC prevented the increase of *IL-1β* and *TNF-α* mRNA expression (Figure 7A), reduced the nuclear translocation of the p65 subunit (Figure 7B), reversed the degradation of IκBα, as well as the increase of nuclear NF-κB p65 levels and concomitant decrease of cytosolic NF-κB p65 levels in HG-treated glomerular mesangial cells (Figures 7C–F). However, compared with a single PDTC treatment, the combination of SA and PDTC did not further prevent the inflammatory injury caused by high glucose. Above results suggested that SA blocked HG-induced inflammatory process by suppressing the NF-κB pathway.

Discussion

Current study evaluated the reno-protective effects and explored underlying molecular mechanisms of SA in STZ-induced diabetic mice. To date, the study provided strong evidence that SA prevented kidney injury during hyperglycemia. It is noteworthy that hyperglycemia is the foremost etiological factor of DKD, which induces profibrotic responses in kidneys of diabetic patients, eventually promoting glomerular sclerosis and interstitial fibrosis (Wu et al., 2020; Zhao et al., 2020). In our present study, SA treatment dose-dependently reduced kidney injury in STZ-treated mice, as evidenced by a decrease in ratio of kidney weight to body weight, serum creatinine, blood urine nitrogen and 24-h urinary protein. Consistently, SA administration ameliorated hyperglycemia induced glomerular morphological changes in STZ-treated mice. In addition, we also explored the beneficial effects of SA on HG-treated glomerular mesangial cells *in vitro*. Under diabetic conditions, glomerular mesangial cells are activated, leading to cell proliferation and excess glomerular ECM deposition in the mesangial region. Besides, glomerular mesangial cells also secrete various inflammatory cytokines, adhesion molecules, chemokines and enzymes in response to HG stimulation (Wei et al., 2021). Previous studies have elucidated that ECM accumulation and glomerular mesangial cells proliferation are known to be intimately associated with diabetes induced glomerular hypertrophy and sclerosis (Tung et al., 2018). In the present study, we found that SA treatment weakened HG-induced TGF-β1 and Col IV expression in glomerular mesangial cells. Consistently, the flow cytometry results revealed that SA treatment reversed glomerular mesangial cells proliferation during hyperglycemia. Above results demonstrated that SA administration alleviated diabetes induced kidney fibrotic process *in vivo* and *in vitro*.

Several inflammatory cytokines participate in the pathophysiology of DKD. Among which, IL-1β and TNF-α are considered to be the representative regulators of inflammation. It was reported that IL-1β in the kidney increased in the rodent animal models of DKD, which was associated with increased production of adhesive molecules, such as intercellular adhesion molecule 1 (ICAM-1) and vascular cell adhesion protein 1 (VCAM-1) (Sassy-Prigent et al., 2000; Navarro-Gonzalez et al., 2011). Similar to IL-1β, TNF-α also exerts various biological effects in DKD, including its direct cytotoxicity to kidney resident cells as well as activation of cell pathways leading to apoptosis and necrosis (Navarro-Gonzalez et al., 2011). Furthermore, TNF-α promotes oxidative process in mesangial cells *via* activating NADPH oxidase, leading to overproduction of reactive oxygen species (Koike et al., 2007). Recently, SA was reported to inhibit the production of inflammatory cytokines: TNF-α and IL-1β in the kidney of cisplatin-induced injury (Branstetter et al., 1989), which was in coincidence with our results in DKD.

Although several innate immune pathways have been postulated in the pathogenesis and progression of DKD, NF-κB signaling pathway is the most well-defined in a sterile glomerular and interstitial inflammatory process (Guijarro and Egido, 2001; Yang et al., 2019; Tang and Yiu, 2020). For instance, it was reported that NF-kB inhibitor reduced macrophage infiltration in the kidney, decreased production of inflammatory cytokines, and consequently reversed kidney dysfunction in diabetic rats (Yang et al., 2019). In addition, PDTC, one of NF-κB inhibitors, prevented IκB phosphorylation, thereby blocking NF-κB translocation to the nucleus, which ultimately reduced the expression of downstream cytokines (Liao et al., 2017). Thus, we continued to explore whether SA exerted beneficial actions *via* inhibition of NF-κB signaling pathway. As expected, SA administration significantly reversed IκB degradation and p65 nuclear translocation in STZ treated mice and HG treated glomerular mesangial cells. Furthermore, although blockage of NF-κB by PDTC or SA significantly attenuated abnormal proliferation and fibrotic molecules expression in HG treated mesangial cells, the combination of SA and PDTC did not further improve the phenomena. Above results demonstrated that SA indeed prevents kidney injury *via* inhibition of NF-κB signaling pathway.

Studies in some rodent models of DKD have shown that immunosuppressive drugs exhibited reno-protective effects. For instance, mycophenolate mofetil (MMF), a classic inosine monophosphate dehydrogenase (IMPDH) inhibitor, was reported to suppress proteinuria and attenuate glomerular sclerosis and interstitial fibrosis in STZ-treated rats. Similar results were reported in an experimental model of T2DM, in which MMF treatment resulted in reduced glomerular and tubulointerstitial inflammatory cell infiltration as well as decreased proteinuria. Despite these promising results in rodent animal models, immunosuppressive interventions are still not a clinical therapeutic option in real patients with DKD because of potential adverse-effects. Interestingly, Tu et al. (Liao et al., 2017) found that SA exerted anti-neuroinflammatory effects because of its highly selective inhibition of IMPDH2. However, other previous studies have demonstrated that SA directly inhibited NF-κB activation (Lee et al., 2015; Kang et al., 2016). Diverse mechanisms of SA may be dependent on different experimental models. In our present study, no significant immunosuppressive effects such as infectious disease or diarrhea were observed in the whole period of SA-treated mice.

Taken together, we speculate that SA may have a direct modulation of NF-κB pathway in STZ-induced diabetic mice, which is worth further exploration in another study.

Conclusion

In summary, the present study demonstrated that SA prevents DKD by ameliorating glomerular pathological changes, decreasing biological parameters, attenuating inflammatory molecules production and secretion, as well as alleviating fibrotic process. *In vitro*, we also found that SA ameliorates inflammatory response and fibrosis in HG-treated glomerular mesangial cells *via* inhibiting NF-κB signaling pathway. These results are promising and may provide new evidence for the potential application of SA in the treatment of DKD.

Data availability statement

The raw data supporting the conclusion of this article will be made available by the authors, without undue reservation.

Ethics statement

The animal study was reviewed and approved by the Animal Ethics Committee of Zhejiang University.

Author contributions

CZ designed the experiments. ZW and ZC carried out most of the experiments and drafted the manuscript. XW, YH, JK, JL, TL, YZ, XL, SW, QZ, and SY collected the animal samples and analyzed the effects of SA by molecular methods in tissues and cells. BH and XZ did animal experiments and recorded the weight and serum glucose.

Funding

This work was supported by the National Natural Science Foundation of China (Nos. 82070833, 82100748, 82100862, and 82000767), Natural Science Foundation of Zhejiang Province (Nos. LZ19H020001, LQ22H050005, and LY22H070001), Zhejiang Medical and Health Science and Technology Project (No. 2022502919).

Conflict of interest

TL was employed by Nanjing Kingmed Center for Clinical Laboratory Co., Ltd.

The remaining authors declare that the research was conducted in the absence of any commercial or financial relationships that could be construed as a potential conflict of interest.

Publisher's note

All claims expressed in this article are solely those of the authors and do not necessarily represent those of their affiliated organizations, or those of the publisher, the editors and the reviewers. Any product that may be evaluated in this article, or claim that may be made by its manufacturer, is not guaranteed or endorsed by the publisher.

References

Abais, J. M., Xia, M., Li, G., Gehr, T. W., Boini, K. M., Li, P. L., et al. (2014). Contribution of endogenously produced reactive oxygen species to the activation of podocyte NLRP3 inflammasomes in hyperhomocysteinemia. *Free Radic. Biol. Med.* 67, 211–220. doi:10.1016/j.freeradbiomed.2013.10.009

Ahmad, I., Li, S., Li, R., Chai, Q., Zhang, L., Wang, B., et al. (2019). The retroviral accessory proteins S2, Nef, and glycoMA use similar mechanisms for antagonizing the host restriction factor SERINC5. *J. Biol. Chem.* 294, 7013–7024. doi:10.1074/jbc.RA119.007662

Alicic, R. Z., Johnson, E. J., and Tuttle, K. R. (2018). Inflammatory mechanisms as new biomarkers and therapeutic targets for diabetic kidney disease. *Adv. Chronic Kidney Dis.* 25, 181–191. doi:10.1053/j.ackd.2017.12.002

Alicic, R. Z., Rooney, M. T., and Tuttle, K. R. (2017). Diabetic kidney disease: Challenges, progress, and possibilities. *Clin. J. Am. Soc. Nephrol.* 12, 2032–2045. doi:10.2215/CJN.11491116

Branstetter, D. G., Stoner, G. D., Budd, C., Conran, P. B., and Goldblatt, P. J. (1989). Relationship between *in utero* development of the mouse liver and tumor development following transplacental exposure to ethylnitrosourea. *Cancer Res.* 49, 3620–3626.

Chu, M. J., Wang, Y. Z., Itagaki, K., Ma, H. X., Xin, P., Zhou, X. G., et al. (2013). Identification of active compounds from Caesalpinia sappan L. extracts suppressing IL-6 production in RAW 264.7 cells by PLS. *J. Ethnopharmacol.* 148, 37–44. doi:10.1016/j.jep.2013.03.050

Guijarro, C., and Egido, J. (2001). Transcription factor-kappa B (NF-kappa B) and renal disease. *Kidney Int.* 59, 415–424. doi:10.1046/j.1523-1755.2001.059002415.x

Kang, L., Zhao, H., Chen, C., Zhang, X., Xu, M., Duan, H., et al. (2016). Sappanone A protects mice against cisplatin-induced kidney injury. *Int. Immunopharmacol.* 38, 246–251. doi:10.1016/j.intimp.2016.05.019

Kanwar, Y. S., Sun, L., Xie, P., Liu, F. Y., and Chen, S. (2011). A glimpse of various pathogenetic mechanisms of diabetic nephropathy. *Annu. Rev. Pathol.* 6, 395–423. doi:10.1146/annurev.pathol.4.110807.092150

Karin, M., and Greten, F. R. (2005). NF-kappaB: Linking inflammation and immunity to cancer development and progression. *Nat. Rev. Immunol.* 5, 749–759. doi:10.1038/nri1703

Kim, Y., and Park, C. W. (2016). Adenosine monophosphate-activated protein kinase in diabetic nephropathy. *Kidney Res. Clin. Pract.* 35, 69–77. doi:10.1016/j.krcp.2016.02.004

Koike, N., Takamura, T., and Kaneko, S. (2007). Induction of reactive oxygen species from isolated rat glomeruli by protein kinase C activation and TNF-alpha

stimulation, and effects of a phosphodiesterase inhibitor. *Life Sci.* 80, 1721–1728. doi:10.1016/j.lfs.2007.02.001

Lee, S., Choi, S. Y., Choo, Y. Y., Kim, O., Tran, P. T., Dao, C. T., et al. (2015). Sappanone A exhibits anti-inflammatory effects *via* modulation of Nrf2 and NF-κB. *Int. Immunopharmacol.* 28, 328–336. doi:10.1016/j.intimp.2015.06.015

Liang, G., Song, L., Chen, Z., Qian, Y., Xie, J., Zhao, L., et al. (2018). Fibroblast growth factor 1 ameliorates diabetic nephropathy by an anti-inflammatory mechanism. *Kidney Int.* 93, 95–109. doi:10.1016/j.kint.2017.05.013

Liao, L. X., Song, X. M., Wang, L. C., Lv, H. N., Chen, J. F., Liu, D., et al. (2017). Highly selective inhibition of IMPDH2 provides the basis of antineuroinflammation therapy. *Proc. Natl. Acad. Sci. U. S. A.* 114, E5986–E5994. doi:10.1073/pnas.1706778114

Lim, A. (2014). Diabetic nephropathy – complications and treatment. *Int. J. Nephrol. Renov. Dis.* 7, 361. doi:10.2147/ijnrd.s40172

Liu, P., Zhang, Z., and Li, Y. (2021). Relevance of the pyroptosis-related inflammasome pathway in the pathogenesis of diabetic kidney disease. *Front. Immunol.* 12, 603416. doi:10.3389/fimmu.2021.603416

Lu, Y., Liu, D., Feng, Q., and Liu, Z. (2020). Diabetic nephropathy: Perspective on extracellular vesicles. *Front. Immunol.* 11, 943. doi:10.3389/fimmu.2020.00943

Navarro-Gonzalez, J. F., Mora-Fernandez, C., Muros de Fuentes, M., and Garcia-Perez, J. (2011). Inflammatory molecules and pathways in the pathogenesis of diabetic nephropathy. *Nat. Rev. Nephrol.* 7, 327–340. doi:10.1038/nrneph.2011.51

Navarro-Gonzalez, J. F., and Mora-Fernandez, C. (2008). The role of inflammatory cytokines in diabetic nephropathy. *J. Am. Soc. Nephrol.* 19, 433–442. doi:10.1681/asn.2007091048

Rayego-Mateos, S., Morgado-Pascual, J. L., Opazo-Rios, L., Guerrero-Hue, M., Garcia-Caballero, C., Vazquez-Carballo, C., et al. (2020). Pathogenic pathways and therapeutic approaches targeting inflammation in diabetic nephropathy. *Int. J. Mol. Sci.* 21, 3798. doi:10.3390/ijms21113798

Sanz, A. B., Sanchez-Nino, M. D., Ramos, A. M., Moreno, J. A., Santamaria, B., Ruiz-Ortega, M., et al. (2010). NF-kappaB in renal inflammation. *J. Am. Soc. Nephrol.* 21, 1254–1262. doi:10.1681/ASN.2010020218

Sassy-Prigent, C., Heudes, D., Mandet, C., Belair, M. F., Michel, O., Perdereau, B., et al. (2000). Early glomerular macrophage recruitment in streptozotocin-induced diabetic rats. *Diabetes* 49, 466–475. doi:10.2337/diabetes.49.3.466

Schena, F. P., and Gesualdo, L. (2005). Pathogenetic mechanisms of diabetic nephropathy. *J. Am. Soc. Nephrol.* 16 (Suppl. 1), S30–S33. doi:10.1681/asn.2004110970

Schlondorff, D., and Banas, B. (2009). The mesangial cell revisited: No cell is an island. *J. Am. Soc. Nephrol.* 20, 1179–1187. doi:10.1681/ASN.2008050549

Shi, X., Li, Y., Wang, Y., Ding, T., Zhang, X., Wu, N., et al. (2021). Pharmacological postconditioning with sappanone A ameliorates myocardial ischemia reperfusion injury and mitochondrial dysfunction *via* AMPK-mediated mitochondrial quality control. *Toxicol. Appl. Pharmacol.* 427, 115668. doi:10.1016/j.taap.2021.115668

Sun, H. J., Xiong, S. P., Cao, X., Cao, L., Zhu, M. Y., Wu, Z. Y., et al. (2021). Polysulfide-mediated sulfhydration of SIRT1 prevents diabetic nephropathy by suppressing phosphorylation and acetylation of p65 NF-κB and STAT3. *Redox Biol.* 38, 101813. doi:10.1016/j.redox.2020.101813

Tang, S. C. W., and Yiu, W. H. (2020). Innate immunity in diabetic kidney disease. *Nat. Rev. Nephrol.* 16, 206–222. doi:10.1038/s41581-019-0234-4

Tuleta, I., and Frangogiannis, N. G. (2021). Diabetic fibrosis. *Biochim. Biophys. Acta. Mol. Basis Dis.* 1867, 166044. doi:10.1016/j.bbadis.2020.166044

Tung, C. W., Hsu, Y. C., Shih, Y. H., Chang, P. J., and Lin, C. L. (2018). Glomerular mesangial cell and podocyte injuries in diabetic nephropathy. *Nephrol. Carlt.* 23 (Suppl. 4), 32–37. doi:10.1111/nep.13451

Wang, M., Chen, Z., Yang, L., and Ding, L. (2021). Sappanone A protects against inflammation, oxidative stress and apoptosis in cerebral ischemia-reperfusion injury by alleviating endoplasmic reticulum stress. *Inflammation* 44, 934–945. doi:10.1007/s10753-020-01388-6

Wei, J., Deng, X., Li, Y., Li, R., Yang, Z., Li, X., et al. (2021). PP2 ameliorates renal fibrosis by regulating the NF-κB/COX-2 and PPARγ/UCP2 pathway in diabetic mice. *Oxid. Med. Cell. Longev.* 2021, 7394344. doi:10.1155/2021/7394344

Wu, J., Lu, K., Zhu, M., Xie, X., Ding, Y., Shao, X., et al. (2020). miR-485 suppresses inflammation and proliferation of mesangial cells in an *in vitro* model of diabetic nephropathy by targeting NOX5. *Biochem. Biophys. Res. Commun.* 521, 984–990. doi:10.1016/j.bbrc.2019.11.020

Yang, H., Xie, T., Li, D., Du, X., Wang, T., Li, C., et al. (2019). Tim-3 aggravates podocyte injury in diabetic nephropathy by promoting macrophage activation *via* the NF-κB/TNF-α pathway. *Mol. Metab.* 23, 24–36. doi:10.1016/j.molmet.2019.02.007

Zhao, L., Zou, Y., and Liu, F. (2020). Transforming growth factor-beta1 in diabetic kidney disease. *Front. Cell Dev. Biol.* 8, 187. doi:10.3389/fcell.2020.00187

Zheng, C., Huang, L., Luo, W., Yu, W., Hu, X., Guan, X., et al. (2019). Inhibition of STAT3 in tubular epithelial cells prevents kidney fibrosis and nephropathy in STZ-induced diabetic mice. *Cell Death Dis.* 10, 848. doi:10.1038/s41419-019-2085-0

Zhou, D., Zhou, M., Wang, Z., Fu, Y., Jia, M., Wang, X., et al. (2019). PGRN acts as a novel regulator of mitochondrial homeostasis by facilitating mitophagy and mitochondrial biogenesis to prevent podocyte injury in diabetic nephropathy. *Cell Death Dis.* 10, 524. doi:10.1038/s41419-019-1754-3

frontiers | Frontiers in Pharmacology

TYPE Original Research
PUBLISHED 06 September 2022
DOI 10.3389/fphar.2022.966645

OPEN ACCESS

EDITED BY
Swayam Prakash Srivastava,
Yale University, United States

REVIEWED BY
Quan Hong,
Chinese PLA General Hospital, China
Aditya Yashwant Sarode,
Columbia University, United States

*CORRESPONDENCE
Xiang-ming Qi,
qxm119@126.com
Yong-gui Wu,
wuyonggui@medmail.com.cn

SPECIALTY SECTION
This article was submitted to Renal Pharmacology,
a section of the journal
Frontiers in Pharmacology

RECEIVED 11 June 2022
ACCEPTED 25 July 2022
PUBLISHED 06 September 2022

CITATION
Wang X, Liu X-q, Jiang L, Huang Y-b, Zeng H-x, Zhu Q-j, Qi X-m and Wu Y-g (2022), Paeoniflorin directly binds to TNFR1 to regulate podocyte necroptosis in diabetic kidney disease. *Front. Pharmacol.* 13:966645. doi: 10.3389/fphar.2022.966645

Paeoniflorin directly binds to TNFR1 to regulate podocyte necroptosis in diabetic kidney disease

Xian Wang[1], Xue-qi Liu[1], Ling Jiang[1], Yue-bo Huang[1], Han-xu Zeng[1], Qi-jin Zhu[1], Xiang-ming Qi[1*†] and Yong-gui Wu[1,2*]

[1]Department of Nephropathy, The First Affiliated Hospital of Anhui Medical University, Hefei, China, [2]Center for Scientific Research of Anhui Medical University, Hefei, China

Necroptosis was elevated in both tubulointerstitial and glomerular renal tissue in patients with diabetic kidney disease (DKD), and was most pronounced on glomerulus in the stage with macroalbuminuria. This study further explored whether paeoniflorin (PF) could affect podocyte necroptosis to protect kidney injure *in vivo* and *in vitro*. Our study firstly verified that there are obvious necroptosis-related changes in the glomeruli of DKD through bioinformatics analysis combined with clinicopathological data. STZ-induced mouse diabetes model and high-glucose induced podocyte injury model were used to evaluate the renoprotection, podocyte injury protection and necroptosis regulation of PF in DKD. Subsequently, the target protein-TNFR1 that PF acted on podocytes was found by computer target prediction, and then molecular docking and Surface plasmon resonance (SPR) experiments were performed to verify that PF had the ability to directly bind to TNFR1 protein. Finally, knockdown of TNFR1 on podocytes *in vitro* verified that PF mainly regulated the programmed necrosis of podocytes induced by high glucose through TNFR1. In conclusion, PF can directly bind and promote the degradation of TNFR1 in podocytes and then regulate the RIPK1/RIPK3 signaling pathway to affect necroptosis, thus preventing podocyte injury in DKD. Thus, TNFR1 may be used as a new potential target to treat DKD.

KEYWORDS

paeoniflorin, tumor necrosis factor receptor 1, podocyte, necroptosis, diabetic kidney disease

1 Introduction

Diabetic kidney disease (DKD) has been the major cause of chronic kidney disease replacing chronic glomerulonephritis in Chinese inpatients (Zhang et al., 2016). An early manifestation of DKD includes microalbuminuria, which is closely related to the damage to the glomerular filtration barrier (GFB). Moreover, to podocytes injury (loss of functions and reduced number), as a key component of GFB, is considered a major contributor to

DKD (Zhang et al., 2020). Therefore, studying the mechanism of podocyte injury may provide a basis for targeted prevention and treatment of DKD.

Transdifferentiation and death were the ultimate outcome of cell damage. Epithelial-mesenchymal transition (EMT) and endothelial-mesenchymal transition (endMT) involve in the renal fibrosis process of DKD (Zeisberg et al., 2003; Zeisberg et al., 2008; Zeng et al., 2019; Chen et al., 2022). Interestingly, markers of mesenchymal cells were also found on podocytes in DKD, suggesting that podocytes also exhibit EMT (Li et al., 2008), which may be regulated by multiple signaling pathways, including TGF-β (Yin et al., 2018), Wnt/β-catenin (Kato et al., 2011), mTOR (Tao et al., 2021), Notch (Nishad et al., 2020), Hedgehog (Lan et al., 2017), SIRT/NF-κB (Wang et al., 2019), DPP-4 (Chang et al., 2017) and non-coding RNA network (Ling et al., 2018). Additionally, the forms of programmed cell death include apoptosis, pyroptosis, necroptosis, and ferroptosis. Apoptosis is regulated by the Bcl-2 or caspase family. Pyroptosis is Gasdermin-dependent cell death. Ferroptosis is iron-dependent and peroxidative-driven, and necroptosis is associated with membrane rupture by p-MLKL. The above forms of cell death have been reported in podocyte injury in DKD (Zhang et al., 2021; Zhu et al., 2021), while unfortunately, the research of necroptosis on podocytes in DKD is still limited to *in vitro* cells (Chung et al., 2022). Our lab recently discovered the activation of necroptosis in DKD tissues glomeruli. Therefore, antagonizing necroptosis may be a therapeutic target for DKD.

In recent years, based on the mechanism research of DKD, some potential drugs have been developed, including glucose cotransporter 2 (SGLT2) inhibitors (Tomita et al., 2020), glucagon-like peptide-1 (GLP-1) inhibitors (Moellmann et al., 2018), dipeptidyl peptidase-4 (DPP-4) inhibitors (Peng et al., 2019), protein kinase C (PKC) inhibitors (Koya et al., 2000), advanced glycation end product (AGE) inhibitors (Sugimoto et al., 2007), aldosterone receptor inhibitors (De Zeeuw et al., 2010), endothelin receptor (ETR) inhibitors (De Zeeuw et al., 2014), transforming growth factor-β (TGF-β) inhibitors (Benigni et al., 2003), Rho kinase (ROCK) inhibitors (Komers et al., 2011) and N-acetyl-seryl-aspartyl-lysyl-proline (AcSDKP) (Srivastava et al., 2020; Wang et al., 2021). However, the clinical application of these drugs in DKD still has a long way to go.

Chinese herbal medicines have been used to treat diseases in China for more than a thousand years, and the efficacy and safety of most of them have been clinically proven. Paeoniflorin (PF), as an active monomer extracted from Paeonia lactiflora, have been reported a protective effect on various organ damage caused by different diseases (Zhang and Wei, 2020). Our previous study found that PF can improve kidney injury in DKD mice model (Zhang et al., 2017). In this study, we further explored whether PF can affect the necroptosis of podocytes and protect their injury in DKD mice.

2 Materials and methods

2.1 Data collection and analysis

This study extracted the specific data information of necroptosis-related genes from three groups of samples found in the GSE142025 dataset (GPL 20301) (Fan et al., 2019) from NCBI-GEO (http://www.ncbi.nlm.nih.gov/geo/), including NC group (n = 9), DKD1 group (albumin to creatinine ratio, ACR 30–300 mg/g, eGFR>90 ml/min·1.73 m^2, n = 6), and DKD2 group (ACR>300 mg/g, eGFR<90 ml/min·1.73 m^2, n = 21; one sample in the DKD2 group was missing). The necroptosis-related genes were queried from AmiGO 2 (http://amigo.geneontology.org/amigo/).

2.2 Patients and specimens

Percutaneous kidney biopsy samples were obtained from patients with DKD between January 2019 and December 2021. The inclusion criteria were: 1) age ≥18 years; 2) diagnosed with diabetes as previous (American Diabetes, 2013); 3) urinary ACR >30 mg/g; 4) diagnosis of DKD by renal biopsy as previous (Tervaert et al., 2010); The exclusion criteria included infection, cancer, autoimmune disease, and severe heart failure of other organs (including heart, liver, respiratory). Additionally, the unaffected portion of tumor nephrectomies were obtained to be as the samples of NC group without diabetes (urinary ACR<30 mg/g).

The study was reviewed and approved by the institutional review board of the First Affiliated Hospital of Anhui Medical University (approval no.: 20,190,454). The participants provided their written informed consent to participate in this study.

2.3 Chemicals and reagents

PF (CAS No: 23,180-57-6, purity = 98.04%), necrostatin-1 (Nec-1, CAS No: 4,311-88-0, purity = 99.82%), and MG132 (CAS No.: 133,407-82-6, purity≥98.0%) were purchased from Macklin Biochemical Co., Ltd. (Shanghai, China). D-glucose, streptozotocin (STZ), and D-mannitol were acquired from Sigma-Aldrich (MO, United States). Anti-RIPK1 (receptor-interacting serine-threonine kinase 1), anti-RIPK3 (receptor-interacting serine-threonine kinase 3), anti-WT-1 (wilms Tumor 1 protein), anti-TNFR1, anti-ubiquitin, anti-β-actin and secondary antibodies were from Proteintech Group, Inc. (Hubei, China). TNFR1 protein was obtained from Abcam (Cambridge, United Kingdom). Anti-SYNPO (synaptopodin) antibody was acquired from Santa Cruz (Santa Cruz Biotechnology. United States). Anti-p-MLKL (phosphorylated mixed-lineage kinase domain-like protein) was obtained from Affinity. Additionally, an immunohistochemistry

kit (PV-9000) and Mayer (ZLI-9620) were acquired from Beijing Zhongshan Biotechnology Inc. (Beijing, China). Periodic acid–Schiff (PAS) kits were purchased from Jiancheng Biotechnology Institute (Nanjing, China).

2.4 Animal model and experimental design

We observed the effect of the whole course or preventive treatment of PF treatment in mice models. Wild-type (WT) C57BL/6J mice (male, 6–8 W, 16–20 g) were obtained from the Animal Department of Anhui Medical University (Hefei, Anhui Province, China). STZ (50 mg/kg/mice) intraperitoneal injection was used to establish a diabetic mouse model (Liu et al., 2022).

Mouse were divided into 6 groups (n = 6/group): normal control (NC) group, NC + PF group (200 mg/kg·d), DKD group, and DKD + PF group (50/100/200 mg/kg·d). The treatment groups were intraperitoneally injected with PF daily, and the non-treatment groups received a 0.9% sodium chloride solution. The treatment lasted for 12 weeks. A preliminary experiment showed that DKD was significantly improved by the administration of PF100 mg/kg·d. Therefore, two additional groups were established: NC + PF100 mg/kg·d and DKD + PF100 mg/kg·d, in which the treatment was given for 6 weeks and then discontinued for the following 6 weeks after the successful production of the diabetes mice model.

Metabolic cages (Hatteras Instruments, Hatteras, NC) were used to collect animal's urine. All animals were raised under standard conditions, and the experiment protocol has been approved by the Ethics Committee of the Animal Research of Anhui Medical University (approval no.: LLSC 20190,519).

2.5 Physical and biochemical analyses

Before the mice were sacrificed, mice's tail vein blood was collected and used to detect fasting blood sugar (FBS). Mice were then weighed and the blood by retro-orbital bleeding was collected under anesthesia. Mice were then euthanized, and the kidneys of the mouse were removed. A mouse albumin ELISA kit (ab108792) (Abcam, Cambridge, United Kingdom) was used to detect 24 h urinary albumin excretion rate (24 h UAER). Orbital blood was used to measure the levels of blood urea nitrogen (BUN), serum creatinine (Scr), and serum alanine transaminase (ALT) according to the kit instructions, respectively (Nanjing Jiancheng Bioengineering Institute, Nanjing, China).

2.6 Kidney histological examination

Kidney tissues were routinely dehydrated, embedded in paraffin, and then cut into 2 μm-thick sections. Periodic Acid-Schiff stain (PAS) stained the tissue sections as previously described (Zhong et al., 2019).

2.7 Transmission electron microscopy

The changes of the basement membrane and foot process were observed under an electron microscope after routine embedding and sectioning of renal tissue, as previously described (Zhong et al., 2019). In addition, the organelles and membranes of podocytes cultured *in vitro* were observed by electron microscope (Huang et al., 2020).

2.8 Molecular docking

The PubChem database (https://pubchem.ncbi.nlm.nih.gov/) was used to acquire the docked compound PF, which was imported into Schrodinger software to hydrogenate, structure optimize, and minimize energy. Afterward, the adjusted molecular structures were saved as ligand molecules for molecular docking. TNF (PDB ID: 7KPA) and TNFRSF1A (tumor necrosis factor receptor superfamily, member 1, APDB ID: 1EXT) protein structures were obtained by homology modeling (Swiss-Model) from the website (https://swissmodel.expasy.org/). All protein structures were processed on Schrodinger's Protein Preparation Wizard platform, including removal of water and ions, protonation, the addition of missing atoms and completion of missing groups, and protein energy minimization. The processing and optimization of small molecules and proteins were performed by the Glide module and Protein Preparation Wizard in the Schrödinger Maestro software, respectively. Receptors were constrained minimized through the OPLS3e force field. We used the interaction interface of TNF with TNFRSF1A to determine the active site of the two docking proteins. By analyzing the action mode of compounds and proteins, the interaction between compounds and target protein residues was obtained, including hydrophobic interaction, hydrogen bonding and π-π interaction, to evaluate the molecular binding activity of compounds.

2.9 Surface plasmon resonance

SPR was used to observe the real-time interaction between PF and TNFR1 using a Biacore T200 (GE, United States). All reagents used in the experiment were prepared according to the instructions. TNFR1 protein was purchased from Macklin Biochemical Co., Ltd. (Shanghai, China) at 10 μg/ml was dialyzed on a Series S Sensor Chip CM5 (10 min activation with 0.5 M EDC/0.25 M NHS in 0.1 M MES, pH 5.5) to obtain

an immobilization signal of 16,131.9 RU. The experimental results were calculated for the equilibrium binding and disassociation constants.

2.10 Mouse podocyte clone 5 culture

MPC5 cells were purchased from the Cell Bank of the Chinese Academy of Sciences (Shanghai, China), differentiated in the environment as previously reported (Zhong et al., 2019), and then cultured in DMEM (5.5 mmol/L glucose, HyClone, United States) containing 10% fetal bovine serum (Gibco, San Diego, CA, United States). Cells were then divided into 8 groups: NC group (5.5 mmol/L glucose), M group (mannitol, 34.5 mmol/L mannitol +5.5 mmol/L glucose), NC+PF (160 μmol/L), HG (high glucose, 40 mmol/L), and HG+PF (40/80/160 μmol/L) containing 1% fetal bovine serum for 48 h. Additionally, another group was treated with HG+PF 80 μmol/L for 24 h and then without PF for 24 h to verify the effect of PF preventive treatment *in vitro*. Moreover, additional cell models were established to observe the effect of PF on podocyte necroptosis *in vitro*, including NC group (5.5 mmol/L glucose), NC + Nec-1 group (5.5 mmol/L glucose +3 μmol/L Nec-1), HG group (high glucose, 40 mmol/L glucose), HG + PF group (80 μmol/L PF), HG + Nec-1 group (3 μmol/L Nec-1), and HG+PF + Nec-1 group.

2.11 Determination of cell vitality

The vitality of MPC5 was determined using MTT (thiazole blue colorimetry) assay. Briefly, MPC5 were treated with HG and/or PF for 48 h, followed by 20 μL of sterile MTT dye (5 mg/ml) for another 4 h. The optical density (OD) at 550 nm wavelength was measured by a microplate reader (Multiskan MK3; Thermo Scientific, Waltham, MA, United States).

2.12 Western blot

The protein was extracted using RIPA buffer (Beyotime, Shanghai, China) to quantify the concentrations using the BCA Kit (Beyotime, Jiangsu, China). Podocyte-rich kidney tissues were isolated as previously described (Wei et al., 2020). The total protein from each sample (20 μg) was loaded, electrophoresed, and then transferred to nitrocellulose membranes (Invitrogen, United States). Samples were then incubated with the corresponding primary antibody: anti-WT-1 (1:1,000, 12609-1-AP), anti-SYNPO (1:1,000, sc-515842), anti-RIPK1 (1:1,000, 17519-1-AP), anti-RIPK3 (1:1,000, 17563-1-AP), anti-p-MLKL (1:1,000, AF7420), TNFR1 (1:1,000, 21574-1-AP), anti-ubiquitin (1:1,000, 10201-2-AP), anti-β-actin (1:10000, 66009-1-Ig), for at least 12 h followed by sealing with blocking buffer (EpiZyme, Shanghai, China) for 10 min, and the secondary antibody (1:10,000, anti-mouse: SA00001-1 or anti-rabbit: SA00001-2) for 1h. The images of the band were developed using SuperSignalTM West Femto Maximum Sensitivity Substrate Kit (thermos scientific, United States) and Amersham Imager 600 (GE, United States), and then analyzed using ImageJ software.

2.13 Ribonucleic acid isolation and real-time polymerase chain reaction

Total RNA extraction of MPC5 and kidney tissues was performed using TRIZOL lysis buffer (Invitrogen, Carlsbad, CA, United States). The concentration and purity were then measured, after which the RNA was reverse transcribed into cDNAs which were amplified by using SYBR Green ER qPCR Supermix (Thermo Fisher Scientific, Waltham, MA) on a T100 thermal cycler (Bio-Rad, Hercules, CA, United States). All primers were shown in Table 1. The target mRNAs were calculated as previously reported (Zhong et al., 2019).

2.14 Co-immunoprecipitation assay

MPC5 cells were divided into 4 groups: HG group (40 mmol/L glucose), HG + MG132 group (4 μmol/L MG132), HG + PF group (80 μmol/l PF), and HG + PF + MG132 group. All MPC5 cells were cultured for 36 h in a regular incubator. After being extracted from MPC5 cells, the total protein was incubated with 15 μL of protein A/G magnetic beads (MedChenExpress, Shanghai, China) overnight at 4°C. Next, the compound was mixed with a TNFR1 antibody (10 μL/tube, 21574-1-AP) at 4°C for 12 h, cleaned by RIPA buffer and boiled at 100°C for 5 min. Finally, the levels of TNFR1 and ubiquitin of the samples were detected using WB.

2.15 Cell transfection

After planted in the 6-well plate, MPC5 cells were transfected with TNFR1 siRNA (Hanbio, Shanghai, China) using a LipofectamineTM 2000 reagent (Invitrogen, Carlsbad, CA, United States) at 37°C for 6 h according to the manufacturer's instructions. Subsequently, the effect of siRNAs was measured by real-time PCR and WB.

2.16 Immunohistochemistry assay

After routine deparaffinization, paraffin sections were heated in a pressure pot for 2 min to retrieve the antigens, incubated with the primary antibody: anti-WT-1 (1:500, 12609-1-AP), anti-SYNPO (1:500, sc-515842), anti-p-MLKL (1:300, AF7420),

TABLE 1 Sequences of the primers.

Genes	Forward (5–3′)	Reverse (5–3′)
Mouse TNFR1	GTGTGGCTGTAAGGAGAACCAG	CACACGGTGTTCTGAGTCTCCT
Mouse TNF-α	GGTGCCTATGTCTCAGCCTCTT	GCCATAGAACTGATGAGAGGGAG
Mouse IL-1β	TGGACCTTCCAGGATGAGGACA	GTTCATCTCGGAGCCTGTAGTG
Mouse β-actin	CATTGCTGACAGGATGCAGAAGG	TGCTGGAAGGTGGACAGTGAGG

TNFR1 (1:300, 21574-1-AP), at 4°C overnight and the secondary antibody at 37°C for 1 h, successively. ImageJ was used to analyze the intensity of DAB staining.

2.17 Immunofluorescence assay

After blocking the non-special antigens with 10% goat serum, the renal tissue sections and cell slides were incubated with the primary antibody with the same concentration in the IHC experiments, and with the fluorescent secondary antibody (1:200, SA00013-1 and SA00013-4) at 37°C for 40 min, finally stained with DAPI (G1012, Servicebio). The images were taken using a fluorescence microscope (Zeiss Spot; Carl Zeiss Ltd., Canada).

2.18 Statistical analysis

R3.6.3 (https://www.r-project.org/) was used for the visualization of the dataset. PASS 15.0 was used to calculate the sample size of clinical trials. SPSS 22.0 was used for data analysis. Mann-Whitney *U*-test was used to calculate the statistical significance of non-normally distributed data. The statistical significance of normally distributed data among groups was calculated by independent samples *t*-test and one-way analysis of variance (ANOVA). Linear correlation analysis was performed using Spearman's test. A $p < 0.05$ was considered to be statistically significant. Data were calculated as the mean ± SD. A *p*-value < 0.05 among groups was identified, followed by mapping with GraphPad Prism 9.3 software (GraphPad Software Inc., San Diego, CA, United States).

3 Results

3.1 The changes of necroptosis in diabetic kidney disease

3.1.1 Different necroptosis-related genes are seen in human kidney tissue with diabetic kidney disease

A total of 17, 155, 27 genes were identified in the dataset. Principal component analysis (PCA) indicated that three groups of samples together were clustering (Supplementary Figure S1). A total of 31 genes related to necroptosis were found in AmiGO 2 (Supplementary Table S1). *Ripk 1*, *ripk 3*, and *mlkl* mRNA, as the key factors in the process of cell necroptosis, showed statistically significant changes and were especially increased in the DKD2 group (Figure 1A).

3.1.2 Different necroptosis-related proteins are seen in human kidney tissue with diabetic kidney disease

The final calculated sample size was n = 3/group, based on the pre-experimental results of IHC staining for p-MLKL staining on glomeruli, the sample ratio (1:1:1), and the dropout rate (20%). The patients' characteristics, which are described in Table 2, revealed no significant differences in age and gender among groups, while SBP and DBP in DKD2 group were higher than in NC and DKD1 group.

The expressions of p-MLKL protein were used as a marker for observing the changes of necroptosis in Human kidney biopsy tissue samples. Because albuminuria in DKD is mainly associated with glomerular damage, this study mainly measured necroptosis-related proteins in the glomeruli. The results of IHC staining indicated that p-MLKL protein was expressed in glomeruli and part of renal tubules, especially in the DKD2 group (Figure 1B and Table 2). Interestingly, the results of double immunofluorescence staining indicated that SYNPO, as a podocyte marker, partially overlapped with p-MLKL protein expression (Figure 1C).

3.1.3 Preliminary exploration of the clinical significance of programmed necrosis in diabetic kidney disease development

In this part of the study, we first briefly compared the clinicopathological data of the two groups of patients in the DKD group. The results indicated significant differences in CHO, LDL, ALB, ApoB, glomerular lesions, IFTA, and interstitial inflammation compared to DKD1 with DKD2 groups (Table 3). The results of correlation analysis between p-MLKL protein and clinicopathological difference indicators indicated that p-MLKL was positively correlated with SBP, CHO, LDL, ApoB, and IFTA, while negatively correlated with ALB (Table 4).

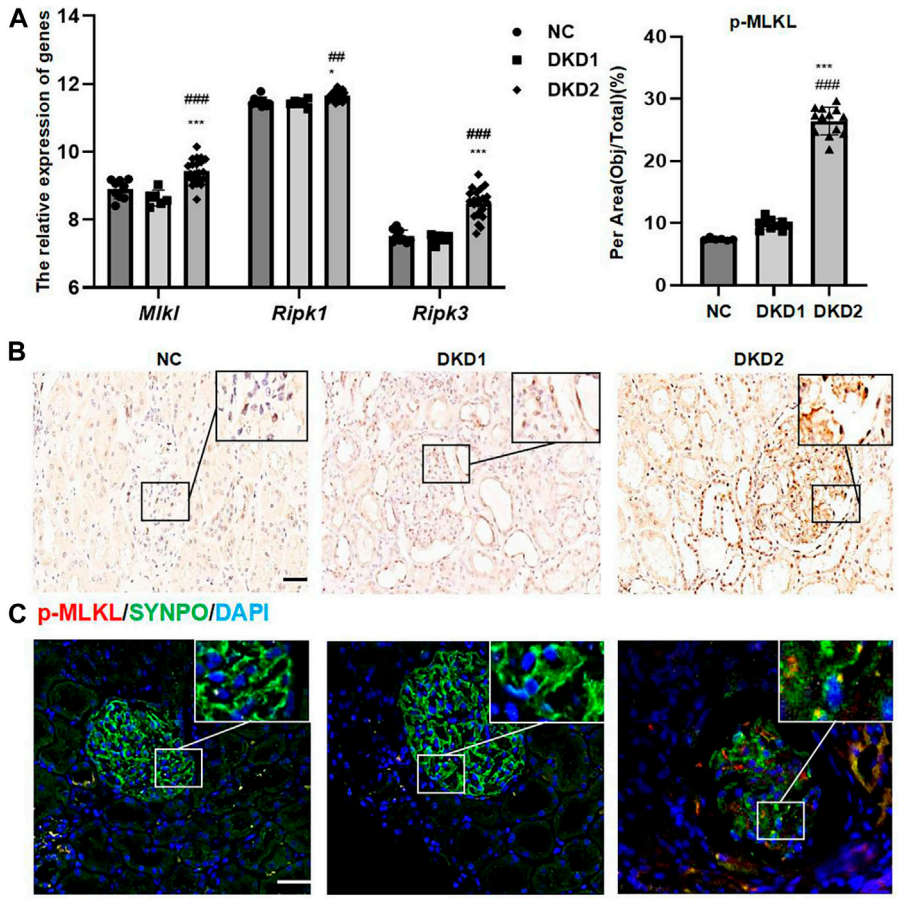

FIGURE 1
Necroptosis-related proteins changed in human kidney tissue with DKD. **(A)** The relative expression of necroptosis-related genes in GSE 142025. **(B)** IHC assay of p-MLKL protein expression in the glomerulus of human renal biopsy tissues. Scale bar = 20 μm. **(C)** IF double staining for p-MLKL and SYNPO in human renal biopsy tissues. Scale bar = 20 μm. Results represent the mean ± SD. $^{*}p < 0.05$, $^{***}p < 0.001$ vs. NC; $^{\#\#}p < 0.01$, $^{\#\#\#}p < 0.001$ vs. DKD1. NC, normal control; DKD, diabetic kidney disease; IHC, immunohistochemistry; IF, immunofluorescence.

TABLE 2 The general characters of all patients.

Parameters	NC(n = 6)	DKD		p-value
		DKD1 (n = 10)	DKD2 (n = 13)	
Age (y)	51.50 (48.25, 54.75)	50.50 (32.75, 52.75)	48.00 (37.00, 53.00)	0.457
Gender (M/F)	4/2	6/4	10/3	0.688
SBP (mmHg)	117.50 ± 5.05	128.30 ± 30.53	149.69 ± 21.79***	0.001
DBP (mmHg)	70.00 ± 5.48	81.00 ± 10.80	93.31 ± 14.10**#	0.001
U-ACR (mg/gcr)	18.96 ± 5.75	85.06 ± 72.75&	3,324.77 ± 2031.77***	0.000
p-MLKL	7.44 ± 0.21	9.85 ± 0.88	26.44 ± 2.24***###	0.000

NC, vs. DKD1 &p< 0.05, NC, vs. DKD2**p< 0.01,***p< 0.001; DKD1 vs. DKD2 #p< 0.05,###p< 0.001; M, male; F, female; SBP, systolic blood pressure; DBP, diastolic blood pressure; U-ACR, urine albumin creatinine ratio; p-MLKL, phosphorylated mixed-lineage kinase domain-like protein.

TABLE 3 The clinical and pathological characters of DKD patients.

Parameters	DKD1 (n = 10)	DKD2 (n = 13)	t (Z)	p-value
DM duration (M)	74.60 ± 64.19	107.69 ± 74.73	1.117	0.276
Scr (μmol/L)	102.95 (49.55, 131.13)	118.40 (93.40,150.40)	(0.806)	0.420
BUN (mmol/L)	8.12 ± 2.01	8.83 ± 3.48	0.575	0.572
UA (μmol/L)	306.10 ± 76.38	352.92 ± 101.82	1.213	0.239
eGFR [ml/min·1.73 m^2]	85.30 ± 36.15	70.77 ± 33.90	0.990	0.333
FBS (mmol/L)	5.54 (4.03, 6.25)	6.84 (5.34, 8.90)	(1.210)	0.226
HbAc1 (%)	7.10 (6.58, 7.70)	7.60 (6.10.8.00)	(0.279)	0.780
CHO (mmol/L)	4.31 ± 1.32	5.92 ± 1.08	3.221	0.004
TG (mmol/L)	1.95 (1.20.2.27)	1.50 (1.37.2.30)	(0.620)	0.535
LDL (mmol/L)	2.46 ± 1.27	3.88 ± 0.85	3.201	0.004
VLDL (mmol/L)	0.72 (0.45.0.84)	0.56 (0.51.0.85)	(0.559)	0.576
HDL (mmol/L)	1.03 ± 0.36	1.24 ± 0.27	1.616	0.121
ALB (g/L)	41.66 ± 2.30	30.68 ± 6.86	-5.393	0.000
ApoA1 (mmol/L)	1.14 (1.01.1.22)	1.30 (1.15.1.40)	(1.850)	0.064
ApoB (mmol/L)	0.86 ± 0.27	1.18 ± 0.28	2.702	0.014
ApoB/ApoA1	0.77 ± 0.24	0.95 ± 0.30	1.440	0.166
Lipoprotein α(mmol/L)	111.00 (46.00,253.00)	328.50 (166.25,626.75)	(1.845)	0.065
Glomerular lesions [n (%)]			(3.052)	0.002
I	0 (0)	0 (0)		
II				
IIa	6 (60.00%)	1 (7.69%)		
IIb	3 (30.00%)	3 (23.08%)		
III	1 (10.00%)	9 (69.23%)		
IV	0	0		
IFTA (0/1/2/3)	3/4/3/0	0/2/9/2	(2.810)	0.005
Interstitial inflammation (0/1/2)	4/6/0	1/7/5	(2.276)	0.023
Arteriolar hyalinosis (0/1/2)	1/6/3	1/4/8	(1.344)	0.179
Arteriosclerosis (0/1/2)	0/8/2	1/7/5	(0.595)	0.552

DM, diabetic metabolism; M, month; NC, normal control; Scr, serum creatinine; BUN, blood urea nitrogen; UA, uric acid; eGFR, estimate glomerular filtration rate; FBS, fasting blood sugar; CHO, cholesterol; TG, triglycerides; LDL, low-density lipoprotein; VLDL, very-low-density lipoprotein; HDL, high-density lipoprotein; ALB, albumin; ApoB, apolipoprotein B; ApoA1, apolipoprotein A1; IFTA, interstitial fibrosis and tubular atrophy.

3.2 Paeoniflorin improves kidney injury caused by diabetic kidney disease *in vitro* and *in vivo*

3.2.1 Paeoniflorin shows renoprotection in streptozotocin-induced diabetic mice

The molecular structure of PF is shown in Figure 2A. We first observed the renoprotective effect of PF in mouse models of DKD (Figure 2B). The results of physiological and biochemical indicators showed that compared with the NC group, DKD group exhibited significantly higher levels of FBG, 24 UAER, and inflammatory markers of renal tissue, including TNF-a and IL-1β mRNA. Compared to the DKD group, 24 UAER and inflammatory markers of renal tissue were all decreased in a dose-dependent manner in PF groups (Figures 2C–F). There was no significant difference in Scr, BUN, ALB, ALT, and kidney/body ratio among groups (Supplementary Figures 2A–E).

TABLE 4 Correlation between p-MLKL in renal tissue and clinical differential indicators.

Parameter	Correlation coefficient (r)	P
SBP	0.453	0.031
DBP	0.362	0.362
CHO	0.475	0.022
LDL	0.437	0.038
ALB	−0.749	0.000
ApoB	0.472	0.031
Glomerular lesions	0.408	0.054
IFTA	0.483	0.020
Interstitial inflammation	0.358	0.094

SBP, systolic blood pressure; DBP, diastolic blood pressure; CHO, cholesterol; LDL, low-density lipoprotein; ALB, albumin; ApoB, apolipoprotein B; IFTA, interstitial fibrosis and tubular atrophy.

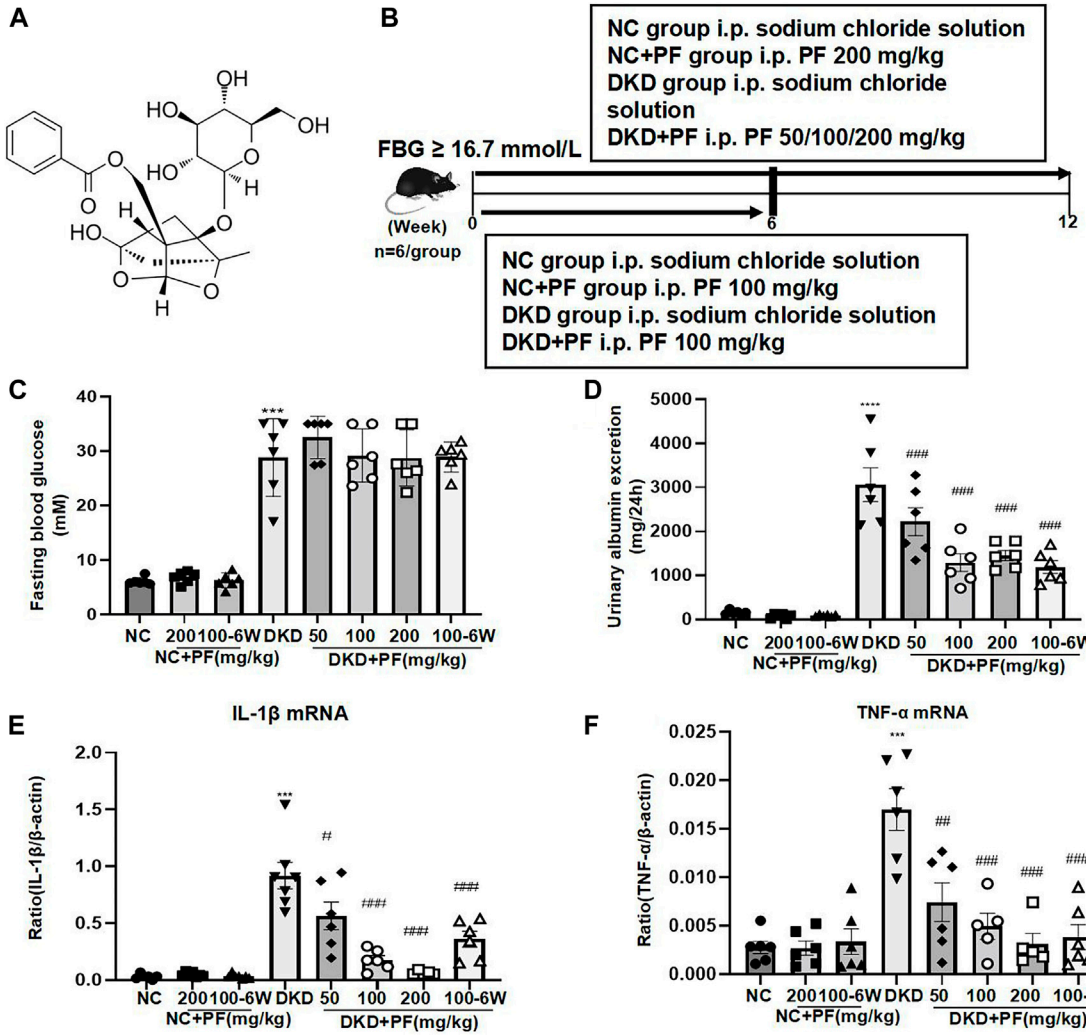

FIGURE 2
Serum and urine biochemical parameters of STZ-induced diabetic mice. **(A)** Molecular structure of PF. **(B)** Study design of the animal experiment and treatment. **(C)** Fasting blood glucose in different groups. **(D)** A 24 h urine albumin excretion in different groups. **(E)** IL-1β mRNA in different groups. **(F)** TNF-α mRNA in different groups. Results represent the mean ± SD for 6 mouse/group. $^{***}p < 0.001$ vs. NC; $^{\#}p < 0.05$, $^{\#\#}p < 0.01$, $^{\#\#\#}p < 0.001$ vs. DKD. FBG, fasting blood glucose; NC, normal control; DKD, diabetic kidney disease; PF, paeoniflorin; STZ, streptozotocin; TNF-α, tumor necrosis factor-α.

Observation of pathological kidney morphology further showed that compared with NC group, the glomerular volume enlarged, the mesangial area widened, foot process width increased and glomerular basement membrane (GBM) thickened in STZ-induced mouse DKD model, those were significantly alleviated after PF treatment (Figure 3). Interestingly, PF improved biochemical and pathological changes in DKD mice in a dose-dependent manner. In STZ-induced diabetic mouse model, PF showed renal protection after only 6 weeks of administration.

3.2.2 PF ameliorates podocyte injury in diabetic kidney disease

3.2.2.1 Paeoniflorin ameliorates podocyte injury in streptozotocin-induced diabetic mice

We examined the protective effect of PF against podocyte injury, a key factor in the pathogenesis of albuminuria during DKD. The results of TEM detection showed that PF could significantly restore the fused foot processes of DKD mice (Figure 3B). Furthermore, the podocyte marker (WT-1) and the podocyte functional protein (SYNPO) were observed by IHC staining and WB. The results showed that the number

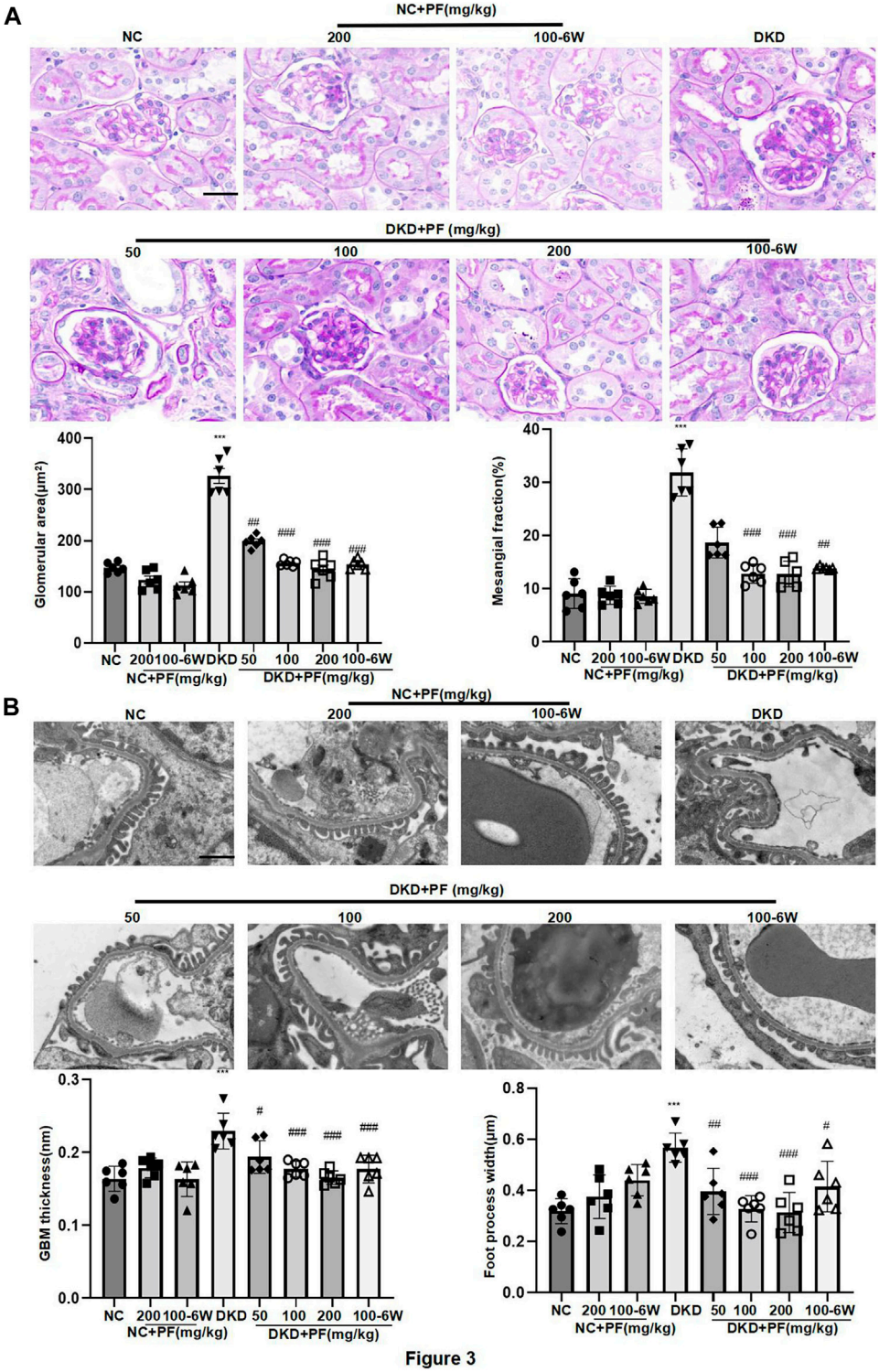

FIGURE 3
Morphological changes of STZ-induced diabetic mice. **(A)** Histopathological examinations of renal tissue sections stained with PAS from different groups, Scale bar = 50 μm. **(B)** Images of podocyte foot processes and glomerular basement membrane observed by TEM, Scale bar = 1 μm. Results represent the mean ± SD for 6 mouse/group. $^{*}p < 0.05$, $^{***}p < 0.001$ vs. NC; $^{\#\#}p < 0.01$, $^{\#\#\#}p < 0.001$ vs. DKD. NC, normal control; PF, paeoniflorin; STZ, streptozotocin; PAS, periodic acid–Schiff; TEM, transmission electron microscopy.

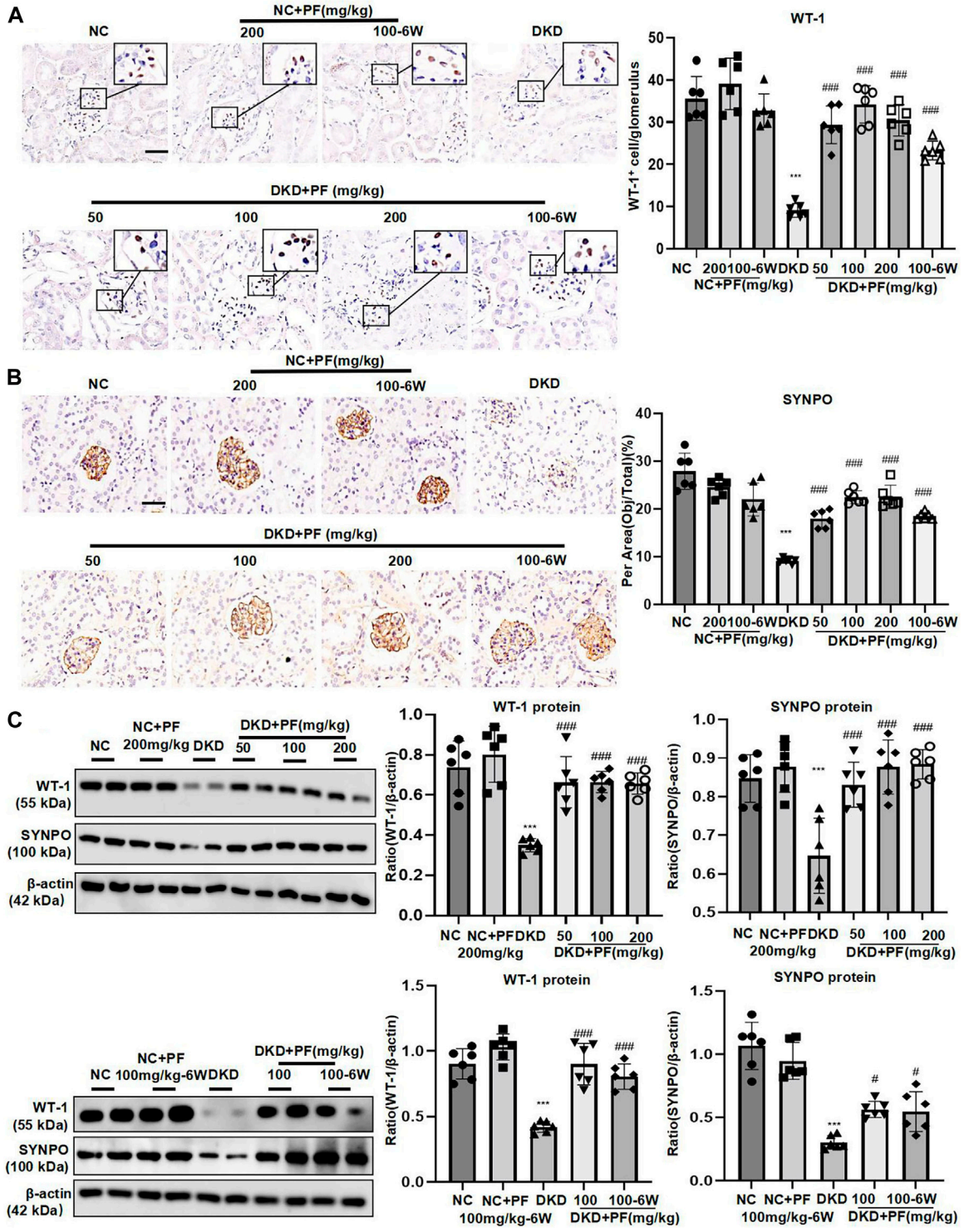

FIGURE 4
PF ameliorates podocyte injury in STZ-induced diabetic mice. **(A)** IHC assay of WT-1 protein expression in the glomerulus. Scale bar = 50 μm. **(B)** IHC assay of SYNPO protein expression in the glomerulus. Scale bar = 50 μm. **(C)** WB assay of WT-1 and SYNPO protein expression in the glomerulus. Data represent the mean ± SD for 6 mouse/group. ***$p < 0.001$ vs. NC; $^{\#}p < 0.05$, $^{\#\#\#}p < 0.001$ vs. DKD. NC, normal control; PF, paeoniflorin; STZ, streptozotocin; DKD, diabetic kidney disease; WT-1, Wilms tumor 1 protein; SYNPO, synaptopodin; IHC, immunohistochemistry; WB, Western blotting.

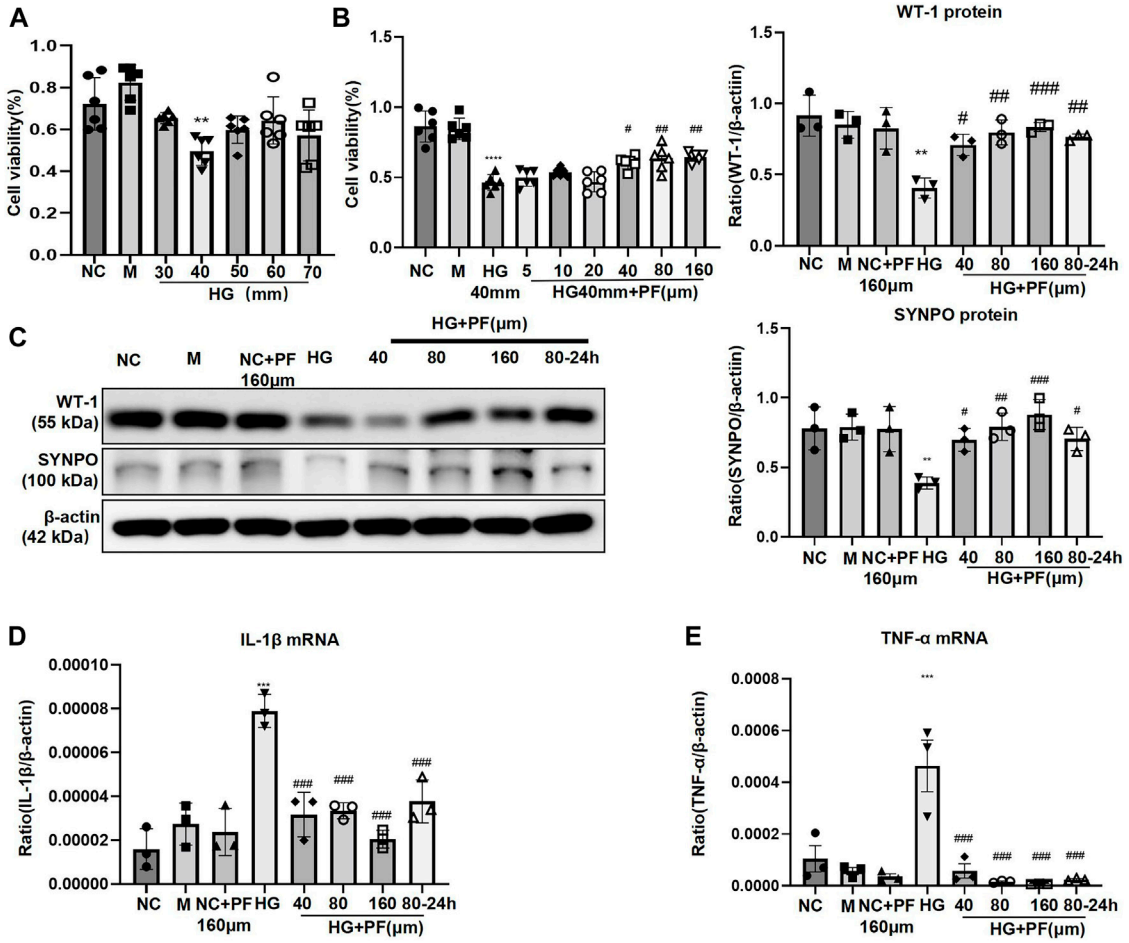

FIGURE 5
PF ameliorates HG-stimulated podocyte injury. **(A)** MTT assay to evaluate the effect of HG on MPC5 cells viability. **(B)** MTT assay to evaluate the effect of PF on HG-stimulated MPC5 cells viability. **(C)** WB assay of WT-1 and SYNPO protein in MPC5 cells. **(D)** IL-1β mRNA in MPC5 cells. **(E)** TNF-α mRNA in MPC5 cells. Results represent the mean ± SD. $^{**}p < 0.01$, $^{***}p < 0.001$ vs. NC; $^{\#}p < 0.05$, $^{\#\#}p < 0.01$, $^{\#\#\#}p < 0.001$ vs. HG. NC, normal control (5.5 mmol/L glucose); HG, high glucose (40 mmol/L); M, mannitol (34.5 mmol/L mannitol +5.5 mmol/L glucose); PF, paeoniflorin; WT-1, Wilms tumor 1 protein; SYNPO, synaptopodin; WB, Western blotting; MPC5, mouse podocyte clone 5; TNF-α, tumor necrosis factor-α.

and function of podocytes were significantly decreased in the STZ-induced mice model, but not in mice treated with PF (Figures 4A–C).

3.2.2.2 Paeoniflorin ameliorates high glucose-stimulated podocyte injury

MTT experiments indicated that 40 mmol/L was the optimal glucose concentration for high glucose-induced podocyte injury (Figure 5A), and 40 μmol/L is the minimum concentration of PF for improving podocyte proliferation (Figure 5B). *In vitro*, the experiments further showed that the expression of WT-1 and SYNPO proteins significantly decreased on podocytes induced by HG (Figure 5C), and the mRNAs of inflammatory factors TNF and IL-1β were significantly increased (Figures 5D,E). Contrary, the above changes in podocytes obviously improved after PF treatment in a dose-dependent manner. In addition, the middle dose (80 μmol/L) was further selected to observe the preventive effect of PF on HG-induced podocyte injury. Similar to the animal experiments, podocyte injury and inflammatory responses were alleviated after PF preventive treatment.

3.3 Paeoniflorin regulates podocyte necroptosis of diabetic kidney disease *in vitro* and *in vivo*

3.3.1 Paeoniflorin regulates podocyte necroptosis in streptozotocin-induced diabetic mice

In STZ-induced diabetic mice models, the p-MLKL protein was mainly expressed on glomeruli and was obviously higher than that in the NC group, which was consistent with clinical data. Contrary, p-MLKL was downregulated especially in the middle

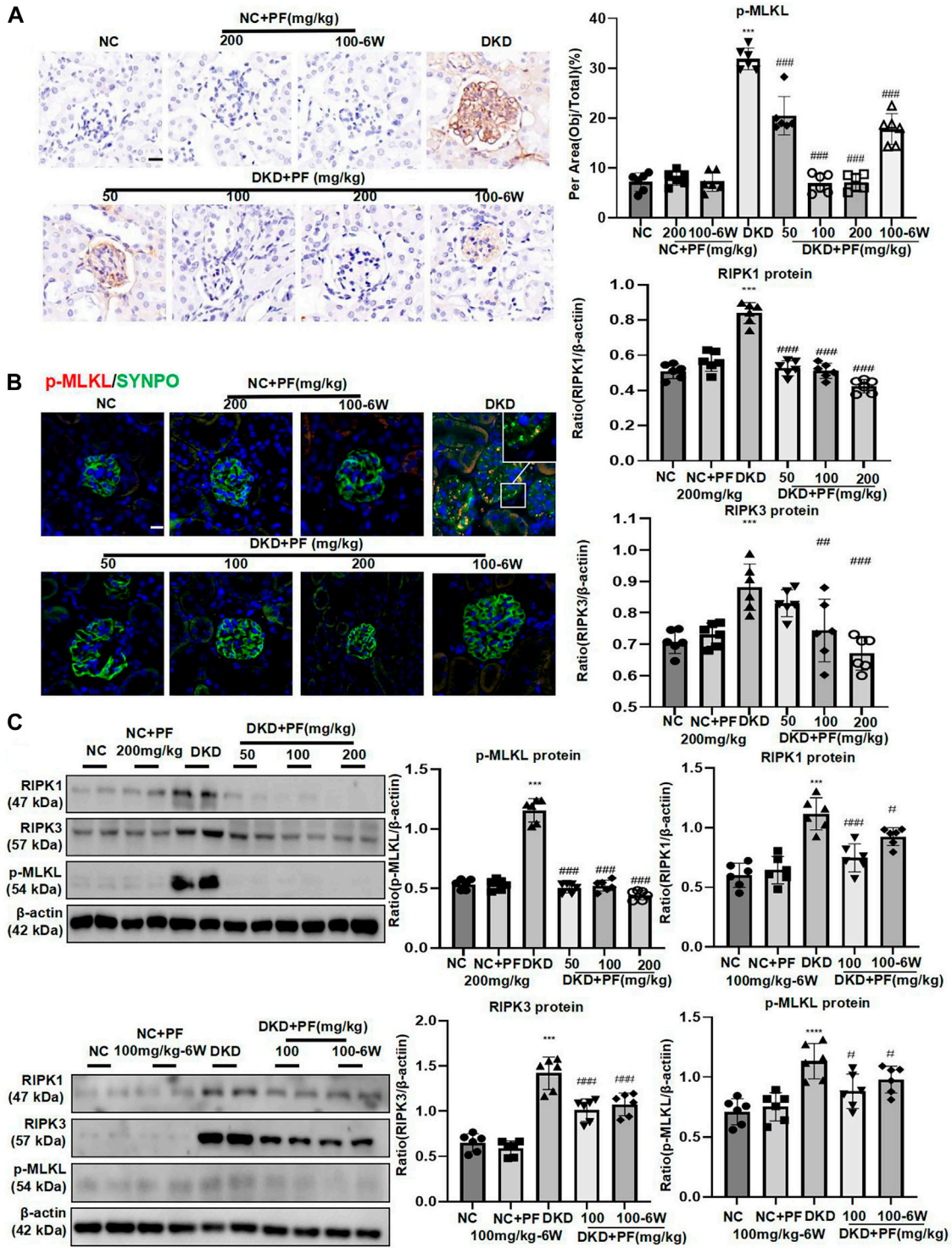

FIGURE 6
PF regulates podocyte necroptosis in STZ-induced diabetic mice. **(A)** IHC assay of p-MLKL protein expression on the glomerulus in STZ-induced diabetic mice. Scale bar = 50 μm. **(B)** IF double staining of p-MLKL and SYNPO proteins expression in renal biopsy samples. Scale bar = 50 μm. **(C)** WB assay of RIPK1, RIPK3, and p-MLKL proteins in STZ-induced diabetic mice. Data represent the mean ± SD for 6 mouse/group. $^{***}p < 0.001$ vs. NC; $^{\#}p < 0.05$, $^{\#\#}p < 0.01$, $^{\#\#\#}p < 0.001$ vs. DKD. NC, normal control; PF, paeoniflorin; STZ, streptozotocin; DKD, diabetic kidney disease; IHC, immunohistochemistry; IF, immunofluorescence; WB, Western blotting; SYNPO, synaptopodin; RIPK1, receptor-interacting serine/threonine kinase 1; RIPK3, receptor-interacting serine/threonine kinase 3; MLKL, mixed-lineage kinase domain-like protein.

and high dose groups of PF. There was no significant difference between NC group and PF group. Research also indicated that IHC results of p-MLKL protein were consistent with WB detection results (Figures 6A,C). IF double staining results showed that SYNPO was co-expressed with p-MLKL in the DKD mice model group, suggesting that necroptosis occurred on podocytes during DKD development (Figure 6B). WB also detected the marker proteins RIPK1 and RIPK3 of the programmed necrosis signaling pathway, suggesting that the protein expression was dramatically increased in DKD group, while decreased after the treatment of PF in a dose-dependent manner. The levels of necroptosis-related proteins also showed similar changes in the PF preventive treatment group with the full course of treatment (Figure 6C).

3.3.2 Paeoniflorin regulates podocyte necroptosis stimulated by high glucose

We further observed the effect of PF on the necroptosis of podocytes induced by HG. IF staining showed that p-MLKL protein level in podocytes significantly increased when induced by HG while decreased after PF treatment (Figure 7A). Furthermore, the observation using TEM showed that the cell membrane integrity of podocytes was damaged by HG-stimulation group, but not in the PF group (Figure 7B).

Moreover, we further detected necroptosis signaling pathway-related proteins by the WB method; the results were consistent with the cell IF results (Figure 7C). It should be mentioned that the changes related to necroptosis in PF groups were dose-dependent, and prevention treatment of PF also exhibited necroptosis modulating effects. Additionally, Nec-1, as an inhibitor of necroptosis, was used as a positive control to confirm that the performance of PF in inhibiting necroptosis of podocytes was similar to that of Nec-1 (Figures 7D,E).

3.4 Paeoniflorin regulates TNFR1 protein expression of diabetic kidney disease *in vitro* and *in vivo*

3.4.1 The changes of TNFR1 in diabetic kidney disease

IHC staining showed that TNFR1 protein was expressed in glomeruli and renal tubules in human kidney tissue. Furthermore, in the NC group, there was a small amount of TNFR1 expression on the glomerulus, which gradually increased with increased urinary albumin (Figure 8A). The results of IF double staining indicated that TNFR1 and p-MLKL co-localized in the glomerulus (Figure 8B).

3.4.2 Paeoniflorin regulates TNFR1 protein expression in streptozotocin-induced diabetic mice and podocytes stimulated by high glucose

IHC and WB showed that the expression of TNFR1 was low under the normal condition, but was increased mainly in the glomerulus of STZ-induced diabetic mice. TNFR1 was dramatically decreased after PF treatment, similar to NC group (Figures 8C,D).

Similarly, TNFR1 protein expression in podocytes was significantly increased after HG-stimulation and decreased after PF treatment (Figure 8E). Interestingly, the experimental results found no change in the level of TNFR1 mRNA after PF treatment *in vitro* and *in vivo* (Figures 8F,G).

Moreover, this study detected the ubiquitination level of TNFR1, purified by COIP method, suggesting that the administration of PF significantly increased the ubiquitination level of TNFR1 protein induced by HG (Figure 8H).

3.5 Paeoniflorin binds directly to TNFR1

Molecular structure screening in Molecular docking is shown in Table 5. We first analyzed the binding mode of TNFR1 to its ligand TNF. The binding score of TNFRSF1A and TNF protein was -56.59 kcal/mol. The binding sites of TNFRSF1A protein included ILE-21, LYS-32, HIS-66, ARG-68, GLU-64, LEU-71, and other amino acid residues, while the binding sites of TNF included TYR-115, PRO-117, TYR-119, LEU-120, GLN-149, GLU-146, ASN-34, and other amino acid residues. The interaction of these reactive amino acids has an important role in stabilizing the two proteins (Figure 9A). Therefore, the amino acids that interact with the two proteins can be used as active sites to bind to small molecules, thereby hindering the binding of the two proteins.

Next, we analyzed the interaction of PF with TNFRSF1A. The main binding sites of PF to TNFRSF1A target were ILE-21, LYS-32, HIS-66, ARG-68, and other amino acid residues. The binding score of PF and TNFRSF1A protein was −8.32 kcal/mol. PF compound contains multiple hydrogen bond donors and acceptors, which can form strong hydrogen bond interactions with the active groups of amino acids such as ILE-21, LYS-32, HIS-66, ARG-68 and so on. The average hydrogen bond distance was 2.5 Å. In addition, the hydrophobic benzene ring of this compound could also form a strong hydrophobic interaction with the amino acid in the active pocket, which was very helpful for stabilizing small molecules (Figure 9B). Therefore, the PF compound had a high degree of matching with the active pocket of TNFRSF1A protein and could form multiple strong hydrogen bond interactions with amino acids in the active site, which had a role in hindering the binding of TNFRSF1A and TNF. In addition, the SPR assay demonstrated the direct binding between PF and TNFR1 protein, with an equilibrium dissociation constant (KD) of 9.859×10^{-8} for steady-state fit, and the combination or separation of PF and TNFR1 was relatively rapid (Figure 9C).

3.6 Paeoniflorin regulates podocyte necroptosis via TNFR1

The effect of siRNAs on TNFR1 knockdown is shown in Figures 10A,B. After knockdown of TNFR1 on podocytes, the

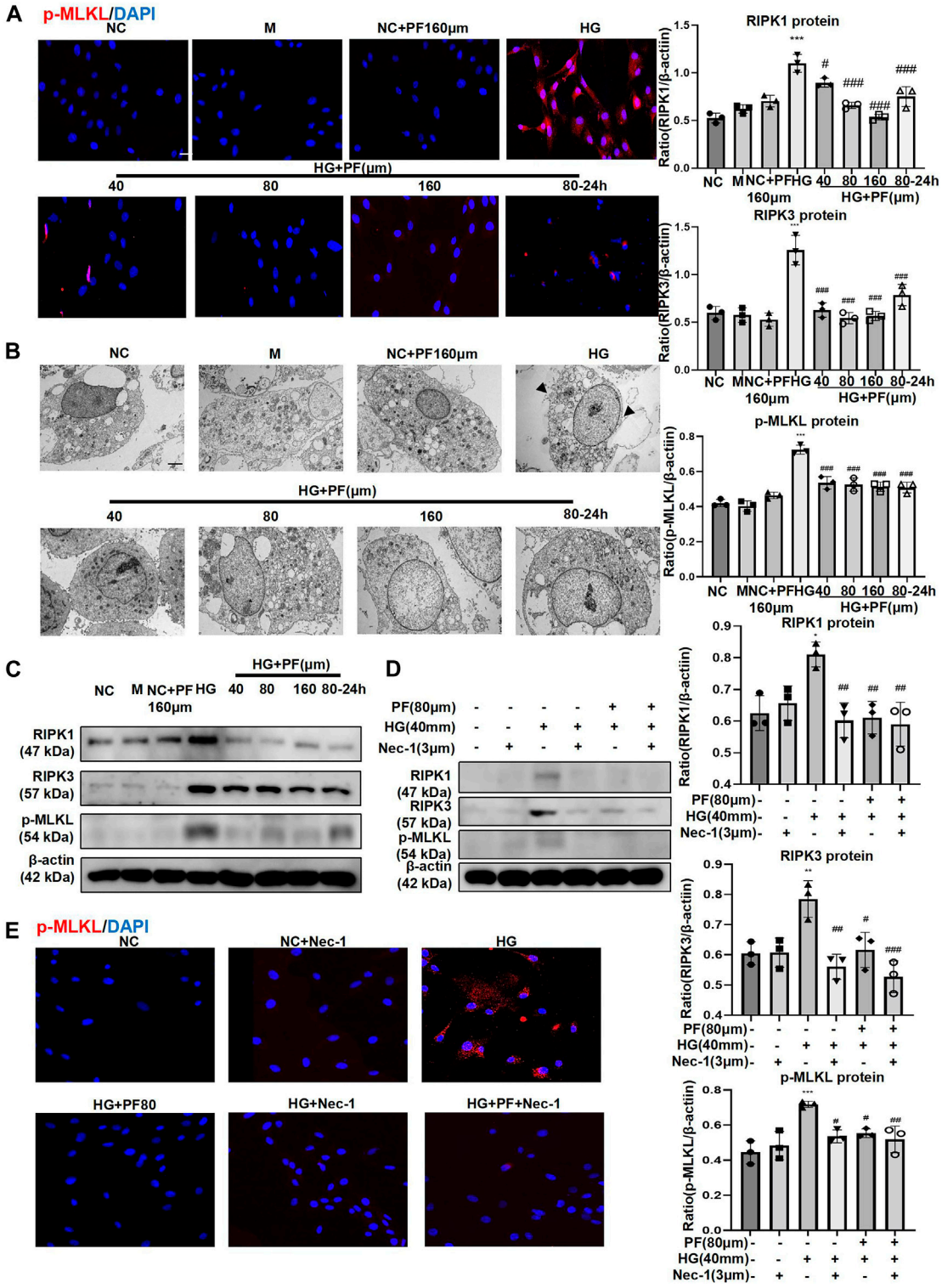

FIGURE 7
PF regulates podocyte necroptosis stimulated by HG. **(A)** IF staining of p-MLKL proteins expression in MPC5 cells stimulated with HG and treated with PF. Scale bar = 50 μm. **(B)** Images of MPC5 cells observed by TEM. **(C)** WB assay of RIPK1, RIPK3, and p-MLKL proteins in MPC5 treated with HG and PF. **(D)** WB assay of RIPK1, RIPK3, and p-MLKL proteins in MPC5 treated by Nec-1. **(E)** IF staining of p-MLKL proteins expression in MPC5 treated by Nec-1. Scale bar = 50 μm. Results represent the mean ± SD. $^{*}p < 0.05$, $^{**}p < 0.01$, $^{***}p < 0.001$ vs. NC; $^{\#}p < 0.05$, $^{\#\#}p < 0.01$, $^{\#\#\#}p < 0.001$ vs. HG. NC, normal control (5.5 mmol/L glucose); HG, high glucose (40 mmol/L); M, mannitol (34.5 mmol/L mannitol +5.5 mmol/L glucose); PF, paeoniflorin; WB, Western blotting; MPC5, mouse podocyte clone 5; Nec-1, necrostatin-1; TEM, transmission electron microscopy; RIPK1, receptor-interacting serine/threonine kinase 1; RIPK3, receptor-interacting serine/threonine kinase three; MLKL, mixed-lineage kinase domain-like protein.

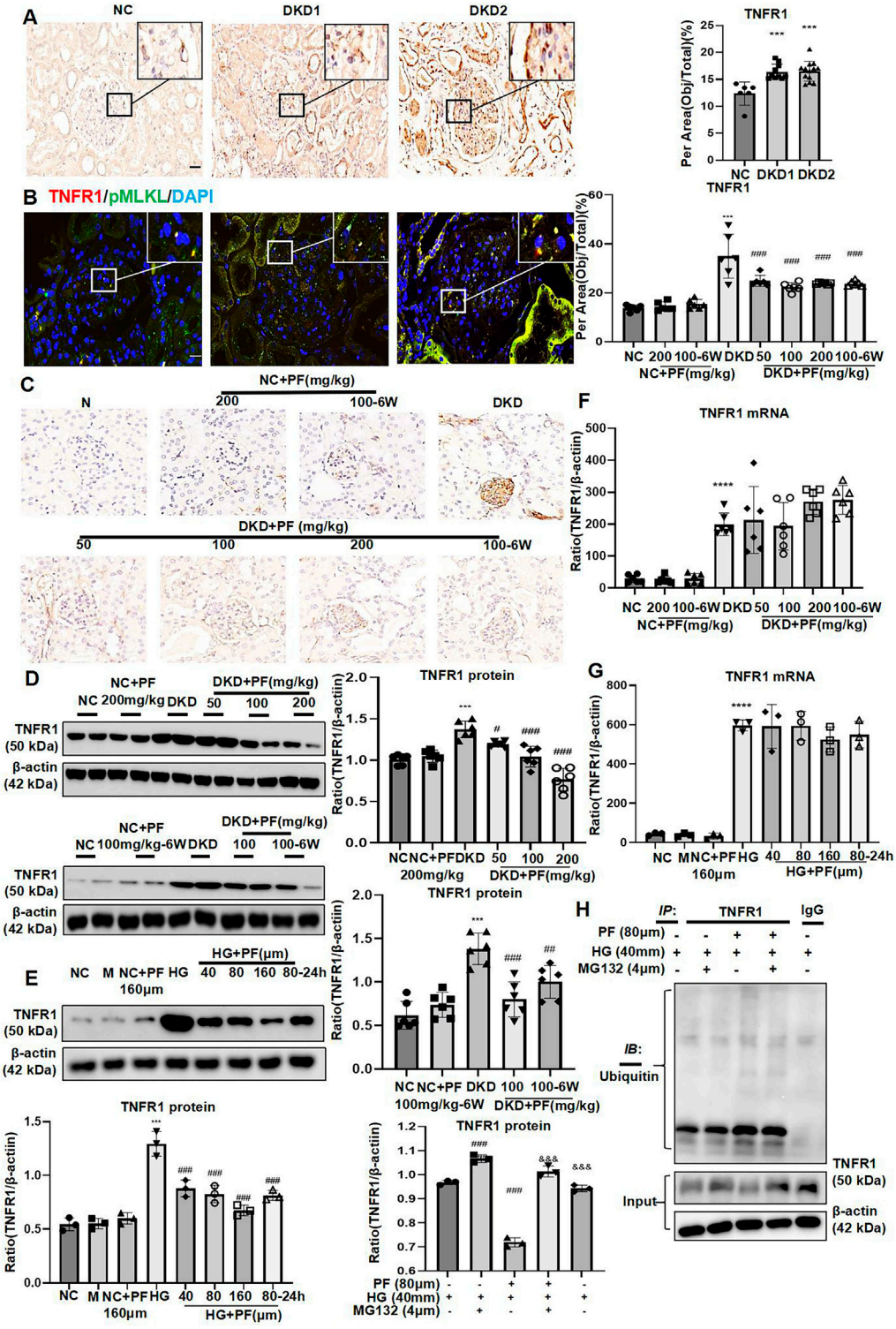

FIGURE 8
PF regulates TNFR1 protein expression *in vivo* and *in vitro*. **(A)** IHC assay of TNFR1 protein expression on the glomerulus of human renal biopsy tissues. Scale bar = 20 μm. **(B)** IF double staining for p-MLKL and TNFR1 in human renal biopsy tissues. Scale bar = 20 μm. **(C)** IHC assay of TNFR1 protein expression on the glomerulus in STZ-induced diabetic mice. Scale bar = 50 μm. **(D)** WB assay of TNFR1 protein in STZ-induced diabetic mice. **(E)** WB assay of TNFR1 protein in MPC5 with HG and PF treatment. **(F)** The levels of TNFR1 mRNA in STZ-induced diabetic mice. **(G)** The levels of TNFR1 mRNA in MPC5 with HG and PF treatment. **(H)** The ubiquitination of TNFR1 in MPC cells. Results represent the mean ± SD. $^{**}p < 0.01$, $^{***}p < 0.001$ vs. NC; $^{\#}p < 0.05$, $^{\#\#}p < 0.01$, $^{\#\#\#}p < 0.001$ vs. HG/DKD; $^{\&\&\&}p < 0.001$ vs. HG+PF. NC, normal control (5.5 mmol/L glucose);
(*Continued*)

FIGURE 8
HG, high glucose (40 mmol/L); M, mannitol (34.5 mmol/L mannitol +5.5 mmol/L glucose); PF, paeoniflorin; STZ, streptozotocin; DKD, diabetic kidney disease; IHC, immunohistochemistry; TNFR1, tumor necrosis factor receptor 1; IF, immunofluorescence; WB, Western blotting; MPC5, mouse podocyte clone 5; RIPK1, receptor-interacting serine/threonine kinase 1; RIPK3, receptor-interacting serine/threonine kinase 3; MLKL, mixed-lineage kinase domain-like protein.

TABLE 5 The molecular docking results of target proteins.

Protein1	Protein2	Binding energy (kcal/mol)	Contact sites (protein1)	Contact sites (protein2)	Combination type
TNFRSF1A	TNF	-56.59	ILE-21, LYS-32, HIS-66, ARG-68, GLU-64, LEU-71	TYR-115, PRO-117, TYR-119, LEU-120, GLN-149, GLU-146, ASN-34	Hydrogen bond, Hydrophobic interaction
TNFRSF1A	PF	-8.32	ILE-21, LYS-32, HIS-66, ARG-68	-	Hydrogen bond, Hydrophobic interaction

PF, paeoniflorin; TNFR1, tumor necrosis factor receptor 1; TNFRSF1A, tumor necrosis factor receptor superfamily, member 1.

levels of inflammatory indicators (IL-1β and TNF-α mRNA), cell injury indicators (WT-1 and SYNPO protein), and necroptosis-related proteins were significantly reduced, similarly to the effect of PF on HG-stimulated podocytes, but the podocyte protection and necroptosis regulation of PF were not improved after TNFR1 knockdown (Figures 10C–F). The p-MLKL IF staining of the cell slides was consistent with the WB results (Figure 10G).

4 Discussion

The mechanism of occurrence and development of DKD is quite complex, requiring the participation of many cells and the regulation of various signaling pathways (Raval et al., 2020). Among them, the formation of proteinuria in the early stage of DKD is closely related to the damage of podocytes, which is irreversible (Sugita et al., 2021). Therefore, exploring podocyte death's occurrence and development mechanism may provide a new way to treat and prevent DKD. To the best of our knowledge, this is the first study that reported the significance of necroptosis in the process of DKD and the inhibitory effect of PF on podocyte necroptosis in DKD through directly binding TNFR1. These results provided a theoretical basis for the application of PF in DKD.

Necroptosis is a form of the programmed cell death initiated by various pattern recognition receptors (PRRs) or cytokines, and mediated by RIPK1, RIPK3, and MLKL. Phosphorylated-MLKL (p-MLKL) acts as an executor that ultimately induces necroptosis by translocating and breaking the cell membrane and eventually resulting in cell death (Seo et al., 2019). In this study, we first observed the dynamic changes of necroptosis in the renal tissues of DKD patients, especially in the glomerulus. The RNA-seq dataset GSE142025 was selected to observe the dynamic changes of necroptosis-related genes in the process of DKD; RNA-seq dataset GSE142025 contains human renal biopsy samples with the microalbumin and macroalbuminuria stages of DKD. The mRNA levels of necroptosis-related genes were dramatically upregulated in DKD patients with macroalbuminuria. RIPK1, RIPK3, and MLKL were identified as key factors in developing necroptosis and the progression of DKD. Interestingly, from the analysis results of this dataset, the necroptosis did not seem to occur at the initial stage of DKD but at the time of progressive exacerbation. However, it should be noted that the actual occurrence of necroptosis requires the formation of p-MLKL, which will be used as a marker for more accurate evaluation of the level of necroptosis in our subsequent study. In addition, necroptosis observed by IHC staining of human kidney tissue was present not only in the tubulointerstitium as in acute kidney injury, but also in the glomerular resident cells of DKD patients, especially of those with macroalbuminuria. This result was consistent with the observations on the above datasets. Furthermore, IHC staining of renal tissue in an STZ-induced mouse diabetes model with macroalbuminuria was used to locate and observe necroptosis. The results showed that the change of p-MLKL was most significant in the glomerulus. This gave us an interesting hint that the glomerulus resident cells showed necroptosis markedly during macroalbuminuria. Therefore, this study focused on detecting necroptosis changes in the glomerulus. Results of correlation analysis showed that glomerulus necroptosis might participate in the progression of renal tissue damage in DKD.

In our study, the results of IF double staining confirmed the presence of necroptosis in podocytes in DKD. The *in vitro* experiments also showed classical changes associated with necroptosis, including the destruction of the cell membrane

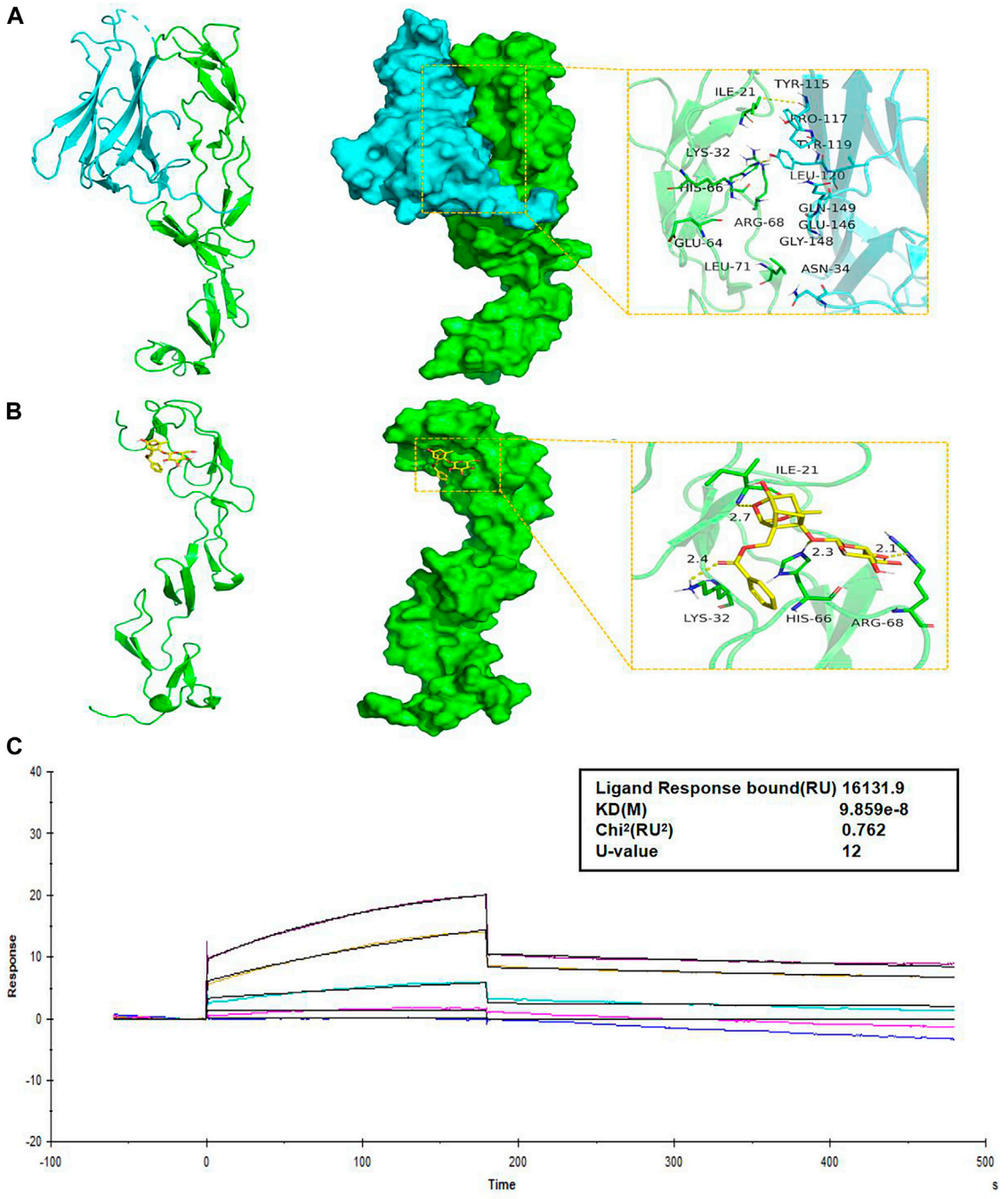

FIGURE 9
PF directly binds to TNFR1. **(A)** The binding mode of the complex TNFRSF1A with TNF. The backbone of protein was rendered in a tube and colored in green. TNFRSF1A (left) and TNF (right) protein were rendered by the surface. The yellow dash represents a hydrogen bond or salt bridge. **(B)** The binding mode of the complex TNFRSF1A with PF. The backbone of protein was rendered in a tube and colored in green. TNFRSF1A protein was rendered by the surface. The yellow dash represents a hydrogen bond or salt bridge. **(C)** SPR assay showed the steady-state fit of binding between PF and TNFR1. TNFR1, tumor necrosis factor receptor 1; TNFRSF1A, tumor necrosis factor receptor superfamily member 1; PF, paeoniflorin; SPR, surface plasmon resonance.

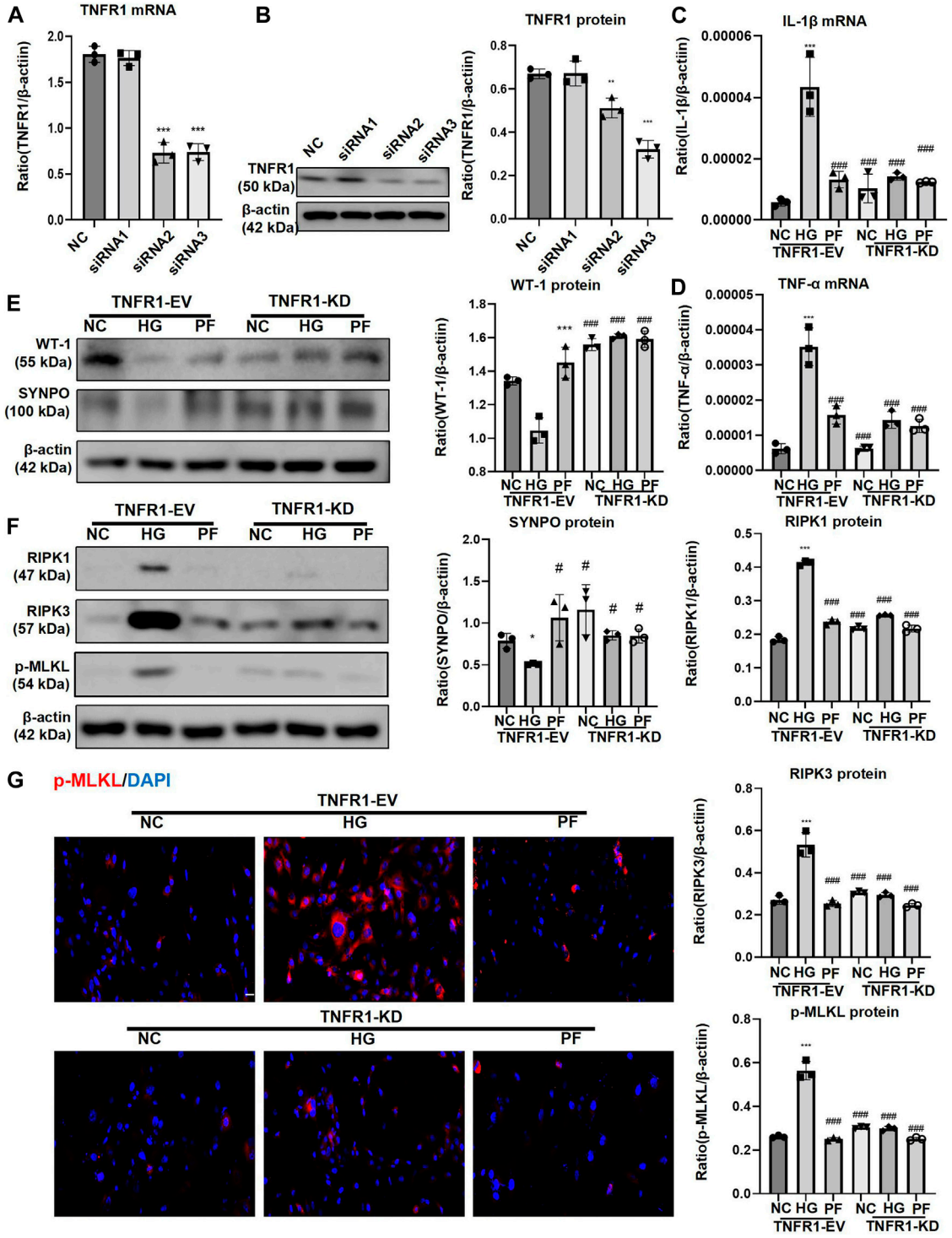

FIGURE 10
PF regulates podocyte necroptosis via TNFR1. **(A)** Real-time PCR assay of TNFR1 in MPC5 cells after TNFR1 knockdown. **(B)** WB assay of TNFR1 protein in MPC5 cells after TNFR1 knockdown. **(C)** The change of IL-1β mRNA in MPC5 cells after TNFR1 knockdown. **(D)** The change of TNF-α mRNA in MPC5 cells after TNFR1 knockdown. **(E)** WB assay of WT-1 and SYNPO proteins in MPC5 cells after TNFR1 knockdown. **(F)** WB assay of necroptosis-related proteins in MPC5 cells after TNFR1 knockdown. **(G)** IF staining of p-MLKL proteins expression in MPC5 cells after TNFR1 knockdown. Scale bar = 50 μm. Results represent the mean ± SD. $^{*}p < 0.05$, $^{***}p < 0.001$ vs. NC; $^{\#}p < 0.05$, $^{\#\#}p < 0.01$, $^{\#\#\#}p < 0.001$ vs. HG. NC, normal control (5.5 mmol/L glucose); HG, high glucose (40 mmol/L); PF, paeoniflorin; TNFR1, tumor necrosis factor receptor 1; IF, immunofluorescence; WB, Western blotting; MPC5, mouse podocyte clone 5; TNF-α, tumor necrosis factor-α; WT-1, Wilms tumor 1 protein; SYNPO, synaptopodin; RIPK1, receptor-interacting serine/threonine kinase 1; RIPK3, receptor-interacting serine/threonine kinase 3; MLKL, mixed-lineage kinase domain-like protein.

and elevated p-MLKL protein in podocytes stimulated by HG. Therefore, amelioration of necroptosis may be a potential measure to protect against podocyte damage in DKD.

In China, the clinical efficacy and safety of some classic Chinese herbal medicines have undergone long-term and sufficient clinical verification. Paeoniflorin has been studied for decades as the main active ingredient of the classic traditional Chinese medicine Paeonia lactiflora. Our previous study found that PF can improve kidney injury in DKD mice model without obvious toxic side effects (Zhang et al., 2017). Furthermore, we validated the advantages of PF for kidney and podocyte, finding that PF can improve renoprotection and alleviate podocyte injury in both the whole administration and prophylactic administration. All roads lead to Rome. These interesting results provided a certain basis for the mobility of PF in clinical application. In exploring the mechanism of PF in DKD, we found that PF can significantly inhibit glomerulus necroptosis in DKD, especially on podocytes, similarly to the classical necroptosis inhibitor, necrostatin-1 (Nec-1).

Subsequent studies focused on the specific mechanisms through which PF affects podocyte necroptosis in DKD. TNFRSF1A (also named TNFR1) was the interacting protein of RIPK1 predicted by the sting website (https://cn.string-db.org/). TNFRs are recognized as the receptor of TNFα, leading to the nitric oxide production (Jha et al., 2020). The levels of TNFR1 in circulation have been associated with the damage of kidney in type 2 diabetes (Fernandez-Real et al., 2012). Interestingly enough, we found in our study that the expression of TNFR1 protein on the glomerulus was obviously upregulated in human and mouse with DKD. Meanwhile, the trend of TNFR1 expression was consistent with the necroptosis marker, p-MLKL. Previous reports have pointed out that the intracellular domain of TNFR1 on the cell membrane can bind to RIPK1 and regulate the phosphorylation of MLKL through RIPK1/RIPK3 signaling pathway, thereby participating in cell necroptosis (Dondelinger et al., 2016). Thus, TNFR1 may be an upstream target protein of necroptosis on podocytes. Unfortunately, there is no report on the clinical application of TNFR1-specific blockers or inhibitors (Al-Lamki and Mayadas, 2015). Animal experiments showed that PF could downregulate the expression of TNFR1 protein on the glomerulus, which was consistent with *in vitro* data on podocytes. Molecular docking further showed that PF and TNFR1 had multiple binding sites, some of which overlapped with TNF-a and TNFR1 binding sites, suggesting that PF may compete with TNF-a to bind TNFR1 for regulating necroptosis. SPR experiments verified the rapid association and dissociation properties of PF with TNFR1, providing a certain basis for the safety of multiple administration of PF. However, it should be noted that in another report, CD40, which was upregulated in podocytes, tubular epithelial cells and various infiltrating cells of human renal tissue with DKD, can change TRAF-binding domains to affect the function of TNFRs. This result was mainly achieved through the effect of $CD40^{-}CD40L$ interacting residues on the binding capacity of TRAF (Sarode et al., 2020). Therefore, we wondered whether PF could also act in a similar manner as CD40.

Next, we explored the specific mechanism of PF in regulating TNFR1. Common mechanisms that affect protein expression include transcription and translation of protein-related genes and protein folding and degradation. The ubiquitin-proteasome system is the main pathway for intracellular protein degradation. The ubiquitination system, consisting of E1 (ubiquitin activation), E2 (ubiquitin binding/carrier), and E3 (ubiquitin ligase), can anchors proteins and transport them to the 26S proteasome for degradation (Wertz and Dixit, 2008). In this study, there was no significant change in TNFR1 mRNA level after PF treatment in DKD modes, suggesting that PF might directly affect the protein level of TNFR1. We tried to clarify the downregulation mechanism of PF in the expression of TNFR1 by focusing on the protein ubiquitination level leading to protein degradation. The further research suggested that the ubiquitination of TNFR1 protein increased in the PF group, suggesting that PF promotes the degradation of TNFR1 protein. Finally, after TNFR1 knockdown, the injury and necroptosis of cultured podocytes stimulated by HG decreased significantly, while PF could no longer exert its protective effects on podocyte injury and regulation of necroptosis. Therefore, we confirmed that PF could directly bind to TNFR1 and increase its degradation to regulate podocyte necroptosis mediated by the RIPK1/RIPK3 signaling pathway in DKD.

Admittedly, this study has a lot of limitations. First, the clinical sample size was not large enough. Also, observation of necroptosis was limited to renal tissue specimens; other types of specimens, including blood and urine, need to be examined in future studies. In addition, due to the limitation of intraperitoneal administration of PF, this study only used STZ-induced mice as a diabetic model. Further studies should be performed to evaluate the role of necroptosis in other types of DKD model.

5 Conclusion

PF can improve renoprotection and alleviate podocyte injury in both the whole administration and prophylactic administration. Furthermore, PF can directly bind and promote the degradation of TNFR1 in podocytes and then regulate the RIPK1/RIPK3 signaling pathway to affect necroptosis, thus preventing podocyte injury in DKD. Thus, TNFR1 may be used as a new potential target to treat DKD.

Data availability statement

The datasets presented in this study can be found in online repositories. The names of the repository/repositories and

accession number(s) can be found in the article/ Supplementary Material.

Ethics statement

The studies involving human participants were reviewed and approved by the First Affiliated Hospital of Anhui Medical University. The patients/participants provided their written informed consent to participate in this study. The animal study was reviewed and approved by Anhui Medical University Experimental Animal Ethics Committee.

Author contributions

X-mQ and Y-gW contributed to design of this study. X-qL and LJ contributed to preparate the original draft. XW wrote the manuscript. Y-bH and H-xZ performed the statistical analysis. Q-jZ contributed to design of the study. All authors reviewed and approved the final manuscript.

Funding

This study was supported by the National Natural Science Foundation of China (Grant No. 81904035) and the Natural Science Foundation of Anhui Province (No. 1908085MH245).

Acknowledgments

The authors thank the Center for Scientific Research of Anhui Medical University for valuable help in our experiment.

Conflict of interest

The authors declare that the research was conducted in the absence of any commercial or financial relationships that could be construed as a potential conflict of interest.

Publisher's note

Supplementary material

The Supplementary Material for this article can be found online at: https://www.frontiersin.org/articles/10.3389/fphar.2022.966645/full#supplementary-material

References

Al-Lamki, R. S., and Mayadas, T. N. (2015). TNF receptors: Signaling pathways and contribution to renal dysfunction. *Kidney Int.* 87, 281–296. doi:10.1038/ki.2014.285

American Diabetes, A. (2013). Diagnosis and classification of diabetes mellitus. *Diabetes Care* 36 (1), S67–S74. doi:10.2337/dc13-s067

Benigni, A., Zoja, C., Corna, D., Zatelli, C., Conti, S., Campana, M., et al. (2003). Add-on anti-TGF-beta antibody to ACE inhibitor arrests progressive diabetic nephropathy in the rat. *J. Am. Soc. Nephrol.* 14, 1816–1824. doi:10.1097/01.asn.0000074238.61967.b7

Chang, Y. P., Sun, B., Han, Z., Han, F., Hu, S. L., Li, X. Y., et al. (2017). Saxagliptin attenuates albuminuria by inhibiting podocyte epithelial- to-mesenchymal transition via SDF-1α in diabetic nephropathy. *Front. Pharmacol.* 8, 780. doi:10.3389/fphar.2017.00780

Chen, Y., Zou, H., Lu, H., Xiang, H., and Chen, S. (2022). Research progress of endothelial-mesenchymal transition in diabetic kidney disease. *J. Cell. Mol. Med.* 26, 3313–3322. doi:10.1111/jcmm.17356

Chung, H., Lee, S. W., Hyun, M., Kim, S. Y., Cho, H. G., Lee, E. S., et al. (2022). Curcumin blocks high glucose-induced podocyte injury via RIPK3-dependent pathway. *Front. Cell Dev. Biol.* 10, 800574. doi:10.3389/fcell.2022.800574

De Zeeuw, D., Agarwal, R., Amdahl, M., Audhya, P., Coyne, D., Garimella, T., et al. (2010). Selective vitamin D receptor activation with paricalcitol for reduction of albuminuria in patients with type 2 diabetes (VITAL study): A randomised controlled trial. *Lancet* 376, 1543–1551. doi:10.1016/S0140-6736(10)61032-X

De Zeeuw, D., Coll, B., Andress, D., Brennan, J. J., Tang, H., Houser, M., et al. (2014). The endothelin antagonist atrasentan lowers residual albuminuria in patients with type 2 diabetic nephropathy. *J. Am. Soc. Nephrol.* 25, 1083–1093. doi:10.1681/ASN.2013080830

Dondelinger, Y., Darding, M., Bertrand, M. J., and Walczak, H. (2016). Poly-ubiquitination in TNFR1-mediated necroptosis. *Cell. Mol. Life Sci.* 73, 2165–2176. doi:10.1007/s00018-016-2191-4

Fan, Y., Yi, Z., D'Agati, V. D., Sun, Z., Zhong, F., Zhang, W., et al. (2019). Comparison of kidney transcriptomic profiles of early and advanced diabetic nephropathy reveals potential new mechanisms for disease progression. *Diabetes* 68, 2301–2314. doi:10.2337/db19-0204

Fernandez-Real, J. M., Vendrell, J., Garcia, I., Ricart, W., and Valles, M. (2012). Structural damage in diabetic nephropathy is associated with TNF-alpha system activity. *Acta Diabetol.* 49, 301–305. doi:10.1007/s00592-011-0349-y

Huang, H., Jin, W. W., Huang, M., Ji, H., Capen, D. E., Xia, Y., et al. (2020). Gentamicin-induced acute kidney injury in an animal model involves programmed necrosis of the collecting duct. *J. Am. Soc. Nephrol.* 31, 2097–2115. doi:10.1681/ASN.2019020204

Jha, M. K., Rao, S. J., Sarode, A. Y., Saha, B., Kar, A., and Pal, J. K. (2020). A Leishmania donovani dominant-negative mutant for eIF2α kinase LdeK1 elicits host-protective immune response. *Parasite Immunol.* 42, e12678. doi:10.1111/pim.12678

Kato, H., Gruenwald, A., Suh, J. H., Miner, J. H., Barisoni-Thomas, L., Taketo, M. M., et al. (2011). Wnt/β-catenin pathway in podocytes integrates cell adhesion, differentiation, and survival. *J. Biol. Chem.* 286, 26003–26015. doi:10.1074/jbc.M111.223164

Komers, R., Oyama, T. T., Beard, D. R., Tikellis, C., Xu, B., Lotspeich, D. F., et al. (2011). Rho kinase inhibition protects kidneys from diabetic nephropathy without reducing blood pressure. *Kidney Int.* 79, 432–442. doi:10.1038/ki.2010.428

Koya, D., Haneda, M., Nakagawa, H., Isshiki, K., Sato, H., Maeda, S., et al. (2000). Amelioration of accelerated diabetic mesangial expansion by treatment with a PKC

beta inhibitor in diabetic db/db mice, a rodent model for type 2 diabetes. *FASEB J.* 14, 439–447. doi:10.1096/fasebj.14.3.439

Lan, X., Wen, H., Cheng, K., Plagov, A., Marashi Shoshtari, S. S., Malhotra, A., et al. (2017). Hedgehog pathway plays a vital role in HIV-induced epithelial-mesenchymal transition of podocyte. *Exp. Cell Res.* 352, 193–201. doi:10.1016/j.yexcr.2017.01.019

Li, Y., Kang, Y. S., Dai, C., Kiss, L. P., Wen, X., and Liu, Y. (2008). Epithelial-to-mesenchymal transition is a potential pathway leading to podocyte dysfunction and proteinuria. *Am. J. Pathol.* 172, 299–308. doi:10.2353/ajpath.2008.070057

Ling, L., Tan, Z., Zhang, C., Gui, S., Hu, Y., and Chen, L. (2018). Long noncoding RNA ENSRNOG00000037522 is involved in the podocyte epithelialmesenchymal transition in diabetic rats. *Int. J. Mol. Med.* 41, 2704–2714. doi:10.3892/ijmm.2018.3457

Moellmann, J., Klinkhammer, B. M., Onstein, J., Stohr, R., Jankowski, V., Jankowski, J., et al. (2018). Glucagon-like peptide 1 and its cleavage products are renoprotective in murine diabetic nephropathy. *Diabetes* 67, 2410–2419. doi:10.2337/db17-1212

Nishad, R., Meshram, P., Singh, A. K., Reddy, G. B., and Pasupulati, A. K. (2020). Activation of Notch1 signaling in podocytes by glucose-derived AGEs contributes to proteinuria. *BMJ Open Diabetes Res. Care* 8, e001203. doi:10.1136/bmjdrc-2020-001203

Peng, C. H., Lin, H. C., Lin, C. L., Wang, C. J., and Huang, C. N. (2019). Abelmoschus esculentus subfractions improved nephropathy with regulating dipeptidyl peptidase-4 and type 1 glucagon-like peptide receptor in type 2 diabetic rats. *J. Food Drug Anal.* 27, 135–144. doi:10.1016/j.jfda.2018.07.004

Raval, N., Kumawat, A., Kalyane, D., Kalia, K., and Tekade, R. K. (2020). Understanding molecular upsets in diabetic nephropathy to identify novel targets and treatment opportunities. *Drug Discov. Today* 25, 862–878. doi:10.1016/j.drudis.2020.01.008

Sarode, A. Y., Jha, M. K., Zutshi, S., Ghosh, S. K., Mahor, H., Sarma, U., et al. (2020). Residue-specific message encoding in CD40-ligand. *iScience* 23, 101441. doi:10.1016/j.isci.2020.101441

Seo, J., Kim, M. W., Bae, K. H., Lee, S. C., Song, J., and Lee, E. W. (2019). The roles of ubiquitination in extrinsic cell death pathways and its implications for therapeutics. *Biochem. Pharmacol.* 162, 21–40. doi:10.1016/j.bcp.2018.11.012

Srivastava, S. P., Goodwin, J. E., Kanasaki, K., and Koya, D. (2020). Metabolic reprogramming by N-acetyl-seryl-aspartyl-lysyl-proline protects against diabetic kidney disease. *Br. J. Pharmacol.* 177, 3691–3711. doi:10.1111/bph.15087

Sugimoto, H., Grahovac, G., Zeisberg, M., and Kalluri, R. (2007). Renal fibrosis and glomerulosclerosis in a new mouse model of diabetic nephropathy and its regression by bone morphogenic protein-7 and advanced glycation end product inhibitors. *Diabetes* 56, 1825–1833. doi:10.2337/db06-1226

Sugita, E., Hayashi, K., Hishikawa, A., and Itoh, H. (2021). Epigenetic alterations in podocytes in diabetic nephropathy. *Front. Pharmacol.* 12, 759299. doi:10.3389/fphar.2021.759299

Tao, M., Zheng, D., Liang, X., Wu, D., Hu, K., Jin, J., et al. (2021). Tripterygium glycoside suppresses epithelialtomesenchymal transition of diabetic kidney disease podocytes by targeting autophagy through the mTOR/Twist1 pathway. *Mol. Med. Rep.* 24, 592. doi:10.3892/mmr.2021.12231

Tervaert, T. W., Mooyaart, A. L., Amann, K., Cohen, A. H., Cook, H. T., Drachenberg, C. B., et al. (2010). Pathologic classification of diabetic nephropathy. *J. Am. Soc. Nephrol.* 21, 556–563. doi:10.1681/ASN.2010010010

Tomita, I., Kume, S., Sugahara, S., Osawa, N., Yamahara, K., Yasuda-Yamahara, M., et al. (2020). SGLT2 inhibition mediates protection from diabetic kidney disease by promoting ketone body-induced mTORC1 inhibition. *Cell Metab.* 32, 404–419. doi:10.1016/j.cmet.2020.06.020

Wang, J., Xiang, H., Lu, Y., Wu, T., and Ji, G. (2021). New progress in drugs treatment of diabetic kidney disease. *Biomed. Pharmacother.* 141, 111918. doi:10.1016/j.biopha.2021.111918

Wang, X., Gao, Y., Tian, N., Wang, T., Shi, Y., Xu, J., et al. (2019). Astragaloside IV inhibits glucose-induced epithelial-mesenchymal transition of podocytes through autophagy enhancement via the SIRT-NF-κB p65 axis. *Sci. Rep.* 9, 323. doi:10.1038/s41598-018-36911-1

Wei, X., Wei, X., Lu, Z., Li, L., Hu, Y., Sun, F., et al. (2020). Activation of TRPV1 channel antagonizes diabetic nephropathy through inhibiting endoplasmic reticulum-mitochondria contact in podocytes. *Metabolism.* 105. 154182. doi:10.1016/j.metabol.2020.154182

Wertz, I. E., and Dixit, V. M. (2008). Ubiquitin-mediated regulation of TNFR1 signaling. *Cytokine Growth Factor Rev.* 19, 313–324. doi:10.1016/j.cytogfr.2008.04.014

Yin, J., Wang, Y., Chang, J., Li, B., Zhang, J., Liu, Y., et al. (2018). Apelin inhibited epithelial-mesenchymal transition of podocytes in diabetic mice through downregulating immunoproteasome subunits β5i. *Cell Death Dis.* 9, 1031. doi:10.1038/s41419-018-1098-4

Zeisberg, E. M., Potenta, S. E., Sugimoto, H., Zeisberg, M., and Kalluri, R. (2008). Fibroblasts in kidney fibrosis emerge via endothelial-to-mesenchymal transition. *J. Am. Soc. Nephrol.* 19, 2282–2287. doi:10.1681/ASN.2008050513

Zeisberg, M., Hanai, J., Sugimoto, H., Mammoto, T., Charytan, D., Strutz, F., et al. (2003). BMP-7 counteracts TGF-beta1-induced epithelial-to-mesenchymal transition and reverses chronic renal injury. *Nat. Med.* 9, 964–968. doi:10.1038/nm888

Zeng, L. F., Xiao, Y., and Sun, L. (2019). A glimpse of the mechanisms related to renal fibrosis in diabetic nephropathy. *Adv. Exp. Med. Biol.* 1165, 49–79. doi:10.1007/978-981-13-8871-2_4

Zhang, L., Long, J., Jiang, W., Shi, Y., He, X., Zhou, Z., et al. (2016). Trends in chronic kidney disease in China. *N. Engl. J. Med.* 375, 905–906. doi:10.1056/NEJMc1602469

Zhang, L., and Wei, W. (2020). Anti-inflammatory and immunoregulatory effects of paeoniflorin and total glucosides of paeony. *Pharmacol. Ther.* 207, 107452. doi:10.1016/j.pharmthera.2019.107452

Zhang, L., Wen, Z., Han, L., Zheng, Y., Wei, Y., Wang, X., et al. (2020). Research progress on the pathological mechanisms of podocytes in diabetic nephropathy. *J. Diabetes Res.* 2020, 7504798. doi:10.1155/2020/7504798

Zhang, Q., Hu, Y., Hu, J. E., Ding, Y., Shen, Y., Xu, H., et al. (2021). Sp1-mediated upregulation of Prdx6 expression prevents podocyte injury in diabetic nephropathy via mitigation of oxidative stress and ferroptosis. *Life Sci.* 278, 119529. doi:10.1016/j.lfs.2021.119529

Zhang, T., Zhu, Q., Shao, Y., Wang, K., and Wu, Y. (2017). Paeoniflorin prevents TLR2/4-mediated inflammation in type 2 diabetic nephropathy. *Biosci. Trends* 11, 308–318. doi:10.5582/bst.2017.01104

Zhong, Y., Lee, K., Deng, Y., Ma, Y., Chen, Y., Li, X., et al. (2019). Arctigenin attenuates diabetic kidney disease through the activation of PP2A in podocytes. *Nat. Commun.* 10, 4523. doi:10.1038/s41467-019-12433-w

Zhu, W., Li, Y. Y., Zeng, H. X., Liu, X. Q., Sun, Y. T., Jiang, L., et al. (2021). Carnosine alleviates podocyte injury in diabetic nephropathy by targeting caspase-1-mediated pyroptosis. *Int. Immunopharmacol.* 101. 108236. doi:10.1016/j.intimp.2021.108236

Glossary

ACR albumin to creatinine ratio
ALB albumin;
ALT serum alanine transaminase
ApoA1 apolipoprotein A1
ApoB apolipoprotein B
BUN blood urea nitrogen
CHO cholesterol
CO-IP co-immunoprecipitation assay
DBP diastolic blood pressure
DEGs differential expression genes
DKD diabetic kidney disease
DM diabetic metabolism
eGFR estimate glomerular filtration rate
endMT endothelial-mesenchymal transition
EMT epithelial-mesenchymal transition
FBS fasting blood sugar
FC fold change
GBM glomerular basement membrane
GFB glomerular filtration barrier
HG high glucose
HDL high-density lipoprotein
IHC immunohistochemistry
IF immunofluorescence
IFTA interstitial fibrosis and tubular atrophy
LDL low-density lipoprotein
M mannitol
MLKL mixed-lineage kinase domain-like protein
MPC5 mouse podocyte clone 5
NC normal control
Nec-1 necrostatin-1
OD optical density
PF paeoniflorin
RIPK1 receptor-interacting serine/threonine kinase 1
RIPK3 receptor-interacting serine/threonine kinase 3
SBP systolic blood pressure
Scr serum creatinine
SPR surface plasmon resonance
SPF specific pathogen-free
STZ streptozotocin
SYNPO synaptopodin
TEM transmission electron microscopy
TNF-α tumor necrosis factor-α
TNFR1 tumor necrosis factor receptor 1
TNFRSF1A tumor necrosis factor receptor superfamily, member 1
TG triglycerides
UAER urinary albumin excretion rate
UA uric acid
VLDL very low-density lipoprotein
WB western blotting
WT wild-type
WT-1 wilms tumor 1 protein.

frontiers | Frontiers in Pharmacology

TYPE Systematic Review
PUBLISHED 16 September 2022
DOI 10.3389/fphar.2022.967317

OPEN ACCESS

EDITED BY
Swayam Prakash Srivastava,
Yale University, United States

REVIEWED BY
Barani Kumar Rajendran,
Yale University, United States
Angel Manuel Sevillano Prieto,
Hospital Universitario 12 de Octubre, Spain

*CORRESPONDENCE
Zongji Zheng,
zhengzongji2014@163.com
Yijie Jia,
yijie0207@126.com

†These authors have contributed equally to this work and share first authorship

SPECIALTY SECTION
This article was submitted to Renal Pharmacology, a section of the journal Frontiers in Pharmacology

RECEIVED 12 June 2022
ACCEPTED 24 August 2022
PUBLISHED 16 September 2022

CITATION
Wu Y, Lin H, Tao Y, Xu Y, Chen J, Jia Y and Zheng Z (2022), Network meta-analysis of mineralocorticoid receptor antagonists for diabetic kidney disease. *Front. Pharmacol.* 13:967317. doi: 10.3389/fphar.2022.967317

Network meta-analysis of mineralocorticoid receptor antagonists for diabetic kidney disease

Yichuan Wu[1,2†], Huanjia Lin[1,2†], Yuan Tao[1,2], Ying Xu[1,2], Jiaqi Chen[1,2], Yijie Jia[1,2*] and Zongji Zheng[1,2*]

[1]Department of Endocrinology and Metabolism, Nanfang Hospital, Southern Medical University, Guangzhou, China, [2]De Feng Academy, Southern Medical University, Guangzhou, China

Diabetic kidney disease (DKD) is one of the major causes of end-stage renal disease (ESRD). To evaluate the efficacy and safety of different types of mineralocorticoid receptor antagonists (MRAs) in diabetic kidney disease patients, we conducted this network meta-analysis by performing a systematic search in PubMed, MEDLINE, EMBASE, Web of Science, the Cochrane Library, and Clinicaltrials.gov. A total of 12 randomized clinical trials with 15,492 patients applying various types of MRAs covering spironolactone, eplerenone, finerenone, esaxerenone, and apararenone were included. The efficacy outcomes were the ratio of urine albumin creatine ratio (UACR) at posttreatment vs. at baseline, change in posttreatment estimated glomerular filtration (eGFR) vs. at baseline, and change in posttreatment systolic blood pressure (SBP) vs. at baseline. The safety outcome was the number of patients suffering from hyperkalemia. High-dose finerenone (MD −0.31, 95% CI: −0.52, −0.11), esaxerenone (MD −0.54, 95% CI: −0.72, −0.30), and apararenone (MD −0.63, 95% CI: −0.90, −0.35) were associated with a superior reduction in proteinuria in patients with DKD. Regarding the change in eGFR, the results of all drugs were similar, and finerenone may have potential superiority in protecting the kidney. Compared with placebo, none of the treatments was associated with a higher probability of controlling systolic blood pressure during treatment. Moreover, spironolactone, esaxerenone, and 20 mg of finerenone presented a higher risk of hyperkalemia. This Bayesian network meta-analysis was the first to explore the optimal alternative among MRAs in the treatment of DKD and revealed the superiority of 20 mg of finerenone among MRAs in treating DKD.

Systematic Review Registration: PROSPERO, identifier (CRD42022313826)

KEYWORDS

diabetic kidney disease (DKD), mineralocorticoid receptor antagonists (MRA), type 2 diabetes, hyperkalemia, network meta-analysis (NMA)

1 Introduction

Diabetic kidney disease, or DKD, is a common type of complication among diabetes patients, whose morbidity has risen sharply in recent years (Tuttle et al., 2014). Additionally, as the leading cause of end-stage renal disease (ESRD), DKD causes huge health and economic burdens for both patients and society (Johansen et al., 2021). Although the mechanism of diabetic kidney disease is still unclear, we and others have revealed that diabetic kidney disease may be related to renal fibrosis, among which the relationship between microRNA (miRNA) crosstalk and renal epithelial tubular cell epithelial-mesenchymal transition (EMT) and endothelial-to-mesenchymal transition (EndMT), leads to fibrosis in kidney. (Wang et al., 2014; Zheng et al., 2016; Jia et al., 2019; Srivastava et al., 2019; Wang et al., 2019; Ding et al., 2021; Zheng Y. et al., 2022). Moreover, sirtuins, which are a part of class III HDAC, are associated with various metabolic signs of progress, for example, aging, apoptosis, and inflammation. Studies have demonstrated that the suppression of SIRT3 protein in diabetic kidneys causes abnormal glycolysis, which is related to fibrosis in the kidney. Also, the SIRT3 protein in endothelial cells is linked with. (Liu et al., 2017; Srivastava et al., 2018).

Various treatments have been performed on DKD, while no single class of drugs has presented outstanding efficacy (Doshi and Friedman, 2017). Therefore, the combination of different kinds of drugs should be considered for managing DKD. Both albuminuria and decreased eGFR can be used for the prediction of DKD (Ninomiya et al., 2009), while albuminuria has been the most investigated sign of DKD in various forms, such as the urine albumin creatine ratio (UACR) (Mogensen, 1984). Studies have shown that DKD may be associated with the hyperactivation of the mineralocorticoid receptor (MR) (Jaisser and Farman, 2016). Mineralocorticoid receptor antagonist (MRA) has been proven to effectively protect the cardiovascular system and the kidney by competitively combining with MR (Draznin et al., 2022). Traditional MRAs include spironolactone and eplerenone; however, they are not widely used clinically owing to the high incidence of hyperkalemia (Bomback et al., 2008). Finerenone is a new nonsteroidal MRA with optimal efficacy and safety in treating patients with DKD (Draznin et al., 2022). As a selective nonsteroidal drug, esaxerenone has been proven to have antihypertensive and renal-protective effects (Jankovic and Jankovic, 2022). Apararenone was shown to protect renal functions in patients with DKD in a phase 2 study (Wada et al., 2021).

The existing evidence for the treatment of MRAs in DKD remains unclear (Draznin et al., 2022). Previous meta-analyses related to mineralocorticoid receptor antagonists were mostly about cardiovascular diseases (Yang et al., 2019). Chen et al. (2021) reported that for those who suffered from acute myocardial infarction, mineralocorticoid receptor antagonists reduced cardiovascular adverse events and all-cause mortality. Moreover, finerenone has been proven effective in treating patients with DKD (D'Marco et al., 2021). However, few trials have directly compared the efficacy and safety of MRAs in patients with DKD, and few studies have compared different kinds of mineralocorticoid receptor antagonists with placebo to compare their efficacy and safety outcomes. As an extension of conventional meta-analysis, network meta-analysis (NMA) can compare the results of a series of drugs for a disease simultaneously in the absence of head-to-head evidence to determine the best treatment.

We performed this systematic review and network meta-analysis of randomized clinical trials to compare both traditional and new MRAs in adults with diabetic kidney disease.

2 Methods

This study was conducted according to the PRISMA Extension Statement for Reporting of Systematic Reviews Incorporating Network Meta-analyses of Health Care Interventions: Checklist and Explanations. The protocol of this study was registered with PROSPERO (CRD42022313826).

2.1 Data sources and search strategies

This network meta-analysis was conducted to compare the effect and safety outcomes of five kinds of MRAs on clinical outcomes. We searched PubMed, MEDLINE, EMBASE, Web of Science, the Cochrane Library, and Clinicaltrials.gov from 1 January 2000, to 23 April 2022. The keywords utilized were as follows: "Diabetic Nephropathy," "Diabetic Kidney Disease," "Diabetic Nephropathies," "Diabetic Glomerulosclerosis," "DN," "Kimmelstiel-Wilson Syndrome," "DKD," "nephropathy, diabetic," "Mineralocorticoid Receptor Antagonist," "MRA," "Aldosterone Receptor Antagonist," "antagonists, mineralocorticoid," "antagonist, aldosterone receptor," "spironolactone," "finerenone," "eplerenone," "esaxerenone," "apararenone," "BAY 94-8862," "MT-3995," and "CS-3150." References cited in identified papers and meta-analyses were reviewed in case of neglect. The details of the search strategy are listed in the Supplementary Table S1.

2.2 Study selection and data extraction

The articles were included if they met the inclusion criteria listed as follows: 1) the patients included in the study were adults suffering from T2DM and chronic kidney disease (CKD); 2) studies conducted as randomized clinical trials of treatment groups utilizing MRA and control group using placebo; 3) studies with outcomes of "UACR" or "eGFR" or "SBP" or "adverse event."

Studies were excluded if 1) they were not randomized clinical trials, such as systemic reviews, comments, or case reports; 2) they focused on nonhuman subjects; 3) the studies only contained treatment groups or the control groups did not use placebo; or 4) they lacked basic data for analysis.

Two investigators independently searched articles and extracted data. Any disagreements concerning data were resolved with the third author. We extracted the name of the first author, year of publication, sample size, interventions, follow-up time, efficacy, and safety outcomes.

2.3 Efficacy and safety outcomes

The efficacy outcomes included the ratio of UACR at posttreatment vs. at baseline, change in posttreatment estimated glomerular filtration (eGFR) vs. at baseline, and change in posttreatment systolic blood pressure (SBP) vs. at baseline. The safety outcome was shown as the number of patients suffering from hyperkalemia. Posttreatment was defined as after the end of the administration of MRAs.

2.4 Risk of bias assessment

We used the Cochrane risk of bias tool to assess risk, including seven sections: random sequence generation, allocation concealment, blinding of personnel and participants, blinding of outcome assessment, selective reporting, method of addressing incomplete data, and other bias. For each part, studies were assessed to have a low, high, or unclear risk of bias. A graphic of bias was generated with Review Manager 5.4 (Cochrane Collaboration, Oxford, United Kingdom). Two authors independently assessed bias and any disagreements were resolved by consensus.

2.5 Statistical analysis

This Bayesian network meta-analysis was conducted by R software utilizing the "gemtc" package, which recalled JAGS in R for Markov chain Monte Carlo (MCMC) sampling. Data were analyzed using a random-effect model. Dichotomous outcomes were evaluated by a binomial likelihood model with a logit link function while continuous outcomes were calculated using a normal likelihood model with an identity link function. Risk ratios (RRs) and 95% credible intervals (95% CIs) were used to evaluate dichotomous outcomes, and for continuous outcomes, mean differences (MDs) and 95% CIs were used. Model convergence was assessed utilizing the Brooks–Gelman–Rubin statistic and trace plots. We generated 50,000 iterations for each analysis and discarded the first 10,000 iterations as a burn-in period. To rank each outcome, we utilized surface under the cumulative ranking area (SUCRA) probabilities. The larger the SUCRA was, the higher the probability of an endpoint event. Nodal analyses were used for heterogeneity checks. Over 50% of I^2 indicated significant heterogeneity while I^2 less than 50% indicated little heterogeneity.

3 Results

3.1 Baseline characteristics of the studies

A total of 12,692 studies were retrieved from the databases mentioned above, and 12 studies of 15,492 patients were eligible for our study. The details of the selection are shown in Figure 1. Spironolactone was utilized in four studies, one for eplerenone, four for finerenone, two for esaxerenone, and one for apararenone. The sample size of each study ranged from 35 to 7,352, while the duration of treatment varied from 12 to 152 weeks. Of all studies, 6 reported the ratio of UACR at posttreatment vs. at baseline, 6 provided data on change in posttreatment eGFR vs. at baseline, 5 submitted data on change in posttreatment SBP vs. at baseline, and 10 studies reported the morbidity of hyperkalemia. The overall details of the eligible studies are shown in Table 1.

According to Figure 2, most studies included used randomized grouping methods and applied at least double-blind methods during the treatment. The risk of bias was mainly caused by blinding methods and other biases. Moreover, some studies only provided their results in graphs rather than specific data, so we were incapable of adding their results into our analysis. In Figure 3, the network plot of the Bayesian NMA, nine interventions were reported in the changes of UACR and eGFR at posttreatment vs. at baseline, eight interventions in the change of SBP at posttreatment vs. at baseline, and eleven in hyperkalemia. The detailed SUCRAs of efficacy and safety outcomes was shown in Table 2. The results of the network meta-analysis were shown in Tables 3–6. Figure 4 reports the SUCRA figure of each outcome, and the heterogeneity plot is shown in Supplementary Figure S1.

3.2 Efficacy outcomes

3.2.1 Ratio of urine albumin creatine ratio at posttreatment vs. at baseline

Compared with placebo, the efficacy of finerenone in reducing albuminuria was observed to be dose-dependent, because a high dose of finerenone could effectively reduce UACR in DKD patients (MD −0.31, 95% CI: −0.52, −0.11), while apararenone (MD −0.63, 95% CI: −0.90, −0.35) and esaxerenone (MD −0.54, 95% CI: −0.72, −0.30) significantly

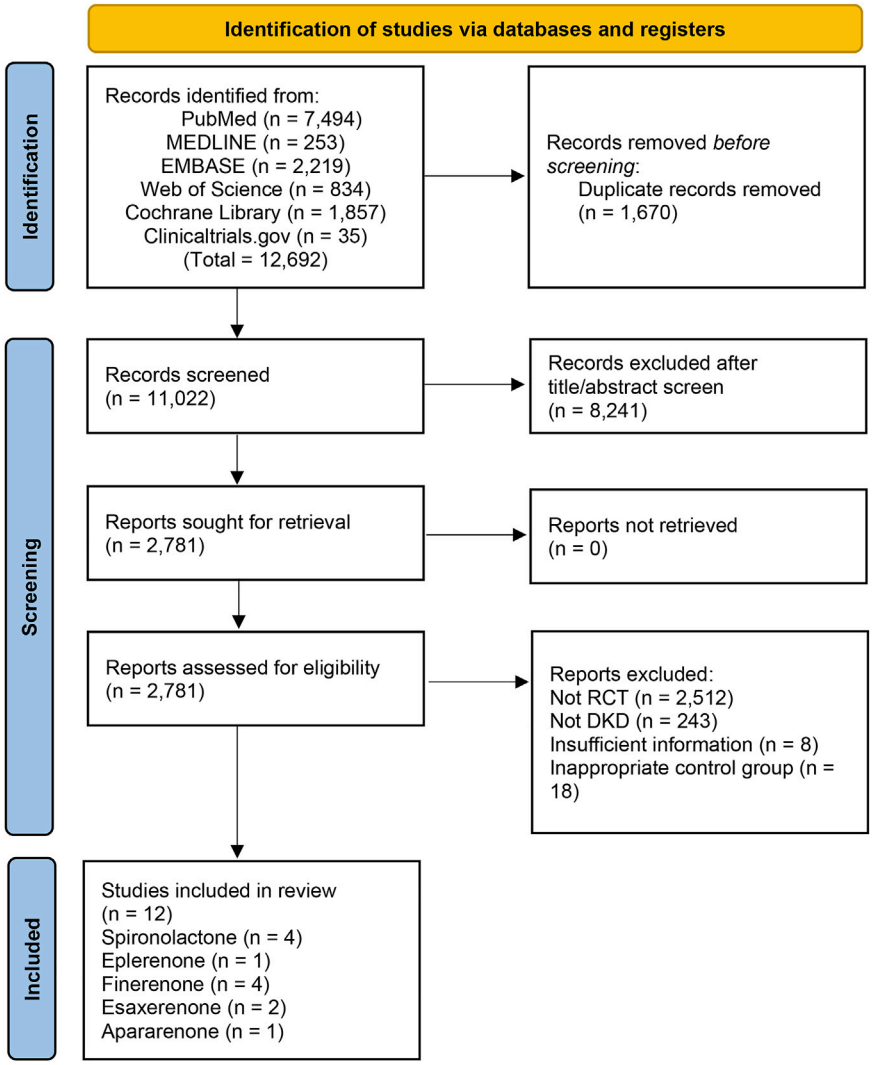

FIGURE 1
PRISMA flow diagram used for study selection.

remised proteinuria in patients with DKD. The results of the network meta-analysis are shown in Figure 5A. Ranking all treatments reported ratio of UACR at posttreatment vs. at baseline, we found that apararenone was superior in reducing proteinuria in patients with DKD (SUCRA 95.88%), followed by esaxerenone (SUCRA 89.04%) and 20 mg of finerenone (SUCRA 71.16%) (Figure 4A).

3.2.2 Change in posttreatment estimated glomerular filtration vs. baseline

We found that all treatments were similar in eGFR change since compared with placebo, none of the drugs showed significant changes in eGFR (Figure 5B). Ranking all treatments that reported changes in eGFR at posttreatment vs. at baseline, we found that 1.25 mg of finerenone was superior in maintaining kidney function in patients with DKD (SUCRA 69.92%), followed by 5 mg of finerenone (SUCRA 66.72%), 2.5 mg of finerenone (SUCRA 56.37%), 7.5 mg of finerenone (SUCRA 51.82%), 15 mg of finerenone (SUCRA 46.56%), 20 mg of finerenone (SUCRA 46.48%), 10 mg of finerenone (SUCRA 39.01%), and esaxerenone (SUCRA 32.67%), while spironolactone had the lowest possibility of maintaining kidney function (SUCRA 14.68%) (Figure 4B).

3.2.3 Change in posttreatment SBP vs. baseline

We found that none of the treatments showed significant changes in SBP (Figure 5C). Ranking all treatments that reported changes in SBP at posttreatment vs. at baseline, we found that spironolactone was superior in reducing SBP (SUCRA 79.19%), followed by 20 mg of finerenone (SUCRA 65.76%), 7.5 mg of

TABLE 1 Baseline characteristics of eligible studies.

Study	Country	Age (T/C)	Sample size (T/C)	Intervention (T/C)	Duration of treatment	Duration of follow-up	Outcomes
Bakris 2015(Bakris et al., 2015)	United States	64.33 ± 9.21/ 63.26 ± 8.68	727/94	RAS blocker + Finerenone (1.25, 2.5, 5, 7.5, 10, 15, 20 mg)/RAS blocker + placebo	90 days	-	①②③④
Bakris 2020(Bakris et al., 2020)	United States	65.4 ± 8.9/ 65.7 ± 9.2	2,833/2,841	RAS blocker + Finerenone (10 mg, 20 mg)/RAS blocker + placebo	44 weeks	-	②④
Katayama 2017(Katayama et al., 2017)	Japan	62.40 ± 9.80/ 66.75 ± 9.02	84/12	RAS blocker + Finerenone (1.25, 2.5, 5, 7.5, 10, 15, 20 mg)/RAS blocker + placebo	90 days	30 days	①③④
Pitt 2021(Pitt et al., 2021)	United States	64.1 ± 9.7/ 64.1 ± 10.0	3,686/3,666	RAS blocker + Finerenone (10 mg, 20 mg)/RAS blocker + placebo	54 weeks	-	①②④
Epstein 2006(Epstein et al., 2006)	United States	60/58	177/91	Eplerenone (50 mg, 100 mg) + enalapril/placebo + enalapril	12 weeks	-	④
Ito 2019(Ito et al., 2019)	Japan	65.3 ± 9.3/ 66.0 ± 10.0	285/73	ACEi/ARB + Esaxerenone (0.625, 1.25, 2.5, 5 mg)/ACEi/ARB + placebo	12 weeks	6 weeks	①②④
Ito 2020(Ito et al., 2020b)	Japan	66 ± 10/ 66 ± 9	222/227	ACEi/ARB + Esaxerenone (1.25–2.5 mg)/ACEi/ARB + placebo	52 weeks	-	①④
Mehdi 2009(Mehdi et al., 2009)	United States	49.3 ± 8.8/ 51.7 ± 9.3	27/27	Lisinopril + Spironolactone (25 mg)/lisinopril + placebo	48 weeks	4 weeks	④
Wada 2021(Wada et al., 2021)	Japan	62.3 ± 9.0/ 60.1 ± 10.0	220/72	ACEi/ARB + Apararenone (2.5, 5, 10 mg)/ACEi/ARB + placebo	24 weeks	8 weeks	①②
Momeni 2015(Momeni et al., 2015)	Iran	58.9 ± 9.3/ 55.4 ± 8.9	20/20	Hydrochlorothiazide + Spironolactone (50 mg)/ hydrochlorothiazide + placebo	12 weeks	-	③
van den Meiracker 2006(van den Meiracker et al., 2006)	Netherland	29-78	24/29	ACEi/ARB + Spironolactone (20–40 mg)/ACEi/ARB + placebo	52 weeks	-	②③④
Kota 2012(Kumar Kota et al., 2012)	India	45.6 ± 13.1/ 48.1 ± 12.5	19/16	ACEi/ARB + Spironolactone (25 mg)/ACEi/ARB + placebo	12 weeks	-	③④

Notes: T, treatment group; C, control group; -, Not mentioned; ①, ratio of UACR at posttreatment vs. at baseline; ②, change in posttreatment eGFR vs. at baseline; ③, change in posttreatment SBP vs. at baseline; ④, morbidity of hyperkalemia.

finerenone (SUCRA 59.81%), 10 mg of finerenone (SUCRA 50.66%), 15 mg of finerenone (SUCRA 48.88%), 2.5 mg of finerenone (SUCRA 41.68%), 5 mg of finerenone (SUCRA 35.96%), and 1.25 mg of finerenone (SUCRA 33.55%) (Figure 4C).

3.3 Safety outcomes

We found that spironolactone (RR 8.4, 95% CI 3.2, 36.0), esaxerenone (RR 4.1, 95% CI 1.8, 11.0), and 20 mg of finerenone (RR 2.0, 95% CI 1.8, 2.3) had significant risks of increasing the morbidity of hyperkalemia (Figure 5D). Ranking all treatments reported morbidity of hyperkalemia at posttreatment vs. at baseline, we found that 10 mg of finerenone was associated with the lowest possibility of leading to hyperkalemia among all drugs (SUCRA 6.36%), followed by 2.5 mg of finerenone (SUCRA 6.58%), 5 mg of finerenone (SUCRA 46.36%), and spironolactone was associated with the highest possibility of increasing the morbidity of hyperkalemia (SUCRA 86.94%) (Figure 4D).

4 Discussion

Although MRAs have been proven effective in decreasing albuminuria in addition to RAAS blockers (Lozano-Maneiro and Puente-Garcia, 2015; Chung et al., 2020), few head-to-head studies have been performed to assess the efficacy of individual MRAs. In addition, previous meta-analyses related to MRAs focused on either a specific kind of MRA (Zhao et al., 2016; Zheng et al., 2022); or different classes of drugs (Elliott and Meyer, 2007), so the existing evidence of MRAs treating DKD is limited. This study suggested the priority of several new nonsteroidal MRAs in reducing albuminuria. None of the treatments included was associated with significant risks of worsening kidney function. The efficacy of MRAs in controlling the systolic blood pressure of DKD patients remains unclear. Meanwhile, spironolactone, esaxerenone, and 20 mg of finerenone demonstrated higher morbidity of hyperkalemia in patients suffering from chronic kidney disease and T2DM.

10.3389/fphar.2022.967317

TABLE 2 SUCRAs of treatments according to efficacy and safety outcomes.

	1.25 mg finerenone	2.5 mg finerenone	5 mg finerenone	7.5 mg finerenone	10 mg finerenone	15 mg finerenone	20 mg finerenone	esaxerenone	eplerenone	Spironolactone	Apararenone
UACR	21.17	19.41	26.86	53.43	51.69	58.69	71.16	89.04	—	—	95.88
eGFR	69.92	56.37	66.72	51.82	39.01	46.56	46.48	32.67	—	14.68	—
SBP	33.55	41.68	35.96	59.81	50.66	48.88	65.76	—	—	79.19	—
Hyperkalemia	68.53	6.58	46.36	47.33	6.36	61.31	53.48	73.23	48.13	86.94	69.36

Our network meta-analysis indicated that several new non-steroidal mineralocorticoid receptor antagonists, including apararenone, esaxerenone, and 20 mg of finerenone, could significantly reduce the UACR in patients with DKD, which is consistent with a recent meta-analysis indicating that finerenone has an optimal effect on albuminuria in patients with DKD (Zheng et al., 2022). While apararenone is still in clinical trials, and esaxerenone is used for hypertension treatment, more trials are needed to systematically evaluate the renoprotection efficacy of esaxerenone and apararenone in patients with DKD. Compared with esaxerenone and apararenone, 20 mg of finerenone included more evidence from thousands of participants, which presented a more comprehensive reflection of its effect.

Both the results of our NMA and ranking SUCRAs revealed that most included MRA could not significantly impact kidney functions, while finerenone was associated with potential priority in protecting kidney function and spironolactone was in connection to the decrease of eGFR, according to the ranking SUCRA, which was consistent with another meta-analysis published before (Pei et al., 2018). Chung et al. (2020) reported that spironolactone significantly decreased eGFR in patients with chronic kidney disease with or without diabetes. For several nonsteroid MRAs, however, eGFR decreased after the administration of MRAs and returned to baseline during the follow-up period, which suggested that no severe damage was caused by drug administration (Ito et al., 2019; Wada et al., 2021). The decrease in eGFR reduction in spironolactone shown in Figure 4 might be related to the acute kidney injury caused by steroidal MRAs, and the potential priority of finerenone in NMA revealed greater benefits of finerenone in kidney protection with no dose-dependency observed (Barrera-Chimal et al., 2022). The possible reasons for the different conclusions about spironolactone in impact on kidney function may be the heterogeneity of eligible studies such as different durations of studies, and different baseline information of patients.

Regarding controlling blood pressure, no significant superiority was observed in spironolactone or finerenone compared with placebo; however, spironolactone may have greater priority in controlling blood pressure compared with finerenone, according to the SUCRAs. As a steroid MRA, spironolactone is known for its antihypertensive efficacy by crossing the blood-brain barrier, binding to mineralocorticoid receptors in the brain, and inhibiting the excitation of central sympathetic activity, thus lowering blood pressure (Gomez-Sanchez and Gomez-Sanchez, 2012). A meta-analysis indicated that for patients with resistant hypertension, spironolactone could effectively control both systolic and diastolic blood pressure (Zhao et al., 2017). Moreover, Lin et al. (2021) showed that spironolactone could reduce the hypertensive situation of patients with diabetes. Hou et al. (2015) revealed that the add-on therapy of spironolactone could slow down the progression of DKD due to its

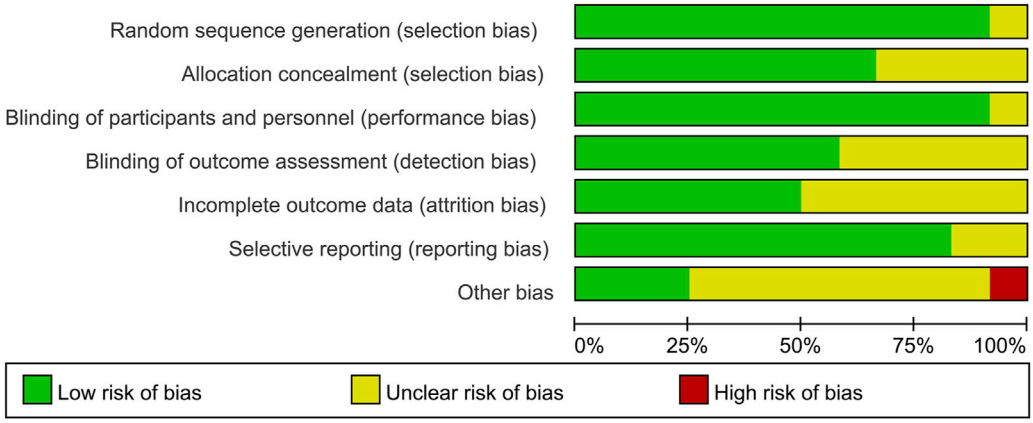

FIGURE 2
Risk of bias graph. The green symbols indicate for low risk of bias, the yellow symbols indicate for unclear risk of bias, and the red symbols indicate for high risk of bias. This figure was generated using Review Manager Version 5.4.

antihypertensive use. However, in our NMA, spironolactone did not demonstrate significant antihypertensive effects. This may be related to the different baselines of patients; some suffered from hypertension, while others did not. Hence, further studies are needed to determine the antihypertensive efficacy of MRAs in DKD patients. For patients with stage 2 to stage 4 CKD and diabetes, finerenone did not show great blood pressure lowering effect compared with steroidal MRAs. However, phase 3 trials of finerenone demonstrated that finerenone could significantly reduce cardiovascular events in patients with T2DM and CKD (Lerma et al., 2022). Esaxerenone has been proven to have greater efficacy in hypertension therapy than recommended doses of eplerenone. (Ito et al., 2020a). Esaxerenone has been put into clinical use in Japan (Wan et al., 2021). Apararenone is still under clinical trials, and its antihypertensive efficacy should be studied further.

Previous studies have reported hyperkalemia as a common adverse event of MRAs. Our NMA showed that spironolactone, esaxerenone, and 20 mg of finerenone could significantly increase the morbidity of hyperkalemia compared with a placebo. The mechanism between MRAs and hyperkalemia has already been revealed. Aldosterone binds to receptors in renal collecting tubules, which can increase epithelial sodium channels (ENaC) and K + -Na + -ATPase to promote reabsorption of Na + as well as the secretion of K+ (Rico-Mesa et al., 2020). MRAs obstruct aldosterone by competitively binding to mineralocorticoid receptors, thus raising serum potassium levels and even leading to hyperkalemia. Previous studies have revealed that spironolactone and eplerenone have a higher proportion of mineralocorticoid receptors in the kidney, while finerenone has less (Kolkhof and Borden, 2012). Therefore, the morbidity of hyperkalemia in patients administered finerenone should be lower. Hou et al. (2015) indicated that spironolactone could significantly increase the serum potassium level in patients with DKD , which is consistent with our study. Zuo and Xu (2019) revealed that for DKD patients, finerenone had a lower risk of causing hyperkalemia than eplerenone and spironolactone. Eplerenone was used for DKD in various animal experiments and was proven to be effective in decreasing proteinuria (Vodosek et al., 2021). Few studies have been published using eplerenone in DKD patients, although with little increase in serum potassium levels, eplerenone has been banned for treating patients with albuminuria and type 2 diabetes for arterial hypertension (Kloner, 2003). The results of our study suggested that only some doses of finerenone were associated with lower risks of hyperkalemia than those administered eplerenone. The possible reasons may be that the clinical evidence of eplerenone treating DKD was limited, while four studies applying finerenone were eligible in our study, and the duration of treatments was also longer, so the exploration of finerenone was also more comprehensive. Moreover, one study of esaxerenone indicated that the increase in serum potassium level may be related to the decrease in eGFR or higher baseline serum potassium content (Kintscher et al., 2021). The serum potassium level of patients receiving apararenone for treatment increased significantly in a dose-dependent manner, but no patients discontinued the treatment because of hyperkalemia (Wada et al., 2021). Considering that more clinical evidence is needed for esaxerenone and apararenone (Kintscher et al., 2021), finerenone may be the optimal treatment for DKD in controlling hyperkalemia among various MRAs at present.

Concerning the cardiovascular outcomes of MRAs for DKD patients, we found that spironolactone and eplerenone have been proven effective in treating hypertension, and one meta-analysis showed that in addition to ACEI/ARB, MRA could significantly

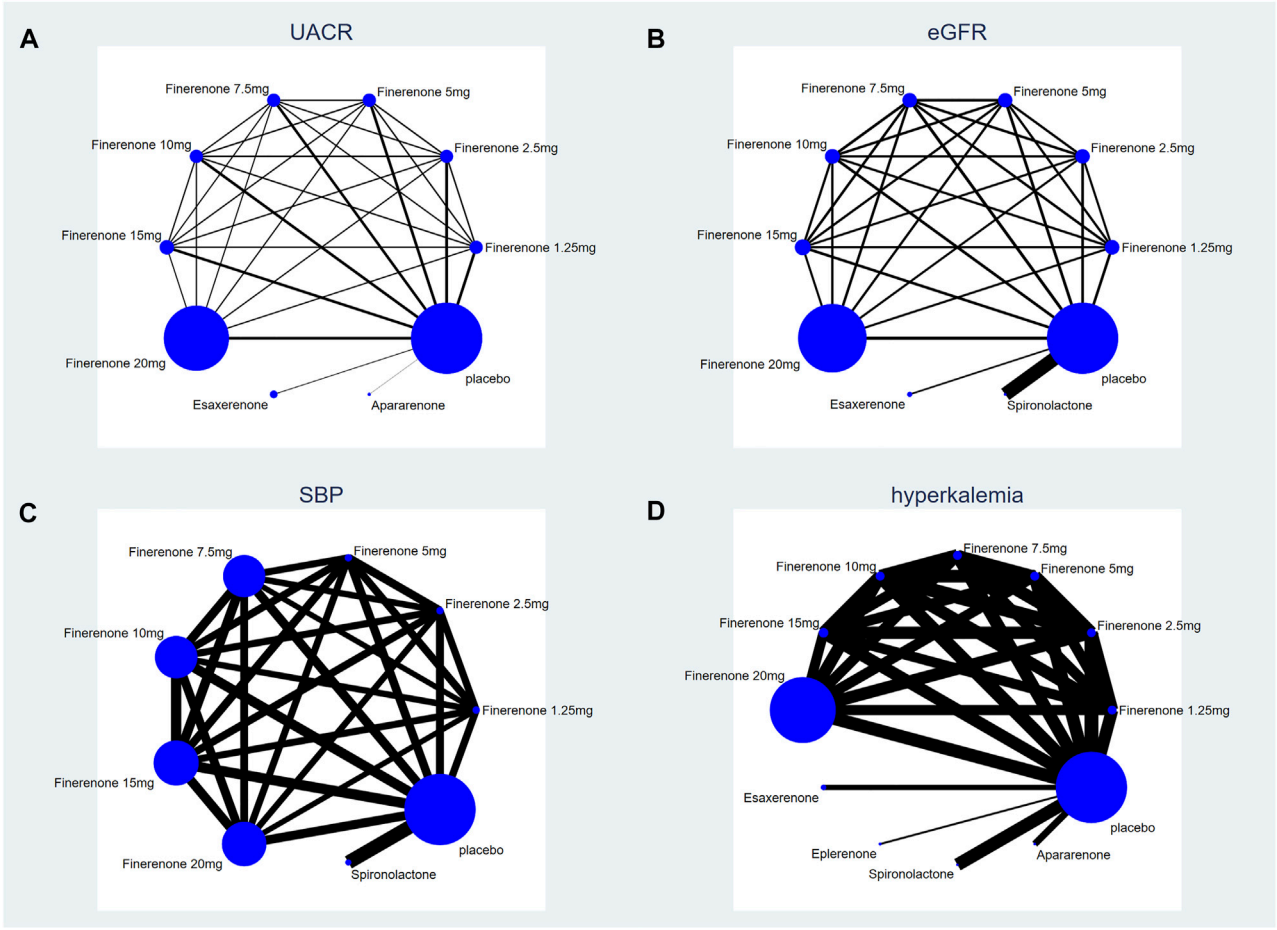

FIGURE 3
Network plot of treatment comparisons. **(A)** UACR at posttreatment vs. at baseline; **(B)** eGFR at posttreatment vs. at baseline; **(C)** SBP at posttreatment vs. at baseline; **(D)** number of patients suffering from hyperkalemia. The size of the blue nodes is proportional to the number of participants included in the interventions. Interventions are shown by lines, whose thickness represents the number of trials included in our study).

reduce systolic and diastolic blood pressure in patients with proteinuric CKD. However, due to the high risk of adverse events such as hyperkalemia and gynecomastia, therapy using spironolactone and eplerenone in proteinuric CKD has been largely replaced by better methods (Lytvyn et al., 2019). Compared with placebo, finerenone could significantly reduce the incidence of cardiovascular outcomes, including cardiovascular death, nonfatal stroke, and nonfatal myocardial infarction, with less hyperkalemia risk (Filippatos et al., 2021). In summary, compared with other MRAs, 20 mg of finerenone has been proven effective in improving proteinuria with more supporting evidence, maintained kidney function, superior cardiovascular protection, and acceptable incidence of an adverse event.

Several new drugs and therapies have been developed for the treatment of diabetic kidney disease. Studies have shown that ACE inhibitors are related to alleviating DKD through DPP-4 and TGFβ pathways. (Srivastava et al., 2020). Some patients in the included studies used sodium-glucose cotransporter-2 (SGLT2) inhibitors for glucose-lowering therapy. Neuen et al. (2022) found that SGLT2 inhibitors can reduce the risk of hyperkalemia in patients with T2DM and chronic kidney disease. Moreover, studies have shown that SGLT2 inhibitors have not only renoprotective but also cardioprotective effects in patients with CKD (Sarafidis et al., 2021). Several MRAs have been proven effective in CKD therapy. However, studies combining MRAs with SGLT2 inhibitors are limited. A preclinical study showed that the combination of finerenone and empagliflozin could improve cardiovascular and renal outcomes in a model with hypertension-induced cardiorenal disease (Kolkhof et al., 2021). Rossing et al. (2022) indicated that receiving SGLT2 inhibitors in addition to finerenone was associated with greater UACR improvement, while kidney and cardiovascular

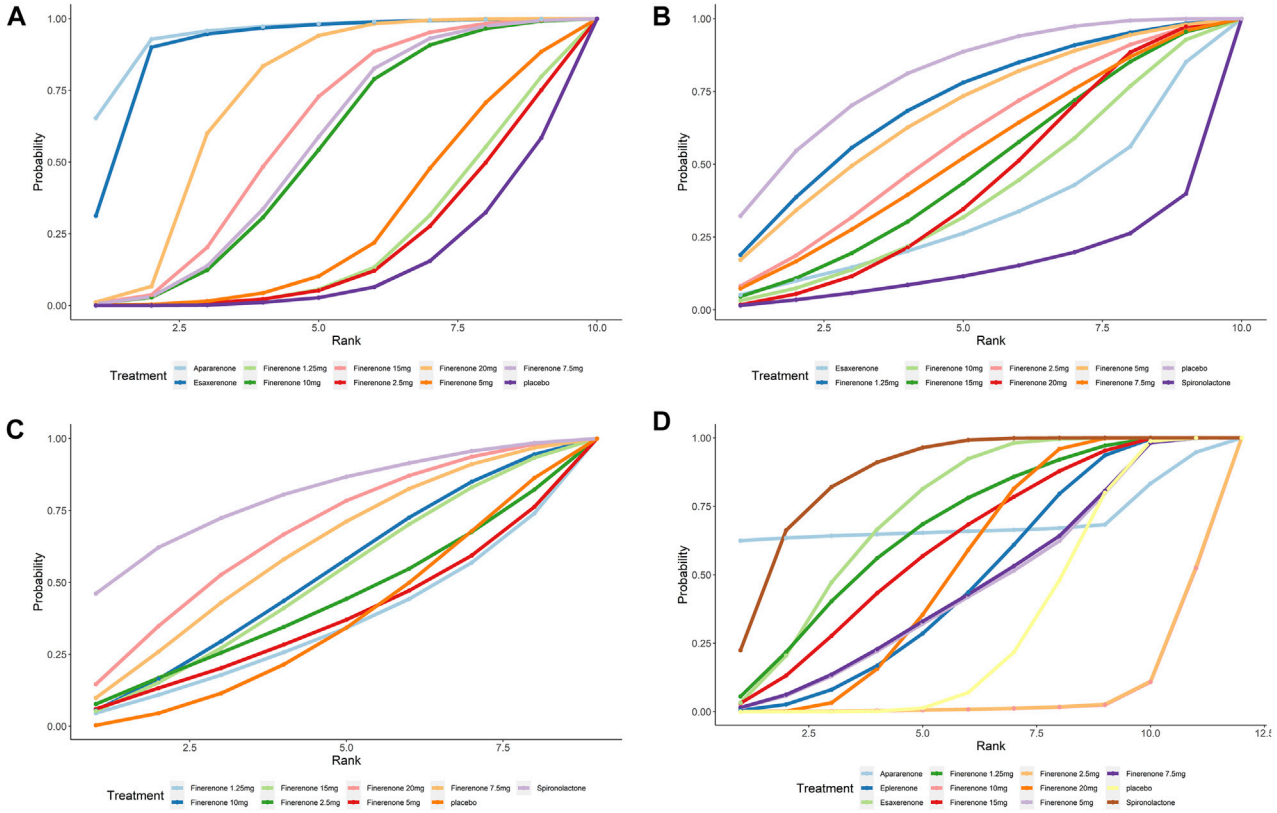

FIGURE 4
SUCRA probabilities for the effectiveness and safety outcomes of interventions. **(A)** UACR at posttreatment vs. at baseline; **(B)** eGFR at posttreatment vs. at baseline; **(C)** SBP at posttreatment vs. at baseline; **(D)** number of patients suffering from hyperkalemia. A higher SUCRA indicates a higher probability that the drug can reach the endpoint. For example, a higher SUCRA in 5A indicates that the drug has a better effect on UACR decrease).

TABLE 3 Network meta-analysis of UACR (lower left).

Finerenone 1.25 mg									
0.99 (0.75, 1.3)	Finerenone 2.5 mg								
1.03 (0.78, 1.36)	1.04 (0.79, 1.37)	Finerenone 5 mg							
1.18 (0.91, 1.53)	1.19 (0.92, 1.55)	1.14 (0.89, 1.48)	Finerenone 7.5 mg						
1.17 (0.9, 1.52)	1.18 (0.9, 1.54)	1.14 (0.87, 1.47)	0.99 (0.77, 1.27)	Finerenone 10 mg					
1.21 (0.92, 1.54)	1.23 (0.93, 1.57)	1.18 (0.9, 1.5)	1.03 (0.79, 1.29)	1.04 (0.8, 1.32)	Finerenone 15 mg				
1.29 (1.01, 1.65)	1.31 (1.02, 1.67)	1.26 (0.98, 1.6)	1.1 (0.87, 1.37)	1.11 (0.88, 1.4)	1.07 (0.86, 1.36)	Finerenone 20 mg			
1.62 (1.1, 2.26)	1.64 (1.11, 2.29)	1.57 (1.07, 2.19)	1.38 (0.93, 1.9)	1.39 (0.95, 1.94)	1.34 (0.94, 1.86)	1.25 (0.91, 1.64)	Esaxerenone		
1.78 (1.18, 2.62)	1.8 (1.2, 2.64)	1.72 (1.15, 2.55)	1.51 (1, 2.2)	1.52 (1.02, 2.24)	1.46 (1, 2.18)	1.37 (0.97, 1.92)	1.09 (0.8, 1.58)	Apararenone	
0.95 (0.7, 1.26)	0.96 (0.71, 1.28)	0.92 (0.69, 1.22)	0.81 (0.6, 1.06)	0.81 (0.61, 1.07)	0.78 (0.6, 1.03)	0.73 (0.59, 0.89)	0.59 (0.48, 0.74)	0.53 (0.41, 0.7)	placebo

TABLE 4 Network meta-analysis of eGFR (lower left).

Finerenone 1.25 mg									
2.44 (0, 5,027.18)	Finerenone 2.5 mg								
1.2 (0, 2,325.71)	0.5 (0, 1,101.05)	Finerenone 5 mg							
3.27 (0, 6,952.97)	1.33 (0, 3,267.24)	2.69 (0, 6,273.5)	Finerenone 7.5 mg						
7.35 (0, 16,355.21)	3.1 (0, 6,306.9)	5.96 (0, 13,186.77)	2.28 (0, 7,065.87)	Finerenone 10 mg					
4.53 (0, 10,182.99)	1.88 (0, 3,976.36)	3.7 (0, 9,554.33)	1.35 (0, 3,320.35)	0.61 (0, 1,425.72)	Finerenone 15 mg				
5.69 (0, 7,004.93)	2.31 (0, 3,046.62)	4.66 (0, 6,051.47)	1.71 (0, 2,364.52)	0.78 (0, 926.75)	1.26 (0, 1,268.32)	Finerenone 20 mg			
14.53 (0, 520,116.44)	6.06 (0, 197,478.6)	11.47 (0, 550,938.04)	4.49 (0, 212,097.79)	1.94 (0, 76,190.83)	3.19 (0, 118,525.24)	2.58 (0, 26,873.07)	Esaxerenone		
212.81 (0.01, 1,714,689.05)	89.78 (0, 779,941.88)	169.75 (0.01, 1,791,763.97)	64.84 (0, 609,453.8)	28.03 (0, 249,203.46)	49.68 (0, 373,124.62)	36.92 (0, 111,704.93)	14.25 (0, 159,865.75)	Spironolactone	
0.54 (0, 868.12)	0.23 (0, 305.37)	0.44 (0, 840.79)	0.17 (0, 272.31)	0.07 (0, 106.41)	0.12 (0, 149.02)	0.09 (0, 24.82)	0.04 (0, 93.71)	0 (0, 3.8)	Placebo

TABLE 5 Network meta-analysis of SBP (lower left).

Finerenone 1.25 mg								
30.61 (0, 3.69e+20)	Finerenone 2.5 mg							
2.65 (0, 2.97e+19)	0.08 (0, 3.21e+17)	Finerenone 5 mg						
3.31e+4 (0, 1.29e+21)	1,032.82 (0, 2.59e+19)	12,053.12 (0, 1.89e+21)	Finerenone 7.5 mg					
1,465.01 (0, 6.84e+19)	39.35 (0, 2.79e+18)	465.79 (0, 4.98e+19)	0.04 (0, 9.22e+11)	Finerenone 10 mg				
712.53 (0, 3.85e+19)	25.26 (0, 1.36e+18)	273.72 (0, 3.45e+19)	0.02 (0, 2.52e+11)	0.61 (0, 8.13e+12)	Finerenone 15 mg			
2.83e+5 (0, 1.36e+22)	8661.49 (0, 3.73e+20)	97,026.08 (0, 1.23e+22)	8.75 (0, 1.05e+14)	215.6 (0, 1.80e+15)	394.28 (0, 8.60e+15)	Finerenone 20 mg		
5.17e+8 (0, 1.35e+28)	1.47e+7 (0, 1.14e+27)	1.77e+8 (0, 2.07e+28)	13,591.8 (0, 1.167e+21)	337,539.68 (0, 3.49e+22)	6.24e+05 (0, 6.16e+22)	1,656.86 (0, 1.36e+20)	Spironolactone	
8.28 (0, 2.53e+17)	0.22 (0, 114e+16)	3 (0, 2.69e+17)	0 (0, 1.58e+9)	0.01 (0, 9.50e+10)	0.01 (0, 1.48e+11)	0 (0, 4.51e+08)	0 (0, 603.71)	Placebo

outcomes remained consistent whether SGLT2 inhibitors were used. In addition, in an extended analysis of dapagliflozin in the treatment of CKD patients with or without diabetes, we found that the efficacy of dapagliflozin in renal protection remains similar in CKD patients with or without MRAs prescribed before (Provenzano et al., 2022). Interrelated to MR, glucocorticoid receptor (GR) is known as an antifibrotic molecule in the development of DKD. Preclinical studies have indicated that diabetes promotes the development of renal fibrosis in mice lack of GR compared to control mice, which is related to abnormal cytokine and chemokine reprogramming and upgraded Wnt signaling. (Srivastava et al., 2021).

Our study has some limitations. First, the number of comparisons and sample size varied, thus some large-sample studies may influence the overall result more than those with small sample sizes. Second, no outcomes included all 12 trials, which may cause potential bias. Third, varied baseline treatments, such as whether ACEIs/ARBs were used during treatment, significantly impacted the clinical outcomes. Fourth, some kinds of drugs had a small number

TABLE 6 Network meta-analysis of hyperkalemia (lower left).

Finerenone 1.25 mg											
1.37e+9 (4.45, 8.69e+28)	Finerenone 2.5 mg										
2.57 (0.22, 84.84)	0 (0, 0.73)	Finerenone 5 mg									
2.5 (0.2, 81.41)	0 (0, 0.69)	0.96 (0.02, 39.89)	Finerenone 7.5 mg								
1.61e+9 (4.85, 1.89e+29)	1.33 (0, 2.08e+22)	5.76e+8 (1.42, 5.58e+28)	5.76e+8 (1.38, 5.91e+28)	Finerenone 10 mg							
1.32 (0.14, 12.45)	0 (0, 0.29)	0.5 (0.01, 6.53)	0.52 (0.02, 6.93)	0 (0, 0.28)	Finerenone 15 mg						
1.78 (0.19, 16.8)	0 (0, 0.37)	0.69 (0.02, 8.72)	0.71 (0.02, 9.34)	0 (0, 0.35)	1.35 (0.14, 12.84)	Finerenone 20 mg					
0.88 (0.08, 9.5)	0 (0, 0.19)	0.33 (0.01, 4.97)	0.34 (0.01, 5.24)	0 (0, 0.18)	0.66 (0.06, 7.13)	0.5 (0.18, 1.14)	Esaxerenone				
2.18 (0.17, 26.32)	0 (0, 0.48)	0.81 (0.02, 13.07)	0.84 (0.02, 14.79)	0 (0, 0.46)	1.64 (0.13, 19.88)	1.24 (0.33, 3.56)	2.49 (0.55, 10.4)	Eplerenone			
0.41 (0.03, 4.89)	0 (0, 0.09)	0.15 (0, 2.54)	0.16 (0, 2.72)	0 (0, 0.08)	0.31 (0.02, 3.75)	0.24 (0.06, 0.64)	0.47 (0.09, 1.94)	0.19 (0.03, 0.98)	Spironolactone		
0 (0, 1.08e+14)	0 (0, 3.78e+7)	0 (0, 3.64e+13)	0 (0, 3.84e+13)	0 (0, 4.79e+7)	0 (0, 8.70e+13)	0 (0, 6.46e+13)	0 (0, 1.74e+14)	0 (0, 5.59e+13)	0 (0, 3.09e+14)	Apararenone	
3.63 (0.39, 34.29)	0 (0, 0.77)	1.4 (0.04, 17.86)	1.45 (0.04, 18.98)	0 (0, 0.71)	2.75 (0.29, 26.11)	2.03 (1.82, 2.27)	4.07 (1.8, 10.89)	1.65 (0.57, 6.03)	8.49 (3.2, 35.66)	1.63e+4 (0, 1.92e+26)	Placebo

10.3389/fphar.2022.967317

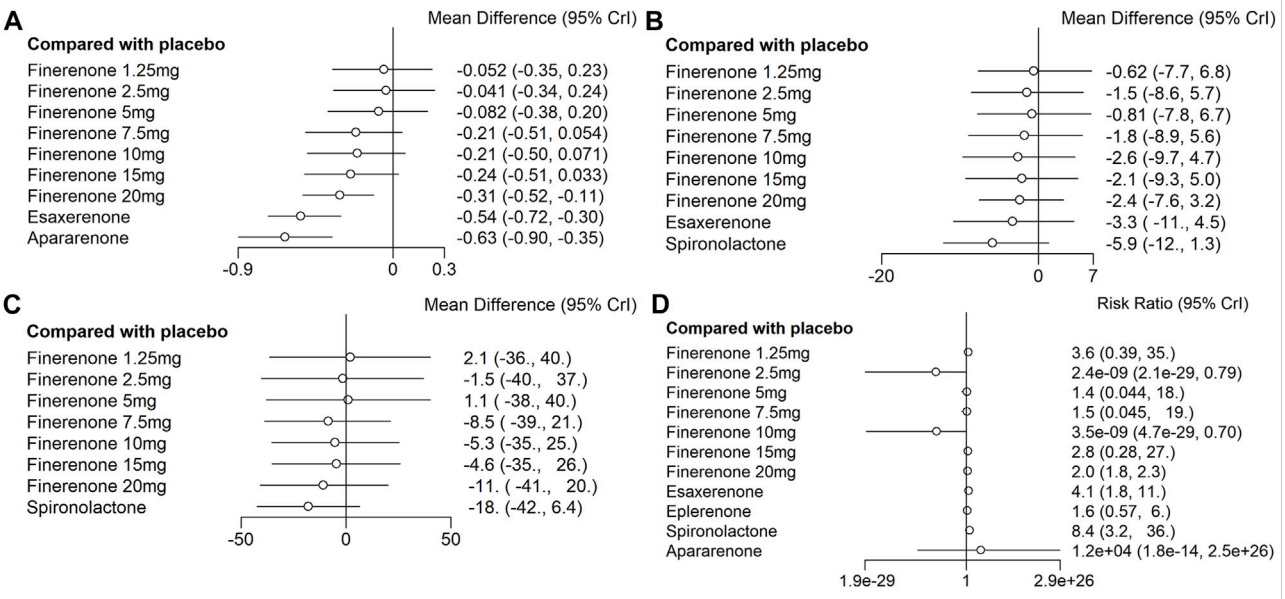

FIGURE 5
Data of network comparison between placebo and MRAs. **(A)** UACR at posttreatment vs. at baseline; **(B)** eGFR at posttreatment vs. at baseline; **(C)** SBP at posttreatment vs. at baseline; **(D)** number of patients suffering from hyperkalemia).

of treatments included, causing unknown bias or uncertainty. Fifth, hyperkalemia was the only adverse event analyzed. Sixth, no subgroup analysis was performed in this NMA. The seventh, head-to-head comparison was absent in this NMA due to the absence of direct comparisons between different MRAs in patients with DKD. Eighth, due to a lack of data, spironolactone and eplerenone were not included in the superiority analysis of UACR, which can be further explored in the future. In the future, relevant trials can focus on the direct head-to-head comparison administrating different kinds of MRAs for DKD patients. Meanwhile, the mechanism of DKD should be explored further and more new therapies and drugs including glycolysis inhibitors, ROCK isoforms, and SIRT3 still need further study.

This study systematically searched existing RCTs of MRAs on patients with DKD, and we may recommend the use of 20 mg finerenone in DKD treatment compared with other types of MRAs based on existing data. Further head-to-head studies combining SGLT2 inhibitors with different MRAs may support this conclusion.

Data availability statement

The original contributions presented in the study are included in the article/Supplementary Material, further inquiries can be directed to the corresponding author.

Author contributions

YW, ZZ, and YJ designed this meta-analysis, YW and HL performed the search strategies and data extraction. YT, YX, and JC helped to assess the quality of the studies. YW wrote the original draft of the manuscript, which was revised by ZZ and YJ. All authors made great contributions to the manuscript and approved it for submission.

Funding

This work was supported by research grants from the National Natural Science Foundation of China (Nos. 82000785 and 81700730), the Natural Science Foundation of Guangdong (Nos. 2019A1515110661 and 2017A030313555), the Guangzhou Science and Technology Project (202201010971), the Outstanding Youth Development Scheme of Nanfang Hospital, Southern Medical University (No. 2019J010), and the Undergraduate Innovation and Entrepreneurship Training Program, Southern Medical University (No. 202112121007).

Acknowledgments

We would like to sincerely express our gratitude for the support of all participants in this study.

Conflict of interest

The authors declare that the research was conducted in the absence of any commercial or financial relationships that could be construed as a potential conflict of interest.

Publisher's note

All claims expressed in this article are solely those of the authors and do not necessarily represent those of their affiliated organizations, or those of the publisher, the editors and the reviewers. Any product that may be evaluated in this article, or claim that may be made by its manufacturer, is not guaranteed or endorsed by the publisher.

Supplementary material

The Supplementary Material for this article can be found online at: https://www.frontiersin.org/articles/10.3389/fphar.2022.967317/full#supplementary-material

References

Bakris, G. L., Agarwal, R., Anker, S. D., Pitt, B., Ruilope, L. M., Rossing, P., et al. (2020). Effect of finerenone on chronic kidney disease outcomes in type 2 diabetes. *N. Engl. J. Med.* 383, 2219–2229. doi:10.1056/NEJMoa2025845

Bakris, G. L., Agarwal, R., Chan, J. C., Cooper, M. E., Gansevoort, R. T., Haller, H., et al. (2015). Effect of finerenone on albuminuria in patients with diabetic nephropathy: A randomized clinical trial. *JAMA* 314, 884–894. doi:10.1001/jama.2015.10081

Barrera-Chimal, J., Lima-Posada, I., Bakris, G. L., and Jaisser, F. (2022). Mineralocorticoid receptor antagonists in diabetic kidney disease - mechanistic and therapeutic effects. *Nat. Rev. Nephrol.* 18, 56–70. doi:10.1038/s41581-021-00490-8

Bomback, A. S., Kshirsagar, A. V., Amamoo, M. A., and Klemmer, P. J. (2008). Change in proteinuria after adding aldosterone blockers to ace inhibitors or angiotensin receptor blockers in ckd: A systematic review. *Am. J. Kidney Dis.* 51, 199–211. doi:10.1053/j.ajkd.2007.10.040

Chen, Q., Zhao, D., Sun, J., and Lu, C. (2021). Aldosterone blockade in acute myocardial infarction: A systematic review and meta-analysis. *Cardiovasc. Ther.* 2021, 1710731. doi:10.1155/2021/1710731

Chung, E. Y., Ruospo, M., Natale, P., Bolignano, D., Navaneethan, S. D., Palmer, S. C., et al. (2020). Aldosterone antagonists in addition to renin angiotensin system Antagonists for preventing the progression of chronic kidney disease. *Cochrane Database Syst. Rev.* 10, CD007004. doi:10.1002/14651858.CD007004.pub4

D'Marco, L., Puchades, M. J., Gandia, L., Forquet, C., Gimenez-Civera, E., Panizo, N., et al. (2021). Finerenone: A potential treatment for patients with chronic kidney disease and type 2 diabetes mellitus. *touchREV. Endocrinol.* 17, 84–87. doi:10.17925/EE.2021.17.2.84

Ding, H., Zhang, L., Yang, Q., Zhang, X., and Li, X. (2021). Epigenetics in kidney diseases. *Adv. Clin. Chem.* 104, 233–297. doi:10.1016/bs.acc.2020.09.005

Doshi, S. M., and Friedman, A. N. (2017). Diagnosis and management of type 2 diabetic kidney disease. *Clin. J. Am. Soc. Nephrol.* 12, 1366–1373. doi:10.2215/CJN.11111016

Draznin, B., Aroda, V. R., Bakris, G., Benson, G., Brown, F. M., Freeman, R., et al. (2022). 11. Chronic kidney disease and risk management: Standards of medical Care in diabetes-2022. *Diabetes Care* 45, S175–S184. doi:10.2337/dc22-S011

Elliott, W. J., and Meyer, P. M. (2007). Incident diabetes in clinical trials of antihypertensive drugs: A network meta-analysis. *Lancet* 369, 201–207. doi:10.1016/S0140-6736(07)60108-1

Epstein, M., Williams, G. H., Weinberger, M., Lewin, A., Krause, S., Mukherjee, R., et al. (2006). Selective aldosterone blockade with eplerenone reduces albuminuria in patients with type 2 diabetes. *Clin. J. Am. Soc. Nephrol.* 1, 940–951. doi:10.2215/CJN.00240106

Filippatos, G., Anker, S. D., Agarwal, R., Pitt, B., Ruilope, L. M., Rossing, P., et al. (2021). Finerenone and cardiovascular outcomes in patients with chronic kidney disease and type 2 diabetes. *Circulation* 143, 540–552. doi:10.1161/CIRCULATIONAHA.120.051898

Gomez-Sanchez, E. P., and Gomez-Sanchez, C. E. (2012). Central regulation of blood pressure by the mineralocorticoid receptor. *Mol. Cell. Endocrinol.* 350, 289–298. doi:10.1016/j.mce.2011.05.005

Hou, J., Xiong, W., Cao, L., Wen, X., and Li, A. (2015). Spironolactone add-on for preventing or slowing the progression of diabetic nephropathy: A meta-analysis. *Clin. Ther.* 37, 2086–2103. doi:10.1016/j.clinthera.2015.05.508

Ito, S., Itoh, H., Rakugi, H., Okuda, Y., Yoshimura, M., and Yamakawa, S. (2020b). Double-blind randomized phase 3 study comparing esaxerenone (Cs-3150) and eplerenone in patients with essential hypertension (Esax-Htn study). *Hypertension* 75, 51–58. doi:10.1161/HYPERTENSIONAHA.119.13569

Ito, S., Kashihara, N., Shikata, K., Nangaku, M., Wada, T., Okuda, Y., et al. (2020a). Esaxerenone (Cs-3150) in patients with type 2 diabetes and microalbuminuria (Esax-Dn): Phase 3 randomized controlled clinical trial. *Clin. J. Am. Soc. Nephrol.* 15, 1715–1727. doi:10.2215/CJN.06870520

Ito, S., Shikata, K., Nangaku, M., Okuda, Y., and Sawanobori, T. (2019). Efficacy and safety of esaxerenone (Cs-3150) for the treatment of type 2 diabetes with microalbuminuria: A randomized, double-blind, placebo-controlled, phase ii trial. *Clin. J. Am. Soc. Nephrol.* 14, 1161–1172. doi:10.2215/CJN.14751218

Jaisser, F., and Farman, N. (2016). Emerging roles of the mineralocorticoid receptor in pathology: Toward new paradigms in clinical Pharmacology. *Pharmacol. Rev.* 68, 49–75. doi:10.1124/pr.115.011106

Jankovic, S. M., and Jankovic, S. V. (2022). Clinical pharmacokinetics and pharmacodynamics of esaxerenone, a novel mineralocorticoid receptor antagonist: A review. *Eur. J. Drug Metab. Pharmacokinet.* 47, 291–308. doi:10.1007/s13318-022-00760-1

Jia, Y., Zheng, Z., Yang, Y., Zou, M., Li, J., Wang, L., et al. (2019). Mir-4756 promotes albumin-induced renal tubular epithelial cell epithelial-to-mesenchymal transition and endoplasmic reticulum stress via targeting Sestrin2. *J. Cell. Physiol.* 234, 2905–2915. doi:10.1002/jcp.27107

Johansen, K. L., Chertow, G. M., Foley, R. N., Gilbertson, D. T., Herzog, C. A., Ishani, A., et al. (2021). Us renal data system 2020 annual data report: Epidemiology of kidney disease in the United States. *Am. J. Kidney Dis.* 77, A7–A8. doi:10.1053/j.ajkd.2021.01.002

Katayama, S., Yamada, D., Nakayama, M., Yamada, T., Myoishi, M., Kato, M., et al. (2017). A randomized controlled study of finerenone versus placebo in Japanese patients with type 2 diabetes mellitus and diabetic nephropathy. *J. Diabetes Complicat.* 31, 758–765. doi:10.1016/j.jdiacomp.2016.11.021

Kintscher, U., Bakris, G. L., and Kolkhof, P. (2021). Novel non-steroidal mineralocorticoid receptor antagonists in cardiorenal disease. *Br. J. Pharmacol.* 179, 3220–3234. doi:10.1111/bph.15747

Kloner, R. A. (2003). New therapy update. Inspra (eplerenone tablets). *Congest. Heart Fail.* 9, 341–342. doi:10.1111/j.1527-5299.2003.03306.x

Kolkhof, P., and Borden, S. A. (2012). Molecular Pharmacology of the mineralocorticoid receptor: Prospects for novel therapeutics. *Mol. Cell. Endocrinol.* 350, 310–317. doi:10.1016/j.mce.2011.06.025

Kolkhof, P., Hartmann, E., Freyberger, A., Pavkovic, M., Mathar, I., Sandner, P., et al. (2021). Effects of finerenone combined with empagliflozin in a model of hypertension-induced end-organ damage. *Am. J. Nephrol.* 52, 642–652. doi:10.1159/000516213

Kumar Kota, S., Jammula, S., Krishna Kota, S., Meher, L. K., and Modi, K. D. (2012). Spironolactone treatment in patients with diabetic microalbuminuria and resistant hypertension. *Int. J. Diabetes Dev. Ctries.* 1, 33–36. doi:10.1007/s13410-012-0063-5

Lerma, E., White, W. B., and Bakris, G. (2022). Effectiveness of nonsteroidal mineralocorticoid receptor antagonists in patients with diabetic kidney disease. *Postgrad. Med.* 1-10, 1–10. doi:10.1080/00325481.2022.2060598

Lin, M., Heizati, M., Wang, L., Nurula, M., Yang, Z., Wang, Z., et al. (2021). A systematic review and meta-analysis of effects of spironolactone on blood pressure,

glucose, lipids, renal function, fibrosis and inflammation in patients with hypertension and diabetes. *Blood Press* 30, 145–153. doi:10.1080/08037051.2021.1880881

Liu, M., Liang, K., Zhen, J., Zhou, M., Wang, X., Wang, Z., et al. (2017). Sirt6 deficiency exacerbates podocyte injury and proteinuria through targeting notch signaling. *Nat. Commun.* 8, 413. doi:10.1038/s41467-017-00498-4

Lozano-Maneiro, L., and Puente-Garcia, A. (2015). Renin-angiotensin-aldosterone system blockade in diabetic nephropathy. Present evidences. *J. Clin. Med.* 4, 1908–1937. doi:10.3390/jcm4111908

Lytvyn, Y., Godoy, L. C., Scholtes, R. A., van Raalte, D. H., and Cherney, D. Z. (2019). Mineralocorticoid antagonism and diabetic kidney disease. *Curr. Diab. Rep.* 19, 4. doi:10.1007/s11892-019-1123-8

Mehdi, U. F., Adams-Huet, B., Raskin, P., Vega, G. L., and Toto, R. D. (2009). Addition of angiotensin receptor blockade or mineralocorticoid antagonism to maximal angiotensin-converting enzyme inhibition in diabetic nephropathy. *J. Am. Soc. Nephrol.* 20, 2641–2650. doi:10.1681/ASN.2009070737

Mogensen, C. E. (1984). Microalbuminuria predicts clinical proteinuria and early mortality in maturity-onset diabetes. *N. Engl. J. Med.* 310, 356–360. doi:10.1056/NEJM198402093100605

Momeni, A., Behradmanesh, M. S., Kheiri, S., and Karami, H. M. (2015). Evaluation of spironolactone plus hydrochlorothiazide in reducing proteinuria in type 2 diabetic nephropathy. *J. Renin. Angiotensin. Aldosterone. Syst.* 16, 113–118. doi:10.1177/1470320313481485

Neuen, B. L., Oshima, M., Agarwal, R., Arnott, C., Cherney, D. Z., Edwards, R., et al. (2022). Sodium-glucose cotransporter 2 inhibitors and risk of hyperkalemia in people with type 2 diabetes: A meta-analysis of individual participant data from randomized, controlled trials. *Circulation* 145, 1460–1470. doi:10.1161/CIRCULATIONAHA.121.057736

Ninomiya, T., Perkovic, V., de Galan, B. E., Zoungas, S., Pillai, A., Jardine, M., et al. (2009). Albuminuria and kidney function independently predict cardiovascular and renal outcomes in diabetes. *J. Am. Soc. Nephrol.* 20, 1813–1821. doi:10.1681/ASN.2008121270

Pei, H., Wang, W., Zhao, D., Wang, L., Su, G. H., and Zhao, Z. (2018). The use of a novel non-steroidal mineralocorticoid receptor antagonist finerenone for the treatment of chronic heart failure: A systematic review and meta-analysis. *Med. Baltim.* 97, e0254. doi:10.1097/MD.0000000000010254

Pitt, B., Filippatos, G., Agarwal, R., Anker, S. D., Bakris, G. L., Rossing, P., et al. (2021). Cardiovascular events with finerenone in kidney disease and type 2 diabetes. *N. Engl. J. Med.* 385, 2252–2263. doi:10.1056/NEJMoa2110956

Provenzano, M., Jongs, N., Vart, P., Stefansson, B. V., Chertow, G. M., Langkilde, A. M., et al. (2022). The kidney protective effects of the sodium-glucose cotransporter-2 inhibitor, dapagliflozin, are present in patients with ckd treated with mineralocorticoid receptor antagonists. *Kidney Int. Rep.* 7, 436–443. doi:10.1016/j.ekir.2021.12.013

Rico-Mesa, J. S., White, A., Ahmadian-Tehrani, A., and Anderson, A. S. (2020). Mineralocorticoid receptor antagonists: A comprehensive review of finerenone. *Curr. Cardiol. Rep.* 22, 140. doi:10.1007/s11886-020-01399-7

Rossing, P., Filippatos, G., Agarwal, R., Anker, S. D., Pitt, B., Ruilope, L. M., et al. (2022). Finerenone in predominantly advanced ckd and type 2 diabetes with or without sodium-glucose cotransporter-2 inhibitor therapy. *Kidney Int. Rep.* 7, 36–45. doi:10.1016/j.ekir.2021.10.008

Sarafidis, P., Papadopoulos, C. E., Kamperidis, V., Giannakoulas, G., and Doumas, M. (2021). Cardiovascular protection with sodium-glucose cotransporter-2 inhibitors and mineralocorticoid receptor antagonists in chronic kidney disease: A milestone achieved. *Hypertension* 77, 1442–1455. doi:10.1161/HYPERTENSIONAHA.121.17005

Srivastava, S. P., Goodwin, J. E., Kanasaki, K., and Koya, D. (2020). Inhibition of angiotensin-converting enzyme ameliorates renal fibrosis by mitigating dpp-4 level and restoring antifibrotic micrornas. *Genes (Basel)* 11 (2), 211. doi:10.3390/genes11020211

Srivastava, S. P., Hedayat, A. F., Kanasaki, K., and Goodwin, J. E. (2019). Microrna crosstalk influences epithelial-to-mesenchymal, endothelial-to-mesenchymal, and macrophage-to-mesenchymal transitions in the kidney. *Front. Pharmacol.* 10, 904. doi:10.3389/fphar.2019.00904

Srivastava, S. P., Li, J., Kitada, M., Fujita, H., Yamada, Y., Goodwin, J. E., et al. (2018). Sirt3 deficiency leads to induction of abnormal glycolysis in diabetic kidney with fibrosis. *Cell Death Dis.* 9, 997. doi:10.1038/s41419-018-1057-0

Srivastava, S. P., Zhou, H., Setia, O., Liu, B., Kanasaki, K., Koya, D., et al. (2021). Loss of endothelial glucocorticoid receptor accelerates diabetic nephropathy. *Nat. Commun.* 12, 2368. doi:10.1038/s41467-021-22617-y

Tuttle, K. R., Bakris, G. L., Bilous, R. W., Chiang, J. L., de Boer, I. H., Goldstein-Fuchs, J., et al. (2014). Diabetic kidney disease: A report from an ada consensus conference. *Diabetes Care* 37, 2864–2883. doi:10.2337/dc14-1296

van den Meiracker, A. H., Baggen, R. G., Pauli, S., Lindemans, A., Vulto, A. G., Poldermans, D., et al. (2006). Spironolactone in type 2 diabetic nephropathy: Effects on proteinuria, blood pressure and renal function. *J. Hypertens.* 24, 2285–2292. doi:10.1097/01.hjh.0000249708.44016.5c

Vodosek, H. N., Bevc, S., Ekart, R., Piko, N., Petreski, T., and Hojs, R. (2021). Mineralocorticoid receptor antagonists in diabetic kidney disease. *Pharm. (Basel)* 14 (6), 561. doi:10.3390/ph14060561

Wada, T., Inagaki, M., Yoshinari, T., Terata, R., Totsuka, N., Gotou, M., et al. (2021). Apararenone in patients with diabetic nephropathy: Results of a randomized, double-blind, placebo-controlled phase 2 dose-response study and open-label extension study. *Clin. Exp. Nephrol.* 25, 120–130. doi:10.1007/s10157-020-01963-z

Wan, N., Rahman, A., and Nishiyama, A. (2021). Esaxerenone, a novel nonsteroidal mineralocorticoid receptor blocker (mrb) in hypertension and chronic kidney disease. *J. Hum. Hypertens.* 35, 148–156. doi:10.1038/s41371-020-0377-6

Wang, L. P., Gao, Y. Z., Song, B., Yu, G., Chen, H., Zhang, Z. W., et al. (2019). Micrornas in the progress of diabetic nephropathy: A systematic review and meta-analysis. *Evid. Based Complement. Altern. Med.* 2019, 3513179. doi:10.1155/2019/3513179

Wang, X., Liu, J., Zhen, J., Zhang, C., Wan, Q., Liu, G., et al. (2014). Histone deacetylase 4 selectively contributes to podocyte injury in diabetic nephropathy. *Kidney Int.* 86, 712–725. doi:10.1038/ki.2014.111

Yang, P., Shen, W., Chen, X., Zhu, D., Xu, X., Wu, T., et al. (2019). Comparative efficacy and safety of mineralocorticoid receptor antagonists in heart failure: A network meta-analysis of randomized controlled trials. *Heart fail. Rev.* 24, 637–646. doi:10.1007/s10741-019-09790-5

Zhao, D., Liu, H., Dong, P., and Zhao, J. (2017). A meta-analysis of add-on use of spironolactone in patients with resistant hypertension. *Int. J. Cardiol.* 233, 113–117. doi:10.1016/j.ijcard.2016.12.158

Zhao, J. V., Xu, L., Lin, S. L., and Schooling, C. M. (2016). Spironolactone and glucose metabolism, a systematic review and meta-analysis of randomized controlled trials. *J. Am. Soc. Hypertens.* 10, 671–682. doi:10.1016/j.jash.2016.05.013

Zheng, Y., Ma, S., Huang, Q., Fang, Y., Tan, H., Chen, Y., et al. (2022). Meta-analysis of the efficacy and safety of finerenone in diabetic kidney disease. *Kidney Blood Press Res (Basel)* 47 (4), 219–228. doi:10.1159/000521908

Zheng, Z., Guan, M., Jia, Y., Wang, D., Pang, R., Lv, F., et al. (2016). The coordinated roles of miR-26a and miR-30c in regulating TGFβ1-induced epithelial-to-mesenchymal transition in diabetic nephropathy. *Sci. Rep.* 6, 37492. doi:10.1038/srep37492

Zheng, Z., Zhang, S., Chen, J., Zou, M., Yang, Y., Lu, W., et al. (2022). The hdac2/sp1/mir-205 feedback loop contributes to tubular epithelial cell extracellular matrix production in diabetic kidney disease. *Clin. Sci.* 136, 223–238. doi:10.1042/CS20210470

Zuo, C., and Xu, G. (2019). Efficacy and safety of mineralocorticoid receptor antagonists with acei/arb treatment for diabetic nephropathy: A meta-analysis. *Int. J. Clin. Pract.* 73, e13413. doi:10.1111/ijcp.13413

frontiers | Frontiers in Pharmacology

TYPE Original Research
PUBLISHED 30 September 2022
DOI 10.3389/fphar.2022.969207

OPEN ACCESS

EDITED BY
Swayam Prakash Srivastava,
Yale University, United States

REVIEWED BY
Ebru Arioglu Inan,
Ankara University, Turkey
Maria Angelica Miglino,
University of São Paulo, Brazil
Naguib Bin Salleh,
University of Malaya, Malaysia

*CORRESPONDENCE
Yong-De Xu,
xuyongd@foxmail.com
Yong Yang,
yongyang301@163.com

†These authors have contributed equally to this work.

SPECIALTY SECTION
This article was submitted to Renal Pharmacology, a section of the journal Frontiers in Pharmacology

RECEIVED 14 June 2022
ACCEPTED 14 September 2022
PUBLISHED 30 September 2022

CITATION
Liu Y, Zheng J-Y, Wei Z-T, Liu S-K, Sun J-L, Mao Y-H, Xu Y-D and Yang Y (2022), Therapeutic effect and mechanism of combination therapy with ursolic acid and insulin on diabetic nephropathy in a type I diabetic rat model.
Front. Pharmacol. 13:969207.
doi: 10.3389/fphar.2022.969207

Therapeutic effect and mechanism of combination therapy with ursolic acid and insulin on diabetic nephropathy in a type I diabetic rat model

Yang Liu[1†], Jin-Yan Zheng[2†], Zhi-Tao Wei[1], Shu-Kun Liu[1], Ji-Lei Sun[1], Yin-Hui Mao[1], Yong-De Xu[3*] and Yong Yang[1*]

[1]Department of Urology, The Affiliated Hospital of Changchun University of Chinese Medicine, Changchun, China, [2]Department of Endocrinology, The Central Hospital of Zibo, Zibo, China, [3]Department of Urology, Beijing Friendship Hospital, Capital Medical University, Beijing, China

This work aims to investigate the therapeutic effect of ursolic acid (UA) plus insulin (In) on diabetic nephropathy (DN) in streptozotocin (STZ)-induced T1DM rats. The experimental groups and operational details are as follows: A total of thirty-two SD rats were divided into four groups: the DN model group (DN, n = 8), DN + In treatment group (DN + In, n = 8), DN + In + UA administration group (DN + In + UA, n = 8), and negative control group (control, n = 8). After 8 weeks, changes in renal function indices and pathological damage were assessed. Additionally, oxidative stress-, apoptosis-, and fibrosis-related proteins in kidney tissue were measured. Compared with the control group, the vehicle group showed higher levels of creatine, blood urea nitrogen, urinary protein, apoptosis, and lipid peroxidation; lower superoxide dismutase levels; more severe levels of pathological kidney damage and renal fibrosis; and a deepened degree of EMT and EndMT. Better outcomes were achieved with the combined treatment than with insulin-only treatment. The improvement of TGF-β1, phosphorylated p38 MAPK, FGFR1, SIRT3 and DPP-4 expression levels in renal tissues after combination therapy was greater than that after insulin-only treatment. This study shows that the combination of insulin and UA significantly improved the pathological changes in the renal tissue of T1DM rats, and the underlying mechanism may be related to improving apoptosis and oxidative stress by regulating p38 MAPK, SIRT3, DPP-4 and FGFR1 levels, thereby blocking TGF-β signaling pathway activation and inhibiting EMT and EndMT processes.

KEYWORDS

ursolic acid, insulin, diabetic nephropathy, oxidative stress, apoptosis, EMT

Introduction

Type 1 diabetes mellitus (T1DM), or insulin-dependent diabetes mellitus, is a disorder caused by an absolute deficiency of insulin, causing persistently elevated blood glucose levels and the eventual development of diabetes mellitus (Abraham et al., 2021). The disease occurs mostly in children and adolescents with rapid onset (Morandi et al., 2021). Patients with T1DM are susceptible to DN due to a chronic absolute deficiency of insulin. As one of the most common and devastating microvascular complications of diabetes, DN seriously affects the lives of patients (Gong et al., 2021). When DN shows obvious symptoms, most of them have developed into advanced stage, As the disease continues to progress, the most common symptom is proteinuria. After persistent proteinuria, the glomerular filtration rate decreases, and when the glomerular filtration rate is significantly lower than normal and a large amount of proteinuria appears, it can quickly progress to renal failure stage (Roumeliotis et al., 2021). Its complex pathogenesis is not yet fully understood, and classical views mainly focus on metabolic and hemodynamic changes (Fu et al., 2022). The lack of attention to the disease and its relationship to unhealthy lifestyles has indirectly elevated its incidence. The current clinical treatment plan for T1DM is dominated by lifelong insulin injection, but it requires patient compliance and adherence to healthy lifestyles (Lecumberri et al., 2018).

Renal fibrosis caused by excessive extracellular matrix (ECM) deposition during DN. Fibroblasts generated by activation during epithelial mesenchymal transition (EMT) and endothelial mesenchymal transition (EndMT) are the main source of renal fibroblasts. Renal fibroblasts play an important role in the process of renal fibrosis. There is a complex regulation of the EMT and EndMT processes, and renal fibrosis is the result of the action of multiple signaling pathways and corresponding cytokines, such as the transforming growth factor-β (TGF-β), MAPK, Gh, Wnt, Notch, and Hedgehog signaling pathways (Zhang et al., 2022). Transforming growth factor-β (TGF-β) has also been shown to be a possible fibrogenic factor involved in DN progression (Wu W. et al., 2021; Zheng et al., 2021; Chen et al., 2022). The p38 pathway is one of the MAPK pathways involved in the pathological process of DN (Cui et al., 2019; Gu et al., 2021). Studies have shown that the TGF-β/Smad and MAPK signaling pathways play an important role in the process of renal fibrosis (Geng et al., 2020). In addition, for endothelial fibroblast growth factor receptor 1 (FGFR1) signaling (Xu et al., 2022), the endothelial Sirtuin3 (SIRT3)-mediated signaling mechanism (Srivastava et al., 2021a) and dipeptidyl peptidase-4 (DPP-4)-mediated signaling mechanism (Li et al., 2021) have also become hotspots for DN research.

Currently, there are many therapeutic strategies for DN, but the effectiveness of treatment varies, among which SIRT3, glycolysis inhibitors, DPP-4 inhibitors (e.g., linagliptin), ROCK inhibitors, mineralocorticoid receptor antagonists, and peptide AcSDKP are more widely used in clinical and scientific research to prevent kidney injury (Castoldi et al., 2013; Zhao et al., 2020). For ACEIs and ARBs, blockers of the common renin-angiotensin-aldosterone system (RAAS), the effects in animal models of DN still vary widely (Srivastava et al., 2020a). In this regard, we need to develop a novel therapeutic approach against DN.

Ursolic acid (UA), a pentacyclic triterpene acid compound, is widely found in natural plants and has attracted much attention in recent years (Balcazar et al., 2021). UA has been shown to have antioxidant, anti-inflammatory, antitumor, neuroprotective, hypoglycemic, and other bioactive effects (Zhou et al., 2021; Liu et al., 2022). Some studies have reported that ursolic acid has been used in the treatment of bone injury (Yu et al., 2015), nonalcoholic fatty liver (Li et al., 2014) and cardiovascular diseases (Xiang et al., 2012). At the same time, abundant evidence suggests that hyperglycemia promotes the excessive production of reactive oxygen species (ROS) and oxidative stress (Tota et al., 2021), which accelerates the apoptosis of podocytes (Jin et al., 2019; Qin et al., 2020) and causes renal fibrosis. As a result, it can be hypothesized that UA can exert a therapeutic effect by inhibiting the fibrotic process through anti-EMT and EndMT processes and antioxidant activity.

Therefore, this study investigated the protective effect of UA combined with insulin on renal injury in type 1 diabetic rats and its mechanism by establishing an STZ-induced type I diabetic rat model to provide a theoretical basis for the clinical application of UA on DN.

Materials and methods

Laboratory animals

Thirty-two 8-week-old male SPF-grade SD rats, weighing 210–240 g, were purchased from the Laboratory Animal Center of Changchun University of Chinese Medicine [Medical Experimental Animal Number SYXK (Ji)2018-0014], and all animal experiments were approved by the Ethics Committee of Changchun University of Chinese Medicine on 6 January 2020. (Changchun, China; Approval No. 2020132). The animals were given a standard pellet diet and tap water, and the experiments began after 1 week of adaptive feeding without abnormalities.

Establishment of the DN rat model

Thirty-two SD male rats were randomly divided into a negative control group (n = 8) and a modeling group (n = 24). STZ (HPLC ≥98%, Sigma, United States) solution was prepared as follows (Zheng et al., 2020): 1 g of STZ was dissolved in 100 ml of citric acid-sodium citrate buffer (0.1 mol/L, pH = 4.5) in an ice bath to a final concentration

of 10 mg/ml; this ready-to-use solution was kept dry and protected from light. Before formal modeling, all rats were weighed, random blood glucose was measured, and the T1DM model was induced after 12 h of fasting without water. The T1DM model was induced by a single intraperitoneal injection of streptozotocin (STZ, 60 mg/kg) in SD rats, and the negative control group was injected intraperitoneally with an equal amount of citrate-sodium citrate buffer. Random blood glucose and body weight measurements were performed daily after injection, and rats with blood glucose >16.67 mmol/L for 3 days, accompanied by obvious symptoms of polyuria, excessive drinking, and excessive eating, were considered successful.

Experimental grouping and treatment

After 4 weeks of modeling, the rats in the model group were rerandomized. The final DM rats were randomly divided into three groups: DN model group (DN, n = 8), DN + insulin treatment group (DN + In, n = 8), DN + In + UA administration group (DN + In + UA, n = 8), and another negative control group (control, n = 8). Rats in the insulin group were given an intraperitoneal injection of glargine insulin (Aventis Pharma, Germany, 1–3 U/100 g) once in the morning and once in the evening, while rats in the UA and insulin combination group were given an intraperitoneal injection of insulin along with UA (HPLC ≥98%, Absin, Shanghai, China, 20 mg/ml) (solvent: DMSO:ddH2O = 1:9, 50 mg/kg) gavage, and all groups were given an equal amount of solvent gavage once daily for 4 weeks. At the end of the study, diabetic rats received approximately 10–12 U/day of insulin based on daily glucose changes.

General index testing

The body weight and tail vein glucose level of each rat were measured before and after modeling and after the last dose of treatment, as were the 24-h diet and water intakes of each group of rats. At the end of the experiment, the rats were anesthetized by intraperitoneal injection of 3% sodium pentobarbital (30 mg/kg), and the right kidney was rapidly removed after the rats were completely anesthetized. Finally, they were euthanized by cervical dragging. The kidney weight was measured, and the kidney index was calculated according to the last weight (kidney mass/body mass).

Testing of biochemical indicators of renal function

During the experiment, metabolic cages were used to collect 24-h urine from rats. Before the rats were euthanized, 4 ml of blood was collected from the carotid artery and centrifuged at 3,500 r/min and 4°C for 20 min. The serum was collected and centrifuged at 4°C (3,500 r/min, 10 min); the supernatant was stored at −20°C for measurement. Serum creatinine (SCr), blood urea nitrogen (BUN), and urine protein content were measured by an automatic biochemical analyzer (Lei Du lives Science and Technology Limited Company, Shenzhen, China).

Renal pathology staining

The kidney tissues of rats in each group were fixed with 4% paraformaldehyde, embedded in paraffin, and routinely sectioned at a thickness of 5 μm. These sections were dehydrated in ethanol, cleared in xylene, dewaxed in xylene, stained with HE, periodic acid-Schiff (PAS), Sirius red and Masson trichrome stained (MTS), dehydrated, cleared, sealed, and photographed microscopically, and morphological changes in the kidney tissues were recorded. A point-counting method on a microscopic grid was used to assess the relative area of each rat glomerular thylakoid stroma in PAS staining. The area of fibrosis in Sirius red- and MTS-stained tissue images was assessed using ImageJ software. For each rat kidney, images of six different fields of view (×40) were randomly evaluated.

Oxidative stress indicator test

An appropriate amount of kidney tissue was removed, and the 10% homogenate was placed in an ice bath to be centrifuged at 4°C (4,000 rpm/min) for 10 min; the supernatant was stored at −20°C. The expression levels of superoxide dismutase (SOD) and malondialdehyde (MDA) in kidney tissues were measured according to the kit instructions (Beyotime Biotechnology, Shanghai, China).

TUNEL fluorescent staining

A reaction solution was added for staining according to the TUNEL kit instructions (Roche, Switzerland). The nuclei were stained blue; positive cells were stained green under the microscope to calculate the apoptotic rate. Apoptotic cells (green) were counted at 200×; six unconnected fields of view were selected for each group to calculate the apoptotic rate as follows: apoptotic rate (%) = (number of TUNEL-positive cells/total number of cells) × 100%.

Immunofluorescence staining

Frozen kidney sections (5 μm) were used for immunofluorescence to express EndMT and EMT levels.

Positive markers for α-smooth muscle actin (α-SMA, Boster, BM0002, 1:500), Vimentin (Servicebio, GB11192, 1:300), E-cadherin (Proteintech, 20874-1-AP, 1:200) and CD31 (Abcam, ab281583, 1:200) were assessed. Briefly, the frozen sections were first dried, washed 3 times (5 min) in PBS solution, and blocked with 2% bovine serum albumin (BSA)/PBS for 30 min at room temperature. Thereafter, specimens in sections were incubated in primary antibody for 90 min, followed by three washes of sections in PBS for 5 min each. Next, the specimens were incubated with secondary antibody for 40 min and washed again 3 times in PBS (5 min each time). Finally, the sections were sealed with a DAPI-containing blocking liquid. Immunolabeled sections were analyzed by fluorescence microscopy. For each kidney section, pictures of six different areas (×400) were taken and analyzed quantitatively.

Immunohistochemical testing

Paraffin sections were dewaxed, hydrated and repaired with high-pressure antigen heat. The sections were sealed and incubated with antibody (Caspase-3:Proteintech,19677-1-AP,1:200; Bax: BOSTER,BA0315-1,1:200; FGFR1:Cell Signaling Technology,#9740,1:500; SIRT3:affinity: AF5135, 1:100; DPP-4: Abcam, ab187048, 1:2000; TGF-β1, Abcam, ab50036,1:200) at 4°C overnight, washed, incubated with secondary antibody at 37°C for 1 h, and washed for DAB color development. Six fields of view were randomly selected from each section under the microscope and saved by video; the macro program for positive expression was set up using ImageJ software to analyze the expression of target proteins in different groups under the same conditions.

Western blotting for protein expression in kidney tissues

Kidney tissues were lysed in RIPA buffer (Beyotime Biotechnology, Shanghai, China); protein concentrations were determined using the BCA Protein Assay Kit (Beyotime Biotechnology). Equal amounts of proteins were resolved by SDS–PAGE, and the proteins were transferred to PVDF membranes and incubated with the appropriate antibodies.

Rabbit anti-rat TGF-β1 antibody (Abcam, ab50036, 1:1,000), phospho-p38 MAPK antibody (Thr180/Tyr182) (Cell Signaling Technology, #4511, 1:1,000), p38 MAPK antibody (Cell Signaling Technology, #8690, 1:1,000) and GAPDH internal reference antibody (Millipore, #3241215, 1:10,000) were added and incubated overnight at 4°C. Development was performed according to the ECL kit instructions, and the protein bands were quantified in grayscale values using Gel EQ Quantity One software (Bio-Rad, United States).

Statistical analyses

SPSS 26.0 statistical software (SPSS Inc., Chicago, IL, United States) was used to analyze the statistical significance of the data. ImageJ software (National Institutes of Health, Bethesda, MD, United States) was used for quantitative analysis of the data. One-way ANOVA was used for comparisons between multiple groups, and Tukey's HSD method was used for two-way comparisons. $p < 0.05$ indicated that the differences were statistically significant.

Results

Comparison of blood glucose in rats

The fasting blood glucose levels of the rats were monitored at 0 h, 72 h, 4, 6 and 8 weeks after 12 h of fasting. FBG was significantly increased in the DN group and maintained at a higher level throughout the experimental period. FBG was significantly lower in the insulin-treated group alone than in the DN group ($p < 0.01$) and was even more significant after the combination of ursolic acid and insulin ($p < 0.01$). These results suggest that UA has a hypoglycemic effect on DN (Figure 1A).

General condition of the rats

By the end of the experiment, there were two dead rats in the DM group and one dead rat in the DM + In group. Compared with the negative control rats, the body weight and renal index of DN rats were significantly higher ($p < 0.01$), indicating that the kidneys of DN rats showed hypertrophy. In contrast, the renal index was significantly lower in both the UA and insulin-treated groups than in the DN group ($p < 0.01$), suggesting that UA could have an ameliorative effect by reducing renal hypertrophy in DN rats (Figures 1B,C). Compared with the negative control rats, the DN rats came out with significantly more food and more drink ($p < 0.01$). In contrast, DN + In + UA treatment groups were more convergent to the normal group rats compared with the DN group ($p < 0.01$), suggesting that UA could alleviate the clinical manifestations of diabetes in the DN rats (Figures 1D,E).

Comparison of renal function and biochemical parameters in rats

Compared with the control group, rats in the DN model group showed significant differences in SCr, BUN and urinary

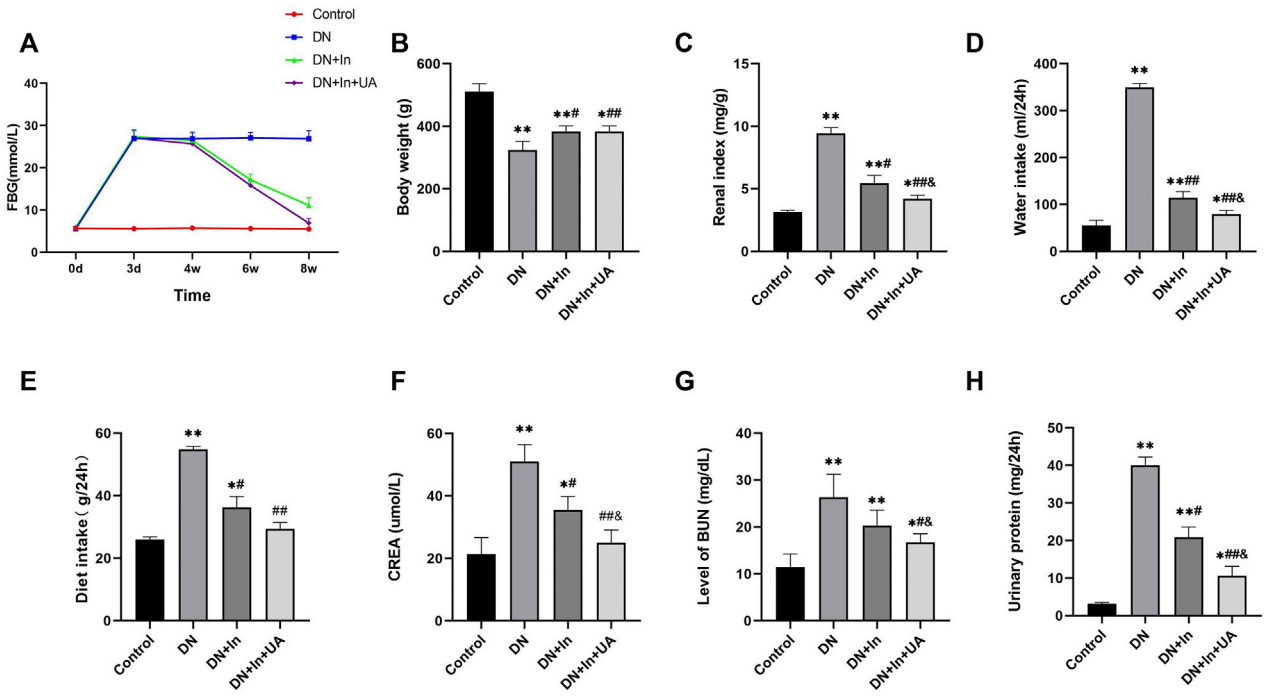

FIGURE 1
General condition of the rats. **(A)** Effect of ursolic acid and insulin on fasting blood glucose levels in diabetic rats. Fasting blood glucose (FBG) levels were correlated with once daily oral UA (50 mg/kg) for a 4-week duration of treatment. **(B–E)** Comparison of the final body weight, renal index, and total daily diet and water intake of the four groups of rats in the final week. **(F–H)** Comparison of blood creatinine, blood urea nitrogen and urine protein levels in the four groups of rats. Data are expressed as the mean ± S.D. (n = 6). *p < 0.05, **p < 0.01 vs. the control group; #p < 0.05, ##p < 0.01 vs. the DN group; and p < 0.05 vs. the DN + In group. Control, control group; DN, diabetic nephropathy model group; DN + In, insulin treatment group; DN + In + UA, insulin and ursolic acid combination therapy group.

protein amount (all p < 0.01); compared with levels in the DN model group, the SCr (p < 0.01), BUN (p < 0.05), and urinary protein volume (p < 0.01) were significantly improved in the combined insulin and UA group compared with the DN model group. There was a significant difference between the SCr, BUN and urine protein levels in the DN + In group and the DN + In + UA combination group (p < 0.05) (Figures 1F–H).

Morphological evaluation of the rat kidney

Based on HE staining, PAS staining, Sirius red staining and MTS, no pathological changes were observed in the kidney tissue of the control group, while the glomerular basement membrane was thickened, the thylakoid matrix was hyperplastic, and glomerulosclerosis was obvious in the DN model group. Compared with the DN model group, the glomerular basement membrane remained thickened, the thylakoid matrix was mildly hyperplastic in the insulin group, and the degree of glomerulosclerosis was reduced; in the UA and insulin combination group, however, the degree of lesion was significantly reduced and normalized (Figures 2A–D). Meanwhile, quantitative analysis of their staining results revealed that fibrosis levels were significantly higher in the DN group than in the control group (p < 0.01), and after treatment, fibrosis improved more significantly in the DN + In + UA group (p < 0.01) and was statistically significant with the DN + In group (p < 0.05) (Figures 2E–G).

Oxidative stress injury in the rat kidney

In the DM model group, the MDA content in the kidney tissue of rats was significantly increased compared with that in the control group, and SOD activity was significantly decreased (both p < 0.01). After treatment, the MDA content in the kidney tissue of rats in the UA + insulin group was significantly decreased, and SOD activity was significantly increased (both p < 0.01). Relative to the MDA content and SOD activity expression in the DN + In group, there was a significant difference in the DN + In + UA group (p < 0.05) (Figures 3A,B).

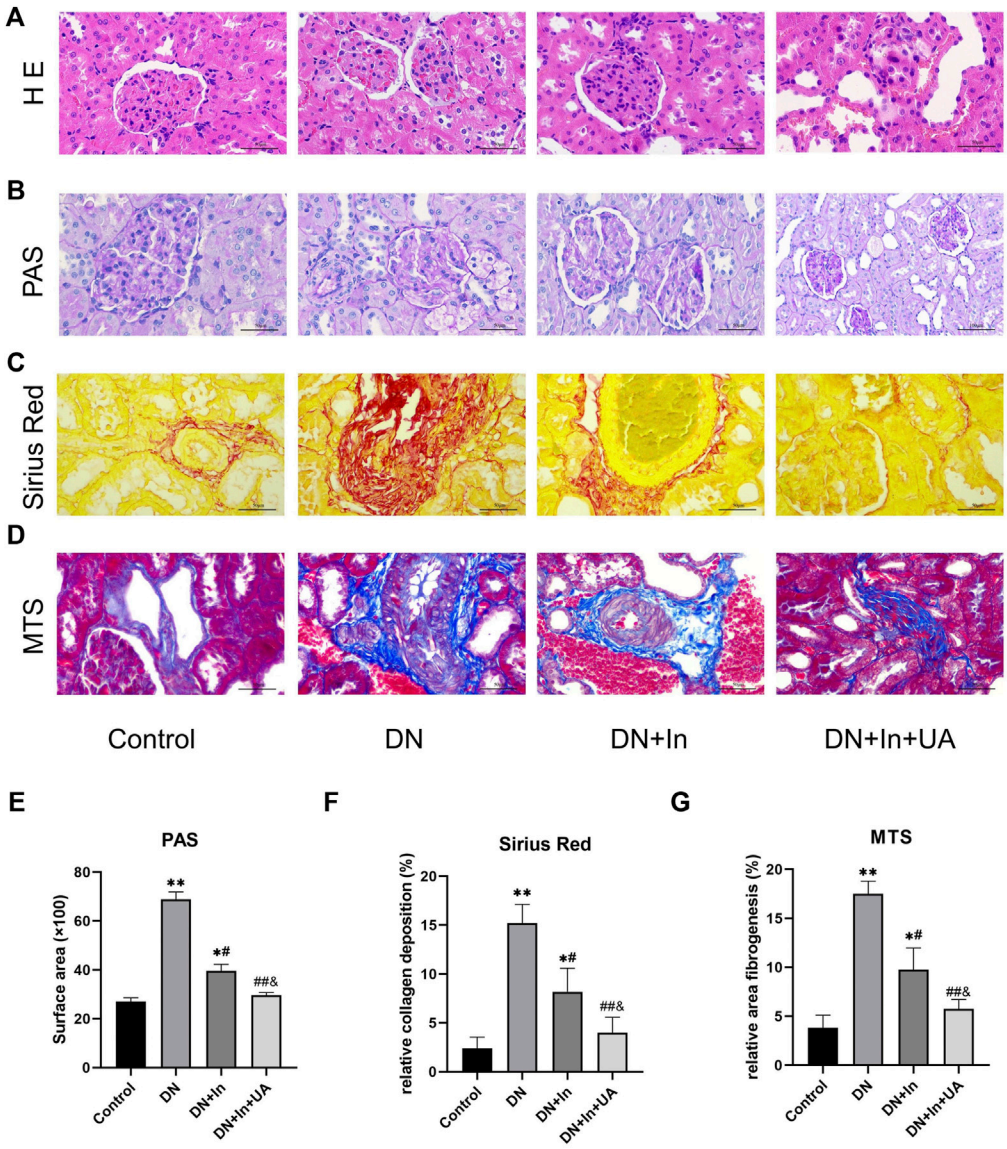

FIGURE 2
Morphological observation of rat kidney. **(A)** Representative images of HE staining of pathological structures of rat kidney. **(B)** PAS, **(C)** Sirius red, **(D)** MTS in the control, DN-, DN + In- and DN + In + UA-treated diabetic kidneys. **(E–G)** Quantitative analysis of PAS, Sirius red, and MTS staining in the four groups of rats. Magnification: ×400, scale bars = 50 μm. Data are expressed as the mean ± S.D. ($n = 5$). *$p < 0.05$, **$p < 0.01$ vs. the control group; #$p < 0.05$, ##$p < 0.01$ vs. the DN group; and $p < 0.05$ vs. the DN + In group.

Detection of apoptosis levels in rat kidney tissues

Renal apoptosis in rats was observed by TUNEL staining (Figures 3C,D). The degree of apoptosis was significantly increased in the DN group of rats compared to the control group ($p < 0.01$). Interestingly, after treatment in the DN + In + UA group, the level of TUNEL-positive cells was significantly reduced ($p < 0.01$), and the level of TUNEL-positive cells in the DN + In + UA group was less than that in the DN + In group ($p < 0.05$).

The expression of the apoptosis-related proteins caspase-3 and Bax was observed by immunohistochemistry (Figure 3E). The expression of caspase-3 (Figure 3F) and Bax (Figure 3G) proteins was greatly increased ($p < 0.01$) in the DN group rats compared to the control group, indicating more severe renal apoptosis. Reassuringly, treatment in the DN + In + UA group significantly reversed the expression of caspase-3 and Bax proteins compared with rats in the DN group ($p < 0.01$). Notably, the expression levels of caspase-3 and Bax proteins were reduced in the DN + In + UA group compared to the DN + In group ($p < 0.05$).

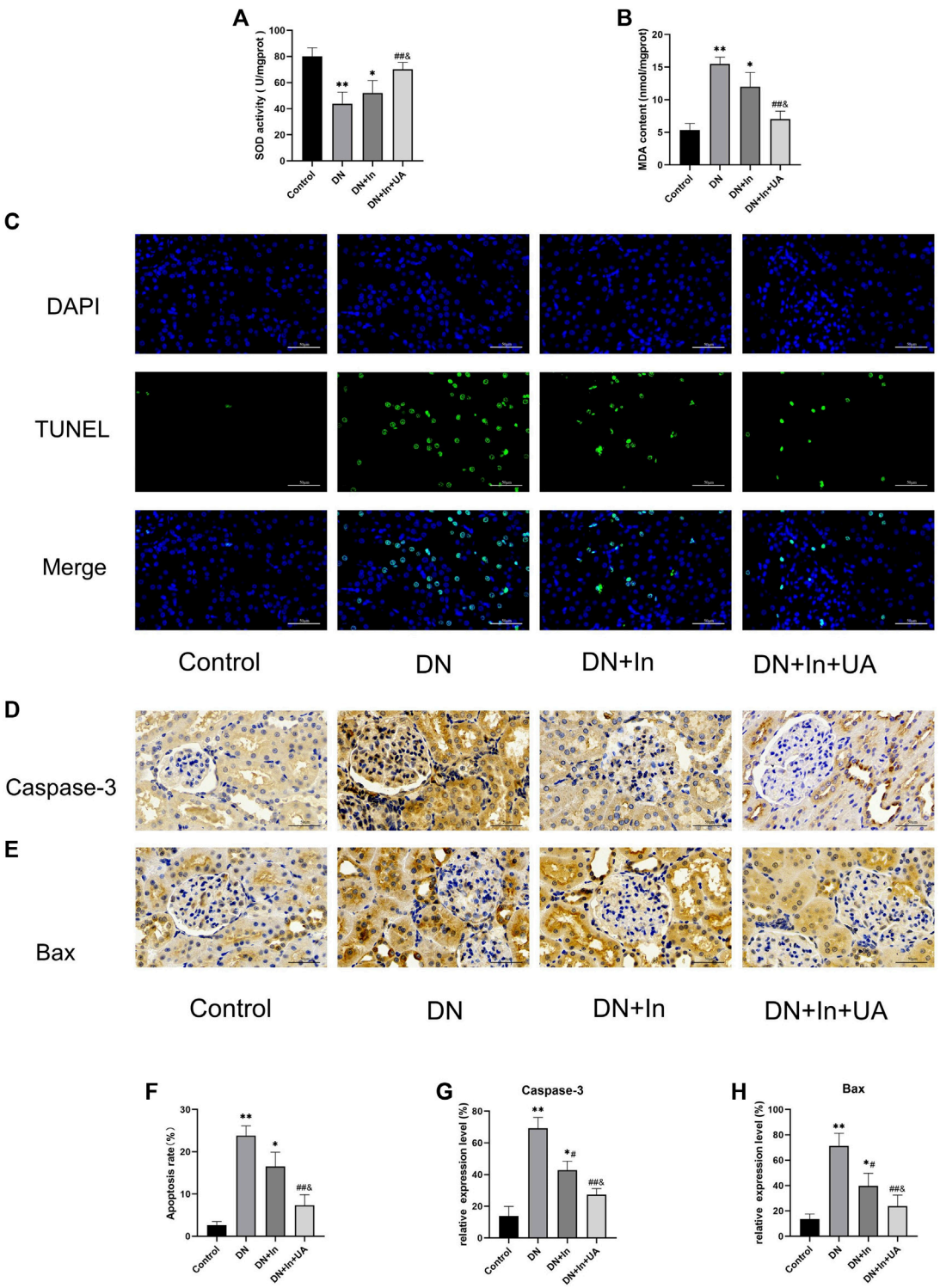

FIGURE 3
Detection of oxidative stress levels and apoptosis indicators in kidney tissues. **(A,B)** The kidney oxidative stress index of rats in each group. **(C)** TUNEL fluorescence staining to detect apoptosis levels in kidney tissue. The nucleus is in blue, and the apoptotic cells are in green. The bottom picture is a composite of both. **(D,E)** Characteristic images of immunohistochemical staining for Caspase-3 and Bax in kidney tissue (×400, scale bars = 50 μm). **(F)** Semiquantitative statistical graph of the percentage of apoptotic cells. **(G,H)** Quantitative analysis of Caspase-3 and Bax expression levels in kidney tissues from the four groups. Magnification: ×400, scale bars = 50 μm. Data are expressed as the mean ± S.D. (n = 6). *$p < 0.05$, **$p < 0.01$ vs. the control group; #$p < 0.05$, ##$p < 0.01$ vs. the DN group; and $p < 0.05$ vs. the DN + In group.

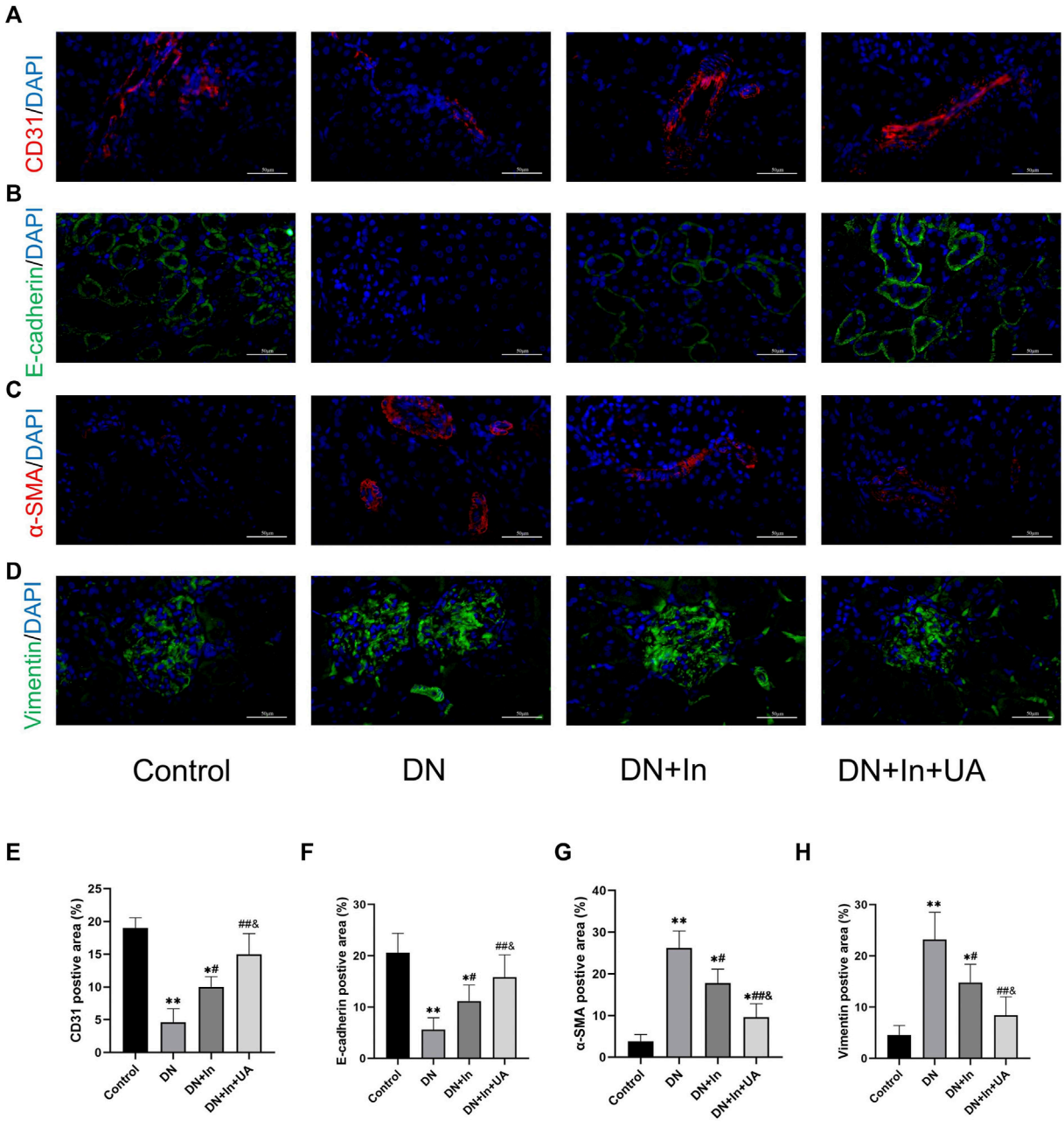

FIGURE 4
EMT and EndMT analysis in kidney tissues. Typical images of the endothelial cell marker **(A)** CD31, the epithelial cell marker **(B)** E-cadherin, and the mesenchymal cell markers **(C)** α-SMA and **(D)** Vimentin. **(E–H)** Quantification of CD31, E-cadherin, α-SMA and Vimentin in diabetic kidney tissues treated with control, DN, DN + In and DN + In + UA. Decreases in the epithelial marker E-cadherin and the endothelial marker CD31, along with increases in the mesenchymal marker α-SMA and Vimentin, were considered to be undergoing EMT and EndMT. Magnification: ×400, scale bars = 50 μm. Data are expressed as the mean ± S.D. (n = 5). *p < 0.05, **p < 0.01 vs. the control group; #p < 0.05, ##p < 0.01 vs. the DN group; and p < 0.05 vs. the DN + In group.

EMT and EndMT expression

In the DN group of rats, we found that the endothelial cell marker CD31 (Figure 4A) and the epithelial cell marker E-cadherin (Figure 4B) were significantly reduced (p < 0.01). CD31 and E-cadherin expression levels were significantly higher in both the DN + In group and DN + In + UA group than in the DN group (p < 0.05; p < 0.01). Notably, CD31 and E-cadherin

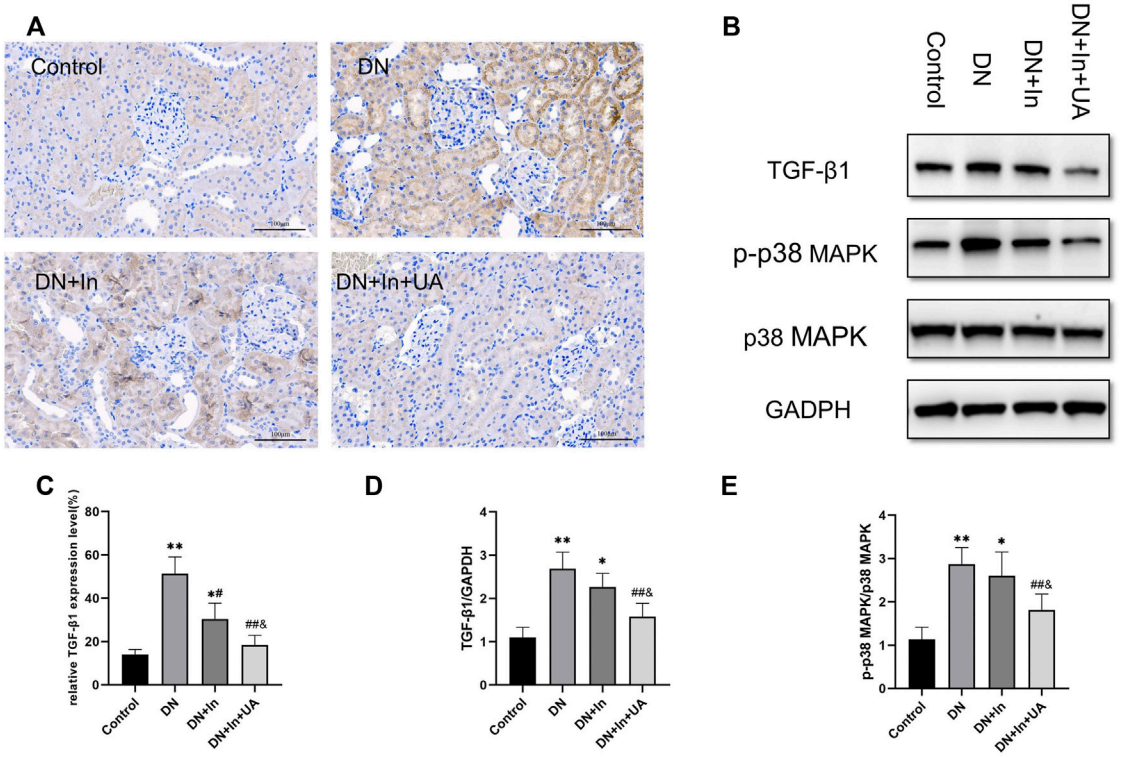

FIGURE 5
Expression of TGF-β1 and p38 signaling factors. **(A)** TGF-β1 expression as assessed by immunohistochemical staining of the kidney. Positive expression of TGF-β1 appears as dark brown granules in the cell membrane and/or cytoplasm (magnification: ×200, scale bars = 100 μm). **(B)** Western blot detection of TGF-β1, p-p38 MAPK and p38 MAPK expression in each group. **(C)** Semiquantitative analysis of the positive expression of TGF-β1 in immunohistochemistry. **(D,E)** Quantitative analysis of TGF-β1 and p-p38 MAPK expression in kidney tissues in Western blot experiments. Data are expressed as the mean ± S.D. ($n = 6$). *$p < 0.05$, **$p < 0.01$ vs. the control group; #$p < 0.05$, ##$p < 0.01$ vs. the DN group; and $p < 0.05$ vs. the DN + In group.

expression levels in the DN + In + UA group remained statistically significant for the DN + In group ($p < 0.05$). Meanwhile, the MSC markers α-SMA (Figure 4C) and Vimentin (Figure 4D) were significantly elevated in the DN group ($p < 0.01$) and significantly decreased after ursolic acid and insulin treatment ($p < 0.01$) but remained statistically significant compared to the DN + In group ($p < 0.05$). It is generally accepted that the epithelial cell marker E-cadherin is associated with a decrease in the endothelial cell marker CD31 and an increase in the mesenchymal cell marker α-SMA and Vimentin is considered to be undergoing EMT and EndMT (Figures 4E–H).

Expression of TGF-β1 in kidney tissues

In immunohistochemical staining, the TGF-β1 expression level was significantly higher in the kidney tissue of the DN model group than in the control group; UA combined with insulin treatment significantly reduced the TGF-β1 expression level ($p < 0.01$). There was a significant difference between the DN + In + UA group and the DN + In treatment group ($p < 0.05$). In the western blot assay, the expression level of TGF-β1 in the kidney tissue of rats in the DN model group was significantly higher than that in the control group ($p < 0.01$); DN + In + UA treatment significantly reduced the expression level of TGF-β1 ($p < 0.01$), and the levels in the DN + In + UA treatment group and the DN + In treatment group were significantly different from each other ($p < 0.05$) (Figures 5A,C).

Western blot detection of p38 MAPK expression in kidney tissues

The level of p-p38 MAPK expression in the kidney tissue of rats in the model group was significantly higher than that in the control group ($p < 0.01$). UA combined with insulin treatment reduced the level of p38 MAPK phosphorylation ($p < 0.01$). There was a statistically significant difference between the

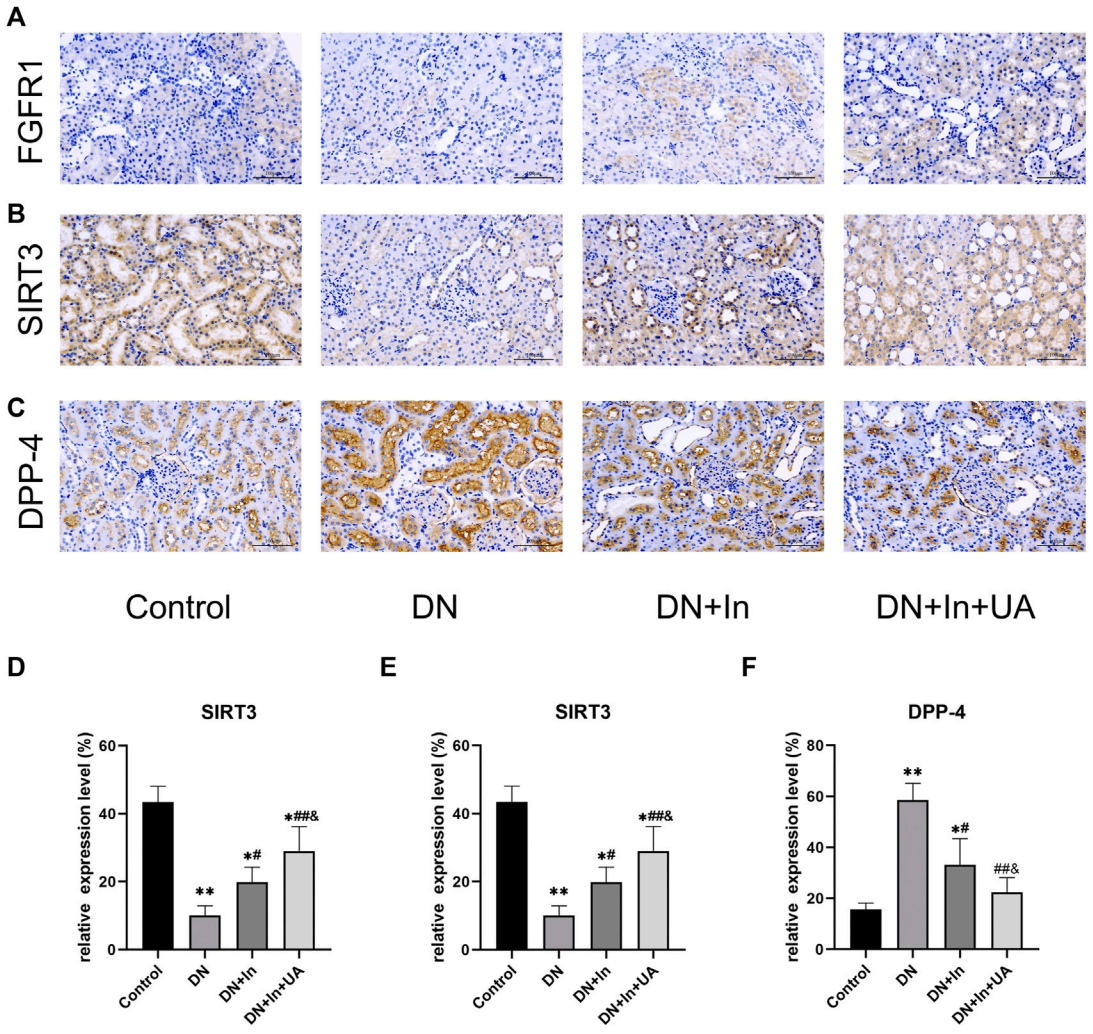

FIGURE 6
Exploration of classical signaling pathways. The expression levels of **(A)** FGFR1, **(B)** SIRT3, and **(C)** DPP-4 in kidney tissues were examined by immunohistochemical staining. **(D–F)** Quantitative analysis of FGFR1, SIRT3 and DPP-4 expression levels in renal tissues of each group. Magnification: ×200, scale bars = 100 μm. Data are expressed as the mean ± S.D. (n = 5). *p < 0.05, **p < 0.01 vs. the control group; #p < 0.05, ##p < 0.01 vs. the DN group; and p < 0.05 vs. the DN + In group.

combined treatment and the insulin alone groups, which were significantly different from each other (p < 0.05). P38 MAPK expression was not significantly different between the groups (p > 0.05) (Figures 5B,D,E).

Exploration of classical signaling pathways

The protein expression levels of FGFR1 (Figure 6A), SIRT3 (Figure 6B), and DPP-4 (Figure 6C) were examined by immunohistochemical staining in kidney tissues. We found that the expression levels of FGFR1 and SIRT3 were significantly lower in the DN group than in the control group (p < 0.01). After combined treatment with ursolic acid and insulin, FGFR1 and SIRT3 expression levels showed a significant increase (p < 0.01) and remained higher than those in the DN + In group (p < 0.05) (Figures 6D,E). In contrast, DPP-4 expression levels in kidney tissues showed the opposite trend. (Figure 6F).

Discussion

Current treatment strategies for DN include glycemic and blood pressure control, a low-protein diet, lipid-lowering drugs, and interference with the renin-angiotensin (RAS) system (Ahola et al., 2021; Zhang and Jiang, 2022). Despite their efficacies, most patients still develop end-stage renal disease, and the lethality rate

remains high. Therefore, better treatments and interventions are needed.

Our experiment showed classic clinical symptoms of "excessive drinking, polyphagia, polyuria, and weight loss" in DN rats, which significantly improved after treatment. We also detected a significant increase in the levels of SCr and BUN, indicating severely impaired renal function, which further elevated 24-h urinary protein in the urine. This is generally considered to be the initial step in DN, from normoalbuminuria to microalbuminuria (Ramaphane et al., 2021). It is well documented that good glycemic control improves microalbuminuria and reduces the risk of nephropathy in diabetic patients (de Boer et al., 2011). After 4 weeks of therapeutic intervention, all treatment groups showed significantly lower indices than those of the model group, and the treatment effect was more effective in the insulin plus UA combination group. This result was also consistent with the results reported by Ma et al. (Mapanga et al., 2009), suggesting that UA has a protective effect on DN renal tissue. DN is characterized by morphological and ultrastructural changes in the kidney. HE, Sirius red, PAS and Masson staining revealed pathological manifestations in DN rats, such as glomerular hypertrophy, a thickened glomerular tubular basement membrane dense layer, glomerular nodular sclerosis and tubulointerstitial fibrosis. After combined treatment with insulin and UA, the above pathological changes were partially reversed. Compared with the insulin group, the combination treatment group had a significant therapeutic effect, which also visually demonstrated the protective effect of UA on DN renal tissue.

We know that the relevant features of STZ-induced animals are similar to the clinical features of human diabetes (Westenfelder et al., 2021). High blood glucose can cause the production of ROS and lipid peroxidation, which can trigger DN (Dai et al., 2021). The aggravation of DN further leads to the aggregation of ROS, which generate lipid peroxides (e.g., MDA), leading to the oxidation of proteins and amino acids to aggravate the progression of the disease. In a basic study, Tong et al. (Tong et al., 2019) demonstrated that ethyl vanillin could protect against the progression to DN from kidney injury by inhibiting oxidative stress and apoptosis, which provided us with ideas for studying the mechanism of UA treatment. The results of the basic experiments conducted by Wang *et al.* showed that UA ameliorated oxidative stress, inflammation and fibrosis in rats with diabetic cardiomyopathy (Wang et al., 2018). The results of this study showed that the SOD levels of DN rats were all significantly reduced, and the lipid peroxide index (the MDA content) was significantly increased. The changes in the MDA and SOD contents reflected the enhanced level of oxidative stress in the kidney tissue of the model group rats, and the above phenomenon was reversed after treatment with insulin and UA, which indicated that UA not only lowered blood glucose but also had good antioxidant ability. Data from the study by Xu et al. further suggest that UA can be used as a protective agent against renal dysfunction through its antioxidant and anti-inflammatory effects (Xu et al., 2018).

In a rat model of diabetes induced by a high-sugar, high-fat diet and STZ intraperitoneal injection, investigators using a combination of UA and other drugs for DN found that its protective effects on the kidney may be related to oxidative stress, renal fibrosis, and anti-apoptosis (Wu et al., 2021b). In this experiment, it was concluded by TUNEL fluorescence staining and expression of Caspase-3 and Bax in immunohistochemistry that apoptosis was increased in the kidney of rats with DN and was significantly reduced after the application of insulin combined with UA treatment, so it is presumed that UA has good anti-apoptotic ability to repair the kidney functional damage in T1DM rats.

In DN, ECM deposition results in renal fibrosis. Fibroblasts produced by activation during EMT and EndMT are the main source of renal fibroblasts. In the present experiment, in the DN group, the decrease in the epithelial cell marker E-cadherin with the endothelial cell marker CD31 and the increase in the mesenchymal cell markers α-SMA and Vimentin indicated that the process of EMT and EndMT was being undergone, and this was improved after treatment. The study shows that TGF-β1 can stimulate the excessive accumulation of ECM through EMT, which leads to renal fibrosis (Gwon et al., 2021). TGF-β1 is involved in renal cell hypertrophy, proliferation and apoptosis in addition to ECM protein synthesis (Zhang et al., 2021). In the present study, the expression level of TGF-β1 was significantly elevated in DN rats, which is consistent with the findings of Barbara et al. in db/db mice (Toffoli et al., 2020). After combined treatment with insulin and UA, the expression level of TGF-β1 was reduced, suggesting that UA may improve the extent of renal fibrosis by reducing TGF-β1 expression. A clinical study by Mumtaz *et al.* also found elevated levels of TGF-β1 expression in DN patients (Takir et al., 2016), which has important implications for the subsequent treatment of DN. The p38 MAPK signaling pathway increases the release of inflammatory mediators by increasing ROS production, regulates the RAS system, affects glomerular thylakoid extracellular matrix formation and degradation, and can be activated by high glucose to accelerate DN (Susztak et al., 2006). In early DN, there are increased levels of p38 MAPK phosphorylation in the glomerulus (Kang et al., 2001). In the western blot assay, the same results were obtained wherein the p-p38 MAPK expression level was significantly increased in the DN group rats; after treatment, the p-p38 MAPK level was able to converge to that of the negative control rats, showing that UA seems to affect the transduction of this signaling pathway during the treatment of DN rats. A number of novel drugs for DN treatment have been shown to affect the expression of p-p38 MAPK and TGF-β1 to improve renal tubulointerstitial fibrosis in experimental animals with DN (Fujita et al., 2004; Cheng et al., 2013; Jiang et al., 2017; Wang et al., 2019a).

There are many ways to treat DN, among which glucagon-like polypeptide-1 (GLP-1) receptor agonists can slow down the progression of DN. DPP-4 inhibitors reduce GLP-1 inactivation by inhibiting the activity of DPP-4 and are currently used in kidney injury due to type 2 diabetes. In our experiment, rats in the DN group also showed an increase in the activity of DPP-4, and the level of DPP-4 expression was significantly reduced after combined treatment with ursolic acid and insulin. A study showed that treatment of rats with DN with linagliptin, a DPP-4 inhibitor, reduced proteinuria and slowed fibrotic kidney damage without affecting blood glucose levels (Sharkovska et al., 2014). Sodium glucose cotransporter 2 (SGLT2) inhibitors are beneficial in the prevention of DN. SGLT2 inhibitors exhibit renoprotective potential that relies in part on inhibition of glucose reabsorption and subsequent aberrant glycolysis in the renal tubules (Li et al., 2020b). Mineralocorticoid receptor antagonist (MRA) can block sodium reabsorption and overactivation of mineralocorticoid receptor (MR) in renal epithelial or vascular tissues mediated by MR, avoiding MR overactivation leading to fibrosis and inflammation and thus protecting the function of the kidney, which has a good prognosis for patients with chronic kidney disease (Oka et al., 2022). It has been shown that diabetes accelerates renal fibrosis in mice lacking the endothelial glucocorticoid receptor (GR) compared to control mice (Srivastava et al., 2021c). These data demonstrate that loss of podocyte GR leads to upregulation of Wnt signaling and disruption in fatty acid metabolism. Podocyte–endothelial cell crosstalk, mediated through GR, is important for glomerular homeostasis, and its disruption likely contributes to DN. It is well documented that deletion of podocyte GR leads to upregulation of Wnt signaling and disruption of fatty acid metabolism, which are important factors that may contribute to DN (Srivastava et al., 2021b).

Although novel hypoglycemic agents, such as GLP-1 analogs, SGLT2 inhibitors, and DPP-4 inhibitors, have made great progress in the protective effects of DN, they still need to be used in combination with RAAS blockers. ACEIs and ARBs are not only effective in controlling blood pressure and reducing urinary protein in the clinical management of early-to mid-stage DN but also in delaying the risk of progression of chronic kidney disease to end-stage renal disease (Deng et al., 2022). In a diabetic mouse model, ACEIs were observed to ameliorate renal fibrosis by attenuating DPP-4 and TGF-β signaling but were not demonstrated by ARBs. Furthermore, the combination of N-acetyl-serinyl-aspartyl-lysinyl-proline (AcSDKP), one of the ACE substrates, with ACEI slightly enhanced the inhibitory effect of ACEI on DPP-4 and related TGF-β signaling and revealed miR-29s and miR-let-7s as key antifibrotic players. Interestingly, ACEIs also restored miR-29 and miR-let-7 family crosstalk in endothelial cells, suggesting that the antifibrotic effects of ACEIs are due to AcSDKP-mediated antifibrotic mechanisms (Srivastava et al., 2020a). This mechanism reprograms central metabolism, including restoration of SIRT3 protein and mitochondrial fatty acid oxidation and inhibition of abnormal glucose metabolism in DN. Inhibition of AcSDKP leads to disruption of renal cellular metabolism and activation of interstitial transformation, leading to severe fibrosis in the diabetic kidney (Srivastava et al., 2020b). In our experiment, it was also found that the SIRT3 protein expression level was significantly reduced in the DN group rats, which was significantly improved by the combined treatment of ursolic acid and insulin. Wang et al. (Wang et al., 2019) found that activation of SIRT3 induced mitochondrial biosynthesis and prevented renal oxidative stress and lipid accumulation through *in vitro* and *in vivo* studies. Endothelial SIRT3 regulates the metabolic transition of myofibroblasts in DN (Srivastava et al., 2021a). We also found a significant reduction in FGFR1 in the kidneys of DN rats, which is the same as that reported in the kidneys of diabetic mice; that is, endothelial-type FGFR1 deficiency contributes to fibrogenesis in DN (Li et al., 2020a). The effect was significantly improved after combined treatment with ursolic acid and insulin. In addition, regulation of NCAM/FGFR1 signaling inhibits the EMT program in human proximal tubular epithelial cells (Životić et al., 2018).

Currently, several miRNAs (e.g., miR-29, Let-7b, miR-21, miR-30b) have been found to be involved in the regulation of EMT and EndMT to affect disease processes such as renal fibrosis (Srivastava et al., 2019). GHOSH et al. (Ghosh et al., 2012) also confirmed that the TGF-β signaling pathway induced EndMT with altered expression levels of multiple miRNAs using miRNA array analysis. Subsequent studies have confirmed that miRNAs can affect renal fibrosis. For example, the miR-29 family directly targets and inhibits the expression level of Smad3, a molecule downstream of the TGF-β signaling pathway, thereby blocking the activation of the TGF-β pathway and inhibiting the EndMT and EMT processes (Chen et al., 2014).

The formation process of renal fibrosis is complex, and there are certain interactions between signaling pathways; therefore, multiple signaling pathways and their cross-relationships can be explored in future studies to gain a comprehensive understanding of the renal fibrosis process and to find the key intersections between signaling pathways, with the aim of finding the exact pathogenesis and the best treatment path for renal fibrosis.

Conclusion

In conclusion, strict glycemic control plus ursolic acid could better reduce the degree of renal histopathological damage, apoptosis and fibrosis in rats. The underlying mechanism may be related to improving apoptosis and oxidative stress by regulating p38 MAPK, SIRT3, DPP-4 and FGFR1 levels, thereby blocking TGF-β signaling pathway activation and inhibiting EMT and EndMT processes.

Data availability statement

The original contributions presented in the study are included in the article/supplementary material, further inquiries can be directed to the corresponding authors.

Ethics statement

The animal study was reviewed and approved by all animal experiments were approved by the Ethics Committee of Changchun University of Traditional Chinese Medicine on 6 January 2020. (Changchun, China; Approval No. 2020132).

Author contributions

YL and J-LS constructed the animal models and performed the functional assays. S-KL and Y-HM performed the histological assays. J-YZ and Y-DX participated in the design of the experimental studies. YY participated in the study design and provided technical support. Z-TW participated in the statistical analysis and images. YL and J-YZ participated in the drafting of the manuscript. YY and Y-DX was involved in the screening and approval of the article. All authors read and approved the final manuscript.

Conflict of interest

The authors declare that the research was conducted in the absence of any commercial or financial relationships that could be construed as a potential conflict of interest.

Publisher's note

All claims expressed in this article are solely those of the authors and do not necessarily represent those of their affiliated organizations, or those of the publisher, the editors and the reviewers. Any product that may be evaluated in this article, or claim that may be made by its manufacturer, is not guaranteed or endorsed by the publisher.

References

Abraham, M., DE Bock, M., Smith, G., Dart, J., Fairchild, J., King, B., et al. (2021). Effect of a hybrid closed-loop system on glycemic and psychosocial outcomes in children and adolescents with type 1 diabetes: A randomized clinical trial. *JAMA Pediatr.* 175, 1227–1235. doi:10.1001/jamapediatrics.2021.3965

Ahola, A., Forsblom, C., Harjutsalo, V., and Groop, P. (2021). Nut consumption is associated with lower risk of metabolic syndrome and its components in type 1 diabetes. *Nutrients* 13, 3909. doi:10.3390/nu13113909

Balcazar, N., Betancur, L. I., Munoz, D. L., Cabrera, F. J., Castano, A., Echeverri, L. F., et al. (2021). Ursolic acid lactone obtained from Eucalyptus tereticornis increases glucose uptake and reduces inflammatory activity and intracellular neutral fat: An *in vitro* study. *Molecules* 26, 2282. doi:10.3390/molecules26082282

Castoldi, G., DI Gioia, C. R. T., Bombardi, C., Preziuso, C., Leopizzi, M., Maestroni, S., et al. (2013). Renal antifibrotic effect of N-acetyl-seryl-aspartyl-lysyl-proline in diabetic rats. *Am. J. Nephrol.* 37, 65–73. doi:10.1159/000346116

Chen, H.-Y., Zhong, X., Huang, X. R., Meng, X.-M., You, Y., Chung, A. C., et al. (2014). MicroRNA-29b inhibits diabetic nephropathy in db/db mice. *Mol. Ther.* 22, 842–853. doi:10.1038/mt.2013.235

Chen, X., Sun, L., Li, D., Lai, X., Wen, S., Chen, R., et al. (2022). Green tea peptides ameliorate diabetic nephropathy by inhibiting the TGF-β/Smad signaling pathway in mice. *Food Funct.* 13, 3258–3270. doi:10.1039/d1fo03615g

Cheng, X., Gao, W., Dang, Y., Liu, X., Li, Y., Peng, X., et al. (2013). Both ERK/MAPK and TGF-Beta/Smad signaling pathways play a role in the kidney fibrosis of diabetic mice accelerated by blood glucose fluctuation. *J. Diabetes Res.* 2013, 463740. doi:10.1155/2013/463740

Cui, F., Tang, L., Gao, Y., Wang, Y., Meng, Y., Shen, C., et al. (2019). Effect of baoshenfang formula on podocyte injury via inhibiting the NOX-4/ROS/p38 pathway in diabetic nephropathy. *J. Diabetes Res.* 2019, 2981705. doi:10.1155/2019/2981705

Dai, X., Liao, R., Liu, C., Liu, S., Huang, H., Liu, J., et al. (2021). Epigenetic regulation of TXNIP-mediated oxidative stress and NLRP3 inflammasome activation contributes to SAHH inhibition-aggravated diabetic nephropathy. *Redox Biol.* 45, 102033. doi:10.1016/j.redox.2021.102033

De Boer, I. H., Rue, T. C., Cleary, P. A., Lachin, J. M., Molitch, M. E., Steffes, M. W., et al. (2011). Long-term renal outcomes of patients with type 1 diabetes mellitus and microalbuminuria: An analysis of the diabetes control and complications trial/epidemiology of diabetes interventions and complications cohort. *Arch. Intern. Med.* 171, 412–420. doi:10.1001/archinternmed.2011.16

Deng, X., Li, D., Tang, Q., and Chen, Y. (2022). ACEI and arb lower the incidence of end-stage renal disease among patients with diabetic nephropathy: A meta-analysis. *Comput. Math. Methods Med.* 2022, 6962654. doi:10.1155/2022/6962654

Fu, J., Shinjo, T., Li, Q., St-Louis, R., Park, K., Yu, M., et al. (2022). Regeneration of glomerular metabolism and function by podocyte pyruvate kinase M2 in diabetic nephropathy. *JCI insight* 7, e155260. doi:10.1172/jci.insight.155260

Fujita, H., Omori, S., Ishikura, K., Hida, M., and Awazu, M. (2004). ERK and p38 mediate high-glucose-induced hypertrophy and TGF-beta expression in renal tubular cells. *Am. J. Physiol. Ren. Physiol.* 286, F120–F126. doi:10.1152/ajprenal.00351.2002

Geng, X. Q., Ma, A., He, J. Z., Wang, L., Jia, Y. L., Shao, G. Y., et al. (2020). Ganoderic acid hinders renal fibrosis via suppressing the TGF-β/Smad and MAPK signaling pathways. *Acta Pharmacol. Sin.* 41, 670–677. doi:10.1038/s41401-019-0324-7

Ghosh, A. K., Nagpal, V., Covington, J. W., Michaels, M. A., and Vaughan, D. E. (2012). Molecular basis of cardiac endothelial-to-mesenchymal transition (EndMT): Differential expression of microRNAs during EndMT. *Cell. Signal.* 24, 1031–1036. doi:10.1016/j.cellsig.2011.12.024

Gong, P., Wang, P., Pi, S., Guo, Y., Pei, S., Yang, W., et al. (2021). Proanthocyanidins protect against cadmium-induced diabetic nephropathy through p38 MAPK and keap1/nrf2 signaling pathways. *Front. Pharmacol.* 12, 801048. doi:10.3389/fphar.2021.801048

Gu, L., Yun-SunTang, H., and Xu, Z. (2021). Huangkui capsule in combination with metformin ameliorates diabetic nephropathy via the Klotho/TGF-β1/p38MAPK signaling pathway. *J. Ethnopharmacol.* 281, 113548. doi:10.1016/j.jep.2020.113548

Gwon, M., An, H., Gu, H., Kim, Y., Han, S., and Park, K. (2021). Apamin inhibits renal fibrosis via suppressing TGF-β1 and STAT3 signaling *in vivo* and *in vitro*. *J. Mol. Med.* 99, 1265–1277. doi:10.1007/s00109-021-02087-x

Jiang, M., Zhang, H., Zhai, L., Ye, B., Cheng, Y., and Zhai, C. (2017). ALA/LA ameliorates glucose toxicity on HK-2 cells by attenuating oxidative stress and apoptosis through the ROS/p38/TGF-β1 pathway. *Lipids Health Dis.* 16, 216. doi:10.1186/s12944-017-0611-6

Jin, J., Shi, Y., Gong, J., Zhao, L., Li, Y., He, Q., et al. (2019). Exosome secreted from adipose-derived stem cells attenuates diabetic nephropathy by promoting autophagy flux and inhibiting apoptosis in podocyte. *Stem Cell Res. Ther.* 10, 95. doi:10.1186/s13287-019-1177-1

Kang, S. W., Adler, S. G., Lapage, J., and Natarajan, R. (2001). p38 MAPK and MAPK kinase 3/6 mRNA and activities are increased in early diabetic glomeruli. *Kidney Int.* 60, 543–552. doi:10.1046/j.1523-1755.2001.060002543.x

Lecumberri, E., Ortega, M., Iturregui, M., Quesada, J. A., Vazquez, C., and Orozco, D. (2018). Quality-of-life and treatment satisfaction in actual clinical practice of patients with Type 1 diabetes mellitus (T1DM) and hypoglycemia treated with insulin degludec. *Curr. Med. Res. Opin.* 34, 1053–1059. doi:10.1080/03007995.2017.1419172

Li, J., Liu, H., Srivastava, S. P., Hu, Q., Gao, R., Li, S., et al. (2020a1979). Endothelial FGFR1 (fibroblast growth factor receptor 1) deficiency contributes differential fibrogenic effects in kidney and heart of diabetic mice. *Hypertension* 76, 1935–1944. doi:10.1161/HYPERTENSIONAHA.120.15587

Li, J., Liu, H., Takagi, S., Nitta, K., Kitada, M., Srivastava, S. P., et al. (2020b). Renal protective effects of empagliflozin via inhibition of EMT and aberrant glycolysis in proximal tubules. *JCI Insight* 5, 129034. doi:10.1172/jci.insight.129034

Li, L., Qian, K., Sun, Y., Zhao, Y., Zhou, Y., Xue, Y., et al. (2021). Omarigliptin ameliorated high glucose-induced nucleotide oligomerization domain-like receptor protein 3 (NLRP3) inflammasome activation through activating adenosine monophosphate-activated protein kinase α (AMPKα) in renal glomerular endothelial cells. *Bioengineered* 12, 4805–4815. doi:10.1080/21655979.2021.1957748

Li, S., Liao, X., Meng, F., Wang, Y., Sun, Z., Guo, F., et al. (2014). Therapeutic role of ursolic acid on ameliorating hepatic steatosis and improving metabolic disorders in high-fat diet-induced non-alcoholic fatty liver disease rats. *PLoS One* 9, e86724. doi:10.1371/journal.pone.0086724

Liu, K., Huang, Y., Wan, P., Lu, Y., Zhou, N., Li, J., et al. (2022). Ursolic acid protects neurons in temporal lobe epilepsy and cognitive impairment by repressing inflammation and oxidation. *Front. Pharmacol.* 13, 877898. doi:10.3389/fphar.2022.877898

Mapanga, R. F., Tufts, M. A., Shode, F. O., and Musabayane, C. T. (2009). Renal effects of plant-derived oleanolic acid in streptozotocin-induced diabetic rats. *Ren. Fail.* 31, 481–491. doi:10.1080/08860220902963558

Morandi, A., Corradi, M., Orsi, S., Piona, C., Zusi, C., Costantini, S., et al. (2021). Oxidative stress in youth with type 1 diabetes: Not only a matter of gender, age, and glycemic control. *Diabetes Res. Clin. Pract.* 179, 109007. doi:10.1016/j.diabres.2021.109007

Oka, T., Sakaguchi, Y., Hattori, K., Asahina, Y., Kajimoto, S., Doi, Y., et al. (2022). Mineralocorticoid receptor antagonist use and hard renal outcomes in real-world patients with chronic kidney disease. *Hypertension* 79, 679–689. doi:10.1161/HYPERTENSIONAHA.121.18360

Qin, X., Zhu, S., Chen, Y., Chen, D., Tu, W., and Zou, H. (2020). Long non-coding RNA (LncRNA) CASC15 is upregulated in diabetes-induced chronic renal failure and regulates podocyte apoptosis. *Med. Sci. Monit.* 26, e919415. doi:10.12659/MSM.919415

Ramaphane, T., Gezmu, A., Tefera, E., Gabaitiri, L., Nchingane, S., Matsheng-Samuel, M., et al. (2021). Prevalence and factors associated with microalbuminuria in pediatric patients with type 1 diabetes mellitus at a large tertiary-level hospital in Botswana. *Diabetes Metab. Syndr. Obes.* 14, 4415–4422. doi:10.2147/DMSO.S322847

Roumeliotis, S., Roumeliotis, A., Georgianos, P., Stamou, A., Manolopoulos, V., Panagoutsos, S., et al. (2021). Oxidized ldl is associated with eGFR decline in proteinuric diabetic kidney disease: A cohort study. *Oxid. Med. Cell. Longev.* 2021, 2968869. doi:10.1155/2021/2968869

Sharkovska, Y., Reichetzeder, C., Alter, M., Tsuprykov, O., Bachmann, S., Secher, T., et al. (2014). Blood pressure and glucose independent renoprotective effects of dipeptidyl peptidase-4 inhibition in a mouse model of type-2 diabetic nephropathy. *J. Hypertens.* 32, 2211–2223. doi:10.1097/HJH.0000000000000328

Srivastava, S. P., Goodwin, J. E., Kanasaki, K., and Koya, D. (2020b). Metabolic reprogramming by N-acetyl-seryl-aspartyl-lysyl-proline protects against diabetic kidney disease. *Br. J. Pharmacol.* 177, 3691–3711. doi:10.1111/bph.15087

Srivastava, S. P., Goodwin, J. E., Kanasaki, K., and Koya, D. (2020a). Inhibition of angiotensin-converting enzyme ameliorates renal fibrosis by mitigating DPP-4 level and restoring antifibrotic MicroRNAs. *Genes* 11, E211. doi:10.3390/genes11020211

Srivastava, S. P., Hedayat, A. F., Kanasaki, K., and Goodwin, J. E. (2019). microRNA crosstalk influences epithelial-to-mesenchymal, endothelial-to-mesenchymal, and macrophage-to-mesenchymal transitions in the kidney. *Front. Pharmacol.* 10, 904. doi:10.3389/fphar.2019.00904

Srivastava, S. P., Li, J., Takagaki, Y., Kitada, M., Goodwin, J. E., Kanasaki, K., et al. (2021a). Endothelial SIRT3 regulates myofibroblast metabolic shifts in diabetic kidneys. *IScience* 24, 102390. doi:10.1016/j.isci.2021.102390

Srivastava, S. P., Zhou, H., Setia, O., Dardik, A., Fernandez-Hernando, C., and Goodwin, J. (2021b). Podocyte glucocorticoid receptors are essential for glomerular endothelial cell homeostasis in diabetes mellitus. *J. Am. Heart Assoc.* 10, e019437. doi:10.1161/JAHA.120.019437

Srivastava, S. P., Zhou, H., Setia, O., Liu, B., Kanasaki, K., Koya, D., et al. (2021c). Loss of endothelial glucocorticoid receptor accelerates diabetic nephropathy. *Nat. Commun.* 12, 2368. doi:10.1038/s41467-021-22617-y

Susztak, K., Raff, A. C., Schiffer, M., and BöTTINGER, E. P. (2006). Glucose-induced reactive oxygen species cause apoptosis of podocytes and podocyte depletion at the onset of diabetic nephropathy. *Diabetes* 55, 225–233. doi:10.2337/diabetes.55.01.06.db05-0894

Takir, M., Unal, A. D., Kostek, O., Bayraktar, N., and Demirag, N. G. (2016). Cystatin-C and TGF-β levels in patients with diabetic nephropathy. *Nefrologia* 36, 653–659. doi:10.1016/j.nefro.2016.06.011

Toffoli, B., Tonon, F., Tisato, V., Michelli, A., Zauli, G., Secchiero, P., et al. (2020). TRAIL treatment prevents renal morphological changes and TGF-β-induced mesenchymal transition associated with diabetic nephropathy. *Clin. Sci.* 134, 2337–2352. doi:10.1042/CS20201004

Tong, Y., Liu, S., Gong, R., Zhong, L., Duan, X., and Zhu, Y. (2019). Ethyl vanillin protects against kidney injury in diabetic nephropathy by inhibiting oxidative stress and apoptosis. *Oxid. Med. Cell. Longev.* 2019, 2129350. doi:10.1155/2019/2129350

Tota, Ł., Matejko, B., Morawska-Tota, M., Pilch, W., Mrozińska, S., Pałka, T., et al. (2021). Changes in oxidative and nitrosative stress indicators and vascular endothelial growth factor After maximum-intensity exercise assessing aerobic capacity in males with type 1 diabetes mellitus. *Front. Physiol.* 12, 672403. doi:10.3389/fphys.2021.672403

Wang, S., Zhou, Y., Zhang, Y., He, X., Zhao, X., Zhao, H., et al. (2019a). Roscovitine attenuates renal interstitial fibrosis in diabetic mice through the TGF-β1/p38 MAPK pathway. *Biomed. Pharmacother. = Biomedecine Pharmacother.* 115, 108895. doi:10.1016/j.biopha.2019.108895

Wang, X.-T., Gong, Y., Zhou, B., Yang, J.-J., Cheng, Y., Zhao, J.-G., et al. (2018). Ursolic acid ameliorates oxidative stress, inflammation and fibrosis in diabetic cardiomyopathy rats. *Biomed. Pharmacother. = Biomedecine Pharmacother.* 97, 1461–1467. doi:10.1016/j.biopha.2017.11.032

Wang, Z., Li, Y., Wang, Y., Zhao, K., Chi, Y., and Wang, B. (2019b). Pyrroloquinoline quinine protects HK-2 cells against high glucose-induced oxidative stress and apoptosis through Sirt3 and PI3K/Akt/FoxO3a signaling pathway. *Biochem. Biophys. Res. Commun.* 508, 398–404. doi:10.1016/j.bbrc.2018.11.140

Westenfelder, C., Hu, Z., Zhang, P., and Gooch, A. (2021). Intraperitoneal administration of human "Neo-Islets", 3-D organoids of mesenchymal stromal and pancreatic islet cells, normalizes blood glucose levels in streptozotocin-diabetic NOD/SCID mice: Significance for clinical trials. *PloS one* 16, e0259043. doi:10.1371/journal.pone.0259043

Wu, W., Huang, X., You, Y., Xue, L., Wang, X., Meng, X., et al. (2021a). Latent TGF-β1 protects against diabetic kidney disease via Arkadia/Smad7 signaling. *Int. J. Biol. Sci.* 17, 3583–3594. doi:10.7150/ijbs.61647

Wu, X., Li, H., Wan, Z., Wang, R., Liu, J., Liu, Q., et al. (2021b). The combination of ursolic acid and empagliflozin relieves diabetic nephropathy by reducing inflammation, oxidative stress and renal fibrosis. *Biomed. Pharmacother. = Biomedecine Pharmacother.* 144, 112267. doi:10.1016/j.biopha.2021.112267

Xiang, M., Wang, J., Zhang, Y., Ling, J., and Xu, X. (2012). Attenuation of aortic injury by ursolic acid through RAGE-Nox-NFκB pathway in streptozocin-induced diabetic rats. *Arch. Pharm. Res.* 35, 877–886. doi:10.1007/s12272-012-0513-0

Xu, H. L., Wang, X. T., Cheng, Y., Zhao, J. G., Zhou, Y. J., Yang, J. J., et al. (2018). Ursolic acid improves diabetic nephropathy via suppression of oxidative stress and inflammation in streptozotocin-induced rats. *Biomed. Pharmacother.* 105, 915–921. doi:10.1016/j.biopha.2018.06.055

Xu, Z., Luo, W., Chen, L., Zhuang, Z., Yang, D., Qian, J., et al. (2022). Ang II (angiotensin II)-Induced FGFR1 (fibroblast growth factor receptor 1) activation in tubular epithelial cells promotes hypertensive kidney fibrosis and injury. *Hypertension* 79, 2028–2041. doi:10.1161/HYPERTENSIONAHA.122.18657

Yu, S. G., Zhang, C. J., Xu, X. E., Sun, J. H., Zhang, L., and Yu, P. F. (2015). Ursolic acid derivative ameliorates streptozotocin-induced diabestic bone deleterious effects in mice. *Int. J. Clin. Exp. Pathol.* 8, 3681–3690.

Zhang, F., and Jiang, X. (2022). The efficacy and safety of canagliflozin in the treatment of patients with early diabetic nephropathy. *J. Physiol. Pharmacol.* 73. doi:10.26402/jpp.2022.1.06

Zhang, Y., Tan, R., Yu, Y., Niu, Y., and Yu, C. (2021). LncRNA GAS5 protects against TGF-β-induced renal fibrosis via the Smad3/miRNA-142-5p axis. *Am. J. Physiol. Ren. Physiol.* 321, F517–F526. doi:10.1152/ajprenal.00085.2021

Zhang, Y., Wang, Y., Zheng, G., Liu, Y., Li, J., Huang, H., et al. (2022). Follistatin-like 1 (FSTL1) interacts with Wnt ligands and Frizzled receptors to enhance Wnt/β-catenin signaling in obstructed kidneys *in vivo*. *J. Biol. Chem.* 298, 102010. doi:10.1016/j.jbc.2022.102010

Zhao, M., Sun, S., Huang, Z., Wang, T., and Tang, H. (2020). Network meta-analysis of novel glucose-lowering drugs on risk of acute kidney injury. *Clin. J. Am. Soc. Nephrol.* 16, 70–78. doi:10.2215/CJN.11220720

Zheng, H. X., Qi, S. S., He, J., Hu, C. Y., Han, H., Jiang, H., et al. (2020). Cyanidin-3-glucoside from black rice ameliorates diabetic nephropathy via reducing blood glucose, suppressing oxidative stress and inflammation, and regulating transforming growth factor β1/smad expression. *J. Agric. Food Chem.* 68, 4399–4410. doi:10.1021/acs.jafc.0c00680

Zheng, W., Qian, C., Xu, F., Cheng, P., Yang, C., Li, X., et al. (2021). Fuxin Granules ameliorate diabetic nephropathy in db/db mice through TGF-β1/Smad and VEGF/VEGFR2 signaling pathways. *Biomed. Pharmacother. = Biomedecine Pharmacother.* 141, 111806. doi:10.1016/j.biopha.2021.111806

Zhou, D., Bao, Q., and Fu, S. (2021). Anticancer activity of ursolic acid on retinoblastoma cells determined by bioinformatics analysis and validation. *Ann. Transl. Med.* 9, 1548. doi:10.21037/atm-21-4617

Životić, M., Tampe, B., MüLLER, G., MüLLER, C., Lipkovski, A., Xu, X., et al. (2018). Modulation of NCAM/FGFR1 signaling suppresses EMT program in human proximal tubular epithelial cells. *PloS One* 13, e0206786. doi:10.1371/journal.pone.0206786

frontiers | Frontiers in Pharmacology

TYPE Review
PUBLISHED 11 October 2022
DOI 10.3389/fphar.2022.998574

OPEN ACCESS

EDITED BY
Swayam Prakash Srivastava,
Yale University, United States

REVIEWED BY
Quan Hong,
Chinese PLA General Hospital, China
Anqun Chen,
Central South University, China
Eun Hee Koh,
University of Ulsan, South Korea

*CORRESPONDENCE
Sijie Zhou,
fcczhousj@zzu.edu.cn
Zhangsuo Liu,
zhangsuoliu@zzu.edu.cn

SPECIALTY SECTION
This article was submitted to Renal Pharmacology,
a section of the journal
Frontiers in Pharmacology

RECEIVED 20 July 2022
ACCEPTED 20 September 2022
PUBLISHED 11 October 2022

CITATION
Wan J, Liu D, Pan S, Zhou S and Liu Z (2022), NLRP3-mediated pyroptosis in diabetic nephropathy.
Front. Pharmacol. 13:998574.
doi: 10.3389/fphar.2022.998574

NLRP3-mediated pyroptosis in diabetic nephropathy

Jiayi Wan [1,2,3,4], Dongwei Liu[1,2,3,4], Shaokang Pan[1,2,3,4], Sijie Zhou[1,2,3,4]* and Zhangsuo Liu[1,2,3,4]*

[1]Traditional Chinese Medicine Integrated Department of Nephrology, The First Affiliated Hospital of Zhengzhou University, Zhengzhou, China, [2]Research Institute of Nephrology, Zhengzhou University, Zhengzhou, China, [3]Henan Province Research Center for Kidney Disease, Zhengzhou, China, [4]Key Laboratory of Precision Diagnosis and Treatment for Chronic Kidney Disease in Henan Province, Zhengzhou, China

Diabetic nephropathy (DN) is the main cause of end-stage renal disease (ESRD), which is characterized by a series of abnormal changes such as glomerulosclerosis, podocyte loss, renal tubular atrophy and excessive deposition of extracellular matrix. Simultaneously, the occurrence of inflammatory reaction can promote the aggravation of DN-induced kidney injury. The most important processes in the canonical inflammasome pathway are inflammasome activation and membrane pore formation mediated by gasdermin family. Converging studies shows that pyroptosis can occur in renal intrinsic cells and participate in the development of DN, and its activation mechanism involves a variety of signaling pathways. Meanwhile, the activation of the NOD-like receptor thermal protein domain associated protein 3 (NLRP3) inflammasome can not only lead to the occurrence of inflammatory response, but also induce pyroptosis. In addition, a number of drugs targeting pyroptosis-associated proteins have been shown to have potential for treating DN. Consequently, the pathogenesis of pyroptosis and several possible activation pathways of NLRP3 inflammasome were reviewed, and the potential drugs used to treat pyroptosis in DN were summarized in this review. Although relevant studies are still not thorough and comprehensive, these findings still have certain reference value for the understanding, treatment and prognosis of DN.

KEYWORDS

diabetic nephropathy, pyroptosis, pathogenesis, signaling pathways, drugs

Introduction

Inflammasomes were first discovered in 2002 as multi-protein complexes with the function of inducing inflammation (Martinon et al., 2002). The assembly and activation of inflammasomes can occur in different organelles such as mitochondria, endoplasmic reticulum, and nucleus (Pandey et al., 2021). Clinical diagnosis of certain diseases and monitoring of treatment response can be realized through inflammasome imaging systems (Nandi et al., 2022). NOD-like receptor thermal protein domain associated protein 3 (NLRP3) inflammasome is a well-studied inflammasome, which is mainly composed of NLRP3, apoptosis-associated speck-like protein containing a caspase

recruitment domain (ASC) and caspase-1, and assembled after pattern recognition receptors (PRRs) receive danger signals (Broz and Dixit, 2016). The activation of NLRP3 inflammasome not only leads to an inflammatory response, but also induces a type of lytic cell death known as pyroptosis (Huang et al., 2021b).

Over long periods of time, the study of pyroptosis was put on hold and was once defined as "apoptosis" (Zychlinsky et al., 1994; Hersh et al., 1999). It was not until 2015 that Academician Shao Feng and his team reported the process of gasdermin D (GSDMD) being cleaved by caspase family that people began to make new breakthroughs in the study of pyroptosis (Shi et al., 2015). Currently, pyroptosis is defined as a member of programmed cell death (PCD), which has crosstalk between apoptosis and autophagy (Doerflinger et al., 2020; Zhang et al., 2021b). Necroptosis, pyroptosis, and ferroptosis are three widely studied non-apoptotic cell deaths. Molecularly, necroptosis is a form of PCD that depends on the sequential activation of receptor interacting serine/threonine kinase 3 (RIPK3) and mixed lineage kinase domains, which can assemble into oligomeric complexes called necrosomes (Linkermann and Green, 2014). Ferroptosis is characterized by the overwhelming, iron-dependent accumulation of lethal lipid ROS, independent of caspases and necrosomes components (Dixon et al., 2012). Apoptosis involves several different activation mechanisms, including the intrinsic and extrinsic pathways, intrinsic endoplasmic reticulum pathway, and these processes dependent on TNF receptors, caspase-3, and Bcl-2 family (Wong, 2011). Pyroptosis mainly depends on the pore-forming properties of the gasdermin family (Yu et al., 2021b). Morphologically, apoptosis is manifested in the formation of apoptotic bodies, cytoplasmic shrinkage, and chromatin condensation; necroptosis is mainly manifested by cell swelling, and there are no obvious involvement of phagocytes and lysosomes; ferroptosis is mainly manifested by mitochondrial changes, including shrinkage, electron-dense ultrastructure, and reduced/disappeared cristae (Galluzzi et al., 2018). It has been recognized that when pyroptosis occurs, deoxyribonucleic acid (DNA) double-strand breaks, cells swell, pores form in the cell membrane, and cells contents leak out, resulting in the destruction of the balance of sodium and potassium ions inside and outside the cells (Kovacs and Miao, 2017). These different cell death modes perform different functions. Although pyroptosis can recruit immune cells to attack pathogens by releasing inflammatory factors, excessive pyroptosis can damage cell membrane integrity and lead to organ damage (Man et al., 2017). Initially, pyroptosis was thought to occur only in immune cells, but a large number of studies have shown that pyroptosis can also occur in other cell types. For instance, pyroptosis can promote the proliferation, invasion, and metastasis of cancer cells, and it can also induce retinopathy under high glucose (HG) stimulation (Zhou and Fang, 2019; Gan et al., 2020).

Diabetic nephropathy (DN) is not only a chronic disease with a complex pathogenesis, but also one of the main factors leading to end-stage renal disease (ESRD) (Ilyas et al., 2017). Based on current epidemiological data, the number of DN patients is expected to increase further in the coming decades (Saeedi et al., 2019). The occurrence of DN can induce a series of abnormal changes such as glomerular hypertrophy, podocyte loss, and mesangial matrix expansion (Alicic et al., 2017). Progressive DN is not only the result of glucose metabolism disorder and reactive oxygen species (ROS) production, but also the result of chronic low-grade inflammation and fibrosis (Rayego-Mateos et al., 2020; Maiti, 2021). Genomics analysis found significant ferroptosis in the DN group (Wang et al., 2022c). It has also been found that necroptosis shares several upstream signaling pathways with apoptosis, and that necroptosis may have a greater impact on podocyte loss in DN than apoptosis under the regulation of ubiquitin C-terminal hydrolase L1 (UCHL1) (Xu et al., 2019). Furthermore, studies have shown that in the DN mouse model, the redox balance in kidney cells was disrupted and pyroptosis was shown to be triggered, resulting in loss of kidney cells and impaired kidney function (Cuevas and Pelegrín, 2021). The release of a large number of pro-inflammatory factors such as Interleukin-1β (IL-1β) and Interleukin-18 (IL-18) will lead to an increase in renal vascular permeability, and the urinary protein excretion rate will further increase (Yaribeygi et al., 2019).

NLRP3 inflammasome-mediated pyroptosis is one of the main activation mechanisms of pyroptosis and also a key step in the activation of inflammatory responses. When the NLRP3 inflammasome is activated, it converts inactive pro-caspase-1 into active cleaved-caspase-1, which subsequently promotes the production of mature IL-1β and IL-18 and cleaves GSDMD. The N-terminal fragment of GSDMD leads to the formation of membrane pores and induces pyroptosis (Wang and Hauenstein, 2020). Meanwhile, the activation of NLRP3 inflammasome can cause the production of a large number of inflammatory factors, which is the pathogenesis of certain inflammatory diseases including DN (Yang et al., 2021b). Hyperglycemia, hyperlipidemia, and hyperuricemia can all activate the NLRP3 inflammasome, and NLRP3 knockout (KO) can attenuate glomerular hypertrophy, glomerulosclerosis, and mesangial matrix expansion in streptozotocin (STZ)-induced diabetic mice (Qiu and Tang, 2016; Wu et al., 2018). Therefore, targeting NLRP3 and GSDMD to inhibit pyroptosis may serve as a potential therapeutic strategy (Newton et al., 2021). In this review, we first introduced three activation mechanisms of pyroptosis and described the correlation between NLRP3 inflammasome activation and pyroptosis, and then we explored several pathways that may lead to NLRP3 inflammasome activation and its effects in pyroptosis.Finally, some potential therapeutic drugs for pyroptosis in DN were summarized.

Three molecular mechanisms of pyroptosis

Canonical inflammasome pathway

Activation of inflammasome and cleavage of gasdermin family are two of the most important processes in the canonical inflammasome pathway. When the recognition of pathogen-associated molecular patterns (PAMPs) and damage-associated molecular patterns (DAMPs) by PRRs was activated by bacteria, viruses and various pathological factors, different inflammasomes were assembled with the participation of adaptor proteins (such as: ASC) and effector proteins (such as: caspase family) (Lin et al., 2020). Subsequently, pro-caspase-1 can be recruited by inflammasomes and activated into cleaved-caspase-1. Cleaved-caspase-1 can activate IL-1β and IL-18. Next, the activated IL-1β and IL-18 can release into the extracellular in a manner independent of the gasdermin family and mediate the inflammatory cascade. However, GSDMD can be cleaved into GSDMD-N-terminal (GSDMD-NT) with pore forming characteristics and GSDMD-C-terminal (GSDMD-CT), which is the key process leading to pyroptosis (Liu et al., 2016b).

The PRR family includes Toll-like receptors (TLRs) and C-type lectin receptors (CLRs), which are mainly located on cell membranes, and NOD-like Receptors (NLRs) and absent in melanoma 2 (AIM2)-like receptors (ALRs), which are mainly located in the cytoplasm (Plato et al., 2015). Different inflammasomes adapt to different activation mechanisms, and their activation signals are diverse, such as ROS generation, endoplasmic reticulum (ER) stress, calcium (Ca^{2+}) overload, and nicotinamide adenine dinucleotide phosphate (NADPH) oxidase (NOXs) activation (Xue et al., 2019). In general, the activation of the NLRP3 inflammasome requires the participation of ASC, but for NLR family CARD domain containing 4 (NLRC4) and NLRP1, they can directly interact with caspase-1 independent of ASC (Zhai et al., 2017; Duncan and Canna, 2018). Additionally, recent studies have shown that Cd exposure can activate AIM2 by increasing oxidative stress (Zhou et al., 2022). Cerebral ischemia/reperfusion (I/R) injury can also induce the release of ectopic dsDNA to promote AIM2 inflammasome assembly and pyroptosis (Li et al., 2019). Moreover, AIM2 has also been identified as a direct target of miR-485, which can inhibit inflammatory response under the action of MEG3 (Liang et al., 2020). It is known that AIM2 inflammasome can also be activated in macrophages to induce GSDMD-dependent pyroptosis (Gao et al., 2019). Interestingly, the expression of GSDMD-N was also significantly increased accompanied by the increase of AIM2 in kidney induced by aldosterone, which aggravated the renal fibrosis (Wu et al., 2022b). Downregulation of AIM2 can reduce the expression of caspase-1, IL-1β, and IL-18 in human glomerular mesangial (HGM) cells (Zhen et al., 2014). Although the above experiments can prove that the AIM2 inflammasome is related to pyroptosis, there is still a gap in the research on whether AIM2 can be a new target for inhibiting pyroptosis in DN.

In addition to AIM2 inflammasome, TLR2, and TLR4 have recently been found to further activate NLRP3 inflammasome by activating nuclear-factor κB (NF-κB) signaling pathway to regulate ozonation-induced pyroptosis (Tian et al., 2021). Meanwhile, the regulation of TLR/NF-κB pathway can also improve renal function and promote renal injury repair (Wang et al., 2019a; Wu et al., 2019). Additionally, Mincle is a C-type lectin receptor whose activation has been shown *in vitro* to promote the release of pro-inflammatory cytokines and pyroptosis of macrophages (Gong et al., 2020). Inhibition of the Mincle/Syk/NF-κB signaling pathway can also reduce the expression of ASC and caspase-1 (He et al., 2022). Although there is still a lack of research on the role of CLRs and TLRs in pyroptosis of DN, their effects on pyroptosis in other cells should not be ignored.

Gasdermin family includes GSDMA, GSDMB, GSDMC, GSDMD, DFNA5, and DFNB59, they are widely expressed in different cells and tissues (Kovacs and Miao, 2017). It has been reported that the N-terminal domain of gasdermin family can bind to phosphorylated phosphatidylinositol and may form pores on lipid membranes (Ding and Shao, 2018). Although such pore formation character of gasdermin family is the molecular basis for pyroptosis, GSDMD is the primary molecule with pore-forming properties in the canonical inflammasome pathway (Ding et al., 2016). And so far, there are no known mechanisms, other than cleavage, for regulating GSDMD (Gao et al., 2022a). GSDME can also mediated pyroptosis, but whether other proteins of gasdermin family can regulate pyroptosis in DN still lacks specific research (Rogers et al., 2019; Li et al., 2021g).

Non-canonical inflammasome pathway

In the non-canonical inflammasome pathway, caspase-4/5/11 can directly respond to the pathogen structural molecules [e.g., lipopolysaccharide (LPS), lipid A] through the caspase recruitment domain (CARD) and lead to the cleavage of GSDMD and the release of IL-1β and IL-18 (Rathinam et al., 2019). The product of this pathway can also induce the activation of caspase-1 and promote IL-1β and IL-18 maturation (Downs et al., 2020). It has been reported that GSDMB does not induce pyroptosis through its N-terminal like other proteins of gasdermin family, but promotes caspase-4 activity by directly binding to the CARD domain of caspase-4 (Chen et al., 2019b). Subsequently, activated caspase-4 can lead to membrane pore formation with the help of GSDMD, followed by potassium influx to activate NLRP3 (Linder and Hornung, 2020). Downregulation of caspase-4 can inhibit the occurrence of TNF-α-induced pyroptosis of human pulmonary artery

endothelial cells (HPAEC) and the activation of GSDMD and GSDME (Wu et al., 2022a). Additionally, leishmania lipophosphoglycan (LPG) and C/EBP homologous protein (CHOP) have also been reported to induce the activation of caspase-11, and activated caspase-11 can directly act on pro-caspase-1 and activate it (Yang et al., 2014; de Carvalho et al., 2019). Caspase-11 has a special recognition mechanism for protein substrates, which is mainly mediated by the P1′-P4′ region of its substrate GSDMD, and caspase-4 and caspase-5 are also regulated by the same mechanism (Bibo-Verdugo et al., 2020). Arginine adenosine-5′-diphosphoribosylation (ADP-ribosylation) of caspase-4/11 can block its recognition and cleavage of GSDMD (Li et al., 2021k). Moreover, CHOP silencing significantly reduced the activity of caspase-11 and the cleavage of GSDMD in renal tubular epithelial cells (Yang et al., 2014; Zhang et al., 2018). The above evidence suggests that inhibiting the activation of non-canonical inflammasome pathway may be a therapeutic target for certain diseases, but this is beyond the scope of this paper. Taking together, the activation of pyroptosis mediated by caspase-4/5/11 has a complex mechanism, and its role in DN still needs to be further explored.

Caspase-3-mediated inflammasome pathway

Traditionally, caspase-3 is the core molecular of apoptosis and caspase-8 is also involved in apoptosis. However, recent studies have shown that caspase-3 was activated during LPS-induced pyroptosis (Hu et al., 2021). In some cases, gasdermin E (DFNA5) can also be cleaved by caspase-3 and lead to a transition from apoptosis to pyroptosis (Wang et al., 2017; Zhang et al., 2021h). Although inflammasome is generally considered to play a major role in the canonical inflammasome pathway, AIM2 inflammasome has recently been found to activate caspase-3 and promote DFNA5 expression (Li et al., 2021i). Zeng et al. (2019) also used NLRP3 specific inhibitors to inhibit the activation of the NLRP3-mediated pyroptosis, finding that ATP induced macrophage pyroptosis *via* the caspase-3/GSDME axis. Meanwhile, activated caspase-3 can also inactivate pore-forming domain (PFD) in GSDMD, inhibiting GSDMD-mediated pyroptosis (Taabazuing et al., 2017). It is worth noting that both GSDMD-NT and GSDME-NT can act on mitochondria and make them generate a large amount of ROS, inducing apoptosis and further stimulating the release of inflammatory substances (Rogers et al., 2019). Besides, caspase-1, which mediates the canonical inflammasome pathway, can not only activate caspase-3/7, but also activate Bid in GSDMD deficient cells and lead to apoptosis by inducing the release of cytochrome C in mitochondrial (Tsuchiya et al., 2019). When caspase-11 is overexpressed, caspase-3 can also be activated to promote apoptosis (Miao et al., 2018). Notably, transfection of podocytes with GSDMD siRNA reversed HG-induced inflammation and apoptosis, which may be related to the blocking of JNK signaling pathway (Li et al., 2021a). Although apoptosis-related proteins were also activated in caspase-3-dependent pyroptosis signaling pathway, pyroptosis activation occurred more rapidly (Tsuchiya, 2021). Interestingly, the expression of autophagy-related proteins light chain (LC) 3 I/II and beclin 1 were also reduced with the inhibition of NLRP3 in podocytes of DN (Hou et al., 2020b). Z-DEVD-FMK, an inhibitor of caspase-3, has also been reported to improve proteinuria and tubulointerstitial fibrosis in DN mice and this nephroprotective effect may be related to the inhibition of GSDME (Wen et al., 2020). Moreover, the studies also showed that programmed cell death-ligand 1 (PD-L1) can activate caspase-8 and specifically cleave GSDMC under the action of TNF-α, and then the pores can form in the cell membrane and the apoptosis can transform into pyroptosis (Hou et al., 2020a). Consequently, there is a crosstalk between apoptosis and pyroptosis and even autophagy. Although the mechanism is not completely clear, it provides a new perspective for understanding PCD. Figure 1 summarized the three molecular mechanisms of pyroptosis.

NLRP3 inflammosome activation and pyroptosis

NLRP3 is a member of the NLRs protein family and also one of the core molecules in the NLRP3 inflammasome. Different domains contained in NLRP3 play different functions. When a leucine-rich repeat (LRR) domain located at the C-terminus is recognized by the ligand, the nucleotide-binding oligomerization domain (NOD) located at the center of the molecule can play an oligomerization role, resulting in conformational rearrangement of NLRP3 and exposing the pyrin domain (PYD) or CARD located at the N-terminus, which subsequently activates the biological effects of the corresponding effector molecules (Inohara et al., 2005). Many studies suggest that inhibiting the expression of NLRP3 has a protective effect on cells (Song et al., 2018a; Wang et al., 2020a). However, it has also been shown that in the unilateral ureter obstruction (UUO) model, Nlrp3−/− increased the damage of renal tubular epithelial cells, and they also suggest that NLRP3 may have an inflammasome-independent role (Pulskens et al., 2014). The reasons for this discrepancy in findings are not fully understood. However, some studies on inflammasome activation did not select cell-specific NLRP3 knockout mice, which may interfere with experimental results due to the inability to distinguish the inflammasomes in the renal

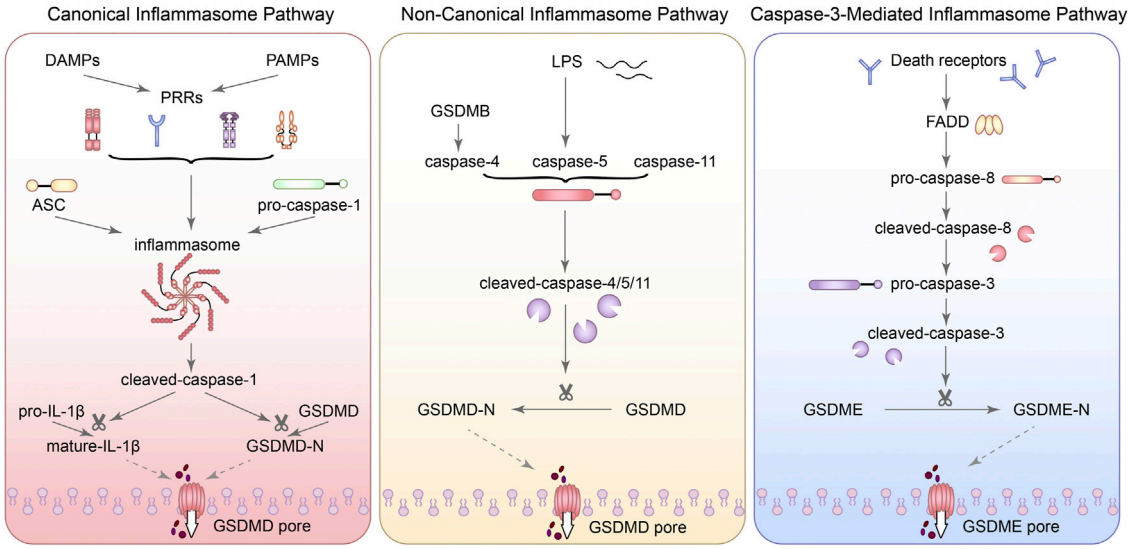

FIGURE 1
The three molecular mechanisms of pyroptosis. (1) In the canonical inflammasome pathway, when the recognition of PAMPs and DAMPs by PRRs was activated, different inflammasomes were assembled with the participation of adaptor proteins (such as: ASC) and effector proteins (such as: caspase family). Subsequently, pro-caspase-1 can be recruited by inflammasomes and activated into cleaved-caspase-1. Cleaved-caspase-1 can activate IL-1β. Next, the activated IL-1β can release into the extracellular. GSDMD can be cleaved into GSDMD-N-terminal (GSDMD-NT) with pore forming characteristics, which is the key process leading to pyroptosis. (2) In the non-canonical inflammasome pathway, caspase-4/5/11 can directly respond to LPS and lead to the cleavage of GSDMD. GSDMB can promote caspase-4 activity by directly binding to the CARD domain of caspase-4. (3) In the caspase-3-mediated inflammasome pathway, GSDME can also be cleaved by caspase-3 and lead to pyroptosis.

parenchyma or phagocytes. It has also been suggested that NLRP3 exerts its function independently of the inflammasome or performs its regulatory role in the form of the NLRP3 inflammasome may be related to different cell types (Komada and Muruve, 2019).

Conventional studies suggest that NLRP3 inflammasome activation is an essential part of the canonical inflammasome pathway. The activation of NLRP3 inflammasome can lead to the cleavage of GSDMD and lytic cell death (Yu et al., 2021b). However, through recent studies in macrophages, Evavold et al. (2018) suggested that GSDMD activation following activation of the NLRP3 inflammasome may determine two distinct cell fates. One induces GSDMD-dependent pyroptosis, while the other induces the indirect release of IL-1 triggered by hyperactivation of cells in a viable state. In other words, even if the NLRP3 inflammasome causes GSDMD to be cleaved by activated caspase-1, pyroptosis does not necessarily occur. Not only that, they also found that the activation of the NLRP3 inflammasome in these two different cell fates is sensitive to different treatments, such as high extracellular potassium concentrations. Meanwhile, several studies in recent years have shown that cytokines can be released from living cells without pyroptosis occurring in the process (Gaidt et al., 2016; Zanoni et al., 2016). Interestingly, GSDMD may also regulate the NLRP3 inflammasome through miR-223 (Kong et al., 2022). Furthermore, in the absence of GSDMD, sustained exposure to LPS can trigger pyroptosis and the release of inflammatory cytokines *via* activation of the caspase-3/GSDME axis. This means that inhibition of GSDMD alone does not completely prevent cytokine secretion and pyroptosis in response to certain inflammatory challenges (Wang et al., 2021a). Consequently, although the advantages and disadvantages of NLRP3 inflammasome blockers, the inhibition of GSDMD-induced pyroptosis and the status of clinical trials have been discussed, the protective effect on cells by inhibiting the activation of the NLRP3 inflammasome is not necessarily related to the inhibition of pyroptosis (Coll et al., 2022). Therefore, when exploring the role of NLRP3 inflammasome inhibitors, it is necessary to verify whether the pyroptosis-associated proteins (such as GSDMD) are regulated accordingly, so as to more accurately understand whether the therapeutic effects of these inhibitors are also related to the regulation of pyroptosis. Despite the many advances made in recent years, the focus on NLRP3 and pyroptosis still leaves gaps in our understanding of the inflammasome. In conclusion, although the activation of the NLRP3 inflammasome does not necessarily lead to pyroptosis, it is still important to review the regulatory pathway of the inflammasome and its potential clinical application as a pre-signal for the activation of the canonical inflammasome pathway of pyroptosis.

NLRP3 inflammosome-dependent pyroptosis regulatory pathways in diabetic nephropathy

It is well known that chronic sterile inflammation in DN is closely related to renal impairment. The inflammatory cascade induced by NLRP3 inflammasome and IL-1β and IL-18 also has a significant impact on the development of DN. Meanwhile, activation of NLRP3 inflammasome is also the key process to initiate pyroptosis. There are multiple recognized mechanisms or pathways for the activation of NLRP3 inflammasome, such as the massive production of mitochondrial ROS, the reduction of intracellular potassium concentration, and the destabilization of lysosomes (Jo et al., 2016; Paik et al., 2021). However, it still remains to be demonstrated whether the protective effects of these signaling pathways by regulating NLRP3 inflammasome activation are related to pyroptosis. Here we describe several possible signaling pathways, hopefully providing a more complete overview.

NF-κB/NLRP3 inflammasome signalling pathway

In general, NF-κB binds with inhibitor of NF-κB (IκB) to anchor in cytoplasm in inactive form, dissociates upon stimulation and exposes the active form of P50/P65 heterodimer. It then enters the nucleus and participates in various reactions (Porta et al., 2020). NF-κB can be activated by a variety of factors, and it can regulate inflammatory response, stress response, pyroptosis and apoptosis (Yu et al., 2020; Yu et al., 2021a; Piao et al., 2021). Recently, evidence from clinical and experimental studies has shown that TLRs can induce sterile tubulointerstitial inflammatory responses through the NF-κB signaling pathway. The NLRP3 inflammasome can be activated by NF-κB during this process, linking the perception of metabolic stress in the DN kidney with the activation of a pro-inflammatory cascade (Tang and Yiu, 2020). In addition, it has also been shown that lncRNA-Gm4419 can directly interact with p50, which can interact with the NLRP3 inflammasome and lead to increased expression of pro-inflammatory cytokines in mesangial cells (MCs) under HG stimulation (Yi et al., 2017). These evidences suggest the existence of the NF-κB/NLRP3 axis in the kidney and its regulatory role in the inflammatory response to DN.

In addition to promoting inflammation, the NF-κB/NLRP3 axis also plays a role in regulating pyroptosis. For example, in renal ischemia-reperfusion injury (IRI), Tisp40-dependent phosphorylation promoted the activation of p65 in tubular epithelial cells (TEC) and triggered GSDMD-mediated pyroptosis (Xiao et al., 2020). In DN, this role in regulating pyroptosis has also been confirmed. For instance, the increased activity of the mammalian target of rapamycin (mTOR) can also promote the activation of NF-κB p65 in podocytes and trigger NLRP3-dependent pyroptosis (Wang et al., 2020d). *In vitro* and *in vivo* experiments demonstrated that the activation of the TLR4/NF-κB signaling pathway also promoted GSDMD expression in tubule cells, although they did not examine whether the NLRP3 inflammasome was activated in this experiment (Wang et al., 2019b). However, in another study, knockdown of lncRNA XIST using lentivirus was found to inhibit NLRP3/GSDMD axis-mediated pyroptosis in HK-2 cells through the microRNA-15b-5p (miR-15b-5p)/TLR4 axis (Xu et al., 2022). Furthermore, Xu et al. (2021b) also constructed a DN mouse model and overexpressed the Forkhead box M1 (FOXM1) which can drive renal tubular regeneration in podocytes. They found that can FOXM1 bind to the Sirtuin 4 (SIRT4) promoter and inhibit the phosphorylation of NF-κB, and then the expression of nephrin (a podocyte marker) was increased while the expression of the NLRP3 inflammasome and cleaved-caspase-1 were decreased. Recently, AMPK was used to inhibit the activation of NF-κB *via* silent mating type information regulation-2 homolog-1 (SIRT1), and the expression of NLRP3, caspase-1, IL-1β, and GSDMD-N were observed to decrease in podocytes of DN mice (Li et al., 2020a). The use of catalpol (Cat) can increase the expression of adenosine 5′-monophosphate (AMP)-activated protein kinase (AMPK) and SIRT1, effectively inhibit pyroptosis in podocytes, and improve the abnormal structure and function in kidney of DN (Chen et al., 2020b). These studies further established a relationship between NLRP3 inflammasome activation and pyroptosis in DN, and also provided a solid theoretical basis for how to regulate pyroptosis and play a protective role by inhibiting the NF-κB/NLRP3 axis.

Recently, Xin et al. (2018) found that X-linked inhibitor of apoptosis protein (XIAP) can also inhibit the activation of NF-κB and alleviate HG-induced podocyte injury and renal fibrosis. Meanwhile, dual specificity phosphatase-4 (DUSP-4) inhibited the sustained activation of p38 and c-Jun N-terminal kinase (JNK) mitogen-activated protein kinase (MAPK) and protected the structure and function of glomeruli and podocytes in DN (Denhez et al., 2019). Inhibition of ROS/MAPK/NF-κB signaling pathway can also inhibit renal dysfunction induced by HG (Chen et al., 2018c). However, inhibition of NF-κB by XIAP or MAPK has not been verified to be related to NLRP3-mediated pyroptosis in the kidney. Interestingly, metformin not only can activate AMPK and inhibit the mTOR pathway to reduce pyroptosis in diabetic cardiomyopathy, but also correct glucose metabolic reprogramming by inhibiting the TLR4/NF-κB signaling pathway and inhibit NLRP3-induced pyroptosis. They also found that downregulation of sodium-glucose cotransporter 1 (SGLT1) also inhibited NF-κB activation and pyroptosis induced by HG (Yang et al., 2019a; Chai et al., 2021; Zhang et al., 2021g). Although it has not been demonstrated that

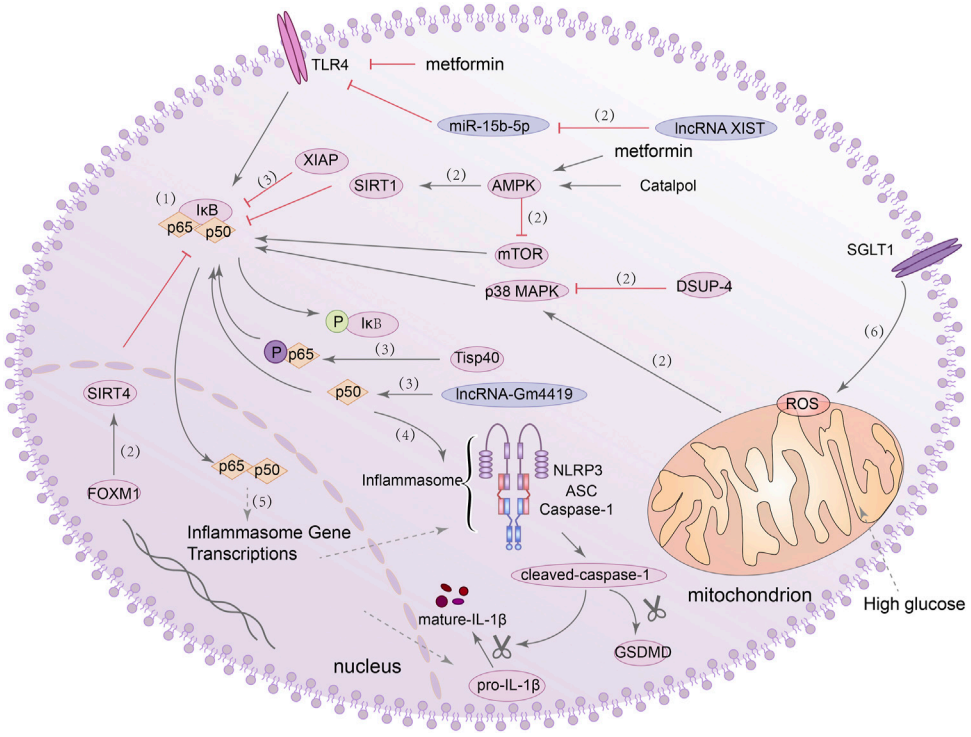

FIGURE 2
NF-κB/NLRP3 signaling pathway is involved in the regulation of pyroptosis. (1) NF-κB binds with IκB in inactive form, dissociates the active form of P50/P65 heterodimer upon stimulation. (2) lncRNA XIST/miR-15b-5p/TLR4/NF-κB signaling pathway, AMPK/SIRT1/NF-κB signaling pathway, AMPK/mTOR/NF-κB signaling pathway, DSUP-4/MAPK/NF-κB signaling pathway, ROS/MAPK signaling pathway and FOXM1/SIRT4/NF-κB signaling pathway, they all can regulate the activation of NF-κB. (3) Tisp40 and lncRNA-Gm4419 can promote the activation of NF-κB p65/p50, and XIAP can inhibit the activation of NF-κB. (4) P50 can act with NLRP3 inflammasome and lead to increased expression of pro-inflammatory cytokines and GSDMD-N. (5) NF-κB can promote the transcription of inflammasome genes. (6) Knockdown of SGLT1 partially reduced pyroptosis, ROS generation and NF-κB activation.

these mechanisms are also present in DN, it is still of interest. In conclusion, these evidences all indicated that the activation of NF-κB/NLRP3 signaling pathway is one of the key factors regulating pyroptosis, and inhibiting the activation of this signaling pathway may inhibit the occurrence of pyroptosis. Figure 2 summarized the functions of different molecules and pathways in NF-κB/NLRP3-mediated pyroptosis.

TXNIP/NLRP3 inflammasome signalling pathway

Generally speaking, thioredoxin-interacting proteins (TXNIP) can inhibit the antioxidant activity of thioredoxin protein (Trx) when interacting with it (Yoshihara, 2020). In order to prove whether TXNIP has an effect on DN, Qi et al. analyzed the transcription profile of proximal renal tubular epithelial cells under HG condition by using cDNA microarray and found significant changes in TXNIP expression compared with the control group (Qi et al., 2007). Continuous overexpression of TXNIP can lead to the increase of ROS expression and progressive renal interstitial fibrosis (Tan et al., 2015). Knockdown of TXNIP can inhibit phenotypic changes in podocytes and the production of ROS induced by HG by reducing the activity of mTOR signaling pathway (Song et al., 2019). Furthermore, downregulation of TXNIP antagonized EMT induced by HG by inhibiting MAPK activation and transforming growth factor β1 (TGF-β1) expression (Wei et al., 2013). These studies all suggested that TXNIP can be a potential target for the treatment of DN. Considering the phenomenon that has been stated before, that is, increased activity of mTOR signaling pathway can promote the activation of NF-κB and then trigger NLRP3-mediated pyroptosis, and inhibiting the activation of MAPK can also protect renal function by inhibiting the activation of NF-κB, it is not difficult to understand that regulating TXNIP may have a regulatory effect on pyroptosis. Moreover, several studies have shown that TXNIP/NLRP3 axis-dependent pyroptosis can be detected in neuron cells, liver cells, intestinal cells and

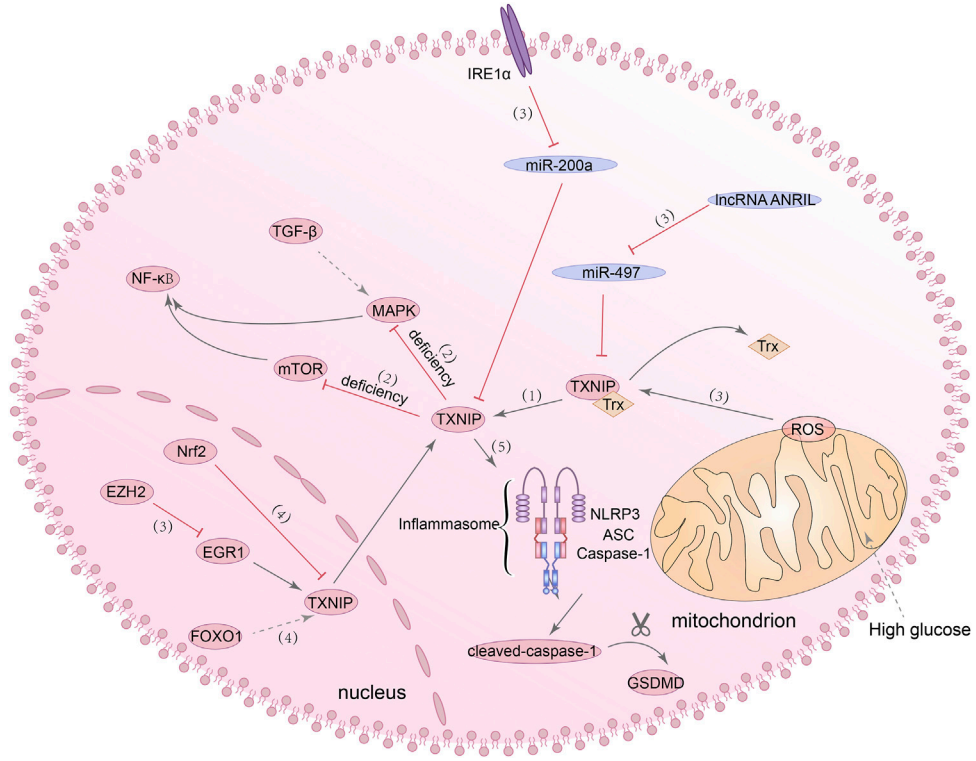

FIGURE 3
TXNIP/NLRP3 signaling pathway is involved in the regulation of pyroptosis. (1) TXNIP can inhibit the antioxidant activity of Trx. (2) The deficiency of TXNIP can inhibit the MAPK/NF-κB signaling pathway and mTOR/NF-κB signaling pathway. (3) IRE1α/miR-200a/TXNIP signaling pathway, ANRIL/miR-497/TXNIP signaling pathway, mROS/TXNIP signaling pathway and EZH2/EGR1/TXNIP/NLRP3 signaling pathway, they all can regulate the activation of TXNIP. (4) Nrf2 can inhibit the expression of TXNIP, and FOXO1 can promote the expression of TXNIP. (5) The interaction of TXNIP with NLRP3 can promote the activation of NLRP3 inflammasome and lead to increased expression of cleaved-caspase-1 and GSDMD-N.

other cells (Heo et al., 2019; Ding et al., 2020; Jia et al., 2020). It can be seen that TXNIP/NLRP3 signaling pathway also has a regulatory effect on pyroptosis.

It has been reported that TXNIP is an NLRP3 binding protein, and its interaction with NLRP3 can promote the activation of NLRP3 inflammasome (Chen et al., 2018b). NLRP3 inflammasome has been found to be activated through mROS/TXNIP/NLRP3 signaling pathway in ischemic acute kidney injury (AKI) (Wen et al., 2018). In the meantime, both *in vitro* and *in vivo* experiments have demonstrated that TXNIP acts as a transcription target of forkhead box O1 (FOXO1). After FOXO1 was knocked out, TXNIP expression and NLRP3 inflammasome activation under HG stimulation were inhibited (Ji et al., 2019; Nyandwi et al., 2020). Besides, inhibition of EZH2/EGR1/TXNIP/NLRP3 signaling pathway and Nrf2/TXNIP/NLRP3 signaling pathway can slow down the progression of DN (Dai et al., 2021; Abd El-Khalik et al., 2022). All of these studies revealed a regulatory role for the TXNIP/NLRP3 axis in DN, but whether NLRP3 inflammasome-dependent pyroptosis is also affected in these processes has not been demonstrated. Of course, in addition to the above-mentioned activation mechanisms of TXNIP/NLRP3 axis, studies have confirmed the other activation mechanisms of TXNIP/NLRP3 axis and their effects on pyroptosis in DN. Wang and Zhao (2021) found that the ANRIL/MIR-497/TXNIP axis was activated in the kidney tissue of diabetic patients, and the high expression of lncRNA-ANRIL can promote the activation of the TXNIP/NLRP3/caspase-1 axis and cause pyroptosis in human kidney-2 (HK-2) cells. ER stress, previously considered as one of the primary culprits leading to the development of DN, has recently been found that one of its pathogenic mechanisms seems to be related to pyroptosis. From *in vitro* experiments to *in vivo*, it has demonstrated that the excessive activation of ER stress sensor inositol-requiring enzyme 1 alpha (IRE1α) can promote the NLRP3-mediated pyroptosis and the expression of TXNIP in renal tubular cells (Ke et al., 2020). Taken together, these evidences suggested that the TXNIP/NLRP3 axis has a role in regulating pyroptosis and is a promising target for the treatment of DN. Figure 3 summarized present studies exploring molecular mechanisms in TXNIP/NLRP3-mediated pyroptosis.

Nrf2/HO-1/NLRP3 inflammasome signalling pathway

Nuclear factor erythroid 2-related factor 2 (Nrf2) can regulate the intracellular redox balance and has anti-inflammatory effects. Under certain stimulation, Nrf2 will be separated from kelch-like ECH-associated protein 1 (Keap1) and translocated to the nucleus to activate its downstream target genes such as heme oxygenase-1 (HO-1) and superoxide dismutase (SOD) (Bellezza et al., 2018). Activation of Nrf2/HO-1 signaling pathway has been reported to inhibit iron death and apoptosis under HG stimulation (Ma et al., 2020; Antar et al., 2022). Meanwhile, a number of studies in DN mouse model have shown that oxidative stress and inflammatory response in kidney can be improved by activating Nrf2/HO-1 signaling pathway (Alaofi, 2020; Lu et al., 2020). These results suggested that the Nrf2/HO-1 signaling pathway may be a potential target for the treatment of DN.

Recent studies have shown that the Nrf2/HO-1 signaling pathway can also regulate the expression of NLRP3. Chen et al. (2019c) and Huang et al. (2020a) demonstrated the inhibitory effect of activation of Nrf2/HO-1 signaling pathway on NLRP3 inflammatory activation in different cells. Additionally, the increased expression of Nrf2 and HO-1 can also reduce the expression of ROS, caspase-1, and IL-1β (Bian et al., 2020a). Subsequently, one study in alveolar macrophage showed that Nrf2/HO-1 signaling also appears to be involved in NLRP3-mediated pyroptosis (Fei et al., 2020). It has been found that in AKI, inhibition of protein arginine methylation transferase 5 (PRMT5) can significantly reduce the expression of ROS, NLRP3 and GSDMD-N of renal tubular cells by activating the Nrf2/HO-1 signaling pathway (Diao et al., 2019). Besides, inhibition of miR-92a-3p can also alleviate NLRP3-mediated pyroptosis in renal ischemia-reperfusion injury (IRI) *via* its potential target Nrf1 (Wang et al., 2020b). The above studies all indicated that the Nrf2/HO-1 axis was closely related to the production of ROS, and the production of mitochondrial ROS was considered to be a regulator of the NLRP3 inflammasome. However, it has been reported that mitochondrial electron transport chain (ETC) maintains the activation of NLRP3 inflammasome by relying on polymerase chain reaction to generate ATP, but no evidence that mitochondrial ROS is essential for this process has been found (Billingham et al., 2022). Generally speaking, pyroptosis mediated by Nrf2/HO-1/NLRP3 pathway can occur in a variety of cells, which can be considered as a potential therapeutic target.

Recently, the studies on Nrf2/HO-1/NLRP3 signaling pathway and pyroptosis in DN have also made many advances. Ab-38b, which has the property of activating Nrf2, inhibited the expression of NLRP3 and IL-1β by HO-1 in mesangial cells of diabetic mouse. However, this study did not examine whether GSDMD expression was also affected (Du et al., 2020). Other evidence suggested that lncRNA-MALAT1 can act as a molecular sponge, leading to downregulation of miR-30c and promoting the NLRP3-dependent pyroptosis in HK2 cells induced by HG (Liu et al., 2020). Furthermore, MALAT1 can increase the expression of NLRP3 in renal tubular epithelial cells and induce pyroptosis by regulating miR-23c and ELAV like RNA binding protein 1 (ELAVL1) (Li et al., 2017). Other studies in diabetes models found that, miR-23a-3p is also a member of the miR-23 family and can negatively regulate its downstream target gene NEK7 and inhibit NEK7-dependent NLRP3 activation (Zhou et al., 2020; Chang et al., 2021). However, these mechanisms have not been tested in kidney cells. Additionally, miR-200c also has the ability to bind MALAT1 and can affect the expression of Nrf2 and HO-1. Atorvastatin can reduce the overexpression of mir-200c induced by HG in podocytes and inhibit oxidative stress and the expression of NLRP3 and GSDMD-N (Zuo et al., 2021). The above evidences all indicated that the Nrf2/HO-1/NLRP3 signaling pathway has the effect of regulating pyroptosis, but more research is needed to explore the possibility of its use as a therapeutic target in DN. Figure 4 summarized the functions of different molecules and pathways in pyroptosis mediated by Nrf2/HO-1/NLRP3 signaling pathway.

HIF-1α/NLRP3 inflammasome signalling pathway

Hypoxia inducible factor 1-alpha (HIF-1α) is an active component of HIF-1, which is regulated by hypoxia and regulates the activity of HIF-1 (Yang et al., 2021a). HIF-1α regulates numerous downstream target genes such as vascular endothelial growth factor (VEGF) and glucose transporter-1 (GLUT-1) (Fan et al., 2019; Hepp et al., 2021). Recently, it was found that VEGF, as one of the downstream target genes of HIF-1α, has the effect of inhibiting pyroptosis in hepatocytes (Zhao et al., 2018a). Meanwhile, overexpression of HIF-2α in macrophages improves insulin resistance and reduces NLRP3 inflammasome activation (Li et al., 2021h). Furthermore, various evidences have shown that accumulation of HIF-1α can significantly increase the expression of NLRP3, GSDMD-N, and cleaved caspase-1 in microglia and cardiomyocytes (Jiang et al., 2020; Yuan et al., 2021). Besides, the inhibition of NF-κB/HIF-1α signaling pathway can alleviate hypoxia-induced pyroptosis in C2C12 myoblasts (Yu et al., 2019). These evidences suggested that HIF-1α has a regulatory effect on NLRP3 inflammasome-mediated pyroptosis.

It is known that HIF-1α is one of the downstream transcription factors of mTOR, and mTOR is one of the downstream targets of PI3K/Akt axis (Appelberg et al., 2020). In the DN mouse model, Leu is an activator of mTOR that can lead to an increase of NLRP3 inflammasome and induce podocytes pyroptosis (Wang et al., 2020d). In addition, caspase-8 can promote the activation of NLRP3 inflammasome by regulating HIF-1α through NF-κB nuclear translocation. Next, mature IL-1β in turn can promote the activation of caspase-8/HIF-1α/NLRP3/NLRP12/NLRC4,

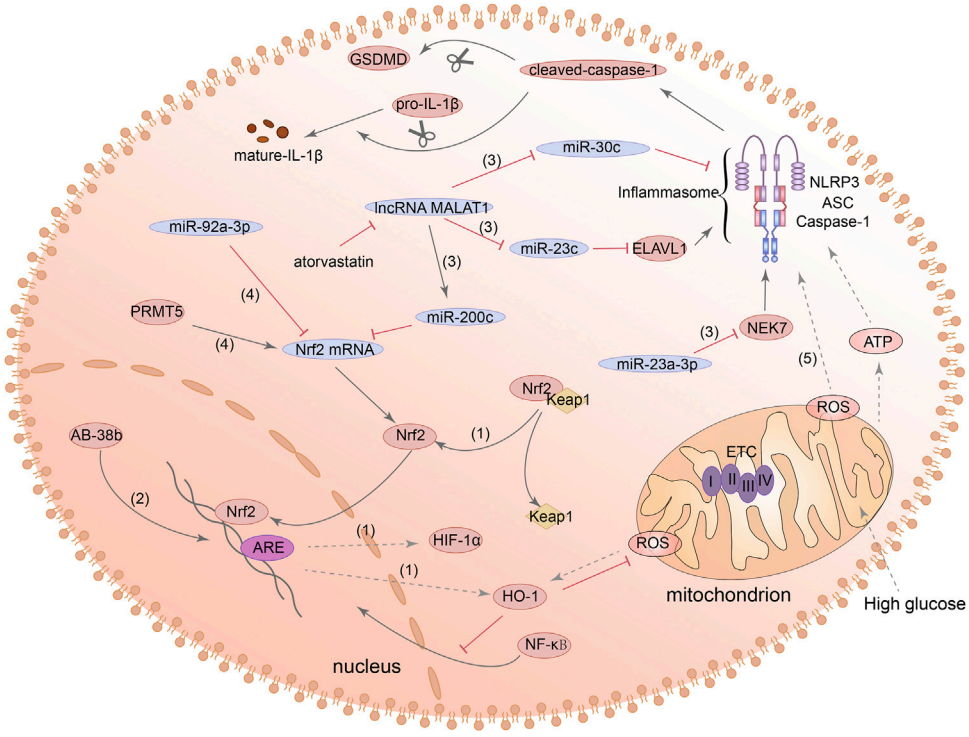

FIGURE 4
Nrf2/HO-1/NLRP3 signaling pathway is involved in the regulation of pyroptosis. (1) Nrf2 can be separated from Keap1 and translocated to the nucleus to activate its downstream target genes such as HO-1 and HIF-1α. (2) Ab-38b can activate Nrf2 and inhibit NLRP3 expression. (3) lncRNA-MALAT1/miR-200c/Nrf2 signaling pathway, MALAT1/miR-23c/ELAVL1/NLRP3 signaling pathway, MALAT1/miR-30c/NLRP3 signaling pathway and miR-23a-3p/NEK7/NLRP3 signaling pathway, they all can regulate the activation of NLRP3. (4) MiR-92a-3p can inhibit the expression of Nrf2, and PRMT5 can promote the expression of Nrf2. (5) Nrf2 can promote the expression of ROS and ROS can lead to the activation of NLRP3 inflammasome and increase the expression of cleaved-caspase-1 and GSDMD-N.

resulting in pyroptosis (Huang et al., 2019; Chen et al., 2020a). In conclusion, although it has not been directly demonstrated whether HIF-1α/NLRP3 is related to pyroptosis, we can still speculate that HIF-1α may be a potential target for NLRP3-mediated pyroptosis in DN. Notably, ASC is one of the key components of the activation of NLRP3 inflammasome, and glycogen synthase kinase-3beta (GSK-3β) can interact with ASC and induce the activation of NLRP3 inflammasome in cardiac fibroblast (Wang et al., 2020c). Simultaneously, inhibition of miR-129 can alter the pyroptosis rate of neuronal cells through IGF-1/GSK3β signaling pathway (Wang et al., 2021b). Meanwhile, Wang et al. also found that inhibition of GSK-3β reduced NLRP3 expression and inhibited pyroptosis in cardiomyocytes (Wang et al., 2022b). Interestingly, several studies have shown that GSK-3β can regulate the expression of HIF-1α (Flügel et al., 2007; Mennerich et al., 2014). However, there is no direct evidence of the relationship between HIF-1α, GSK-3β and pyroptosis of renal cells in DN. Consequently, the mechanism between HIF-1α, GSK-3β and NLRP3-dependent pyroptosis in DN needs to be further explored. Figure 5 summarized present studies exploring molecular mechanisms in HIF-1α/NLRP3-mediated pyroptosis.

PTEN/PI3K/Akt inflammasome signalling pathway

Phosphatase and tensin homologue (PTEN) is a newly discovered tumor suppressor gene, whose protein products have the functions of dephosphorylating and can regulate apoptosis, cell metastasis and cell growth (Khokhar et al., 2020). A recent study found that podocyte dysfunction and proteinuria seem to be related to the reduced expression of PTEN in mouse models of DN (Lin et al., 2015). Another study showed that epithelial-mesenchymal transformation (EMT) of renal tubular epithelial cells induced by HG was also aggravated by the decreased expression of PTEN, and the mechanism may be related to peroxisome proliferator-activated receptor gamma (PPARγ) (Yan et al., 2019). Meanwhile, in a streptozotocin (STZ)-induced diabetic mouse model, upregulation of PTEN can reduce the phosphorylation levels of phosphoinositide 3-kinases (PI3K) and protein kinase B (Akt/PKB), thereby alleviating inflammation and renal interstitial fibrosis in DN (Song et al., 2020). These studies demonstrated the protective effect of PTEN on DN kidney cells. Interestingly, methyltransferase-like protein 3 (METTL3) can modify PTEN,

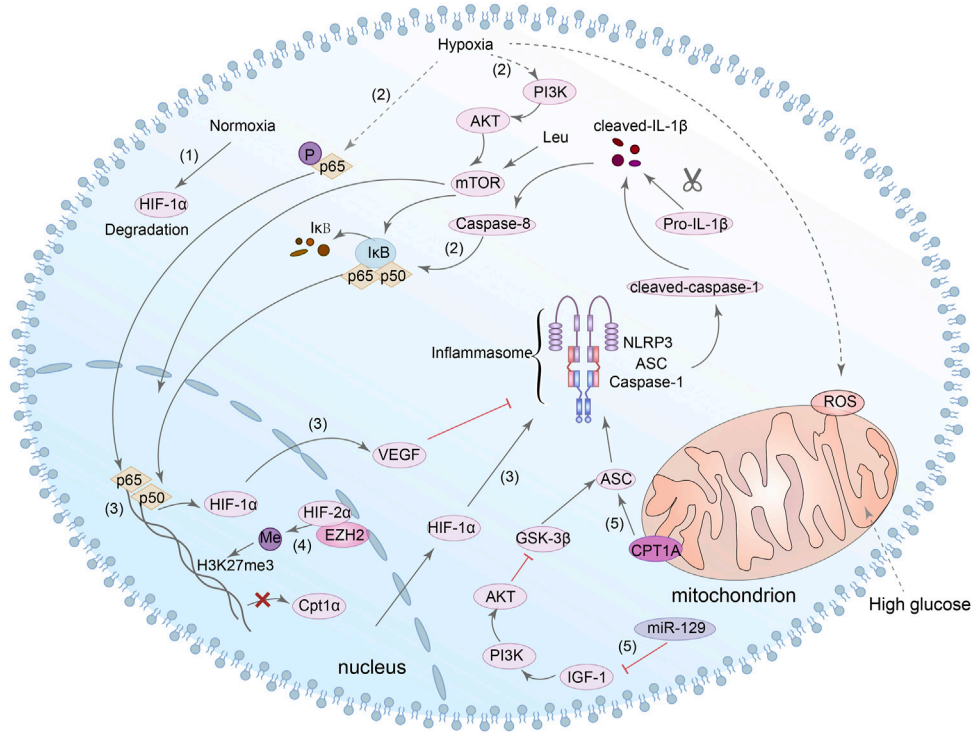

FIGURE 5
HIF-1α/NLRP3 signaling pathway is involved in the regulation of pyroptosis. (1) HIF-1α can be degraded in normoxia. (2) In hypoxia, NF-κB and PI3K/Akt/mTOR/NF-κB signaling pathway can be activated, and caspase-8 can also promote the nuclear translocation of NF-κB. (3) NF-κB directly bound to the HIF-1α promoter and enhanced its transcription. HIF-1α could modulate the activation of the NLRP3 inflammasome, and the increase in VEGF-A can also result in NLRP3 inflammasome activation. (4) HIF-2α binds directly to the Cpt1a promoter and inhibits the expression of it. HIF-2α can also regulate the H3K27me3 methylation during NLRP3 inflammasome activation. (5) Both Cpt1a and miR-129/IGF-1/PI3K/Akt/GSK3β signaling pathway can regulate the expression of ASC which is involved in the activation of NLRP3 inflammasome.

and the increased expression of METTL3 has a specific inhibitory effect on pyroptosis of podocytes under HG condition (Liu et al., 2021a). Meanwhile, experiments in the human retinal pigment epithelium (RPE) cell line and cardiomyocyte also demonstrated that METTL3 overexpression can inhibit PTEN and increase the phosphorylation level of Akt (Zha et al., 2020). Next, activation of SIRT1 can also inhibit ROS generation and NLRP3 inflammasome activation through the activation of Akt signaling pathway (Han et al., 2020). Besides, other studies have also shown that NLRP3-mediated pyroptosis can also be affected by PI3K/Akt pathway in liver cells (Li et al., 2018b). The PTEN/PI3K/Akt signaling pathway will be affected when the level of ROS *in vivo* incresed, resulting in increased expression of NLRP3, caspase-1 and GSDMD-N (Zhang et al., 2021c). It can be seen that the PTEN/PI3K/Akt signaling pathway also has a role in regulating NLRP3-mediated pyroptosis.

To further investigate the relationship between PTEN and pyroptosis, Zhao et al. (2020) induced macrophages with LPS and found that the activation of NLRP3 was inhibited with Akt by increasing the phosphorylation of NLRP3 at S5 and decreasing the ubiquitination at lysine 496. Furthermore, as a component of NLRP3 inflammasome, DEAD-box helicase 3 X-linked (DDX3X) can be phosphorylated by Akt and affect the function of NLRP3 inflammasome (Guo et al., 2021). These evidences suggested that Akt has a direct role in regulating NLRP3. Moreover, other studies suggested that the activation of mTOR, which is the downstream target of PI3K/Akt, can also promote NLRP3-mediated pyroptosis, and PTEN can directly interact with NLRP3 to activate NLRP3 inflammasome (Huang et al., 2020c; Wang et al., 2020d). However, none of the above-mentioned mechanisms have been confirmed in the DN kidney model, and further verification is required. Figure 6 shows the potential mechanism of pyroptosis mediated by PTEN/PI3K/Akt signaling pathway.

Pyroptosis and renal cells in diabetic nephropathy

The intrinsic cells of kidney include mesangial cells, capillary endothelial cells, podocytes, renal tubular epithelial cells and renal interstitial fibroblasts. Among them, the glomerular capillary endothelial cells, basement membrane and podocytes constitute

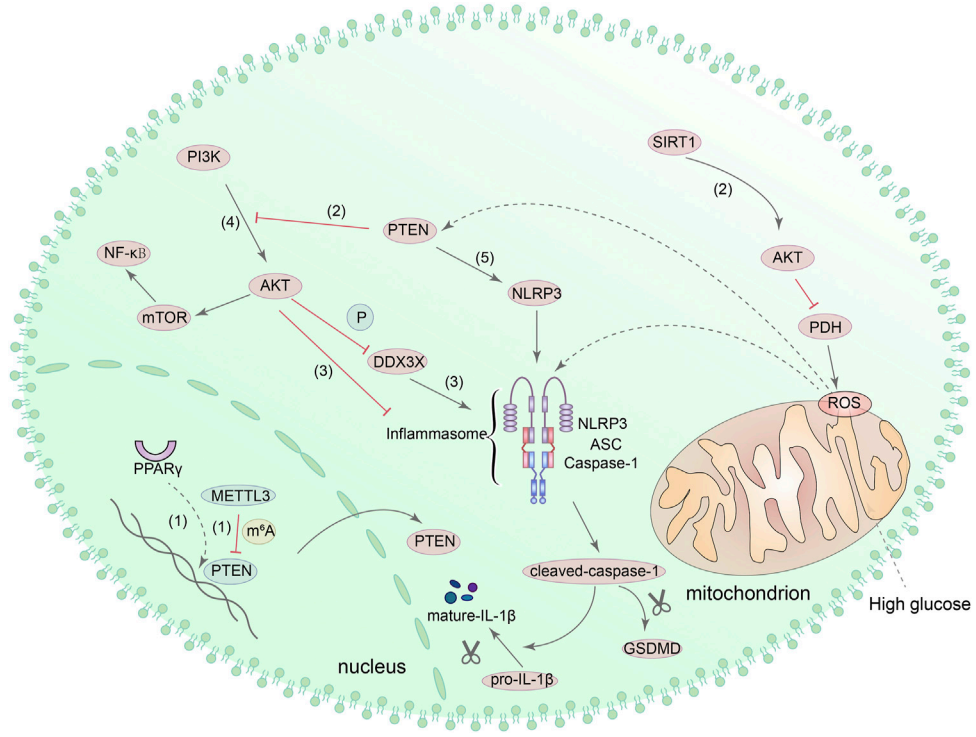

FIGURE 6
PTEN/PI3K/Akt signaling pathway is involved in the regulation of pyroptosis. (1) PPAR can regulate the transcription of PTEN, and METTL3 can also modify PTEN. (2) Upregulation of PTEN can reduce the phosphorylation of PI3K and Akt. SIRT1 can interact with Akt directly, consequently promoting the activity of Akt and inhibiting the production of ROS *via* Akt/PDH axis. (3) DDX3X can be phosphorylated by Akt, and Akt can increase the phosphorylation of NLRP3. (4) PI3K/Akt/mTOR/NF-κB signaling pathway can also regulate pyroptosis mediated by NLRP3 inflammasome. (5) PTEN directly interacts with NLRP3 and enables NLRP3 inflammasome assembly and activation.

the glomerular filtration barrier. The progression of DN is associated with glomerular basement membrane (GBM) thickening, podocytes injury and interstitial fibrosis caused by various factors. In recent years, it has been found that GSDMD and GSDME related to pyroptosis are widely distributed in tissues such as placenta, heart, brain, intestine, and kidney (Ruan et al., 2020). Inhibition of pyroptosis seems to be a new way to delay the development of DN. Here, we reviewed the situation of pyroptosis in podocytes, renal tubular epithelial cells, and kidney endothelial cells.

Pyroptosis of podocytes in diabetic nephropathy

Because of the notoriously difficult to regenerate, damage to podocytes will lead to damage to the glomerular filtration barrier and the occurrence of proteinuria. Recent studies have shown that the inhibition of pyroptosis as well as the inhibition of apoptosis or autophagy can protect the podocytes structure and function from damage. For instance, combined treatment with mycophenolate mofetil, tacrolimus, and steroids significantly inhibited the activation of NLRP3 and caspase-1 and reduced GSDMD-N levels in lupus nephritis models (Cao et al., 2021). The use of superoxide dismutase-mimic agent and glyburide can also inhibit pyroptosis and NLRP3 inflammatory activation in HIV by inhibiting production of ROS (Haque et al., 2016). Zhang et al. (2021a) also stimulated mouse podocytes with the soluble complement complex C5b-9 and found that a long-chain noncoding RNA (lncRNA) KCNQ1OT1 can interact with miR-486a-3p and induce pyroptosis in podocytes by affecting the transcriptional activity of NLRP3. These results suggested that the inhibition of NLRP3 inflammasome may have a regulatory effect on pyroptosis in podocytes.

In addition to hyperglycemia and other factors involved in the progression of DN, overactivation of pyroptosis in podocytes is also one of the important factors leading to cell loss and dysfunction. Qian et al. demonstrated that excessive activation of pyroptosis mediated by caspase-11/4 and GSDMD in HFD/STZ-induced DN mice can lead to podocyte injury (Cheng et al., 2021). Furthermore, the level of miR-21-5p in exosomes derived from macrophages was increased in response to HG stimulation, and inhibition of miR-21-5p can reduce the production of ROS and the expression of NLRP3, caspase-1 and IL-1β in podocytes (Ding et al., 2021b). In addition, the purinergic P2X7 receptor

(P2X7R) expressed in podocytes can lead to the opening of ligand-gated ion channels and potassium outflow in response to ATP stimulation. Next, assembly and activation of NLRP3 inflammasome can be initiated due to reduced intracellular potassium ion level (Wang et al., 2018). However, in the latter two experiments, although changes in NLRP3 expression levels were confirmed, changes in GSDMD were not detected. All in all, it can be seen that the over-activation of pyroptosis has a significant impact on podocyte injury in DN. However, more studies are needed to confirm the activation mechanism of pyroptosis by different signaling pathways as described before, and we also need to find more effective therapeutic targets.

Pyroptosis of renal tubular epithelial cells in diabetic nephropathy

From developmental studies, we have learned that the effect of renal tubular epithelial cells injury on DN seems to be no less than that of glomerular cells injury. DN is a syndrome characterized by renal ischemia and hypoxia, and renal tubular epithelial cells are very sensitive to hypoxia. Moreover, the exacerbation of renal tubular interstitial fibrosis will eventually lead to irreversible renal damage. Consequently, the study on the mechanism of renal tubular epithelial cells injury has been paid more and more attention in recent years. Some studies have found that when renal tubular epithelial cells are exposed to excessive molybdenum or cadmium, they can not only induce autophagy, but also activate the ROS/NLRP3/caspase-1 signaling pathway and lead to pyroptosis (Wei et al., 2020; Zhang et al., 2021b). Moretti J et al. found that caspase-11 can promote GSDMD cleavage and membrane translocation in renal tubular cells in AKI, and scanning electron microscope (SEM) results further confirmed the formation of small protrusion bodies (indicating pore formation in the membrane) (Miao et al., 2019). Previous studies have also shown that the activation of TNF-α/caspase-3/GSDME axis in ureteral can lead to pyroptosis and cell damage (Li et al., 2021j). When GSDME was inhibited, pyroptosis and the transcription of pro-inflammatory cytokines induced by AKI were alleviated (Xia et al., 2021). These evidences highlight the possibility of GSDMD or GSDME-mediated pyroptosis in renal tubular epithelial cells.

To investigate the mechanism of the NLRP3 inflammasome in DN tubular cells, Ding et al. found decreased miR-10a/b expression and increased NLRP3 inflammasome activation in db/db and STZ-treated mice. The reason may be related to the fact that miR-10a/b can target the 3′ untranslated region of NLRP3 mRNA and inhibit the assembly of NLRP3 inflammasome (Ding et al., 2021a). Furthermore, other studies have demonstrated NLRP3 inflammasome activation and pyroptosis in DN tubular cells. Wang et al. (2022d) found that miR-93-5p can also bind to NLRP3 and regulate pyroptosis of renal tubular epithelial cells in DN. At the same time, under the regulation of Wilms tumor 1-associating protein (WTAP), NLRP3 was methylated and pyroptosis was induced in HK-2 cells (Lan et al., 2022). Han et al. (2022) also found that overexpression of transcription factor EB (TFEB) can reduce the level of ROS and inhibit pyroptosis. Additionally, it was found that the cleavage of GSDME at 267–270 can be inhibited by inhibiting the activity of caspase-3 in STZ-induced diabetic mice, and tubulointerstitial fibrosis was improved (Wen et al., 2020). This result again demonstrated the role of the caspase-3/GSDME axis on tubular cell injury in DN. What's more, some evidence emphasizes that lncRNA GAS5 and circACTR2, which function as molecular sponges, can affect the expression of NLRP3, caspase-1, GSDMD-N and IL-1β in renal tubular epithelial cells under HG conditions (Xie et al., 2019; El-Lateef et al., 2022). Vascular cell adhesion protein 1(VCAM1) has also been found to be positively correlated with pyroptosis and immune cell infiltration (Jia et al., 2021). All these evidences indicated that inhibition of pyroptosis has a protective effect on DN tubular cells. In addition, other studies have demonstrated that under HG conditions, the activation of NLRP3 inflammasome can be mediated by CD36 under and inhibited with OPTN by enhancing mitochondrial phagocytosis (Chen et al., 2019a; Hou et al., 2021). However, they did not examine whether the expression of GSDMD changed in the process. In short, pyroptosis in renal tubular epithelial cells of DN is regulated by different mechanisms, and inhibition of it has the potential to be a therapeutic target for slowing the progression of DN.

MicroRNAs (miRNAs) are a class of noncoding RNAs with potential roles in regulating the pathogenesis of various diseases. For instance, increased expression of miR-34a has been found in renal tubular epithelial cells from patients with renal fibrosis and mice with UUO (Liu et al., 2019c). The miR-21 in exosomes from renal tubular epithelial cells may accelerate the development of renal fibrosis through the PTEN/Akt axis (Zhao et al., 2021). Many studies have also reported the potential role of miRNAs in DN (Dewanjee and Bhattacharjee, 2018). For instance, miR-483-5p expression was reduced in HG-stimulated renal tubular epithelial cells, which attenuated its restriction on MAPK1 and TIMP2 mRNAs, ultimately promoting renal interstitial fibrosis (Liu et al., 2021b). In the STZ-induced diabetic mice, renal fibrosis was reduced by modulating the miR-21/Smad7 signaling pathway (Liu et al., 2019a). Furthermore, inhibition of miR-122-5p, miR-133b, and miR-199b can attenuate EMT of renal tubular epithelial cells in diabetic mice (Sun et al., 2018; Zang et al., 2022). Interestingly, miRNAs were also found to have regulatory roles of pyroptosis in tubular epithelial cells. For example, regulation of ANRIL/miR-497/TXNIP and miR-667-5p/NLRC4 axis can both promote the progression of pyroptosis in DN (Wang and Zhao, 2021; Li et al., 2022c). Collectively,

different miRNAs may be potential strategies for the treatment of EMT and pyroptosis of renal tubular epithelial cells in DN.

Pyroptosis of glomerular endothelial cells in diabetic nephropathy

Glomerular endothelial cells (GECs) are more susceptible to damage by circulating substances in the blood as the first barrier of the glomerular filtration membrane. Meanwhile, GECs are rich in mitochondria and require a lot of energy. Impaired GECs can affect hemodynamic and are closely related to the production of proteinuria. Moreover, renal tubular epithelial cells can release cytokines through autocrine or paracrine mechanisms and induce inflammatory responses to impair glomerular structure and function. Subsequently, damaged GECs can reduce blood supply to the renal tubules, leading to increased damage of renal tubules (Chen et al., 2020c). It can be seen that the effect of GECs damage on DN is also very important.

There is a close relationship between endothelial dysfunction and various diseases in humans. For example, in hyperuricemia, pyroptosis in human umbilical vein endothelial cells (HUVEC) can be promoted by regulating NLRP3 expression (Chi et al., 2021). The activation of the ROS/NLRP3/caspase-1 signaling pathway induced by oxidative stress can also lead to endothelial dysfunction and pyroptosis in chronic kidney disease (CKD) (Tang et al., 2019). Several studies have demonstrated that hyperglycemia can also adversely affect structure and function of GECs. For instance, in the DN mouse model, the overexpression of METTL14 induced by HG can promote apoptosis and inflammation in GECs (Li et al., 2021d). Moreover, loss of autophagy in endothelial cells altered the phenotype of GECs and led to sparse capillaries in the glomeruli of diabetic animals (Lenoir et al., 2015). It is worth noting that some recent studies have shown that the pyroptosis also exists in GECs. For instance, Han et al. (2021) regulated GSDMD expression by inhibiting interferon regulatory factor 2 (Irf2), which improved endothelial pyroptosis in DN. The use of NaB can also ameliorate HG-induced GECs damage by modulating the canonical inflammasome pathway *via* the NF-κB/IκB-α signaling pathway (Gu et al., 2019). However, there are still few studies on the role of NLRP3 inflammasome-mediated pyroptosis in GECs, and further research is needed.

Epithelial-to-mesenchymal transition and endothelial-to-mesenchymal transition and pyroptosis in diabetic nephropathy

DN is histologically characterized by the excessive deposition of extracellular matrix (ECM) in glomerular mesangium, GBM, and tubulointerstitium (Steffes et al., 1989; Mason and Wahab, 2003). It has been suggested that activated fibroblasts/myofibroblasts are the main cells for the accumulation of ECM and that both epithelial-to-mesenchymal transition (EMT) and endothelial-to-mesenchymal transition (EndMT) can lead to the increase of fibroblasts (Kalluri and Neilson, 2003; Potenta et al., 2008). Numerous studies have shown that EMT in renal tubular epithelial cells is a key process in tubulointerstitial fibrosis (TIF) and also one of the key reasons for the progression of renal fibrosis in DN (LeBleu et al., 2013; Lovisa et al., 2015). Rather than being directly transformed into myofibroblasts, renal epithelial cells secrete cytokines and chemokines to promote the development of fibrosis (Carew et al., 2012). When EMT occurs, cell adhesion molecules, including E-cadherin and the zonula occludens (ZO-1) protein-1, are lost and replaced by the mesenchymal marker alpha-smooth muscle actin (α-SMA) and the intermediate filament proteins (Sun et al., 2020). EndMT refers to the transition from endothelial cells (ECs) to mesenchymal cells and can be considered as a special type of EMT that occurs in ECs. When EndMT occurs, the endothelial phenotypes are lost and mesenchymal-like characteristics are acquired in endothelial cells (Liang et al., 2016). In DN, EMT can occur in renal tubular epithelial cells and podocytes, while EndMT can occur in glomerular endothelial cells (Loeffler and Wolf, 2015; Tu et al., 2019; Shi et al., 2020). Inhibition of EMT or EndMT in renal cells can alleviate renal fibrosis in DN (Liu et al., 2016a; Shang et al., 2017).

Connective tissue growth factor (CTGF/CCN2), TGF-β1, IL-6, and sonic hedgehog (SHH) are all key regulators of renal fibrosis (Lovisa et al., 2015). Although there are many pro-fibrotic factors can affect renal function, the TGF-β/Smad signaling pathway is considered to be one of the major pathways that orchestrate renal fibrosis (Zheng et al., 2021). Numerous studies have shown that TGF-β can induce EMT and EndMT in renal cells of DN (Wang et al., 2014; Sun et al., 2018; Guan et al., 2022). Sustained HG levels induce the expression of TGF-β, which subsequently activates Smad 2/3 through phosphorylation. Inhibiting p53-mediated nuclear translocation of Smad2/3 may be an effective strategy to prevent diabetes-induced renal fibrosis (Higgins et al., 2018). Interestingly, Zhang et al. (2019c) found that silencing of GSDMD significantly reduced TGF-β expression in fibroblast-like synoviocytes. Moreover, Li et al. (2022b) also demonstrated in HG-induced renal tubular epithelial cells that regulation of TGFB1 can regulate pyroptosis and inhibit cellular inflammation and cell death. Although these studies suggest that the TGF-β signaling pathway may have a regulatory role in pyroptosis of DN, the specific mechanism still needs to be confirmed by more studies.

The Wnt/β-Catenin signaling pathway has also been shown to regulate EMT and EndMT in DN kidney cells (Li et al., 2015; Zhang et al., 2019b). However, there are two opposing views on the role of Wnt/β-Catenin axis in DN. It has been suggested that

under conditions of high glucose or diabetes, the decreased secretion of some Wnt proteins can induce apoptosis and EMT in mesangial cells (Lin et al., 2006; Lin et al., 2008; Beaton et al., 2016). However, it has also been suggested that nitric oxide (NO) donor treatment can inhibit diabetes-mediated oxidative stress and reduce the expression of TGF-β1 (Hsu et al., 2015). Notably, it was found in breast cancer cells that inhibition of the wnt/*β*-Catenin signaling pathway can inhibite EMT and the expression of NLRP3 and IL-1β (Zheng et al., 2020). The use of siRNA or drugs to inhibit the expression of *β*-Catenin can inhibit the activation of NLRP3 inflammasome, which may be related to the fact that *β*-Catenin can interact with NLRP3 and promote the association of NLRP3 with ASC (Huang et al., 2020b). Furthermore, inhibiting the expression of TXNIP can also inhibit the Wnt/*β*-Catenin signaling pathway (Dong et al., 2020). Meanwhile, TXNIP can regulate NLRP3-mediated pyroptosis as previously described. Collectively, these studies suggest that the wnt/*β*-Catenin signaling pathway may have a regulatory effect on NLRP3, but no studies have directly demonstrated the role of the Wnt/*β*-Catenin axis in renal cells pyroptosis of DN.

Glucocorticoid receptor (GR), presenting in almost every tissue of the body, is a nuclear hormone receptor and the target of a number of synthetic steroids (Goodwin et al., 2013). The expression of *α*-SMA and *β*-Catenin were significantly increased after endothelial GR knockout in diabetic mice, and then EndMT was induced by upregulating Wnt signaling (Srivastava et al., 2021c). Additionally, loss of podocyte GR can also lead to the upregulation of Wnt signaling, the disruption of fatty acid metabolism, and the exacerbated glomerular fibrosis (Srivastava et al., 2021b). GR has also been shown to be a inducer of EMT in breast cancer cells (Shi et al., 2019), and overexpression of the homeobox protein HOX-A13 (HOXA13) in renal tubular epithelial cells can inhibit EMT by activating GR signaling (Peng et al., 2016). However, the regulation effect of EMT has not been demonstrated in DN kidney cells. Interestingly, studies have shown that inhibition of CASP1/NLRP3 expression increased GR levels (Paugh et al., 2015), and glucocorticoids can activate NF-κB/NLRP3 signaling pathway through GR (Feng et al., 2019). However, whether GR is involved in NLRP3-mediated pyroptosis in DN is still unclear.

Fibroblast growth factor receptors (FGFRs) are tyrosine kinase receptors that mediate biological responses by binding to fibroblast growth factors (FGFs) (Itoh and Ornitz, 2004). Specific knockout of FGFR1 in endothelial cells can lead to the activation of TGF-β signaling and exacerbate EndMT (Chen et al., 2014). Li et al. (2020b) also demonstrated that FGFR1 was a critical regulator of EndMT-associated EMT activation in diabetic kidneys in diabetic kidneys. FGF21, a potential diabetes drug, can inhibit the phosphorylation of tyrosine kinase *via* FGFR1. And tyrosine kinase can regulate the activation of NLRP3 inflammasome through phosphorylation of ASC. FGF21 can also significantly inhibit the expression of the expression of caspase-1 and IL-1β and improve vascular intimal hyperplasia in diabetic mice (Wei et al., 2019). FGFR1 has also been implicated in the PI3K/Akt signaling pathway, and knockdown of FGFR1 reduced the expression of TLR4 and NLRP3 in periodontitis (Huang et al., 2021a). However, whether FGFR is also involved in NLRP3-mediated pyroptosis in DN remains unclear.

Notch signaling is activated by interaction between Notch receptors and their ligands, which is a common mechanism of proteinuria in kidney disease (Murea et al., 2010). The expression of snail1 is directly regulated by the Notch signaling pathway, and the Notch/snail signaling pathway has been shown to regulate HG-induced EMT in renal tubular epithelial cells (Yang et al., 2017). In HUVECs, inhibition of Notch signaling can also significantly attenuate TGF-β1-induced EndMT (Yang et al., 2020). However, the regulatory effect of Notch signaling on EndMT in DN kidney has not been precisely studied. In addition to regulating EMT and EndMT, Notch1 signaling has also been reported to promote the activation of Snail and inhibit NLRP3 function in models of hepatic injury (Jin et al., 2020). Silencing of Notch1 in keloid fibroblasts fibroblasts also markedly inhibited the expression of the NLRP3 inflammasome and *α*-SMA (Lee et al., 2020). These findings suggest a possible regulatory role of Notch signaling on NLRP3, but whether it regulates pyroptosis in DN remains unclear.

The hedgehog interacting protein (Hhip) is a signaling molecule in the hedgehog pathway whose expression is quiescent after birth (Bishop et al., 2009). The activation of hedgehog signaling has been shown to be associated with EMT in liver cancer cells (Ding et al., 2017). In the UUO model, inhibition of hedgehog signaling pathway was also demonstrated to improve EMT in HK-2 cells (Li et al., 2021c). In the DN model, Zhao et al. found that hyperglycemia stimulated the expression of the Hhip by enhancing the generation of ROS, and TGF-β1/Smad2 pathway was also activated, which promoted the transition of glomerular endothelial cells to the mesenchyme. In addition, they found that Hhip expression was also increased in mouse podocytes cultured in a HG environment, resulting in podocyte loss and the activation of TGF-β1 and α-SMA (Zhao et al., 2018b). Furthermore, the use of the hedgehog inhibitor GANT-61 can also attenuate the expression of caspase-1, IL-1β, and IL-18 in chondrocyte (Liu et al., 2019b). However, there is no evidence to directly demonstrate the relationship between hedgehog and pyroptosis in DN.

Sirtuin3 (SIRT3) is a mitochondrial nicotinamide adenine dinucleotide (NAD+)-dependent deacetylase that can effectively prevent the development of DN, whether by regulating the AMPK/SIRT3 signaling pathway or the SIRT3/SOD2 signaling pathway (Liu et al., 2019d; Guan et al., 2021; Wongmekiat et al., 2021; Li et al., 2022a). Under HG conditions, the expression of SIRT3 was inhibited in HK-2 cells, and glycolysis was abnormally altered, ultimately leading to EMT (Li et al., 2020c). Srivastava

et al. (2021a) also constructed endothelial SIRT3 knockout mice model and found that loss of SIRT3 accelerated EndMT in diabetic kidneys. Mechanistically, SIRT3 in endothelial cells can regulate glucose and lipid metabolism and mesenchymal transdifferentiation by regulating TGF-β/Smad3 axis. These evidences suggest that SIRT3 has a key role in diabetic renal fibrosis. In addition to regulating the process of renal fibrosis, SIRT3 has also been found to regulate the activation of inflammasomes. Guan et al. (2021) found that SIRT3 interacted with NLRC4 to promote its activation in macrophages, and SIRT3 is indispensable for the activation of the NLRP3 inflammasome. However, Liu et al. (2018) suggest that NLRP3 inflammasome activation was increased in SIRT3-deficient macrophages. In addition, studies have shown that cardiomyocyte pyroptosis can be reduced by activating the Nrf2/SIRT3 signaling pathway (Gu et al., 2021). However, there is no direct evidence that the role of SIRT3 in regulating NLRP3 inflammasome activation and pyroptosis is also present in DN kidney cells.

Dipeptidyl peptidase-4 (DPP-4) is a cell surface serine protease that cleaves various substrates, while dipeptidyl peptidase-4 inhibitors (DPP-4i) have the ability to inhibit DPP-4 enzyme activity under diabetic conditions. Therefore, DPP-4 inhibitors have been developed as novel agents for glycemic control in the clinic (Muskiet et al., 2014). Inhibition of DPP-4 activity can improve insulin sensitivity and reduce angiotensin II receptor-1 (AT-1) -mediated tubular-interstitial EMT (Huang et al., 2016). Reduction of DPP-4 expression in podocytes of diabetic rat can restore stromal cell-derived factor 1 α (SDF-1α) levels and may attenuate EMT through the activation of the PKA pathway (Chang et al., 2017). Additionally, linagliptin can also inhibit EndMT by inhibiting the activity of DPP-4, and improve renal fibrosis in STZ-induced diabetic mice. These evidences suggest that DPP-4 can also regulate EMT and EndMT. Furthermore, the use of linagliptin can reduce the expression of ASC, NALP3 and IL-1β in cardiomyocytes of db/db mice (Birnbaum et al., 2019). DPP-4i sitagliptin and omarigliptin can also inhibit NLRP3 expression in macrophages and HG-induced human glomerular endothelial cells (Dai et al., 2014; Li et al., 2021b). However, whether DPP-4i can also inhibit NLRP3-mediated pyroptosis in DN kidney cells remains to be verified.

Pyroptosis and drugs in diabetic nephropathy

Because the complex pathogenesis of DN is not completely clear, the current treatment methods are still not enough to effectively delay the progression of DN. More and more evidences indicated that pyroptosis is one of the mechanisms of cell injury in DN. Therefore, therapeutic drugs targeting pyroptosis and their mechanism are worth exploring.

Therapeutic drugs targeting NLRP3 inflammasome

One of the most characteristic of pyroptosis is activation of inflammasome. BAY 11–7082 is an NF-κB inhibitor that can inhibit NLRP3 inflammasome activation by inhibiting NLRP3-ATPase activity, and this effect is independent of its inhibitory effect on the NF-κB pathway (Juliana et al., 2010). Multiple studies have shown that BAY 11–7082 can reverse the activation of NLRP3 inflammasome-mediated pyroptosis, although this has not been validated in DN kidney cells (Qiu et al., 2017; Qiu et al., 2019). Meanwhile, the expressions of NLRP3, caspase-1 and IL-1β were reduced in db/db mice and HG-induced mesangial cells by the selective NLRP3 inhibitor MCC950. However, body weight and blood glucose levels were not affected (Zhang et al., 2019a). Moreover, it has been confirmed that the use of MCC950 can reduce the expression of pyroptosis-related proteins such as GSDMD in HG-stimulated podocytes (Liu et al., 2021a). Wang et al. also found that after Fucoidan (FPS) treatment, AMPK/mammalian target of rapamycin complex 1 (mTORC1)/NLRP3 signaling axis was regulated and podocyte pyroptosis was inhibited in DN rats (Wang et al., 2022a). Geniposide (GE) can effectively reduce the expression of NLRP3, cleaved-caspase-1 and GSDMD-N in HG-induced podocytes, and the mechanism may be related to the APMK/SIRT1/NF-κB signaling pathway (Li et al., 2020a). Another study found that the effect of saxagliptin in delaying the progression of DN also seems to be related to the inhibition of NLRP3 inflammasome activation (Birnbaum et al., 2016). Additionally, the glucagon-like peptide-1 analog liraglutide, a drug that can reduce the risk of adverse renal outcomes in diabetic patients, can also inhibit NLRP3-mediated pyroptosis in cardiomyocytes (Chen et al., 2018a). Furthermore, the administration of quercetin and allopurinol to high-fat diet (HFD) and STZ-induced diabetic mice significantly reduced the expression of NLRP3, caspase-1, IL-1β, and IL-18, but their effects on pyroptosis still require more experimental validation (Wang et al., 2012). Recently, the experiments in other cells have also found that Kuijieling (KJL), rosuvastatin (RVS), vitamin D (VD), and Kanglexin (KLX) can also inhibit NLRP3 inflammasome-mediated pyroptosis, but whether these drugs act on pyroptosis in DN kidney is still lacking specific research (Bian et al., 2020b; Chen et al., 2021; Zhang et al., 2021f; Jie et al., 2021). Overall, some of the above studies have demonstrated the inhibitory effect of certain drugs on NLRP3-mediated pyroptosis in DN kidney cells, but some only demonstrated the inhibitory effect of drugs on NLRP3 inflammasome activation, and did not detect pyroptosis. However, targeting the NLRP3 inflammasome to treat DN still has certain potential.

Therapeutic drugs targeting reactive oxygen species

In DN, the imbalance of oxidation/antioxidant in renal cells will lead to excessive production of ROS and decreased expression of Nrf2 and other antioxidant factors, which can eventually lead to various forms of cell death. Punicalagin (PU) is a polyphenol that can reduce ROS production and exert antioxidant effects by promoting the production of SOD. The activation of TXNIP/NLRP3 axis was inhibited due to reduced ROS production, suggesting that this may be the mechanism by which PU inhibited pyroptosis of renal cells in diabetic mice (An et al., 2020). Besides, the pyroptosis induced by I/R was inhibited with salvianolic acid B (Sal B) by promoting the accumulation of Nrf2 through its antioxidant properties, although its effectiveness has not been demonstrated in DN (Pang et al., 2020). Since mitochondrial dysfunction is inseparable from the increase of ROS production, Yang et al. (2019b) treated DN mice with mitochondria-targeted peptide (MTP)-131/SS31, a mitochondria-targeted antioxidant peptide. The results showed that hydrogen peroxide (H2O2) and other free radicals were eliminated, accompanied by decreased expression of dynamin-related protein 1 (Drp1), caspase-1, and IL-1β, but whether GSDMD was cleaved in this process still needs further study. Moreover, Qu et al. (2022) demonstrated that pyrroloquinoline quinone (PQQ) can reduce mitochondrial dysfunction and ROS production, and improved renal fibrosis induced by hyperglycemia. In addition, Gao et al. (2022b) restored mitochondrial morphology by culturing podocytes with sialic acid precursor N-acetylmannosamine (ManNAc) and inhibited HG-induced pyroptosis by ROS/NLRP3 signaling pathway. These evidences suggested that DN can be improved by inhibiting pyroptosis by ameliorating mitochondrial dysfunction or reducing ROS production.

Therapeutic drugs targeting caspase1/GSDMD

GSDMD is the most frequently studied protein with pore-forming characteristic that can be cleaved by cleaved-caspase-1. In the treatment of multiple sclerosis, when GSDMD reacts with dimethyl fumarate (DMF) to lead to succination, its reaction with caspase-1 will be restricted and pyroptosis will be inhibited (Humphries et al., 2020). Targeting caspase1/GSDMD in DN has also achieved good results. Han et al. (2021) observed amelioration of renal injury in stz-induced diabetic mice after injecting with hirudin, which may be related to the inhibition of Irf2/GSDMD axis. As an inhibitor of caspase-1, Vx-765 can improve the dysfunction of renal tubular epithelial cells in DN and regulate pyroptosis without affecting blood glucose levels or body weight (Wen et al., 2022). Other studies have shown that carnosine can inhibit HG-induced podocyte pyroptosis through its target caspase-1 (Zhu et al., 2021). Additionally, Sodium butyrate (NaB) can also inhibit pyroptosis by inhibiting caspase1/GSDMD axis in HG induced glomerular endothelial cells (GECs) (Gu et al., 2019). Taken together, these evidences suggested that caspase1/GSDMD axis may serve as one of the therapeutic targets for DN.

Chinese proprietary medicine targeting pyroptosis in diabetic nephropathy

Due to the limitations of current drugs for the treatment of DN, the therapeutic effect of the Chinese proprietary medicine (CPM) has also begun to attract widespread attention. It has been reported that ginsenoside compound K (CK) with hypoglycemic effect can not only inhibit the activation of TXNIP/NLRP3 signaling pathway and the production of IL-1β and IL-18, but also reduce blood glucose, serum creatinine, and 24-h urine protein of the DN mice (Song et al., 2018b). Meanwhile, the activation of NLRP3 inflammasome and pyroptosis can be inhibited by ginsenoside Rg1 in podocytes of diabetic mice *via* mTOR/NF-κB/NLRP3 axis (Wang et al., 2020d). Additionally, ginsenoside Rg5 can also significantly inhibit the activation of NF-κB/NLRP3 axis and the phosphorylation of the three subfamilies of MAPK (Zhu et al., 2020). However, although they demonstrated inhibition of NLRP3 by these drugs, whether this renoprotective effect is also related to NLRP3 inflammasome-mediated pyroptosis remains to be verified. Furthermore, GSDMD-dependent pyroptosis can be inhibited by regulating TGF-β1 in HK-2 cells treated with Tanshinone IIA (Li et al., 2022b). Tangshen formula (TSF) can inhibit pyroptosis by regulating the TXNIP-NLRP3-GSDMD signaling pathway in HK-2 cells. Yi Shen Pai Du Formula (YSPDF) can regulate the Nrf2/HO-1 signaling pathway and reduces the generation of ROS and the expression of NLRP3, ASC, and caspase-1 in DN (Li et al., 2020d; Zhang et al., 2021d). Recently, it was also found that tetrahydroxy stilbene glucoside (TSG), the total flavonoids of Astragalus (TFA), Huangkwai capsule (HKC), and artificially cultivated Ophiocordyceps sinensis (ACOS) could improve kidney injury in DN. Their therapeutic mechanism may be related to the activation of PTEN/PI3K/Akt axis, TLR4/NF-κB axis, and the activation of NLRP3 inflammasome associated with P2X7R (Li et al., 2018a; Wang et al., 2018; Han et al., 2019; Liu et al., 2021a). Although some of these drugs only demonstrated an effect on NLRP3 inflammasome or caspase family and not indicated whether other pyroptosis markers such as GSDMD were also affected in the processes, the use of CPM to treat DN by inhibiting pyroptosis still has a lot of research value. Supplementary Table S1 summarized the drugs mentioned above related to NLRP3 inflammasome and pyroptosis.

Potential drugs that have been evaluated for diabetic nephropathy treatment

Abnormal glucose metabolism also plays a contributing role in the development of DN. Impaired glycolysis may lead to disturbance of podocyte energy supply in DN and affect podocyte cytoskeletal structure (Luo et al., 2022). It has been reported that glucose fluctuation (GF) can also induce kidney injury, and regulation of HIF-1α/miR-210/ISCU/FeS signaling pathway can antagonize GF-induced kidney damage in glomerular mesangial cells (GMCs) by regulating aerobic glycolysis (Xu et al., 2021a). It has also been shown that glycolysis also plays a key role in pyroptosis of LPS-stimulated macrophages, and glycolysis inhibitors can inhibit HIF-1α downregulation and pyroptosis (Aki et al., 2020). Moreover, the use of glycolysis inhibitor 2-deoxy-D-glucose (2-DG) can also inhibit LPS-induced pyroptosis in microglial (Li et al., 2021e). However, the role of glycolysis inhibitors in pyroptosis of DN has not yet been demonstrated. SIRT3 is a major mitochondrial deacetylase involved in the activation of many oxidative pathways. In clinical trials and the diabetic animal models, Li et al. found that SIRT3 deficiency can promote abnormal glycolysis and HIF-1α accumulation, and the abnormal glycolysis is associated with the increased mesenchymal transition rate (Srivastava et al., 2018). Resveratrol (RES) has the effect of activating SIRT3 and can effectively reduce blood sugar levels without any side effects, and RES can also reduce urinary albumin excretion in DN patients (Sattarinezhad et al., 2019; Gowd et al., 2020). Moreover, RES can promote mitophagy to inhibit NLRP3 inflammasome activation and can inhibit pyroptosis through SIRT1 (Chou et al., 2019; Fan et al., 2021). Honokiol (HKL) is also an activator of SIRT3 and can inhibit the expression of NLRP3, caspase-1, GSDMD by activating Nrf2 in human bronchial epithelial cells (Liu et al., 2021c). Although these evidences suggest that regulation of SIRT3 has a protective effect on cells and may also regulate NLRP3 inflammasome-mediated pyroptosis, there is no direct evidence for the role of SIRT3 activators in pyroptosis of DN. DPP-4 is a member of serine proteases and plays a major role in glucose metabolism. DPP-4 inhibitors are a class of antidiabetic drugs and have nephroprotective properties (Gupta and Sen, 2019). Saxagliptin and linagliptin are both DPP-4 inhibitors and both have the potential to reduce proteinuria in patients with type 2 diabetes (Groop et al., 2015; Mosenzon et al., 2017). In db/db mice, linagliptin can also inhibit renal inflammation and fibrosis induced by C-reactive protein (CRP)/CD32b/NF-κB axis (Tang et al., 2021). Interestingly, studies have found that linagliptin can reduce the expression of ASC, NLRP3, IL-1β, TNF-α, and inhibit apoptosis in db/db mice, and this effect is dependent on the activation of p38 and the inhibition of TLR4 expression (Birnbaum et al., 2019). But another study found that DPP-4i not only activated the ROS/NRF2/HO-1 axis in breast cancer cells, but also triggered ROS-dependent NF-κB activation. Moreover, DPP-4i also triggered ROS/NF-κB-dependent NLRP3 inflammasome activation (Li et al., 2021f). Although no studies have shown the relationship between DPP-4i and NLRP3 inflammasome-mediated pyroptosis in DN, these evidences may provide new insights into the unexpected side effects of DPP-4i in diabetic patients with other diseases.

Early stages of DN are characterized by elevated glomerular filtration rate (GFR) and increased filtration fraction (FF) (Hannedouche et al., 1990; Komers et al., 2011). The RhoA/ROCK axis plays a role in the control of vascular tone in the kidney. The Rho-associated kinases (ROCK) inhibitors Y27632 and fasudil were examined to have renoprotective effects on DN (Komers et al., 2011). Fasudil also ameliorated albuminuria and glomerular hypertrophy in DN mice by downregulating HIF-1α expression (Matoba et al., 2013). Furthermore, the application of fasudil can reduce proteinuria and improve renal prognosis by inhibiting ROCK activity in diabetic patients (Matoba et al., 2021). Studies have also shown that fasudil can inhibit NF-κB nuclear translocation and TGF-β1 expression in STZ-induced diabetic rats (Xie et al., 2013). ROCK Inhibitor-Y27632 can also reverse the expression of NF-κB, NLRP3, ASC, and caspase-1 induced by ventilator-induced lung injury (VILI) (Zhang et al., 2021e). However, studies on whether ROCK inhibitors also have an effect on NLRP3-mediated pyroptosis are still lacking. Mineralocorticoid receptor (MR) has a role in regulating the transcription of target genes, and both elevated aldosterone levels and MR hyperactivation can lead to salt and water retention and hypertension (Tirosh et al., 2010). Mineralocorticoid receptor antagonists (MRA) also have therapeutic effects on eGFR, proteinuria, and hyperkalemia in diabetic rats and patients with CKD (Bhuiyan et al., 2019; Baran et al., 2021; Patel et al., 2021). ACE inhibitors (ACEIs) and AT1 receptor antagonists (ARBs) are thought to reduce the progression of ESRD in diabetic patients, and their effects have been extensively validated in DN patients and mouse models (Zheng et al., 2006; Nakagawa, 2010; Tesch et al., 2019). In clinical trials, the combination of MRA and ACEI/ARB significantly reduced urinary albumin excretion and urinary albumin-creatinine ratio and significantly increased the risk of hyperkalemia (Sun et al., 2017). Furthermore, N-acetyl-seryl-aspartyl-lysyl-proline (AcSDKP) is considered to be one of many anti-fibrotic molecules that ACE inhibitors exert their anti-fibrotic effects, and the inhibition of AcSDKP can lead to the activation of mesenchymal transition and renal fibrosis in diabetic mice (Castoldi et al., 2013; Nitta et al., 2016; Srivastava et al., 2020). Studies have also shown that AcSDKP can also predict changes in renal function in normoproteinuric diabetic patients (Nitta et al., 2019), and AcSDKP levels are also associated with sodium intake (Kwakernaak et al., 2013). These findings provide many clues for the anti-fibrotic effect of AcSDKP in human kidney disease. Interestingly, one study demonstrated that the activation of MR was involved in the NLRP3/caspase-1 axis-induced

pyroptosis of UUO model (Ma et al., 2019). Studies have also shown that AcSDKP was found to increase Akt phosphorylation in cancer cells (Hu et al., 2013). Meanwhile, we have previously described the potential impact of the PI3K/Akt signaling pathway on pyroptosis. Taking together, although the above-mentioned drugs have been used clinically, there are still many gaps in the research on their mechanism.

Future directions and perspective in diabetic nephropathy

Many of the studies discussed above clearly demonstrated that NLRP3-dependent pyroptosis occurs during the progression of DN, and the inhibition of NLRP3 inflammasome activation through different signaling pathways can inhibit pyroptosis and ameliorate renal injury. However, several remaining issues must be addressed. First, NLRP3 inflammasome activation does not necessarily lead to pyroptosis, so are the protective effects of some NLRP3 inflammasome inhibitors related to the inhibition of pyroptosis? What conditions can trigger NLRP3 inflammasome-mediated pyroptosis? Second, whether some of our proposed signaling pathways can trigger pyroptosis by activating the expression of NLRP3 in DN kidneys is still lacking in specific studies. Meanwhile, are there other signaling pathways that can also activate NLRP3 inflammasome assembly and trigger pyroptosis? Furthermore, EMT and EndMT also appear to be linked to pyroptosis. Therefore, can exploring this potential link also provide new perspectives for DN treatment and find more effective therapeutic targets? Finally, many drugs have been discovered to have therapeutic effects on DN, and they can inhibit the expression of NLRP3. However, studies are still lacking to show whether their mechanisms are also related to pyroptosis. May further investigation of the mechanism of these drugs and their possible side effects on some concomitant diseases provide more effective options for clinical application?

Conclusion

In this review, we summarized three mechanisms of pyroptosis and discussed the relationship between pyroptosis and NLRP3 inflammasome activation. In addition, we explored several pathways related to NLRP3 inflammasome activation, involving NF-κB, TXNIP, Nrf2, PI3K/Akt and other important signaling molecules. These pathways are linked to each other, complicating the activation mechanisms of NLRP3 inflammasome. However, the inhibition of NLRP3 inflammasome, caspase-1, GSDMD and other proteins in pyroptosis can alleviate the kidney damage in DN. In conclusion, the research on the mechanism of NLRP3 inflammasome-mediated pyroptosis in DN is still ongoing, and more effective drugs are expected to be found.

Author contributions

JW and SZ decided to elaborate this subject and helped revise the manuscript and made a contribution of literature collection. DL and SP were responsible for collection of published paper and drove the manuscript. ZL helped revise the manuscript. All authors took part in the critical reading and revision of the manuscript and definitively approved the edition to be published.

Funding

This study was supported by grants from the General Program of the National Natural Science Foundation of China General Project (No. 81970633), the National Natural Science Young Scientists Foundation of China (No. 81800648), and Excellent Young Scientists Fund Program of the Natural Science Foundation of Henan Province (No. 202300410363).

Acknowledgments

We are grateful for the feedback provided by the reviewers and editor which were extremely useful to the final draft of the manuscript. We are especially grateful to the professional English editing service from Charlesworth. Lastly, thanks to all involved in this study.

Conflict of interest

The authors declare that the research was conducted in the absence of any commercial or financial relationships that could be construed as a potential conflict of interest.

Publisher's note

Supplementary material

The Supplementary Material for this article can be found online at: https://www.frontiersin.org/articles/10.3389/fphar.2022.998574/full#supplementary-material

References

Abd El-Khalik, S. R., Nasif, E., Arakeep, H. M., and Rabah, H. (2022). The prospective ameliorative role of zinc oxide nanoparticles in STZ-induced diabetic nephropathy in rats: Mechanistic targeting of autophagy and regulating Nrf2/TXNIP/NLRP3 inflammasome signaling. *Biol. Trace Elem. Res.* 200 (4), 1677–1687. doi:10.1007/s12011-021-02773-4

Aki, T., Funakoshi, T., Noritake, K., Unuma, K., and Uemura, K. (2020). Extracellular glucose is crucially involved in the fate decision of LPS-stimulated RAW264.7 murine macrophage cells. *Sci. Rep.* 10 (1), 10581. doi:10.1038/s41598-020-67396-6

Alaofi, A. L. (2020). Sinapic acid ameliorates the progression of streptozotocin (STZ)-Induced diabetic nephropathy in rats via NRF2/HO-1 mediated pathways. *Front. Pharmacol.* 11, 1119. doi:10.3389/fphar.2020.01119

Alicic, R. Z., Rooney, M. T., and Tuttle, K. R. (2017). Diabetic kidney disease: Challenges, progress, and possibilities. *Clin. J. Am. Soc. Nephrol.* 12 (12), 2032–2045. doi:10.2215/CJN.11491116

An, X., Zhang, Y., Cao, Y., Chen, J., Qin, H., and Yang, L. (2020). Punicalagin protects diabetic nephropathy by inhibiting pyroptosis based on TXNIP/NLRP3 pathway. *Nutrients* 12 (5), E1516. doi:10.3390/nu12051516

Antar, S. A., Abdo, W., Taha, R. S., Farage, A. E., El-Moselhy, L. E., Amer, M. E., et al. (2022). Telmisartan attenuates diabetic nephropathy by mitigating oxidative stress and inflammation, and upregulating Nrf2/HO-1 signaling in diabetic rats. *Life Sci.* 291, 120260. doi:10.1016/j.lfs.2021.120260

Appelberg, S., Gupta, S., Svensson Akusjärvi, S., Ambikan, A. T., Mikaeloff, F., Saccon, E., et al. (2020). Dysregulation in Akt/mTOR/HIF-1 signaling identified by proteo-transcriptomics of SARS-CoV-2 infected cells. *Emerg. Microbes Infect.* 9 (1), 1748–1760. doi:10.1080/22221751.2020.1799723

Baran, W., Krzemińska, J., Szlagor, M., Wronka, M., Młynarska, E., Franczyk, B., et al. (2021). Mineralocorticoid receptor antagonists-use in chronic kidney disease. *Int. J. Mol. Sci.* 22 (18), 9995. doi:10.3390/ijms22189995

Beaton, H., Andrews, D., Parsons, M., Murphy, M., Gaffney, A., Kavanagh, D., et al. (2016). Wnt6 regulates epithelial cell differentiation and is dysregulated in renal fibrosis. *Am. J. Physiol. Ren. Physiol.* 311 (1), F35–F45. doi:10.1152/ajprenal.00136.2016

Bellezza, I., Giambanco, I., Minelli, A., and Donato, R. (2018). Nrf2-Keap1 signaling in oxidative and reductive stress. *Biochim. Biophys. Acta. Mol. Cell Res.* 1865 (5), 721–733. doi:10.1016/j.bbamcr.2018.02.010

Bhuiyan, A. S., Rafiq, K., Kobara, H., Masaki, T., Nakano, D., and Nishiyama, A. (2019). Effect of a novel nonsteroidal selective mineralocorticoid receptor antagonist, esaxerenone (CS-3150), on blood pressure and renal injury in high salt-treated type 2 diabetic mice. *Hypertens. Res.* 42 (6), 892–902. doi:10.1038/s41440-019-0211-0

Bian, H., Wang, G., Huang, J., Liang, L., Zheng, Y., Wei, Y., et al. (2020a). Dihydrolipoic acid protects against lipopolysaccharide-induced behavioral deficits and neuroinflammation via regulation of Nrf2/HO-1/NLRP3 signaling in rat. *J. Neuroinflammation* 17 (1), 166. doi:10.1186/s12974-020-01836-y

Bian, Y., Li, X., Pang, P., Hu, X.-L., Yu, S.-T., Liu, Y.-N., et al. (2020b). Kanglexin, a novel anthraquinone compound, protects against myocardial ischemic injury in mice by suppressing NLRP3 and pyroptosis. *Acta Pharmacol. Sin.* 41 (3), 319–326. doi:10.1038/s41401-019-0307-8

Bibo-Verdugo, B., Snipas, S. J., Kolt, S., Poreba, M., and Salvesen, G. S. (2020). Extended subsite profiling of the pyroptosis effector protein gasdermin D reveals a region recognized by inflammatory caspase-11. *J. Biol. Chem.* 295 (32), 11292–11302. doi:10.1074/jbc.RA120.014259

Billingham, L. K., Stoolman, J. S., Vasan, K., Rodriguez, A. E., Poor, T. A., Szibor, M., et al. (2022). Mitochondrial electron transport chain is necessary for NLRP3 inflammasome activation. *Nat. Immunol.* 23 (5), 692–704. doi:10.1038/s41590-022-01185-3

Birnbaum, Y., Bajaj, M., Qian, J., and Ye, Y. (2016). Dipeptidyl peptidase-4 inhibition by Saxagliptin prevents inflammation and renal injury by targeting the Nlrp3/ASC inflammasome. *BMJ Open Diabetes Res. Care* 4 (1), e000227. doi:10.1136/bmjdrc-2016-000227

Birnbaum, Y., Tran, D., Bajaj, M., and Ye, Y. (2019). DPP-4 inhibition by linagliptin prevents cardiac dysfunction and inflammation by targeting the Nlrp3/ASC inflammasome. *Basic Res. Cardiol.* 114 (5), 35. doi:10.1007/s00395-019-0743-0

Bishop, B., Aricescu, A. R., Harlos, K., O'Callaghan, C. A., Jones, E. Y., and Siebold, C. (2009). Structural insights into hedgehog ligand sequestration by the human hedgehog-interacting protein HHIP. *Nat. Struct. Mol. Biol.* 16 (7), 698–703. doi:10.1038/nsmb.1607

Broz, P., and Dixit, V. M. (2016). Inflammasomes: Mechanism of assembly, regulation and signalling. *Nat. Rev. Immunol.* 16 (7), 407–420. doi:10.1038/nri.2016.58

Cao, H., Liang, J., Liu, J., He, Y., Ke, Y., Sun, Y., et al. (2021). Novel effects of combination therapy through inhibition of caspase-1/gasdermin D induced-pyroptosis in lupus nephritis. *Front. Immunol.* 12, 720877. doi:10.3389/fimmu.2021.720877

Carew, R. M., Wang, B., and Kantharidis, P. (2012). The role of EMT in renal fibrosis. *Cell Tissue Res.* 347 (1), 103–116. doi:10.1007/s00441-011-1227-1

Castoldi, G., di Gioia, C. R. T., Bombardi, C., Preziuso, C., Leopizzi, M., Maestroni, S., et al. (2013). Renal antifibrotic effect of N-acetyl-seryl-aspartyl-lysyl-proline in diabetic rats. *Am. J. Nephrol.* 37 (1), 65–73. doi:10.1159/000346116

Chai, Q., Meng, Z., Lu, D., Zhang, Z., Liu, M., and Wu, W. (2021). Intermittent high glucose induces pyroptosis of rat H9C2 cardiomyocytes via sodium-glucose cotransporter 1. *Mol. Cell. Biochem.* 476 (6), 2479–2489. doi:10.1007/s11010-021-04104-6

Chang, H., Chang, H., Cheng, T., Lee, G. D., Chen, X., and Qi, K. (2021). Micro-ribonucleic acid-23a-3p prevents the onset of type 2 diabetes mellitus by suppressing the activation of nucleotide-binding oligomerization-like receptor family pyrin domain containing 3 inflammatory bodies-caused pyroptosis through negatively regulating NIMA-related kinase 7. *J. Diabetes Investig.* 12 (3), 334–345. doi:10.1111/jdi.13396

Chang, Y.-P., Sun, B., Han, Z., Han, F., Hu, S.-L., Li, X.-Y., et al. (2017). Saxagliptin attenuates albuminuria by inhibiting podocyte epithelial- to-mesenchymal transition via SDF-1α in diabetic nephropathy. *Front. Pharmacol.* 8, 780. doi:10.3389/fphar.2017.00780

Chen, A., Chen, Z., Xia, Y., Lu, D., Yang, X., Sun, A., et al. (2018a). Liraglutide attenuates NLRP3 inflammasome-dependent pyroptosis via regulating SIRT1/NOX4/ROS pathway in H9c2 cells. *Biochem. Biophys. Res. Commun.* 499 (2), 267–272. doi:10.1016/j.bbrc.2018.03.142

Chen, A., Chen, Z., Zhou, Y., Wu, Y., Xia, Y., Lu, D., et al. (2021). Rosuvastatin protects against coronary microembolization-induced cardiac injury via inhibiting NLRP3 inflammasome activation. *Cell Death Dis.* 12 (1), 78. doi:10.1038/s41419-021-03389-1

Chen, D., Dixon, B. J., Doycheva, D. M., Li, B., Zhang, Y., Hu, Q., et al. (2018b). IRE1α inhibition decreased TXNIP/NLRP3 inflammasome activation through miR-17-5p after neonatal hypoxic-ischemic brain injury in rats. *J. Neuroinflammation* 15 (1), 32. doi:10.1186/s12974-018-1077-9

Chen, H., Deng, Y., Gan, X., Li, Y., Huang, W., Lu, L., et al. (2020a). NLRP12 collaborates with NLRP3 and NLRC4 to promote pyroptosis inducing ganglion cell death of acute glaucoma. *Mol. Neurodegener.* 15 (1), 26. doi:10.1186/s13024-020-00372-w

Chen, J., Yang, Y., Lv, Z., Shu, A., Du, Q., Wang, W., et al. (2020b). Study on the inhibitive effect of Catalpol on diabetic nephropathy. *Life Sci.* 257, 118120. doi:10.1016/j.lfs.2020.118120

Chen, K., Feng, L., Hu, W., Chen, J., Wang, X., Wang, L., et al. (2019a). Optineurin inhibits NLRP3 inflammasome activation by enhancing mitophagy of renal tubular cells in diabetic nephropathy. *FASEB J. Official Publ. Fed. Am. Soc. For Exp. Biol.* 33 (3), 4571–4585. doi:10.1096/fj.201801749RRR

Chen, M.-F., Liou, S.-S., Hong, T.-Y., Kao, S.-T., and Liu, I. M. (2018c). Gigantol has protective effects against high glucose-evoked nephrotoxicity in mouse glomerulus mesangial cells by suppressing ROS/MAPK/NF-κB signaling pathways. *Mol. (Basel, Switz.* 24 (1), E80. doi:10.3390/molecules24010080

Chen, P.-Y., Qin, L., Tellides, G., and Simons, M. (2014). Fibroblast growth factor receptor 1 is a key inhibitor of TGFβ signaling in the endothelium. *Sci. Signal.* 7 (344), ra90. doi:10.1126/scisignal.2005504

Chen, Q., Shi, P., Wang, Y., Zou, D., Wu, X., Wang, D., et al. (2019b). GSDMB promotes non-canonical pyroptosis by enhancing caspase-4 activity. *J. Mol. Cell Biol.* 11 (6), 496–508. doi:10.1093/jmcb/mjy056

Chen, S.-J., Lv, L.-L., Liu, B.-C., and Tang, R.-N. (2020c). Crosstalk between tubular epithelial cells and glomerular endothelial cells in diabetic kidney disease. *Cell Prolif.* 53 (3), e12763. doi:10.1111/cpr.12763

Chen, Z., Zhong, H., Wei, J., Lin, S., Zong, Z., Gong, F., et al. (2019c). Inhibition of Nrf2/HO-1 signaling leads to increased activation of the NLRP3 inflammasome in osteoarthritis. *Arthritis Res. Ther.* 21 (1), 300. doi:10.1186/s13075-019-2085-6

Cheng, Q., Pan, J., Zhou, Z.-L., Yin, F., Xie, H.-Y., Chen, P.-P., et al. (2021). Caspase-11/4 and gasdermin D-mediated pyroptosis contributes to podocyte injury in mouse diabetic nephropathy. *Acta Pharmacol. Sin.* 42 (6), 954–963. doi:10.1038/s41401-020-00525-z

Chi, K., Geng, X., Liu, C., Zhang, Y., Cui, J., Cai, G., et al. (2021). LncRNA-HOTAIR promotes endothelial cell pyroptosis by regulating the miR-22/NLRP3 axis in hyperuricaemia. *J. Cell. Mol. Med.* 25 (17), 8504–8521. doi:10.1111/jcmm.16812

Chou, X., Ding, F., Zhang, X., Ding, X., Gao, H., and Wu, Q. (2019). Sirtuin-1 ameliorates cadmium-induced endoplasmic reticulum stress and pyroptosis through XBP-1s deacetylation in human renal tubular epithelial cells. *Arch. Toxicol.* 93 (4), 965–986. doi:10.1007/s00204-019-02415-8

Coll, R. C., Schroder, K., and Pelegrín, P. (2022). NLRP3 and pyroptosis blockers for treating inflammatory diseases. *Trends Pharmacol. Sci.* 43 (8), 653–668. doi:10.1016/j.tips.2022.04.003

Cuevas, S., and Pelegrín, P. (2021). Pyroptosis and redox balance in kidney diseases. *Antioxid. Redox Signal.* 35 (1), 40–60. doi:10.1089/ars.2020.8243

Dai, X., Liao, R., Liu, C., Liu, S., Huang, H., Liu, J., et al. (2021). Epigenetic regulation of TXNIP-mediated oxidative stress and NLRP3 inflammasome activation contributes to SAHH inhibition-aggravated diabetic nephropathy. *Redox Biol.* 45, 102033. doi:10.1016/j.redox.2021.102033

Dai, Y., Dai, D., Wang, X., Ding, Z., and Mehta, J. L. (2014). DPP-4 inhibitors repress NLRP3 inflammasome and interleukin-1beta via GLP-1 receptor in macrophages through protein kinase C pathway. *Cardiovasc. Drugs Ther.* 28 (5), 425–432. doi:10.1007/s10557-014-6539-4

de Carvalho, R. V. H., Andrade, W. A., Lima-Junior, D. S., Dilucca, M., de Oliveira, C. V., Wang, K., et al. (2019). Leishmania lipophosphoglycan triggers caspase-11 and the non-canonical activation of the NLRP3 inflammasome. *Cell Rep.* 26 (2), 429–437. doi:10.1016/j.celrep.2018.12.047

Denhez, B., Rousseau, M., Dancosst, D.-A., Lizotte, F., Guay, A., Auger-Messier, M., et al. (2019). Diabetes-induced DUSP4 reduction promotes podocyte dysfunction and progression of diabetic nephropathy. *Diabetes* 68 (5), 1026–1039. doi:10.2337/db18-0837

Dewanjee, S., and Bhattacharjee, N. (2018). MicroRNA: A new generation therapeutic target in diabetic nephropathy. *Biochem. Pharmacol.* 155, 32–47. doi:10.1016/j.bcp.2018.06.017

Diao, C., Chen, Z., Qiu, T., Liu, H., Yang, Y., Liu, X., et al. (2019). Inhibition of PRMT5 attenuates oxidative stress-induced pyroptosis via activation of the Nrf2/HO-1 signal pathway in a mouse model of renal ischemia-reperfusion injury. *Oxid. Med. Cell. Longev.* 2019, 2345658. doi:10.1155/2019/2345658

Ding, H., Li, J., Li, Y., Yang, M., Nie, S., Zhou, M., et al. (2021a). MicroRNA-10 negatively regulates inflammation in diabetic kidney via targeting activation of the NLRP3 inflammasome. *Mol. Ther.* 29 (7), 2308–2320. doi:10.1016/j.ymthe.2021.03.012

Ding, J., and Shao, F. (2018). Growing a gasdermin pore in membranes of pyroptotic cells. *EMBO J.* 37 (15), e100067. doi:10.15252/embj.2018100067

Ding, J., Wang, K., Liu, W., She, Y., Sun, Q., Shi, J., et al. (2016). Pore-forming activity and structural autoinhibition of the gasdermin family. *Nature* 535 (7610), 111–116. doi:10.1038/nature18590

Ding, J., Zhou, X.-T., Zou, H.-Y., and Wu, J. (2017). Hedgehog signaling pathway affects the sensitivity of hepatoma cells to drug therapy through the ABCC1 transporter. *Lab. Invest.* 97 (7), 819–832. doi:10.1038/labinvest.2017.34

Ding, R., Ou, W., Chen, C., Liu, Y., Li, H., Zhang, X., et al. (2020). Endoplasmic reticulum stress and oxidative stress contribute to neuronal pyroptosis caused by cerebral venous sinus thrombosis in rats: Involvement of TXNIP/peroxynitrite-NLRP3 inflammasome activation. *Neurochem. Int.* 141, 104856. doi:10.1016/j.neuint.2020.104856

Ding, X., Jing, N., Shen, A., Guo, F., Song, Y., Pan, M., et al. (2021b). MiR-21-5p in macrophage-derived extracellular vesicles affects podocyte pyroptosis in diabetic nephropathy by regulating A20. *J. Endocrinol. Invest.* 44 (6), 1175–1184. doi:10.1007/s40618-020-01401-7

Dixon, S. J., Lemberg, K. M., Lamprecht, M. R., Skouta, R., Zaitsev, E. M., Gleason, C. E., et al. (2012). Ferroptosis: An iron-dependent form of nonapoptotic cell death. *Cell* 149 (5), 1060–1072. doi:10.1016/j.cell.2012.03.042

Doerflinger, M., Deng, Y., Whitney, P., Salvamoser, R., Engel, S., Kueh, A. J., et al. (2020). Flexible usage and interconnectivity of diverse cell death pathways protect against intracellular infection. *Immunity* 53 (3), 533–547. doi:10.1016/j.immuni.2020.07.004

Dong, F., Dong, S., Liang, Y., Wang, K., Qin, Y., and Zhao, X. (2020). miR-20b inhibits the senescence of human umbilical vein endothelial cells through regulating the Wnt/β-catenin pathway via the TXNIP/NLRP3 axis. *Int. J. Mol. Med.* 45 (3), 847–857. doi:10.3892/ijmm.2020.4457

Downs, K. P., Nguyen, H., Dorfleutner, A., and Stehlik, C. (2020). An overview of the non-canonical inflammasome. *Mol. Asp. Med.* 76, 100924. doi:10.1016/j.mam.2020.100924

Du, L., Wang, J., Chen, Y., Li, X., Wang, L., Li, Y., et al. (2020). Novel biphenyl diester derivative AB-38b inhibits NLRP3 inflammasome through Nrf2 activation in diabetic nephropathy. *Cell Biol. Toxicol.* 36 (3), 243–260. doi:10.1007/s10565-019-09501-8

Duncan, J. A., and Canna, S. W. (2018). The NLRC4 inflammasome. *Immunol. Rev.* 281 (1), 115–123. doi:10.1111/imr.12607

El-Lateef, A. E. A., El-Shemi, A. G. A., Alhammady, M. S., Yuan, R., and Zhang, Y. (2022). LncRNA NEAT2 modulates pyroptosis of renal tubular cells induced by high glucose in diabetic nephropathy (DN) by via miR-206 regulation. *Biochem. Genet.* 60, 1733–1747. doi:10.1007/s10528-021-10164-6

Evavold, C. L., Ruan, J., Tan, Y., Xia, S., Wu, H., and Kagan, J. C. (2018). The pore-forming protein gasdermin D regulates interleukin-1 secretion from living macrophages. *Immunity* 48 (1), 35–44. doi:10.1016/j.immuni.2017.11.013

Fan, J., Lv, H., Li, J., Che, Y., Xu, B., Tao, Z., et al. (2019). Roles of Nrf2/HO-1 and HIF-1α/VEGF in lung tissue injury and repair following cerebral ischemia/reperfusion injury. *J. Cell. Physiol.* 234 (6), 7695–7707. doi:10.1002/jcp.27767

Fan, W., Chen, S., Wu, X., Zhu, J., and Li, J. (2021). Resveratrol relieves gouty arthritis by promoting mitophagy to inhibit activation of NLRP3 inflammasomes. *J. Inflamm. Res.* 14, 3523–3536. doi:10.2147/JIR.S320912

Fei, L., Jingyuan, X., Fangte, L., Huijun, D., Liu, Y., Ren, J., et al. (2020). Preconditioning with rHMGB1 ameliorates lung ischemia-reperfusion injury by inhibiting alveolar macrophage pyroptosis via the Keap1/Nrf2/HO-1 signaling pathway. *J. Transl. Med.* 18 (1), 301. doi:10.1186/s12967-020-02467-w

Feng, X., Zhao, Y., Yang, T., Song, M., Wang, C., Yao, Y., et al. (2019). Glucocorticoid-driven NLRP3 inflammasome activation in hippocampal microglia mediates chronic stress-induced depressive-like behaviors. *Front. Mol. Neurosci.* 12, 210. doi:10.3389/fnmol.2019.00210

Flügel, D., Görlach, A., Michiels, C., and Kietzmann, T. (2007). Glycogen synthase kinase 3 phosphorylates hypoxia-inducible factor 1alpha and mediates its destabilization in a VHL-independent manner. *Mol. Cell. Biol.* 27 (9), 3253–3265. doi:10.1128/MCB.00015-07

Gaidt, M. M., Ebert, T. S., Chauhan, D., Schmidt, T., Schmid-Burgk, J. L., Rapino, F., et al. (2016). Human monocytes engage an alternative inflammasome pathway. *Immunity* 44 (4), 833–846. doi:10.1016/j.immuni.2016.01.012

Galluzzi, L., Vitale, I., Aaronson, S. A., Abrams, J. M., Adam, D., Agostinis, P., et al. (2018). Molecular mechanisms of cell death: Recommendations of the nomenclature committee on cell death 2018. *Cell Death Differ.* 25 (3), 486–541. doi:10.1038/s41418-017-0012-4

Gan, J., Huang, M., Lan, G., Liu, L., and Xu, F. (2020). High glucose induces the loss of retinal pericytes partly via NLRP3-caspase-1-GSDMD-mediated pyroptosis. *Biomed. Res. Int.* 2020, 4510628. doi:10.1155/2020/4510628

Gao, J., Peng, S., Shan, X., Deng, G., Shen, L., Sun, J., et al. (2019). Inhibition of AIM2 inflammasome-mediated pyroptosis by Andrographolide contributes to amelioration of radiation-induced lung inflammation and fibrosis. *Cell Death Dis.* 10 (12), 957. doi:10.1038/s41419-019-2195-8

Gao, W., Li, Y., Liu, X., Wang, S., Mei, P., Chen, Z., et al. (2022a). TRIM21 regulates pyroptotic cell death by promoting Gasdermin D oligomerization. *Cell Death Differ.* 29 (2), 439–450. doi:10.1038/s41418-021-00867-z

Gao, Y., Ma, Y., Xie, D., and Jiang, H. (2022b). ManNAc protects against podocyte pyroptosis via inhibiting mitochondrial damage and ROS/NLRP3 signaling pathway in diabetic kidney injury model. *Int. Immunopharmacol.* 107, 108711. doi:10.1016/j.intimp.2022.108711

Gong, W., Zheng, T., Guo, K., Fang, M., Xie, H., Li, W., et al. (2020). Mincle/syk signalling promotes intestinal mucosal inflammation through induction of macrophage pyroptosis in crohn's disease. *J. Crohns Colitis* 14 (12), 1734–1747. doi:10.1093/ecco-jcc/jjaa088

Goodwin, J. E., Feng, Y., Velazquez, H., and Sessa, W. C. (2013). Endothelial glucocorticoid receptor is required for protection against sepsis. *Proc. Natl. Acad. Sci. U. S. A.* 110 (1), 306–311. doi:10.1073/pnas.1210200110

Gowd, V., Kang, Q., Wang, Q., Wang, Q., Chen, F., and Cheng, K.-W. (2020). Resveratrol: Evidence for its nephroprotective effect in diabetic nephropathy. *Adv. Nutr.* 11 (6), 1555–1568. doi:10.1093/advances/nmaa075

Groop, P.-H., Cooper, M. E., Perkovic, V., Sharma, K., Schernthaner, G., Haneda, M., et al. (2015). Dipeptidyl peptidase-4 inhibition with linagliptin and effects on hyperglycaemia and albuminuria in patients with type 2 diabetes and renal dysfunction: Rationale and design of the MARLINA-T2D™ trial. *Diab. Vasc. Dis. Res.* 12 (6), 455–462. doi:10.1177/1479164115579002

Gu, J., Huang, H., Liu, C., Jiang, B., Li, M., Liu, L., et al. (2021). Pinocembrin inhibited cardiomyocyte pyroptosis against doxorubicin-induced cardiac dysfunction via regulating Nrf2/Sirt3 signaling pathway. *Int. Immunopharmacol.* 95, 107533. doi:10.1016/j.intimp.2021.107533

Gu, J., Huang, W., Zhang, W., Zhao, T., Gao, C., Gan, W., et al. (2019). Sodium butyrate alleviates high-glucose-induced renal glomerular endothelial cells damage via inhibiting pyroptosis. *Int. Immunopharmacol.* 75, 105832. doi:10.1016/j.intimp.2019.105832

Guan, C., Huang, X., Yue, J., Xiang, H., Shaheen, S., Jiang, Z., et al. (2021). SIRT3-mediated deacetylation of NLRC4 promotes inflammasome activation. *Theranostics* 11 (8), 3981–3995. doi:10.7150/thno.55573

Guan, G., Xie, J., Dai, Y., and Han, H. (2022). TFPI2 suppresses the interaction of TGF-β2 pathway regulators to promote endothelial-mesenchymal transition in diabetic nephropathy. *J. Biol. Chem.* 298 (3), 101725. doi:10.1016/j.jbc.2022.101725

Guo, X., Chen, S., Yu, W., Chi, Z., Wang, Z., Xu, T., et al. (2021). AKT controls NLRP3 inflammasome activation by inducing DDX3X phosphorylation. *FEBS Lett.* 595 (19), 2447–2462. doi:10.1002/1873-3468.14175

Gupta, S., and Sen, U. (2019). More than just an enzyme: Dipeptidyl peptidase-4 (DPP-4) and its association with diabetic kidney remodelling. *Pharmacol. Res.* 147, 104391. doi:10.1016/j.phrs.2019.104391

Han, J., Zuo, Z., Shi, X., Zhang, Y., Peng, Z., Xing, Y., et al. (2021). Hirudin ameliorates diabetic nephropathy by inhibiting Gsdmd-mediated pyroptosis. *Cell Biol. Toxicol.* doi:10.1007/s10565-021-09622-z

Han, N., Wang, Z., Luo, H., Chi, Y., Zhang, T., Wang, B., et al. (2022). Effect and mechanism of TFEB on pyroptosis in HK-2 cells induced by high glucose. *Biochem. Biophys. Res. Commun.* 610, 162–169. doi:10.1016/j.bbrc.2022.04.062

Han, W., Ma, Q., Liu, Y., Wu, W., Tu, Y., Huang, L., et al. (2019). Huangkui capsule alleviates renal tubular epithelial-mesenchymal transition in diabetic nephropathy via inhibiting NLRP3 inflammasome activation and TLR4/NF-κB signaling. *Phytomedicine* 57, 203–214. doi:10.1016/j.phymed.2018.12.021

Han, Y., Sun, W., Ren, D., Zhang, J., He, Z., Fedorova, J., et al. (2020). SIRT1 agonism modulates cardiac NLRP3 inflammasome through pyruvate dehydrogenase during ischemia and reperfusion. *Redox Biol.* 34, 101538. doi:10.1016/j.redox.2020.101538

Hannedouche, T. P., Delgado, A. G., Gnionsahe, D. A., Boitard, C., Lacour, B., and Grünfeld, J. P. (1990). Renal hemodynamics and segmental tubular reabsorption in early type 1 diabetes. *Kidney Int.* 37 (4), 1126–1133. doi:10.1038/ki.1990.95

Haque, S., Lan, X., Wen, H., Lederman, R., Chawla, A., Attia, M., et al. (2016). HIV promotes NLRP3 inflammasome complex activation in murine HIV-associated nephropathy. *Am. J. Pathol.* 186 (2), 347–358. doi:10.1016/j.ajpath.2015.10.002

He, X., Huang, Y., Liu, Y., Zhang, X., Yue, P., Ma, X., et al. (2022). BAY61-3606 attenuates neuroinflammation and neurofunctional damage by inhibiting microglial Mincle/Syk signaling response after traumatic brain injury. *Int. J. Mol. Med.* 49 (1), 5. doi:10.3892/ijmm.2021.5060

Heo, M. J., Kim, T. H., You, J. S., Blaya, D., Sancho-Bru, P., and Kim, S. G. (2019). Alcohol dysregulates miR-148a in hepatocytes through FoxO1, facilitating pyroptosis via TXNIP overexpression. *Gut* 68 (4), 708–720. doi:10.1136/gutjnl-2017-315123

Hepp, M., Werion, A., De Greef, A., de Ville de Goyet, C., de Bournonville, M., Behets, C., et al. (2021). Oxidative stress-induced Sirtuin1 downregulation correlates to HIF-1α, GLUT-1, and VEGF-A upregulation in Th1 autoimmune hashimoto's thyroiditis. *Int. J. Mol. Sci.* 22 (8), 3806. doi:10.3390/ijms22083806

Hersh, D., Monack, D. M., Smith, M. R., Ghori, N., Falkow, S., and Zychlinsky, A. (1999). The Salmonella invasin SipB induces macrophage apoptosis by binding to caspase-1. *Proc. Natl. Acad. Sci. U. S. A.* 96 (5), 2396–2401. doi:10.1073/pnas.96.5.2396

Higgins, S. P., Tang, Y., Higgins, C. E., Mian, B., Zhang, W., Czekay, R.-P., et al. (2018). TGF-β1/p53 signaling in renal fibrogenesis. *Cell. Signal.* 43, 1–10. doi:10.1016/j.cellsig.2017.11.005

Hou, J., Zhao, R., Xia, W., Chang, C.-W., You, Y., Hsu, J.-M., et al. (2020a). PD-L1-mediated gasdermin C expression switches apoptosis to pyroptosis in cancer cells and facilitates tumour necrosis. *Nat. Cell Biol.* 22 (10), 1264–1275. doi:10.1038/s41556-020-0575-z

Hou, Y., Lin, S., Qiu, J., Sun, W., Dong, M., Xiang, Y., et al. (2020b). NLRP3 inflammasome negatively regulates podocyte autophagy in diabetic nephropathy. *Biochem. Biophys. Res. Commun.* 521 (3), 791–798. doi:10.1016/j.bbrc.2019.10.194

Hou, Y., Wang, Q., Han, B., Chen, Y., Qiao, X., and Wang, L. (2021). CD36 promotes NLRP3 inflammasome activation via the mtROS pathway in renal tubular epithelial cells of diabetic kidneys. *Cell Death Dis.* 12 (6), 523. doi:10.1038/s41419-021-03813-6

Hsu, Y.-C., Lee, P.-H., Lei, C.-C., Ho, C., Shih, Y.-H., and Lin, C.-L. (2015). Nitric oxide donors rescue diabetic nephropathy through oxidative-stress-and nitrosative-stress-mediated Wnt signaling pathways. *J. Diabetes Investig.* 6 (1), 24–34. doi:10.1111/jdi.12244

Hu, B., Zhang, Q., Gao, X., Xu, K., and Tang, B. (2021). Monitoring the activation of caspases-1/3/4 for describing the pyroptosis pathways of cancer cells. *Anal. Chem.* 93 (35), 12022–12031. doi:10.1021/acs.analchem.1c02158

Hu, P., Li, B., Zhang, W., Li, Y., Li, G., Jiang, X., et al. (2013). AcSDKP regulates cell proliferation through the PI3KCA/Akt signaling pathway. *PloS One* 8 (11), e79321. doi:10.1371/journal.pone.0079321

Huang, C.-N., Wang, C.-J., Yang, Y.-S., Lin, C.-L., and Peng, C.-H. (2016). Hibiscus sabdariffa polyphenols prevent palmitate-induced renal epithelial mesenchymal transition by alleviating dipeptidyl peptidase-4-mediated insulin resistance. *Food Funct.* 7 (1), 475–482. doi:10.1039/c5fo00464k

Huang, C., Zhang, C., Yang, P., Chao, R., Yue, Z., Li, C., et al. (2020a). Eldecalcitol inhibits LPS-induced NLRP3 inflammasome-dependent pyroptosis in human gingival fibroblasts by activating the Nrf2/HO-1 signaling pathway. *Drug Des. devel. Ther.* 14, 4901–4913. doi:10.2147/DDDT.S269223

Huang, J.-J., Xia, J., Huang, L.-L., and Li, Y.-C. (2019). HIF-1α promotes NLRP3 inflammasome activation in bleomycin-induced acute lung injury. *Mol. Med. Rep.* 20 (4), 3424–3432. doi:10.3892/mmr.2019.10575

Huang, L., Luo, R., Li, J., Wang, D., Zhang, Y., Liu, L., et al. (2020b). β-catenin promotes NLRP3 inflammasome activation via increasing the association between NLRP3 and ASC. *Mol. Immunol.* 121, 186–194. doi:10.1016/j.molimm.2020.02.017

Huang, X., Shen, H., Liu, Y., Qiu, S., and Guo, Y. (2021a). Fisetin attenuates periodontitis through FGFR1/TLR4/NLRP3 inflammasome pathway. *Int. Immunopharmacol.* 95, 107505. doi:10.1016/j.intimp.2021.107505

Huang, Y., Wang, H., Hao, Y., Lin, H., Dong, M., Ye, J., et al. (2020c). Myeloid PTEN promotes chemotherapy-induced NLRP3-inflammasome activation and antitumour immunity. *Nat. Cell Biol.* 22 (6), 716–727. doi:10.1038/s41556-020-0510-3

Huang, Y., Xu, W., and Zhou, R. (2021b). NLRP3 inflammasome activation and cell death. *Cell. Mol. Immunol.* 18 (9), 2114–2127. doi:10.1038/s41423-021-00740-6

Humphries, F., Shmuel-Galia, L., Ketelut-Carneiro, N., Li, S., Wang, B., Nemmara, V. V., et al. (2020). Succination inactivates gasdermin D and blocks pyroptosis. *Sci. (New York, N.Y.)* 369 (6511), 1633–1637. doi:10.1126/science.abb9818

Ilyas, Z., Chaiban, J. T., and Krikorian, A. (2017). Novel insights into the pathophysiology and clinical aspects of diabetic nephropathy. *Rev. Endocr. Metab. Disord.* 18 (1), 21–28. doi:10.1007/s11154-017-9422-3

Inohara, C., McDonald, C., Nuñez, G., and Nunez, G. (2005). NOD-LRR proteins: Role in host-microbial interactions and inflammatory disease. *Annu. Rev. Biochem.* 74, 355–383. doi:10.1146/annurev.biochem.74.082803.133347

Itoh, N., and Ornitz, D. M. (2004). Evolution of the fgf and fgfr gene families. *Trends Genet.* 20 (11), 563–569. doi:10.1016/j.tig.2004.08.007

Ji, L., Wang, Q., Huang, F., An, T., Guo, F., Zhao, Y., et al. (2019). FOXO1 overexpression attenuates tubulointerstitial fibrosis and apoptosis in diabetic kidneys by ameliorating oxidative injury via TXNIP-TRX. *Oxid. Med. Cell. Longev.* 2019, 3286928. doi:10.1155/2019/3286928

Jia, Y., Cui, R., Wang, C., Feng, Y., Li, Z., Tong, Y., et al. (2020). Metformin protects against intestinal ischemia-reperfusion injury and cell pyroptosis via TXNIP-NLRP3-GSDMD pathway. *Redox Biol.* 32, 101534. doi:10.1016/j.redox.2020.101534

Jia, Y., Xu, H., Yu, Q., Tan, L., and Xiong, Z. (2021). Identification and verification of vascular cell adhesion protein 1 as an immune-related hub gene associated with the tubulointerstitial injury in diabetic kidney disease. *Bioengineered* 12 (1), 6655–6673. doi:10.1080/21655979.2021.1976540

Jiang, Q., Geng, X., Warren, J., Eugene Paul Cosky, E., Kaura, S., Stone, C., et al. (2020). Hypoxia inducible factor-1α (HIF-1α) mediates NLRP3 inflammasome-dependent-pyroptotic and apoptotic cell death following ischemic stroke. *Neuroscience* 448, 126–139. doi:10.1016/j.neuroscience.2020.09.036

Jie, F., Xiao, S., Qiao, Y., You, Y., Feng, Y., Long, Y., et al. (2021). Kuijieling decoction suppresses NLRP3-Mediated pyroptosis to alleviate inflammation and experimental colitis *in vivo* and *in vitro*. *J. Ethnopharmacol.* 264, 113243. doi:10.1016/j.jep.2020.113243

Jin, Y., Li, C., Xu, D., Zhu, J., Wei, S., Zhong, A., et al. (2020). Jagged1-mediated myeloid Notch1 signaling activates HSF1/Snail and controls NLRP3 inflammasome activation in liver inflammatory injury. *Cell. Mol. Immunol.* 17 (12), 1245–1256. doi:10.1038/s41423-019-0318-x

Jo, E.-K., Kim, J. K., Shin, D.-M., and Sasakawa, C. (2016). Molecular mechanisms regulating NLRP3 inflammasome activation. *Cell. Mol. Immunol.* 13 (2), 148–159. doi:10.1038/cmi.2015.95

Juliana, C., Fernandes-Alnemri, T., Wu, J., Datta, P., Solorzano, L., Yu, J.-W., et al. (2010). Anti-inflammatory compounds parthenolide and Bay 11-7082 are direct inhibitors of the inflammasome. *J. Biol. Chem.* 285 (13), 9792–9802. doi:10.1074/jbc.M109.082305

Kalluri, R., and Neilson, E. G. (2003). Epithelial-mesenchymal transition and its implications for fibrosis. *J. Clin. Invest.* 112 (12), 1776–1784. doi:10.1172/JCI20530

Ke, R., Wang, Y., Hong, S., and Xiao, L. (2020). Endoplasmic reticulum stress related factor IRE1α regulates TXNIP/NLRP3-mediated pyroptosis in diabetic nephropathy. *Exp. Cell Res.* 396 (2), 112293. doi:10.1016/j.yexcr.2020.112293

Khokhar, M., Roy, D., Modi, A., Agarwal, R., Yadav, D., Purohit, P., et al. (2020). Perspectives on the role of PTEN in diabetic nephropathy: An update. *Crit. Rev. Clin. Lab. Sci.* 57 (7), 470–483. doi:10.1080/10408363.2020.1746735

Komada, T., and Muruve, D. A. (2019). The role of inflammasomes in kidney disease. *Nat. Rev. Nephrol.* 15 (8), 501–520. doi:10.1038/s41581-019-0158-z

Komers, R., Oyama, T. T., Beard, D. R., and Anderson, S. (2011). Effects of systemic inhibition of Rho kinase on blood pressure and renal haemodynamics in diabetic rats. *Br. J. Pharmacol.* 162 (1), 163–174. doi:10.1111/j.1476-5381.2010.01031.x

Kong, X., Gao, M., Liu, Y., Zhang, P., Li, M., Ma, P., et al. (2022). GSDMD-miR-223-NLRP3 axis involved in B(a)P-induced inflammatory injury of alveolar epithelial cells. *Ecotoxicol. Environ. Saf.* 232, 113286. doi:10.1016/j.ecoenv.2022.113286

Kovacs, S. B., and Miao, E. A. (2017). Gasdermins: Effectors of pyroptosis. *Trends Cell Biol.* 27 (9), 673–684. doi:10.1016/j.tcb.2017.05.005

Kwakernaak, A. J., Waanders, F., Slagman, M. C. J., Dokter, M. M., Laverman, G. D., de Boer, R. A., et al. (2013). Sodium restriction on top of renin-angiotensin-aldosterone system blockade increases circulating levels of N-acetyl-seryl-aspartyl-lysyl-proline in chronic kidney disease patients. *J. Hypertens.* 31 (12), 2425–2432. doi:10.1097/HJH.0b013e328364f5de

Lan, J., Xu, B., Shi, X., Pan, Q., and Tao, Q. (2022). WTAP-mediated N^6-methyladenosine modification of NLRP3 mRNA in kidney injury of diabetic nephropathy. *Cell. Mol. Biol. Lett.* 27 (1), 51. doi:10.1186/s11658-022-00350-8

LeBleu, V. S., Taduri, G., O'Connell, J., Teng, Y., Cooke, V. G., Woda, C., et al. (2013). Origin and function of myofibroblasts in kidney fibrosis. *Nat. Med.* 19 (8), 1047–1053. doi:10.1038/nm.3218

Lee, S., Kim, S. K., Park, H., Lee, Y. J., Park, S. H., Lee, K. J., et al. (2020). Contribution of autophagy-notch1-mediated NLRP3 inflammasome activation to chronic inflammation and fibrosis in keloid fibroblasts. *Int. J. Mol. Sci.* 21 (21), E8050. doi:10.3390/ijms21218050

Lenoir, O., Jasiek, M., Hénique, C., Guyonnet, L., Hartleben, B., Bork, T., et al. (2015). Endothelial cell and podocyte autophagy synergistically protect from diabetes-induced glomerulosclerosis. *Autophagy* 11 (7), 1130–1145. doi:10.1080/15548627.2015.1049799

Li, F., Chen, Y., Li, Y., Huang, M., and Zhao, W. (2020a). Geniposide alleviates diabetic nephropathy of mice through AMPK/SIRT1/NF-κB pathway. *Eur. J. Pharmacol.* 886, 173449. doi:10.1016/j.ejphar.2020.173449

Li, H., Zhao, K., and Li, Y. (2021a). Gasdermin D protects mouse podocytes against high-glucose-induced inflammation and apoptosis via the C-jun N-terminal kinase (JNK) pathway. *Med. Sci. Monit.* 27, e928411. doi:10.12659/MSM.928411

Li, J., Liu, H., Srivastava, S. P., Hu, Q., Gao, R., Li, S., et al. (2020b1979). Endothelial FGFR1 (fibroblast growth factor receptor 1) deficiency contributes differential fibrogenic effects in kidney and heart of diabetic mice. *Hypertension* 76 (6), 1935–1944. doi:10.1161/HYPERTENSIONAHA.120.15587

Li, J., Liu, H., Takagi, S., Nitta, K., Kitada, M., Srivastava, S. P., et al. (2020c). Renal protective effects of empagliflozin via inhibition of EMT and aberrant glycolysis in proximal tubules. *JCI Insight* 5 (6), 129034. doi:10.1172/jci.insight.129034

Li, J., Wang, B., Zhou, G., Yan, X., and Zhang, Y. (2018a). Tetrahydroxy stilbene glucoside alleviates high glucose-induced MPC5 podocytes injury through suppression of NLRP3 inflammasome. *Am. J. Med. Sci.* 355 (6), 588–596. doi:10.1016/j.amjms.2018.03.005

Li, L., Chen, L., Zang, J., Tang, X., Liu, Y., Zhang, J., et al. (2015). C3a and C5a receptor antagonists ameliorate endothelial-myofibroblast transition via the Wnt/β-catenin signaling pathway in diabetic kidney disease. *Metabolism.* 64 (5), 597–610. doi:10.1016/j.metabol.2015.01.014

Li, L., Qian, K., Sun, Y., Zhao, Y., Zhou, Y., Xue, Y., et al. (2021b). Omarigliptin ameliorated high glucose-induced nucleotide oligomerization domain-like receptor protein 3 (NLRP3) inflammasome activation through activating adenosine monophosphate-activated protein kinase α (AMPKα) in renal glomerular endothelial cells. *Bioengineered* 12 (1), 4805–4815. doi:10.1080/21655979.2021.1957748

Li, L., Zhou, G., Fu, R., He, Y., Xiao, L., Peng, F., et al. (2021c). Polysaccharides extracted from balanophora polyandra Griff (BPP) ameliorate renal Fibrosis and EMT via inhibiting the Hedgehog pathway. *J. Cell. Mol. Med.* 25 (6), 2828–2840. doi:10.1111/jcmm.16313

Li, M., Deng, L., and Xu, G. (2021d). METTL14 promotes glomerular endothelial cell injury and diabetic nephropathy via m6A modification of α-klotho. *Mol. Med.* 27 (1), 106. doi:10.1186/s10020-021-00365-5

Li, M., Lu, H., Wang, X., Duan, C., Zhu, X., Zhang, Y., et al. (2021e). Pyruvate kinase M2 (PKM2) interacts with activating transcription factor 2 (ATF2) to bridge glycolysis and pyroptosis in microglia. *Mol. Immunol.* 140, 250–266. doi:10.1016/j.molimm.2021.10.017

Li, N., Zhao, T., Cao, Y., Zhang, H., Peng, L., Wang, Y., et al. (2020d). Tangshen formula attenuates diabetic kidney injury by imparting anti-pyroptotic effects *via* the TXNIP-NLRP3-GSDMD Axis. *Front. Pharmacol.* 11, 623489. doi:10.3389/fphar.2020.623489

Li, Q., Liao, J., Chen, W., Zhang, K., Li, H., Ma, F., et al. (2022a). NAC alleviative ferroptosis in diabetic nephropathy via maintaining mitochondrial redox homeostasis through activating SIRT3-SOD2/Gpx4 pathway. *Free Radic. Biol. Med.* 187, 158–170. doi:10.1016/j.freeradbiomed.2022.05.024

Li, R., Zeng, X., Yang, M., Feng, J., Xu, X., Bao, L., et al. (2021f). Antidiabetic DPP-4 inhibitors reprogram tumor microenvironment that facilitates murine breast cancer metastasis through interaction with cancer cells *via* a ROS-NF-κb-NLRP3 Axis. *Front. Oncol.* 11, 728047. doi:10.3389/fonc.2021.728047

Li, W., Sun, J., Zhou, X., Lu, Y., Cui, W., and Miao, L. (2021g). Mini-review: GSDME-mediated pyroptosis in diabetic nephropathy. *Front. Pharmacol.* 12, 780790. doi:10.3389/fphar.2021.780790

Li, X.-Q., Yu, Q., Fang, B., Zhang, Z.-L., and Ma, H. (2019). Knockdown of the AIM2 molecule attenuates ischemia-reperfusion-induced spinal neuronal pyroptosis by inhibiting AIM2 inflammasome activation and subsequent release of cleaved caspase-1 and IL-1β. *Neuropharmacology* 160, 107661. doi:10.1016/j.neuropharm.2019.05.038

Li, X., Zeng, L., Cao, C., Lu, C., Lian, W., Han, J., et al. (2017). Long noncoding RNA MALAT1 regulates renal tubular epithelial pyroptosis by modulated miR-23c targeting of ELAVL1 in diabetic nephropathy. *Exp. Cell Res.* 350 (2), 327–335. doi:10.1016/j.yexcr.2016.12.006

Li, X., Zhang, X., Xia, J., Zhang, L., Chen, B., Lian, G., et al. (2021h). Macrophage HIF-2α suppresses NLRP3 inflammasome activation and alleviates insulin resistance. *Cell Rep.* 36 (8), 109607. doi:10.1016/j.celrep.2021.109607

Li, Y., Deng, X., Zhuang, W., Li, Y., Xue, H., Lv, X., et al. (2022b). Tanshinone IIA down-regulates -transforming growth factor beta 1 to relieve renal tubular epithelial cell inflammation and pyroptosis caused by high glucose. *Bioengineered* 13 (5), 12224–12236. doi:10.1080/21655979.2022.2074619

Li, Y., Wang, W., Li, A., Huang, W., Chen, S., Han, F., et al. (2021i). Dihydroartemisinin induces pyroptosis by promoting the AIM2/caspase-3/DFNA5 axis in breast cancer cells. *Chem. Biol. Interact.* 340, 109434. doi:10.1016/j.cbi.2021.109434

Li, Y., Yu, W., Xiong, H., and Yuan, F. (2022c). Circ_0000181 regulates miR-667-5p/NLRC4 axis to promote pyroptosis progression in diabetic nephropathy. *Sci. Rep.* 12 (1), 11994. doi:10.1038/s41598-022-15607-7

Li, Y., Yuan, Y., Huang, Z.-X., Chen, H., Lan, R., Wang, Z., et al. (2021j). GSDME-mediated pyroptosis promotes inflammation and fibrosis in obstructive nephropathy. *Cell Death Differ.* 28 (8), 2333–2350. doi:10.1038/s41418-021-00755-6

Li, Z., Liu, W., Fu, J., Cheng, S., Xu, Y., Wang, Z., et al. (2021k). Shigella evades pyroptosis by arginine ADP-riboxanation of caspase-11. *Nature* 599 (7884), 290–295. doi:10.1038/s41586-021-04020-1

Li, Z., Zhao, F., Cao, Y., Zhang, J., Shi, P., Sun, X., et al. (2018b). DHA attenuates hepatic ischemia reperfusion injury by inhibiting pyroptosis and activating PI3K/Akt pathway. *Eur. J. Pharmacol.* 835, 1–10. doi:10.1016/j.ejphar.2018.07.054

Liang, J., Wang, Q., Li, J.-Q., Guo, T., and Yu, D. (2020). Long non-coding RNA MEG3 promotes cerebral ischemia-reperfusion injury through increasing pyroptosis by targeting miR-485/AIM2 axis. *Exp. Neurol.* 325, 113139. doi:10.1016/j.expneurol.2019.113139

Liang, X., Duan, N., Wang, Y., Shu, S., Xiang, X., Guo, T., et al. (2016). Advanced oxidation protein products induce endothelial-to-mesenchymal transition in human renal glomerular endothelial cells through induction of endoplasmic reticulum stress. *J. Diabetes Complicat.* 30 (4), 573–579. doi:10.1016/j.jdiacomp.2016.01.009

Lin, C.-L., Wang, J.-Y., Huang, Y.-T., Kuo, Y.-H., Surendran, K., and Wang, F.-S. (2006). Wnt/beta-catenin signaling modulates survival of high glucose-stressed mesangial cells. *J. Am. Soc. Nephrol.* 17 (10), 2812–2820. doi:10.1681/ASN.2005121355

Lin, C.-L., Wang, J.-Y., Ko, J.-Y., Surendran, K., Huang, Y.-T., Kuo, Y.-H., et al. (2008). Superoxide destabilization of beta-catenin augments apoptosis of high-glucose-stressed mesangial cells. *Endocrinology* 149 (6), 2934–2942. doi:10.1210/en.2007-1372

Lin, J., Cheng, A., Cheng, K., Deng, Q., Zhang, S., Lan, Z., et al. (2020). New insights into the mechanisms of pyroptosis and implications for diabetic kidney disease. *Int. J. Mol. Sci.* 21 (19), E7057. doi:10.3390/ijms21197057

Lin, J., Shi, Y., Peng, H., Shen, X., Thomas, S., Wang, Y., et al. (2015). Loss of PTEN promotes podocyte cytoskeletal rearrangement, aggravating diabetic nephropathy. *J. Pathol.* 236 (1), 30–40. doi:10.1002/path.4508

Linder, A., and Hornung, V. (2020). Irgm2 and Gate-16 put a break on caspase-11 activation. *EMBO Rep.* 21 (11), e51787. doi:10.15252/embr.202051787

Linkermann, A., and Green, D. R. (2014). Necroptosis. *N. Engl. J. Med.* 370 (5), 455–465. doi:10.1056/NEJMra1310050

Liu, B.-H., Tu, Y., Ni, G.-X., Yan, J., Yue, L., Li, Z.-L., et al. (2021a). Total flavones of *Abelmoschus manihot* ameliorates podocyte pyroptosis and injury in high glucose conditions by targeting METTL3-dependent m^6A modification-mediated NLRP3-inflammasome activation and PTEN/PI3K/Akt signaling. *Front. Pharmacol.* 12, 667644. doi:10.3389/fphar.2021.667644

Liu, C., Zhuo, H., Ye, M.-Y., Huang, G.-X., Fan, M., and Huang, X.-Z. (2020). LncRNA MALAT1 promoted high glucose-induced pyroptosis of renal tubular epithelial cell by sponging miR-30c targeting for NLRP3. *Kaohsiung J. Med. Sci.* 36 (9), 682–691. doi:10.1002/kjm2.12226

Liu, D., Liu, F., Li, Z., Pan, S., Xie, J., Zhao, Z., et al. (2021b). HNRNPA1-mediated exosomal sorting of miR-483-5p out of renal tubular epithelial cells promotes the progression of diabetic nephropathy-induced renal interstitial fibrosis. *Cell Death Dis.* 12 (3), 255. doi:10.1038/s41419-021-03460-x

Liu, H., Wang, X., Liu, S., Li, H., Yuan, X., Feng, B., et al. (2016a). Effects and mechanism of miR-23b on glucose-mediated epithelial-to-mesenchymal transition in diabetic nephropathy. *Int. J. Biochem. Cell Biol.* 70, 149–160. doi:10.1016/j.biocel.2015.11.016

Liu, L., Wang, Y., Yan, R., Liang, L., Zhou, X., Liu, H., et al. (2019a). BMP-7 inhibits renal fibrosis in diabetic nephropathy via miR-21 downregulation. *Life Sci.* 238, 116957. doi:10.1016/j.lfs.2019.116957

Liu, P., Huang, G., Wei, T., Gao, J., Huang, C., Sun, M., et al. (2018). Sirtuin 3-induced macrophage autophagy in regulating NLRP3 inflammasome activation. *Biochim. Biophys. Acta. Mol. Basis Dis.* 1864 (3), 764–777. doi:10.1016/j.bbadis.2017.12.027

Liu, Q., Wu, Z., Hu, D., Zhang, L., Wang, L., and Liu, G. (2019b). Low dose of indomethacin and Hedgehog signaling inhibitor administration synergistically attenuates cartilage damage in osteoarthritis by controlling chondrocytes pyroptosis. *Gene* 712, 143959. doi:10.1016/j.gene.2019.143959

Liu, X., Zhang, Z., Ruan, J., Pan, Y., Magupalli, V. G., Wu, H., et al. (2016b). Inflammasome-activated gasdermin D causes pyroptosis by forming membrane pores. *Nature* 535 (7610), 153–158. doi:10.1038/nature18629

Liu, Y., Bi, X., Xiong, J., Han, W., Xiao, T., Xu, X., et al. (2019c). MicroRNA-34a promotes renal fibrosis by downregulation of klotho in tubular epithelial cells. *Mol. Ther.* 27 (5), 1051–1065. doi:10.1016/j.ymthe.2019.02.009

Liu, Y., Zhou, J., Luo, Y., Li, J., Shang, L., Zhou, F., et al. (2021c). Honokiol alleviates LPS-induced acute lung injury by inhibiting NLRP3 inflammasome-mediated pyroptosis via Nrf2 activation *in vitro* and *in vivo*. *Chin. Med.* 16 (1), 127. doi:10.1186/s13020-021-00541-z

Liu, Z., Liu, H., Xiao, L., Liu, G., Sun, L., and He, L. (2019d). STC-1 ameliorates renal injury in diabetic nephropathy by inhibiting the expression of BNIP3 through the AMPK/SIRT3 pathway. *Lab. Invest.* 99 (5), 684–697. doi:10.1038/s41374-018-0176-7

Loeffler, I., and Wolf, G. (2015). Epithelial-to-Mesenchymal transition in diabetic nephropathy: Fact or fiction? *Cells* 4 (4), 631–652. doi:10.3390/cells4040631

Lovisa, S., LeBleu, V. S., Tampe, B., Sugimoto, H., Vadnagara, K., Carstens, J. L., et al. (2015). Epithelial-to-mesenchymal transition induces cell cycle arrest and parenchymal damage in renal fibrosis. *Nat. Med.* 21 (9), 998–1009. doi:10.1038/nm.3902

Lu, C., Fan, G., and Wang, D. (2020). Akebia Saponin D ameliorated kidney injury and exerted anti-inflammatory and anti-apoptotic effects in diabetic nephropathy by activation of NRF2/HO-1 and inhibition of NF-KB pathway. *Int. Immunopharmacol.* 84, 106467. doi:10.1016/j.intimp.2020.106467

Luo, Q., Liang, W., Zhang, Z., Zhu, Z., Chen, Z., Hu, J., et al. (2022). Compromised glycolysis contributes to foot process fusion of podocytes in diabetic kidney disease: Role of ornithine catabolism. *Metabolism.* 134, 155245. doi:10.1016/j.metabol.2022.155245

Ma, H., Wang, X., Zhang, W., Li, H., Zhao, W., Sun, J., et al. (2020). Melatonin suppresses ferroptosis induced by high glucose via activation of the Nrf2/HO-1 signaling pathway in type 2 diabetic osteoporosis. *Oxid. Med. Cell. Longev.* 2020, 9067610. doi:10.1155/2020/9067610

Ma, X., Chang, Y., Xiong, Y., Wang, Z., Wang, X., and Xu, Q. (2019). Eplerenone ameliorates cell pyroptosis in contralateral kidneys of rats with unilateral ureteral obstruction. *Nephron* 142 (3), 233–242. doi:10.1159/000497489

Maiti, A. K. (2021). Development of biomarkers and molecular therapy based on inflammatory genes in diabetic nephropathy. *Int. J. Mol. Sci.* 22 (18), 9985. doi:10.3390/ijms22189985

Man, S. M., Karki, R., and Kanneganti, T.-D. (2017). Molecular mechanisms and functions of pyroptosis, inflammatory caspases and inflammasomes in infectious diseases. *Immunol. Rev.* 277 (1), 61–75. doi:10.1111/imr.12534

Martinon, F., Burns, K., and Tschopp, J. (2002). The inflammasome: A molecular platform triggering activation of inflammatory caspases and processing of proIL-beta. *Mol. Cell* 10 (2), 417–426. doi:10.1016/s1097-2765(02)00599-3

Mason, R. M., and Wahab, N. A. (2003). Extracellular matrix metabolism in diabetic nephropathy. *J. Am. Soc. Nephrol.* 14 (5), 1358–1373. doi:10.1097/01.asn.0000065640.77499.d7

Matoba, K., Kawanami, D., Okada, R., Tsukamoto, M., Kinoshita, J., Ito, T., et al. (2013). Rho-kinase inhibition prevents the progression of diabetic nephropathy by downregulating hypoxia-inducible factor 1α. *Kidney Int.* 84 (3), 545–554. doi:10.1038/ki.2013.130

Matoba, K., Sekiguchi, K., Nagai, Y., Takeda, Y., Takahashi, H., Yokota, T., et al. (2021). Renal ROCK activation and its pharmacological inhibition in patients with diabetes. *Front. Pharmacol.* 12, 738121. doi:10.3389/fphar.2021.738121

Mennerich, D., Dimova, E. Y., and Kietzmann, T. (2014). Direct phosphorylation events involved in HIF-α regulation: The role of GSK-3β. *Hypoxia Auckl. N.Z.)* 2, 35–45. doi:10.2147/HP.S60703

Miao, N., Wang, B., Xu, D., Wang, Y., Gan, X., Zhou, L., et al. (2018). Caspase-11 promotes cisplatin-induced renal tubular apoptosis through a caspase-3-dependent pathway. *Am. J. Physiol. Ren. Physiol.* 314 (2), F269–F279. doi:10.1152/ajprenal.00091.2017

Miao, N., Yin, F., Xie, H., Wang, Y., Xu, Y., Shen, Y., et al. (2019). The cleavage of gasdermin D by caspase-11 promotes tubular epithelial cell pyroptosis and urinary IL-18 excretion in acute kidney injury. *Kidney Int.* 96 (5), 1105–1120. doi:10.1016/j.kint.2019.04.035

Mosenzon, O., Leibowitz, G., Bhatt, D. L., Cahn, A., Hirshberg, B., Wei, C., et al. (2017). Effect of saxagliptin on renal outcomes in the SAVOR-TIMI 53 trial. *Diabetes Care* 40 (1), 69–76. doi:10.2337/dc16-0621

Murea, M., Park, J.-K., Sharma, S., Kato, H., Gruenwald, A., Niranjan, T., et al. (2010). Expression of Notch pathway proteins correlates with albuminuria, glomerulosclerosis, and renal function. *Kidney Int.* 78 (5), 514–522. doi:10.1038/ki.2010.172

Muskiet, M. H. A., Smits, M. M., Morsink, L. M., and Diamant, M. (2014). The gut-renal axis: Do incretin-based agents confer renoprotection in diabetes? *Nat. Rev. Nephrol.* 10 (2), 88–103. doi:10.1038/nrneph.2013.272

Nakagawa, T. (2010). Diabetic nephropathy: Aldosterone breakthrough in patients on an ACEI. *Nat. Rev. Nephrol.* 6 (4), 194–196. doi:10.1038/nrneph.2010.32

Nandi, D., Farid, N. S. S., Karuppiah, H. A. R., and Kulkarni, A. (2022). Imaging approaches to monitor inflammasome activation. *J. Mol. Biol.* 434 (4), 167251. doi:10.1016/j.jmb.2021.167251

Newton, K., Dixit, V. M., and Kayagaki, N. (2021). Dying cells fan the flames of inflammation. *Sci. (New York, N.Y.)* 374 (6571), 1076–1080. doi:10.1126/science.abi5934

Nitta, K., Nagai, T., Mizunuma, Y., Kitada, M., Nakagawa, A., Sakurai, M., et al. (2019). N-Acetyl-seryl-aspartyl-lysyl-proline is a potential biomarker of renal function in normoalbuminuric diabetic patients with eGFR ≥ 30 ml/min/1.73 m2. *Clin. Exp. Nephrol.* 23 (8), 1004–1012. doi:10.1007/s10157-019-01733-6

Nitta, K., Shi, S., Nagai, T., Kanasaki, M., Kitada, M., Srivastava, S. P., et al. (2016). Oral administration of N-Acetyl-seryl-aspartyl-lysyl-proline ameliorates kidney disease in both type 1 and type 2 diabetic mice via a therapeutic regimen. *Biomed. Res. Int.* 2016, 9172157. doi:10.1155/2016/9172157

Nyandwi, J. B., Ko, Y. S., Jin, H., Yun, S. P., Park, S. W., and Kim, H. J. (2020). Rosmarinic acid inhibits oxLDL-induced inflammasome activation under high-glucose conditions through downregulating the p38-FOXO1-TXNIP pathway. *Biochem. Pharmacol.* 182, 114246. doi:10.1016/j.bcp.2020.114246

Paik, S., Kim, J. K., Silwal, P., Sasakawa, C., and Jo, E.-K. (2021). An update on the regulatory mechanisms of NLRP3 inflammasome activation. *Cell. Mol. Immunol.* 18 (5), 1141–1160. doi:10.1038/s41423-021-00670-3

Pandey, A., Shen, C., Feng, S., and Man, S. M. (2021). Cell biology of inflammasome activation. *Trends Cell Biol.* 31 (11), 924–939. doi:10.1016/j.tcb.2021.06.010

Pang, Y., Zhang, P.-C., Lu, R.-R., Li, H.-L., Li, J.-C., Fu, H.-X., et al. (2020). Andrade-oliveira salvianolic acid B modulates caspase-1-mediated pyroptosis in

renal ischemia-reperfusion injury via Nrf2 pathway. *Front. Pharmacol.* 11, 541426. doi:10.3389/fphar.2020.541426

Patel, V., Joharapurkar, A., and Jain, M. (2021). Role of mineralocorticoid receptor antagonists in kidney diseases. *Drug Dev. Res.* 82 (3), 341–363. doi:10.1002/ddr.21760

Paugh, S. W., Bonten, E. J., Savic, D., Ramsey, L. B., Thierfelder, W. E., Gurung, P., et al. (2015). NALP3 inflammasome upregulation and CASP1 cleavage of the glucocorticoid receptor cause glucocorticoid resistance in leukemia cells. *Nat. Genet.* 47 (6), 607–614. doi:10.1038/ng.3283

Peng, L., He, Q., Li, X., Shuai, L., Chen, H., Li, Y., et al. (2016). HOXA13 exerts a beneficial effect in albumin-induced epithelial-mesenchymal transition via the glucocorticoid receptor signaling pathway in human renal tubular epithelial cells. *Mol. Med. Rep.* 14 (1), 271–276. doi:10.3892/mmr.2016.5247

Piao, C. H., Fan, Y., Nguyen, T. V., Shin, H. S., Kim, H. T., Song, C. H., et al. (2021). $PM_{2.5}$ exacerbates oxidative stress and inflammatory response through the Nrf2/NF-κB signaling pathway in OVA-induced allergic rhinitis mouse model. *Int. J. Mol. Sci.* 22 (15), 8173. doi:10.3390/ijms22158173

Plato, A., Hardison, S. E., and Brown, G. D. (2015). Pattern recognition receptors in antifungal immunity. *Semin. Immunopathol.* 37 (2), 97–106. doi:10.1007/s00281-014-0462-4

Porta, C., Consonni, F. M., Morlacchi, S., Sangaletti, S., Bleve, A., Totaro, M. G., et al. (2020). Tumor-derived prostaglandin E2 promotes p50 NF-κB-Dependent differentiation of monocytic MDSCs. *Cancer Res.* 80 (13), 2874–2888. doi:10.1158/0008-5472.CAN-19-2843

Potenta, S., Zeisberg, E., and Kalluri, R. (2008). The role of endothelial-to-mesenchymal transition in cancer progression. *Br. J. Cancer* 99 (9), 1375–1379. doi:10.1038/sj.bjc.6604662

Pulskens, W. P., Butter, L. M., Teske, G. J., Claessen, N., Dessing, M. C., Flavell, R. A., et al. (2014). Nlrp3 prevents early renal interstitial edema and vascular permeability in unilateral ureteral obstruction. *PloS One* 9 (1), e85775. doi:10.1371/journal.pone.0085775

Qi, W., Chen, X., Gilbert, R. E., Zhang, Y., Waltham, M., Schache, M., et al. (2007). High glucose-induced thioredoxin-interacting protein in renal proximal tubule cells is independent of transforming growth factor-beta1. *Am. J. Pathol.* 171 (3), 744–754. doi:10.2353/ajpath.2007.060813

Qiu, Y.-Y., and Tang, L.-Q. (2016). Roles of the NLRP3 inflammasome in the pathogenesis of diabetic nephropathy. *Pharmacol. Res.* 114, 251–264. doi:10.1016/j.phrs.2016.11.004

Qiu, Z., He, Y., Ming, H., Lei, S., Leng, Y., and Xia, Z.-Y. (2019). Lipopolysaccharide (LPS) aggravates high glucose- and hypoxia/reoxygenation-induced injury through activating ROS-dependent NLRP3 inflammasome-mediated pyroptosis in H9C2 cardiomyocytes. *J. Diabetes Res.* 2019, 8151836. doi:10.1155/2019/8151836

Qiu, Z., Lei, S., Zhao, B., Wu, Y., Su, W., Liu, M., et al. (2017). NLRP3 inflammasome activation-mediated pyroptosis aggravates myocardial ischemia/reperfusion injury in diabetic rats. *Oxid. Med. Cell. Longev.* 2017, 9743280. doi:10.1155/2017/9743280

Qu, X., Zhai, B., Liu, Y., Chen, Y., Xie, Z., Wang, Q., et al. (2022). Pyrroloquinoline quinone ameliorates renal fibrosis in diabetic nephropathy by inhibiting the pyroptosis pathway in C57BL/6 mice and human kidney 2 cells. *Biomed. Pharmacother. = Biomedecine Pharmacother.* 150, 112998. doi:10.1016/j.biopha.2022.112998

Rathinam, V. A. K., Zhao, Y., and Shao, F. (2019). Innate immunity to intracellular LPS. *Nat. Immunol.* 20 (5), 527–533. doi:10.1038/s41590-019-0368-3

Rayego-Mateos, S., Morgado-Pascual, J. L., Opazo-Ríos, L., Guerrero-Hue, M., García-Caballero, C., Vázquez-Carballo, C., et al. (2020). Pathogenic pathways and therapeutic approaches targeting inflammation in diabetic nephropathy. *Int. J. Mol. Sci.* 21 (11), E3798. doi:10.3390/ijms21113798

Rogers, C., Erkes, D. A., Nardone, A., Aplin, A. E., Fernandes-Alnemri, T., and Alnemri, E. S. (2019). Gasdermin pores permeabilize mitochondria to augment caspase-3 activation during apoptosis and inflammasome activation. *Nat. Commun.* 10 (1), 1689. doi:10.1038/s41467-019-09397-2

Ruan, J., Wang, S., and Wang, J. (2020). Mechanism and regulation of pyroptosis-mediated in cancer cell death. *Chem. Biol. Interact.* 323, 109052. doi:10.1016/j.cbi.2020.109052

Saeedi, P., Petersohn, I., Salpea, P., Malanda, B., Karuranga, S., Unwin, N., et al. (2019). Global and regional diabetes prevalence estimates for 2019 and projections for 2030 and 2045: Results from the international diabetes federation diabetes atlas, 9th edition. *Diabetes Res. Clin. Pract.* 157, 107843. doi:10.1016/j.diabres.2019.107843

Sattarinezhad, A., Roozbeh, J., Shirazi Yeganeh, B., Omrani, G. R., and Shams, M. (2019). Resveratrol reduces albuminuria in diabetic nephropathy: A randomized double-blind placebo-controlled clinical trial. *Diabetes Metab.* 45 (1), 53–59. doi:10.1016/j.diabet.2018.05.010

Shang, J., Zhang, Y., Jiang, Y., Li, Z., Duan, Y., Wang, L., et al. (2017). NOD2 promotes endothelial-to-mesenchymal transition of glomerular endothelial cells via MEK/ERK signaling pathway in diabetic nephropathy. *Biochem. Biophys. Res. Commun.* 484 (2), 435–441. doi:10.1016/j.bbrc.2017.01.155

Shi, J., Zhao, Y., Wang, K., Shi, X., Wang, Y., Huang, H., et al. (2015). Cleavage of GSDMD by inflammatory caspases determines pyroptotic cell death. *Nature* 526 (7575), 660–665. doi:10.1038/nature15514

Shi, S., Song, L., Yu, H., Feng, S., He, J., Liu, Y., et al. (2020). Knockdown of LncRNA-H19 ameliorates kidney fibrosis in diabetic mice by suppressing miR-29a-mediated EndMT. *Front. Pharmacol.* 11, 586895. doi:10.3389/fphar.2020.586895

Shi, W., Wang, D., Yuan, X., Liu, Y., Guo, X., Li, J., et al. (2019). Glucocorticoid receptor-IRS-1 axis controls EMT and the metastasis of breast cancers. *J. Mol. Cell Biol.* 11 (12), 1042–1055. doi:10.1093/jmcb/mjz001

Song, S., Qiu, D., Luo, F., Wei, J., Wu, M., Wu, H., et al. (2018a). Knockdown of NLRP3 alleviates high glucose or TGFB1-induced EMT in human renal tubular cells. *J. Mol. Endocrinol.* 61 (3), 101–113. doi:10.1530/JME-18-0069

Song, S., Qiu, D., Shi, Y., Wang, S., Zhou, X., Chen, N., et al. (2019). Thioredoxin-interacting protein deficiency alleviates phenotypic alterations of podocytes via inhibition of mTOR activation in diabetic nephropathy. *J. Cell. Physiol.* 234, 16485–16502. doi:10.1002/jcp.28317

Song, W., Wei, L., Du, Y., Wang, Y., and Jiang, S. (2018b). Protective effect of ginsenoside metabolite compound K against diabetic nephropathy by inhibiting NLRP3 inflammasome activation and NF-κB/p38 signaling pathway in high-fat diet/streptozotocin-induced diabetic mice. *Int. Immunopharmacol.* 63, 227–238. doi:10.1016/j.intimp.2018.07.027

Song, Y., Liu, W., Tang, K., Zang, J., Li, D., and Gao, H. (2020). Mangiferin alleviates renal interstitial fibrosis in streptozotocin-induced diabetic mice through regulating the PTEN/PI3K/Akt signaling pathway. *J. Diabetes Res.* 2020, 9481720. doi:10.1155/2020/9481720

Srivastava, S. P., Goodwin, J. E., Kanasaki, K., and Koya, D. (2020). Metabolic reprogramming by N-acetyl-seryl-aspartyl-lysyl-proline protects against diabetic kidney disease. *Br. J. Pharmacol.* 177 (16), 3691–3711. doi:10.1111/bph.15087

Srivastava, S. P., Li, J., Kitada, M., Fujita, H., Yamada, Y., Goodwin, J. E., et al. (2018). SIRT3 deficiency leads to induction of abnormal glycolysis in diabetic kidney with fibrosis. *Cell Death Dis.* 9 (10), 997. doi:10.1038/s41419-018-1057-0

Srivastava, S. P., Li, J., Takagaki, Y., Kitada, M., Goodwin, J. E., Kanasaki, K., et al. (2021a). Endothelial SIRT3 regulates myofibroblast metabolic shifts in diabetic kidneys. *IScience* 24 (5), 102390. doi:10.1016/j.isci.2021.102390

Srivastava, S. P., Zhou, H., Setia, O., Dardik, A., Fernandez-Hernando, C., and Goodwin, J. (2021b). Podocyte glucocorticoid receptors are essential for glomerular endothelial cell homeostasis in diabetes mellitus. *J. Am. Heart Assoc.* 10 (15), e019437. doi:10.1161/JAHA.120.019437

Srivastava, S. P., Zhou, H., Setia, O., Liu, B., Kanasaki, K., Koya, D., et al. (2021c). Loss of endothelial glucocorticoid receptor accelerates diabetic nephropathy. *Nat. Commun.* 12 (1), 2368. doi:10.1038/s41467-021-22617-y

Steffes, M. W., Osterby, R., Chavers, B., and Mauer, S. M. (1989). Mesangial expansion as a central mechanism for loss of kidney function in diabetic patients. *Diabetes* 38 (9), 1077–1081. doi:10.2337/diab.38.9.1077

Sun, L.-J., Sun, Y.-N., Shan, J.-P., and Jiang, G.-R. (2017). Effects of mineralocorticoid receptor antagonists on the progression of diabetic nephropathy. *J. Diabetes Investig.* 8 (4), 609–618. doi:10.1111/jdi.12629

Sun, X., Huang, K., Haiming, X., Lin, Z., Yang, Y., Zhang, M., et al. (2020). Connexin 43 prevents the progression of diabetic renal tubulointerstitial fibrosis by regulating the SIRT1-HIF-1α signaling pathway. *Clin. Sci.* 134 (13), 1573–1592. doi:10.1042/CS20200171

Sun, Z., Ma, Y., Chen, F., Wang, S., Chen, B., and Shi, J. (2018). miR-133b and miR-199b knockdown attenuate TGF-β1-induced epithelial to mesenchymal transition and renal fibrosis by targeting SIRT1 in diabetic nephropathy. *Eur. J. Pharmacol.* 837, 96–104. doi:10.1016/j.ejphar.2018.08.022

Taabazuing, C. Y., Okondo, M. C., and Bachovchin, D. A. (2017). Pyroptosis and apoptosis pathways engage in bidirectional crosstalk in monocytes and macrophages. *Cell Chem. Biol.* 24 (4), 507–514. doi:10.1016/j.chembiol.2017.03.009

Tan, C. Y. R., Weier, Q., Zhang, Y., Cox, A. J., Kelly, D. J., and Langham, R. G. (2015). Thioredoxin-interacting protein: A potential therapeutic target for treatment of progressive fibrosis in diabetic nephropathy. *Nephron* 129 (2), 109–127. doi:10.1159/000368238

Tang, P. M.-K., Zhang, Y.-Y., Hung, J. S.-C., Chung, J. Y.-F., Huang, X.-R., To, K.-F., et al. (2021). DPP4/CD32b/NF-κB circuit: A novel druggable target for inhibiting CRP-driven diabetic nephropathy. *Mol. Ther.* 29 (1), 365–375. doi:10.1016/j.ymthe.2020.08.017

Tang, S. C. W., and Yiu, W. H. (2020). Innate immunity in diabetic kidney disease. *Nat. Rev. Nephrol.* 16 (4), 206–222. doi:10.1038/s41581-019-0234-4

Tang, Y.-S., Zhao, Y.-H., Zhong, Y., Li, X.-Z., Pu, J.-X., Luo, Y.-C., et al. (2019). Neferine inhibits LPS-ATP-induced endothelial cell pyroptosis via regulation of ROS/NLRP3/Caspase-1 signaling pathway. *Inflamm. Res.* 68 (9), 727–738. doi:10.1007/s00011-019-01256-6

Tesch, G. H., Pullen, N., Jesson, M. I., Schlerman, F. J., and Nikolic-Paterson, D. J. (2019). Combined inhibition of CCR2 and ACE provides added protection against progression of diabetic nephropathy in Nos3-deficient mice. *Am. J. Physiol. Ren. Physiol.* 317 (6), F1439–F1449. doi:10.1152/ajprenal.00340.2019

Tian, L., Yan, J., Li, K., Zhang, W., Lin, B., Lai, W., et al. (2021). Ozone exposure promotes pyroptosis in rat lungs via the TLR2/4-NF-κB-NLRP3 signaling pathway. *Toxicology* 450, 152668. doi:10.1016/j.tox.2020.152668

Tirosh, A., Garg, R., and Adler, G. K. (2010). Mineralocorticoid receptor antagonists and the metabolic syndrome. *Curr. Hypertens. Rep.* 12 (4), 252–257. doi:10.1007/s11906-010-0126-2

Tsuchiya, K., Nakajima, S., Hosojima, S., Thi Nguyen, D., Hattori, T., Manh Le, T., et al. (2019). Caspase-1 initiates apoptosis in the absence of gasdermin D. *Nat. Commun.* 10 (1), 2091. doi:10.1038/s41467-019-09753-2

Tsuchiya, K. (2021). Switching from apoptosis to pyroptosis: Gasdermin-elicited inflammation and antitumor immunity. *Int. J. Mol. Sci.* 22 (1), E426. doi:10.3390/ijms22010426

Tu, Q., Li, Y., Jin, J., Jiang, X., Ren, Y., and He, Q. (2019). Curcumin alleviates diabetic nephropathy via inhibiting podocyte mesenchymal transdifferentiation and inducing autophagy in rats and MPC5 cells. *Pharm. Biol.* 57 (1), 778–786. doi:10.1080/13880209.2019.1688843

Wang, C., Hou, X.-X., Rui, H.-L., Li, L.-J., Zhao, J., Yang, M., et al. (2018). Artificially cultivated Ophiocordyceps sinensis alleviates diabetic nephropathy and its podocyte injury via inhibiting P2X7R expression and NLRP3 inflammasome activation. *J. Diabetes Res.* 2018, 1390418. doi:10.1155/2018/1390418

Wang, C., Pan, Y., Zhang, Q.-Y., Wang, F.-M., and Kong, L.-D. (2012). Quercetin and allopurinol ameliorate kidney injury in STZ-treated rats with regulation of renal NLRP3 inflammasome activation and lipid accumulation. *PloS One* 7 (6), e38285. doi:10.1371/journal.pone.0038285

Wang, C., Yang, T., Xiao, J., Xu, C., Alippe, Y., Sun, K., et al. (2021a). NLRP3 inflammasome activation triggers gasdermin D-independent inflammation. *Sci. Immunol.* 6 (64), eabj3859. doi:10.1126/sciimmunol.abj3859

Wang, F., Wang, L., Sui, G., Yang, C., Guo, M., Xiong, X., et al. (2021b). Inhibition of miR-129 improves neuronal pyroptosis and cognitive impairment through IGF-1/gsk3β signaling pathway: An *in vitro* and *in vivo* study. *J. Mol. Neurosci.* 71 (11), 2299–2309. doi:10.1007/s12031-021-01794-x

Wang, H.-Q., Wang, S.-S., Chiufai, K., Wang, Q., and Cheng, X.-L. (2019a). Umbelliferone ameliorates renal function in diabetic nephropathy rats through regulating inflammation and TLR/NF-κB pathway. *Chin. J. Nat. Med.* 17 (5), 346–354. doi:10.1016/S1875-5364(19)30040-8

Wang, J.-Y., Gao, Y.-B., Zhang, N., Zou, D.-W., Wang, P., Zhu, Z.-Y., et al. (2014). miR-21 overexpression enhances TGF-β1-induced epithelial-to-mesenchymal transition by target smad7 and aggravates renal damage in diabetic nephropathy. *Mol. Cell. Endocrinol.* 392 (1-2), 163–172. doi:10.1016/j.mce.2014.05.018

Wang, J., and Zhao, S.-M. (2021). LncRNA-antisense non-coding RNA in the INK4 locus promotes pyroptosis via miR-497/thioredoxin-interacting protein axis in diabetic nephropathy. *Life Sci.* 264, 118728. doi:10.1016/j.lfs.2020.118728

Wang, L., and Hauenstein, A. V. (2020). The NLRP3 inflammasome: Mechanism of action, role in disease and therapies. *Mol. Asp. Med.* 76, 100889. doi:10.1016/j.mam.2020.100889

Wang, M.-Z., Wang, J., Cao, D.-W., Tu, Y., Liu, B.-H., Yuan, C.-C., et al. (2022a). Fucoidan alleviates renal fibrosis in diabetic kidney disease *via* inhibition of NLRP3 inflammasome-mediated podocyte pyroptosis. *Front. Pharmacol.* 13, 790937. doi:10.3389/fphar.2022.790937

Wang, Q., Ou, Y., Hu, G., Wen, C., Yue, S., Chen, C., et al. (2020a). Naringenin attenuates non-alcoholic fatty liver disease by down-regulating the NLRP3/NF-κB pathway in mice. *Br. J. Pharmacol.* 177 (8), 1806–1821. doi:10.1111/bph.14938

Wang, R., Zhao, H., Zhang, Y., Zhu, H., Su, Q., Qi, H., et al. (2020b). Identification of MicroRNA-92a-3p as an essential regulator of tubular epithelial cell pyroptosis by targeting Nrf1 via HO-1. *Front. Genet.* 11, 616947. doi:10.3389/fgene.2020.616947

Wang, S.-H., Cui, L.-G., Su, X.-L., Komal, S., Ni, R.-C., Zang, M.-X., et al. (2022b). GSK-3β-mediated activation of NLRP3 inflammasome leads to pyroptosis and apoptosis of rat cardiomyocytes and fibroblasts. *Eur. J. Pharmacol.* 920, 174830. doi:10.1016/j.ejphar.2022.174830

Wang, S., Su, X., Xu, L., Chang, C., Yao, Y., Komal, S., et al. (2020c). Glycogen synthase kinase-3β inhibition alleviates activation of the NLRP3 inflammasome in myocardial infarction. *J. Mol. Cell. Cardiol.* 149, 82–94. doi:10.1016/j.yjmcc.2020.09.009

Wang, T., Gao, Y., Yue, R., Wang, X., Shi, Y., Xu, J., et al. (2020d). Ginsenoside Rg1 alleviates podocyte injury induced by hyperlipidemia via targeting the mTOR/NF-B/NLRP3 Axis. *Evid. Based. Complement. Altern. Med.* 2020, 2735714. doi:10.1155/2020/2735714

Wang, X., Jiang, L., Liu, X.-Q., Huang, Y.-B., Zhu, W., Zeng, H.-X., et al. (2022c). Identification of genes reveals the mechanism of cell ferroptosis in diabetic nephropathy. *Front. Physiol.* 13, 890566. doi:10.3389/fphys.2022.890566

Wang, Y., Ding, L., Wang, R., Guo, Y., Yang, Z., Yu, L., et al. (2022d). Circ_0004951 promotes pyroptosis of renal tubular cells *via* the NLRP3 inflammasome in diabetic kidney disease. *Front. Med.* 9, 828240. doi:10.3389/fmed.2022.828240

Wang, Y., Gao, W., Shi, X., Ding, J., Liu, W., He, H., et al. (2017). Chemotherapy drugs induce pyroptosis through caspase-3 cleavage of a gasdermin. *Nature* 547 (7661), 99–103. doi:10.1038/nature22393

Wang, Y., Zhu, X., Yuan, S., Wen, S., Liu, X., Wang, C., et al. (2019b). TLR4/NF-κB signaling induces GSDMD-related pyroptosis in tubular cells in diabetic kidney disease. *Front. Endocrinol.* 10, 603. doi:10.3389/fendo.2019.00603

Wei, J., Shi, Y., Hou, Y., Ren, Y., Du, C., Zhang, L., et al. (2013). Knockdown of thioredoxin-interacting protein ameliorates high glucose-induced epithelial to mesenchymal transition in renal tubular epithelial cells. *Cell. Signal.* 25 (12), 2788–2796. doi:10.1016/j.cellsig.2013.09.009

Wei, W., Li, X.-X., and Xu, M. (2019). Inhibition of vascular neointima hyperplasia by FGF21 associated with FGFR1/Syk/NLRP3 inflammasome pathway in diabetic mice. *Atherosclerosis* 289, 132–142. doi:10.1016/j.atherosclerosis.2019.08.017

Wei, Z., Nie, G., Yang, F., Pi, S., Wang, C., Cao, H., et al. (2020). Inhibition of ROS/NLRP3/Caspase-1 mediated pyroptosis attenuates cadmium-induced apoptosis in duck renal tubular epithelial cells. *Environ. Pollut.* 273, 115919. doi:10.1016/j.envpol.2020.115919

Wen, S., Deng, F., Li, L., Xu, L., Li, X., and Fan, Q. (2022). VX-765 ameliorates renal injury and fibrosis in diabetes by regulating caspase-1-mediated pyroptosis and inflammation. *J. Diabetes Investig.* 13 (1), 22–33. doi:10.1111/jdi.13660

Wen, S., Wang, Z.-H., Zhang, C.-X., Yang, Y., and Fan, Q.-L. (2020). Caspase-3 promotes diabetic kidney disease through gasdermin E-mediated progression to secondary necrosis during apoptosis. *Diabetes Metab. Syndr. Obes.* 13, 313–323. doi:10.2147/DMSO.S242136

Wen, Y., Liu, Y.-R., Tang, T.-T., Pan, M.-M., Xu, S.-C., Ma, K.-L., et al. (2018). mROS-TXNIP axis activates NLRP3 inflammasome to mediate renal injury during ischemic AKI. *Int. J. Biochem. Cell Biol.* 98, 43–53. doi:10.1016/j.biocel.2018.02.015

Wong, R. S. Y. (2011). Apoptosis in cancer: From pathogenesis to treatment. *J. Exp. Clin. Cancer Res.* 30, 87. doi:10.1186/1756-9966-30-87

Wongmekiat, O., Lailerd, N., Kobroob, A., and Peerapanyasut, W. (2021). Protective effects of purple rice husk against diabetic nephropathy by modulating PGC-1α/SIRT3/SOD2 signaling and maintaining mitochondrial redox equilibrium in rats. *Biomolecules* 11 (8), 1224. doi:10.3390/biom11081224

Wu, M., Han, W., Song, S., Du, Y., Liu, C., Chen, N., et al. (2018). NLRP3 deficiency ameliorates renal inflammation and fibrosis in diabetic mice. *Mol. Cell. Endocrinol.* 478, 115–125. doi:10.1016/j.mce.2018.08.002

Wu, X. Y., Yu, J., and Tian, H. M. (2019). Effect of SOCS1 on diabetic renal injury through regulating TLR signaling pathway. *Eur. Rev. Med. Pharmacol. Sci.* 23 (18), 8068–8074. doi:10.26355/eurrev_201909_19023

Wu, Y., Pan, B., Zhang, Z., Li, X., Leng, Y., Ji, Y., et al. (2022a1979). Caspase-4/11-Mediated pulmonary artery endothelial cell pyroptosis contributes to pulmonary arterial hypertension. *Hypertension* 79 (3), 536–548. doi:10.1161/HYPERTENSIONAHA.121.17868

Wu, Y., Yang, H., Xu, S., Cheng, M., Gu, J., Zhang, W., et al. (2022b1979)., 136. London, England, 103–120. doi:10.1042/CS20211075AIM2 inflammasome contributes to aldosterone-induced renal injury via endoplasmic reticulum stress*Clin. Sci.*1

Xia, W., Li, Y., Wu, M., Jin, Q., Wang, Q., Li, S., et al. (2021). Gasdermin E deficiency attenuates acute kidney injury by inhibiting pyroptosis and inflammation. *Cell Death Dis.* 12 (2), 139. doi:10.1038/s41419-021-03431-2

Xiao, C., Zhao, H., Zhu, H., Zhang, Y., Su, Q., Zhao, F., et al. (2020). Tisp40 induces tubular epithelial cell GSDMD-mediated pyroptosis in renal ischemia-reperfusion injury via NF-κB signaling. *Front. Physiol.* 11, 906. doi:10.3389/fphys.2020.00906

Xie, C., Wu, W., Tang, A., Luo, N., and Tan, Y. (2019). lncRNA GAS5/miR-452-5p reduces oxidative stress and pyroptosis of high-glucose-stimulated renal tubular cells. *Diabetes Metab. Syndr. Obes.* 12, 2609–2617. doi:10.2147/DMSO.S228654

Xie, X., Peng, J., Chang, X., Huang, K., Huang, J., Wang, S., et al. (2013). Activation of RhoA/ROCK regulates NF-κB signaling pathway in experimental diabetic nephropathy. *Mol. Cell. Endocrinol.* 369 (1-2), 86–97. doi:10.1016/j.mce.2013.01.007

Xin, R., Sun, X., Wang, Z., Yuan, W., Jiang, W., Wang, L., et al. (2018). Apocynin inhibited NLRP3/XIAP signalling to alleviate renal fibrotic injury in rat diabetic nephropathy. *Biomed. Pharmacother. = Biomedecine Pharmacother.* 106, 1325–1331. doi:10.1016/j.biopha.2018.07.036

Xu, J., Wang, Q., Song, Y.-F., Xu, X.-H., Zhu, H., Chen, P.-D., et al. (2022). Long noncoding RNA X-inactive specific transcript regulates NLR family pyrin domain containing 3/caspase-1-mediated pyroptosis in diabetic nephropathy. *World J. Diabetes* 13 (4), 358–375. doi:10.4239/wjd.v13.i4.358

Xu, W.-L., Liu, S., Li, N., Ye, L.-F., Zha, M., Li, C.-Y., et al. (2021a). Quercetin antagonizes glucose fluctuation induced renal injury by inhibiting aerobic glycolysis via HIF-1α/miR-210/ISCU/FeS pathway. *Front. Med.* 8, 656086. doi:10.3389/fmed.2021.656086

Xu, X., Zhang, L., Hua, F., Zhang, C., Zhang, C., Mi, X., et al. (2021b). FOXM1-activated SIRT4 inhibits NF-κB signaling and NLRP3 inflammasome to alleviate kidney injury and podocyte pyroptosis in diabetic nephropathy. *Exp. Cell Res.* 408 (2), 112863. doi:10.1016/j.yexcr.2021.112863

Xu, Y., Gao, H., Hu, Y., Fang, Y., Qi, C., Huang, J., et al. (2019). High glucose-induced apoptosis and necroptosis in podocytes is regulated by UCHL1 via RIPK1/RIPK3 pathway. *Exp. Cell Res.* 382 (2), 111463. doi:10.1016/j.yexcr.2019.06.008

Xue, Y., Enosi Tuipulotu, D., Tan, W. H., Kay, C., and Man, S. M. (2019). Emerging activators and regulators of inflammasomes and pyroptosis. *Trends Immunol.* 40 (11), 1035–1052. doi:10.1016/j.it.2019.09.005

Yan, R., Wang, Y., Shi, M., Xiao, Y., Liu, L., Liu, L., et al. (2019). Regulation of PTEN/AKT/FAK pathways by PPARγ impacts on fibrosis in diabetic nephropathy. *J. Cell. Biochem.* 120, 6998–7014. doi:10.1002/jcb.27937

Yang, C., Zhong, Z.-F., Wang, S.-P., Vong, C.-T., Yu, B., and Wang, Y.-T. (2021a). HIF-1: Structure, biology and natural modulators. *Chin. J. Nat. Med.* 19 (7), 521–527. doi:10.1016/S1875-5364(21)60051-1

Yang, F., Qin, Y., Wang, Y., Meng, S., Xian, H., Che, H., et al. (2019a). Metformin inhibits the NLRP3 inflammasome via AMPK/mTOR-dependent effects in diabetic cardiomyopathy. *Int. J. Biol. Sci.* 15 (5), 1010–1019. doi:10.7150/ijbs.29680

Yang, G., Zhao, Z., Zhang, X., Wu, A., Huang, Y., Miao, Y., et al. (2017). Effect of berberine on the renal tubular epithelial-to-mesenchymal transition by inhibition of the Notch/snail pathway in diabetic nephropathy model KKAy mice. *Drug Des. devel. Ther.* 11, 1065–1079. doi:10.2147/DDDT.S124971

Yang, J.-R., Yao, F.-H., Zhang, J.-G., Ji, Z.-Y., Li, K.-L., Zhan, J., et al. (2014). Ischemia-reperfusion induces renal tubule pyroptosis via the CHOP-caspase-11 pathway. *Am. J. Physiol. Ren. Physiol.* 306 (1), F75–F84. doi:10.1152/ajprenal.00117.2013

Yang, M., Wang, X., Han, Y., Li, C., Wei, L., Yang, J., et al. (2021b). Targeting the NLRP3 inflammasome in diabetic nephropathy. *Curr. Med. Chem.* 28 (42), 8810–8824. doi:10.2174/0929867328666210705153109

Yang, R., Yang, F., Hu, Y., Chen, M., Liu, Y., Li, J., et al. (2020). Hepatocyte growth factor Attenuates the development of TGF-β1- induced EndMT through down-regulating the Notch signaling. *Endocr. Metab. Immune Disord. Drug Targets* 20 (5), 781–787. doi:10.2174/1871530319666191023141638

Yang, S.-K., Li, A.-M., Han, Y.-C., Peng, C.-H., Song, N., Yang, M., et al. (2019b). Mitochondria-targeted peptide SS31 attenuates renal tubulointerstitial injury via inhibiting mitochondrial fission in diabetic mice. *Oxid. Med. Cell. Longev.* 2019, 2346580. doi:10.1155/2019/2346580

Yaribeygi, H., Atkin, S. L., and Sahebkar, A. (2019). Interleukin-18 and diabetic nephropathy: A review. *J. Cell. Physiol.* 234 (5), 5674–5682. doi:10.1002/jcp.27427

Yi, H., Peng, R., Zhang, L.-Y., Sun, Y., Peng, H.-M., Liu, H.-D., et al. (2017). LincRNA-Gm4419 knockdown ameliorates NF-κB/NLRP3 inflammasome-mediated inflammation in diabetic nephropathy. *Cell Death Dis.* 8 (2), e2583. doi:10.1038/cddis.2016.451

Yoshihara, E. (2020). TXNIP/TBP-2: A master regulator for glucose homeostasis. *Antioxidants (Basel, Switz.* 9 (8), E765. doi:10.3390/antiox9080765

Yu, H., Lin, L., Zhang, Z., Zhang, H., and Hu, H. (2020). Targeting NF-κB pathway for the therapy of diseases: Mechanism and clinical study. *Signal Transduct. Target. Ther.* 5 (1), 209. doi:10.1038/s41392-020-00312-6

Yu, H., Yao, S., Zhou, C., Fu, F., Luo, H., Du, W., et al. (2021a). Morroniside attenuates apoptosis and pyroptosis of chondrocytes and ameliorates osteoarthritic development by inhibiting NF-κB signaling. *J. Ethnopharmacol.* 266, 113447. doi:10.1016/j.jep.2020.113447

Yu, L.-M., Zhang, W.-H., Han, X.-X., Li, Y.-Y., Lu, Y., Pan, J., et al. (2019). Hypoxia-induced ROS contribute to myoblast pyroptosis during obstructive sleep apnea via the NF-B/HIF-1 signaling pathway. *Oxid. Med. Cell. Longev.* 2019, 4596368. doi:10.1155/2019/4596368

Yu, P., Zhang, X., Liu, N., Tang, L., Peng, C., and Chen, X. (2021b). Pyroptosis: Mechanisms and diseases. *Signal Transduct. Target. Ther.* 6 (1), 128. doi:10.1038/s41392-021-00507-5

Yuan, D., Guan, S., Wang, Z., Ni, H., Ding, D., Xu, W., et al. (2021). HIF-1α aggravated traumatic brain injury by NLRP3 inflammasome-mediated pyroptosis and activation of microglia. *J. Chem. Neuroanat.* 116, 101994. doi:10.1016/j.jchemneu.2021.101994

Zang, L., Gao, F., Huang, A., Zhang, Y., Luo, Y., Chen, L., et al. (2022). Icariin inhibits epithelial mesenchymal transition of renal tubular epithelial cells via regulating the miR-122-5p/FOXP2 axis in diabetic nephropathy rats. *J. Pharmacol. Sci.* 148 (2), 204–213. doi:10.1016/j.jphs.2021.10.002

Zanoni, I., Tan, Y., Di Gioia, M., Broggi, A., Ruan, J., Shi, J., et al. (2016). An endogenous caspase-11 ligand elicits interleukin-1 release from living dendritic cells. *Sci. (New York, N.Y.)* 352 (6290), 1232–1236. doi:10.1126/science.aaf3036

Zeng, C.-Y., Li, C.-G., Shu, J.-X., Xu, L.-H., Ouyang, D.-Y., Mai, F.-Y., et al. (2019). ATP induces caspase-3/gasdermin E-mediated pyroptosis in NLRP3 pathway-blocked murine macrophages. *Apoptosis* 24 (9-10), 703–717. doi:10.1007/s10495-019-01551-x

Zha, X., Xi, X., Fan, X., Ma, M., Zhang, Y., and Yang, Y. (2020). Overexpression of METTL3 attenuates high-glucose induced RPE cell pyroptosis by regulating miR-25-3p/PTEN/Akt signaling cascade through DGCR8. *Aging* 12 (9), 8137–8150. doi:10.18632/aging.103130

Zhai, Z., Liu, W., Kaur, M., Luo, Y., Domenico, J., Samson, J. M., et al. (2017). NLRP1 promotes tumor growth by enhancing inflammasome activation and suppressing apoptosis in metastatic melanoma. *Oncogene* 36 (27), 3820–3830. doi:10.1038/onc.2017.26

Zhang, C., Gong, Y., Li, N., Liu, X., Zhang, Y., Ye, F., et al. (2021a). Long noncoding RNA Kcnq1ot1 promotes sC5b-9-induced podocyte pyroptosis by inhibiting miR-486a-3p and upregulating *NLRP3*. *Am. J. Physiol. Cell Physiol.* 320 (3), C355–C364. doi:10.1152/ajpcell.00403.2020

Zhang, C., Hu, Z., Hu, R., Pi, S., Wei, Z., Wang, C., et al. (2021b). New insights into crosstalk between pyroptosis and autophagy co-induced by molybdenum and cadmium in duck renal tubular epithelial cells. *J. Hazard. Mat.* 416, 126138. doi:10.1016/j.jhazmat.2021.126138

Zhang, C., Lin, T., Nie, G., Hu, R., Pi, S., Wei, Z., et al. (2021c). Cadmium and molybdenum co-induce pyroptosis via ROS/PTEN/PI3K/AKT axis in duck renal tubular epithelial cells. *Environ. Pollut.* 272, 116403. doi:10.1016/j.envpol.2020.116403

Zhang, C., Zhu, X., Li, L., Ma, T., Shi, M., Yang, Y., et al. (2019a). A small molecule inhibitor MCC950 ameliorates kidney injury in diabetic nephropathy by inhibiting NLRP3 inflammasome activation. *Diabetes Metab. Syndr. Obes.* 12, 1297–1309. doi:10.2147/DMSO.S199802

Zhang, L., Shen, Z.-Y., Wang, K., Li, W., Shi, J.-M., Osoro, E. K., et al. (2019b). C-reactive protein exacerbates epithelial-mesenchymal transition through Wnt/β-catenin and ERK signaling in streptozocin-induced diabetic nephropathy. *FASEB J. Official Publ. Fed. Am. Soc. For Exp. Biol.* 33 (5), 6551–6563. doi:10.1096/fj.201801865RR

Zhang, L., Zhang, L., Huang, Z., Xing, R., Li, X., Yin, S., et al. (2019c). Increased HIF-1 in knee osteoarthritis aggravate synovial fibrosis via fibroblast-like synoviocyte pyroptosis. *Oxid. Med. Cell. Longev.* 2019, 6326517. doi:10.1155/2019/6326517

Zhang, Q., Liu, X., Sullivan, M. A., Shi, C., and Deng, B. (2021d). Protective effect of yi shen Pai Du formula against diabetic kidney injury via inhibition of oxidative stress, inflammation, and epithelial-to-mesenchymal transition in *db/db* mice. *Oxid. Med. Cell. Longev.* 2021, 7958021. doi:10.1155/2021/7958021

Zhang, S., Zhu, L., Dai, H., and Pan, L. (2021e). Silencing ROCK1 ameliorates ventilator-induced lung injury in mice by inhibiting macrophages' NLRP3 signaling. *Int. Immunopharmacol.* 101 (1), 108208. doi:10.1016/j.intimp.2021.108208

Zhang, X., Shang, X., Jin, S., Ma, Z., Wang, H., Ao, N., et al. (2021f). Vitamin D ameliorates high-fat-diet-induced hepatic injury via inhibiting pyroptosis and alters gut microbiota in rats. *Arch. Biochem. Biophys.* 705, 108894. doi:10.1016/j.abb.2021.108894

Zhang, Y., Liu, W., Zhong, Y., Li, Q., Wu, M., Yang, L., et al. (2021g). Metformin corrects glucose metabolism reprogramming and NLRP3 inflammasome-induced pyroptosis via inhibiting the TLR4/NF-B/PFKFB3 signaling in trophoblasts: Implication for a potential therapy of preeclampsia. *Oxid. Med. Cell. Longev.* 2021, 1806344. doi:10.1155/2021/1806344

Zhang, Z., Shao, X., Jiang, N., Mou, S., Gu, L., Li, S., et al. (2018). Caspase-11-mediated tubular epithelial pyroptosis underlies contrast-induced acute kidney injury. *Cell Death Dis.* 9 (10), 983. doi:10.1038/s41419-018-1023-x

Zhang, Z., Zhang, H., Li, D., Zhou, X., Qin, Q., and Zhang, Q. (2021h). Caspase-3-mediated GSDME induced Pyroptosis in breast cancer cells through the ROS/JNK signalling pathway. *J. Cell. Mol. Med.* 25 (17), 8159–8168. doi:10.1111/jcmm.16574

Zhao, H., Huang, H., Alam, A., Chen, Q., Suen, K. C., Cui, J., et al. (2018a). VEGF mitigates histone-induced pyroptosis in the remote liver injury associated with renal allograft ischemia-reperfusion injury in rats. *Am. J. Transpl.* 18 (8), 1890–1903. doi:10.1111/ajt.14699

Zhao, S., Li, W., Yu, W., Rao, T., Li, H., Ruan, Y., et al. (2021). Exosomal miR-21 from tubular cells contributes to renal fibrosis by activating fibroblasts via targeting PTEN in obstructed kidneys. *Theranostics* 11 (18), 8660–8673. doi:10.7150/thno.62820

Zhao, W., Shi, C.-S., Harrison, K., Hwang, I.-Y., Nabar, N. R., Wang, M., et al. (2020)., 205. Baltimore, Md, 2255–2264. doi:10.4049/jimmunol.2000649AKT regulates NLRP3 inflammasome activation by phosphorylating NLRP3 serine 5*J. Immunol.*8

Zhao, X.-P., Chang, S.-Y., Liao, M.-C., Lo, C.-S., Chenier, I., Luo, H., et al. (2018b). Hedgehog interacting protein promotes fibrosis and apoptosis in glomerular endothelial cells in murine diabetes. *Sci. Rep.* 8 (1), 5958. doi:10.1038/s41598-018-24220-6

Zhen, J., Zhang, L., Pan, J., Ma, S., Yu, X., Li, X., et al. (2014). AIM2 mediates inflammation-associated renal damage in Hepatitis B virus-associated glomerulonephritis by regulating caspase-1, IL-1β, and IL-18. *Mediat. Inflamm.* 2014, 190860. doi:10.1155/2014/190860

Zheng, F., Zeng, Y. J., Plati, A. R., Elliot, S. J., Berho, M., Potier, M., et al. (2006). Combined AGE inhibition and ACEi decreases the progression of established diabetic nephropathy in B6 db/db mice. *Kidney Int.* 70 (3), 507–514. doi:10.1038/sj.ki.5001578

Zheng, Q., Yao, D., Cai, Y., and Zhou, T. (2020). NLRP3 augmented resistance to gemcitabine in triple-negative breast cancer cells via EMT/IL-1β/Wnt/β-catenin signaling pathway. *Biosci. Rep.* 40 (7), BSR20200730. doi:10.1042/BSR20200730

Zheng, W., Qian, C., Xu, F., Cheng, P., Yang, C., Li, X., et al. (2021). Fuxin Granules ameliorate diabetic nephropathy in db/db mice through TGF-β1/Smad and VEGF/VEGFR2 signaling pathways. *Biomed. Pharmacother. = Biomedecine Pharmacother.* 141, 111806. doi:10.1016/j.biopha.2021.111806

Zhou, C.-B., and Fang, J.-Y. (2019). The role of pyroptosis in gastrointestinal cancer and immune responses to intestinal microbial infection. *Biochim. Biophys. Acta. Rev. Cancer* 1872 (1)–10. doi:10.1016/j.bbcan.2019.05.001

Zhou, J., Zeng, L., Zhang, Y., Wang, M., Li, Y., Jia, Y., et al. (2022). Cadmium exposure induces pyroptosis in testicular tissue by increasing oxidative stress and activating the AIM2 inflammasome pathway. *Sci. Total Environ.* 847, 157500. doi:10.1016/j.scitotenv.2022.157500

Zhou, X., Wang, Q., Nie, L., Zhang, P., Zhao, P., Yuan, Q., et al. (2020). Metformin ameliorates the NLPP3 inflammasome mediated pyroptosis by inhibiting the expression of NEK7 in diabetic periodontitis. *Arch. Oral Biol.* 116, 104763. doi:10.1016/j.archoralbio.2020.104763

Zhu, W., Li, Y.-Y., Zeng, H.-X., Liu, X.-Q., Sun, Y.-T., Jiang, L., et al. (2021). Carnosine alleviates podocyte injury in diabetic nephropathy by targeting caspase-1-mediated pyroptosis. *Int. Immunopharmacol.* 101 (2), 108236. doi:10.1016/j.intimp.2021.108236

Zhu, Y., Zhu, C., Yang, H., Deng, J., and Fan, D. (2020). Protective effect of ginsenoside Rg5 against kidney injury via inhibition of NLRP3 inflammasome activation and the MAPK signaling pathway in high-fat diet/streptozotocin-induced diabetic mice. *Pharmacol. Res.* 155, 104746. doi:10.1016/j.phrs.2020.104746

Zuo, Y., Chen, L., He, X., Ye, Z., Li, L., Liu, Z., et al. (2021). Atorvastatin regulates MALAT1/miR-200c/NRF2 activity to protect against podocyte pyroptosis induced by high glucose. *Diabetes Metab. Syndr. Obes.* 14, 1631–1645. doi:10.2147/DMSO.S298950

Zychlinsky, A., Fitting, C., Cavaillon, J. M., and Sansonetti, P. J. (1994). Interleukin 1 is released by murine macrophages during apoptosis induced by Shigella flexneri. *J. Clin. Invest.* 94 (3), 1328–1332. doi:10.1172/JCI117452

frontiers | Frontiers in Pharmacology

TYPE Original Research
PUBLISHED 17 October 2022
DOI 10.3389/fphar.2022.964234

OPEN ACCESS

EDITED BY
Divya Bhatia,
Cornell University, United States

REVIEWED BY
Francesco Locatelli,
Alessandro Manzoni Hospital, Italy
Edwin Patino,
NewYork-Presbyterian, United States

*CORRESPONDENCE
Peng Yi,
yipeng2008@163.com
Gaoxiao Zhang,
zhanggaoxiao2005@163.com
Yewei Sun,
yxy0723@163.com

†These authors have contributed equally to this work

SPECIALTY SECTION
This article was submitted to Renal Pharmacology, a section of the journal Frontiers in Pharmacology

RECEIVED 08 June 2022
ACCEPTED 03 October 2022
PUBLISHED 17 October 2022

CITATION
Cen Y, Wang P, Gao F, Jing M, Zhang Z, Yi P, Zhang G, Sun Y and Wang Y (2022), Tetramethylpyrazine nitrone activates hypoxia-inducible factor and regulates iron homeostasis to improve renal anemia.
Front. Pharmacol. 13:964234.
doi: 10.3389/fphar.2022.964234

Tetramethylpyrazine nitrone activates hypoxia-inducible factor and regulates iron homeostasis to improve renal anemia

Yun Cen[1,2†], Peile Wang[2†], Fangfang Gao[2], Mei Jing[2], Zaijun Zhang[2], Peng Yi[2*], Gaoxiao Zhang[2*], Yewei Sun[2*] and Yuqiang Wang[2]

[1]Department of Intensive Care Unit, The First Affiliated Hospital of Jinan University and Institute of New Drug Research, Jinan University College of Pharmacy, Guangzhou, China, [2]Institute of New Drug Research and Guangzhou Key Laboratory of Innovative Chemical Drug Research in Cardio-cerebrovascular Diseases, Jinan University College of Pharmacy, Guangzhou, China

Renal anemia is one of the most common complications of chronic kidney disease and diabetic kidney disease. Despite the progress made in recent years, there is still an urgent unmet clinical need for renal anemia treatment. In this research, we investigated the efficacy and mechanism of action of the novel tetramethylpyrazine nitrone (TBN). Animal models of anemia including the streptozotocin (STZ)-induced spontaneously hypertensive rats (SHR) and the cisplatin (CDDP)-induced C57BL/6J mice are established to study the TBN's effects on expression of hypoxia-inducible factor and erythropoietin. To explore the mechanism of TBN's therapeutic effect on renal anemia, cobalt chloride ($CoCl_2$) is used in Hep3B/HepG2 cells to simulate a hypoxic environment. TBN is found to increase the expression of hypoxia-inducible factor HIF-1α and HIF-2α under hypoxic conditions and reverse the reduction of HIFs expression caused by saccharate ferric oxide (SFO). TBN also positively regulates the AMPK pathway. TBN stimulates nuclear transcription and translation of erythropoietin by enhancing the stability of HIF-1α expression. TBN has a significant regulatory effect on several major biomarkers of iron homeostasis, including ferritin, ferroportin (FPN), and divalent metal transporter-1 (DMT1). In conclusion, TBN regulates the AMPK/mTOR/4E-BP1/HIFs pathway, and activates the hypoxia-inducible factor and regulates iron homeostasis to improve renal anemia.

KEYWORDS

tetramethylpyrazine nitrone, renal anemia, hypoxia-inducible factor, AMPK/mTOR pathway, iron homeostasis

Introduction

In the United States, anemia is twice as prevalent in patients with chronic kidney disease (CKD) than in the general population (Stauffer and Fan, 2014). Anemia is a widespread and problematic complication in CKD (Kassebaum et al., 2014; St Peter et al., 2018). Hypertension is not only the main risk factor but also one of the most common co-morbidities of diabetic kidney disease (DKD) (Stanton, 2016). Every 10 mmHg increase in mean systolic blood pressure induces a 15% increase in developing microalbuminuria (Retnakaran et al., 2006). Hence, diabetic patients with concomitant hypertension have a much higher risk of developing DKD than diabetic patients without. DKD patients are 2–10 folds more likely to have anemia than non-diabetic nephropathy patients (Loutradis et al., 2016; Astor et al., 2002). The reduction of erythropoietin (EPO) production by renal tubular fibroblasts is the primary cause of CKD-related anemia (Olmos et al., 2018). When kidney function decreases, patients have inadequate serum iron, resulting in decreased transfers of iron into the bone marrow, further impairing erythropoiesis (Mikhail et al., 2017; Gafter-Gvili et al., 2019).

Anemia occurs at an early stage and can be observed even before any demonstrable changes in renal function take place (Thomas, 2007). The etiology and pathophysiology of anemia are multi-factorial, including iron deficiencies, chronic diseases, and bone marrow diseases (Crathorne et al., 2016). EPO analogues and iron replacement are the current treatments for anemia, but the Food and Drug Administration (FDA) has issued a warning for the usage of EPO analogues because their usage results in a greater risk of serious side effects (Besarab et al., 2015).

Although a relative deficiency of EPO production is the main cause of anemia in CKD, iron metabolism is closely regulated at various stages of the red blood cell (RBC) life cycle. Human serum iron levels are tightly controlled by iron efflux transporter FPN and the hormone hepcidin (Billesbølle et al., 2020). The process by which erythroblasts disintegrate into reticulocytes is iron-dependent (Yilmaz et al., 2011). Serum transferrin (Tf) binds to the iron in the gastrointestinal tract. Following this, iron is transported to the liver or spleen for storage or to the bone marrow for erythropoiesis (Wish, 2006). Divalent metal transporter-1 (DMT1) and duodenal cytochrome b reductase (DCYTB) are activated by HIF-2α during HIF signaling regulation of transferrin receptor (TfR) and iron transport gene Tf expression (Batchelor et al., 2020).

HIF-1α synthesis is regulated by mammalian target of rapamycin complex 1 (mTORC1) on a translational level through co-operative regulation of 4E-binding protein 1 (4E-BP1). Cobalt metal is genotoxic, creating oxidative DNA damage through reactive oxygen species and inhibits DNA repair (Simonsen et al., 2012). Cobalt (Co^{2+}) stabilizes the transcriptional activator HIF and therefore imitates hypoxic conditions and urges EPO production (Simonsen et al., 2012).

TBN is a novel nitrone derivative of tetramethylpyrazine, a principal active ingredient of the herbal medicine Ligusticum Chuanxiong armed with a powerful free radical scavenger (Sun et al., 2008; Tian et al., 2010; Sun et al., 2012). The structure of TBN is shown in Supplementary Figure S1. Our previous studies have found that TBN was effective in improving renal functions in DKD at the early stage both in rats and monkeys (Jing et al., 2021), however, its effects on renal anemia have not been explored. As DKD and renal anemia are commonly concomitant, herein we investigated whether TBN is effective in alleviating renal anemia and its mechanism of action *in vitro* and in animal models of CKD and DKD.

Materials and methods

Animal model

All animal care and experimental protocols were approved by the Institutional Animal Care and Use Committee of the Guangzhou University of Chinese Medicine (Guangzhou, China). All animal experiments complied with the US National Institutes of Health guide for the care and use of laboratory animals (NIH Publications No. 8023, revised 1978).

The 11-week-old male SHR rats and normal Wistar Kyoto rats (WKY) were obtained from Beijing Vital River Laboratory Animal Technology Co, Ltd, China. The rats were housed 3–4 per cage on a 12 h light/dark cycle with standard rodent chow and water *ad libitum* in a temperature (20–25°C) and humidity (30%–50%) under the control of an animal facility. Animals (weighing 300 ± 10 g, 200 ± 10 g) were divided into the following four groups: 1) normal WKY group (WKY-Ctrl); 2) non-diabetic SHR group (SHR-Ctrl); 3) STZ-induced diabetic SHR group (SHR-STZ); 4) TBN-treated STZ-induced diabetic SHR group (60 mg/kg) (SHR-STZ-TBN 60). For diabetic rats, blood glucose levels were measured 3 days after the intraperitoneal injection of STZ (55 mg/kg, STZ, Sigma-Aldrich) and the rats with blood glucose concentrations lower than 16.7 mmol/L were excluded. Three weeks after STZ injection, rats were administered intragastric TBN (60 mg/kg) twice a day for 6 weeks.

The 8-week-old male C57BL/6J mice were obtained from Guangdong Medical Laboratory Animal Centre, China. The mice were housed 6 per cage on a 12 h light/dark cycle with standard rodent chow and water *ad libitum* in a temperature (20–25°C) and humidity (30%–50%) under the control of the animal facility. For the CDDP-induced C57BL/6J mice renal anemia model, male C57BL/6J mice were randomly divided into 6 groups: control group (Control), vehicle-treated CDDP group (Model), CDDP-TBN low-dose group (10 mg/kg, TBN 10), CDDP-TBN medium-dose group (30 mg/kg, TBN 30), CDDP-TBN high-dose group (60 mg/kg, TBN 60), and CDDP-Roxadustat (10 mg/kg) group (Roxadustat). The control group

was injected with an equal volume of normal saline. The other groups were injected with CDDP (5 mg/kg, CDDP, Sigma-Aldrich) intraperitoneally once a week for a total of 4 weeks. From the fifth week of the CDDP injection to the end of the eighth week, the TBN and Roxadustat treatment groups were respectively given TBN and Roxadustat by intragastric administration, with TBN administered twice a day, and Roxadustat once every other day.

Metabolic measurements

In the SHR, blood glucose and pressure levels were measured at the third and ninth weeks. Bodyweight was measured weekly. After 6 weeks of TBN treatment, the rats were sacrificed; blood and tissue samples were harvested and processed for the following research. Blood glucose, blood urea nitrogen (BUN), serum iron, and Tf were measured *via* an automatic biochemical analyser (Hitachi AutoAnalyzer 7100, Hitachi Co. Ltd., and Tokyo, Japan). The sera from SHR were assayed using Rat EPO ELISA Kits (BioLegend, Inc., San Diego, CA, United States) and Rat Hepcidin ELISA Kits (Biovision, Milpitas, CA, United States), after which blood samples were collected and centrifuged for 10 min at 3,000 g.

Blood pressure measurement

Systolic and diastolic blood pressures were non-invasively measured *via* a calibrated-catheter tail-cuff system (CODA, Kent Scientific, and Torrington, CT). Rats were kept in compatible size holders on a comfortable and warm pad during the measurement. Blood pressure was monitored before and after TBN administration, respectively. Blood pressure measurements were conducted at the same time each day.

Blood analysis

Mouse whole blood collected from the caudal vein was analyzed by an Automatic five-category blood analyser. Mouse blood was taken by an abdominal aortic method and serum was separated by centrifugation with 3,000 g/10 min. In the fourth and eighth weeks after the start of the experiment, when the animals were awake, blood was collected from the tail vein, and the whole blood haemoglobin (Hb), RBC, and haematocrit (HCT) were measured with the Automatic Five-category Blood Analyser. Blood serum EPO (BioLegend, Inc., San Diego, CA, United States), serum Hepcidin (Biovision, Milpitas, CA, United States), serum catalase (CAT), and serum Glutathione peroxidase (GPx) concentrations were quantified by mouse ELISA kit.

H&E staining and PAS staining

The kidneys and livers were excised for histological analysis and stored at −80°C. A portion of the renal cortex and right lobe of the liver were reserved for biochemical analysis. The glomerular area was measured with H&E staining and the tubular injury was assessed by PAS staining. The malnutrition inflammation scores of the liver were quantified by H&E staining. After fixing in 4% paraformaldehyde for 24 h, kidneys and livers were embedded in paraffin and cut into 5 μm slices. The tissue sections were dewaxed and then stained with haematoxylin, after which they were washed with acid-alcohol and stained with eosin (Nanjing Jiancheng Bioengineering Institute, China). For PAS staining, slides were incubated with Alcian blue and Schiff's reagent to stain the acidic mucins and neutral mucins respectively. The slides were examined using a Fluorescence Inversion Microscope System (Olympus Corporation, CKX41).

Immunohistochemistry assay

The tissue sections were deparaffinized and rehydrated. For retrieving antigens, slides were heated in 10 mmol/L sodium citrate-hydrochloric acid buffer (Beyotime Biotechnology, China), and then incubated with blocking buffer (10% horse serum and 3% Triton X-100) at room temperature for 2 h. Afterward, the kidney sections were incubated with primary antibody HIF-2α (Abcam, Cambridge, MA, 1:300) at 4°C overnight, then incubated with secondary antibody for 2 h at room temperature. The DAB kit was used to visualize the antibody binding in the kidney sections. The nucleus was stained with haematoxylin as a counter stain. Photomicrographs were taken by Fluorescence Inversion Microscope System (Olympus Corporation, CKX41).

Cell culture and transfection

Hep3B and HepG2 cells were cultured in DMEM medium augmented with 10% heat-inactivated fetal bovine serum and 1% penicillin/streptomycin solution at 37°C with 5% CO_2 and 95% air. In a hypoxic environment, the cells were incubated accompanied by 50 μM $CoCl_2$ for 24 h. After $CoCl_2$-induction, Hep3B and HepG2 cells were hatched with TBN (30, 100, and 300 μM) under hypoxic conditions for 24 h. In order to assess protein stability, cells were incubated in the existence of $CoCl_2$ with or without TBN for 24 h and then treated with 2.5 μg/ml cycloheximide (CHx) for indicated times. In SFO stimulation experiments, Hep3B cells were incubated with 200 μg/ml SFO in presence of TBN (300 μM) under hypoxia for 24 h.

Western blot analysis

For preparing total protein, the kidney and liver tissues were lysed in RIPA lysis buffer (Beyotime Biotechnology, China) containing 1% PMSF (Beyotime Biotechnology, China) and 1% phosphatase inhibitors (Cell Signaling Technology, Danvers, MA, 1: 100). The concentration of protein was measured by BCA assay and total protein was separated by 10% SDS-PAGE and then transferred to PVDF membranes (0.45 μm, Immobilon-P, United States). After blocking with 5% skim milk for 2 h at room temperature, membranes were incubated with primary antibody HIF-1α (Cell Signaling Technology, Danvers, MA, 1:2000), HIF-2α (Abcam, Cambridge, MA, 1:1000), NRF2 (Abcam, Cambridge, MA, 1: 1000), HO-1 (Novus, Littleton, Colorado, United States, 1:1000), ferritin (Cell Signaling Technology, Danvers, MA, 1:1000), FPN (Cell Signaling Technology, Danvers, MA, 1:1000), Prolyl hydroxylase inhibitor (PHD3) (Cell Signaling Technology, Danvers, MA, 1:1000), factor-inhibiting HIF (FIH) (Cell Signaling Technology, Danvers, MA, 1:1000), DMT1 (Cell Signaling Technology, Danvers, MA, 1:1000), p-mTOR (Cell Signaling Technology, Danvers, MA, 1:1000), mTOR (Cell Signaling Technology, Danvers, MA, 1:1000), p-AMPK (Cell Signaling Technology, Danvers, MA, 1:1000), AMPK (Cell Signaling Technology, Danvers, MA, 1:1000), p-ULK1 (Cell Signaling Technology, Danvers, MA, 1:1000), ULK1 (Cell Signaling Technology, Danvers, MA, 1:1000), LC3 II (Cell Signaling Technology, Danvers, MA, 1:1000), GADPH (Cell Signaling Technology, Danvers, MA, 1:1000) and β-actin (Cell Signaling Technology, Danvers, MA, 1:1000) overnight at 4°C. Then, the PVDF membranes were incubated with anti-rabbit IgG antibody (Cell Signaling Technology, Danvers, MA, 1:2000) and anti-mouse IgG antibody (Cell Signaling Technology, Danvers, MA, 1:2000) respectively for 2 h at room temperature. Immunoreactive bands were visualized by the ECL detection system (Amersham Imager 600, GE, United States).

Immunofluorescence microscopy

Before being fixed in paraformaldehyde for 15 min at room temperature, cells were cultured and incubated on confocal small dishes. After washing three times with PBS, cells were treated with 0.3% v/v Triton X-100 in PBS for 10 min. After washing three times with PBS, cells were blocked with 10% v/v FBS in PBS for 1–2 h. Cells were then incubated with primary antibodies HIF-1α (1:300, diluted in Immune Primary Antibody Diluent) and HIF-2α (1:300, diluted in Immune Primary Antibody Diluent) overnight. Next day, the cells were washed three times before being incubated with fluorochrome-conjugated secondary anti-rabbit antibody or anti-mouse antibody, and DAPI for 1–2 h, and were washed three times with PBS and dropped anti-fluorescence quencher. Cells were examined and scanned on a fluorescence microscope.

Intracellular reactive oxygen species detection

Intracellular reactive oxidative species (ROS) were determined using 2′, 7′-dichlorofluorescin diacetate (DCFH-DA; Sigma-Aldrich, St Louis, MO, United States). Hep3B cells were incubated with SFO and TBN for 24 h and then 10 mM DCFH-DA was added at 37°C for 30–40 min. After washing, the ROS production was measured using quantitative measurements by fluorescence microscopy (FilterMax F3 Multi-Mode Microplate Readers, Molecular Devices, and Sunnyvale, CA, United States).

QPCR analysis

Total RNA was extracted from HepG2 cells using Trizol according to the manufacturer's protocol. Complementary DNA was synthesized using the All-in-One TM First-Strand cDNA Synthesis kit. Quantitative reverse transcription-polymerase chain reaction (qRT-PCR) was carried out in an ABI 7900 real-time PCR system (Illumina, San Diego, CA, United States) for 40 cycles using the All-in-One TM qPCR SYBR Green Mix. The results were expressed as the means of fold changes in target gene expression relative to GADPH, $n = 3$.

Statistical analysis

GraphPad Prism 8.0 software (San Diego, CA, United States) was used to analyse the data. The data were expressed as the mean ± SEM. Comparisons among multiple groups were analysed using one-way ANOVA or two-way ANOVA by Dunnett's test, as appropriate. $p < 0.05$ was considered statistically significant.

Results

Tetramethylpyrazine nitrone alleviated streptozotocin-induced kidney damage and ameliorated anemia in the spontaneously hypertensive rats

After injection of STZ, the body weight of rats was significantly reduced about 39.4%, which indicated that STZ induced a stable and reliable diabetic mellitus condition in SHR rats (Figure 1A). The systolic and diastolic pressures of SHR rats were significantly higher than in the WKY rats and TBN treatment did not affect blood pressure (Figures 1B,C). In SHR-STZ rats, the blood glucose level was approximately four times higher than that of the SHR-Ctrl rats. There was a non-significant trend of decrease in the blood glucose level in the TBN-treated than untreated SHR-STZ group at 9-weeks (Figure 1D). The urea nitrogen level was significantly elevated in the STZ-induced rats compared to that of the SHR rats (Figure 1E).

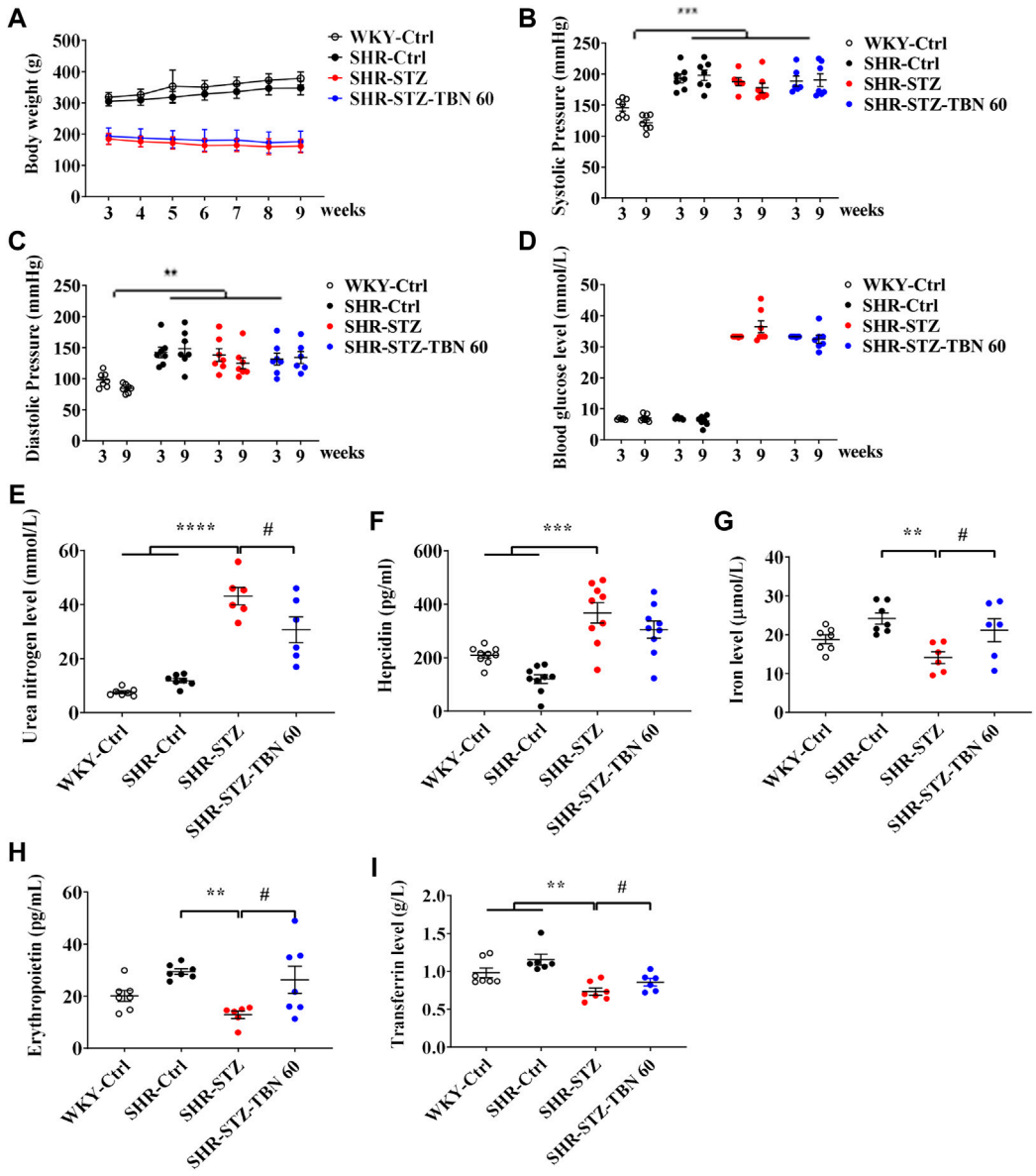

FIGURE 1
Effects of TBN on STZ-induced diabetic SHR rats. 11-week-old SHR rats are injected with a single dose of STZ (55 mg/kg) to induce diabetes. Shown are the effects of STZ and TBN on **(A)** body weight; **(B,C)** systolic pressure and diastolic pressure; **(D)** blood glucose level; **(E)** urea nitrogen level in diabetic-SHR rats treated with TBN. The changes of **(F)** hepcidin, **(G)** iron level, **(H)** EPO, and **(I)** Tf level in the serum of SHR rats after TBN treatment (n = 6–9 for each group). Data are presented as mean ± SEM; **$p < 0.01$; ***$p < 0.001$; ****$p < 0.0001$ vs. WKY-control, SHR-control; $^{\#}p < 0.05$ vs. SHR-STZ. WKY, Wistar-Kyoto; STZ, streptozotocin; SHR, spontaneously hypertensive rat; EPO, Erythropoietin; Tf, transferrin.

TBN treatment significantly reversed the increase in circulating urea nitrogen levels (Figure 1E).

We found that the levels of EPO and iron in SHR rats were increased compared with those of WKY rats before STZ treatment although the difference did not reach statistical significance. After STZ treatment, the hepcidin level was suppressed in SHR rats. STZ treatment promoted hepcidin expression and TBN alleviated the effects of STZ (Figure 1F). Furthermore, EPO and iron levels in the serum of SHR-STZ group were significantly lowered than those that in the SHR-Ctrl group. However, TBN treatment increased the levels of both serum iron level and EPO (Figures 1G,H). Tf is a biomarker for diagnosing anemia and monitoring treatment. In the DKD-SHR rats, expression of Tf was much lower than that in SHR rats; TBN elevated Tf levels by a statistically significant amount (Figure 1I). These results demonstrated that TBN ameliorated anemia in the diabetic SHR.

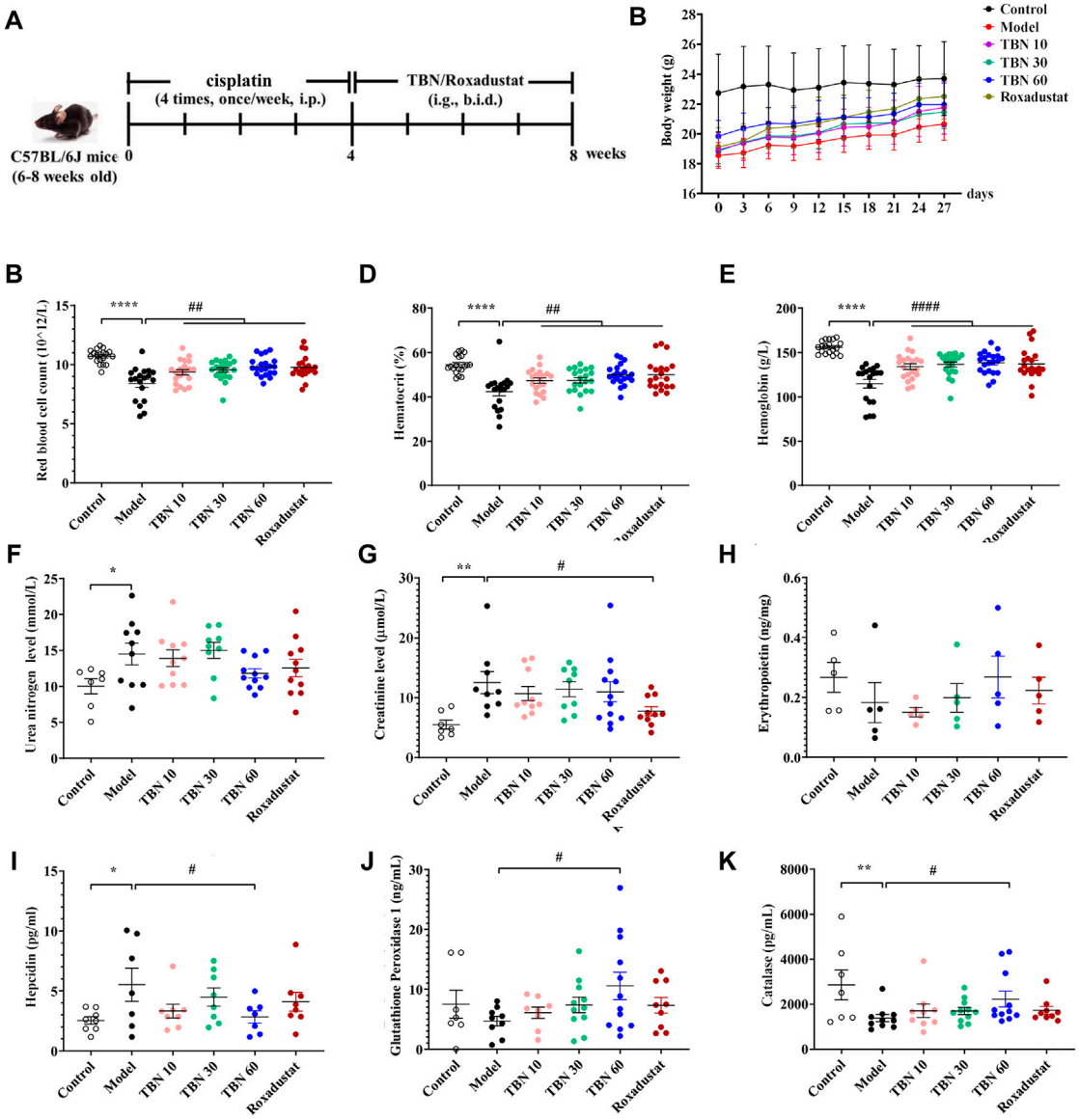

FIGURE 2
TBN ameliorates renal anemia in CDDP-induced mice. **(A)** Experimental flow chart, **(B)** Body weight. Blood measurements including **(C)** RBC count, **(D)** HCT and **(E)** Hb in C57BL/6J mice [n = 19–21 for each group in Figure **(A–E)**]. Levels of **(F)** Urea nitrogen level, **(G)** Creatinine after TBN treatment in C57BL/6J mice. Levels of **(H)** EPO, **(I)** hepcidin, subsequent to TBN treatment in C57Bl/6J mice. The effect of TBN in **(J)** GPx, **(K)** CAT (n = 7–8 for control group in Figure **(F–G)**, **(I–K)**; n = 7–12 for the other group in Figure **(F–G)**, **(I–K)**; n = 5 for each group in Figure **(H)**. Data are presented as mean ± SEM; $^{*}p < 0.05$; $^{**}p < 0.01$; $^{****}p < 0.0001$; vs. Control; $^{\#}p < 0.05$; $^{\#\#}p < 0.01$; $^{\#\#\#\#}p < 0.0001$ vs. vehicle-treated CDDP group. CDDP, cisplatin; RBC count, red blood cell count; HCT, hematocrit; Hb, hemoglobin; EPO, Erythropoietin; CAT, catalase; GPx, glutathione peroxidase. Model: vehicle-treated CDDP group.

Tetramethylpyrazine nitrone alleviated cisplatin-induced anemia in the C57BL/6J mice

In order to explore whether TBN ameliorates anemia in the CKD anemia model, CDDP was administered to produce the CKD anemia model (Wu et al., 2018). The flow chart of the experiment was shown in Figure 2A. Four weeks after CDDP administration, the body weight of mice was significantly decreased (approximately 25%) as shown in Figure 2B. In contrast to normal mice, the CDDP-induced mice exhibit reduced RBC count, HCT and Hb. The TBN treated CDDP-induced mice exhibit higher RBC counts, HCT, and Hb than those in the CDDP-induced (Model) TBN-untreated group. Hb levels in the CDDP-administered anemic mice (120 g/

L) were up-regulated by TBN to close to the normal levels (160 g/L), performing on par with the positive drug Roxadustat, and treatment with TBN stopped the development of CDDP-induced anemia (Figures 2C–E). The decreased RBC count and HCT level were reversed with TBN treatment dose-dependently, and the effects of a high dose of TBN (60 mg/kg) were similar to that of the positive control Roxadustat. There was no statistically significant difference in urea nitrogen and creatinine between the cisplatin-induced renal anemia group and the TBN-treated groups (Figures 2F,G). Roxadustat similarly reduced the creatinine level (Figure 2G).

There was a non-significant trend of decrease in the EPO levels after 8 weeks of CDDP administration in the model group than the control group. TBN treatment caused a dose-dependent increase in EPO levels. However, there were no statistically significant differences in serum EPO levels between the vehicle-treated CDDP group and the TBN- or Roxadustat-treated groups (Figure 2H). Hepcidin, which plays an inhibitory role in the regulation of iron balance in the body, leading to iron deficiency and anemia due to the premature overexpression of hepcidin, is a biomarker for the diagnosis and treatment monitoring of anemia. TBN diminished CDDP's effects, and CDDP treatment increased hepcidin expression (Figure 2I). These data showed that TBN reduces the severity of anemia in C57BL/6J mice.

We had found that TBN had significant free radical scavenging activity against some of the most damaging radicals, including superoxide, hydroxyl and peroxynitrite (Zhang et al., 2018). To investigate whether TBN influenced peroxide levels, the amount of GPx, an important peroxide decomposing enzyme widely present in the body, was measured in the sera of C57BL/6J mice. TBN (60 mg/kg) significantly increased the level of GPx in comparison to Roxadustat. Similar to the increase in GPx, TBN also increased the level of CAT at high doses (Figures 2J,K).

Tetramethylpyrazine nitrone improved anemia through activating hypoxia-inducible factor in streptozotocin-induced SHR rats and cisplatin-induced C57BL/6J mice

In the kidney tissues of C57BL/6J anemic mice, after immunofluorescence co-staining, areas where significant differences were found that TBN increased the synthesis of not only HIF-2α but also HIF-1α, and TBN affected HIF-1α more than HIF-2α (Figure 3A). To further explore the protective effect of TBN in STZ-induced renal injury, we investigated the pathological changes in rat kidneys through imaging. Hypertension seemed to have little effect on renal tissue when compared to what was seen in WKY rats. Remarkably, STZ induced an abnormal glomerular hypertrophy, but TBN treatment ameliorated the effect of STZ (Figure 3B). The tubular injury shown with PAS staining demonstrated that TBN treatment partially reversed the STZ damage (Figure 3B). The H&E staining and PAS staining results indicated that TBN significantly reduced STZ-induced damage in SHR rats with DKD. We evaluated the effects of TBN on HIF-2α and HO-1 in STZ-induced DKD anemia rats and the effects of TBN on HIF-1α and HIF-2α in CDDP-induced C57BL/6J anemic mice. TBN treatment increased the HIF-2α level (Figures 3C,D). HO-1 showed a similar change to that of HIF-2α (Figures 3C,E). These results suggested that TBN can prevent renal anemia by activating HIFs in STZ-induced SHR rats and CDDP-induced mice.

Next, the liver injury was analysed through PAS staining. Microscopically, the mice treated with CDDP exhibited inflammation in the hepatic lobules as well as a small amount of hepatocyte necrosis, nucleus lysis, and increased cytoplasmic eosinophilia, with no obvious inflammation in the portal area (Figures 3F,G). Remarkably, these pathological injuries were reduced after TBN treatment. The mice treated with Roxadustat exhibited little improvement (Figures 3F,G). These results indicated that TBN can improve renal function in rats and liver function in mice.

Tetramethylpyrazine nitrone increased synthesis and nuclear expression of hypoxia-inducible factor under hypoxic conditions

To further confirm whether TBN increased HIFs synthesis, $CoCl_2$ was used to produce hypoxic conditions. As seen through Western blot, HIF-2α expression increased significantly after TBN treatment under hypoxic conditions both in Hep3B and HepG2 cells, while HIF-1α expression increased only in Hep3B cell after TBN treatment (Figures 4A–F). Hypoxia leads to increased expression of HIF, which then binds to the EPO gene enhancer, resulting in transcriptional activation (Semenza and Wang, 1992). We found that TBN can promote both HIF-1α and HIF-2α nuclear expression in Hep3B cells (Figures 4G,H), suggesting that TBN increased EPO through activating HIF-1α synthesis and nuclear expression. Then we examined the expression of HIF-1α, HIF-2α, PHD3 and HIF-1α target genes as well as EPO, by qRT-PCR. As shown in Figures 4I–L, TBN promoted the expression of HIFs and EPO and decreased PHD3 in the hypoxic environment. These results demonstrated that TBN effectively induced HIFs synthesis and nuclear expression to regulate EPO.

Tetramethylpyrazine nitrone regulated HIF-1α synthesis in a translation-dependent fashion

Superfluous iron produces hydroxyl radicals through the Fenton reaction that can cause oxidative stress (Kruszewski,

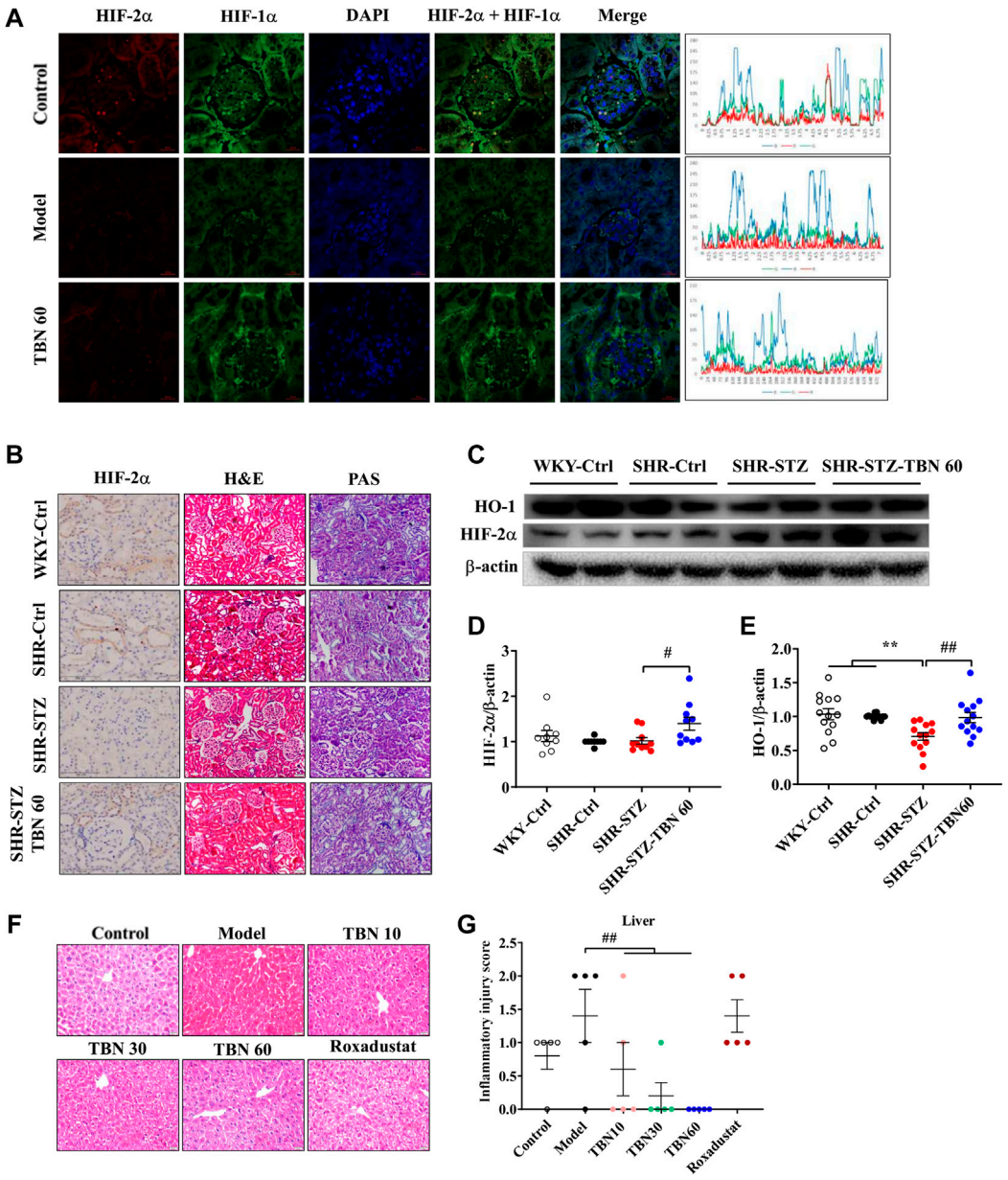

FIGURE 3
TBN increases the expression of HIF-1α and HIF-2α in CDDP-induced anemia C57BL/6J mice and SHR rats. **(A)** Representative images of the expression of HIF-1α and HIF-2α by immunofluorescence co-staining experiment, (original magnification: ×630). Scale bar, 20 μm. The Y-axis is the average value of fluorescence intensity obtained by immunofluorescence analysis through Image J software. The peaks as shown along with the immunofluorescence images represent the highest expression of the whole images. The X-axis is the length of the images. The formula of fluorescence intensity in a specific area is as follows: Mean fluorescence intensity (Mean) = Total fluorescence intensity (IntDen)/Area of the region (Area). Mean: Mean gray value, IntDen: Integrated Density. **(B)** Representative images of H&E staining and PAS staining (original magnification: ×200) of kidney tissue. Scale bar, 50 μm. Representative Immunohistochemistry staining of HIF-2α (original magnification: ×400). Scale bar: 100 μm. **(C–E)** Representative western blot of HIF-2α and HO-1 (n = 8 for each group in Figure **(D)**; n = 13 for each group in Figure **(E)**. **(F,G)** Representative images of HE staining (×200) of liver tissue and inflammatory injury score in CDDP-induced C57BL/6J mice (n = 5 for each group in Figure **(G)**. $^{**}p < 0.01$ vs. SHR-control; $^{\#}p < 0.05$; $^{\#\#}p < 0.01$ vs. SHR-STZ. $^{\#\#}p < 0.01$ vs. vehicle-treated CDDP group. HIF, hypoxia-inducible factor; CDDP, cisplatin.

2003). In earlier research, SFO administration is found to reduce EPO mRNA expression; HIF-1α and HIF-2α mRNA and protein levels are also reduced by SFO treatment in HepG2 cells (Oshima et al., 2017). The research suggests that SFO inhibited the expression and translation of HIFs and its target gene EPO. To explore whether TBN increased the number of HIFs at the translation step, we thus used SFO (200 μg/ml) with and without TBN in Hep3B and HepG2 cells to examine the change in HIF-1α

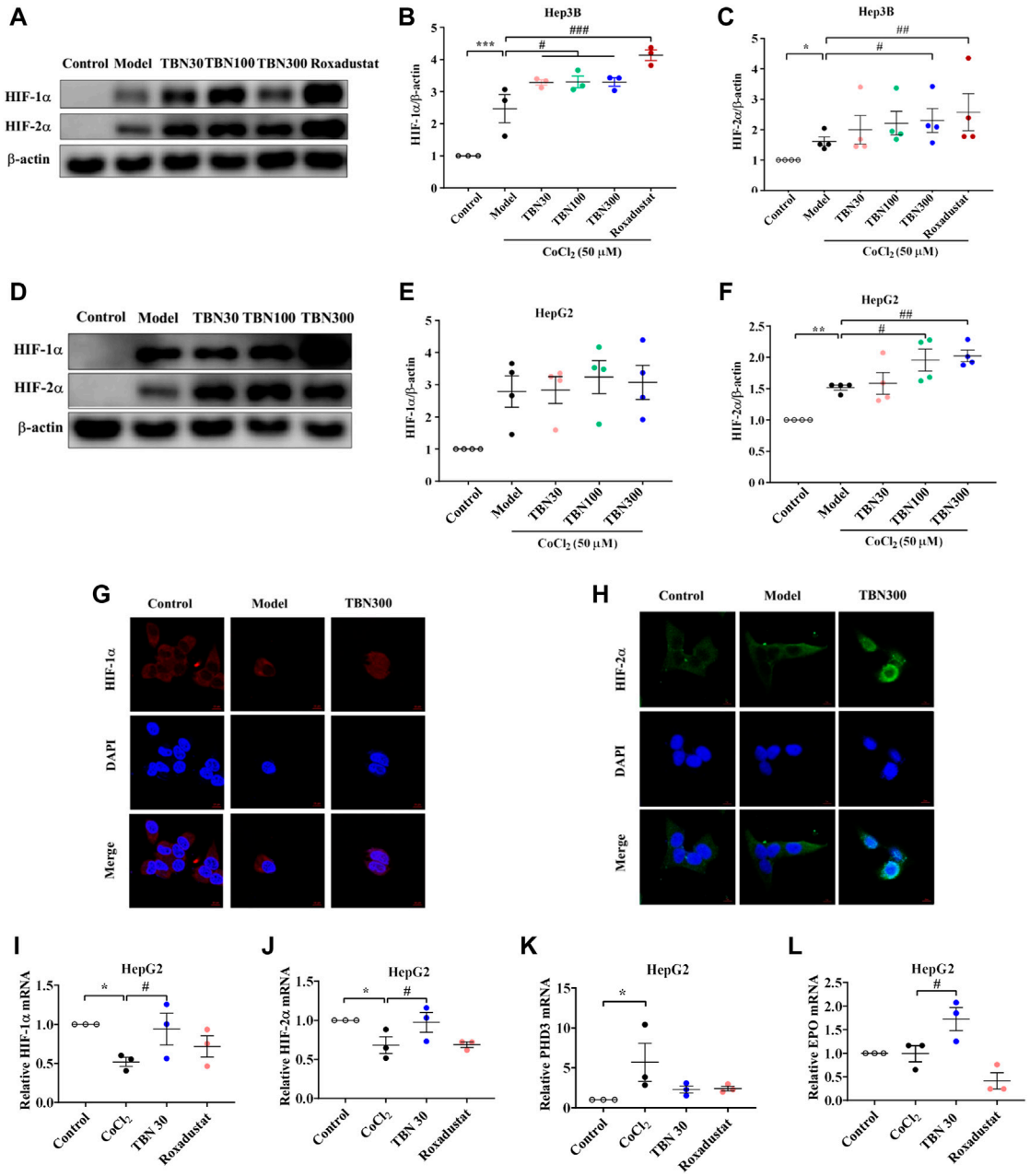

FIGURE 4
TBN increases the expression of HIF-1α and HIF-2α in $CoCl_2$-induced Hep3B and HepG2 cells. **(A–C)** Effects of TBN on expression of HIF-1α and HIF-2α in $CoCl_2$-induced Hep3B cells. **(D–F)** Representative western blots of HIF-1α and HIF-2α in HepG2 cells. **(G,H)** HIF-1α and HIF-2α nuclear expression in Hep3B cells, (original magnification: ×630). Scale bar, 10 μm. **(I–L)** HIF-1α, HIF-2α, PHD3 and EPO mRNA expression in HepG2 cells. [n = 3–4 for each group in Figure **(A–L)**]. *$p < 0.05$; **$p < 0.01$; ***$p < 0.001$; vs. Control; $^{\#}p < 0.05$; $^{\#\#}p < 0.01$; $^{\#\#\#}p < 0.001$ vs. $CoCl_2$-induced Model. HIF, hypoxia-inducible factor; $CoCl_2$, cobalt chloride. Model: $CoCl_2$-induced group.

and HIF-2α levels. As our results shown (Figures 5A–F), TBN reversed the down-regulation of HIFs seen with SFO, which confirms our hypothesis.

TBN regulated HIF-1α at both the mRNA and protein levels. To explore the effect of TBN treatment in the stage of HIFs' protein synthesis, CHx, a protein translational inhibitor, is used in HepG2 cells to investigate HIF-1α levels over time. In this study, as shown in Figures 5G,H, the half-life of HIF-1α was extended to 2 h with TBN treatment, while that without TBN was 0.5 h. These results indicated that TBN further stabilized HIF-1α in hypoxic conditions.

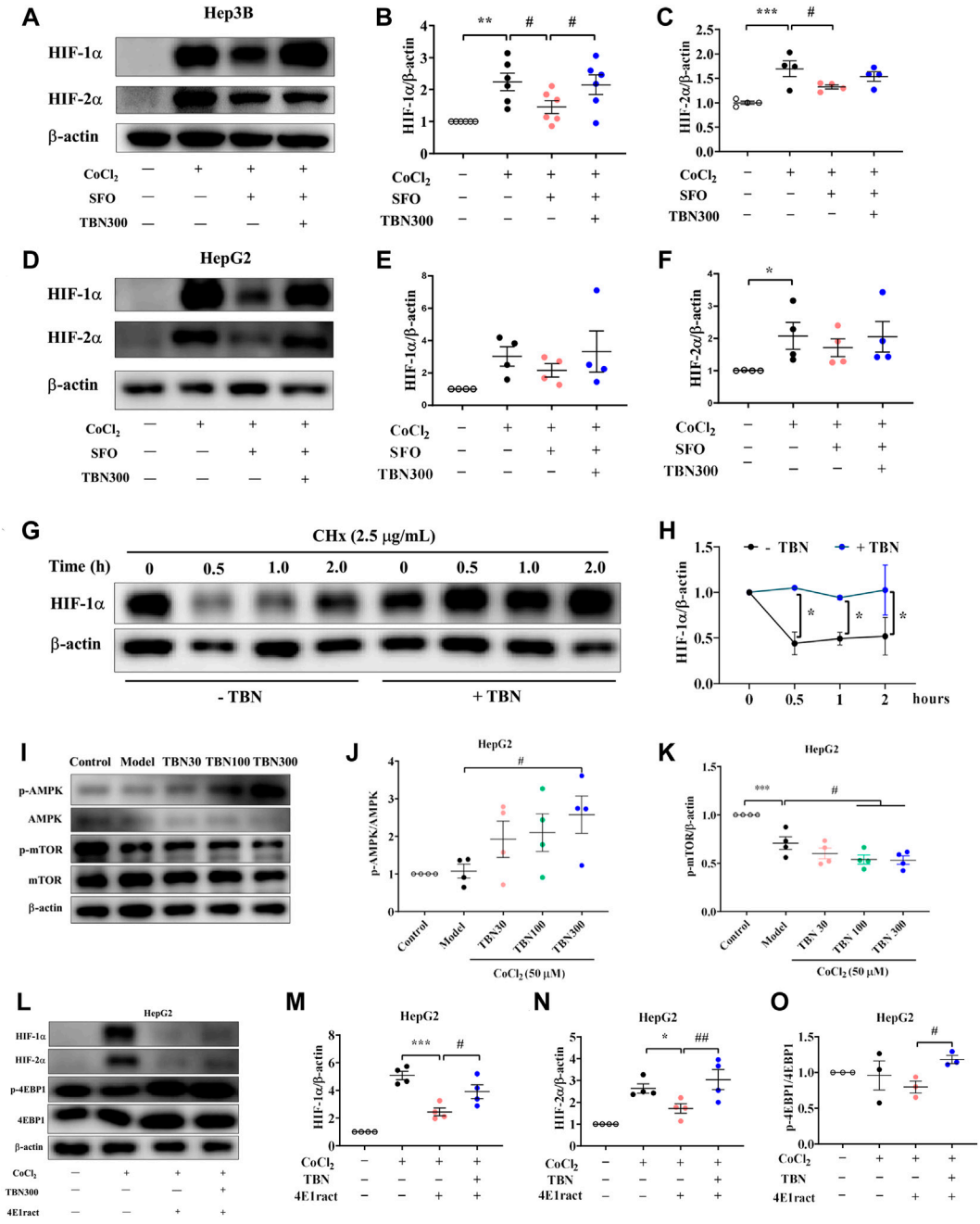

FIGURE 5
(A–F) TBN reverses the suppressive action of SFO on $CoCl_2$-induced increments of HIF-1α and HIF-2α protein expression in Hep3B and HepG2 cells. **(G,H)** TBN effects on HIF-1α and HIF-2α protein levels in Hep3B cells by western blot analysis. **(I–K)** Effects of TBN on expression of AMPK/mTOR in $CoCl_2$-induced HepG2 cells. **(L–O)** HIF-1α, HIF-2α and p-4EBP1 expression with or without 4E1rcat in HepG2 cells. [n = 3–6 for each group in Figure **(A–O)**]. *p < 0.05; **p < 0.01; ***p < 0.001 vs. Control; $^{\#}p$ < 0.05 vs. $CoCl_2$-induced Model, $CoCl_2$-SFO-induced group. *p < 0.05; ***p < 0.001; vs. 4E1rcat-induced group; $^{\#}p$ < 0.05; $^{\#\#}p$ < 0.01 vs. TBN group. SFO: saccharate ferric oxide; $CoCl_2$: cobalt chloride; HIF: hypoxia-inducible factor.

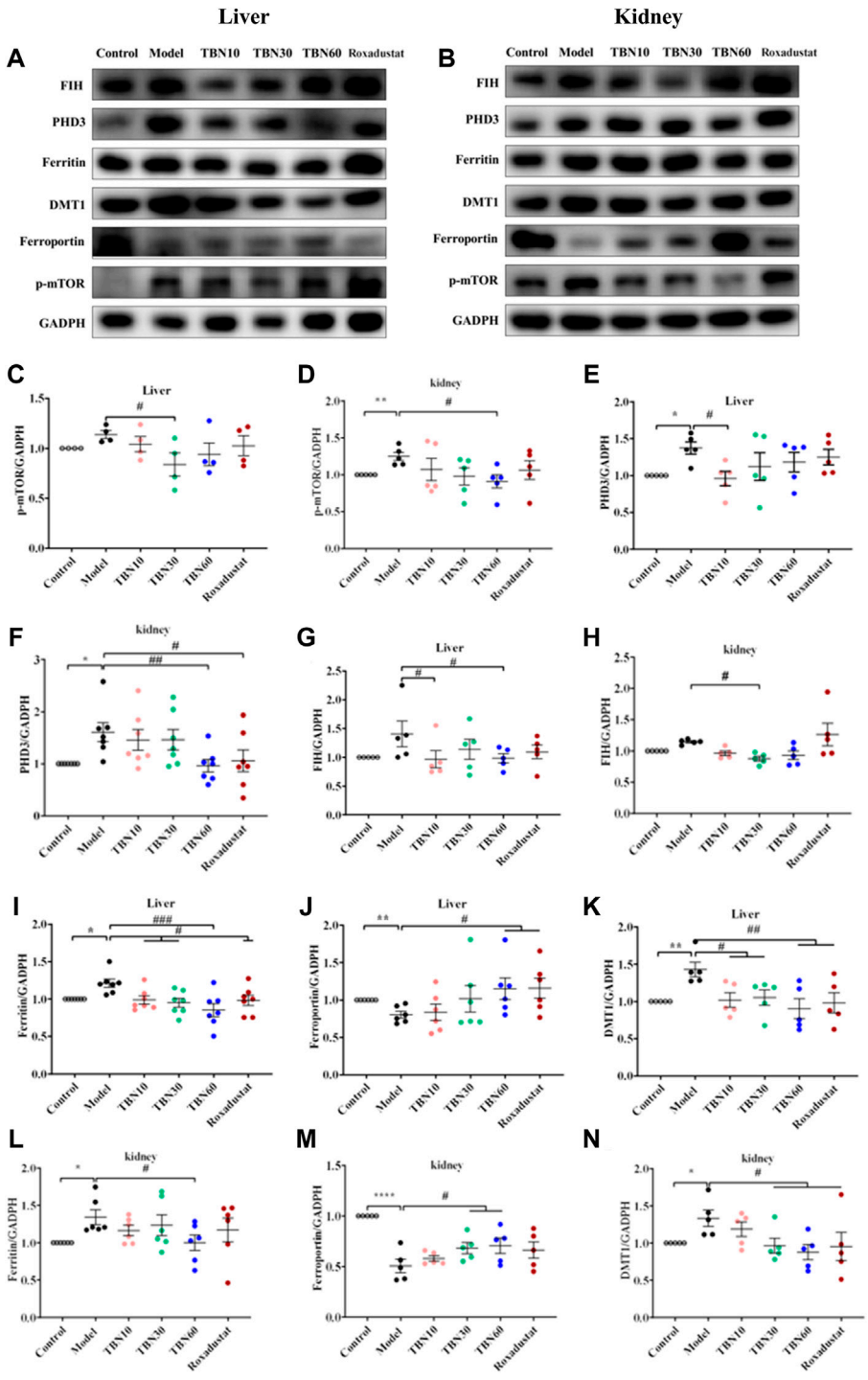

FIGURE 6
TBN effect in iron metabolism in CDDP-induced C57BL/6J mice. **(A–D)** Representative western blots of p-mTOR in liver and kidney tissue. **(A,B,E–H)** Representative western blots of PHD3, FIH of liver and kidney tissue. **(A,B,I–N)** Representative western blots of ferritin, FPN and DMT1 both in liver and kidney tissue. [n = 4–7 for each group in Figure **(A–N)**]. *p < 0.05; **p < 0.01; ****p < 0.0001 vs. Control; $^{\#}p$ < 0.05; $^{\#\#}p$ <0.01; $^{\#\#\#}p$ < 0.001 vs. vehicle-treated CDDP group. CDDP, cisplatin; FPN, ferroportin; DMT1, Divalent metal transporter-1; FIH, factor-inhibiting HIF. Model: vehicle-treated CDDP group.

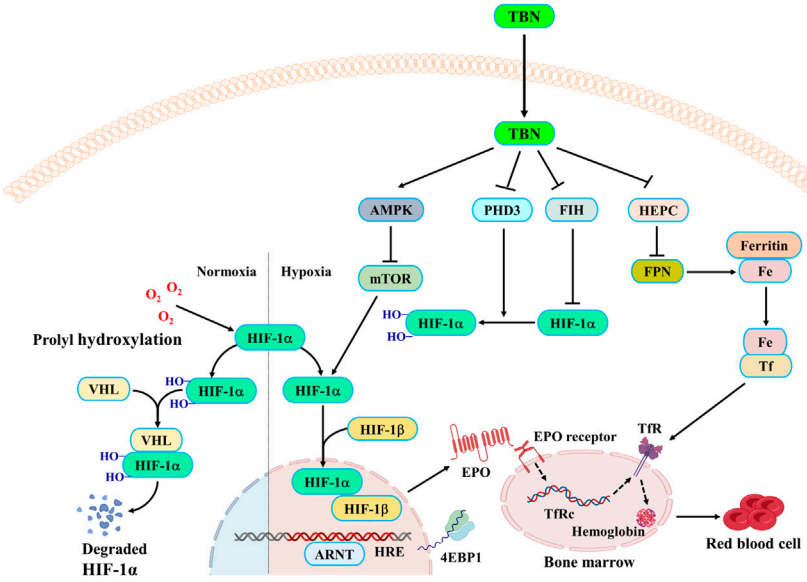

FIGURE 7
TBN mechanism of action in anemia.

Tetramethylpyrazine nitrone regulated hypoxia-inducible factor *via* AMPK/mTOR to influence translation and maintain iron homeostasis

It has been well demonstrated that the mammalian target of rapamycin (mTOR) pathway modulates HIF-1α expression *via* different external stimuli (Sudhagar et al., 2011). TBN can scavenge free radicals and increase AMPK expression and decrease mTOR expression (Supplementary Figure S2; Figures 5I–K). This had also been verified in HK-2 cells, shown in Supplementary Figure S3 and Supplementary Figure S4. In HepG2 cells, we used 4E1rcat (10 μM), which was the direct inhibitor of 4EBP1, to examine whether TBN can still cause changes in HIF-1α and HIF-2α levels. As the results shown (Figures 5L–O), 4E1rcat decreased HIFs and TBN reversed the down-regulation of HIFs, which demonstrated that the effects of TBN on HIFs is *via* the mTOR/4E-BP1 pathway. Hence, based on these results, we examined whether or not the phosphorylation of mTOR impacted the effects of TBN in CDDP-induced C57BL/6J mice. Compared to the normal mice, the expression of the phosphorylation status of mTOR (Ser2448) significantly increased (approximately 10%–20%) in CDDP-CKD mice in both liver and kidney, while TBN dose-dependently reversed the increase in p-mTOR in the kidney (Figures 6A–D).

TBN reduced the expressions of PHD3 and FIH (Figures 6A,B,E–H), which regulates two different degradation pathways separately. One degradation pathway is through prolyl hydroxylase, which hydroxylates of HIF-α leading to the recognition of HIF-α by Von Hippel–Lindau protein (pVHL) and subsequent degradation *via* the ubiquitin-proteasome system. Another degradation pathway is through inhibition of FIH, which prevents HIF-α from associating with the coactivator p300/CBP, resulting in a reduction of HIF-mediated transcription. The precise mechanism of action of how TBN regulates the expression levels of PHD3 and FIH is not understood. We speculated that TBN does not activate HIF by directly acting on PHD and FIH since previous studies had demonstrated that TBN acts by scavenging ROS (Wu et al., 2019; Jing et al., 2021). We demonstrated that TBN scavenged ROS in $CoCl_2$-induced Hep3B and $CoCl_2$-induced HepG2 cells (Supplementary Figure S2).

TBN inhibited hepcidin in CDDP-induced C57BL/6J mice and improved serum iron and Tf levels in STZ-induced SHR rats, which suggested that TBN may have effects on iron stores and metabolism. It was reported that stabilization of HIFs leads to regulation of EPO biosynthesis and iron homeostasis. Thus, we determined whether TBN treatment impacted iron absorption and transportation from kidney and liver to plasma *via* western blot; specifically, we examined the levels of ferritin, FPN, and DMT1 in the liver and kidney in CDDP-induced C57BL/6J mice. The results in Figures 6A,B,I–N showed that treatment with TBN significantly increased FPN levels in both organs, while DMT1 and ferritin protein levels decreased with TBN treatment when compared to the vehicle-treated CDDP group. These results demonstrated that TBN can impact iron homeostasis and regulate HIFs to improve anemia.

Discussion

Approximate 40% of the people with diabetes ultimately develop DKD, of which may further progress into ESRD (Reddy et al., 2013). The clinical manifestations of DKD include progressive decline in the glomerular filtration rate, microalbuminuria, glomerular hypertrophy and thickening of the glomerular basement membrane, glomerular sclerosis and interstitial fibrosis. Eventually, these effects result in renal failure, requiring either dialysis or renal replacement therapy. To date, there are only a few promising options available for the treatment of DKD in clinical practice.

Many studies have found that hypertension is an important risk factor in the progression of chronic renal failure, as hypertension exacerbates diabetic kidney damage in diabetic patients (James et al., 2015). Thus, in this study, the DKD rat model induced by STZ in SHR rats was chosen. The coexistence of diabetes and hypertension exuberates renal function, increases albuminuria, and promotes the progression of DKD. The symptoms and pathological characteristics of DKD in SHR rats resemble that of DKD in patients (Elmarakby et al., 2012). Our results shown that TBN decreased the level of urea nitrogen and ameliorated kidney injury (Figure 1E), suggesting that TBN was a potential DKD treatment.

Anemia often appears earlier in DKD than in other types of CKD. EPO is important for RBC production. Thus, patients with diabetes are vulnerable to EPO deficiency and are twice as likely to have anemia as compared with those non-diabetic CKD patients (Thomas et al., 2006). Compared to non-diabetic patients, anemia in those with renal insufficiency occurs earlier and more seriously (Wang et al., 1995; Haase, 2010; Suzuki and Yamamoto, 2016). More recently, it has been shown that disordered iron homeostasis is another vital factor resulting in renal anemia (Panwar and Gutiérrez, 2016). As shown in our results, TBN was effective at promoting EPO synthesis in STZ-induced DKD in SHR rats. TBN also improved iron levels and enhances the function of iron by increasing Tf expression and suppressing hepcidin expression. These results demonstrated that TBN significantly improved renal anemia (Figures 1F–I). On the other hand, HIF-2α is sensitive to oxygen levels and cellular iron (Mastrogiannaki et al., 2009; Shah et al., 2009). HIF-2α plays an essential role in the absorption of iron during systemic iron deficiency (Anderson et al., 2011; Taylor et al., 2011; Ramakrishnan et al., 2015). Immunohistochemistry (IHC) and western blot results demonstrated that TBN increases expression of HIF-2α and HO-1. The effects of TBN to ameliorate renal anemia in DKD rats were due to their ability to scavenge free radicals, reduce oxidative stress, and activate the AMPK/mTOR/HIF pathway (Figure 3C–E, 5I–K; Supplementary Figures S2, S3).

Previous studies have shown that 15 mg/kg of CDDP caused CKD characterized by a sustained reduction in eGFR and reduced kidney mass. Two weeks after the second dose of CDDP, both of these features of CKD are typically present, indicating that the disease model has been established (Landau et al., 2019). In this CDDP-induced model, TBN effectively relieved the symptoms of anemia and increased the levels of the RBC count, HCT, Hb and EPO (Figures 2C–E,H). TBN also increased stabilization of HIF-1α and HIF-2α and the transcriptional activation of the EPO gene in hypoxic conditions (Figures 4A–F,I–L). The down-regulation of the expression of hepcidin in the serum treated with TBN was not dose-dependent. We thought that this result may be an artefact due to coincidental individual differences in the mice. These findings shown that the increased synthesis and stable expression of HIFs can effectively improve the expression of EPO and the decline of blood cell function caused by anemia. Furthermore, TBN treatment rapidly increased HIF-1α and HIF-2α synthesis both in C57BL/6J mice and hepatoma cells. TBN also affected the stability of HIF-1α and the transcription of its mRNA. TBN significantly blocked the degradation pathway of HIFs by inhibiting the expression of the PHD3 and FIH proteins (Figures 6A,B,E–H).

In renal anemia, iron is secluded in macrophages, intestinal iron absorption is diminished, and erythropoiesis is impaired by the low amounts of iron (Weiss and Goodnough, 2005; Goodnough et al., 2010; Ganz, 2011). Iron cannot be directly absorbed by the body; rather, a unique transportation pathway is required for iron to be absorbed into the blood, and it needs to be delivered to the bloodstream in a soluble form for use by cells and tissues. Thus, the regulation of the iron metabolism is important for the maintenance of a healthy physiological state of the human body. Our results found that TBN enhanced the FPN levels in the livers of mice with renal anemia. Through binding to FPN, hepcidin induces its internalization, therefore limiting iron export (Bârsan et al., 2015). Ferritin is an acute phase product and, as such, is frequently elevated in patients with CKD. TBN can reverse this increase in CKD (Figures 6A,B,I,J,L,M). High levels of dietary iron produce an increase in DMT1 expression in hepatocytes, promoting iron acquisition, whereas low levels decrease hepatic DMT1 expression, causing a reduction in iron accumulation (Oates et al., 2000; Trinder et al., 2000). Higher ROS levels are present in DMT1-mutant erythrocytes (Zidova et al., 2014). The loss of DMT1 is suggested to protect against oxidative damage to the pancreas and help to maintain insulin sensitivity despite iron overload (Jia et al., 2013). The anti-oxidative stress properties of TBN caused DMT1 inhibition, as DMT1 caused oxidative damage and ROS accumulation (Figures 6K,N).

Recently, researchers find that mTORC1 regulates HIF-1α protein accumulation *via* promoting the transcription of HIF-1α mRNA, which is blocked by either knockdown or inhibition of the STAT3 (Luo et al., 2021). Furthermore, studies find that STAT3 is directly phosphorylated by mTORC1 on Ser727 under hypoxic conditions, thus promoting HIF-1α mRNA transcription. mTORC1 regulates HIF-1α synthesis on a translational level through co-operative regulation of both ribosomal protein S6K1 and initiation factor 4E-BP1, while HIF-1α degradation is not affected (Jia et al., 2013). Under hypoxic conditions, TBN promoted the stable expression of

HIF-1α and HIF-2α in the nucleus by promoting the expression of HIF-1α and HIF-2α (Figures 4G,H). The combination of HIF-1α and HIF-1α forms aggregate and further promotes the transcription and synthesis of EPO. TBN improved the synthesis rate of HIF-1α (Figures 5G,H). On the other hand, TBN can positively regulate the AMPK/mTOR/4EBP1 pathway. However, there is no corresponding experimental data to support whether there is a direct correlation between the effects of TBN on HIFs and mTOR. The molecular mechanism by which TBN regulates HIFs may be multi-faceted (Figure 7). It increases the expression of protein, the synthesis rate and reduces the degradation of HIFs. TBN was most likely responsible for promoting HIF transcription and translation by activating the AMPK pathway. Therefore, exploring the molecular mechanisms of TBN on HIFs in more detail is needed (Sudhagar et al., 2011).

Data availability statement

The original contributions presented in the study are included in the article/Supplementary Materials, further inquiries can be directed to the corresponding authors.

Ethics statement

The animal study was reviewed and approved by all animal care and experimental protocols by the Institutional Animal Care and Use Committee of the Guangzhou University of Chinese Medicine (Guangzhou, China).

Author contributions

YC, PW, YS, PY, and GZ designed the study. YC and FG carried out the experiments. YC and PW did all of the experiments except for some cell experiments, data analysis and assisted in automated image analysis of electron micrographs. YC, YW, and ZZ wrote the manuscript. MJ provided critical review of the manuscript.

Funding

This work was partially supported by grants from the National Natural Science Foundation of China (NSFC 82003821, 81872842, 82073821) and Guangdong Research and Development Project (2020A1515011060, 2021A0505080012, 2022A1515012655).

Acknowledgments

Many thanks to Linda Wang for editing this manuscript.

Conflict of interest

YW, YS, ZZ, PY, and GZ are shareholders of Guangzhou Magpie Pharmaceuticals, Inc.

The remaining authors declare that the research was conducted in the absence of any commercial or financial relationships that could be construed as a potential conflict of interest.

Publisher's note

All claims expressed in this article are solely those of the authors and do not necessarily represent those of their affiliated organizations, or those of the publisher, the editors and the reviewers. Any product that may be evaluated in this article, or claim that may be made by its manufacturer, is not guaranteed or endorsed by the publisher.

Supplementary material

The Supplementary Material for this article can be found online at: https://www.frontiersin.org/articles/10.3389/fphar.2022.964234/full#supplementary-material

References

Anderson, E. R., Xue, X., and Shah, Y. M. (2011). Intestinal hypoxia-inducible factor-2alpha (HIF-2alpha) is critical for efficient erythropoiesis. *J. Biol. Chem.* 286, 19533–19540. doi:10.1074/jbc.M111.238667

Astor, B. C., Muntner, P., and Levin, A. (2002). Association of Kidney Function With Anemia: The Third National Health and Nutrition Examination Survey (1988–1994). *Archives of Internal Medicine* 162, 1401–1408.

Bârsan, L., Stanciu, A., Stancu, S., Căpuşă, C., Brătescu, L., Mandache, E., et al. (2015). Bone marrow iron distribution, hepcidin, and ferroportin expression in renal anemia. *Hematology* 20, 543–552. doi:10.1179/1607845415Y.0000000004

Batchelor, E. K., Kapitsinou, P., Pergola, P. E., Kovesdy, C. P., and Jalal, D. I. (2020). Iron deficiency in chronic kidney disease: Updates on pathophysiology, diagnosis, and treatment. *J. Am. Soc. Nephrol.* 31, 456–468. doi:10.1681/ASN.2019020213

Besarab, A., Provenzano, R., Hertel, J., Zabaneh, R., Klaus, S. J., Lee, T., et al. (2015). Randomized placebo-controlled dose-ranging and pharmacodynamics study of roxadustat (FG-4592) to treat anemia in nondialysis-dependent chronic kidney disease (NDD-CKD) patients. *Nephrol. Dial. Transpl.* 30, 1665–1673. doi:10.1093/ndt/gfv302

Billesbølle, C. B., Azumaya, C. M., and Kretsch, R. C (2020). Structure of hepcidin-bound ferroportin reveals iron homeostatic mechanisms. *Nature* 586, 807–811.

Crathorne, L., Huxley, N., Haasova, M., Snowsill, T., Jones-Hughes, T., Hoyle, M., et al. (2016). The effectiveness and cost-effectiveness of erythropoiesis-stimulating agents (epoetin and darbepoetin) for treating cancer treatment-induced anaemia (including review of technology appraisal no. 142): A systematic review and economic model. *Health Technol. Assess.* 20, 1–588. v-vi. doi:10.3310/hta20130

Elmarakby, A. A., Faulkner, J., Baban, B., and Sullivan, J. C. (2012). Induction of hemeoxygenase-1 reduces renal oxidative stress and inflammation in diabetic spontaneously hypertensive rats. *Int. J. Hypertens.* 2012, 957235. doi:10.1155/2012/957235

Gafter-Gvili, A., Schechter, A., and Rozen-Zvi, B. (2019). Iron deficiency anemia in chronic kidney disease. *Acta Haematol.* 142, 44–50. doi:10.1159/000496492

Ganz, T. (2011). Hepcidin and iron regulation, 10 years later. *Blood* 117, 4425–4433. doi:10.1182/blood-2011-01-258467

Goodnough, L. T., Nemeth, E., and Ganz, T. (2010). Detection, evaluation, and management of iron-restricted erythropoiesis. *Blood* 116, 4754–4761. doi:10.1182/blood-2010-05-286260

Haase, V. H. (2010). Hypoxic regulation of erythropoiesis and iron metabolism. *Am. J. Physiol. Ren. Physiol.* 299, F1–F13. doi:10.1152/ajprenal.00174.2010

James, M. T., Grams, M. E., Woodward, M., Elley, C. R., Green, J. A., Wheeler, D. C., et al. (2015). A meta-analysis of the association of estimated GFR, albuminuria, diabetes mellitus, and hypertension with acute kidney injury. *Am. J. Kidney Dis.* 66, 602–612. doi:10.1053/j.ajkd.2015.02.338

Jia, X., Kim, J., Veuthey, T., Lee, C. H., and Wessling-Resnick, M. (2013). Glucose metabolism in the Belgrade rat, a model of iron-loading anemia. *Am. J. Physiol. Gastrointest. Liver Physiol.* 304, G1095–G1102. doi:10.1152/ajpgi.00453.2012

Jing, M., Cen, Y., Gao, F., Wang, T., Jiang, J., Jian, Q., et al. (2021). Nephroprotective effects of tetramethylpyrazine nitrone TBN in diabetic kidney disease. *Front. Pharmacol.* 12, 680336. doi:10.3389/fphar.2021.680336

Kassebaum, N. J., Jasrasaria, R., Naghavi, M., Wulf, S. K., Johns, N., Lozano, R., et al. (2014). A systematic analysis of global anemia burden from 1990 to 2010. *Blood* 123, 615–624. doi:10.1182/blood-2013-06-508325

Kruszewski, M. (2003). Labile iron pool: The main determinant of cellular response to oxidative stress. *Mutat. Res.* 531, 81–92. doi:10.1016/j.mrfmmm.2003.08.004

Landau, S. I., Guo, X., Velazquez, H., Torres, R., Olson, E., Garcia-Milian, R., et al. (2019). Regulated necrosis and failed repair in cisplatin-induced chronic kidney disease. *Kidney Int.* 95, 797–814. doi:10.1016/j.kint.2018.11.042

Loutradis, C., Skodra, A., and Georgianos, P. (2016). Diabetes mellitus increases the prevalence of anemia in patients with chronic kidney disease: A nested case-control study. *World J. Nephrol.* 5, 358–366.

Luo, Y., Guo, J., Zhang, P., Cheuk, Y. C., Jiang, Y., Wang, J., et al. (2021). Mesenchymal stem cell protects injured renal tubular epithelial cells by regulating mTOR-mediated Th17/treg Axis. *Front. Immunol.* 12, 684197. doi:10.3389/fimmu.2021.684197

Mastrogiannaki, M., Matak, P., Keith, B., Simon, M. C., Vaulont, S., and Peyssonnaux, C. (2009). HIF-2alpha, but not HIF-1alpha, promotes iron absorption in mice. *J. Clin. Invest.* 119, 1159–1166. doi:10.1172/JCI38499

Mikhail, A., Brown, C., Williams, J. A., Mathrani, V., Shrivastava, R., Evans, J., et al. (2017). Renal association clinical practice guideline on anaemia of chronic kidney disease. *BMC Nephrol.* 18, 345. doi:10.1186/s12882-017-0688-1

Oates, P. S., Jeffrey, G. P., Basclain, K. A., Thomas, C., and Morgan, E. H. (2000). Iron excretion in iron-overloaded rats following the change from an iron-loaded to an iron-deficient diet. *J. Gastroenterol. Hepatol.* 15, 665–674. doi:10.1046/j.1440-1746.2000.02210.x

Olmos, G., MuñOZ-FéLIX, J. M., Mora, I., MüLLER, A. G., Ruiz-Torres, M. P., LóPEZ-Novoa, J. M., et al. (2018). Impaired erythropoietin synthesis in chronic kidney disease is caused by alterations in extracellular matrix composition. *J. Cell. Mol. Med.* 22, 302–314. doi:10.1111/jcmm.13319

Oshima, K., Ikeda, Y., Horinouchi, Y., Watanabe, H., Hamano, H., Kihira, Y., et al. (2017). Iron suppresses erythropoietin expression via oxidative stress-dependent hypoxia-inducible factor-2 alpha inactivation. *Lab. Invest.* 97, 555–566. doi:10.1038/labinvest.2017.11

Panwar, B., and Gutiérrez, O. M. (2016). Disorders of iron metabolism and anemia in chronic kidney disease. *Semin. Nephrol.* 36, 252–261. doi:10.1016/j.semnephrol.2016.05.002

Ramakrishnan, S. K., Anderson, E. R., Martin, A., Centofanti, B., and Shah, Y. M. (2015). Maternal intestinal HIF-2α is necessary for sensing iron demands of lactation in mice. *Proc. Natl. Acad. Sci. U. S. A.* 112, E3738–E3747. doi:10.1073/pnas.1504891112

Reddy, M. A., Tak Park, J., and Natarajan, R. (2013). Epigenetic modifications in the pathogenesis of diabetic nephropathy. *Semin. Nephrol.* 33, 341–353. doi:10.1016/j.semnephrol.2013.05.006

Retnakaran, R., Cull, C. A., and Thorne, K. I. (2006). Risk Factors for Renal Dysfunction in Type 2 Diabetes. *Diabetes* 55, 1832

Semenza, G. L., and Wang, G. L. (1992). A nuclear factor induced by hypoxia via de novo protein synthesis binds to the human erythropoietin gene enhancer at a site required for transcriptional activation. *Mol. Cell. Biol.* 12, 5447–5454. doi:10.1128/mcb.12.12.5447

Shah, Y. M., Matsubara, T., Ito, S., Yim, S. H., and Gonzalez, F. J. (2009). Intestinal hypoxia-inducible transcription factors are essential for iron absorption following iron deficiency. *Cell Metab.* 9, 152–164. doi:10.1016/j.cmet.2008.12.012

Simonsen, L. O., Harbak, H., and Bennekou, P. (2012). Cobalt metabolism and toxicology--a brief update. *Sci. Total Environ.* 432, 210–215. doi:10.1016/j.scitotenv.2012.06.009

Stanton, R. C. (2016). Diabetic Kidney Disease and Hypertension. *Exp Clin Endocrinol Diabetes* 124, 93–98.

St Peter, W. L., Guo, H., Kabadi, S., Gilbertson, D. T., Peng, Y., Pendergraft, T., et al. (2018). Prevalence, treatment patterns, and healthcare resource utilization in Medicare and commercially insured non-dialysis-dependent chronic kidney disease patients with and without anemia in the United States. *BMC Nephrol.* 19, 67. doi:10.1186/s12882-018-0861-1

Stauffer, M. E., and Fan, T. (2014). Prevalence of anemia in chronic kidney disease in the United States. *PLoS One* 9, e84943. doi:10.1371/journal.pone.0084943

Sun, Y., Jiang, J., Zhang, Z., Yu, P., Wang, L., Xu, C., et al. (2008). Antioxidative and thrombolytic TMP nitrone for treatment of ischemic stroke. *Bioorg. Med. Chem.* 16, 8868–8874. doi:10.1016/j.bmc.2008.08.075

Sun, Y., Yu, P., Zhang, G., Wang, L., Zhong, H., Zhai, Z., et al. (2012). Therapeutic effects of tetramethylpyrazine nitrone in rat ischemic stroke models. *J. Neurosci. Res.* 90, 1662–1669. doi:10.1002/jnr.23034

Suzuki, N., and Yamamoto, M. (2016). Roles of renal erythropoietin-producing (REP) cells in the maintenance of systemic oxygen homeostasis. *Pflugers Arch.* 468, 3–12. doi:10.1007/s00424-015-1740-2

Sudhagar, S., Sathya, S., and Lakshmi, B. S. (2011). Rapid non-genomic signalling by 17β-oestradiol through c-Src involves mTOR-dependent expression of HIF-1α in breast cancer cells. *Br. J. Cancer* 105, 953–960. doi:10.1038/bjc.2011.349

Taylor, M., Qu, A., Anderson, E. R., Matsubara, T., Martin, A., Gonzalez, F. J., et al. (2011). Hypoxia-inducible factor-2α mediates the adaptive increase of intestinal ferroportin during iron deficiency in mice. *Gastroenterology* 140, 2044–2055. doi:10.1053/j.gastro.2011.03.007

Thomas, M. C. (2007). Anemia in diabetes: Marker or mediator of microvascular disease? *Nat. Clin. Pract. Nephrol.* 3, 20–30. doi:10.1038/ncpneph0378

Thomas, M. C., Cooper, M. E., Rossing, K., and Parving, H. H. (2006). Anaemia in diabetes: Is there a rationale to TREAT? *Diabetologia* 49, 1151–1157. doi:10.1007/s00125-006-0215-6

Tian, Y., Liu, Y., Chen, X., Zhang, H., Shi, Q., Zhang, J., et al. (2010). Tetramethylpyrazine promotes proliferation and differentiation of neural stem cells from rat brain in hypoxic condition via mitogen-activated protein kinases pathway *in vitro*. *Neurosci. Lett.* 474, 26–31. doi:10.1016/j.neulet.2010.02.066

Trinder, D., Oates, P. S., Thomas, C., Sadleir, J., and Morgan, E. H. (2000). Localisation of divalent metal transporter 1 (DMT1) to the microvillus membrane of rat duodenal enterocytes in iron deficiency, but to hepatocytes in iron overload. *Gut* 46, 270–276. doi:10.1136/gut.46.2.270

Wang, G. L., Jiang, B. H., Rue, E. A., and Semenza, G. L. (1995). Hypoxia-inducible factor 1 is a basic-helix-loop-helix-PAS heterodimer regulated by cellular O2 tension. *Proc. Natl. Acad. Sci. U. S. A.* 92, 5510–5514. doi:10.1073/pnas.92.12.5510

Weiss, G., and Goodnough, L. T. (2005). Anemia of chronic disease. *N. Engl. J. Med.* 352, 1011–1023. doi:10.1056/NEJMra041809

Wish, J. B. (2006). Assessing iron status: Beyond serum ferritin and transferrin saturation. *Clin. J. Am. Soc. Nephrol.* 1, S4–S8. doi:10.2215/CJN.01490506

Wu, Y., Jiang, Z., Li, Z., Gu, J., You, Q., and Zhang, X. (2018). Click chemistry-based discovery of [3-Hydroxy-5-(1 H-1, 2, 3-triazol-4-yl)picolinoyl]glycines as orally active hypoxia-inducing factor prolyl hydroxylase inhibitors with favorable safety profiles for the treatment of anemia. *J. Med. Chem.* 61, 5332–5349. doi:10.1021/acs.jmedchem.8b00549

Wu, L., Su, Z., Zha, L., Zhu, Z., Liu, W., Sun, Y., et al. (2019). Tetramethylpyrazine nitrone reduces oxidative stress to alleviate cerebral vasospasm in experimental subarachnoid hemorrhage models. *Neuromolecular Med.* 21, 262–274. doi:10.1007/s12017-019-08543-9

Yilmaz, M. I., Solak, Y., Covic, A., Goldsmith, D., and Kanbay, M. (2011). Renal anemia of inflammation: The name is self-explanatory. *Blood Purif.* 32, 220–225. doi:10.1159/000328037

Zhang, G., Zhang, T., Wu, L., Zhou, X., Gu, J., Li, C., et al. (2018). Neuroprotective effect and mechanism of action of tetramethylpyrazine nitrone for ischemic stroke therapy. *Neuromolecular Med.* 20, 97–111. doi:10.1007/s12017-018-8478-x

Zidova, Z., Kapralova, K., Koralkova, P., Mojzikova, R., Dolezal, D., Divoky, V., et al. (2014). DMT1-mutant erythrocytes have shortened life span, accelerated glycolysis and increased oxidative stress. *Cell. Physiol. biochem.* 34, 2221–2231. doi:10.1159/000369665

frontiers | Frontiers in Pharmacology

TYPE Review
PUBLISHED 03 November 2022
DOI 10.3389/fphar.2022.1055296

OPEN ACCESS

EDITED BY
Divya Bhatia,
Cornell University, United States

REVIEWED BY
Krishna Murthy Nakuluri,
The University of Iowa, United States
Ping Fu,
Sichuan University, China

*CORRESPONDENCE
Dan-Qian Chen,
chendanqian2013@163.com
Ping Li,
lp8675@163.com

SPECIALTY SECTION
This article was submitted to Renal Pharmacology,
a section of the journal
Frontiers in Pharmacology

RECEIVED 27 September 2022
ACCEPTED 24 October 2022
PUBLISHED 03 November 2022

CITATION
Chen D-Q, Wu J and Li P (2022), Therapeutic mechanism and clinical application of Chinese herbal medicine against diabetic kidney disease. *Front. Pharmacol.* 13:1055296. doi: 10.3389/fphar.2022.1055296

Therapeutic mechanism and clinical application of Chinese herbal medicine against diabetic kidney disease

Dan-Qian Chen[1]*, Jun Wu[2] and Ping Li[3]*

[1]Department of Emergency, China-Japan Friendship Hospital, Beijing, China, [2]Shandong College of Traditional Chinese Medicine, Yantai, Shandong, China, [3]Beijing Key Lab for Immune-Mediated Inflammatory Diseases, Institute of Clinical Medical Sciences, China-Japan Friendship Hospital, Beijing, China

Diabetic kidney disease (DKD) is the major complications of type 1 and 2 diabetes, and is the predominant cause of chronic kidney disease and end-stage renal disease. The treatment of DKD normally consists of controlling blood glucose and improving kidney function. The blockade of renin-angiotensin-aldosterone system and the inhibition of sodium glucose cotransporter 2 (SGLT2) have become the first-line therapy of DKD, but such treatments have been difficult to effectively block continuous kidney function decline, eventually resulting in kidney failure and cardiovascular comorbidities. The complex mechanism of DKD highlights the importance of multiple therapeutic targets in treatment. Chinese herbal medicine (active compound, extract and formula) synergistically improves metabolism regulation, suppresses oxidative stress and inflammation, inhibits mitochondrial dysfunction, and regulates gut microbiota and related metabolism *via* modulating GLP-receptor, SGLT2, Sirt1/AMPK, AGE/RAGE, NF-κB, Nrf2, NLRP3, PGC-1α, and PINK1/Parkin pathways. Clinical trials prove the reliable evidences for Chinese herbal medicine against DKD, but more efforts are still needed to ensure the efficacy and safety of Chinese herbal medicine. Additionally, the ideal combined therapy of Chinese herbal medicine and conventional medicine normally yields more favorable benefits on DKD treatment, laying the foundation for novel strategies to treat DKD.

KEYWORDS

diabetic kidney disease, Chinese herbal medicine, therapeutic mechanism, clinical application, metabolism regulation

Introduction

Diabetic kidney disease (DKD), also called diabetic nephropathy (DN), is a microvascular complication of diabetes mellitus (DM) and characterized by microalbuminuria, declined glomerular filtration rate (GFR), and high risk of cardiovascular disease and stroke. DKD results in high morbidity and mortality worldwide (Koye et al., 2018). Clinically, DKD is defined as the presence of

TABLE 1 The commonly used drugs in DKD treatment.

Treatment goal	Common drugs/cautions
Diet and lifestyle	Exercises, loss of weight, smoking cessation, protein intake, carbohydrate intake, fat intake, sodium intake and vitamin intake
Glucose control	Metformin, thiazolidinediones, GLP-1 analogues, DPP-4 inhibitors, and SGLT2 inhibitors
Hypertension control	ACEIs/ARBs, MRAs, CCBs, β-blocker, and diuretics
Albuminuria	ACEIs, ARBs, SGLT2 inhibitors, MRAs, and calcitriol impurities D
Blood lipid regulation	Statins and fibrates
Uric acid control	Diet control, allopurinol, and febuxostat

ARBs, angiotensin receptor blockers; ACEIs, angiotensin-converting enzyme inhibitors; CCBs, calcium channel blockers; DPP-4, dipeptidyl peptidase-4; GLP-1, glucagon-like peptide-1; MRAs, mineralocorticoid receptor antagonists; SGLT2, sodium/glucose cotransporter 2.

persistently increased urinary albumin (>300 mg/day) or urinary albumin-to-creatinine ratio (UACR>30 mg/g), accompanied by declined kidney function, eventually to end-stage renal disease (ESRD). According to pathological changes, DKD involves thickening of glomerular basement membrane, mesangial expansion, nodular sclerosis, and diabetic glomerulosclerosis (Thomas et al., 2015; Anders et al., 2018). DKD is the major complications of type 1 and 2 diabetes, and is the predominant cause of CKD that accounts for almost 50% of ESRD cases (Barrera-Chimal and Jaisser, 2020). Once DKD enters the dialysis stage, the economic burden of the patient and society greatly increases (Koye et al., 2018).

DKD treatment in early stage mainly focuses on the prevention of DM by the management of diet and lifestyle and glucose control. Once microalbuminuria occurred, the treatment needs to pay additional attention on alleviating and delaying albuminuria. Treatment targets hypertension, blood fat and uric acid also exhibit beneficial effect. The commonly used drugs are listed in Table 1. Although metformin, angiotensin-converting enzyme inhibitors (ACEIs), angiotensin receptor blockers (ARBs), glucagon-like peptide-1 (GLP-1) analogues and dipeptidyl peptidase-4 (DPP-4) inhibitors delay kidney function decline, the application of these drugs are limited. Recently, sodium glucose cotransporter 2 (SGLT2) inhibitor, as a novel type of hypoglycemic drugs, attaches a lot attention due to obvious advantages. SGLT2 excretes sugar directly through the kidneys, and only works when blood sugar exceeds the renal glucose threshold (Alicic et al., 2018). Functionally, SGLT2 inhibitors inhibit renal glucose reabsorption in the early proximal tubule, thereby lowering urinary glucose excretion and decreasing the glucose burden. In the diabetic nephron, compensatory upregulation and overexpression of the activity of SGLT2 glucose and sodium reabsorption in the proximal convoluted tubule results in decreased delivery of solutes to the macula densa. In the diabetic nephron with SGLT inhibition, lowering SGLT2-driven sodium-coupled glucose transport in the proximal convoluted tubule normalizes solute delivery to the macula densa, resulting in increasing solute and water reabsorption. However, adverse effects are unavoidable due to its mechanism, such as urinary tract infection and diabetic ketoacidosis. Therefore, the development of novel drugs and alternative strategies are urgently needed.

Overview of the pathophysiological mechanism and therapeutic target of diabetic kidney disease

Renin-angiotensin-aldosterone system

According to the characteristics of DKD, its pathophysiological mechanisms include hemodynamic and nonhemodynamic mechanisms (Figure 1). In the early phase of DKD, intraglomerular hypertension and single-nephron hyperfiltration are responsible for renal injury (Tonneijck et al., 2017). The improvement of preglomerular (afferent) and postglomerular (efferent) arteriolar tone has therefore exhibited beneficial effects on DKD treatment. The renin-angiotensin-aldosterone system (RAAS) controls water and salt metabolisms, but during DKD process the overactivation of RAAS facilitates efferent constriction and intraglomerular hypertension to promotes disease progression (Warren et al., 2019). The inhibition of RAAS, such as ACEIs and ARBs, has been used as the first-line therapy for DKD treatment by maintaining arteriolar tone balance and decreasing albuminuria (Chen et al., 2018a). However, dual RAAS blockade exerts side effects for DKD treatment indicating the harm of efferent arteriole (Parving et al., 2012; Fried et al., 2013). The combined therapy of mineralocorticoid receptor antagonists (MRAs) with ACEIs or ARBs significantly decreases albuminuria and protects glomerular structure (Zhou et al., 2016; Barrera-Chimal et al., 2019; Barrera-Chimal et al., 2022). Notably, finerenone, a kind of MRAs, has been attracted a lot of attention for DKD treatment. Compared with placebo, finerenone treatment decreases albuminuria and lowers the risks of DKD progression and cardiovascular events in patients with CKD and type 2 diabetes (Bakris et al., 2020; Filippatos et al., 2021; Pitt et al., 2021). Additionally, angiotensin-converting enzyme 2 (ACE2)/Ang(1-7) axis exhibits protection on DKD treatment in animal studies (Chou et al., 2013; Liu et al., 2020a), indicating a promising therapeutic target against DKD. Additionally, RAAS also participates in DKD progression *via* nonhemodynamic mechanisms. The upregulation of Ang II contributes to DKD progression by activating proinflammatory and profibrotic

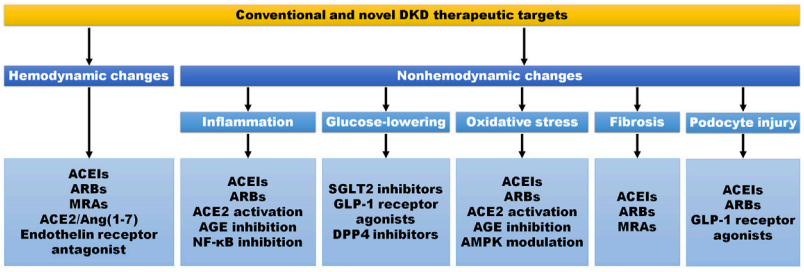

FIGURE 1
Conventional and novel DKD therapeutic targets and strategies. The therapeutic strategy of DKD includes hemodynamic and nonhemodynamic aspects. The improvement of hemodynamic changes, the glucose-lowering therapy, and the suppression of inflammation, oxidative stress, fibrosis and podocyte injury are the main therapeutic targets. ACE2, angiotensin-converting enzyme 2; ACEIs, angiotensin-converting enzyme inhibitors; AGE, advanced glycation end-product; AMPK, adenosine monophosphate-activated protein kinase; ARBs, angiotensin receptor blockers; DPP-4, dipeptidyl peptidase-4; GLP-1, glucagon-like peptide-1; MRAs, mineralocorticoid receptor antagonists; NF-κB, nuclear factor-kappa B; SGLT2, sodium glucose cotransporter 2.

effects (Yang et al., 2016b; Chen L. et al., 2017), while recombinant ACE2 attenuates DKD progression by suppressing oxidative stress, fibrosis, and mesangial cell proliferation (Malek et al., 2021).

Endothelin receptor

The endothelin system accounts for sodium and water metabolism. Endothelin B receptor is responsible for the natriuresis and vasodilatation at the proximal tubule, whereas endothelin A receptor activation is involved in sodium retention and vasoconstriction (Stuart et al., 2013). Endothelin receptor antagonists reduce albuminuria and prevent renal function decline by dilating the efferent arteriole. According to both short-term and long-term clinical trials, treatment with atrasentan, the selective endothelin A receptor antagonist, significantly reduces albuminuria without inducing obvious sodium retention (Kohan et al., 2015), and decreases the risk of renal events in patients with diabetes and CKD (Heerspink et al., 2019).

Sodium glucose cotransporter 2

For glucose-lowering therapies, SGLT2 inhibition and GLP-1 receptor agonists are the common choice for DKD treatment. The uptake and consumption of circulating glucose, the release of glucose by gluconeogenesis, and the reabsorption of glucose from glomerular filtrate are the main ways to maintain glucose homeostasis in the kidney (Alicic et al., 2018). SGLT2 controls tubular glucose reabsorption, and SGLT2 inhibition exhibits strong renal protection against DKD. SGLT2 inhibition improves solute delivery to the macula densa and reactivates tubuloglomerular feedback by reducing sodium and chloride reabsorption in the proximal tubule, which facilitates the reversal of afferent vasodilation and the normalization of glomerular hemodynamics. Several large clinical trials have proved the effective protection of empagliflozin and canagliflozin in patients with type 2 diabetes and CKD (Yale et al., 2013; Yale et al., 2014; Wanner et al., 2016; Cherney et al., 2017). Beyond the hemodynamic effect, reduced glucose uptake through the proximal tubular cells by SGLT2 inhibition alleviates DKD by inhibiting hyperglycemia-related tubulointerstitial injury (Anders et al., 2018; Kalantar-Zadeh et al., 2021).

Glucagon-like peptide-1 and dipeptidyl peptidase-4

GLP-1 is secreted after food ingestion and reduces postprandial glucose levels by promoting insulin secretion, inhibiting glucagon release, delaying gastric emptying, and decreasing hepatic glucose production (Müller et al., 2019). The deletion of GLP-1 in animal model results in reduced albuminuria and mesangial expansion (Fujita et al., 2014). GLP-1 is degraded by the enzyme DPP-4 in a short time indicating that DPP-4 inhibition is suitable for clinical application rather than GLP-1 (Müller et al., 2019). Two type compounds GLP-1 receptor agonists and DPP-4 inhibitors are therefor used to treat DKD. Large clinical trials have confirmed the beneficial effects of GLP-1 receptor agonists on cardiovascular, mortality, and kidney outcomes in patients with type 2 diabetes, including lixisenatide, liraglutide, semaglutide, exenatide, albiglutide, dulaglutide, and oral semaglutide (Kristensen et al., 2019; Yamada et al., 2021). GLP-1 receptor agonist, liraglutide, also coordinates lipogenic and lipolytic signals and protects renal mitochondria function against renal injury by regulating sirtuin 1 (Sirt1)/AMP-activated kinase protein (AMPK)/peroxlsome proliferator-activated

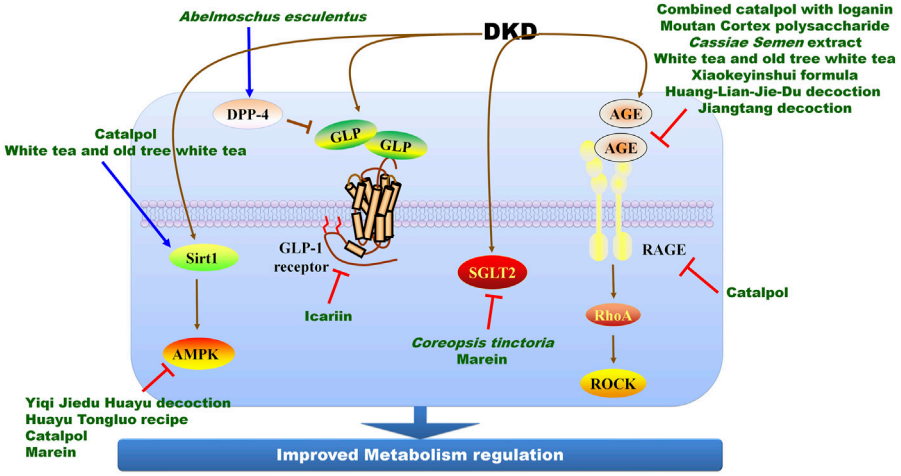

FIGURE 2
The molecular mechanisms and therapeutic targets of Chinese herbal medicine against DKD *via* improving metabolism regulation. AGE, advanced glycation end-product; AMPK, adenosine monophosphate-activated protein kinase; DPP-4, dipeptidyl peptidase-4; RAGE, receptors of AGE; GLP, glucagon-like peptide-1; ROCK, Rho-associated coiled-coil containing kinase; Sirt1, sirtuin 1.

receptor-γ coactlvator-1α (PGC-1α) pathways (Wang et al., 2018). The possible mechanisms of DPP-4 inhibitors for treatment of DKD is a proximally acting natriuresis that increases sodium excretion and triggers tubuloglomerular feedback (Crajoinas et al., 2011). Large clinical trials indicate that DPP-4 inhibitors, dulaglutide and albiglutide, significantly decrease the frequency of major cardiovascular events in patients with type 2 diabetes and CKD (Hernandez et al., 2018; Gerstein et al., 2019). In addition to hemodynamic mechanism, DPP-4 inhibitors reduce albuminuria, alleviate glomerular sclerosis, and suppress oxidative stress and inflammation (Cappetta et al., 2019; Marques et al., 2019).

Overview of Chinese herbal medicine in diabetic kidney disease treatment

A large number of studies have shown that Chinese herbal medicine has exhibited favorable efficacy on DKD treatment in clinics for decades, and has been the primary and additional treatment regimen. Chinese herbal medicine not only functions on abovementioned hemodynamic mechanisms also targets oxidative stress, glucose-lowering, inflammation, fibrosis, and podocyte injury to exert beneficial effects on DKD treatment (Chen et al., 2018b; Chen et al., 2019a), which attaches a lot attention. Notably, Chinese herbal medicine has been widely used to treat DKD clinically and yielded satisfactory results, which is recognized as a promisingly alternative therapy. Chinese herbal medicines are important sources for DKD treatment that prevents DKD and delays DKD progression by targeting multiple targets rather than single targets, including compounds, extracts, and Chinese herbal formulas. The present study aims to review the application of Chinese herbal medicines on DKD treatment in recent 3 years. We start from introducing DKD mechanisms and therapeutic targets, then summarize the advances on the therapeutic mechanisms and clinical application of Chinese herbal medicines on DKD treatment, and conclude by commenting on promising therapeutic candidates from Chinese herbal medicines to highlight the importance and capacity of Chinese herbal medicines on DKD treatment.

Therapeutic mechanism of Chinese herbal medicine in diabetic kidney disease treatment

Metabolism regulation

Numerous Chinese herbal medicines have exhibited beneficial efficacy on DKD treatment in clinics. Here, we describe only some of the important findings for the sake of brevity, and introduce these important findings according to their potential therapeutic targets (Figure 2; Table 2). By targeting DPP-4 and GLP-1 receptor, *Abelmoschus esculentus* significantly inhibits oxidative stress and renal fibrosis to improve kidney function and alleviate diabetic renal damage in streptozocin (STZ)-induced model (Peng et al., 2019). Icariin, a flavonoid extracted from *Herba epimedii*, activates GLP-1 receptor to alleviate tubulointerstitial fibrosis in DKD rats (Jia et al., 2021). Beyond to GLP-1 receptor, icariin alleviates inflammation by inducing NOD-like receptor thermal protein domain associated protein 3 (NLRP3) inactivation and G

TABLE 2 Therapeutic mechanisms and targets of Chinese herbal medicine in DKD treatment.

Chinese herbal medicine	Classification	Therapeutic mechanisms and targets	Reference
Abelmoschus esculentus	Herbal extract	Inhibiting DPP-4 and activating GLP-1 receptor	Peng et al. (2019)
Icariin	Active compound	Activating GLP-1 receptor, inactivating NLRP3, activating GPER *via* Keap1-Nrf2/HO-1 axis and inhibiting TLR4/NF-κB pathway	Qiao et al. (2018), Wang et al. (2020), Jia et al. (2021), Qi et al. (2021), Ding et al. (2022), and Zang et al. (2022)
Catalpol	Active compound	Modulating RAGE/RhoA/ROCK AMPK/Sirt1/NF-κB pathways	Chen Y. et al. (2019), Chen et al. (2020a), Chen et al. (2020b), and Shu et al. (2021)
Combined catalpol and loganin	Active compound	Inhibiting AGE/RAGE pathway	Chen et al. (2020b)
Novel polysaccharide	Active compound	Inhibiting AGEs and RAGEs levels	Lian et al. (2021)
Cassiae Semen extract	Herbal extract	Inhibiting AGEs and RAGEs levels	Wang et al. (2019)
White tea and old tree white tea	Herbal extract	Activating Sirt1/AMPK pathway	Xia et al. (2021)
Xiaokeyinshui formula	Formula	Inhibiting AGE/RAGE pathway	Zhou et al. (2020)
Huang-Lian-Jie-Du decoction	Formula	Inhibiting AGE/RAGE pathway	Tang et al. (2022)
Jiangtang decoction	Formula	Inhibiting AGE/RAGE pathway	Hong et al. (2017)
Coreopsis tinctoria	Herbal extract	Inhibiting SGLT2 and modulating NF-κB pathway	Yao et al. (2019) and Yu et al. (2019)
Marein and flavanomarein	Active compounds	Inhibiting SGLT2, and activating AMPK/ACC/PGC-1α pathway	Guo et al. (2020) and Zhang et al. (2020a)
Yiqi Jiedu Huayu decoction	Formula	Modulating AMPK pathway	Xuan et al. (2021)
Huayu Tongluo recipe	Formula	Modulating AMPK pathway	Li et al. (2021)
Curcumin	Active compounds	Activating Nrf2, inhibiting NF-κB, NADPH oxidase and PKCβII/p66Shc axis, and inhibiting NLRP3 inflammasome activity	Lu et al. (2017), Ghasemi et al. (2019), AlTamimi et al. (2021), and Xie et al. (2021)
Fructus Arctii	Herbal extract	Inhibiting ER stress signal transduction pathway	Zhang et al. (2019a)
Arctigenin	Active compounds	Enhancing PP2A activity	Zhong et al. (2019)
Baicalin	Active compounds	Inhibiting MAPK pathway	Ma et al. (2021)
Ellagic acid	Active compounds	Inhibiting MAPK pathway	Lin et al. (2021)
Astragaloside IV	Active compounds	Inhibiting NLRP3 inflammasome	Feng et al. (2021)
Yi Shen Pai Du Formula	Formula	Activating Nrf2 pathway	Zhang et al. (2021a)
Tangshen Formula	Formula	Modulating TXNIP-NLRP3-GSDMD axis	Li et al. (2020)
Berberine	Active compounds	Activating AMPK pathway to elevate PGC-1α, inhibiting Drp1-mediated mitochondrial fission and dysfunction, and stimulating the positive feedback loop of C/EBPβ/Gas5/miR-18a-5p	Qin et al. (2019), Qin et al. (2020), Rong et al. (2021), and Xu et al. (2021a)
Rhodiola rosea Salidroside	Herbal extract	Promoting mitochondrial DNA copy and electron transport chain proteins by enhancing Sirt1 and PGC-1α expression	Wang et al. (2013) and Xue et al. (2019)
Salidroside	Active compounds	Suppressing TXNIP-NLRP3 inflammasome pathway	Wu et al. (2016) and Wang et al. (2017)
Resveratrol	Active compounds	Suppressing mitochondrial oxidative stress	Zhang et al. (2019c)
4-O-methylhonokiol	Active compounds	Activating AMPK/PGC-1α/CPT1B pathway and activating Nrf2/SOD2 pathway	Ma et al. (2019)
Tangshen Formula and morroniside	Formula, Active compounds	Activating PGC-1α-LXR-ABCA1 pathway	Liu et al. (2018) and Gao et al. (2021a)
Astragaloside II	Active compounds	Upregulating PINK1 and Parkin	Su et al. (2021a)
Astragaloside IV	Active compounds	Inhibiting cytochrome c release and mitochondrial membrane potential	Xing et al. (2021) and Zang et al. (2021)
Combined Ginsenoside Rb1 and aldose therapy	Active compounds	Alleviating mitochondrial damage	He et al. (2022)
Quercetin	Active compounds	Modulating HIF-1α/miR-210/ISCU/FeS pathway	Xu et al. (2021b)
Andrographolide	Active compounds	Suppressing mitochondrial ROS-mediated NLRP3 inflammasome activation	Liu et al. (2021b)
Huangqi-Danshen decoction	Formula	Suppressing PINK1/Parkin-mediated mitophagy	Liu et al. (2020b)

(Continued on following page)

TABLE 2 (*Continued*) Therapeutic mechanisms and targets of Chinese herbal medicine in DKD treatment.

Chinese herbal medicine	Classification	Therapeutic mechanisms and targets	Reference
Punicalagin	Active compounds	Reshaping gut microbial ecology, reversing gut barrier dysfunction, and reducing serum lipopolysaccharide and diamine oxidase levels	Hua et al. (2022)
Polysaccharide	Active compounds	Reconstructing gut microbiota, improving intestinal barrier function, ameliorating serum proinflammatory mediators, and upregulating short-chain fatty acid level	Zhang et al. (2022)
Qing-Re-Xiao-Zheng formula	Formula	Modulating gut microbiota-bile acid axis *via* farnesoid X receptor	Gao et al. (2021)
QiDiTangShen granules	Formula	Modulating gut microbiota-bile acid axis *via* farnesoid X receptor	Wei et al. (2021)
Shenyan Kangfu tablet	Formula	Improving intestinal microbiota *via* elevated *Firmicutes* and reduced *Bacteroidetes* abundance	Chen et al. (2021)
San-Huang-Yi-Shen capsule	Formula	The improvement of gut microbiota by modulating arginine biosynthesis, TCA cycle, tyrosine metabolism, and arginine and proline metabolism	Su et al. (2021b)
Tangshen Formula	Formula	Regulating gut microbiota to reducing lipopolysaccharide and indoxyl sulfate levels	Zhao et al. (2020)

ABCA1, ATP-binding cassette transporter A1; ACC, acetyl-CoA carboxylase; AGE, advanced glycation end-product; AMPK, adenosine monophosphate-activated protein kinase; CPT1B, carnitine palmitoyltransferase 1B; DPP-4, dipeptidyl peptidase-4; EBPβ, enhancer binding protein beta; ER, endoplasmic reticulum; Gas5, growth arrest-specific 5; GLP-1, glucagon-like peptide-1; GPER, G protein-coupled estrogen receptor; GSDMD, gasdermin D; HO-1, heme oxygenase-1; Keap1, kelch-1ike ECH- associated protein l; LXR, liver X receptor; MAPK, mitogen-activated protein kinase; NF-κB, nuclear factor-kappa B; NLRP3, NOD-like receptor thermal protein domain associated protein 3; PGC-1α, peroxlsome proliferator-activated receptor-γ coactlvator-1α; PINK1, PTEN induced putative kinase 1; PKCβII, Significant up-regulation of the protein kinase Cβ II; PP2A, protein phosphatase 2 A; RAGE, receptors of AGE; ROCK, Rho-associated coiled-coil containing kinase; ROS, reactive oxygen species; SGLT2, sodium glucose cotransporter 2; Sirt1, sirtuin 1; SOD2, superoxide dismutase 2; TLR4, toll-like receptor 4; TXNIP, thioredoxin-interacting protein.

protein-coupled estrogen receptor (GPER) activation *via* Kelch-1ike ECH-associated protein l (Keap1)-nuclear factor-erythroid-2-related factor 2 (Nrf2)/heme oxygenase-1 (HO-1) axis and inhibiting toll-like receptor 4 (TLR4)/nuclear factor-kappa B (NF-κB) signal pathway (Qiao et al., 2018; Wang et al., 2020; Qi et al., 2021; Ding et al., 2022), and prevents epithelial-mesenchymal transition (EMT) of tubular epithelial cells *via* modulating the miR-122-5p/forkhead box p2 axis against DKD (Zang et al., 2022).

Advanced glycation end-products (AGEs) are the non-enzymatic glycation products between the aldehyde group of saccharide and amino group of protein, lipid, or nucleic acid. AGEs result in the irreversible transformation of protein by glycation and facilitate DKD progression. The accumulation of AGEs and receptors of AGEs (RAGEs) accelerate glomerulus and tubule injury, and progressive proteinuria (Tang et al., 2021). AGE/AGE pathway is the pivotal therapeutic target of Chinese herbal medicine. Catalpol, an iridoid glycoside isolated from the root of *Rehmannia glutinosa*, significantly alleviates AGE/RAGE-induced endothelial dysfunction and inflammation in DKD mice and delays DKD progression *via* RAGE/RhoA/Rho-associated coiled-coil containing kinase (ROCK) pathway (Shu et al., 2021). The combined therapy of catalpol with loganin isolated from *Cornus officinalis* cooperatively prevents podocyte apoptosis by targeting AGE/RAGE pathway, and exerts stronger effects than used alone against DKD (Chen et al., 2020b). Catalpol also stabilizes podocyte cytoskeleton and enhances injured podocyte autophagy to prevent DKD by suppressing mammalian target of rapamycin activity and promoting transcription factor EB nuclear translocation, and inhibits oxidative stress and inflammation *via* AMPK/Sirt1/NF-κB pathway (Chen Y. et al., 2019; Chen et al., 2020a). The novel polysaccharide isolated from *Moutan Cortex* significantly reduces serum AGE and RAGE levels to prevent DKD progression in rat model (Lian et al., 2021). In addition to active compounds from Chinese herbal medicine, *Cassiae Semen* extract obviously controls glucose and lipid metabolism, and suppresses oxidative stress and inflammatory responses *via* regulating AGEs and RAGEs against DKD in STZ-induced rat model (Wang et al., 2019). White tea and old tree white tea ameliorate AGE accumulation in kidney of STZ-induced mouse model, and alleviate oxidative stress and inflammation *via* activating Sirt1/AMPK pathway (Xia et al., 2021). Additionally, Chinese herbal formula including Xiaokeyinshui formula, Huang-Lian-Jie-Du decoction and Jiangtang decoction exhibit renal protective effects in DKD animal models *via* regulating AGE/RAGE pathway (Hong et al., 2017; Zhou et al., 2020; Tang et al., 2022).

SGLT2 is an important therapeutic target of Chinese herbal medicine. *Coreopsis tinctoria* Nutt is widely used to treat high blood pressure and diarrhea, and SGLT2 is its potential therapeutic target. Its alcohol extract protects diabetic kidney injury in db/db mice by suppressing miR-192- and miR-200b-mediated phosphatase and tensin homolog deleted on

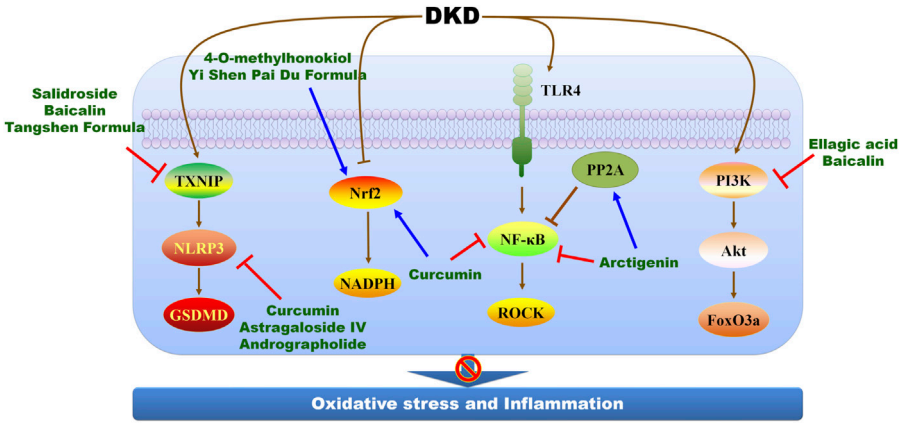

FIGURE 3
The molecular mechanisms and therapeutic targets of Chinese herbal medicine against DKD *via* suppressing oxidative stress and inflammation. FoxO3a, forkhead box transcription factor 3a; GSDMD, gasdermin D; NF-κB, nuclear factor-kappa B; NLRP3, NOD-like receptor thermal protein domain associated protein 3; Nrf2, nuclear factor-erythroid 2-related factor 2; PI3K, phosphoinositide 3-kinase; PP2A, protein phosphatase 2 A; ROCK, Rho-associated coiled-coil containing kinase; TLR4, toll-like receptor 4; TXNIP, thioredoxin-interacting protein.

chromosome ten (PTEN)/phosphoinositide 3-kinase (PI3K)/AKT pathway (Yu et al., 2019), while its ethyl acetate extract controls transforming growth factor-β1/Smads, AMPK, and NF-κB signaling pathways to delay DKD progression (Yao et al., 2019). Further study shows that marein and flavanomarein are the active compounds of *C. tinctoria* to prevent DKD progression. Marein directly inhibits SGLT2 expression and then activates AMPK/acetyl-CoA carboxylase (ACC)/PGC-1α pathway to correct hyperglycemia and dyslipidemia and diabetic kidney injury in db/db mice (Guo et al., 2020). Spleen tyrosine kinase are the potential therapeutic target of flavanomarein to ameliorate high glucose-induced extracellular matrix (ECM) against DKD (Zhang et al., 2020a). Additionally, Yiqi Jiedu Huayu decoction and Huayu Tongluo recipe suppress diabetic kidney injury in STZ-induced rat model *via* modulating AMPK pathway (Li et al., 2021; Xuan et al., 2021).

The inhibition of oxidative stress and inflammation

Oxidative stress and inflammation drive the development of DKD, and several novel mediators are involved in such process, including tonicity-responsive enhancer-binding protein, apoptosis signal-regulating kinase 1, serine/threonine protein kinase 25, and receptor activator of NF-κB (Chen et al., 2017a; Chen et al., 2017b; Liles et al., 2018; Chen et al., 2019b; Cansby et al., 2020; Choi et al., 2020; Ke et al., 2021; Liu et al., 2022b). Additionally, superoxide dismutase (SOD), glutathione peroxidase, malondialdehyde are considered as biomarkers of oxidative stress to evaluate the effects of Chinese herbal medicine on DKD treatment (Zhou et al., 2022). Even mechanistic studies concerning DKD progress develop a lot, mechanistic studies concerning Chinese herbal medicine against DKD is relatively hysteretic, in that most of Chinese herbal medicine alleviates oxidative stress and inflammation in DKD by modulating NF-κB and Nrf2 pathways (Figure 3; Table 2). Curcumin significantly ameliorates albumin/protein urea and increased creatinine clearance in STZ-induced DKD rats, which involves the activation of Nrf2 and the inhibition of NF-κB, NADPH oxidase and significant up-regulation of the protein kinase Cβ II (PKCβII)/p66^{Shc} axis (AlTamimi et al., 2021). The inhibition of NLRP3 inflammasome activity and the downregulation of kidney injury molecule 1 and neutrophil gelatinase-associated lipocalin are also therapeutic targets of curcumin to suppress oxidative stress against DKD progression (Lu et al., 2017; Ghasemi et al., 2019). The combination of curcumin with antihyperglycemic agents exerts stronger effects against diabetic complications by maintaining Nrf2 pathway homeostasis (Xie et al., 2021). *Fructus Arctii* attenuates proteinuria in patients with diabetics, and arctigenin, a lignan extracted from *F. Arctii*, reduces proteinuria and podocyte injury in diabetes mouse models. Arctigenin enhances protein phosphatase 2 A (PP2A) activity to alleviate p65-mediated inflammation *in vivo*, and blocks endoplasmic reticulum (ER) stress signal transduction pathway to suppress apoptosis in high glucose-induced HK2 cells (Zhang et al., 2019a; Zhong et al., 2019). Specific deletion of PP2A in podocyte weakens the efficiency of arctigenin, indicating PP2A as the therapeutic target of arctigenin (Zhong et al., 2019).

Beyond to NF-κB and Nrf2 pathways, the suppression of mitogen-activated protein kinase (MAPK)-mediated inflammatory signaling pathway is therapeutic target of

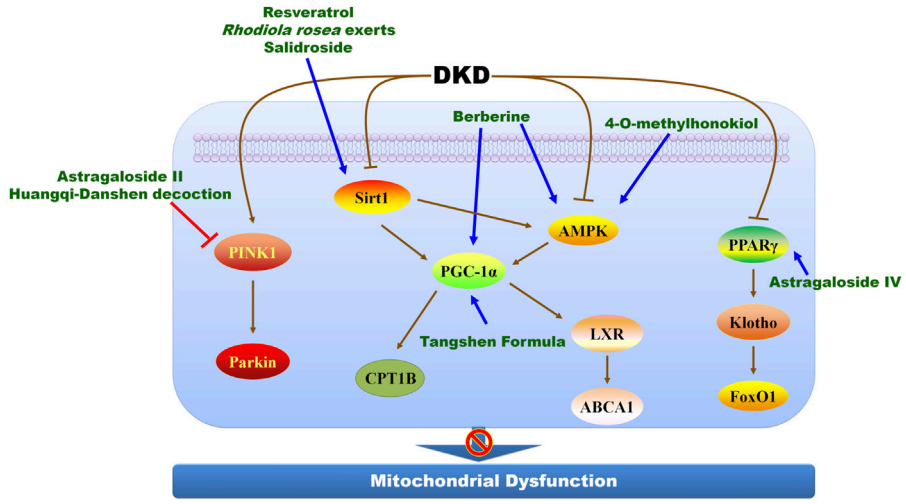

FIGURE 4
The molecular mechanisms and therapeutic targets of Chinese herbal medicine against DKD *via* alleviating mitochondrial dysfunction. ABCA1, ATP-binding cassette transporter A1; AMPK, adenosine monophosphate-activated protein kinase; CPT1B, carnitine palmitoyltransferase 1B; FoxO1, forkhead box transcription factor 1; LXR, liver X receptor; PGC-1α, peroxlsome proliferator-activated receptor-γ coactlvator-1α; PINK1, PTEN induced putative kinase 1; PPARγ, peroxisome proliferator-activated receptor gamma; Sirt1, sirtuin 1.

baicalin. Baicalin attenuates diabetic conditions, proteinuria, renal histopathological changes, and alleviates oxidative stress and inflammation in DKD animal model *via* Nrf2 and MAPK pathways (Ma et al., 2021). Ellagic acid alleviates high glucose-induced mesangial cell injury and inflammation in a concentration-dependent manner, and the underlying mechanisms involve in the activation of PI3K/Akt signaling pathway and the suppression of forkhead box transcription factor 3a (FoxO) 3a during DKD (Lin et al., 2021). Astragaloside IV alleviates podocyte injury and delays DKD progression in db/db mice *via* suppressing NLRP3 inflammasome-mediated inflammation (Feng et al., 2021). Yi Shen Pai Du Formula inhibits oxidative stress, inflammation, and EMT to delay DKD progression in db/db *via* activating Nrf2 pathway (Zhang et al., 2021a). Tangshen Formula, a Chinese formulation, exerts beneficial effects against DKD by modulating thioredoxin-interacting protein (TXNIP)-NLRP3-gasdermin D (GSDMD) axis-mediated pyroptosis in STZ-induced rat model and AGE-induced HK-2 cells (Li et al., 2020).

The modulation of mitochondrial dysfunction

PGC-1α is a prominent modulator of mitochondrial biogenesis and an attractive therapeutic target in DKD treatment (Li and Susztak, 2016; Long et al., 2016; Trembinski et al., 2020), and several Chinese herbal medicines and their active compounds exert renoprotection against DKD by modulating PGC-1α (Figure 4; Table 2). Metabolomic research proves that the abnormality on mitochondrial fuel usage and mitochondrial dysfunction occurs in patients with DKD, and berberine, the main active compounds of *Rhizoma coptidis* and *Cortex phellodendri*, modulates PGC-1α to alleviate mitochondrial injury in direct and indirect pathways. Berberine facilitates mitochondrial energy homeostasis and fatty acid oxidation by directly activating PGC-1α signaling pathway and protects glomerular podocytes *via* inhibiting dynamin-related protein 1-mediated mitochondrial fission and dysfunction in db/db mice model and cultured podocytes (Qin et al., 2019; Qin et al., 2020). Berberine activates AMPK pathway to upregulate PGC-1α that reduces fatty acid oxidation, lipid deposition, and protects mitochondria to mitigate diabetic renal tubulointerstitial injury (Rong et al., 2021). Additionally, berberine modulates mitochondrial reactive oxygen species (ROS) generation by stimulating the positive feedback loop of CCAAT enhancer binding protein beta (C/EBPβ)/growth arrest-specific 5 (Gas5)/miR-18a-5p (Xu et al., 2021a). The ethanol extract of *Rhodiola rosea* exerts beneficial protection in STZ-induced model in the early nephropathy in type 2 diabetic rats (Wang et al., 2013). Further study identifies salidroside as a major active compound of *R. rosea* to treat DKD. Salidroside markedly improves renal structures and reverses the downregulation of nephrin and podocin in patients with DKD. Mechanistically, salidroside treatment promotes mitochondrial DNA copy and electron transport chain proteins by enhancing Sirt1 and PGC-1α expression in STZ-induced mice (Xue et al., 2019). Salidroside

also suppresses oxidative stress and ECM accumulation by modulating TXNIP-NLRP3 inflammasome pathway (Wang et al., 2017), and reduces proteinuria by attenuating caveolin-1 phosphorylation and albumin transcytosis across glomerular endothelial cells (Wu et al., 2016). Resveratrol, a potent Sirt1 agonist, attenuates podocyte damage in diabetic mice by suppressing mitochondrial oxidative stress (Zhang et al., 2019c), while 4-O-methylhonokiol, isolated from *Magnolia stem bark*, protects against STZ-induced DKD by activating AMPK/PGC-1α/carnitine palmitoyltransferase 1B (CPT1B)-mediated fatty acid oxidation and Nrf2/SOD2-mediated anti-oxidative stress (Ma et al., 2019). Notably, Tangshen Formula and its active compounds morroniside enhances renal cholesterol efflux to ameliorates tubular epithelial injury in db/db mice by activating PGC-1α-liver X receptor (LXR)-ATP-binding cassette transporter A1 (ABCA1) pathway (Liu et al., 2018; Gao et al., 2021a), indicating a promising candidate for DKD treatment.

Other potential therapeutic targets are also proved, including PTEN induced putative kinase 1 (PINK1) and peroxisome proliferator-activated receptor (PPAR) (Figure 4; Table 2). Several studies show the renoprotective effects of astragaloside II and astragaloside IV, active compounds of *Astragalus membranes*, referring to the improvement of mitochondrial dysfunction. Astragaloside II and astragaloside IV obviously ameliorate albuminuria in DKD animal models and prevent podocyte injury from high glucose (Su et al., 2021a; Xing et al., 2021; Zang et al., 2021). Astragaloside II suppresses mitochondrial dysfunction of podocyte injury *via* upregulating PINK1 and Parkin, and astragaloside IV inhibits cytochrome c release and mitochondrial membrane potential to protect podocyte against DKD (Su et al., 2021a; Zang et al., 2021). Astragaloside II also mitigates podocyte apoptosis against DKD *via* suppressing transient receptor potential channel 6-mediated $Ca2^{+}$ influx, and astragaloside IV activates PPARγ-Klotho-FoxO1 pathway to alleviate podocyte apoptosis (Xing et al., 2021; Zang et al., 2021). Ginsenoside Rb1 combines with aldose reductase to alleviate mitochondrial damage and podocyte apoptosis thereby delaying the progression of DKD (He et al., 2022). Quercetin, an active compound from *Panax notoginseng*, antagonizes glucose fluctuation-caused kidney injury by inhibiting aerobic glycolysis *via* hypoxia inducible factor-1 alpha (HIF-1α)/miR-210/ISCU/FeS pathway in glomerular mesangial cells (Xu et al., 2021b). Andrographolide isolated from *Andrographis paniculate* suppresses mitochondrial ROS-mediated NLRP3 inflammasome activation to ameliorate mitochondrial dysfunction during DKD (Liu et al., 2021b). Chinese herbal formula Huangqi-Danshen decoction delay DKD progress by suppressing PINK1/Parkin-mediated mitophagy (Liu et al., 2020b). Additionally, signal transducer and activator of transcription 3 is also a potential therapeutic target to modulate mitochondrial homeostasis through SDF-1α/CXCR4 pathway to ameliorate renal tubular injury in DKD (Zhang et al., 2020b).

The regulation of gut microbiota and related metabolism

Emerging evidences have confirmed the relationship between the dysfunction of gut microbiota and related metabolism and the progression of DKD indicating the importance of kidney-gut axis (Winther et al., 2020; Yang et al., 2021). According to 16S rRNA sequencing and metabolomic results, the gut microbiota structure, phenylalanine and tryptophan metabolic pathways are significantly altered in patients with DKD (Zhang et al., 2021b). Phenyl sulfate is a gut microbiota-derived metabolite, and its level increases with the progression of diabetes in rat model. Phenyl sulfate obviously contributes to albuminuria and could be used as a biomarker for DKD (Kikuchi et al., 2019). Trimethylamine *N*-oxide (TMAO) is a gut microbiota-derived metabolite, and serum TMAO closely relates to and mediates impaired renal function (Winther et al., 2019). As an important component of innate immunity, mitochondrial antiviral signaling protein (MAVS) maintains intestinal integrity. DKD contributes to the impairment of MAVS signaling in the kidney and intestine thus leading to the disrupted homeostasis, indicating that maintaining intestinal homeostasis may functions a novel therapeutic approach for DKD treatment (Linh et al., 2022).

Notably, gut microbiota and related metabolism are the potential therapeutic target of Chinese herbal medicine against DKD (Table 2). Punicalagin isolated from *Punica granatum* reshapes gut microbial ecology, reverses gut barrier dysfunction, and reduces serum lipopolysaccharide and diamine oxidase levels to delay DKD progression (Hua et al., 2022). Functioning as a prebiotic, the polysaccharide extracted from *M. Cortex* reconstructs gut microbiota, improves intestinal barrier function, ameliorates serum proinflammatory mediators, and upregulates short-chain fatty acid level by controlling *Lactobacillus* and *Muribaculaceae_unclassified* abundance in gut of DKD rat model (Zhang et al., 2022). Qing-Re-Xiao-Zheng formula reverses gut dysbiosis and inhibits generation of gut-derived LPS, and suppresses DKD-related inflammation by reducing TLR4 and NF-κB expression in DKD mouse model (Gao et al., 2021b). QiDiTangShen granules exert good efficacy on alleviating proteinuria in DKD mice model, and the underlying mechanisms involves the modulation of gut microbiota-bile acid axis *via* farnesoid X receptor (Wei et al., 2021). Shenyan Kangfu tablet, a prescription of traditional Chinese medicine, attenuates stimulated blood glucose and glycosylated hemoglobin (HbA1c) levels and alleviates renal dysfunction and inflammation in db/db mice. The underlying mechanisms refer to suppressed renal inflammatory signaling cascades and improved intestinal microbiota *via* elevated

Firmicutes and reduced *Bacteroidetes* abundance (Chen et al., 2021). San-Huang-Yi-Shen capsule exhibits beneficial effects against DKD in clinics. The mechanism involves the improvement of gut microbiota by modulating arginine biosynthesis, tricarboxylic acid (TCA) cycle, tyrosine metabolism, and arginine and proline metabolism (Su et al., 2021b). In addition to above-mentioned mechanisms, Tangshen Formula attenuates diabetic renal injury and inflammation by regulating gut microbiota to reducing lipopolysaccharide and indoxyl sulfate levels (Zhao et al., 2020).

Clinical application of Chinese herbal medicine in diabetic kidney disease treatment

Even a lot of work engages to elucidate the underlying mechanisms of Chinese herbal medicine, the lack of high-quality evidences from clinical trials significantly hinders the application of Chinese herbal medicine worldwide. Here, we summarize randomized clinical trials (RCTs) of Chinese herbal medicine against DKD to highlight its beneficial efficacy, and found that Chinese herbal medicine can be used as the primary and additional treatment regimen for DKD in clinics.

Single use of Chinese herbal medicine shows beneficial efficacy on DKD treatment. A retrospective study reports the beneficial efficacy of a traditional Chinese medicine, Shenzhuo formula, on patients with DKD. The changes in estimated GFR (eGFR), creatinine clearance, serum creatinine, blood urea nitrogen, albuminuria, HbA1c, blood pressure, and lipid profile are observed. Compared with the baseline, serum creatinine significantly decreases, and estimated glomerular filtration rate (eGFR) and creatinine clearance increases after intervention at 1, 3, 6, 9, 12, and 18 months. Shenzhuo formula also reduces HbA1c, lipid levels and blood pressure (Tian et al., 2015). A multicenter, parallel-control, open-label, RCT investigates the effect of Zicuiyin decoction on DKD treatment, and the primary outcome is the change of eGFR. Zicuiyin decoction significantly increases eGFR and decreases serum creatinine to alleviate DKD *via* correcting gut microbiota dysbiosis (Liu et al., 2022a). Additionally, a single-blind, randomized, controlled preliminary study explores the efficacy of the acupressure at Sanyinjiao for DKD treatment, and the primary outcome measure is the UACR or logarithmic transformed UACR (log-UACR) changes. The difference in UACR and log-UACR before and after the study was higher in the Sanyinjiao group than in the sham groups, and the acupressure at Sanyinjiao for 8 weeks helps to decrease albuminuria in patients with early DKD indicated by eGFR and HbA1c (Chuang et al., 2020).

Combined therapy of Chinese herbal medicine and ARB/ACEI also exhibit favorable efficacy on DKD treatment. Huangkui capsule from traditional Chinese medicine is made from the ethanol extract of flowers in *Abelmoschus manihot*. A multicenter randomized double-blind parallel controlled clinical trial is designed to evaluate the effect of combined Huangkui capsule and irbesartan treatment on DKD, and the primary outcomes are changed values of albumin-to-creatinine ratio from baseline after treatment. Combined Huangkui capsule and irbesartan treatment exhibits beneficial effect on alleviating albuminuria in patients with type 2 diabetes and DKD (Zhao et al., 2022). Additionally, single Huangkui capsule therapy and combined Huangkui capsule and losartan therapy exert favorable therapeutic effect against primary glomerular disease in a prospective, multicenter randomized controlled clinical trial (Zhang et al., 2014). A multicenter double-blinded randomized placebo-controlled trial shows that accompanying by conventional ARB or ACEI treatment, Tangshen Formula treatment for continuous 24 weeks exhibits obviously beneficial efficacy compared with placebo on decreasing proteinuria and improving eGFR in DKD patients with macroalbuminuria (Li et al., 2015). In this study, primary outcomes are urinary protein level, measured by urinary albumin excretion rate (UAER) for participants with microalbuminuria, 24-h urinary protein for participants with macroalbuminuria. Except for UAER, Tangshen Formula treatment exhibits favorable effects on other primary outcomes. Further investigation indicates that urinary liver-type fatty acid binding protein is identified as the biomarker for the severity of DKD and the effects of Tangshen Formula against DKD (Yang et al., 2016a). The on-going RCT of Tangshen Formula aims to investigate its effectiveness and safety on treating type 2 DKD patients with macroalbuminuria (Yan et al., 2016). The meta-analysis of RCTs shows the satisfied efficacy of combined *Tripterygium wilfordii* Hook, tripterygium glycosides, Ophiocordyceps sinensis, or Jinshuibao with conventional ACEI or ARB treatment against DKD (Luo et al., 2015; Lu et al., 2018; Zhang et al., 2019b; Ren et al., 2019; Wu et al., 2020; Yang et al., 2020).

Notably, several RCT protocols have been designed to provide solid evidences for combined Chinese herbal medicine and conventional ARB or ACEI therapy against DKD. An assessor-blind, parallel, pragmatic randomized controlled clinical trial registered in Hong Kong has been engaged to evaluate the effectiveness of add-on astragalus in clinics. This trial plans to enroll 181 patients with type 2 diabetes, stage 2-3 CKD and macroalbuminuria who receive 48 weeks of add-on astragalus or standard medical care (Chan et al., 2021). A double-blind, placebo-controlled, randomized trial is designed to explore the efficacy and safety of combined Liuwei Dihuang pills with conventional metformin and ARB therapy against DKD for 4 weeks treatment and 12 weeks follow-up, and 24 h urinary protein levels from the baseline to the end of the treatment phase is the primary outcome (Liao et al., 2020). A prospective, single-center RCT aims to investigate the efficacy and safety of

combined *Tripterygium* glycosides and ARB therapy for DKD treatment. The primary endpoint is 24 h proteinuria decreased level after treatment for 48 weeks (Lengnan et al., 2020).

Conclusion and perspectives

DKD is the leading cause of CKD and ESRD worldwide. Although the drug development of RAAS and SGLT2 inhibitors has been evolved, a large proportion of DKD patients still needs dialysis and renal transplantation. The beneficial efficacy of Chinese herbal medicine in clinical application attracts a lot attention as an alternative therapy. DKD progression is normally considered irreversible, while Chinese herbal medicine gives us hope. Reliable evidences from RCTs show that Tangshen Formula and *T. wilfordii* Hook extract significantly reduce proteinuria and elevate eGFR compared with ARB or ACEI (Ge et al., 2013; Li et al., 2015; Liu et al., 2021a). Chinese herbal medicine normally targets multiple and synergetic targets to alleviate DKD due to multiple active compounds, including the improvement of metabolism regulation, the inhibition of oxidative stress and inflammation, the modulation of mitochondrial dysfunction, and the regulation of gut microbiota and related metabolism. Notably, we notice that many Chinese herbal medicines synergistically target multiple key factors and pathways to ameliorate DKD, including icariin, catalpol, *C. tinctoria*, salidroside, and 4-O-methylhonokiol (Table 2). These promising candidates highlight the advantage that synergistically targeting multiple key factors and pathways is the important strategy to facilitate drug development for DKD treatment. These also highlight the importance and urgency to discover and identify the novel therapeutic target. Another advantage of Chinese herbal medicine is its clinical experience for thousands of years in east Asia. Chinese herbal medicine has been still used for prevent and treat DKD today, and many high-quality clinical evidences confirm the efficacy of combined Chinese herbal medicine and conventional western medicine, such as Tangshen Formula, Xiaokeyinshui formula, and *T. wilfordii*, which provide an alternative strategy for DKD treatment.

However, some limitations hinder the recognition and extensive use of Chinese herbal medicine beyond east Asia. One is that the lack of high-quality evidence to identify therapeutic mechanism of Chinese herbal medicine. Most research reported the modulation of Chinese herbal medicine on common mechanism rather than specific and targeted mechanism *via* high throughput analysis. Considerable work needs to be done to identify targeted mechanism of Chinese herbal medicine on DKD treatment. The multiple active compounds of Chinese herbal medicine contribute to the beneficial efficacy to alleviate DKD, but also results in the difficulty to control the quality of Chinese herbal medicine. The identification of active compounds and establishment of corresponding quality control system are necessary to ensure the efficacy and safety of Chinese herbal medicine. Additionally, strict and standardized toxicological research is essential to ensure the acceptable side effect. The proper dosage and duration of Chinese herbal medicine should be investigated in preclinical and clinical trial to ensure favorable efficacy. The lack of high-quality evidence from clinical medicine significantly hinders the extensive use of Chinese herbal medicine, and more efforts are needed to solve this problem. Fortunately, RCTs and mechanism studies of some Chinese herbal medicines have been completed and some is ongoing. For example, the clinical efficacy of Tangshen Formula has been investigated by RCTs, and Tangshen Formula exerts better efficacy in reducing albuminuria and elevating eGFR (Li et al., 2015). Meanwhile, mechanism studies show that Tangshen Formula synergistically targets multiple key factors or pathways to ameliorate DKD *via* modulating pyroptosis, enhancing renal cholesterol efflux, reshaping gut microbiota, and suppressing inflammation (Liu et al., 2018; Li et al., 2020; Zhao et al., 2020). Tangshen Formula sets up a good example that provides reliable evidences for clinical trial and therapeutic mechanism.

Given that many Chinese herbal medicines have yet to be investigated using a modern pharmacological approach, we anticipate many of them could be completed in the future. Chinese herbal medicine has its own advantages in treating DKD, including multiple therapeutic targets and rich clinical experience. New guidelines concerning Chinese herbal medicine against DKD are needed to assure safety and efficacy to amplify its application in treating DKD worldwide.

Author contributions

D-QC conceptualized and wrote the manuscript. D-QC, JW, and PL revised the manuscript and approved the submitted version.

Funding

This study was supported by the National Natural Science Foundation of China (Grant Nos. 82174296, 82104511), and the Project funded by China Postdoctoral Science Foundation (Grant Nos. 2021M693579).

Conflict of interest

The authors declare that the research was conducted in the absence of any commercial or financial relationships that could be construed as a potential conflict of interest.

Publisher's note

References

Alicic, R. Z., Johnson, E. J., and Tuttle, K. R. (2018). SGLT2 inhibition for the prevention and treatment of diabetic kidney disease: a review. *Am. J. Kidney Dis.* 72 (2), 267–277. doi:10.1053/j.ajkd.2018.03.022

ALTamimi, J. Z., AlFaris, N. A., Al-Farga, A. M., Alshammari, G. M., BinMowyna, M. N., and Yahya, M. A. (2021). Curcumin reverses diabetic nephropathy in streptozotocin-induced diabetes in rats by inhibition of PKCβ/p(66)Shc axis and activation of FOXO-3a. *J. Nutr. Biochem.* 87, 108515. doi:10.1016/j.jnutbio.2020.108515

Anders, H. J., Huber, T. B., Isermann, B., and Schiffer, M. (2018). CKD in diabetes: diabetic kidney disease versus nondiabetic kidney disease. *Nat. Rev. Nephrol.* 14 (6), 361–377. doi:10.1038/s41581-018-0001-y

Bakris, G. L., Agarwal, R., Anker, S. D., Pitt, B., Ruilope, L. M., Rossing, P., et al. (2020). Effect of finerenone on chronic kidney disease outcomes in type 2 diabetes. *N. Engl. J. Med.* 383 (23), 2219–2229. doi:10.1056/NEJMoa2025845

Barrera-Chimal, J., and Jaisser, F. (2020). Pathophysiologic mechanisms in diabetic kidney disease: A focus on current and future therapeutic targets. *Diabetes Obes. Metab.* 22, 16–31. doi:10.1111/dom.13969

Barrera-Chimal, J., Girerd, S., and Jaisser, F. (2019). Mineralocorticoid receptor antagonists and kidney diseases: Pathophysiological basis. *Kidney Int.* 96 (2), 302–319. doi:10.1016/j.kint.2019.02.030

Barrera-Chimal, J., Lima-Posada, I., Bakris, G. L., and Jaisser, F. (2022). Mineralocorticoid receptor antagonists in diabetic kidney disease - mechanistic and therapeutic effects. *Nat. Rev. Nephrol.* 18 (1), 56–70. doi:10.1038/s41581-021-00490-8

Cansby, E., Caputo, M., Gao, L., Kulkarni, N. M., Nerstedt, A., Ståhlman, M., et al. (2020). Depletion of protein kinase STK25 ameliorates renal lipotoxicity and protects against diabetic kidney disease. *JCI Insight* 5 (24), 140483. doi:10.1172/jci.insight.140483

Cappetta, D., Ciuffreda, L. P., Cozzolino, A., Esposito, G., Scavone, C., Sapio, L., et al. (2019). Dipeptidyl peptidase 4 inhibition ameliorates chronic kidney disease in a model of salt-dependent hypertension. *Oxid. Med. Cell. Longev.* 2019, 8912768. doi:10.1155/2019/8912768

Chan, K. W., Kwong, A. S. K., Tsui, P. N., Cheung, S. C. Y., Chan, G. C. W., Choi, W. F., et al. (2021). Efficacy, safety and response predictors of adjuvant astragalus for diabetic kidney disease (READY): Study protocol of an add-on, assessor-blind, parallel, pragmatic randomised controlled trial. *BMJ Open* 11 (1), e042686. doi:10.1136/bmjopen-2020-042686

Chen, D. Q., Cao, G., Chen, H., Liu, D., Su, W., Yu, X. Y., et al. (2017a). Gene and protein expressions and metabolomics exhibit activated redox signaling and wnt/β-catenin pathway are associated with metabolite dysfunction in patients with chronic kidney disease. *Redox Biol.* 12, 505–521. doi:10.1016/j.redox.2017.03.017

Chen, D. Q., Chen, H., Chen, L., Vaziri, N. D., Wang, M., Li, X. R., et al. (2017b). The link between phenotype and fatty acid metabolism in advanced chronic kidney disease. *Nephrol. Dial. Transpl.* 32 (7), 1154–1166. doi:10.1093/ndt/gfw415

Chen, L., Chen, D. Q., Wang, M., Liu, D., Chen, H., Dou, F., et al. (2017). Role of RAS/Wnt/β-catenin axis activation in the pathogenesis of podocyte injury and tubulo-interstitial nephropathy. *Chem. Biol. Interact.* 273, 56–72. doi:10.1016/j.cbi.2017.05.025

Chen, D. Q., Feng, Y. L., Cao, G., and Zhao, Y. Y. (2018a). Natural products as a source for antifibrosis therapy. *Trends Pharmacol. Sci.* 39 (11), 937–952. doi:10.1016/j.tips.2018.09.002

Chen, D. Q., Hu, H. H., Wang, Y. N., Feng, Y. L., Cao, G., and Zhao, Y. Y. (2018b). Natural products for the prevention and treatment of kidney disease. *Phytomedicine* 50, 50–60. doi:10.1016/j.phymed.2018.09.182

Chen, D. Q., Cao, G., Chen, H., Argyopoulos, C. P., Yu, H., Su, W., et al. (2019a). Identification of serum metabolites associating with chronic kidney disease progression and anti-fibrotic effect of 5-methoxytryptophan. *Nat. Commun.* 10 (1), 1476. doi:10.1038/s41467-019-09329-0

Chen, D. Q., Feng, Y. L., Chen, L., Liu, J. R., Wang, M., Vaziri, N. D., et al. (2019b). Poricoic acid A enhances melatonin inhibition of AKI-to-CKD transition by regulating Gas6/Axl-NF-κB/Nrf2 axis. *Free Radic. Biol. Med.* 134, 484–497. doi:10.1016/j.freeradbiomed.2019.01.046

Chen, Y., Liu, Q., Shan, Z., Mi, W., Zhao, Y., Li, M., et al. (2019). Catalpol ameliorates podocyte injury by stabilizing cytoskeleton and enhancing autophagy in diabetic nephropathy. *Front. Pharmacol.* 10, 1477. doi:10.3389/fphar.2019.01477

Chen, J., Yang, Y., Lv, Z., Shu, A., Du, Q., Wang, W., et al. (2020). Study on the inhibitive effect of Catalpol on diabetic nephropathy. *Life Sci.* 257, 118120. doi:10.1016/j.lfs.2020.118120

Chen, Y., Chen, J., Jiang, M., Fu, Y., Zhu, Y., Jiao, N., et al. (2020). Loganin and catalpol exert cooperative ameliorating effects on podocyte apoptosis upon diabetic nephropathy by targeting AGEs-RAGE signaling. *Life Sci.* 252, 117653. doi:10.1016/j.lfs.2020.117653

Chen, Q., Ren, D., Wu, J., Yu, H., Chen, X., Wang, J., et al. (2021). Shenyan Kangfu tablet alleviates diabetic kidney disease through attenuating inflammation and modulating the gut microbiota. *J. Nat. Med.* 75 (1), 84–98. doi:10.1007/s11418-020-01452-3

Cherney, D. Z. I., Zinman, B., Inzucchi, S. E., Koitka-Weber, A., Mattheus, M., von Eynatten, M., et al. (2017). Effects of empagliflozin on the urinary albumin-to-creatinine ratio in patients with type 2 diabetes and established cardiovascular disease: an exploratory analysis from the EMPA-REG OUTCOME randomised, placebo-controlled trial. *Lancet. Diabetes Endocrinol.* 5 (8), 610–621. doi:10.1016/s2213-8587(17)30182-1

Choi, S. Y., Lee-Kwon, W., and Kwon, H. M. (2020). The evolving role of TonEBP as an immunometabolic stress protein. *Nat. Rev. Nephrol.* 16 (6), 352–364. doi:10.1038/s41581-020-0261-1

Chou, C. H., Chuang, L. Y., Lu, C. Y., and Guh, J. Y. (2013). Interaction between TGF-β and ACE2-Ang-(1-7)-Mas pathway in high glucose-cultured NRK-52E cells. *Mol. Cell. Endocrinol.* 366 (1), 21–30. doi:10.1016/j.mce.2012.11.004

Chuang, S. M., Lee, C. C., Lo, W. Y., and Hsieh, C. L. (2020). Effect of acupressure at Sanyinjiao on albuminuria in patients with early diabetic nephropathy: A single-blind, randomized, controlled preliminary study. *Explore (NY)* 16 (3), 165–169. doi:10.1016/j.explore.2019.09.001

Crajoinas, R. O., Oricchio, F. T., Pessoa, T. D., Pacheco, B. P., Lessa, L. M., Malnic, G., et al. (2011). Mechanisms mediating the diuretic and natriuretic actions of the incretin hormone glucagon-like peptide-1. *Am. J. Physiol. Ren. Physiol.* 301 (2), F355–F363. doi:10.1152/ajprenal.00729.2010

Ding, X., Zhao, H., and Qiao, C. (2022). Icariin protects podocytes from NLRP3 activation by Sesn2-induced mitophagy through the Keap1-Nrf2/HO-1 axis in diabetic nephropathy. *Phytomedicine.* 99, 154005. doi:10.1016/j.phymed.2022.154005

Feng, H., Zhu, X., Tang, Y., Fu, S., Kong, B., and Liu, X. (2021). Astragaloside IV ameliorates diabetic nephropathy in db/db mice by inhibiting NLRP3 inflammasome-mediated inflammation. *Int. J. Mol. Med.* 48 (2), 164. doi:10.3892/ijmm.2021.4996

Filippatos, G., Anker, S. D., Agarwal, R., Pitt, B., Ruilope, L. M., Rossing, P., et al. (2021). Finerenone and cardiovascular outcomes in patients with chronic kidney disease and type 2 diabetes. *Circulation* 143 (6), 540–552. doi:10.1161/circulationaha.120.051898

Fried, L. F., Emanuele, N., Zhang, J. H., Brophy, M., Conner, T. A., Duckworth, W., et al. (2013). Combined angiotensin inhibition for the treatment of diabetic nephropathy. *N. Engl. J. Med.* 369 (20), 1892–1903. doi:10.1056/NEJMoa1303154

Fujita, H., Morii, T., Fujishima, H., Sato, T., Shimizu, T., Hosoba, M., et al. (2014). The protective roles of GLP-1R signaling in diabetic nephropathy: Possible mechanism and therapeutic potential. *Kidney Int.* 85 (3), 579–589. doi:10.1038/ki.2013.427

Gao, J., Liu, P., Shen, Z., Xu, K., Wu, C., Tian, F., et al. (2021). Morroniside promotes PGC-1α-mediated cholesterol efflux in sodium palmitate or high glucose-induced mouse renal tubular epithelial cells. *Biomed. Res. Int.* 2021, 9942152. doi:10.1155/2021/9942152

Gao, Y., Yang, R., Guo, L., Wang, Y., Liu, W. J., Ai, S., et al. (2021). Qing-Re-Xiao-Zheng formula modulates gut microbiota and inhibits inflammation in mice with diabetic kidney disease. *Front. Med.* 8, 719950. doi:10.3389/fmed.2021.719950

Ge, Y., Xie, H., Li, S., Jin, B., Hou, J., Zhang, H., et al. (2013). Treatment of diabetic nephropathy with tripterygium wilfordii Hook F extract: a prospective, randomized, controlled clinical trial. *J. Transl. Med.* 11, 134. doi:10.1186/1479-5876-11-134

Gerstein, H. C., Colhoun, H. M., Dagenais, G. R., Diaz, R., Lakshmanan, M., Pais, P., et al. (2019). Dulaglutide and cardiovascular outcomes in type 2 diabetes (REWIND): a double-blind, randomised placebo-controlled trial. *Lancet* 394 (10193), 121–130. doi:10.1016/s0140-6736(19)31149-3

Ghasemi, H., Einollahi, B., Kheiripour, N., Hosseini-Zijoud, S. R., and Farhadian Nezhad, M. (2019). Protective effects of curcumin on diabetic nephropathy via attenuation of kidney injury molecule 1 (KIM-1) and neutrophil gelatinase-associated lipocalin (NGAL) expression and alleviation of oxidative stress in rats with type 1 diabetes. *Iran. J. Basic Med. Sci.* 22 (4), 376–383. doi:10.22038/ijbms.2019.31922.7674

Guo, Y., Ran, Z., Zhang, Y., Song, Z., Wang, L., Yao, L., et al. (2020). Marein ameliorates diabetic nephropathy by inhibiting renal sodium glucose transporter 2 and activating the AMPK signaling pathway in db/db mice and high glucose-treated HK-2 cells. *Biomed. Pharmacother.* 131, 110684. doi:10.1016/j.biopha.2020.110684

He, J. Y., Hong, Q., Chen, B. X., Cui, S. Y., Liu, R., Cai, G. Y., et al. (2022). Ginsenoside Rb1 alleviates diabetic kidney podocyte injury by inhibiting aldose reductase activity. *Acta Pharmacol. Sin.* 43 (2), 342–353. doi:10.1038/s41401-021-00788-0

Heerspink, H. J. L., Parving, H. H., Andress, D. L., Bakris, G., Correa-Rotter, R., Hou, F. F., et al. (2019). Atrasentan and renal events in patients with type 2 diabetes and chronic kidney disease (SONAR): a double-blind, randomised, placebo-controlled trial. *Lancet* 393 (10184), 1937–1947. doi:10.1016/s0140-6736(19)30772-x

Hernandez, A. F., Green, J. B., Janmohamed, S., D'Agostino, R. B., Sr., Granger, C. B., et al. (2018). Albiglutide and cardiovascular outcomes in patients with type 2 diabetes and cardiovascular disease (harmony outcomes): a double-blind, randomised placebo-controlled trial. *Lancet* 392 (10157), 1519–1529. doi:10.1016/s0140-6736(18)32261-x

Hong, J. N., Li, W. W., Wang, L. L., Guo, H., Jiang, Y., Gao, Y. J., et al. (2017). Jiangtang decoction ameliorate diabetic nephropathy through the regulation of PI3K/Akt-mediated NF-κB pathways in KK-Ay mice. *Chin. Med.* 12, 13. doi:10.1186/s13020-017-0134-0

Hua, Q., Han, Y., Zhao, H., Zhang, H., Yan, B., Pei, S., et al. (2022). Punicalagin alleviates renal injury via the gut-kidney axis in high-fat diet-induced diabetic mice. *Food Funct.* 13 (2), 867–879. doi:10.1039/d1fo03343c

Jia, Z., Wang, K., Zhang, Y., Duan, Y., Xiao, K., Liu, S., et al. (2021). Icariin ameliorates diabetic renal tubulointerstitial fibrosis by restoring autophagy via regulation of the miR-192-5p/GLP-1R pathway. *Front. Pharmacol.* 12, 720387. doi:10.3389/fphar.2021.720387

Kalantar-Zadeh, K., Jafar, T. H., Nitsch, D., Neuen, B. L., and Perkovic, V. (2021). Chronic kidney disease. *Lancet* 398 (10302), 786–802. doi:10.1016/s0140-6736(21)00519-5

Ke, G., Chen, X., Liao, R., Xu, L., Zhang, L., Zhang, H., et al. (2021). Receptor activator of NF-κB mediates podocyte injury in diabetic nephropathy. *Kidney Int.* 100 (2), 377–390. doi:10.1016/j.kint.2021.04.036

Kikuchi, K., Saigusa, D., Kanemitsu, Y., Matsumoto, Y., Thanai, P., Suzuki, N., et al. (2019). Gut microbiome-derived phenyl sulfate contributes to albuminuria in diabetic kidney disease. *Nat. Commun.* 10 (1), 1835. doi:10.1038/s41467-019-09735-4

Kohan, D. E., Lambers Heerspink, H. J., Coll, B., Andress, D., Brennan, J. J., Kitzman, D. W., et al. (2015). Predictors of atrasentan-associated fluid retention and change in albuminuria in patients with diabetic nephropathy. *Clin. J. Am. Soc. Nephrol.* 10 (9), 1568–1574. doi:10.2215/cjn.00570115

Koye, D. N., Magliano, D. J., Nelson, R. G., and Pavkov, M. E. (2018). The global epidemiology of diabetes and kidney disease. *Adv. Chronic Kidney Dis.* 25 (2), 121–132. doi:10.1053/j.ackd.2017.10.011

Kristensen, S. L., Rørth, R., Jhund, P. S., Docherty, K. F., Sattar, N., Preiss, D., et al. (2019). Cardiovascular, mortality, and kidney outcomes with GLP-1 receptor agonists in patients with type 2 diabetes: a systematic review and meta-analysis of cardiovascular outcome trials. *Lancet. Diabetes Endocrinol.* 7 (10), 776–785. doi:10.1016/s2213-8587(19)30249-9

Lengnan, X., Ban, Z., Haitao, W., Lili, L., Aiqun, C., Huan, W., et al. (2020). Tripterygium wilfordii Hook F treatment for stage IV diabetic nephropathy: Protocol for a prospective, randomized controlled trial. *Biomed. Res. Int.* 2020, 9181037. doi:10.1155/2020/9181037

Li, S. Y., and Susztak, K. (2016). The long noncoding RNA Tug1 connects metabolic changes with kidney disease in podocytes. *J. Clin. Invest.* 126 (11), 4072–4075. doi:10.1172/jci90828

Li, P., Chen, Y., Liu, J., Hong, J., Deng, Y., Yang, F., et al. (2015). Efficacy and safety of tangshen formula on patients with type 2 diabetic kidney disease: a multicenter double-blinded randomized placebo-controlled trial. *PLoS One* 10 (5), e0126027. doi:10.1371/journal.pone.0126027

Li, N., Zhao, T., Cao, Y., Zhang, H., Peng, L., Wang, Y., et al. (2020). Tangshen formula attenuates diabetic kidney injury by imparting anti-pyroptotic effects via the TXNIP-NLRP3-GSDMD Axis. *Front. Pharmacol.* 11, 623489. doi:10.3389/fphar.2020.623489

Li, Y., Guo, S., Yang, F., Liu, L., and Chen, Z. (2021). Huayu Tongluo recipe attenuates renal oxidative stress and inflammation through the activation of AMPK/Nrf2 signaling pathway in streptozotocin- (STZ-) induced diabetic rats. *Evid. Based. Complement. Altern. Med.* 2021, 5873007. doi:10.1155/2021/5873007

Lian, Y., Zhu, M., Chen, J., Yang, B., Lv, Q., Wang, L., et al. (2021). Characterization of a novel polysaccharide from Moutan Cortex and its ameliorative effect on AGEs-induced diabetic nephropathy. *Int. J. Biol. Macromol.* 176, 589–600. doi:10.1016/j.ijbiomac.2021.02.062

Liao, T., Zhao, K., Huang, Q., Tang, S., Chen, K., Xie, C., et al. (2020). A randomized controlled clinical trial study protocol of Liuwei Dihuang pills in the adjuvant treatment of diabetic kidney disease. *Med. Baltim.* 99 (31), e21137. doi:10.1097/md.0000000000021137

Liles, J. T., Corkey, B. K., Notte, G. T., Budas, G. R., Lansdon, E. B., Hinojosa-Kirschenbaum, F., et al. (2018). ASK1 contributes to fibrosis and dysfunction in models of kidney disease. *J. Clin. Invest.* 128 (10), 4485–4500. doi:10.1172/jci99768

Lin, W., Liu, G., Kang, X., Guo, P., Shang, Y., Du, R., et al. (2021). Ellagic acid inhibits high glucose-induced injury in rat mesangial cells via the PI3K/Akt/FOXO3a signaling pathway. *Exp. Ther. Med.* 22 (3), 1017. doi:10.3892/etm.2021.10449

Linh, H. T., Iwata, Y., Senda, Y., Sakai-Takemori, Y., Nakade, Y., Oshima, M., et al. (2022). Intestinal bacterial translocation contributes to diabetic kidney disease. *J. Am. Soc. Nephrol.* 33, 1105–1119. doi:10.1681/asn.2021060843

Liu, P., Peng, L., Zhang, H., Tang, P. M., Zhao, T., Yan, M., et al. (2018). Tangshen formula attenuates diabetic nephropathy by promoting ABCA1-mediated renal cholesterol efflux in db/db mice. *Front. Physiol.* 9, 343. doi:10.3389/fphys.2018.00343

Liu, Q., Lv, S., Liu, J., Liu, S., Wang, Y., and Liu, G. (2020). Mesenchymal stem cells modified with angiotensin-converting enzyme 2 are superior for amelioration of glomerular fibrosis in diabetic nephropathy. *Diabetes Res. Clin. Pract.* 162, 108093. doi:10.1016/j.diabres.2020.108093

Liu, X., Lu, J., Liu, S., Huang, D., Chen, M., Xiong, G., et al. (2020). Huangqi-Danshen decoction alleviates diabetic nephropathy in db/db mice by inhibiting PINK1/Parkin-mediated mitophagy. *Am. J. Transl. Res.* 12 (3), 989–998.

Liu, P., Zhang, J., Wang, Y., Shen, Z., Wang, C., Chen, D. Q., et al. (2021). The active compounds and therapeutic target of tripterygium wilfordii Hook. f. in attenuating proteinuria in diabetic nephropathy: A review. *Front. Med.* 8, 747922. doi:10.3389/fmed.2021.747922

Liu, W., Liang, L., Zhang, Q., Li, Y., Yan, S., Tang, T., et al. (2021). Effects of andrographolide on renal tubulointerstitial injury and fibrosis. Evidence of its mechanism of action. *Phytomedicine.* 91, 153650. doi:10.1016/j.phymed.2021.153650

Liu, J., Gao, L. D., Fu, B., Yang, H. T., Zhang, L., Che, S. Q., et al. (2022). Efficacy and safety of Zicuiyin decoction on diabetic kidney disease: A multicenter, randomized controlled trial. *Phytomedicine.* 100, 154079. doi:10.1016/j.phymed.2022.154079

Liu, P., Zhang, J., Wang, Y., Wang, C., Qiu, X., and Chen, D. Q. (2022). Natural products against renal fibrosis via modulation of SUMOylation. *Front. Pharmacol.* 13, 800810. doi:10.3389/fphar.2022.800810

Long, J., Badal, S. S., Ye, Z., Wang, Y., Ayanga, B. A., Galvan, D. L., et al. (2016). Long noncoding RNA Tug1 regulates mitochondrial bioenergetics in diabetic nephropathy. *J. Clin. Invest.* 126 (11), 4205–4218. doi:10.1172/jci87927

Lu, M., Yin, N., Liu, W., Cui, X., Chen, S., and Wang, E. (2017). Curcumin ameliorates diabetic nephropathy by suppressing NLRP3 inflammasome signaling. *Biomed. Res. Int.* 2017, 1516985. doi:10.1155/2017/1516985

Lu, Q., Li, C., Chen, W., Shi, Z., Zhan, R., and He, R. (2018). Clinical efficacy of Jinshuibao capsules combined with angiotensin receptor blockers in patients with early diabetic nephropathy: A meta-analysis of randomized controlled trials. *Evid. Based. Complement. Altern. Med.* 2018, 6806943. doi:10.1155/2018/6806943

Luo, Y., Yang, S. K., Zhou, X., Wang, M., Tang, D., Liu, F. Y., et al. (2015). Use of Ophiocordyceps sinensis (syn. Cordyceps sinensis) combined with angiotensin-converting enzyme inhibitors (ACEI)/angiotensin receptor blockers (ARB) versus ACEI/ARB alone in the treatment of diabetic kidney disease: a meta-analysis. *Ren. Fail.* 37 (4), 614–634. doi:10.3109/0886022x.2015.1009820

Ma, T., Zheng, Z., Guo, H., Lian, X., Rane, M. J., Cai, L., et al. (2019). 4-O-methylhonokiol ameliorates type 2 diabetes-induced nephropathy in mice likely by activation of AMPK-mediated fatty acid oxidation and Nrf2-mediated anti-oxidative stress. *Toxicol. Appl. Pharmacol.* 370, 93–105. doi:10.1016/j.taap.2019.03.007

Ma, L., Wu, F., Shao, Q., Chen, G., Xu, L., and Lu, F. (2021). Baicalin alleviates oxidative stress and inflammation in diabetic nephropathy via Nrf2 and MAPK signaling pathway. *Drug Des. devel. Ther.* 15, 3207–3221. doi:10.2147/dddt.S319260

Malek, V., Suryavanshi, S. V., Sharma, N., Kulkarni, Y. A., Mulay, S. R., and Gaikwad, A. B. (2021). Potential of renin-angiotensin-aldosterone system modulations in diabetic kidney disease: Old players to new hope. *Rev. Physiol. Biochem. Pharmacol.* 179, 31–71. doi:10.1007/112_2020_50

Marques, C., Gonçalves, A., Pereira, P. M. R., Almeida, D., Martins, B., Fontes-Ribeiro, C., et al. (2019). The dipeptidyl peptidase 4 inhibitor sitagliptin improves oxidative stress and ameliorates glomerular lesions in a rat model of type 1 diabetes. *Life Sci.* 234, 116738. doi:10.1016/j.lfs.2019.116738

Müller, T. D., Finan, B., Bloom, S. R., D'Alessio, D., Drucker, D. J., Flatt, P. R., et al. (2019). Glucagon-like peptide 1 (GLP-1). *Mol. Metab.* 30, 72–130. doi:10.1016/j.molmet.2019.09.010

Parving, H. H., Brenner, B. M., McMurray, J. J., de Zeeuw, D., Haffner, S. M., Solomon, S. D., et al. (2012). Cardiorenal end points in a trial of aliskiren for type 2 diabetes. *N. Engl. J. Med.* 367 (23), 2204–2213. doi:10.1056/NEJMoa1208799

Peng, C. H., Lin, H. C., Lin, C. L., Wang, C. J., and Huang, C. N. (2019). Abelmoschus esculentus subfractions improved nephropathy with regulating dipeptidyl peptidase-4 and type 1 glucagon-like peptide receptor in type 2 diabetic rats. *J. Food Drug Anal.* 27 (1), 135–144. doi:10.1016/j.jfda.2018.07.004

Pitt, B., Filippatos, G., Agarwal, R., Anker, S. D., Bakris, G. L., Rossing, P., et al. (2021). Cardiovascular events with finerenone in kidney disease and type 2 diabetes. *N. Engl. J. Med.* 385 (24), 2252–2263. doi:10.1056/NEJMoa2110956

Qi, M. Y., He, Y. H., Cheng, Y., Fang, Q., Ma, R. Y., Zhou, S. J., et al. (2021). Icariin ameliorates streptozocin-induced diabetic nephropathy through suppressing the TLR4/NF-κB signal pathway. *Food Funct.* 12 (3), 1241–1251. doi:10.1039/d0fo02335c

Qiao, C., Ye, W., Li, S., Wang, H., and Ding, X. (2018). Icariin modulates mitochondrial function and apoptosis in high glucose-induced glomerular podocytes through G protein-coupled estrogen receptors. *Mol. Cell. Endocrinol.* 473, 146–155. doi:10.1016/j.mce.2018.01.014

Qin, X., Zhao, Y., Gong, J., Huang, W., Su, H., Yuan, F., et al. (2019). Berberine protects glomerular podocytes via inhibiting drp1-mediated mitochondrial fission and dysfunction. *Theranostics* 9 (6), 1698–1713. doi:10.7150/thno.30640

Qin, X., Jiang, M., Zhao, Y., Gong, J., Su, H., Yuan, F., et al. (2020). Berberine protects against diabetic kidney disease via promoting PGC-1α-regulated mitochondrial energy homeostasis. *Br. J. Pharmacol.* 177 (16), 3646–3661. doi:10.1111/bph.14935

Ren, D., Zuo, C., and Xu, G. (2019). Clinical efficacy and safety of tripterygium wilfordii Hook in the treatment of diabetic kidney disease stage IV: A meta-analysis of randomized controlled trials. *Med. Baltim.* 98 (11), e14604. doi:10.1097/md.0000000000014604

Rong, Q., Han, B., Li, Y., Yin, H., Li, J., and Hou, Y. (2021). Berberine reduces lipid accumulation by promoting fatty acid oxidation in renal tubular epithelial cells of the diabetic kidney. *Front. Pharmacol.* 12, 729384. doi:10.3389/fphar.2021.729384

Shu, A., Du, Q., Chen, J., Gao, Y., Zhu, Y., Lv, G., et al. (2021). Catalpol ameliorates endothelial dysfunction and inflammation in diabetic nephropathy via suppression of RAGE/RhoA/ROCK signaling pathway. *Chem. Biol. Interact.* 348, 109625. doi:10.1016/j.cbi.2021.109625

Stuart, D., Chapman, M., Rees, S., Woodward, S., and Kohan, D. E. (2013). Myocardial, smooth muscle, nephron, and collecting duct gene targeting reveals the organ sites of endothelin A receptor antagonist fluid retention. *J. Pharmacol. Exp. Ther.* 346 (2), 182–189. doi:10.1124/jpet.113.205286

Su, J., Gao, C., Xie, L., Fan, Y., Shen, Y., Huang, Q., et al. (2021). Astragaloside II ameliorated podocyte injury and mitochondrial dysfunction in streptozotocin-induced diabetic rats. *Front. Pharmacol.* 12, 638422. doi:10.3389/fphar.2021.638422

Su, X., Yu, W., Liu, A., Wang, C., Li, X., Gao, J., et al. (2021). San-huang-yi-shen capsule ameliorates diabetic nephropathy in rats through modulating the gut microbiota and overall metabolism. *Front. Pharmacol.* 12, 808867. doi:10.3389/fphar.2021.808867

Tang, G., Li, S., Zhang, C., Chen, H., Wang, N., and Feng, Y. (2021). Clinical efficacies, underlying mechanisms and molecular targets of Chinese medicines for diabetic nephropathy treatment and management. *Acta Pharm. Sin. B* 11 (9), 2749–2767. doi:10.1016/j.apsb.2020.12.020

Tang, D., He, W. J., Zhang, Z. T., Shi, J. J., Wang, X., Gu, W. T., et al. (2022). Protective effects of Huang-Lian-Jie-Du Decoction on diabetic nephropathy through regulating AGEs/RAGE/Akt/Nrf2 pathway and metabolic profiling in db/db mice. *Phytomedicine.* 95, 153777. doi:10.1016/j.phymed.2021.153777

Thomas, M. C., Brownlee, M., Susztak, K., Sharma, K., Jandeleit-Dahm, K. A., Zoungas, S., et al. (2015). Diabetic kidney disease. *Nat. Rev. Dis. Prim.* 1, 15018. doi:10.1038/nrdp.2015.18

Tian, J., Zhao, L., Zhou, Q., Liu, W., Chen, X., Lian, F., et al. (2015). Efficacy of Shenzhuo formula on diabetic kidney disease: a retrospective study. *J. Tradit. Chin. Med.* 35 (5), 528–536. doi:10.1016/s0254-6272(15)30135-7

Tonneijck, L., Muskiet, M. H., Smits, M. M., van Bommel, E. J., Heerspink, H. J., van Raalte, D. H., et al. (2017). Glomerular hyperfiltration in diabetes: Mechanisms, clinical significance, and treatment. *J. Am. Soc. Nephrol.* 28 (4), 1023–1039. doi:10.1681/asn.2016060666

Trembinski, D. J., Bink, D. I., Theodorou, K., Sommer, J., Fischer, A., van Bergen, A., et al. (2020). Aging-regulated anti-apoptotic long non-coding RNA Sarrah augments recovery from acute myocardial infarction. *Nat. Commun.* 11 (1), 2039. doi:10.1038/s41467-020-15995-2

Wang, Z. S., Gao, F., and Lu, F. E. (2013). Effect of ethanol extract of Rhodiola rosea on the early nephropathy in type 2 diabetic rats. *J. Huazhong Univ. Sci. Technol. Med. Sci.* 33 (3), 375–378. doi:10.1007/s11596-013-1127-6

Wang, S., Zhao, X., Yang, S., Chen, B., and Shi, J. (2017). Salidroside alleviates high glucose-induced oxidative stress and extracellular matrix accumulation in rat glomerular mesangial cells by the TXNIP-NLRP3 inflammasome pathway. *Chem. Biol. Interact.* 278, 48–53. doi:10.1016/j.cbi.2017.10.012

Wang, C., Li, L., Liu, S., Liao, G., Li, L., Chen, Y., et al. (2018). GLP-1 receptor agonist ameliorates obesity-induced chronic kidney injury via restoring renal metabolism homeostasis. *PLoS One* 13 (3), e0193473. doi:10.1371/journal.pone.0193473

Wang, Q., Zhou, J., Xiang, Z., Tong, Q., Pan, J., Wan, L., et al. (2019). Anti-diabetic and renoprotective effects of Cassiae Semen extract in the streptozotocin-induced diabetic rats. *J. Ethnopharmacol.* 239, 111904. doi:10.1016/j.jep.2019.111904

Wang, K., Zheng, X., Pan, Z., Yao, W., Gao, X., Wang, X., et al. (2020). Icariin prevents extracellular matrix accumulation and ameliorates experimental diabetic kidney disease by inhibiting oxidative stress via GPER mediated p62-dependent Keap1 degradation and Nrf2 activation. *Front. Cell Dev. Biol.* 8, 559. doi:10.3389/fcell.2020.00559

Wanner, C., Inzucchi, S. E., Lachin, J. M., Fitchett, D., von Eynatten, M., Mattheus, M., et al. (2016). Empagliflozin and progression of kidney disease in type 2 diabetes. *N. Engl. J. Med.* 375 (4), 323–334. doi:10.1056/NEJMoa1515920

Warren, A. M., Knudsen, S. T., and Cooper, M. E. (2019). Diabetic nephropathy: an insight into molecular mechanisms and emerging therapies. *Expert Opin. Ther. Targets* 23 (7), 579–591. doi:10.1080/14728222.2019.1624721

Wei, H., Wang, L., An, Z., Xie, H., Liu, W., Du, Q., et al. (2021). QiDiTangShen granules modulated the gut microbiome composition and improved bile acid profiles in a mouse model of diabetic nephropathy. *Biomed. Pharmacother.* 133, 111061. doi:10.1016/j.biopha.2020.111061

Winther, S. A., Øllgaard, J. C., Tofte, N., Tarnow, L., Wang, Z., Ahluwalia, T. S., et al. (2019). Utility of plasma concentration of trimethylamine N-oxide in predicting cardiovascular and renal complications in individuals with type 1 diabetes. *Diabetes Care* 42 (8), 1512–1520. doi:10.2337/dc19-0048

Winther, S. A., Henriksen, P., Vogt, J. K., Hansen, T. H., Ahonen, L., Suvitaival, T., et al. (2020). Gut microbiota profile and selected plasma metabolites in type 1 diabetes without and with stratification by albuminuria. *Diabetologia* 63 (12), 2713–2724. doi:10.1007/s00125-020-05260-y

Wu, D., Yang, X., Zheng, T., Xing, S., Wang, J., Chi, J., et al. (2016). A novel mechanism of action for salidroside to alleviate diabetic albuminuria: effects on albumin transcytosis across glomerular endothelial cells. *Am. J. Physiol. Endocrinol. Metab.* 310 (3), E225–E237. doi:10.1152/ajpendo.00391.2015

Wu, X., Huang, Y., Zhang, Y., He, C., Zhao, Y., Wang, L., et al. (2020). Efficacy of tripterygium glycosides combined with ARB on diabetic nephropathy: a meta-analysis. *Biosci. Rep.* 40 (11), BSR20202391. doi:10.1042/bsr20202391

Xia, X., Wang, X., Wang, H., Lin, Z., Shao, K., Xu, J., et al. (2021). Ameliorative effect of white tea from 50-year-old tree of Camellia sinensis L. (Theaceae) on kidney damage in diabetic mice via SIRT1/AMPK pathway. *J. Ethnopharmacol.* 272, 113919. doi:10.1016/j.jep.2021.113919

Xie, T., Chen, X., Chen, W., Huang, S., Peng, X., Tian, L., et al. (2021). Curcumin is a potential adjuvant to alleviates diabetic retinal injury via reducing oxidative stress and maintaining Nrf2 pathway homeostasis. *Front. Pharmacol.* 12, 796565. doi:10.3389/fphar.2021.796565

Xing, L., Fang, J., Zhu, B., Wang, L., Chen, J., Wang, Y., et al. (2021). Astragaloside IV protects against podocyte apoptosis by inhibiting oxidative stress via activating PPARγ-Klotho-FoxO1 axis in diabetic nephropathy. *Life Sci.* 269, 119068. doi:10.1016/j.lfs.2021.119068

Xu, J., Liu, L., Gan, L., Hu, Y., Xiang, P., Xing, Y., et al. (2021). Berberine acts on C/EBPβ/lncRNA gas5/miR-18a-5p loop to decrease the mitochondrial ROS generation in HK-2 cells. *Front. Endocrinol.* 12, 675834. doi:10.3389/fendo.2021.675834

Xu, W. L., Liu, S., Li, N., Ye, L. F., Zha, M., Li, C. Y., et al. (2021). Quercetin antagonizes glucose fluctuation induced renal injury by inhibiting aerobic glycolysis via HIF-1α/miR-210/ISCU/FeS pathway. *Front. Med.* 8, 656086. doi:10.3389/fmed.2021.656086

Xuan, C., Xi, Y. M., Zhang, Y. D., Tao, C. H., Zhang, L. Y., and Cao, W. F. (2021). Yiqi Jiedu Huayu decoction alleviates renal injury in rats with diabetic nephropathy by promoting autophagy. *Front. Pharmacol.* 12, 624404. doi:10.3389/fphar.2021.624404

Xue, H., Li, P., Luo, Y., Wu, C., Liu, Y., Qin, X., et al. (2019). Salidroside stimulates the Sirt1/PGC-1α axis and ameliorates diabetic nephropathy in mice. *Phytomedicine* 54, 240–247. doi:10.1016/j.phymed.2018.10.031

Yale, J. F., Bakris, G., Cariou, B., Yue, D., David-Neto, E., Xi, L., et al. (2013). Efficacy and safety of canagliflozin in subjects with type 2 diabetes and chronic kidney disease. *Diabetes Obes. Metab.* 15 (5), 463–473. doi:10.1111/dom.12090

Yale, J. F., Bakris, G., Cariou, B., Nieto, J., David-Neto, E., Yue, D., et al. (2014). Efficacy and safety of canagliflozin over 52 weeks in patients with type 2 diabetes mellitus and chronic kidney disease. *Diabetes Obes. Metab.* 16 (10), 1016–1027. doi:10.1111/dom.12348

Yamada, T., Wakabayashi, M., Bhalla, A., Chopra, N., Miyashita, H., Mikami, T., et al. (2021). Cardiovascular and renal outcomes with SGLT-2 inhibitors versus GLP-1 receptor agonists in patients with type 2 diabetes mellitus and chronic kidney disease: a systematic review and network meta-analysis. *Cardiovasc. Diabetol.* 20 (1), 14. doi:10.1186/s12933-020-01197-z

Yan, M., Wen, Y., Yang, L., Wu, X., Lu, X., Zhang, B., et al. (2016). Chinese herbal medicine tangshen formula treatment of patients with type 2 diabetic kidney disease with macroalbuminuria: Study protocol for a randomized controlled trial. *Trials* 17 (1), 259. doi:10.1186/s13063-016-1385-2

Yang, X., Zhang, B., Lu, X., Yan, M., Wen, Y., Zhao, T., et al. (2016). Effects of tangshen formula on urinary and plasma liver-type fatty acid binding protein levels in patients with type 2 diabetic kidney disease: Post-hoc findings from a multi-center, randomized, double-blind, placebo-controlled trial investigating the efficacy and safety of tangshen formula in patients with type 2 diabetic kidney disease. *BMC Complement. Altern. Med.* 16, 246. doi:10.1186/s12906-016-1228-4

Yang, X. H., Pan, Y., Zhan, X. L., Zhang, B. L., Guo, L. L., and Jin, H. M. (2016). Epigallocatechin-3-gallate attenuates renal damage by suppressing oxidative stress in diabetic db/db mice. *Oxid. Med. Cell. Longev.* 2016, 2968462. doi:10.1155/2016/2968462

Yang, X., Hu, C., Wang, S., and Chen, Q. (2020). Clinical efficacy and safety of Chinese herbal medicine for the treatment of patients with early diabetic nephropathy: A protocol for systematic review and meta-analysis. *Med. Baltim.* 99 (29), e20678. doi:10.1097/md.0000000000020678

Yang, G., Wei, J., Liu, P., Zhang, Q., Tian, Y., Hou, G., et al. (2021). Role of the gut microbiota in type 2 diabetes and related diseases. *Metabolism.* 117, 154712. doi:10.1016/j.metabol.2021.154712

Yao, L., Li, J., Li, L., Li, X., Zhang, R., Zhang, Y., et al. (2019). Coreopsis tinctoria Nutt ameliorates high glucose-induced renal fibrosis and inflammation via the TGF-β1/SMADS/AMPK/NF-κB pathways. *BMC Complement. Altern. Med.* 19 (1), 14. doi:10.1186/s12906-018-2410-7

Yu, S., Zhao, H., Yang, W., Amat, R., Peng, J., Li, Y., et al. (2019). The alcohol extract of Coreopsis tinctoria Nutt ameliorates diabetes and diabetic nephropathy in db/db mice through miR-192/miR-200b and PTEN/AKT and ZEB2/ECM pathways. *Biomed. Res. Int.* 2019, 5280514. doi:10.1155/2019/5280514

Zang, Y., Liu, S., Cao, A., Shan, X., Deng, W., Li, Z., et al. (2021). Astragaloside IV inhibits palmitic acid-induced apoptosis through regulation of calcium homeostasis in mice podocytes. *Mol. Biol. Rep.* 48 (2), 1453–1464. doi:10.1007/s11033-021-06204-4

Zang, L., Gao, F., Huang, A., Zhang, Y., Luo, Y., Chen, L., et al. (2022). Icariin inhibits epithelial mesenchymal transition of renal tubular epithelial cells via regulating the miR-122-5p/FOXP2 axis in diabetic nephropathy rats. *J. Pharmacol. Sci.* 148 (2), 204–213. doi:10.1016/j.jphs.2021.10.002

Zhang, L., Li, P., Xing, C. Y., Zhao, J. Y., He, Y. N., Wang, J. Q., et al. (2014). Efficacy and safety of Abelmoschus manihot for primary glomerular disease: a prospective, multicenter randomized controlled clinical trial. *Am. J. Kidney Dis.* 64 (1), 57–65. doi:10.1053/j.ajkd.2014.01.431

Zhang, J., Cao, P., Gui, J., Wang, X., Han, J., Wang, Y., et al. (2019). Arctigenin ameliorates renal impairment and inhibits endoplasmic reticulum stress in diabetic db/db mice. *Life Sci.* 223, 194–201. doi:10.1016/j.lfs.2019.03.037

Zhang, L., Yang, L., Shergis, J., Zhang, L., Zhang, A. L., Guo, X., et al. (2019). Chinese herbal medicine for diabetic kidney disease: a systematic review and meta-analysis of randomised placebo-controlled trials. *BMJ Open* 9 (4), e025653. doi:10.1136/bmjopen-2018-025653

Zhang, T., Chi, Y., Kang, Y., Lu, H., Niu, H., Liu, W., et al. (2019). Resveratrol ameliorates podocyte damage in diabetic mice via SIRT1/PGC-1α mediated attenuation of mitochondrial oxidative stress. *J. Cell. Physiol.* 234 (4), 5033–5043. doi:10.1002/jcp.27306

Zhang, N. N., Kang, J. S., Liu, S. S., Gu, S. M., Song, Z. P., Li, F. X., et al. (2020). Flavanomarein inhibits high glucose-stimulated epithelial-mesenchymal transition in HK-2 cells via targeting spleen tyrosine kinase. *Sci. Rep.* 10 (1), 439. doi:10.1038/s41598-019-57360-4

Zhang, Q., He, L., Dong, Y., Fei, Y., Wen, J., Li, X., et al. (2020). Sitagliptin ameliorates renal tubular injury in diabetic kidney disease via STAT3-dependent mitochondrial homeostasis through SDF-1α/CXCR4 pathway. *Faseb J.* 34 (6), 7500–7519. doi:10.1096/fj.201903038R

Zhang, Q., Liu, X., Sullivan, M. A., Shi, C., and Deng, B. (2021a). Protective effect of yi shen Pai Du formula against diabetic kidney injury via inhibition of oxidative stress, inflammation, and epithelial-to-mesenchymal transition in db/db mice. *Oxid. Med. Cell. Longev.* 2021, 7958021. doi:10.1155/2021/7958021

Zhang, Q., Zhang, Y., Zeng, L., Chen, G., Zhang, L., Liu, M., et al. (2021b). The role of gut microbiota and microbiota-related serum metabolites in the progression of diabetic kidney disease. *Front. Pharmacol.* 12, 757508. doi:10.3389/fphar.2021.757508

Zhang, M., Yang, L., Zhu, M., Yang, B., Yang, Y., Jia, X., et al. (2022). Moutan Cortex polysaccharide ameliorates diabetic kidney disease via modulating gut microbiota dynamically in rats. *Int. J. Biol. Macromol.* 206, 849–860. doi:10.1016/j.ijbiomac.2022.03.077

Zhao, T., Zhang, H., Yin, X., Zhao, H., Ma, L., Yan, M., et al. (2020). Tangshen formula modulates gut Microbiota and reduces gut-derived toxins in diabetic nephropathy rats. *Biomed. Pharmacother.* 129, 110325. doi:10.1016/j.biopha.2020.110325

Zhao, J., Tostivint, I., Xu, L., Huang, J., Gambotti, L., Boffa, J. J., et al. (2022). Efficacy of combined Abelmoschus manihot and irbesartan for reduction of albuminuria in patients with type 2 diabetes and diabetic kidney disease: A multicenter randomized double-blind parallel controlled clinical trial. *Diabetes Care* 45 (7), e113–e115. doi:10.2337/dc22-0607

Zhong, Y., Lee, K., Deng, Y., Ma, Y., Chen, Y., Li, X., et al. (2019). Arctigenin attenuates diabetic kidney disease through the activation of PP2A in podocytes. *Nat. Commun.* 10 (1), 4523. doi:10.1038/s41467-019-12433-w

Zhou, G., Johansson, U., Peng, X. R., Bamberg, K., and Huang, Y. (2016). An additive effect of eplerenone to ACE inhibitor on slowing the progression of diabetic nephropathy in the db/db mice. *Am. J. Transl. Res.* 8 (3), 1339–1354.

Zhou, J., Pan, J., Xiang, Z., Wang, Q., Tong, Q., Fang, J., et al. (2020). Xiaokeyinshui extract combination, a berberine-containing agent, exerts anti-diabetic and renal protective effects on rats in multi-target mechanisms. *J. Ethnopharmacol.* 262, 113098. doi:10.1016/j.jep.2020.113098

Zhou, Q., Han, C., Wang, Y., Fu, S., Chen, Y., and Chen, Q. (2022). The effect of Chinese medicinal formulas on biomarkers of oxidative stress in STZ-induced diabetic kidney disease rats: A meta-analysis and systematic review. *Front. Med.* 9, 848432. doi:10.3389/fmed.2022.848432

frontiers | Frontiers in Pharmacology

TYPE Original Research
PUBLISHED 22 November 2022
DOI 10.3389/fphar.2022.1018720

OPEN ACCESS

EDITED BY
Swayam Prakash Srivastava,
Yale University, United States

REVIEWED BY
Lin Zhang,
Sichuan University, China
Khadija Banu,
Yale University, United States

*CORRESPONDENCE
Xiaoling Cai,
dr_junel@sina.com
Linong Ji,
jiln@bjmu.edu.cn

†These authors have contributed equally to this work

SPECIALTY SECTION
This article was submitted to Renal Pharmacology,
a section of the journal
Frontiers in Pharmacology

RECEIVED 13 August 2022
ACCEPTED 02 November 2022
PUBLISHED 22 November 2022

CITATION
Hu S, Lin C, Cai X, Zhu X, Lv F, Yang W and Ji L (2022), Disparities in efficacy and safety of sodium-glucose cotransporter 2 inhibitor among patients with different extents of renal dysfunction: A systematic review and meta-analysis of randomized controlled trials.
Front. Pharmacol. 13:1018720.
doi: 10.3389/fphar.2022.1018720

Disparities in efficacy and safety of sodium-glucose cotransporter 2 inhibitor among patients with different extents of renal dysfunction: A systematic review and meta-analysis of randomized controlled trials

Suiyuan Hu†, Chu Lin†, Xiaoling Cai*, Xingyun Zhu, Fang Lv, Wenjia Yang and Linong Ji*

Department of Endocrinology and Metabolism, Peking University People's Hospital, Beijing, China

Background: The pleiotropic efficacy of SGLT2is in patients with different eGFR levels has not been well-understood. This systematic review and meta-analysis assessed the disparities in the efficacy and safety of SGLT2i treatment across stratified renal function.

Methods: We searched four databases from inception to December 2021. We included randomized controlled trials (RCTs) with reported baseline eGFR levels and absolute changes from baseline in at least one of the following outcomes: HbA1c, body weight, blood pressure, and eGFR. Continuous outcomes were evaluated as the weighted mean differences (WMDs) and 95% confidence intervals (CIs). Categorical outcomes were evaluated as odds ratios (ORs) and accompanying 95% CIs.

Results: In total, 86 eligible RCTs were included. SGLT2is produces a substantial benefit in glycemic control, weight control, and blood pressure control even in patients with impaired renal function. HbA1c and weight reductions observed in SGLT2i users were generally parallel with the renal function levels, although there was an augmented weight reduction in severe renal dysfunction stratum [HbA1c: −0.49% (−0.58 to −0.39%) for normal renal function, −0.58% (−0.66 to −0.50%) for mild renal function impairment, −0.22% (−0.35 to −0.09%) for moderate renal function impairment, and −0.13% (−0.67 to 0.42%) for severe renal function impairment ($p < 0.001$ for subgroup differences); weight: −2.12 kg (−2.66 to −1.59 kg) for normal renal function, −2.06 kg (−2.31 to −1.82 kg) for mild renal function impairment; −1.23 kg (−1.59 to −0.86 kg) for moderate renal function impairment; −1.88 kg (−3.04 to −0.72 kg) for severe renal function impairment ($p = 0.002$ for subgroup differences)]. However, the blood pressure reduction observed in SGLT2i users was independent of renal function. When compared with the placebo, the occurrence of hypoglycemia was more

frequent in patients with favorable renal function rather than in those with substantial renal dysfunction.

Conclusion: The HbA1c and body weight reductions observed in SGLT2i users were generally parallel with their baseline eGFR levels, while blood pressure reductions in SGLT2i users were independent of their baseline eGFR levels. Consistently, when compared with the placebo, hypoglycemia was more frequent in patients with favorable renal function, where the HbA1c reduction was profound.

KEYWORDS

renal function impairment, sodium-glucose cotransporter 2 (SGLT2) inhibitor, blood glucose, weight, blood pressure, estimated glomerular alteration rate (eGFR)

Introduction

Sodium-glucose cotransporter 2 inhibitors (SGLT2is) have gained extensive attention in recent years as a novel type of anti-hyperglycemic drugs due to their additional cardiovascular and renal benefits beyond blood glucose control (Nair and Wilding, 2010; Bailey, 2011). SGLT2is exert their function by blocking SGLT2, which plays an important role in glucose reabsorption (Vallon and Thomson, 2017).

Available evidence showed that there was a significant difference in urinary glucose excretion (UGE) induced by SGLT2i among patients with different levels of renal function. UGE gradually decreased with worsening renal impairment, indicated by a reduction in the estimated glomerular filtration rate (eGFR). Therefore, it is important to explore whether the benefits of SGLT2 inhibition on blood glucose control, weight and blood pressure reduction, and eGFR preservation are fairly comparable in patients with impaired renal function to those with normal renal function. However, SGLT2is are generally contraindicated in patients with severe renal impairment (eGFR <30 ml/min per 1.73 m^2) due to concerns that SGLT2 inhibition may increase the risk of acute kidney injury (Levey et al., 2011; Scheen, 2015; Zhang et al., 2018; Davidson, 2019). Few studies have assessed the exact role of SGLT2is in patients with different baseline renal function. However, the pleiotropic efficacy and safety outcomes of SGLT2is in patients with different eGFR levels have not been well-characterized. In this systematic review and meta-analysis, we aimed to assess the similarities and disparities regarding the efficacy and safety of SGLT2is across stratified renal function.

Material and methods

Data sources and searches

Conforming to the recommendations from the Cochrane Handbook for Systematic Reviews for meta-analysis, we conducted systematic searches manually in PubMed, Medline, Embase, and Cochrane Central Register of Controlled Trials (CENTRAL) databases. The systematic database research was first conducted in May 2021 and updated in December 2021. We used the following medical subject headings and free-text search terms: SGLT2 inhibitors, canagliflozin, dapagliflozin, empagliflozin, ertugliflozin, ipragliflozin, luseogliflozin, remogliflozin, sotagliflozin, tofogliflozin, and randomized controlled trial (RCT). We also screened references of existing reviews in this field in order to identify every possibly eligible relevant study.

Study selection

Studies were included if they met the following criteria: 1) RCTs of SGLT2i; 2) RCTs with reported baseline eGFR levels and absolute changes from baseline in at least one of the following outcomes: glycated hemoglobin (HbA1c) levels, body weight, blood pressure, and eGFR; 3) studies published in English. There were no restrictions on the length of the follow-up. Two investigators (CL and SH) independently browsed the titles, abstracts, full texts, and supplementary materials of potentially eligible studies. Any disagreements were resolved by consensus with a third investigator (XZ).

Data extraction and quality assessment

Two investigators (CL and SH) used predefined forms to record data from eligible studies, including study characteristics (first author, publication year, study design, sample size, and mean duration of follow-up), participant characteristics (age, sex, duration of diabetes, baseline eGFR, baseline HbA1c level, blood pressure, and body weight), therapeutic intervention (subtypes of SGLT2i and dosages), comparison groups (placebo or active agent control), and outcomes of interest (changes in HbA1c level, body weight, blood pressure, and eGFR in treatment and control groups). Adverse events such as urinary tract infection, genital infection, amputation, hypovolemia, orthostatic

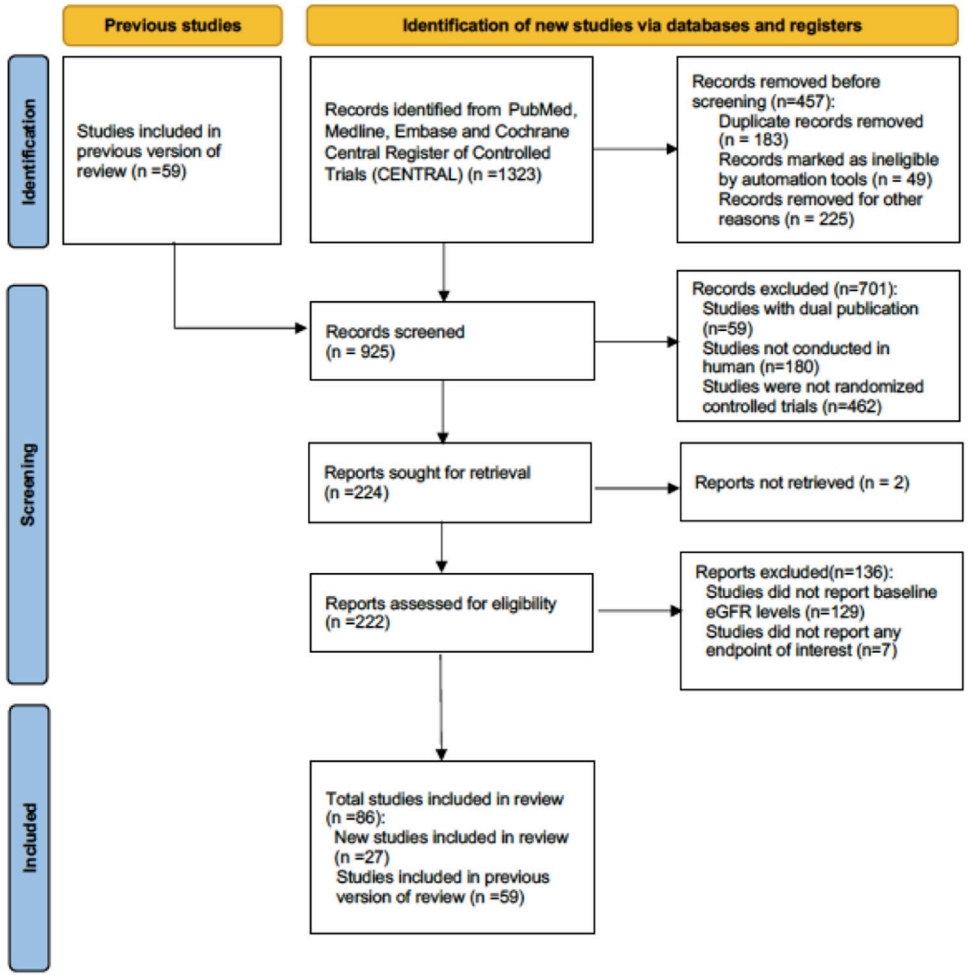

FIGURE 1
Flowchart of the included studies.

hypotension, bone fracture, diabetic ketoacidosis and hypoglycemia were also collected for evaluations of safety as additional outcomes. Study quality was evaluated by using the Cochrane risk of bias tool. A third investigator (FL) checked for the accuracy of the abstractions and study quality evaluation. Any disagreement among investigators would be resolved by consensus.

Data synthesis and analysis

The efficacy outcomes included changes in HbA1c, body weight, systolic and dilated blood pressure, and eGFR. The safety outcomes included the incidence of urinary tract infection, genital infection, amputation, hypovolemia, orthostatic hypotension, bone fracture, diabetic ketoacidosis, and hypoglycemia. Continuous outcomes were evaluated as the weighted mean differences (WMDs) and 95% confidence intervals (CIs). Categorical outcomes were evaluated as odds ratios (ORs) and accompanying 95% CIs. The degree of between-study heterogeneity was evaluated through Higgins I^2 statistics. An I^2 level more than 50% was considered a high level of heterogeneity. A fixed-effect model was used when I^2 <50%, and a random-effect model was used when $I^2 \geq 50\%$. Data were represented graphically in forest plots. Publication bias was assessed using funnel plots.

Subgroup analyses were conducted based on baseline eGFR levels. We divided the enrolled patients into four subgroups with the cut-off values at 90, 60, and 45 ml/min per 1.73 m^2: normal renal function, defined as eGFR ≥90 ml/min/1.73 m^2; mild renal function impairment, defined as 90 > eGFR ≥60 ml/min per 1.73 m^2; moderate renal function impairment, defined as 60 > eGFR ≥45 ml/min per 1.73 m^2; severe renal function impairment, defined as eGFR<45 ml/

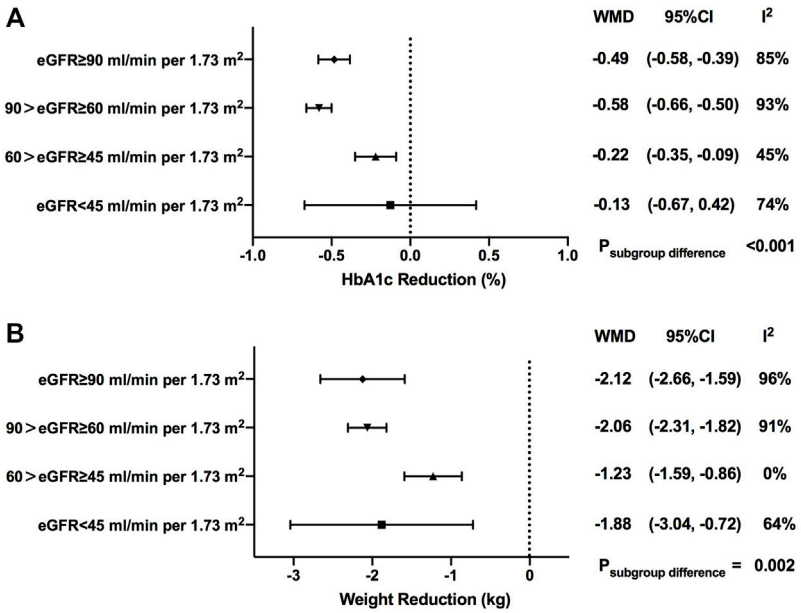

FIGURE 2
HbA1c and weight changes of SGLT2i treatment in patients with different levels of renal function. HbA1c, glycosylated hemoglobin; eGFR, estimated glomerular filtrationrate; WMD, weighted mean differences; 95% CIs, 95% confidence intervals.

min per 1.73 m^2. Meta-analyses were performed by the Review Manager statistical package (version 5.3, Nordic Cochrane Centre, Copenhagen, Denmark) and STATA, version 11.0 (STATA, College Station, TX, United States). A *p*-value less than 0.05 was considered statistically significant for all analyses. This meta-analysis was registered on the PROSPERO platform as CRD42022297648.

Results

Characteristics of included studies

A total of 86 RCTs were included, with 72 placebo-controlled studies and 14 active agent-controlled studies (Figure 1). Eight types of SGLT2is, namely, canagliflozin, dapagliflozin, empagliflozin, ertugliflozin, ipragliflozin, luseogliflozin, sotagliflozin, and tofogliflozin, were assessed. The trial durations ranged from 4 to 135 weeks. Among all included studies, the mean baseline the eGFR ranged from 22.00 to 154.48 ml/min per 1.73 m^2. The numbers of patients with normal renal function, mild renal impairment, moderate renal impairment, and severe renal impairment were 12,069, 37,533, 1,642, and 15,477, respectively. Baseline characteristics of included studies are summarized in Supplementary Table S1. The risk of bias for RCTs was systematically evaluated by the Cochrane tool, and the overall risk of bias and selective reporting was low (Supplementary Table S2). The funnel plots generally displayed even distributions, which indicated no signs of publication bias (Supplementary Figure S1).

Effects of SGLT2is on HbA1c

As shown in our results, greater HbA1c reductions were observed in patients with SGLT2i treatment *versus* control (WMD, -0.53%, 95% CI, -0.59 to -0.47%, $p < 0.001$). When stratified by baseline eGFR levels, it was revealed that the HbA1c reduction effect of SGLT2is was attenuated in patients with worse renal impairment, with -0.49% (-0.58 to -0.39%) in normal renal function, -0.58% (-0.66 to -0.50%) in mild renal function impairment, -0.22% (-0.35 to -0.09%) in moderate renal function impairment, and -0.13% (-0.67 to 0.42%) in severe renal function impairment ($p < 0.001$ for subgroup differences) (Figure 2A, Supplementary Figure S2).

When stratified by different drug categories, it was indicated that HbA1c changes with ertugliflozin users [-0.67% (-0.85 to -0.49%) in normal renal function, -0.60% (-0.93 to -0.26%) in mild renal function impairment, and -0.09% (-0.24 to 0.06%) in moderate renal function impairment ($p < 0.001$ for subgroup differences)] and HbA1c changes with luseogliflozin users [-1.13% (-1.34 to -0.92%) in mild renal function impairment and -0.20% (-0.42 to 0.02%) in moderate renal function impairment ($p < 0.001$ for subgroup differences)] basically

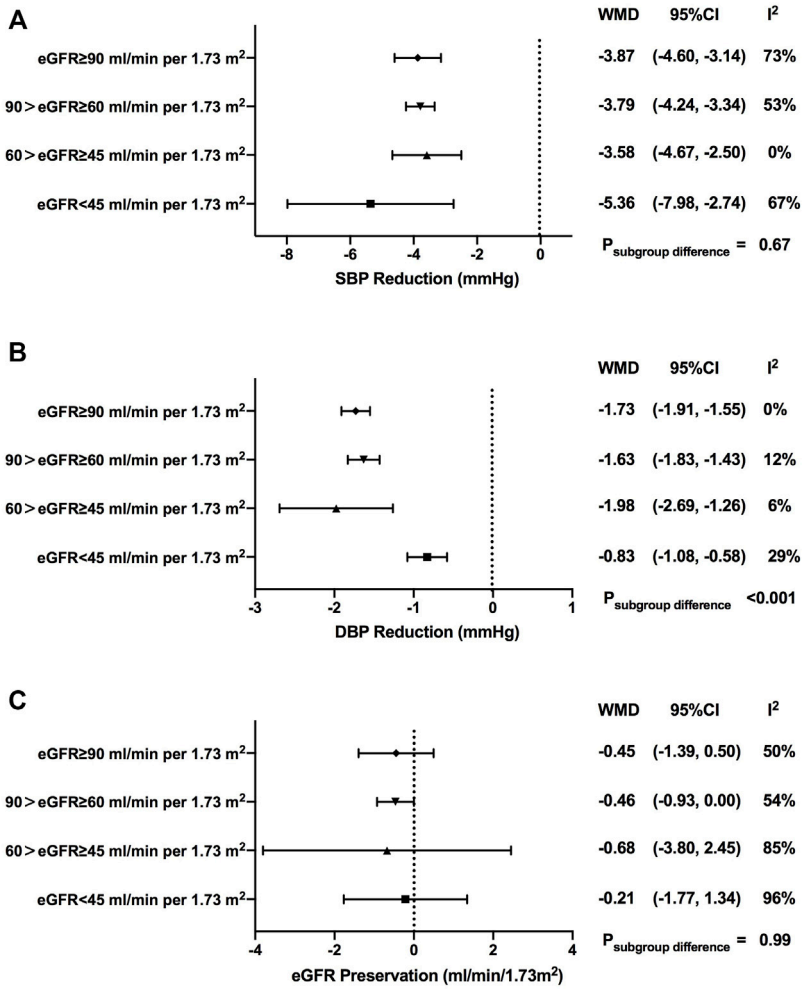

FIGURE 3
Blood pressure and eGFR changes of SGLT2i treatment in patients with different levels of renal function. SBP, systolic blood pressure; DBP, diastolic blood pressure; eGFR, estimated glomerular filtrationrate; WMD, weighted mean differences; 95% CIs, 95% confidence intervals.

followed the similar pattern as the overall trend, with a precipitous deceleration in blood glucose improvement observed in the subgroup of eGFR <60 ml/min per 1.73 m^2. However, no statistically significant subgroup difference was found in other subtypes of SGLT2is in HbA1c reduction when stratified by renal function (Supplementary Table S3). When stratified by the follow-up period, a similar changing trend pattern was observed in HbA1c reduction among different renal function groups with a follow-up less than 1 year (Supplementary Table S4).

Effects of SGLT2is on body weight

In total, weight loss was more profound in the SGLT2i treatment group when compared with the control one (WMD, -2.05 kg, 95% CI, -2.31 to -1.79 kg, $p < 0.001$). Generally speaking, compared with patients with normal renal function, the magnitude of body weight reduction started to decline in the subgroup of patients with mild-to-moderate renal function impairment [-2.12 kg (-2.66 to -1.59 kg) in normal renal function; -2.06 kg (-2.31 to -1.82 kg) in mild renal function impairment; -1.23 kg (-1.59 to -0.86 kg) in moderate renal function impairment), but not in the subgroup with severe renal function impairment [-1.88 kg (-3.04 to -0.72 kg)]. Significant differences in body weight reduction were observed among patients at different stages of renal function ($p = 0.002$) (Figure 2B, Supplementary Figure S3).

When stratified by different drug categories, it was revealed that weight reduction effects of canagliflozin [-2.5 kg (-3.05 to -1.95 kg) in normal renal function; -1.73 kg (-2.05 to -1.42 kg) in mild renal function impairment; $p = 0.02$ for subgroup

differences] and of empagliflozin [-2.17 kg (-2.64 to -1.69 kg) in normal renal function; -1.93 kg (-2.11 to -1.75 kg) in mild renal function impairment; -1.17 kg (-1.75 to -0.59 kg) in moderate renal function impairment; -1.00 kg (-2.57 to 0.57 kg) in severe renal function impairment; $p = 0.03$ for subgroup differences] gradually declined as renal impairment got worse. The results of other subtypes of SGLT2is are also summarized in Supplementary Table S3.

When stratified by the follow-up period, no significant changing trend patterns were identified in patients with a follow-up less or more than 1 year (Supplementary Table S4).

Effects of SGLT2is on blood pressure

SGLT2i treatment contributed to greater reductions for both systolic blood pressure (SBP) and diastolic blood pressure (DBP) when compared with control treatment [WMD, -3.87 mmHg, 95% CI, -4.30 to -3.44 mmHg for SBP, $p < 0.001$; WMD, -1.51 mmHg, 95% CI, -1.62 to -1.39 mmHg for DBP, $p < 0.001$] (Figure 3A and Figure 3B).

In terms of SBP, although there were no significant differences among subgroups with different renal function, SGLT2i-mediated blood pressure reduction seemed to be weakened when renal function got worse (WMD, -3.87 mmHg, 95% CI, -4.60 to -3.14 mmHg in normal renal function; WMD, -3.79 mmHg, 95% CI, -4.24 to -3.34 mmHg in mild renal function impairment; WMD, -3.58 mmHg, 95% CI, -4.67 to -2.50 mmHg in moderate renal function impairment; $p = 0.67$ for subgroup differences). Exceptionally, the greatest reduction of SBP was observed in individuals in the severe renal function impairment groups (WMD, -5.36 mmHg, 95% CI, -7.98 to -2.74 mmHg) (Supplementary Figure S4).

Subgroup analyses showed that there were no significant differences in SBP reduction among subgroups with different renal functions when stratified by different drug categories (Supplementary Table S3) or stratified by the follow-up period (Supplementary Table S4).

As for DBP, there was a prominent decrease in DBP in individuals with severe renal function impairment [-1.73 mmHg (-1.91 to -1.55 mmHg) in normal renal function; -1.63 mmHg (-1.83 to -1.43 mmHg) in mild renal function impairment; -1.98 mmHg (-2.69 to -1.26 mmHg) in moderate renal function impairment; -0.83 mmHg (-1.08 to -0.58 mmHg) in severe renal function impairment; $p < 0.001$ for subgroup differences] (Supplementary Figure S5).

A gradual decrease in DBP reduction was observed as renal function got worse in dapagliflozin users (WMD, -1.80 mmHg, 95% CI, -2.02 to -1.59 mmHg in normal renal function; WMD, -0.73 mmHg, 95% CI, -1.45 to -0.01 mmHg in mild renal function impairment; WMD, -0.47 mmHg, 95% CI, -2.62 to 1.68 mmHg in severe renal function impairment; $p = 0.01$ for subgroup differences). No clear changing trend pattern was found in subgroup analyses of the follow-up period (Supplementary Table S3 and Supplementary Table S4).

Effects of SGLT2is on eGFR

Over the follow-up time ranging from 4 to 135 weeks, SGLT2i treatment failed to contribute to eGFR preservation compared with control treatment (WMD, -0.48 ml/min/1.73 m^2, 95% CI, -0.87 to -0.08 ml/min/1.73 m^2, $p = 0.02$). Such fluctuations of the eGFR showed no notable change pattern as renal function declined, which were comparable among subgroups with different levels of renal function [-0.45 ml/min/1.73 m^2 (-1.39 to 0.50 ml/min/1.73 m^2) in normal renal function; -0.46 ml/min/1.73 m^2 (-0.93 to 0.00 ml/min/1.73 m^2) in mild renal function impairment; -0.68 ml/min/1.73 m^2 (-3.80 to 2.45 ml/min/1.73 m^2) in moderate renal function impairment; -0.21 ml/min/1.73 m^2 (-1.77 to 1.34 ml/min/1.73 m^2) in severe renal function impairment; $p = 0.99$ for subgroup differences)] (Figure 3C and Supplementary Figure S6).

In subgroup analyses for different drug categories, greater eGFR decline was found with sotagliflozin and luseogliflozin treatment [-1.22 ml/min/1.73 m^2 (-1.47 to -0.97 ml/min/1.73 m^2), $p < 0.001$ for sotagliflozin; -2.09 ml/min/1.73 m^2 (-3.54 to -0.63 ml/min/1.73 m^2), $p = 0.005$ for luseogliflozin]. Significant eGFR decline *versus* control was observed when the follow-up duration was less than 1 year (Supplementary Table S3 and Supplementary Table S4).

Effects of SGLT2is on adverse events

In addition, we compared several major adverse events (AEs) between SGLT2i treatment and the control group. Overall, compared with the control group, the risks of urinary tract infection (OR = 1.07, 95% CI, 1.00 to 1.14, $I^2 = 0\%$), genital infection (OR = 3.69, 95% CI, 3.23 to 4.20, $I^2 = 0\%$), hypovolemia (OR = 1.24, 95% CI, 1.13 to 1.35, $I^2 = 0\%$), and diabetic ketoacidosis (OR = 2.23, 95% CI, 1.59 to 3.11, $I^2 = 25\%$) were significantly increased in SGLT2i users (Supplementary Figures S7–S14). The risk of hypovolemia was significantly increased in subgroups with normal renal function and severe renal function impairment [OR = 1.65 (95% CI, 1.08–2.53) in normal renal function, $p = 0.02$; OR = 1.12 (95% CI, 0.99–1.26) in mild renal function impairment, $p = 0.06$; OR = 1.65 (95% CI, 0.82–3.3) in moderate renal function impairment, $p = 0.16$; OR = 1.37 (95% CI, 1.18–1.6) in severe renal function impairment, $p < 0.001$; $p = 0.07$ for subgroup differences] (Figure 4). The risk of hypoglycemia was not increased in SGLT2i users across different renal

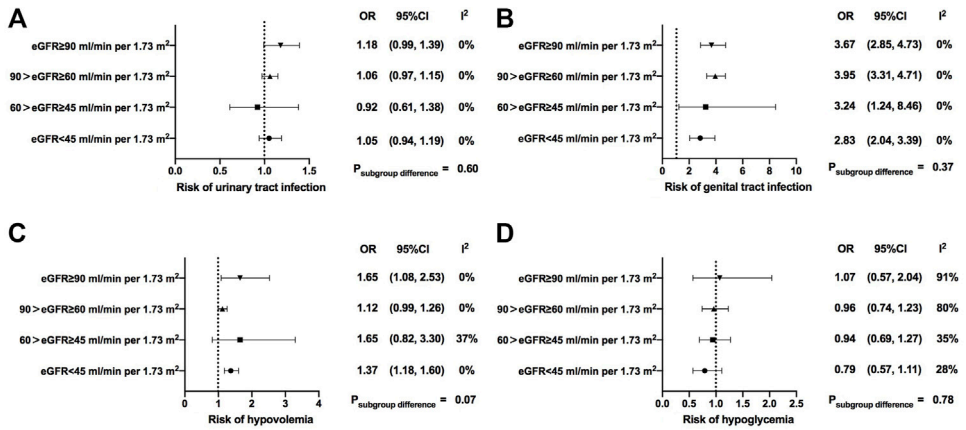

FIGURE 4
Safety of SGLT2i treatment in patients with different levels of renal function. eGFR, estimated glomerular filtrationrate; OR, odds ratio; 95% CIs, 95% confidence intervals.

function strata in the overall analysis (Figure 4). However, when compared with the placebo, the incidence of hypoglycemia in SGLT2i users was only significantly increased in patients with normal renal function and the effect sizes gradually decreased as renal function getting worse in patients treated with SGLT2is [OR = 1.57 (95% CI, 1.29–1.91) in normal renal function; OR = 1.07 (95% CI, 0.98–1.16) in mild renal function impairment; OR = 0.94 (95% CI, 0.74–1.19) in moderate renal function impairment; OR = 0.80 (95% CI, 0.62–1.05) in severe renal function impairment; $p < 0.001$ for subgroup differences] (Supplementary Table S6).

Discussion

With the aim to compare the pleiotropic properties of SGLT2is among individuals with varying levels of renal function, we found that SGLT2is produced a substantial benefit in blood glucose improvement, weight, and blood pressure reduction even in patients with impaired renal function. We also found that the effects of SGLT2is on blood glucose, weight, and blood pressure control varied among different renal function groups, some were parallel with the renal function levels while others were not.

Glycemic control

As it was suggested that SGLT2is exerted their glucose-lowering effect mainly through glycosuria (DeFronzo et al., 2012; Washburn and Poucher, 2013; Abdul-Ghani and DeFronzo, 2014; Hasan et al., 2014; Palmer et al., 2021), previous studies showed that SGLT2i-mediated urinary glucose excretion was renal function-dependent, reducing with progressed renal function impairment (Scheen, 2015; Hu et al., 2022). Consistent with previous studies, we suggested a greater reduction in HbA1c levels in patients treated with SGLT2is than non-SGLT2i users, which was attenuated by the decreased level of eGFR.

Weight loss

On the basis of our studies, it was suggested that a statistically significant difference in SGLT2i-related weight loss was found among different renal functions. As we mentioned before, UGE of SGLT2is is declining with decreasing renal function. Likewise, we did observe the weight reduction effects of SGLT2is were weakened as renal function got worse. Thus, it was reasonable to speculate that urinary glucose excretion and its associated energy loss might play a predominant role in weight control for SGLT2is.

Of course, reduction in body weight with SGLT2is therapy was considered a result of the combination of several systemic factors, including increased excretion of glucose (Abdul-Ghani et al., 2012), reductions in adipose tissue mass (both visceral and subcutaneous) (Bolinder et al., 2012; Cefalu et al., 2013), preservation of lean tissue mass, and loss of extracellular fluid (Schork et al., 2019). However, we also observed a sudden increase in weight loss in patients with severe renal function impairment. Perhaps, there were other compensatory mechanisms that potentially triggered lipolysis, and in turn, led to weight loss during the treatment of SGLT2is in patients with severe renal impairment. It remains to be elucidated with further investigations.

Reduction in systemic blood pressure

In line with previous analyses, our data suggested that SGLT2i treatment was associated with a reduction in systemic blood pressure (Foote et al., 2012; Monami et al., 2014). The initial reduction in extracellular fluid volume (Lambers Heerspink et al., 2013; Vasilakou et al., 2013; Baker et al., 2014; Oliva and Bakris, 2014; Scheen, 2015; Thomas and Cherney, 2018), a further loss in body mass, modulation of the RAAS (Burns and Cherney, 2019), and reduced plasma uric acid levels (Zhao et al., 2018) are likely to lead to reduction in blood pressure.

Interestingly, we found there was a difference in the SGLT2i effect on systolic and diastolic blood pressure. The magnitudes of SBP reduction among different subgroups were comparable. Even in patients with severe impaired renal function, SGLT2is were comparably effective in lowering systolic blood pressure. However, in terms of DBP, we observed a general trend toward more pronounced blood pressure reduction in individuals with better renal function.

Possible mechanisms for the aforementioned findings might be explained as follows. Greater use of antihypertensive medications (including diuretics) was found in patients with worsening chronic kidney disease (CKD) (Cherney et al., 2018). At the same time, patients with CKD exhibited sodium-sensitive phenotypes, leading to significant blood pressure–lowering effects from natriuretic agents (Luzardo et al., 2015). Also, natriuresis and urinary volume were increased in patients with T2D when given empagliflozin in combination with a thiazide or a loop diuretic, compared with either therapy alone (Heise et al., 2016). Thus, drug–drug interaction might partly explain the preserved effect of SGLT2is on SBP with lower eGFRs. However, as CKD developed and progressed, decreasing aortic compliance led to a consequent drop in the diastolic vascular flow and pressure (Inserra et al., 2021). Thus, it possibly made sense that less reduction in DBP with SGLT2is would occur in severe renal function impairment since baseline levels stayed low, either. As mentioned previously, the pathophysiology for BP lowering with SGLT2is has been attributed to several factors. More mechanisms on SGLT2i′ BP- lowering effects among different renal functions remained to be explored further.

Preservation of renal function

Although SGLT2is caused an initial and small reduction in eGFR in the early stage of treatment (Perkovic et al., 2019), previous studies found the reversal of these small changes in eGFR with long-term treatment and that SGLT2is could maintain long-term renoprotective effects ultimately (Pareek et al., 2016).

Similar to existing studies, we observed a transient reduction in eGFR compared with controls when the follow-up duration was less than 1 year. However, we did not see preservation of renal function in SGLT2is compared with controls in the extended follow-up time. Since renal benefits of SGLT2is have been confirmed in several large RCT trials, we summed up the following reasons that may lead to the negative results in our data.

First, the clinical trials reflecting changes in the eGFR included in our analysis were limited, and the sample size was insufficient. Second, as we could see in the dapagliflozin and empagliflozin subgroup, patients with normal renal function or mild renal insufficiency accounted for the majority. However, changes in the eGFR in these patients were quite slight. Third, the difference in the eGFR slope between SGLT2is and control arms varied during follow-up, which was seen in CANVAS、DAPA-HF、and EMPEROR studies (Neuen et al., 2018; Jhund et al., 2021; Zannad et al., 2021).

In CANVAS, participants who received canagliflozin experienced a decline in the eGFR within the first 13 weeks. While after week 13, the annual decline in the eGFR was significantly slower in all subgroups (Neuen et al., 2018). Likewise, after day 14, the rate of decline of the eGFR was steeper in the placebo group than in the dapagliflozin group in DAPA-HF (Jhund et al., 2021). In EMPEROR-Reduced trial, at week 4, the eGFR stabilized and recovered toward baseline, whereas progressive decline was observed in the placebo group (Zannad et al., 2021). However, in our study, we compared only changes in the eGFR but not the slope. Therefore, it is very critical to select the appropriate time point for subgroup analyses. Apparently, we had already seen a significant difference in eGFR changes between SGLT2i treatment and controls when taking “1 year” as the time point. In addition, as seen in Supplementary Table S1, the number of studies with follow-up longer than 1 year was limited. Also, when followed for more than 1 year, though it was not statistically significant, we found an increase in the eGFR in patients with mild-to-moderate renal function impairment when treated with SGLT2 inhibitors compared to controls. Therefore, studies with longer follow-up are needed to further identify the optimal time point at which the gap in eGFR changes appeared between SGLT2 inhibition and controls.

Safety

In our analyses, incidences of urinary tract infection, genital infection, hypovolemia, and diabetic ketoacidosis were higher in the SGLT2i users. At the same time, compared to the placebo, fewer episodes of hypoglycemia were reported in patients with deteriorating renal function, which made sense as urinary glucose excretion reduced with progressed renal function impairment (Scheen, 2015; Hu et al., 2022). Nevertheless, the risks of other AEs like genital infection and diabetic ketoacidosis were comparable among different renal functions. In addition, we observed a significantly increased risk of hypovolemia in patients with normal renal function and severe renal function

impairment. Diuretic effects of SGLT2i led to a decrease in plasma volume and were related to a higher risk of volume depletion (Delanaye and Scheen, 2021). Meanwhile, since hypertension and edema are common comorbidities and complications in patients with CKD (Kidney Disease: Improving Global Outcomes KDIGO Blood Pressure Work Group, 2021), concomitant antihypertensive medications, including diuretics, might also be applied in these patients, which might also be associated with the increased risk of hypovolemia. Moreover, cardiovascular autonomic dysfunction in patients with advanced CKD and end-stage kidney disease (ESKD) might also be associated with the increased incidence of hypovolemia and hypotension (Soomro and Charytan, 2021; Shubrook et al., 2022). However, further analyses were limited due to insufficient information of baseline medications and cardiovascular profiles. Considering certain active comparators with an increased risk of hypoglycemia, such as sulfonylureas and insulin, might lead to a biased hypoglycemia evaluation, we conducted a further sensitivity analysis with only placebo-controlled RCTs. We found that, when compared with the placebo, the risk of hypoglycemia during SGLT2i treatment was elevated in patients with favorable renal function rather than those with renal dysfunction, which was consistent with the decreasing UGE and HbA1c reductions observed in SGLT2i users as the renal function deteriorates. Therefore, SGLT2i was generally well-tolerated in patients with renal impairments in terms of hypoglycemia.

Strengths and limitations

To our knowledge, our study is currently the largest systematic review showing the effect of administration of SGLT2is on different renal function stratifications. Our data provide strong evidence for the clinical application of SGLT2is in patients with CKD. This study has some limitations, though. First, we did not include studies without presenting data regarding changes in HbA1c, weight, blood pressure, and eGFR, and thus data collection might be incomplete. Second, because of the current eGFR-based limitations on the use of SGLT2is, inclusion criteria bias made the sample size unevenly distributed among different stratifications. We were limited to drawing a definite conclusion concerning the efficacies of SGLT2is in patients at an advanced stage of CKD in the case of a relatively small number of participants, especially for patients with an eGFR below 30 ml/min per 1.73 m^2. Further investigations are needed to further assess SGLT2i′s effects in the population with severe renal dysfunction. Furthermore, high urine protein levels are associated with rapid decline in kidney function (Levey et al., 2020), and research studies have shown that SGLT2is reduce albuminuria with consequent benefits on kidney outcomes in patients with diabetes (Shah et al., 2022). However, given that the RCTs included in our analyses provided quite limited data regarding changes in uACR levels, we were unable to conduct a convincing analysis focusing on the SGLT2i-induced uACR changes among groups with different renal functions in our analysis. Further explorations are needed to test SGLT2i′s effects on the uACR levels in patients with declining renal function. Moreover, since we included studies with different populations, different drug types, different dosages, and follow-up periods, the potential heterogeneity lying in our analyses might influence our results. To cope with this issue, we conducted multiple subgroup analyses to control the potential bias. In addition, we performed a sensitivity analysis with only placebo-controlled RCTs to exclude the influence of active agent comparators. It turned out that most results were generally consistent with the overall analyses (Supplementary Table S6 and Supplementary Table S7). At the same time, given that a duration of less than 12 weeks might not be sufficient to evaluate the effect of HbA1c or change of eGFR, we also performed a sensitivity analysis after deleting RCTs with follow-up periods less than 12 weeks to exclude possible influences. It turned out that most results were generally consistent with the results in the overall analyses (Supplementary Table S8). However, there is no denying that the data should still be interpreted with caution. Moreover, certain unmeasured confounding factors such as baseline cardiovascular status, concomitant medications, and diet intakes were unable to be adjusted for now. More investigations are still needed for further evaluations.

Conclusion

In conclusion, SGLT2is contributed to an improved glycemic control, body weight, and blood pressure reduction, even in patients with renal insufficiency. The HbA1c and body weight reductions observed in SGLT2i users were generally parallel with patients' baseline eGFR levels, while blood pressure reductions in SGLT2i users were independent of baseline eGFR levels. Consistently, when compared with the placebo, risk of hypoglycemia with SGLT2i treatment was more frequent in patients with favorable renal function, where the HbA1c reduction was profound.

Data availability statement

The original contributions presented in the study are included in the article/Supplementary Materials; further inquiries can be directed to the corresponding authors.

Ethics statement

Ethical review and approval was not required for the study on human participants in accordance with the local legislation and

institutional requirements. Written informed consent for participation was not required for this study in accordance with the national legislation and the institutional requirements.

Author contributions

LJ and XC conceptualized this study and designed the systematic review protocol; SH, CL, and XZ performed the study selection and data extraction; SH and CL performed the statistical analyses; SH, CL, and XC prepared the outlines and wrote the manuscript. All authors contributed to the critical revision of manuscript drafts.

Funding

This work was supported by the National Natural Science Foundation of China (No. 81970698 and No. 81970708) and Beijing Natural Science Foundation (No. 7202216). The funding agencies had no roles in the study design, data collection or analysis, decision to publish, or preparation of the manuscript.

Acknowledgments

We thank the doctors, nurses, and technicians for their practical during the study at the Department of Endocrinology and Metabolism in Peking University People's Hospital.

Conflict of interest

LJ has received fees for lecture presentations and for consulting from AstraZeneca, Merck, Metabasis, MSD, Novartis, Eli Lilly, Roche, Sanofi-Aventis, and Takeda. All authors have completed the ICMJE uniform disclosure form at www.icmje.org/coi_disclosure.pdf (available on request from the corresponding author) and declare. No other support from any organization for the submitted work other than that described previously.

The remaining authors declare that the research was conducted in the absence of any commercial or financial relationships that could be construed as a potential conflict of interest.

Publisher's note

Supplementary material

The Supplementary Material for this article can be found online at: https://www.frontiersin.org/articles/10.3389/fphar.2022.1018720/full#supplementary-material

References

Abdul-Ghani, M. A., and DeFronzo, R. A. (2014). Lowering plasma glucose concentration by inhibiting renal sodium-glucose cotransport. *J. Intern. Med.* 276 (4), 352–363. doi:10.1111/joim.12244

Abdul-Ghani, M. A., Norton, L., and DeFronzo, R. A. (2012). Efficacy and safety of SGLT2 inhibitors in the treatment of type 2 diabetes mellitus. *Curr. Diab. Rep.* 12 (3), 230–238. doi:10.1007/s11892-012-0275-6

Bailey, C. J. (2011). Renal glucose reabsorption inhibitors to treat diabetes. *Trends Pharmacol. Sci.* 32 (2), 63–71. doi:10.1016/j.tips.2010.11.011

Baker, W. L., Smyth, L. R., Riche, D. M., Bourret, E. M., Chamberlin, K. W., and White, W. B. (2014). Effects of sodium-glucose co-transporter 2 inhibitors on blood pressure: A systematic review and meta-analysis. *J. Am. Soc. Hypertens.* 8 (4), 262–275. doi:10.1016/j.jash.2014.01.007

Bolinder, J., Ljunggren, Ö., Kullberg, J., Johansson, L., Wilding, J., Langkilde, A. M., et al. (2012). Effects of dapagliflozin on body weight, total fat mass, and regional adipose tissue distribution in patients with type 2 diabetes mellitus with inadequate glycemic control on metformin. *J. Clin. Endocrinol. Metab.* 97 (3), 1020–1031. doi:10.1210/jc.2011-2260

Burns, K. D., and Cherney, D. (2019). Renal angiotensinogen and sodium-glucose cotransporter-2 inhibition: Insights from experimental diabetic kidney disease. *Am. J. Nephrol.* 49 (4), 328–330. doi:10.1159/000499598

Cefalu, W. T., Leiter, L. A., Yoon, K. H., Arias, P., Niskanen, L., Xie, J., et al. (2013). Efficacy and safety of canagliflozin versus glimepiride in patients with type 2 diabetes inadequately controlled with metformin (CANTATA-SU): 52 week results from a randomised, double-blind, phase 3 non-inferiority trial. *Lancet* 382 (9896), 941–950. doi:10.1016/s0140-6736(13)60683-2

Cherney, D. Z. I., Cooper, M. E., Tikkanen, I., Pfarr, E., Johansen, O. E., Woerle, H. J., et al. (2018). Pooled analysis of Phase III trials indicate contrasting influences of renal function on blood pressure, body weight, and HbA1c reductions with empagliflozin. *Kidney Int.* 93 (1), 231–244. doi:10.1016/j.kint.2017.06.017

Davidson, J. A. (2019). SGLT2 inhibitors in patients with type 2 diabetes and renal disease: Overview of current evidence. *Postgrad. Med.* 131 (4), 251–260. doi:10.1080/00325481.2019.1601404

DeFronzo, R. A., Davidson, J. A., and Del Prato, S. (2012). The role of the kidneys in glucose homeostasis: A new path towards normalizing glycaemia. *Diabetes Obes. Metab.* 14 (1), 5–14. doi:10.1111/j.1463-1326.2011.01511.x

Delanaye, P., and Scheen, A. J. (2021). The diuretic effects of SGLT2 inhibitors: A comprehensive review of their specificities and their role in renal protection. *Diabetes Metab.* 47 (6), 101285. doi:10.1016/j.diabet.2021.101285

Foote, C., Perkovic, V., and Neal, B. (2012). Effects of SGLT2 inhibitors on cardiovascular outcomes. *Diab. Vasc. Dis. Res.* 9 (2), 117–123. doi:10.1177/1479164112441190

Hasan, F. M., Alsahli, M., and Gerich, J. E. (2014). SGLT2 inhibitors in the treatment of type 2 diabetes. *Diabetes Res. Clin. Pract.* 104 (3), 297–322. doi:10.1016/j.diabres.2014.02.014

Heise, T., Jordan, J., Wanner, C., Heer, M., Macha, S., Mattheus, M., et al. (2016). Acute pharmacodynamic effects of empagliflozin with and without diuretic agents in patients with type 2 diabetes mellitus. *Clin. Ther.* 38 (10), 2248–2264. doi:10.1016/j.clinthera.2016.08.008

Hu, S., Lin, C., Cai, X., Zhu, X., Lv, F., Nie, L., et al. (2022). The urinary glucose excretion by sodium-glucose cotransporter 2 inhibitor in patients with different levels of renal function: A systematic review and meta-analysis. *Front. Endocrinol.* 12, 814074. doi:10.3389/fendo.2021.814074

Inserra, F., Forcada, P., Castellaro, A., and Castellaro, C. (2021). Chronic kidney disease and arterial stiffness: A two-way path. *Front. Med.* 8, 765924. doi:10.3389/fmed.2021.765924

Jhund, P. S., Solomon, S. D., Docherty, K. F., Heerspink, H. J. L., Anand, I. S., Böhm, M., et al. (2021). Efficacy of dapagliflozin on renal function and outcomes in patients with Heart failure with reduced ejection fraction: Results of DAPA-HF. *Circulation* 143 (4), 298–309. doi:10.1161/CIRCULATIONAHA.120.050391

Kidney Disease: Improving Global Outcomes KDIGO Blood Pressure Work Group (2021). KDIGO 2021 clinical practice guideline for the management of blood pressure in chronic kidney disease. *Kidney Int.* 99 (3S), S1–S87. doi:10.1016/j.kint.2020.11.003

Lambers Heerspink, H. J., de Zeeuw, D., Wie, L., Leslie, B., and List, J. (2013). Dapagliflozin a glucose-regulating drug with diuretic properties in subjects with type 2 diabetes. *Diabetes Obes. Metab.* 15 (9), 853–862. doi:10.1111/dom.12127

Levey, A. S., de Jong, P. E., Coresh, J., El Nahas, M., Astor, B. C., Matsushita, K., et al. (2011). The definition, classification, and prognosis of chronic kidney disease: A KDIGO controversies conference report. *Kidney Int.* 80 (1), 17–28. doi:10.1038/ki.2010.483

Levey, A. S., Gansevoort, R. T., Coresh, J., Inker, L. A., Heerspink, H. L., Grams, M. E., et al. (2020). Change in albuminuria and gfr as end points for clinical trials in early stages of CKD: A scientific workshop sponsored by the national kidney foundation in collaboration with the us food and drug administration and European medicines agency. *Am. J. Kidney Dis.* 75 (1), 84–104. doi:10.1053/j.ajkd.2019.06.009

Luzardo, L., Noboa, O., and Boggia, J. (2015). Mechanisms of salt-sensitive hypertension. *Curr. Hypertens. Rev.* 11 (1), 14–21. doi:10.2174/1573402111666150530204136

Monami, M., Nardini, C., and Mannucci, E. (2014). Efficacy and safety of sodium glucose co-transport-2 inhibitors in type 2 diabetes: A meta-analysis of randomized clinical trials. *Diabetes Obes. Metab.* 16 (5), 457–466. doi:10.1111/dom.12244

Nair, S., and Wilding, J. P. (2010). Sodium glucose cotransporter 2 inhibitors as a new treatment for diabetes mellitus. *J. Clin. Endocrinol. Metab.* 95 (1), 34–42. doi:10.1210/jc.2009-0473

Neuen, B. L., Ohkuma, T., Neal, B., Matthews, D. R., de Zeeuw, D., Mahaffey, K. W., et al. (2018). Cardiovascular and renal outcomes with canagliflozin according to baseline kidney function. *Circulation* 138 (15), 1537–1550. doi:10.1161/CIRCULATIONAHA.118.035901

Oliva, R. V., and Bakris, G. L. (2014). Blood pressure effects of sodium-glucose co-transport 2 (SGLT2) inhibitors. *J. Am. Soc. Hypertens.* 8 (5), 330–339. doi:10.1016/j.jash.2014.02.003

Palmer, S. C., Tendal, B., Mustafa, R. A., Vandvik, P. O., Li, S., Hao, Q., et al. (2021). Sodium-glucose cotransporter protein-2 (SGLT-2) inhibitors and glucagon-like peptide-1 (GLP-1) receptor agonists for type 2 diabetes: Systematic review and network meta-analysis of randomised controlled trials. *BMJ* 372, m4573. doi:10.1136/bmj.m4573

Pareek, A., Chandurkar, N., and Naidu, K. (2016). Empagliflozin and progression of kidney disease in type 2 diabetes. *N. Engl. J. Med.* 375 (18), 1800. doi:10.1056/NEJMc1611290

Perkovic, V., Jardine, M. J., Neal, B., Bompoint, S., Heerspink, H. J. L., Charytan, D. M., et al. (2019). Canagliflozin and renal outcomes in type 2 diabetes and nephropathy. *N. Engl. J. Med.* 380 (24), 2295–2306. doi:10.1056/NEJMoa1811744

Scheen, A. J. (2015). Pharmacokinetics, pharmacodynamics and clinical use of SGLT2 inhibitors in patients with type 2 diabetes mellitus and chronic kidney disease. *Clin. Pharmacokinet.* 54 (7), 691–708. doi:10.1007/s40262-015-0264-4

Schork, A., Saynisch, J., Vosseler, A., Jaghutriz, B. A., Heyne, N., Peter, A., et al. (2019). Effect of SGLT2 inhibitors on body composition, fluid status and renin-angiotensin-aldosterone system in type 2 diabetes: A prospective study using bioimpedance spectroscopy. *Cardiovasc. Diabetol.* 18 (1), 46. doi:10.1186/s12933-019-0852-y

Shah, N., Perkovic, V., and Kotwal, S. (2022). Impact of SGLT2 inhibitors on the kidney in people with type 2 diabetes and severely increased albuminuria. *Expert Rev. Clin. Pharmacol.* 15 (7), 827–842. doi:10.1080/17512433.2022.2108402

Shubrook, J. H., Neumiller, J. J., and Wright, E. (2022). Management of chronic kidney disease in type 2 diabetes: Screening, diagnosis and treatment goals, and recommendations. *Postgrad. Med.* 134 (4), 376–387. doi:10.1080/00325481.2021.2009726

Soomro, Q. H., and Charytan, D. M. (2021). Cardiovascular autonomic nervous system dysfunction in chronic kidney disease and end-stage kidney disease: Disruption of the complementary forces. *Curr. Opin. Nephrol. Hypertens.* 30 (2), 198–207. doi:10.1097/mnh.0000000000000686

Thomas, M. C., and Cherney, D. Z. I. (2018). The actions of SGLT2 inhibitors on metabolism, renal function and blood pressure. *Diabetologia* 61 (10), 2098–2107. doi:10.1007/s00125-018-4669-0

Vallon, V., and Thomson, S. C. (2017). Targeting renal glucose reabsorption to treat hyperglycaemia: The pleiotropic effects of SGLT2 inhibition. *Diabetologia* 60 (2), 215–225. doi:10.1007/s00125-016-4157-3

Vasilakou, D., Karagiannis, T., Athanasiadou, E., Mainou, M., Liakos, A., Bekiari, E., et al. (2013). Sodium-glucose cotransporter 2 inhibitors for type 2 diabetes: A systematic review and meta-analysis. *Ann. Intern. Med.* 159 (4), 262–274. doi:10.7326/0003-4819-159-4-201308200-00007

Washburn, W. N., and Poucher, S. M. (2013). Differentiating sodium-glucose co-transporter-2 inhibitors in development for the treatment of type 2 diabetes mellitus. *Expert Opin. Investig. Drugs* 22 (4), 463–486. doi:10.1517/13543784.2013.774372

Zannad, F., Ferreira, J. P., Pocock, S. J., Zeller, C., Anker, S. D., Butler, J., et al. (2021). Cardiac and kidney benefits of empagliflozin in Heart failure across the spectrum of kidney function: Insights from EMPEROR-reduced. *Circulation* 143 (4), 310–321. doi:10.1161/CIRCULATIONAHA.120.051685

Zhang, L., Zhang, M., Lv, Q., and Tong, N. (2018). Efficacy and safety of sodium-glucose cotransporter 2 inhibitors in patients with type 2 diabetes and moderate renal function impairment: A systematic review and meta-analysis. *Diabetes Res. Clin. Pract.* 140, 295–303. doi:10.1016/j.diabres.2018.03.047

Zhao, Y., Xu, L., Tian, D., Xia, P., Zheng, H., Wang, L., et al. (2018). Effects of sodium-glucose co-transporter 2 (SGLT2) inhibitors on serum uric acid level: A meta-analysis of randomized controlled trials. *Diabetes Obes. Metab.* 20 (2), 458–462. doi:10.1111/dom.13101

frontiers | Frontiers in Pharmacology

TYPE Systematic Review
PUBLISHED 24 November 2022
DOI 10.3389/fphar.2022.986186

OPEN ACCESS

EDITED BY
Swayam Prakash Srivastava,
Yale University, United States

REVIEWED BY
Aditya Yashwant Sarode,
Columbia University, United States
Hotimah Masdan Salim,
Nahdlatul Ulama University of Surabaya, Indonesia

*CORRESPONDENCE
Weijing Liu,
liuweijing-1977@hotmail.com
Wenjing Zhao,
zhaowenjing@bjzhongyi.com
Yaoxian Wang,
wyx3203@sina.com

†These authors have contributed equally to this work

SPECIALTY SECTION
This article was submitted to Renal Pharmacology, a section of the journal Frontiers in Pharmacology

RECEIVED 04 July 2022
ACCEPTED 02 November 2022
PUBLISHED 24 November 2022

CITATION
Tian L, Ai S, zheng H, Yang H, Zhou M, Tang J, Liu W, Zhao W and Wang Y (2022), Cardiovascular and renal outcomes with sodium glucose co-transporter 2 inhibitors in patients with type 2 diabetes mellitus: A system review and network meta-analysis. *Front. Pharmacol.* 13:986186. doi: 10.3389/fphar.2022.986186

Cardiovascular and renal outcomes with sodium glucose co-transporter 2 inhibitors in patients with type 2 diabetes mellitus: A system review and network meta-analysis

Lei Tian[1†], Sinan Ai[2†], Huijuan zheng[2], Hanwen Yang[3], Mengqi Zhou[2], Jingyi Tang[2], Weijing Liu[2*], Wenjing Zhao[1*] and Yaoxian Wang[2*]

[1]Department of Nephrology, Beijing Hospital of Traditional Chinese Medicine, Capital Medical University, Beijing, China, [2]Renal Research Institution of Beijing University of Chinese Medicine, Key Laboratory of Chinese Internal Medicine of Ministry of Education and Beijing, Dongzhimen Hospital Affiliated to Beijing University of Chinese Medicine, Beijing, China, [3]China-Japan Friendship Hospital, Beijing, China

Cardiovascular and renal impairment are the most common complications of type 2 diabetes mellitus (T2DM). As an emerging class of glucose-lowing agents sodium glucose co-transporter 2 (SGLT2), possesses beneficial effects on cardiovascular and renal outcomes in patients with T2DM. The aim of this study is to assess the efficacy of different SGLT2 inhibitors for cardiovascular and renal outcomes for patients with T2DM when compared with placebo. We performed a systematic search of PubMed, Embase, and the Cochrane library from inception through November 2021. Randomized clinical trials enrolling participants with T2DM were included, in which SGLT2 inhibitors were compared with each other or placebo. The primary outcomes including all-caused mortality, Cardiovascular outcomes (cardiovascular mortality, hospitalization for heart failure), and the renal composite outcomes (worsening persistent microalbuminuria or macroalbuminuria, new or worsening chronic kidney disease, doubling of serum creatinine, end-stage renal disease, renal transplant, or renal death). The data for the outcomes were pooled and recorded as Hazard rations (HRs) with 95% confidence intervals (CLs). Two researcher independently screened the trials and drawn the data. Ten trials enrolling 68,723 patients were included. Compared with placebo groups, Canagliflozin [HR, 0.85 (95%CI, 0.75–0.98)], ertugliflozin [HR, 0.93 (95%

Abbreviations: T2DM, Type 2 diabetes mellitus; SGLT-2, Sodium-glucose cotransporter-2; DKD, diabetic kidney disease; ESRD, End-stage renal disease; RCT, Randomized controlled trial; PRISMA, Preferred reporting items for systematic reviews and meta-analyses; FDA, Food and Drug Administration; MACE, Major adverse cardiovascular events; HR, Hazard ratios; CI, Confidence interval; eGFR, Estimated glomerular filtration rate; BP, Blood pressure; CVOT, Cardiovascular Outcomes Trials; NHE, Na + -H+ exchanger; KB, Ketone bodies; FFA, Free fatty acid; BCAA, branched-chain amino acid; LV, left ventricular; CV, Cardio vascular; SGLT-1, sodium–glucose co-transporter type 1 inhibitor; HIF1, hypoxia-inducible factor 1.

CI, 0.78–1.11)], and sotagliflozin [HR, 0.94 (95%CI, 0.79–1.12)] were associated with a reduction in all-cause mortality. Canagliflozin [HR, 0.84 (95%CI, 0.72–0.97)], dapagliflozin [HR, 0.88 (95%CI, 0.79–0.99)], empagliflozin [HR, 0.62 (95%CI, 0.49–0.78)], ertugliflozin [HR, 0.92 (95%CI, 0.77–1.10)], and sotagliflozin [HR, 0.88 (95%CI, 0.73–1.06)] were associated with a reduction in cardiovascular mortality; Canagliflozin [HR, 0.64 (95%CI, 0.53–0.77)], dapagliflozin [HR, 0.71 (95%CI, 0.63–0.81)], empagliflozin [HR, 0.65 (95%CI, 0.50–0.85)], ertugliflozin [HR, 0.70 (95%CI, 0.54–0.90)], and sotagliflozin [HR, 0.66 (95%CI, 0.56–0.77)] were associated with a reduction in hospitalization for heart failure. Dapagliflozin [HR, 0.55 (95%CI, 0.47–0.63)], Empagliflozin [HR, 0.54 (95%CI, 0.39–0.74)], canagliflozin [HR, 0.64 (95%CI, 0.54–0.75)], sotagliflozin [HR, 0.71 (95%CI, 0.46–1.09)], and ertugliflozin [HR, 0.81 (95%CI, 0.63–1.04)] were associated with a reduction in the renal composite outcome. All SGLT2 inhibitors showed a reduction in cardiovascular mortality, hospitalization for heart failure, renal composite outcomes and all-cause mortality. Canagliflozin and empagliflozin seemed to have the same efficacy in reducing hospitalization for heart failure, but empagliflozin had advantage in reducing cardiovascular mortality, whereas dapagliflozin most likely showed the best renal composite outcomes.

KEYWORDS

sodium glucose co-transporter 2 (SGLT2) inhibitors, type 2 diabetes mellitus, network meta-analysis, cardiovascular outcomes, renal outcomes

1 Introduction

In 2021, the number of diabetic patients was estimated to be approximately 537 million, and by 2045, the prevalence is expected to reach 783 million (International Diabetes Foundation, 2021). The most frequent feature of diabetic patients is chronic or periodic hyperglycemia, which results in impaired organ function, such as macrovascular disease (including heart and brain disease), microvascular disease (including kidney and eye disease), as well as peripheral neuropathy (like paresthesia in hands and feet) (Bjornstad et al., 2021). Cardiovascular and renal impairment are the most common complications (Koye et al., 2018; Deng et al., 2021). Approximately half of the patients with type 2 diabetes mellitus (T2DM) develop diabetic kidney disease (DKD), which is the leading cause of end-stage renal disease (Anders et al., 2018; Umanath and Lewis, 2018). Additionally, the main cause of morbidity and mortality in patients with T2DM is cardiovascular complications (Lloyd-Jones et al., 2009; Fox et al., 2015). Thus, when choosing hypoglycemic drugs, lowering the blood glucose levels should be considered the primary therapeutic strategy as well as preventing cardiovascular and renal complications in patients with T2DM. Many antidiabetic medications are approved to treat patients with T2DM, such as metformin, insulin, and glitazones, but they have significant limitations for improving cardiovascular and renal function, and some may have side effects (Gilbert and Krum, 2015; Packer, 2018). Even the use of specific antidiabetic medications or intensive hypoglycemic may be related with adverse cardiovascular and renal vascular events antidiabetic medication. For example, the safety of sulfonylureas and insulin in heart failure is unclear. Thiazolidinediones (glitazones) have been showed to increased risk of cardiovascular events, so they should not be used in patients with heart failure or patients at high risk of heart failure (Gilbert and Krum, 2015; Seferović et al., 2018). A meta-analysis of thiazolidinediones further demonstrated that in patients with type 2 diabetes, rosiglitazone was associated with significantly higher odds of congestive heart failure, myocardial infarction, and death in real-world settings compared with pioglitazone (Loke et al., 2011).

As an emerging class of glucose-lowing agents, the pharmacodynamic mechanism of sodium glucose transporter 2 (SGLT2) inhibitors are to inhibit the glucose reabsorption in the proximal tubule and increase urinary glucose excretion to lower hyperglycemia (Nauck, 2014; Gallo et al., 2015). Additionally, SGLT2 inhibitors' mechanism of action is insulin-independent and islet β-cell failure for antidiabetic therapies is not involved. The drug was also shown to be effective at all stages of T2DM for patients without renal impairment (Washburn, 2012; van Baar et al., 2018). The beneficial effects of SGLT2 inhibitors on patients with T2DM include the hypoglycemic effect as well as reducing body weight, increasing urinary sodium excretion, contracting intravascular volume, and changing renal hemodynamics (DeFronzo et al., 2017; Thomas and Cherney, 2018; Neuen et al., 2019). These effects might improve blood pressure, intrarenal blood flow, and albuminuria, and reduce the risk of cardiovascular and renal complications in patients with T2DM (DeFronzo et al., 2017; Thomas and Cherney, 2018). The Empagliflozin Cardiovascular Outcome Event Trial (EMPA-REG-OUTCOME) first reported

that empagliflozin could reduce the risk of major adverse cardiovascular events (MACEs) including cardiovascular death, nonfatal stroke, and myocardial infarction, as well as prevent kidney disease end points, such as serum creatinine doubling, renal failure, and renal death (Zinman et al., 2015). Subsequently, the Canagliflozin Cardiovascular Assessment Study (CANVAS) program and the Dapagliflozin Effect on Cardiovascular Events-Thrombosis in Myocardial Infarction 58 (DECLARE-TIMI-58) trials, which were multi-center randomized controlled trials (RCTs), confirmed that these SGLT2s significantly protected against cardiovascular and renal events compared with placebo treatment in patients with T2DM (Neal et al., 2017; Wiviott et al., 2019). The result of the Canagliflozin and Renal Endpoints in Diabetes with Established Nephropathy Clinical Evaluation (CREDENCE) trial, which was a recent novel multicenter international clinical trial, indicated that canagliflozin remarkably reduced MACE and renal events in patients with T2DM and chronic kidney disease (Perkovic et al., 2019). As a gold standard phase III clinical trial, these results all confirmed the profitable effects of SGLT2 inhibitors on cardiovascular and renal outcomes in patients with T2DM. Some published systematic reviews and meta-analysis have summarized the effects of SGLT2 inhibitors on cardiovascular and renal outcomes in patients with T2DM, which suggests that SGLT2 inhibitors reduce the risk of cardiovascular and renal events with no additional safety concerns (Neuen et al., 2019; Toyama et al., 2019; Zelniker et al., 2019). On the basis of the encouraging results for SGLT2 inhibitors in preventing cardiovascular and renal events during clinical trials with patients with T2DM, the drug has been widely recommended among antidiabetic medications for patients with diabetes. SGLT2 inhibitors include canagliflozin, dapagliflozin, tofogliflozin, luseogliflozin, ipragliflozin, empagliflozin, ertugliflozin, and sotagliflozin (an inhibitor of SGLT2 and SGLT1). The following four SGLT2 inhibitors have been approved by the U.S. Food and Drug Administration (FDA) for the treatment of hyperglycemia as monotherapy or in combination with other glucose-lowering agents for patients with T2DM: canagliflozin, dapagliflozin, empagliflozin, and ertugliflozin (Tuttle et al., 2021). Several oral SGLT2 inhibitors are available to choose from, and determining the best SGLT2 inhibitor to prescribe for patients with T2DM who may have difference cardiovascular and renal risk can be difficult. Several previous network analyses with multiple categories of antidiabetic medications, including SGLT2 inhibitors, evaluated the efficacy of these drugs on cardiovascular and renal outcomes in patients with T2DM, but the conclusions were either uncertain or lacked relevance (Palmer et al., 2021).

Therefore, we performed a network meta-analysis to assess the benefits and limits of different of SGLT2 inhibitors for cardiovascular and renal outcomes in patients with T2DM. The aim of our analysis was to offer evidence for the clinical application of SGLT2 inhibitors in patients with T2DM.

2 Methods

2.1 Data sources and searches

This systematic review article was conducted in accordance with the Preferred Reporting Items for Systematic Reviews and Meta-Analyses (PRISMA-NMA). The network meta-analysis systematic review protocol was registered in the PROSPERO database (International Prospective Register of Systematic Reviews, https://www.crd.york.ac.uk/prospero, registration number CRD42020202202). A systematic search of PubMed, Embase, and the Cochrane library was performed from database inception to 11 November 2021 using the search terms “diabetes mellitus”, “type 2 diabetes”, “type II diabetes”, “sodium-glucose transporter two inhibitors”, “sodium glucose transporter two inhibitor”, “SGLT2 inhibitor”, “sodium glucose transporter II inhibitor”, “canagliflozin”, “dapagliflozin”, “empagliflozin”, “ertugliflozin”, “tofogliflozin”, “ipragliflozin”, and “remogliflozin”. The searches were limited to English-language articles. The selected documents were edited and managed using a bibliographic database created in EndNote X9.1(US) and duplicate documents were removed.

2.2 Study selection

We screened trials account of the following inclusion criteria. 1) They were randomized clinical trials (RCTs) that compared SGLT2 inhibitors (including dapagliflozin, canagliflozin, tofogliflozin, luseogliflozin, ipragliflozin, empagliflozin, ertugliflozin, or sotagliflozin) with placebo or other glucose-lowering treatments. 2) The participants were male or female individuals with T2DM who were ≥18 years old, and had HbA1c levels between 6.5% and 10.5%. 3) The duration of medication was ≥13 weeks 4) The outcomes of the trials included at least one cardiovascular or renal outcomes. The exclusion criteria were as follows. 1) The patients had type 1 diabetes mellitus or a history of hereditary glucose or galactose malabsorption. 2) The trials did not specify the inclusion or exclusion criteria. 3) Repeated use of data for secondary analyses. 4) Preclinical research of animal models.

2.3 Data extraction and quality assessment

Trial Selection and data extraction were conducted independently by two authors (LT and SA) based on the inclusion and exclusion criteria. The titles and abstracts of the trials were screened by two investigators (HZ and HY). Data were

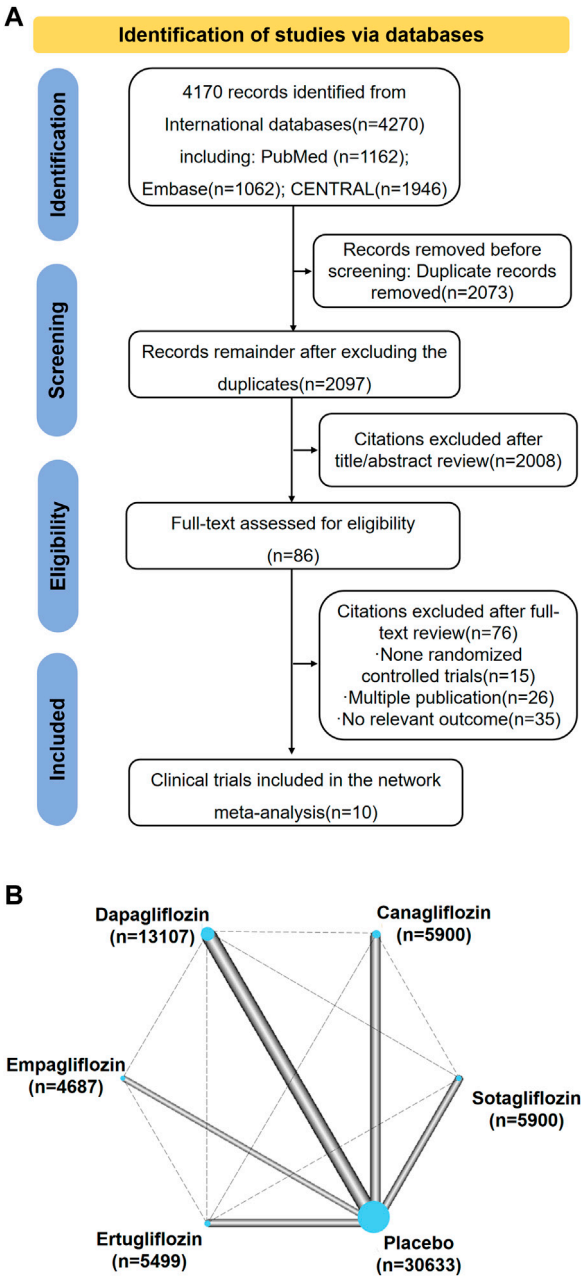

FIGURE 1
(A) Summary of Study Identification for Network Meta-analyses. **(B)** Network Plot for All Studies. Graphical representation of network for all induced trials. Connecting solid lines represent head-to-head comparisons between drugs, indicated by nodes. The thickness of lines between nodes is proportional to the number of trials comparing the treatments. The sizes of the nodes are proportional to the number of patients in each treatment which is marked below drugs. The control group is compared with each drug class. This is accounted for within the network model and does not constitute duplication of participants.

extracted using piloted forms in Microsoft Excel 2016 (US), and quality evaluation were conducted independently and in duplicate by two investigators (LT and SA). Disagreements were settled by deliberation with a third reviewer (WL and YW).

The outcomes in our network meta-analysis were mainly including the cardiovascular, renal outcome and all-cause mortality. Cardiovascular outcome included cardiovascular mortality, hospitalization for heart failure. Renal composite outcome was defined as a composite of doubling of serum creatinine level, initiation of renal-replacement therapy, or renal death.

The quality of the included studies and risk of trial bias were assessed using the Cochrane risk of bias assessment tool, which included randomization, quality of blinding, allocation concealment, and reporting bias categories. For each category, the trial was graded as high, low, or unclear. Two reviewers independently performed the data extraction and quality evaluation, and if there were any disagreements, they were resolved by discussion. The analyses were performed using Review Manager v5.1 (Cochrane Collaboration, http://www.cochrane.org).

2.4 Data synthesis and analysis

We used frequentist network meta-analysis. Hazard ratios (HRs) with 95% confidence intervals (CIs) were used to investigate the effects of cardiovascular and renal events. We used a frequentist approach to compare the effect of different SGLT2 inhibitor classes on these outcomes. The statistical package "netmeta" in R (version 4.1.2) was used for data processing. We used the forest function in "netmeta" package to plot the comparison forest, obtaining indirect comparison results and overall ranking by comparing to each intervention. Furthermore, the "netmeta" package can rank each intervention in order of merit by calculating the P-score of each intervention in the study. P-score from 0 to 1 was used to determine the probability of a treatment being the most effective (0 represents the worst; 1 represents the best). All the analyses results and plots were generated in R.

3 Results

There were 4,170 records identified during the searches. Among them, 2,097 records remained after duplicates were excluded, but 2,008 additional records were excluded after reviewing their titles and abstracts, leaving 89 records for full-text review. Among them, ten trials were included for the network meta-analysis (Figures 1A,B). These trails consist of CANVAS, CANVAS-R, CREDENCE,

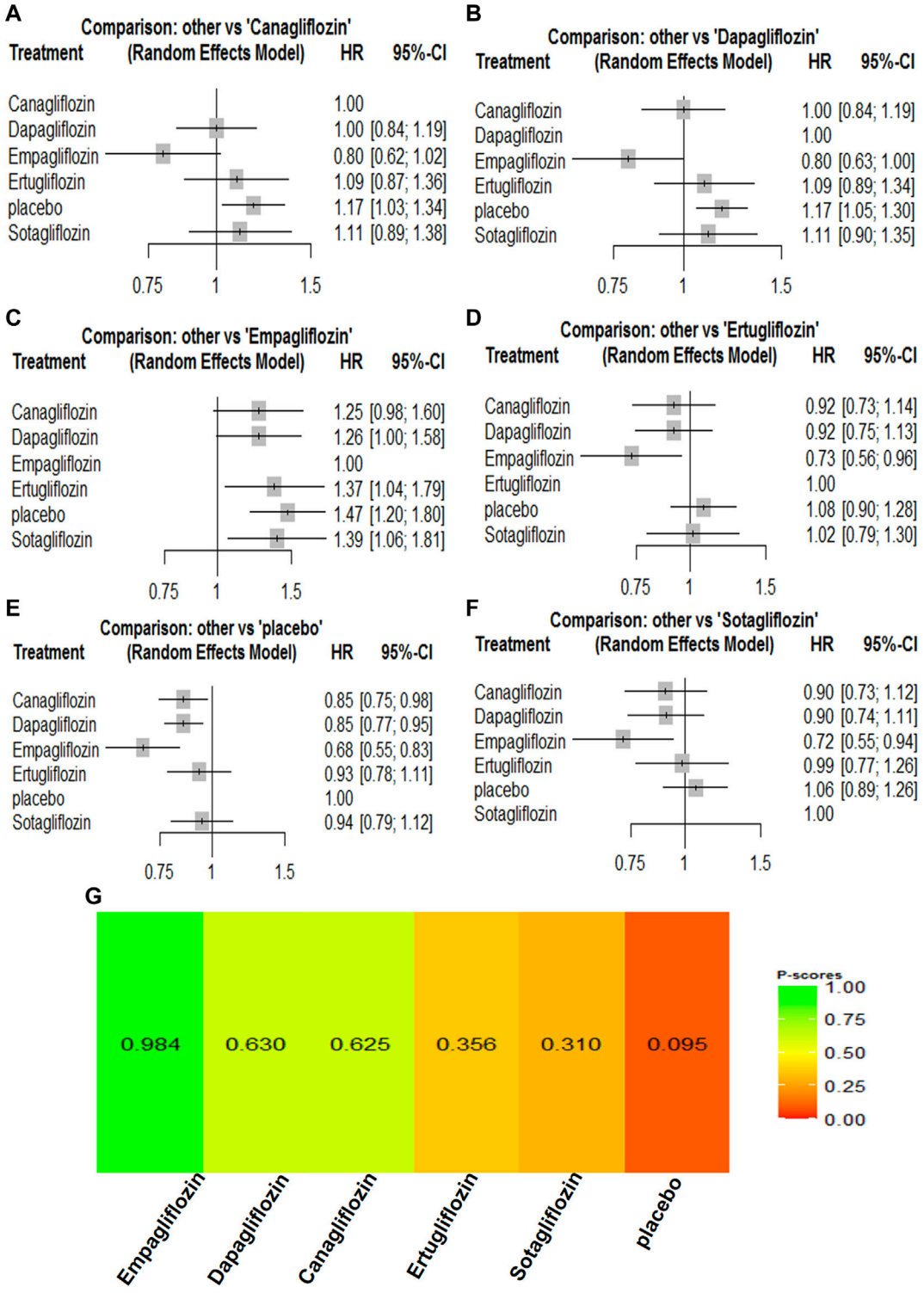

FIGURE 2
Forest Plots and Ranking Plots of Network Meta-analysis of all trials for All-cause Mortality. **(A)** Forest Plots of other drugs compare to canagliflozin. **(B)** Forest Plots of other drugs compare to dapagliflozin. **(C)** Forest Plots of other drugs compare to empagliflozin. **(D)** Forest Plots of other drugs compare to ertugliflozin. **(E)** Forest Plots of other drugs compare to placebo. **(F)** Forest Plots of other drugs compare to sotagliflozin. All outcomes are expressed as hazard ratios (HRs) for treatment vs the comparator and 95% credible intervals (95%-CI). For example, the HRs in all-cause mortality for dapagliflozin compared to canagliflozin is 1.00 (95%-CI 0.84 to 1.19). The x-axis scale indicates the range of the HRs. **(G)** Ranking Plots of Network Meta-analysis. Plots below the forest plots show for the rank of each drug class and ranking descending from left to right, The p-score represents the power of the ranking.

DECLARE-TIMI58, DAPA-CKD, DAPA-HF, EMPA-REG, VERTIS-CV, SCORED, and SOLOIST-WHF (Zinman et al., 2015; Neal et al., 2017; McMurray et al., 2019; Perkovic et al., 2019; Wiviott et al., 2019; Cannon et al., 2020; Bhatt et al., 2021a; Bhatt et al., 2021b; Wheeler et al., 2021). The characteristics of the included trials are presented in Supplementary Table S1. There were 67,823 patients with T2DM who were randomly assigned to the SGLT2 inhibitor treatment or a comparator treatment (placebo or other SGLT2 inhibitor). Among the ten trials, the CREDENCE, SCORED, and DAPA-CKD trials enrolled patients who had both T2DM and kidney disease. The SOLOIST-WHF and DAPA-HF trials enrolled patients who had both T2DM and heart failure. All trials reported all-cause mortality. However, hospitalization for heart failure was not reported in DAPA-CKD, and renal composite outcomes were not reported in the SOLOIST-WHF and DAPA-HF trials. All trials compared a SGLT2 inhibitor with placebo.

3.1 Risk of bias and publication bias

The Cochrane Collaboration risk of bias assessment tool indicated that all of the included trials used randomized sequence generation, and the methods used and allocation concealment were clearly stated. All the trials included blinding for the participants and investigators. All included trials were categorized as having a low risk of detection bias, attrition bias, reporting bias, and other bias. All of the trials were assessed as having a low risk of publication bias.

3.2 Network meta-analyses of SGLT2 inhibitors on all-cause mortality

All the included trials reported all-cause mortality for the 67,823 participants. There were 4,824 events (7.11%) among the 67,823 participants. Compared with the placebo groups, canagliflozin [HR, 0.85 (95%CI, 0.75–0.98)], dapagliflozin [HR, 0.85 (95%CI, 0.77–0.95)], empagliflozin [HR, 0.68 (95%CI, 0.55–0.83)], ertugliflozin [HR, 0.93 (95%CI, 0.78–1.11)], and sotagliflozin [HR, 0.94 (95%CI, 0.79–1.12)] were associated with reductions in all-cause mortality (Supplementary Table S2; and Figure 2). The P-score rank showed the drug rankings for reducing all-cause mortality, which were as follows: empagliflozin > dapagliflozin > canagliflozin > ertugliflozin > sotagliflozin (Figure 2).

3.3 Network meta-analyses of SGLT2 inhibitors on cardiovascular outcomes

For cardiovascular outcomes, nine trials that had enrolled 67,823 participants reported cardiovascular mortality and hospitalization for heart failure. All SGLT2 inhibitors lowered the risk of all-cause mortality and hospitalization for heart failure when compared with placebo (Supplementary Table S2). Empagliflozin [HR, 0.74 (95%CI, 0.56–0.97)] was associated with a reduction in cardiovascular mortality compared with canagliflozin. Canagliflozin [HR, 0.95 (95%CI, 0.78–1.15)] was associated with a reduction in cardiovascular mortality compared with dapagliflozin, while dapagliflozin [HR, 1.00 (95%CI, 0.80–1.24)] was associated with a reduction in cardiovascular mortality compared with sotagliflozin. Compared with ertugliflozin, sotagliflozin [HR, 0.96 (95%CI, 0.74–1.25)] reduced the risk of a cardiovascular mortality event. The cardiovascular mortality rankings were as follows: empagliflozin > canagliflozin > dapagliflozin > sotagliflozin > ertugliflozin (Supplementary Table S2; Figure 3). Canagliflozin [HR, 0.99 (95%CI, 0.71–1.36)] was associated with fewer hospitalizations compared with empagliflozin. Empagliflozin [HR, 0.99 (95%CI, 0.72–1.34)] was associated with a reduction in hospitalization for heart failure compared with sotagliflozin, while sotagliflozin [HR, 0.94 (95%CI, 0.70–1.27)] was associated with a reduction in hospitalization for heart failure compared with ertugliflozin. Ertugliflozin [HR, 0.98 (95%CI, 0.74–1.30)] was associated with a reduction in hospitalization for heart failure compared with dapagliflozin. The rankings for reducing hospitalization for heart failure were as follows: canagliflozin > empagliflozin > sotagliflozin > ertugliflozin > dapagliflozin (Supplementary Table S2; Figure 4). Canagliflozin and empagliflozin seemed to have the same efficacy in reducing hospitalization for heart failure, but empagliflozin had advantage in reducing cardiovascular mortality.

3.4 Network meta-analyses of SGLT2 inhibitors on composite renal outcome

A composite renal outcome consisted of new or worsening persistent microalbuminuria or macroalbuminuria, new or worsening chronic kidney disease, doubling of serum creatinine, end-stage renal disease, renal transplant, or renal death. For the composite renal outcomes, nine trials enrolling 63,079 patients were included. Compared with the control groups, canagliflozin [HR, 0.64 (95%CI, 0.54–0.75)], dapagliflozin [HR, 0.55 (95%CI, 0.47–0.63)], empagliflozin [HR, 0.54 (95%CI, 0.39–0.74)], ertugliflozin [HR, 0.70 (95%CI, 0.54–0.90)], and sotagliflozin [HR, 0.66 (95%CI, 0.56–0.77)] were associated with a reduction in the renal composite outcome. Dapagliflozin [HR, 1.01 (95%CI, 0.71–1.43)] was associated with a reduction in the renal composite compared with empagliflozin, while empagliflozin [HR, 0.85 (95%CI, 0.60–1.21)] was associated with a reduction in the renal composite compared with canagliflozin. Canagliflozin [HR, 0.90 (95%CI, 0.57–1.41)] was associated with a reduction in the renal composite compared

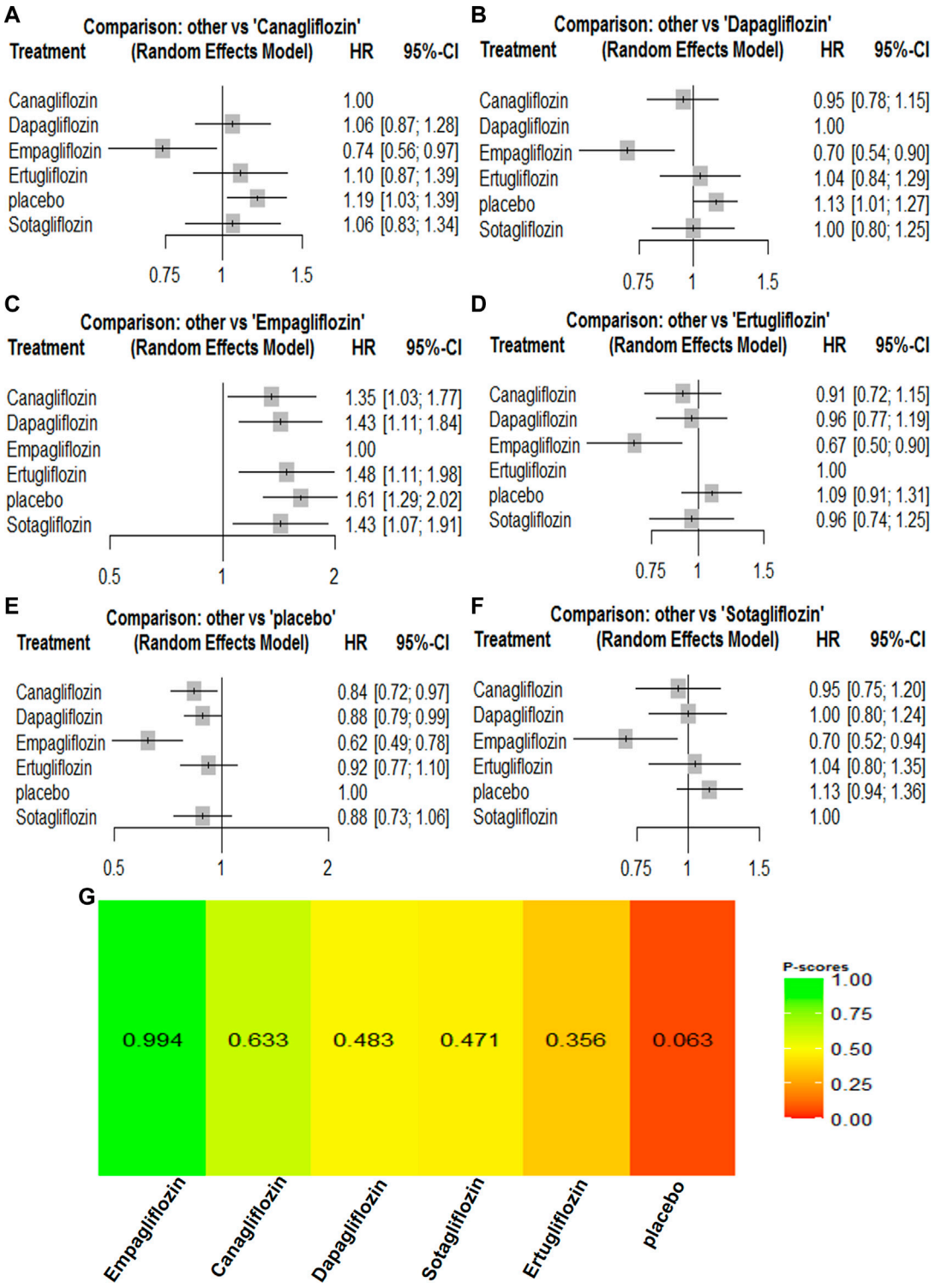

FIGURE 3
Forest Plots and Ranking Plots of Network Meta-analysis of all trials for Cardiovascular Mortality. **(A)** Forest Plots of other drugs compare to placebo. **(B)** Forest Plots of other drugs compare to dapagliflozin. **(C)** Forest Plots of other drugs compare to empagliflozin. **(D)** Forest Plots of other drugs compare to ertugliflozin. **(E)** Forest Plots of other drugs compare to canagliflozin. **(F)** Forest Plots of other drugs compare to sotagliflozin. All effect estimates are expressed as hazard ratios (HRs) for treatment vs the comparator and 95% credible intervals (95%-CI). For example, the HRs in cardiovascular mortality for dapagliflozin compared to canagliflozin is 1.06 (95%-CI 0.87 to 1.28). The x-axis scale indicates the range of the HRs. **(G)** Ranking Plots of Network Meta-analysis. Plots below the forest plots show for the rank of each drug class and ranking descending from left to right, The p-score represents the power of the ranking.

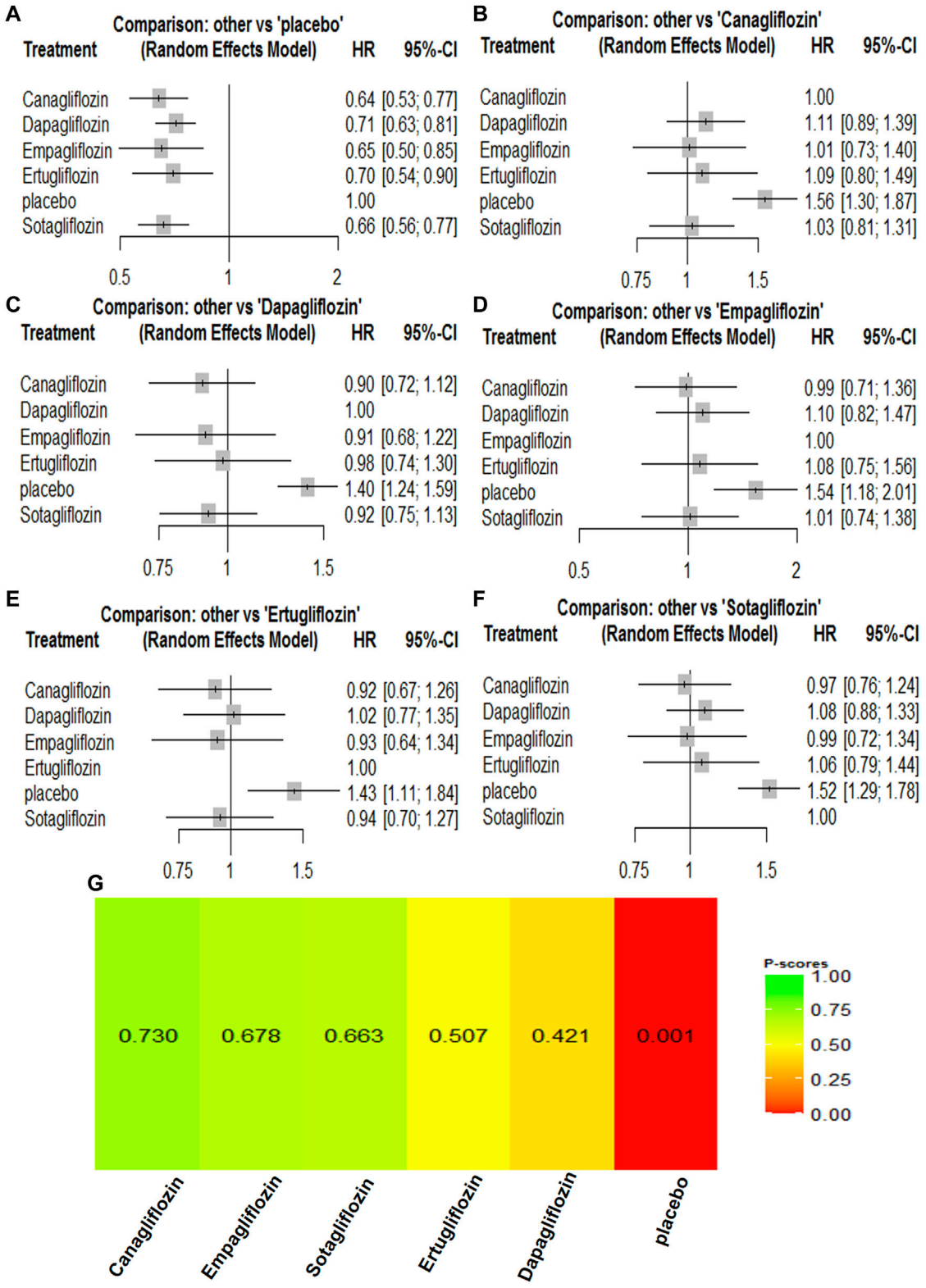

FIGURE 4
Forest Plots and Ranking Plots of Network Meta-analysis of all trials for Hospitalization for Heart Failure. **(A)** Forest Plots of other drugs compare to canagliflozin. **(B)** Forest Plots of other drugs compare to dapagliflozin. **(C)** Forest Plots of other drugs compare to empagliflozin. **(D)** Forest Plots of other drugs compare to ertugliflozin. **(E)** Forest Plots of other drugs compare to placebo. **(F)** Forest Plots of other drugs compare to sotagliflozin. All effect estimates are expressed as hazard ratios (HRs) for treatment vs the comparator and 95% credible intervals (95%-CI). For example, the HRs in hospitalization for heart failure for canagliflozin compared to placebo is 0.64 (95%-CI 0.53 to 0.77). The x-axis scale indicates the range of the HRs. **(G)** Ranking Plots of Network Meta-analysis. Plots below the forest plots show for the rank of each drug class and ranking descending from left to right, The p-score represents the power of the ranking.

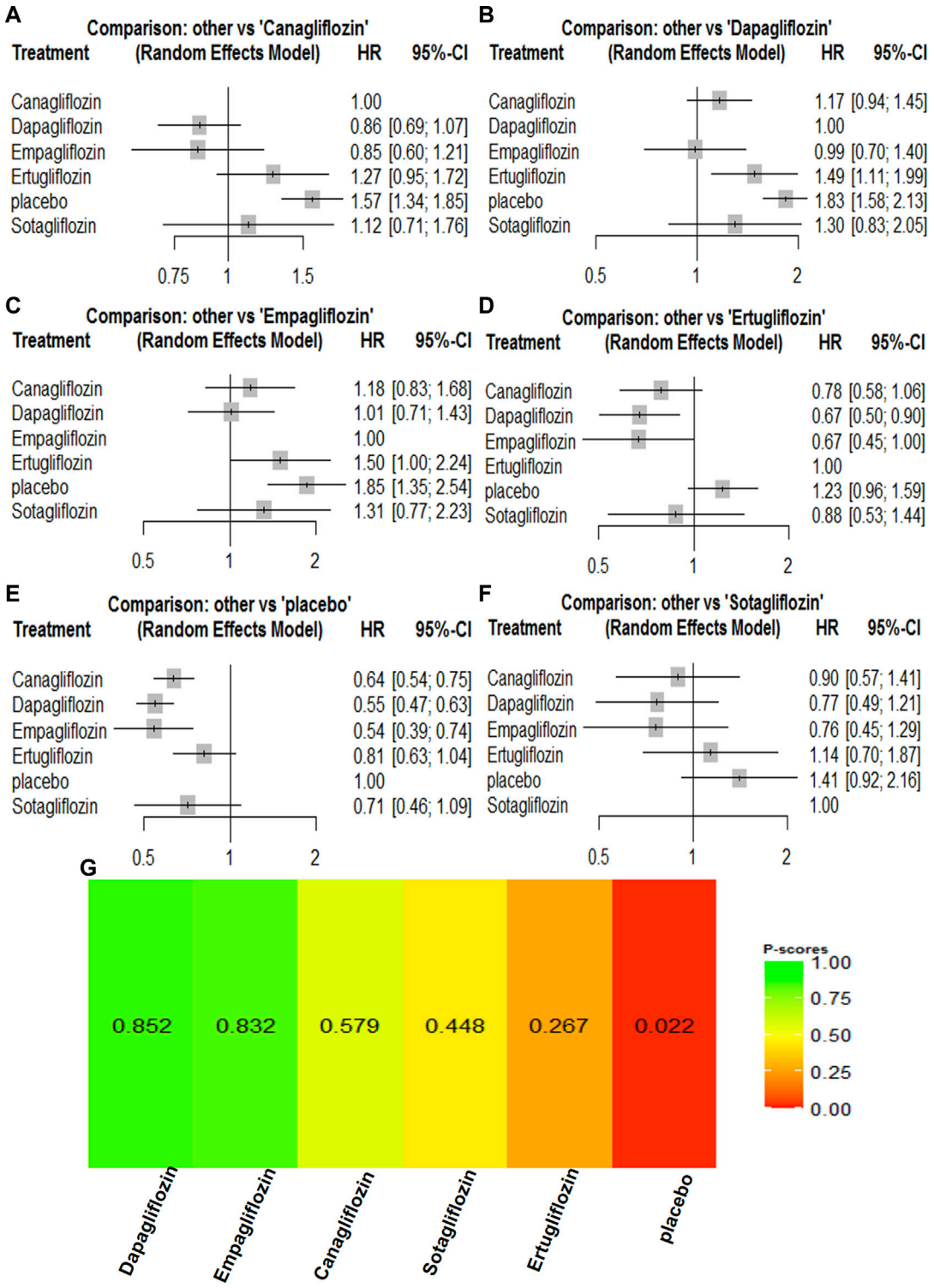

FIGURE 5
Forest Plots and Ranking Plots of Network Meta-analysis of all trials for Composite Renal Outcome. **(A)** Forest Plots of other drugs compare to canagliflozin. **(B)** Forest Plots of other drugs compare to dapagliflozin. **(C)** Forest Plots of other drugs compare to empagliflozin. **(D)** Forest Plots of other drugs compare to ertugliflozin. **(E)** Forest Plots of other drugs compare to placebo. **(F)** Forest Plots of other drugs compare to sotagliflozin. All effect estimates are expressed as hazard ratios (HRs) for treatment vs the comparator and 95% credible intervals (95%-CI). For example, the HRs in composite renal outcome for dapagliflozin compared to canagliflozin is 0.86 (95%-CI 0.69 to 1.07). The x-axis scale indicates the range of the HRs. **(G)** Ranking Plots of Network Meta-analysis. Plots below the forest plots show for the rank of each drug class and ranking descending from left to right, The p-score represents the power of the ranking.

with sotagliflozin, while sotagliflozin [HR, 0.88 (95%CI, 0.53–1.44)] was associated with a reduction in the renal composite compared with ertugliflozin. Dapagliflozin was most likely to have the best results for renal composite outcomes, and the rankings for the renal composite outcome results were as follows: dapagliflozin > empagliflozin > canagliflozin > sotagliflozin > ertugliflozin (Supplementary Table S2; Figure 5).

4 Discussion

This network meta-analysis was the first to incorporate the large and recently published randomized controlled trial about SGLT2 inhibitors in the management of T2DM. SGLT2 inhibitors are the latest recommended first-line hypoglycemic drugs, and our study including dapagliflozin, canagliflozin, tofogliflozin, luseogliflozin, ipragliflozin, empagliflozin, ertugliflozin, and sotagliflozin to provide evidence to help select the most appropriate SGLT2 inhibitor for patients with different cardiovascular and renal complication risk factors. The results of our network meta-analysis suggested the following: 1) For cardiovascular outcomes, all SGLT2 inhibitors reduced the risk of all-cause mortality and hospitalization for heart failure compared with placebo, and the rankings for cardiovascular mortality were empagliflozin > canagliflozin > dapagliflozin > sotagliflozin > ertugliflozin, while the rankings for reduced hospitalization for heart failure were canagliflozin > empagliflozin > sotagliflozin > ertugliflozin > dapagliflozin. 2) For a renal composite outcome, dapagliflozin was the most likely to show the best renal composite outcomes compared with the control group. The rankings were dapagliflozin > empagliflozin > canagliflozin > sotagliflozin > ertugliflozin.

T2DM is a systemic metabolic disease that affects the microvascular and macrovascular systems. Hyperglycemia is the primary risk factor for microvascular complications, such as nephropathy, retinopathy, and neuropathy ((UKPDS) Group, 1998; Diabetes Control and Complications Trial Research Group, 1994). Meaningful benefits of improved blood glucose on macrovascular complications were more pronounced after 10 years or more (Holman et al., 2008). SGLT2 inhibitors may be vital blood glucose lowering agents for T2DM treatment because they exert multiple beneficial metabolic effects such as controlling body weight, uric acid levels, and blood pressure (BP) (Toyama et al., 2019). For cardiovascular events, the precise mechanism of the SGLT2 inhibitor-induced cardiovascular benefit remains to be determined, but previous studies have shown that SGLT2 inhibitors may prevent cardiovascular outcomes by regulating dyslipidemia, restoring normal endothelial function, inhibiting cardiac remodeling, and inhibiting the evolution of monocyte–macrophage foam cells (Terasaki et al., 2015; Kang et al., 2020; Lee et al., 2020; Park et al., 2021). Previous reports suggested that SGLT2 inhibitors may also lead to vasodilation and positive inotropic effects at the angiotensin type II receptor during simultaneous blockade of the renin–angiotensin–aldosterone system (the RAAS hypothesis) (Filippatos et al., 2019). All the above are possible mechanisms of the cardioprotective effect of SGLT2 inhibitors. In addition, Previous meta-analysis showed a moderate benefit of SGLT2 inhibitors for major adverse atherosclerotic cardiovascular events and a significant benefit in reducing hospitalizations for heart failure and renal disease progression, regardless of the presence of atherosclerotic cardiovascular disease or a history of heart failure, but there are differences in the dose, efficacy, and safety among different SGLT2 inhibitors (Zelniker et al., 2019). In 2015, Empagliflozin as a SGLT2 inhibitor first published data with (Cardio vascular) CV outcomes. Compared with other SGLT2 inhibitors, empagliflozin has the highest selectivity for SGLT2. Although SGLT2 expression in the myocardium is negligible, SGLT2 inhibitors can directly reduce Na + -H+ exchanger (NHE) activity in cardiomyocytes through the binding site of SGLT2 on NHE. It is well known that failing cardiomyocytes display enhanced intracellular sodium levels, at least in part on account of increased activity of the sarcolemmal NHE, resulting in associated Ca^{2+} efflux from mitochondria leading to exacerbation of cell function and reduced antioxidant capacity (Darmellah et al., 2007; Bell and Yellon, 2018; Bertero et al., 2018). Thus, SGLT2 inhibitors can reduce the incidence of ventricular arrhythmias and sudden cardiac death by reducing cardiomyocyte NHE activity leading to a reduction in intracellular sodium and restoration of mitochondrial calcium handling, as well as sudden cardia death. The hypothesis may the advantage effects of empagliflozin on cardiovascular mortality. Previous studies have also found that Empagliflozin has a direct pleiotropic effect on isolated failing human myocardium, as well as on the diastolic function of healthy and diseased mouse myocardium, which has direct pleiotropic effects on the myocardium by improving myocardial diastolic stiffness and diastolic function, and these effects were not related to diabetes (Pabel et al., 2018). Empagliflozin switches myocardial fuel utilization from the low-yield energy-producing glucose metabolism to (ketone bodies) KB (free fatty acid) FFA, and (branched -chain amino acid) BCAA, thereby ameliorating myocardial energy, boosting (left ventricular) LV systolic function, as well as improving adverse LV remodeling (Santos-Gallego et al., 2019). Moreover, canagliflozin seemed to have the same efficacy in reducing hospitalization for heart failure as empagliflozin. Canagliflozin is also a low-potency sodium–glucose co-transporter type 1 (SGLT1) inhibitor, which may distinguish it from other SGLT2 inhibitors (Scheen, 2015). The SGLT1 transporters are more widely distributed in heart.

SGLT1 is the major transporter for intestinal glucose absorption, and intestinal inhibition of SGLT1 results in glucose–galactose malabsorption, which may also show better hypoglycemic results with canagliflozin. Another meta-analysis also indicated that canagliflozin, which is a SGLT2 inhibitor only, decreases systolic blood pressure in a dose-dependent manner (0.87 mmHg for every additional 100 mg of canagliflozin), which may explain its additional cardiovascular benefits (Baker et al., 2014).

In terms of renal events, previous studies have not fully revealed the mechanism by which SGLT2 inhibitors benefit renal outcomes in individuals with T2DM. The nephroprotective effect of SGLT2 inhibitors in patients with T2DM may involve multiple mechanisms, which mainly include the following aspects: 1) SGLT2 inhibitors inhibit proximal tubular sodium reabsorption, which results in increased sodium delivery to the juxtaglomerular apparatus, decreased intraglomerular pressure, and normalized ultrafiltration, which decreases the kidney's injury and reduces albuminuria (Vallon and Thomson, 2017); 2) reduced activation of the intrarenal renin–angiotensin–aldosterone system, which lowers blood pressure and helps to reduce glomerular hyperfiltration (Ravindran and Munusamy, 2022). Some reports speculate that SGLT2 inhibitors show similar effects as that of angiotensin blockade, leading to a decrease in the initiation and functional decline in the estimated glomerular filtration rate (eGFR), which may contribute to long-term preservation of renal function (Nespoux and Vallon, 2018); 3) increased ketone bodies in individuals with type 2 diabetes. Similar to fatty acids, ketone bodies could be used as an alternative fuel for mitochondria to synthesize ATP. Moreover, erythropoietin levels were also increased, which could improve renal tissue oxygenation, transfer fuel selection from glucose to ketone bodies, help to improve mitochondrial function, and help to attenuate inflammation (Ferrannini, 2017); and 4) protect against hypoxia and oxidative stress, regulate autophagy, and improve fibrosis. The results of our analysis indicated that dapagliflozin has the best effect on renal outcomes in patients with T2DM. However, there has been no report on the possible mechanism by which dapagliflozin has better renal events than other SGLT2 inhibitors.

A main limitation of this network analysis is the heterogeneity of the included trials. The sources of this heterogeneity mainly include differences in clinical settings as well as differences in national and ethnic groups, although the consistency of the findings alleviates this concern. Moreover, in individual trials, patients included differences in baseline renal function levels, which may affect renal outcomes. The definition of the cardiovascular risk was inconsistent across the trials that were included in the network analysis of patients with an increased cardiovascular risk.

5 Conclusion

In conclusion, our network analysis incorporating the latest and most comprehensive RCTs for SGLT2 inhibitors established a solid evidence base that verified a prominent effect of dapagliflozin and canagliflozin on renal and cardiovascular outcomes compared with similar SGLT2 inhibitors. These class agents also reduced all-cause mortality and showed benefits regardless of the patient's sex or if they had diabetes.

Data availability statement

The original contributions presented in the study are included in the article/Supplementary Material, further inquiries can be directed to the corresponding authors.

Author contributions

LT: Conceptualization, Methodology and Writing. SA: Software and Original draft preparation. HZ: Data curation, MZ: Assessed the risk of bias. HY: Supervision. JT: Validation. WL: Reviewing and Editing. WZ: Manuscript polishing and correction. YW: Conceived and designed the experiments.

Funding

This study was supported by and The National Natural Youth Science Foundation of China (no. 82104847) and National Natural Science Foundation of China (Grant Nos. 81774298) and the Natural Science Foundation of Beijing (No.7222271).

Conflict of interest

The authors declare that the research was conducted in the absence of any commercial or financial relationships that could be construed as a potential conflict of interest.

Publisher's note

Supplementary material

The Supplementary Material for this article can be found online at: https://www.frontiersin.org/articles/10.3389/fphar.2022.986186/full#supplementary-material

References

Anders, H. J., Huber, T. B., Isermann, B., and Schiffer, M. (2018). CKD in diabetes: Diabetic kidney disease versus nondiabetic kidney disease. *Nat. Rev. Nephrol.* 14 (6), 361–377. doi:10.1038/s41581-018-0001-y

Baker, W. L., Smyth, L. R., Riche, D. M., Bourret, E. M., Chamberlin, K. W., and White, W. B. (2014). Effects of sodium-glucose co-transporter 2 inhibitors on blood pressure: A systematic review and meta-analysis. *J. Am. Soc. Hypertens.* 8 (4), 262–275. doi:10.1016/j.jash.2014.01.007

Bell, R. M., and Yellon, D. M. (2018). SGLT2 inhibitors: Hypotheses on the mechanism of cardiovascular protection. *Lancet. Diabetes Endocrinol.* 6 (6), 435–437. doi:10.1016/S2213-8587(17)30314-5

Bertero, E., Prates Roma, L., Ameri, P., and Maack, C. (2018). Cardiac effects of SGLT2 inhibitors: The sodium hypothesis. *Cardiovasc. Res.* 114 (1), 12–18. doi:10.1093/cvr/cvx149

Bhatt, D. L., Szarek, M., Pitt, B., Cannon, C. P., Leiter, L. A., McGuire, D. K., et al. (2021). Sotagliflozin in patients with diabetes and chronic kidney disease. *N. Engl. J. Med.* 384 (2), 129–139. doi:10.1056/NEJMoa2030186

Bhatt, D. L., Szarek, M., Steg, P. G., Cannon, C. P., Leiter, L. A., McGuire, D. K., et al. (2021). Sotagliflozin in patients with diabetes and recent worsening heart failure. *N. Engl. J. Med.* 384 (2), 117–128. doi:10.1056/NEJMoa2030183

Bjornstad, P., Drews, K. L., Caprio, S., Gubitosi-Klug, R., Nathan, D. M., Tesfaldet, B., et al. (2021). Long-term complications in youth-onset type 2 diabetes. *N. Engl. J. Med.* 385 (5), 416–426. doi:10.1056/NEJMoa2100165

Cannon, C. P., Pratley, R., Dagogo-Jack, S., Mancuso, J., Huyck, S., Masiukiewicz, U., et al. (2020). Cardiovascular outcomes with ertugliflozin in type 2 diabetes. *N. Engl. J. Med.* 383 (15), 1425–1435. doi:10.1056/NEJMoa2004967

Darmellah, A., Baetz, D., Prunier, F., Tamareille, S., Rücker-Martin, C., and Feuvray, D. (2007). Enhanced activity of the myocardial Na+/H+ exchanger contributes to left ventricular hypertrophy in the goto-kakizaki rat model of type 2 diabetes: Critical role of akt. *Diabetologia* 50 (6), 1335–1344. doi:10.1007/s00125-007-0628-x

DeFronzo, R. A., Norton, L., and Abdul-Ghani, M. (2017). Renal, metabolic and cardiovascular considerations of SGLT2 inhibition. *Nat. Rev. Nephrol.* 13 (1), 11–26. doi:10.1038/nrneph.2016.170

Deng, Y., Li, N., Wu, Y., Wang, M., Yang, S., Zheng, Y., et al. (2021). Global, regional, and national burden of diabetes-related chronic kidney disease from 1990 to 2019. *Front. Endocrinol.* 12, 672350. doi:10.3389/fendo.2021.672350

Diabetes Control and Complications Trial Research Group (1994). Effect of intensive diabetes treatment on the development and progression of long-term complications in adolescents with insulin-dependent diabetes mellitus: Diabetes Control and Complications Trial. Diabetes Control and Complications Trial Research Group. *J. Pediatr.* 125 (2), 177–188. doi:10.1016/s0022-3476(94)70190-3

Ferrannini, E. (2017). Sodium-glucose Co-transporters and their inhibition: Clinical physiology. *Cell Metab.* 26 (1), 27–38. doi:10.1016/j.cmet.2017.04.011

Filippatos, T. D., Liontos, A., Papakitsou, I., and Elisaf, M. S. (2019). SGLT2 inhibitors and cardioprotection: A matter of debate and multiple hypotheses. *Postgrad. Med.* 131 (2), 82–88. doi:10.1080/00325481.2019.1581971

Fox, C. S., Golden, S. H., Anderson, C., Bray, G. A., Burke, L. E., de Boer, I. H., et al. (2015). Update on prevention of cardiovascular disease in adults with type 2 diabetes mellitus in light of recent evidence: A scientific statement from the American heart association and the American diabetes association. *Diabetes care* 38 (9), 1777–1803. doi:10.2337/dci15-0012

Gallo, L. A., Wright, E. M., and Vallon, V. (2015). Probing SGLT2 as a therapeutic target for diabetes: Basic physiology and consequences. *Diab. Vasc. Dis. Res.* 12 (2), 78–89. doi:10.1177/1479164114561992

Gilbert, R. E., and Krum, H. (2015). Heart failure in diabetes: Effects of anti-hyperglycaemic drug therapy. *Lancet (London, Engl.* 385 (9982), 2107–2117. doi:10.1016/S0140-6736(14)61402-1

Holman, R. R., Paul, S. K., Bethel, M. A., Matthews, D. R., and Neil, H. A. (2008). 10-year follow-up of intensive glucose control in type 2 diabetes. *N. Engl. J. Med.* 359 (15), 1577–1589. doi:10.1056/NEJMoa0806470

International Diabetes Foundation (2021). *IDF diabetes atlas*. Brussels, Belgium: International Diabetes Foundation.

Kang, Y., Zhan, F., He, M., Liu, Z., and Song, X. (2020). Anti-inflammatory effects of sodium-glucose co-transporter 2 inhibitors on atherosclerosis. *Vasc. Pharmacol.* 133, 106779. doi:10.1016/j.vph.2020.106779

Koye, D. N., Magliano, D. J., Nelson, R. G., and Pavkov, M. E. (2018). The global epidemiology of diabetes and kidney disease. *Adv. Chronic Kidney Dis.* 25 (2), 121–132. doi:10.1053/j.ackd.2017.10.011

Lee, S. G., Lee, S. J., Lee, J. J., Kim, J. S., Lee, O. H., Kim, C. K., et al. (2020). Anti-Inflammatory effect for atherosclerosis progression by sodium-glucose cotransporter 2 (SGLT-2) inhibitor in a normoglycemic rabbit model. *Korean Circ. J.* 50 (5), 443–457. doi:10.4070/kcj.2019.0296

Lloyd-Jones, D., Adams, R., Carnethon, M., De Simone, G., Ferguson, T. B., Flegal, K., et al. (2009). Heart disease and stroke statistics--2009 update: A report from the American heart association statistics committee and stroke statistics subcommittee. *Circulation* 119 (3), e21–e181. doi:10.1161/CIRCULATIONAHA.108.191261

Loke, Y. K., Kwok, C. S., and Singh, S. (2011). Comparative cardiovascular effects of thiazolidinediones: Systematic review and meta-analysis of observational studies. *BMJ Clin. Res. ed)* 342, d1309. doi:10.1136/bmj.d1309

McMurray, J. J. V., Solomon, S. D., Inzucchi, S. E., Køber, L., Kosiborod, M. N., Martinez, F. A., et al. (2019). Dapagliflozin in patients with heart failure and reduced ejection fraction. *N. Engl. J. Med.* 381 (21), 1995–2008. doi:10.1056/NEJMoa1911303

Nauck, M. A. (2014). Update on developments with SGLT2 inhibitors in the management of type 2 diabetes. *Drug Des. devel. Ther.* 8, 1335–1380. doi:10.2147/DDDT.S50773

Neal, B., Perkovic, V., Mahaffey, K. W., de Zeeuw, D., Fulcher, G., Erondu, N., et al. (2017). Canagliflozin and cardiovascular and renal events in type 2 diabetes. *N. Engl. J. Med.* 377 (7), 2099–2657. doi:10.1056/NEJMc1712572

Nespoux, J., and Vallon, V. (2018). SGLT2 inhibition and kidney protection. *Clin. Sci. (1979)* 132 (12), 1329–1339. doi:10.1042/CS20171298

Neuen, B. L., Young, T., Heerspink, H. J. L., Neal, B., Perkovic, V., Billot, L., et al. (2019). SGLT2 inhibitors for the prevention of kidney failure in patients with type 2 diabetes: A systematic review and meta-analysis. *Lancet. Diabetes Endocrinol.* 7 (11), 845–854. doi:10.1016/S2213-8587(19)30256-6

Pabel, S., Wagner, S., Bollenberg, H., Bengel, P., Kovács, Á., Schach, C., et al. (2018). Empagliflozin directly improves diastolic function in human heart failure. *Eur. J. Heart Fail.* 20 (12), 1690–1700. doi:10.1002/ejhf.1328

Packer, M. (2018). Have we really demonstrated the cardiovascular safety of anti-hyperglycaemic drugs? Rethinking the concepts of macrovascular and microvascular disease in type 2 diabetes. *Diabetes Obes. Metab.* 20 (5), 1089–1095. doi:10.1111/dom.13207

Palmer, S. C., Tendal, B., Mustafa, R. A., Vandvik, P. O., Li, S., Hao, Q., et al. (2021). Sodium-glucose cotransporter protein-2 (SGLT-2) inhibitors and glucagon-like peptide-1 (GLP-1) receptor agonists for type 2 diabetes: Systematic review and network meta-analysis of randomised controlled trials. *BMJ Clin. Res. ed* 372, m4573. doi:10.1136/bmj.m4573

Park, S. H., Belcastro, E., Hasan, H., Matsushita, K., Marchandot, B., Abbas, M., et al. (2021). Angiotensin II-induced upregulation of SGLT1 and 2 contributes to human microparticle-stimulated endothelial senescence and dysfunction: Protective effect of gliflozins. *Cardiovasc. Diabetol.* 20 (1), 65. doi:10.1186/s12933-021-01252-3

Perkovic, V., Jardine, M. J., Neal, B., Bompoint, S., Heerspink, H. J. L., Charytan, D. M., et al. (2019). Canagliflozin and renal outcomes in type 2 diabetes and nephropathy. *N. Engl. J. Med.* 380 (24), 2295–2306. doi:10.1056/NEJMoa1811744

Ravindran, S., and Munusamy, S. (2022). Renoprotective mechanisms of sodium-glucose co-transporter 2 (SGLT2) inhibitors against the progression of diabetic kidney disease. *J. Cell. Physiol.* 237 (2), 1182–1205. doi:10.1002/jcp.30621

Santos-Gallego, C. G., Requena-Ibanez, J. A., San Antonio, R., Ishikawa, K., Watanabe, S., Picatoste, B., et al. (2019). Empagliflozin ameliorates adverse left ventricular remodeling in nondiabetic heart failure by enhancing myocardial energetics. *J. Am. Coll. Cardiol.* 73 (15), 1931–1944. doi:10.1016/j.jacc.2019.01.056

Scheen, A. J. (2015). Pharmacodynamics, efficacy and safety of sodium-glucose co-transporter type 2 (SGLT2) inhibitors for the treatment of type 2 diabetes mellitus. *Drugs* 75 (1), 33–59. doi:10.1007/s40265-014-0337-y

Seferović, P. M., Petrie, M. C., Filippatos, G. S., Anker, S. D., Rosano, G., Bauersachs, J., et al. (2018). Type 2 diabetes mellitus and heart failure: A position statement from the heart failure association of the European society of cardiology. *Eur. J. Heart Fail.* 20 (5), 853–872. doi:10.1002/ejhf.1170

Terasaki, M., Hiromura, M., Mori, Y., Kohashi, K., Nagashima, M., Kushima, H., et al. (2015). Amelioration of hyperglycemia with a sodium-glucose cotransporter 2 inhibitor prevents macrophage-driven atherosclerosis through macrophage foam cell formation suppression in type 1 and type 2 diabetic mice. *PloS one* 10 (11), e0143396. doi:10.1371/journal.pone.0143396

Thomas, M. C., and Cherney, D. Z. I. (2018). The actions of SGLT2 inhibitors on metabolism, renal function and blood pressure. *Diabetologia* 61 (10), 2098–2107. doi:10.1007/s00125-018-4669-0

Toyama, T., Neuen, B. L., Jun, M., Ohkuma, T., Neal, B., Jardine, M. J., et al. (2019). Effect of SGLT2 inhibitors on cardiovascular, renal and safety outcomes in patients with type 2 diabetes mellitus and chronic kidney disease: A systematic review and meta-analysis. *Diabetes Obes. Metab.* 21 (5), 1237–1250. doi:10.1111/dom.13648

Tuttle, K. R., Brosius, F. C., 3rd, Cavender, M. A., Fioretto, P., Fowler, K. J., Heerspink, H. J. L., et al. (2021). SGLT2 inhibition for CKD and cardiovascular disease in type 2 diabetes: Report of a scientific workshop sponsored by the national kidney foundation. *Am. J. Kidney Dis.* 77 (1), 94–109. doi:10.1053/j.ajkd.2020.08.003

(UKPDS) Group (1998). Intensive blood-glucose control with sulphonylureas or insulin compared with conventional treatment and risk of complications in patients with type 2 diabetes (UKPDS 33). UK Prospective Diabetes Study (UKPDS) Group. *Lancet London, Engl.* 352 (9131), 837–853.

Umanath, K., and Lewis, J. B. (2018). Update on diabetic nephropathy: Core curriculum 2018. *Am. J. Kidney Dis.* 71 (6), 884–895. doi:10.1053/j.ajkd.2017.10.026

Vallon, V., and Thomson, S. C. (2017). Targeting renal glucose reabsorption to treat hyperglycaemia: The pleiotropic effects of SGLT2 inhibition. *Diabetologia* 60 (2), 215–225. doi:10.1007/s00125-016-4157-3

van Baar, M. J. B., van Ruiten, C. C., Muskiet, M. H. A., van Bloemendaal, L., Ijzerman, R. G., and van Raalte, D. H. (2018). SGLT2 inhibitors in combination therapy: From mechanisms to clinical considerations in type 2 diabetes management. *Diabetes care* 41 (8), 1543–1556. doi:10.2337/dc18-0588

Washburn, W. N. (2012). Sodium glucose co-transporter 2 (SGLT2) inhibitors: Novel antidiabetic agents. *Expert Opin. Ther. Pat.* 22 (5), 483–494. doi:10.1517/13543776.2012.680437

Wheeler, D. C., Stefánsson, B. V., Jongs, N., Chertow, G. M., Greene, T., Hou, F. F., et al. (2021). Effects of dapagliflozin on major adverse kidney and cardiovascular events in patients with diabetic and non-diabetic chronic kidney disease: A prespecified analysis from the DAPA-CKD trial. *Lancet. Diabetes Endocrinol.* 9 (1), 22–31. doi:10.1016/S2213-8587(20)30369-7

Wiviott, S. D., Raz, I., Bonaca, M. P., Mosenzon, O., Kato, E. T., Cahn, A., et al. (2019). Dapagliflozin and cardiovascular outcomes in type 2 diabetes. *N. Engl. J. Med.* 380 (4), 347–357. doi:10.1056/NEJMoa1812389

Zelniker, T. A., Wiviott, S. D., Raz, I., Im, K., Goodrich, E. L., Bonaca, M. P., et al. (2019). SGLT2 inhibitors for primary and secondary prevention of cardiovascular and renal outcomes in type 2 diabetes: A systematic review and meta-analysis of cardiovascular outcome trials. *Lancet (London, Engl.* 393 (10166), 31–39. doi:10.1016/S0140-6736(18)32590-X

Zinman, B., Wanner, C., Lachin, J. M., Fitchett, D., Bluhmki, E., Hantel, S., et al. (2015). Empagliflozin, cardiovascular outcomes, and mortality in type 2 diabetes. *N. Engl. J. Med.* 373 (22), 2117–2128. doi:10.1056/NEJMoa1504720

frontiers | Frontiers in Pharmacology

TYPE Original Research
PUBLISHED 06 January 2023
DOI 10.3389/fphar.2022.1035755

OPEN ACCESS

EDITED BY
Jun-Yan Liu,
Chongqing Medical University, China

REVIEWED BY
Krishna Prahlad Maremanda,
Texas A&M University, United States
Dharmani Devi Murugan,
University of Malaya, Malaysia

*CORRESPONDENCE
Zhaoli Gao,
gaozhaoli123@126.com
Xianhua Li,
lixianhua7075@sina.com

SPECIALTY SECTION
This article was submitted to Renal Pharmacology, a section of the journal Frontiers in Pharmacology

RECEIVED 03 September 2022
ACCEPTED 14 December 2022
PUBLISHED 06 January 2023

CITATION
Song Y, Yu H, Sun Q, Pei F, Xia Q, Gao Z and Li X (2023), Grape seed proanthocyanidin extract targets p66Shc to regulate mitochondrial biogenesis and dynamics in diabetic kidney disease.
Front. Pharmacol. 13:1035755.
doi: 10.3389/fphar.2022.1035755

Grape seed proanthocyanidin extract targets p66Shc to regulate mitochondrial biogenesis and dynamics in diabetic kidney disease

Yiyun Song[1,2], Hui Yu[1,2], Qiaoling Sun[1,2], Fei Pei[1,2], Qing Xia[1,2], Zhaoli Gao[2,3]* and Xianhua Li[1,2]*

[1]Department of Nephrology, Qilu Hospital of Shandong University, Jinan, Shandong, China, [2]Cheeloo College of Medicine, Shandong University, Jinan, Shandong, China, [3]Department of Nephrology, Qilu Hospital of Shandong University (Qingdao), Qingdao, Shandong, China

Mitochondrial biogenesis and dynamics are associated with renal mitochondrial dysfunction and the pathophysiological development of diabetic kidney disease (DKD). Decreased p66Shc expression prevents DKD progression by significantly regulating mitochondrial function. Grape seed proanthocyanidin extract (GSPE) is a potential therapeutic medicine for multiple kinds of diseases. The effect of GSPE on the mitochondrial function and p66Shc in DKD has not been elucidated. Hence, we decided to identify p66Shc as a therapeutic target candidate to probe whether GSPE has a renal protective effect in DKD and explored the underlying mechanisms. Methods. *In vivo*, rats were intraperitoneally injected with streptozotocin (STZ) and treated with GSPE. Biochemical changes, mitochondrial morphology, the ultrastructure of nephrons, and protein expression of mitochondrial biogenesis (SIRT1, PGC-1α, NRF1, TFAM) and dynamics (DRP1, MFN1) were determined. *In vitro*, HK-2 cells were transfected with p66Shc and treated with GSPE to evaluate changes in cell apoptosis, reactive oxygen species (ROS), mitochondrial quality, the protein expression. Results. *In vivo*, GSPE significantly improved the renal function of rats, with less proteinuria and a lower apoptosis rate in the injured renal tissue. Besides, GSPE treatment increased SIRT1, PGC-1α, NRF1, TFAM, and MFN1 expression, decreased p66Shc and DRP1 expression. *In vitro*, overexpression of p66Shc decreased the resistance of HK-2 cells to high glucose toxicity, as shown by increased apoptosis and ROS production, decreased mitochondrial quality and mitochondrial biogenesis, and disturbed mitochondrial dynamic homeostasis, ultimately leading to mitochondrial dysfunction. While GSPE treatment reduced p66Shc expression and reversed these changes. Conclusion. GSPE can maintain the balance between mitochondrial biogenesis and dynamics by negatively regulating p66Shc expression.

KEYWORDS

diabetic kidney disease, grape seed proanthocyanidin extract, mitochondrial biogenesis, mitochondrial dynamics, p66Shc

1 Introduction

Diabetic kidney disease (DKD), as the major microvascular complication of diabetes, has become the leading cause of end-stage renal disease worldwide. In recent years, although great progress has been made in the clinical therapies of diabetes, the process of DKD is still uncontrollable (Lytvyn et al., 2020). Thus, further study of its pathogenesis and search for valid therapeutic targets are crucial for the prognosis of DKD.

The conventional perspective of the pathology of DKD emphasized that podocyte injury is often the first target of hyperglycemic damage (Lassen and Daehn, 2020). Recently, renal tubular epithelial cell apoptosis and tubular atrophy have been recognized as indicators of the severity and progression of DKD (Gilbert, 2017). Numerous studies have found that mitochondrial dysfunction plays a crucial role in the pathobiology of DKD accompanied by renal tubular epithelial cell injury (Xiao et al., 2017; Forbes and Thorburn, 2018; Jiang et al., 2019). Hyperglycemia directly damages mitochondria, resulting in the overproduction of reactive oxygen species (ROS), fragmentation of mitochondria, and reduced efficiency of mitochondrial biogenesis ultimately leading to mitochondrial dysfunction (Galvan et al., 2017). Sirtuin 1(SIRT1)/Peroxisome proliferator-activated receptor-γ coactivator-1α (PGC-1α) pathway and their target genes nuclear respiratory factor (NRF1) and mitochondrial transcription factor A (TFAM) play a critical role in mitochondrial biogenesis (Yacoub et al., 2014; Xue et al., 2019). Several evidence suggest that increased mitochondrial fission and decreased fusion lead to mitochondrial fragmentation in DKD. Mitofusins 1 (MFN1) and dynamin-related protein 1 (Drp1) have been shown to be major regulators in the maintenance of mitochondrial dynamic homeostasis (Rovira-Llopis et al., 2017).

The 66 kDa Src homology two domain-containing protein (p66Shc) is a recognized intracellular critical factor that participates in regulating aging and metabolic disorders (Mir et al., 2020). In the recent past, p66Sch has been reported to be a novel renal marker that plays a significant role in the development of DKD (Xu et al., 2016). Recent studies have illustrated that the expression of p66Shc is increased in podocytes of the kidney of diabetic patients (Zheng et al., 2020). Under hyperglycemia conditions, p66Shc is phosphorylated at Ser36 and translocated into mitochondria, releasing cytochrome c and disrupting the electron transport chain (Giorgio et al., 2005; Mir et al., 2020). Besides, p66Shc can affect mitochondrial dynamics while participating in mitochondrial biogenesis by regulating SIRT1 expression (Qu et al., 2018; Wang et al., 2020). These events generate large quantities of ROS, reduce mitochondrial quality and activate apoptotic mechanisms (Giorgio et al., 2005). Furthermore, the genetic deletion of p66Shc significantly attenuated renal oxidative stress and pathological lesions and safely protected the kidneys of DKD (Menini et al., 2006; Sun et al., 2010). Hence, inhibition of p66Shc expression is a promising approach for the treatment of DKD.

Grape seed proanthocyanidin extract (GSPE) is an effective natural plant polyphenolic antioxidant (Prasain et al., 2009), which exhibits lots of effects, such as anti-inflammatory, antioxidant, and antitumor activities in a variety of diseases (Zhan et al., 2016; Serrano et al., 2017; Hao et al., 2018; Yang et al., 2018). Our previous study demonstrated that GSPE reduced proteinuria and attenuated endoplasmic reticulum stress in diabetic rats (Li et al., 2017; Gao et al., 2018). Thus, we propose that GSPE may serve as a potential therapeutic medicine in protecting the kidney from hyperglycemic toxicity. However, there are few studies on the effect of GSPE on p66Shc in DKD, and convincing studies are needed. Therefore, we identified p66Shc as a therapeutic candidate target to probe whether GSPE has a renoprotective effect in DKD and to explore the underlying mechanisms.

2 Materials and methods

2.1 Experimental animal

40 male Sprague-Dawley (SD, 190 ± 10g, 7 weeks old) rats were obtained from Shandong University Animal Experiment Center (Jinan, China). The rats were housed with a 12 h light/dark cycle and free access to food and water at a temperature of 20°C–25°C and humidity of 40–60%. The rats were randomly divided into four groups: control group, control + GSPE group, diabetic model (DM) group, and DM + GSPE group. Diabetic rats were induced with SD rats *via* a single intraperitoneal injection of 40 mg/kg streptozotocin (STZ), freshly dissolved in 0.1 mol/L citrate buffer (pH 4.3). The control animals were given a single intraperitoneal injection with an equal volume of citrate buffer. Rats with blood glucose levels ≥16.7 mmol/L were successfully modeled for diabetes. According to the report, GSPE at a concentration of 250 mg/kg exhibited the most potent renoprotection (Zhan et al., 2016). Therefore, we choose this concentration for the following experiments. After diabetic model formation, rats in the DM + GSPE group and the control + GSPE group were given 250 mg/kg/d GSPE by intragastric administration and maintained for 12 weeks. The control group and DM group were filled with the same amount of physiological saline. Rats in the control group and the control + GSPE group were fed a normal diet. At the same time, the remaining rats in the DM group and the DM + GSPE group were fed a high-sucrose-high-fat diet. At the end of the experiment, all 10 rats survived in the control group and control + GSPE group, six rats survived in the DM group, and seven in the DM + GSPE

group. All experiments involving animals were conducted in strict accordance with the procedure which was approved by the Institutional Animal Care and Use Committee of Shandong University.

2.2 Metabolic Measurements

Metabolic Measurements: The rats' body weights and random blood glucose levels were measured at the end of the experiment. After 12 weeks of treatment, the rat's urine was collected for urinary albumin analysis. At the time that the rats were sacrificed, blood and tissue samples were harvested and processed for various studies. Metabolic conditions were measured using an automatic biochemical analyzer (Hitachi AutoAnalyzer 7100, Hitachi, Japan).

2.3 Assessment of renal tissue morphology and transmission electron microscopy

The kidneys were excised for histological analysis. The sections of renal biopsy from rats were stained with Hematoxylin and Eosin (HE) or periodic acid Schiff (PAS) staining. According to the methods from the literature (Lu et al., 2017), the degree of damage in each glomerulus was assessed using a semiquantitative scoring method. The glomerular matrix expansion index (GMI) was then calculated. The ultrastructure of podocytes and mitochondria in renal tissue was observed using transmission electron microscopy (TEM).

2.4 TUNEL staining

Apoptosis was detected with a Terminal deoxynucleotidyl transferase dUTP nick-end labeling (TUNEL) kit (11684817910, Roche, Switzerland), according to the manufacturer's instructions. Nuclei were visualized by staining with DAPI for 5 min at room temperature. Digital images were captured using a fluorescence microscope (Nikon Eclipse C1, Nikon, Japan). The percentage of the positive cells was analyzed by ImageJ software.

2.5 Immunohistochemistry

The expression of SIRT1, PGC-1α, NRF1, TFAM, Cleaved caspase-3, MFN1, DRP1, and p66Shc in kidney tissues of different groups was detected by immunohistochemistry analysis. The average optical density (AOD) was quantified with ImageJ software.

2.6 Western blotting assay

Renal tissues and cells were lysed using RIPA lysis fluid. The protein concentration was determined using a BCA protein assay kit (P0010S, Beyotime, China). Equal amounts of protein were subjected to electrophoresis on sodium dodecyl sulfate-polyacrylamide gels (SDS-PAGE) and then transferred to polyvinylidene difluoride (PVDF) membranes. The membranes were blocked with 5% nonfat milk and incubated with one of the following primary antibodies: anti-Cleaved caspase-3 (9661/R, 1:1000, Cell Signaling Technology, United States), anti-SIRT1(ab189494, 1:1000, Abcam, UK), anti-PGC-1α(ab191838, 1:1000, Abcam, UK), anti-NRF1(ab175932, 1:1000, Abcam, UK), anti-TFAM(A13552, 1:1000, Abclonal, China), anti-MFN1(13798-1-AP, 1:1000, Proteintech, China), anti-DRP1 (ab184247, 1:1000, Abcam, UK), anti-p66Shc (ab33770, 1:1000, Abcam, UK), anti-cytochrome C(CytoC) (ab133504, 1:5000, Abcam, UK), anti- DIABLO (ab32023, 1:1000, Abcam, UK), overnight at 4°C. After washing with TBST, the PVDF membranes were incubated with a secondary antibody at 37°C for 1 h. The protein bands on the PVDF membranes were observed.

2.7 Cell culture and treatment

Human kidney proximal tubular cells (HK-2 cells) were maintained in Dulbecco's modified Eagle medium (DMEM) containing 10% fetal bovine serum. The cells were placed in a CO_2 incubator at 37°C. Cells in the logarithmic phase were taken for the subsequent experiment. HK-2 cells were subjected to 5.5 mmol/L glucose as normal glucose (NG) or 30 mmol/L glucose as high glucose (HG) administration. Cells were treated with 10 μg/ml GSPE for 24 h at 37°C according to previous research (Cai et al., 2016). The grouping flow chart is shown in Figure 1 as well.

2.8 Transfection

tHK-2 cells were seeded in six-well plates. Cell transfection was performed at a concentration of 100 nmol/L using Lipofectamine 2000 (11668019, Invitrogen, United States) according to the manufacturer's instructions. HK-2 cells grown in NG were transfected with negative control (NC) plasmid and p66Shc plasmid to overexpression of p66Shc (over-p66Shc) for 48 h. In parallel, cells grown in HG were transfected with siRNA against p66Shc (si-p66Shc), or siRNA negative control (si-NC). After transfection for 48 h, HK-2 cells were then treated with 10 μg/ml GSPE. 24 h after, cells were harvested and utilized for various studies. The efficiency of transfection with p66Shc was determined by western blotting assay and real-time quantitative reverse transcription-polymerase chain reaction (qRT-PCR) (Primer sequences: p66Shc forward primer, ATCACT CTCACCG TCTCCACCAG; reverse primer,

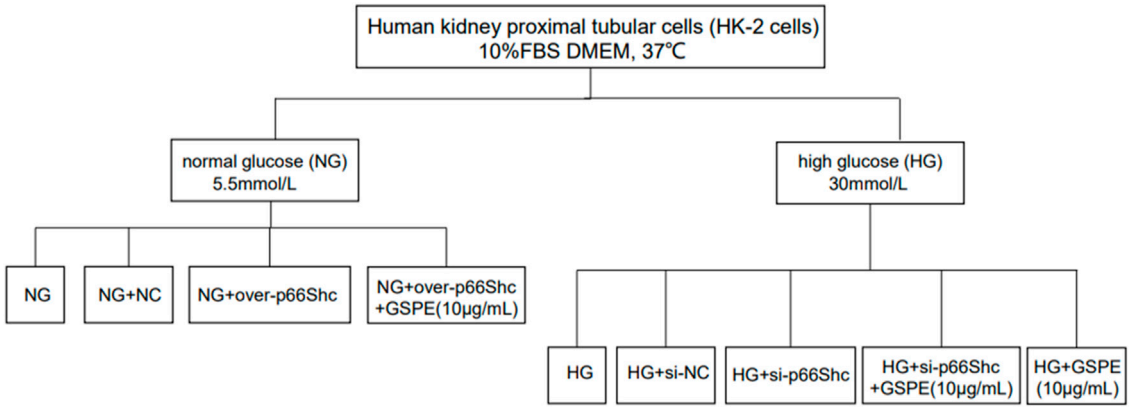

FIGURE 1
The grouping flow chart.

TCTTTGGCAACATAGGC GACATACTC. β-actin forward primer, ACACTGTGCCCATCTACG; reverse primer, TGT CACGCACGATTTCC).

2.9 Measurement of apoptosis and superoxide generation

The commonly used apoptosis kit (AP105, MultiSciences, China) was performed for apoptosis assessment. The ratio of apoptotic cells was assessed by flow cytometry. Mitochondrial superoxide generation was detected using MitoSOX red mitochondrial superoxide indicator (40778ES50, Yeasen, China). 2′,7′-Dichlorodihydrofluorescein diacetate (DCFH-DA, S0033S-1, Beyotime, China) were used to assess intracellular superoxide production in HK-2 cells, respectively.

2.10 Measurement of mitochondrial membrane potential (Δψm)

JC-1 probe (C2006, Beyotime, China) was carried out for Δψm detection according to the instruction. The results were assessed by flow cytometry.

2.11 Measurement of the activity of mitochondrial respiratory chain enzyme complexes I and III

The activity of complexes I and III was measured with Micro Mitochondrial Respiratory Chain Complex III Activity Assay Kit (BC3245, Solarbio, China) and Micro Mitochondrial Respiratory Chain Complex I Activity Assay Kit (BC0515, Solarbio, China) according to the manufacturer's instructions.

2.12 Statistical analyses

GraphPad Prism 6 (GraphPad Software, Inc., San Diego, United States) was used for statistical analyses. One-way analysis of variance (ANOVA) was employed for comparisons between groups. Post-hoc Tukey's honestly significant difference test was performed for multiple comparisons. Data were presented as mean ± SD. $p < 0.05$ was considered statistically significant.

3 Results

3.1 The levels of biochemical indicators in GSPE-treated diabetic rats

Compared with the control group, blood glucose, urinary albumin, and serum creatinine were significantly increased in the DM group, but these indicators were reduced in the DM + GSPE group in comparison with the DM group ($p < 0.05$, Table 1). Meanwhile, compared with the control group, the rats' body weights were significantly decreased in the DM and control + GSPE groups ($p < 0.05$, Table 1), but left unchanged between DM and DM + GSPE groups ($p > 0.05$, Table 1). Blood glucose levels in the control + GSPE group were lower than in the control group ($p < 0.05$, Table 1). Moreover, urinary albumin and serum creatinine were not significantly different between the control group and the control + GSPE group ($p > 0.05$, Table 1).

3.2 Effects on diabetic renal tissues architecture induced by GSPE

We performed the histological examination of renal tissues from all groups. As shown in HE and PAS staining (Figure 2A),

TABLE 1 Characteristics of the rats at the end of the experiment. Mean ± SD.

	Control n = 10	Control+GSPE n = 10	DM n = 6	DM+GSPE n = 7
Body weight (g)	424.3 ± 28.92	376.6 ± 17.77a	321.3 ± 15.22a	341.7 ± 18.28
Blood glucose (mmol/L)	8.36 ± 3.6	3.89 ± 2.29a	38.95 ± 4.41a	27.88 ± 4.26b
Serum creatinine (μmol/L)	39.7 ± 2.67	40.9 ± 2.69	57 ± 3.74a	44.57 ± 3.69b
Urinary albumin (mg/L)	1.23 ± 0.23	1.59 ± 0.94	11.03 ± 3.73a	4.18 ± 2.09b

[a]$p < 0.05$ vs. control.
[b]$p < 0.05$ vs. DM group.

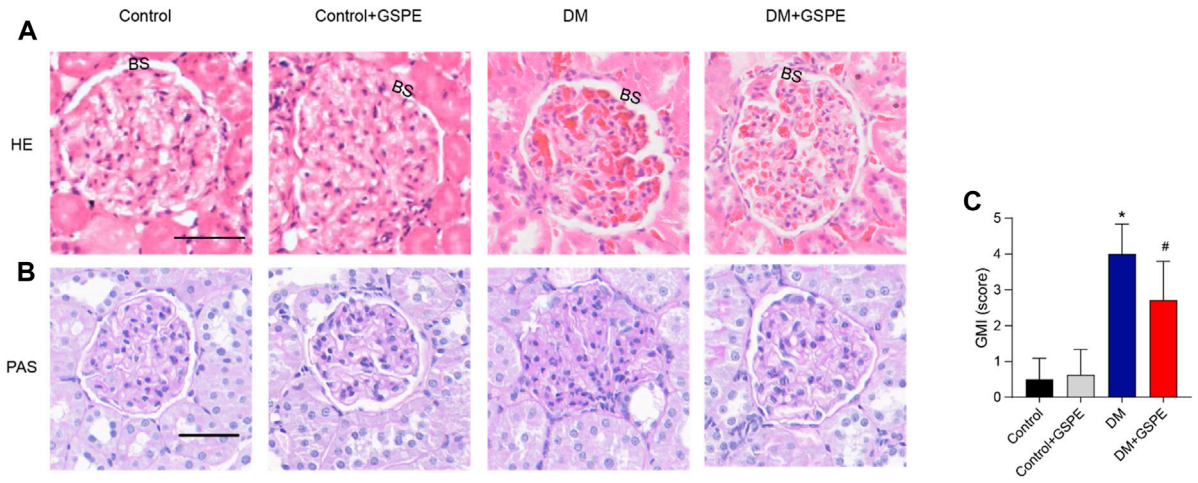

FIGURE 2
Histopathology evaluation of the kidneys of all rats from all experimental groups as stained by HE and PAS staining. Upper panel **(A)** represented images stained by HE (original magnification, ×200). Lower panel **(B,C)** showed images stained by PAS (Scale bars, 50 μm Original magnification, ×200) and the analysis of the GMI (Mean ± SD. n = 6. $*p < 0.05$ vs. control; $\#p < 0.05$ vs. DM group). The images of control and control + GSPE-treated rats showed normal kidney structures with normal glomerulus, normal size Bowman's space (BS). The images of DM rats showed obvious mesangial expansion and glomerulosclerosis. Note the increase in the capsule as well as in Bowman's space. The images of DM + GSPE rats showed almost normal histological features with the almost normal structure of glomerulus, reduced mesangial expansion and Bowman's space (BS).

the renal tubules and glomerular structure of the control group and control + GSPE group were natural. The extracellular matrix (ECM), mesangial cell proliferation, Bowman's space, and glomerulosclerosis increased in the DM group. For GSPE-treated diabetic rats, the situation of these pathological changes was greatly gotten better. The mesangial expansion was assessed by GMI, and the mesangial expansion level in the DM group was significantly larger than that of the control group but inhibited after GSPE treatment ($p < 0.05$, Figure 2B).

3.3 Ultrastructural changes of renal tissues in GSPE-treated diabetic rats

The ultrastructural changes in podocytes and mitochondrial morphology were observed through a transmission electron microscope (TEM). As presented in Figure 3, diabetic rats exhibited apparent foot process fusion and glomerular basement membrane (GBM) thickening. However, GSPE treatment considerably reversed these changes in diabetic rats. Elongated rodlike-shaped mitochondria were observed in the control group. The majority of mitochondria were spherical shapes in the DM group. A partial mitochondrial fragmentation was rescued in cells treated with GSPE.

3.4 Effect of GSPE on renal cell apoptosis in diabetic rats

The cell apoptosis of each group was evaluated by TUNEL assays. Compared to the control group, apoptosis was

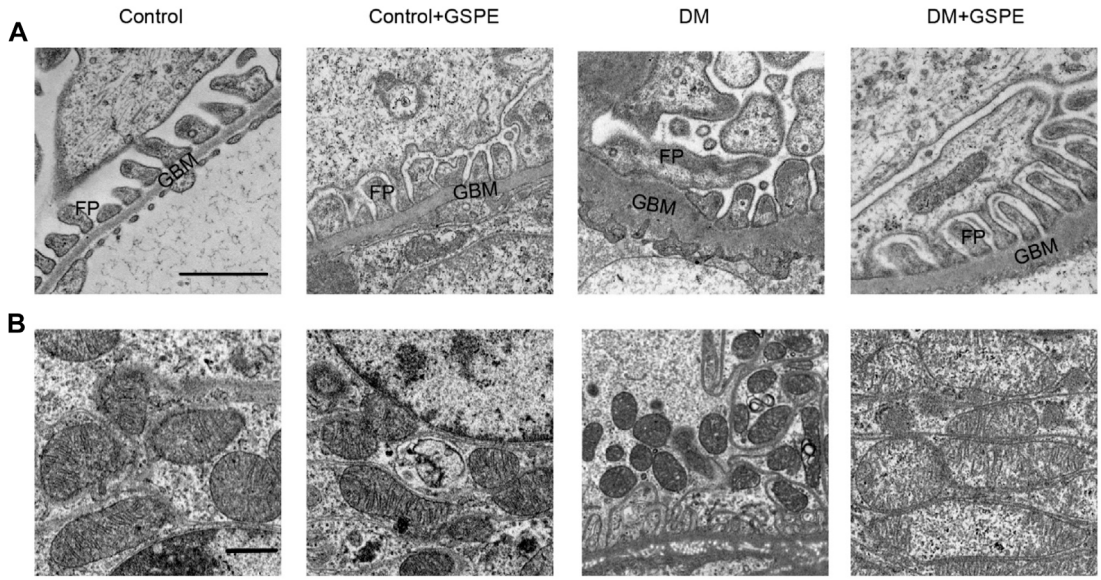

FIGURE 3
Electron microscopy delineated ultrastructural changes of podocyte and mitochondria in kidney biopsies in each group. **(A)** The images of podocytes were taken by electron microscopy (Scale bars, 1 μm Original magnification, ×10000). **(B)** The images of mitochondria were taken by electron microscopy (Scale bars, 1 μm Original magnification, ×3000). GBM: glomerular basement membrane. FP: foot processes.

statistically increased in diabetic rats ($p < 0.05$, Figures 4A, B), especially in renal tubular epithelial cells. And GSPE significantly reduced cell apoptosis ($p < 0.05$, Figures 4A, B). Furthermore, western blotting assay and immunohistochemical staining also showed that apoptosis-related protein Cleaved caspase-3 expression was increased in diabetic rats, and GSPE partially inhibited this increase ($p < 0.05$, Figures 4C, D).

3.5 Expression of related factors in diabetic rats with GSPE treatment

The role of GSPE in mitochondrial biogenesis and dynamics of DKD progression was verified by immunohistochemical staining and western blotting assay. The results showed that compared with the control group, the relative expression of mitochondrial biogenesis-related proteins (SIRT1, PGC-1α, NRF1, and TFAM) and MFN1 decreased, while Drp1 and p66Shc increased simultaneously in the renal tissue of the DM group ($p < 0.05$, Figures 5A–G). However, the expression of these proteins reversed with the treatment of GSPE ($p < 0.05$, Figures 5A–G). Western blotting analysis was consistent with immunohistochemical results ($p < 0.05$, Figures 6A, B).

3.6 The efficiency of transfection was testified

To clarify the influence of p66Shc, HK-2 cells were divided into NG, NG + over-p66Shc, NG + NC, HG, HG + si-p66Shc, and HG + si-NC groups. The efficiency of transfection was analyzed by qRT-PCR and western blotting assay. The results showed that the relative expression of p66Shc in the NG + over-p66Shc group was significantly higher ($p < 0.05$, Figure 7A), and that in HG + si-p66Shc group was lower than those in the HG group ($p < 0.05$, Figure 7B). There were no statistically significant differences in mRNA and protein expression between HG and HG + si-NC groups, as well as NG and NG + NC groups ($p > 0.05$, Figures 7A, B), excluding the effect of transfection on cells.

3.7 Effect of GSPE on HK-2 cells apoptosis in each group

To determine the effect of GSPE, the appropriate GSPE concentration (10 μg/ml) was adopted to treat HK-2 cells. Flow cytometry was performed to detect the apoptotic level. The apoptosis of HK-2 cells significantly increased in HG and

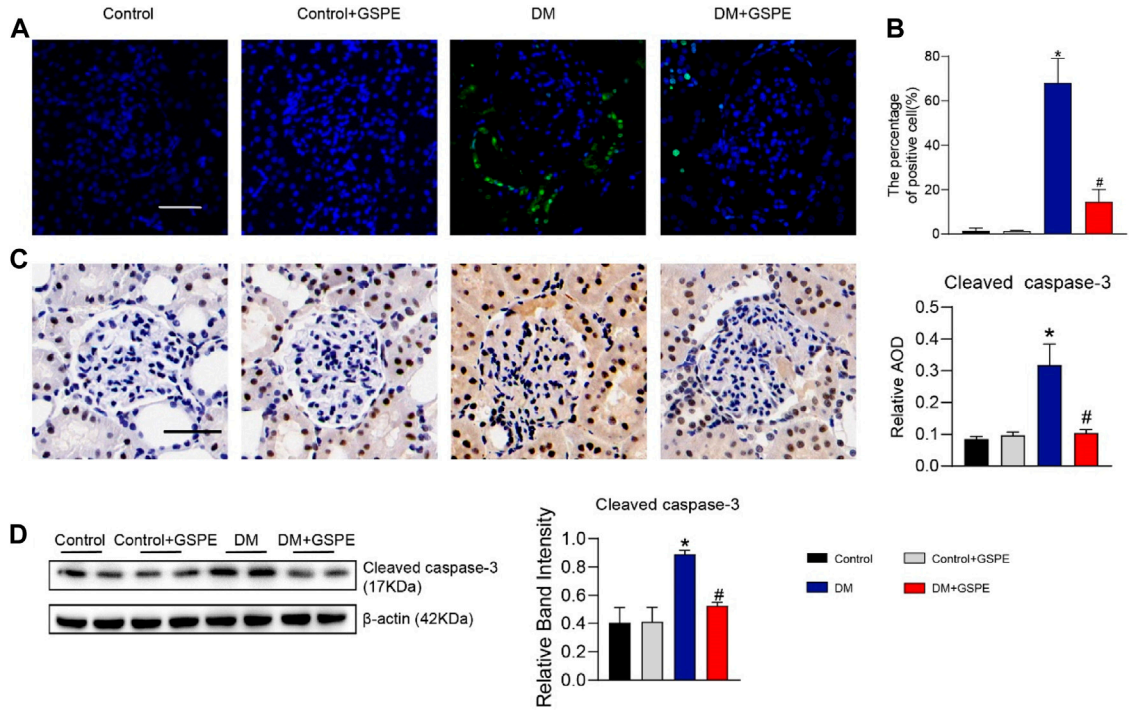

FIGURE 4
(A) The images of cell apoptosis of rat renal tissue. Scale bars, 50 μm. **(B)** Evaluation of apoptosis rate in renal tissue of rats in each group. Mean ± SD. n = 6. ∗$p < 0.05$ vs. control; #$p < 0.05$ vs. DM group. **(C)** Immunohistochemistry delineated the localization and changes in the expression of Cleaved caspase-3 proteins and quantification of relative AOD in each group. (Scale bars, 50 μm Original magnification, ×200) Mean ± SD. n = 6. ∗$p < 0.05$ vs. control; #$p < 0.05$ vs. DM group. **(D)** Western blot for determining the protein levels of Cleaved caspase-3 and quantification of bands in each group. Mean ± SD. n = 6. ∗$p < 0.05$ vs. control; #$p < 0.05$ vs. DM group.

NG + over-p66Shc groups as compared with the NG group ($p < 0.05$, Figure 8A). After treatment with GSPE or transfection of si-p66Shc inhibited cell apoptosis ($p < 0.05$, Figure 8A). In addition, the trend of apoptosis-associated proteins Cleaved caspase-3, Cyto C and DIABLO expression is consistent with apoptosis of flow cytometry ($p < 0.05$, Figure 8B).

3.8 GSPE alleviates intracellular and mitochondrial ROS generation

DCFH-DA and MitoSOX fluorescent probes were conducted to detect intracellular and mitochondrial oxidative stress. Intracellular and mitochondrial ROS level was markedly increased in HK-2 cells exposed to HG conditions ($p < 0.05$, Figures 9A, B). The level of ROS increased significantly in the NG + over-p66Shc group as compared with the NG group ($p < 0.05$, Figures 9A, B). However, these changes were significantly attenuated by GSPE treatment or transfection of si-p66Shc ($p < 0.05$, Figures 9A, B).

3.9 Improvement of mitochondrial quality induced by GSPE

Previous reports have shown that mitochondrial damage is usually accompanied by a decrease in Δψm and the activity of the mitochondrial respiratory chain (Forbes and Thorburn, 2018). We evaluated the transformation of each group on Δψm by JC-1 staining. In healthy mitochondria, JC-1 mainly concentrates as aggregate and emits red fluorescence. In contrast, in mitochondria with reduced Δψm, JC-1 presents mainly in monomeric form and emits green fluorescence. The ratio of red to green fluorescence serves as an indicator of changes in Δψm. The Δψm decreased in HG and NG + over-p66Shc groups, while that was upregulated after si-p66Shc and GSPE treatment ($p < 0.05$, Figure 10A). As shown in Figure 9B, the mitochondrial respiratory chain enzyme complexes Ⅰ and Ⅲ were conspicuously decreased in HK-2 cells by transfection of over-p66Shc or HG treatment. GSPE or transfection of si-p66Shc can increase the activity of mitochondrial respiratory chain enzyme complexes Ⅰ and Ⅲ ($p < 0.05$, Figure 10B).

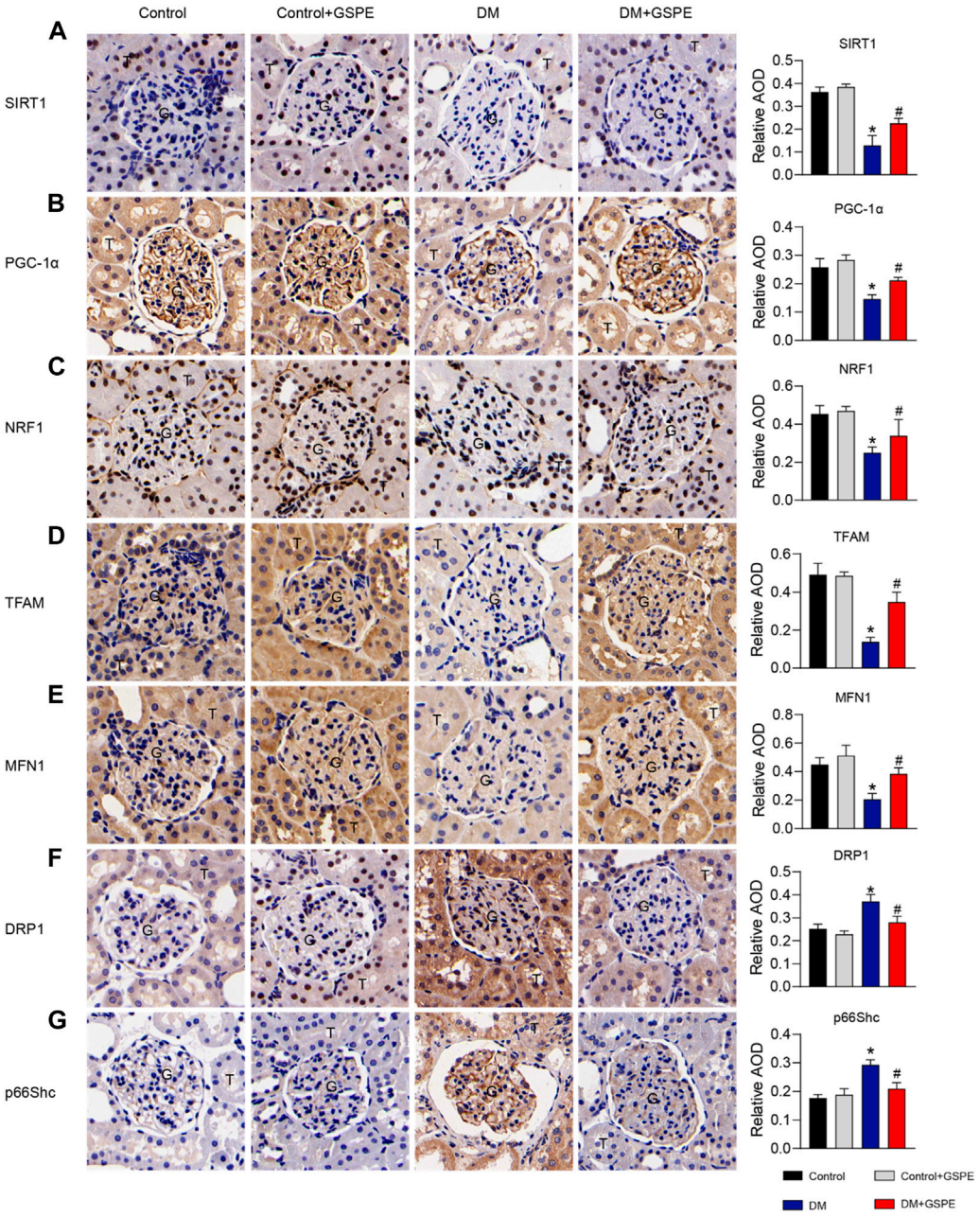

FIGURE 5
Immunohistochemistry delineated the localization and changes in the expression of proteins and quantification of relative AOD in each group. **(A)** SIRT1 is expressed in the nuclei of renal tubules. **(B)** PGC-1α is expressed in the cytoplasm of renal glomeruli and tubules. **(C)** NRF1 is expressed in the nuclei of renal tubules and partly glomeruli. **(D)** TFAM is expressed in the cytoplasm of renal glomeruli and tubules. **(E)** MFN1 is expressed in the cytoplasm of renal glomeruli and tubules. **(F)** DRP1 is expressed in the cytoplasm of renal tubules and partly glomeruli. **(G)** P66Shc is expressed in the cytoplasm of glomeruli and some tubules. Scale bars: 50 μm. Original magnification, ×200. Mean ± SD. n = 6. $*p < 0.05$ vs. control; $\#p < 0.05$ vs. DM group. G: glomeruli. T: tubule.

3.10 GSPE exerts kidney protection by inhibiting p66Shc activity in DKD

The effect of GSPE on p66Shc expression in HK-2 cells was evaluated. Western blotting results revealed that p66Shc expression in the NG + over-p66Shc + GSPE group was less than that in the NG + over-p66Shc group ($p < 0.05$, Figures 11A, B). And the expression of p66Shc markedly decreased after GSPE intervention in HK-2 cells exposed to HG conditions ($p < 0.05$, Figures 11A, B), which was consistent with animal experiments.

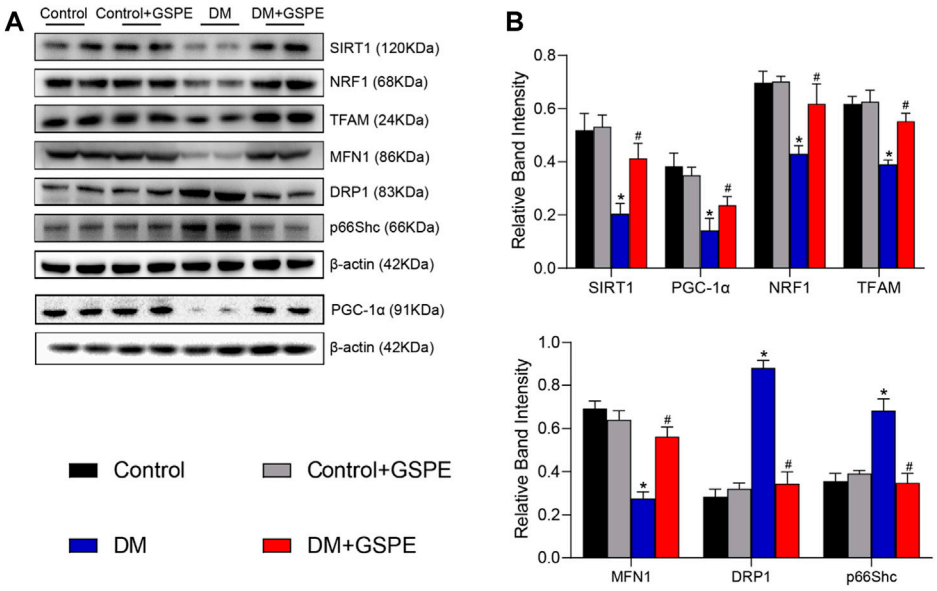

FIGURE 6
(A) Western blot for determining the protein levels of SIRT1, PGC-1α, NRF1, TFAM, MFN1, DRP1 and p66Shc in renal tissue of the rats in each group. **(B)** Quantification of bands in Figure 5A. Mean ± SD. n = 6. *$p < 0.05$ vs. control; #$p < 0.05$ vs. DM group.

3.11 Expression of related factors in HK-2 cells with GSPE treatment

Western blotting analysis showed that the relative expression of mitochondrial biogenesis-related proteins (SIRT1, PGC-1α, NRF1, and TFAM) and MFN1 were conspicuously decreased after HG treatment as well as transfection of over-p66Shc ($p < 0.05$, Figures 11A, B). While the protein level of Drp1 increased ($p < 0.05$, Figures 11A, B). Whereas p66Shc gene disruption and GSPE treatment reversed the above changes ($p < 0.05$, Figures 11A, B). This coincides with the above results of animal experiments.

4 Discussion

DKD is a major microvascular complication in patients with diabetes mellitus and one of the leading causes of end-stage renal disease, contributing to severe morbidity and mortality (Global, 2020). It is characterized by microalbuminuria, glomerulosclerosis, excessive deposition of ECM protein, and GBM thickening, which eventually leads to renal failure (Oshima et al., 2021).

A well-established diabetic rat model with an intraperitoneal injection of STZ partly destroys the function of pancreatic β cells (Lenzen, 2008). Meanwhile, high-sucrose-high-fat diet-induced insulin resistance in rats. High glucose-induced rat models of DKD were established in our present research to investigate the mechanism of GSPE. We could observe hyperglycemia and weight loss in diabetic rats. Urinary albumin and serum creatinine were increased, and glomerular structure was destroyed with obvious ECM and mesangial cell proliferation accompanied by foot process fusion in diabetic rats. These findings indicated the successful rat model of DKD. Moreover, our observation demonstrated that apoptosis of renal tubules was much more than that of glomeruli in diabetic rats, which confirmed the important role of tubular injury in the early stage of DKD. GSPE was demonstrated to decrease blood glucose, relieve renal dysfunction and proteinuria, and alleviate renal damage in diabetic rats. Furthermore, foot process fusion was reduced, and ECM proliferation was alleviated in diabetic rats, indicating that renal structural damage was relieved by GSPE treatment. In addition, there were a large number of apoptosis in HK-2 cells cultured with high glucose *in vitro*. In contrast, the abnormal apoptosis of HK-2 cells was reduced in HG + GSPE incubation, indicating that diabetic renal injury was relieved by GSPE treatment. The above events suggested that GSPE treatment could protect the kidney from high glucose toxicity, thereby alleviating metabolic disorders, reducing renal structural damage, and improving the clinical symptoms of DKD. However, it is worth noting that GSPE also had hypoglycemic and weight-reducing effects in healthy rats. The mechanisms of GSPE affecting metabolism may be affecting the function of pancreatic β-cells, preventing the effect of a high-fat diet on pancreatic insulin secretion,

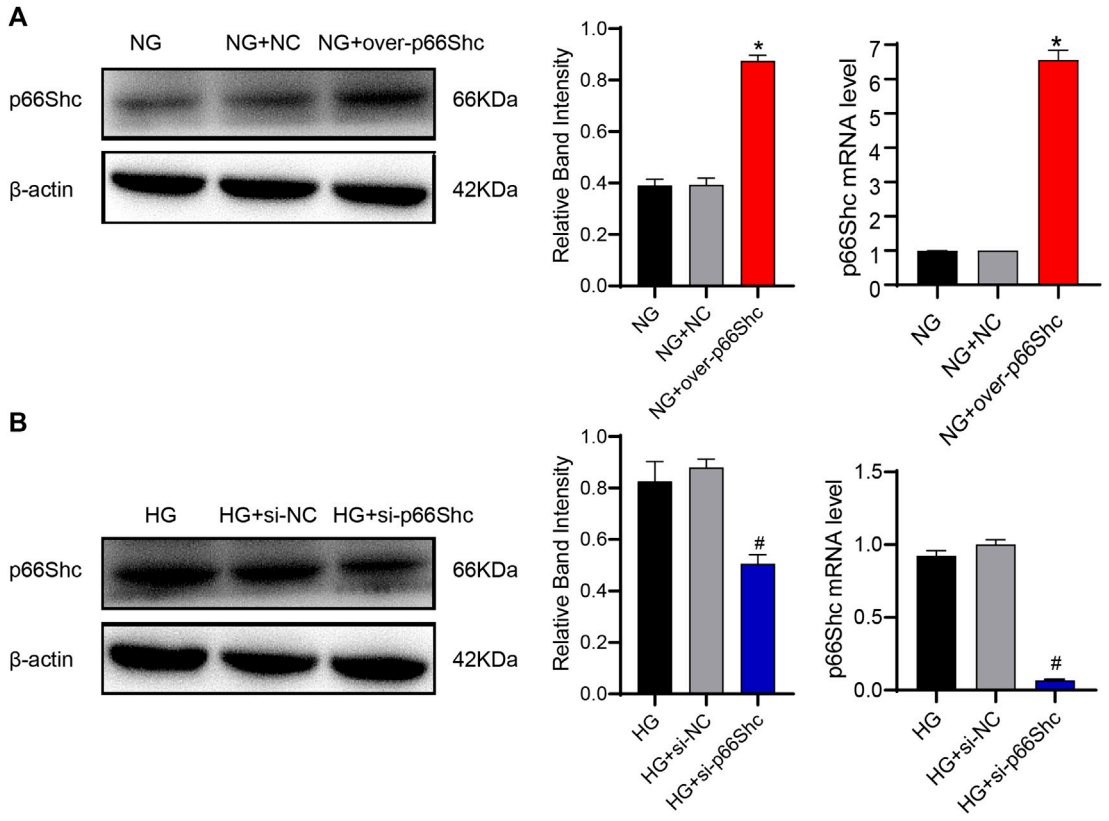

FIGURE 7
(A) Transfection efficiency of over-p66Shc was determined by qRT-PCR and western blotting assay. Mean ± SD. n = 3. $*p < 0.05$ vs. NG group. **(B)** Transfection efficiency of si-p66Shc was determined by qRT-PCR and western blotting assay. Mean ± SD. n = 3. $\#p < 0.05$ vs. HG group.

regulating intestinal microflora, and upregulating intestinal GLP-1 receptor expression (Liu et al., 2020; Grau-Bové et al., 2021).

Accumulating evidence has demonstrated that hyperglycemia, high ROS production, and mitochondrial dysfunction are implicated in the development of DKD (Brownlee, 2005; Reidy et al., 2014; Jha et al., 2016). Among these factors, mitochondrial dysfunction is currently regarded as the key factor in the progression of DKD (Forbes and Thorburn, 2018; Qin et al., 2020). Mitochondrial biogenesis and dynamics are essential in sustaining mitochondrial homeostasis and quality (Bhargava and Schnellmann, 2017). Mitochondrial biogenesis, the generation of new mitochondria, is a complex process involving mtDNA replication and protein synthesis, which is regulated by mitochondrial and nuclear genomes (Scarpulla et al., 2012). PGC-1α is a master regulator of mitochondrial biogenesis, that coordinates the transcriptional machinery leading to increased mitochondrial mass, thus allowing the tissue to adapt to increased energetic demands (Lagouge et al., 2006). SIRT1 is a key regulator of energy and metabolic homeostasis (Rodgers et al., 2005). It is known that SIRT1 activates the PGC-1α-mediated transcription of nuclear and mitochondrial genes encoding proteins during mitochondrial proliferation and energy production (Popov, 2020). Subsequently, PGC-1α initiates the activation of NRF1, which then promotes TFAM activation (Hao et al., 2021). Once activated, TFAM translocates to the mitochondrial matrix and stimulates mtDNA replication and protein translation. On the other hand, mitochondrial dynamics, which contains two reverse processes, fission and fusion, directly contribute to the morphological changes in mitochondria. Previous studies have shown that hyperglycemia of diabetes directly promotes the fragmentation of mitochondria *via* activation of fission (Diaz-Morales et al., 2016). The fission process is mediated by a family of dynamin-related proteins (Drps), particularly Drp1 (Qin et al., 2019). Like fission, fusion controlled by MFN1 is critical for mitochondrial function (Youle and van der Bliek, 2012). Under TEM observation, normal mitochondria were usually in a fused state with a elongated rod shape. In contrast, the majority of mitochondria were spherical shape in the DM group, which was attributed to

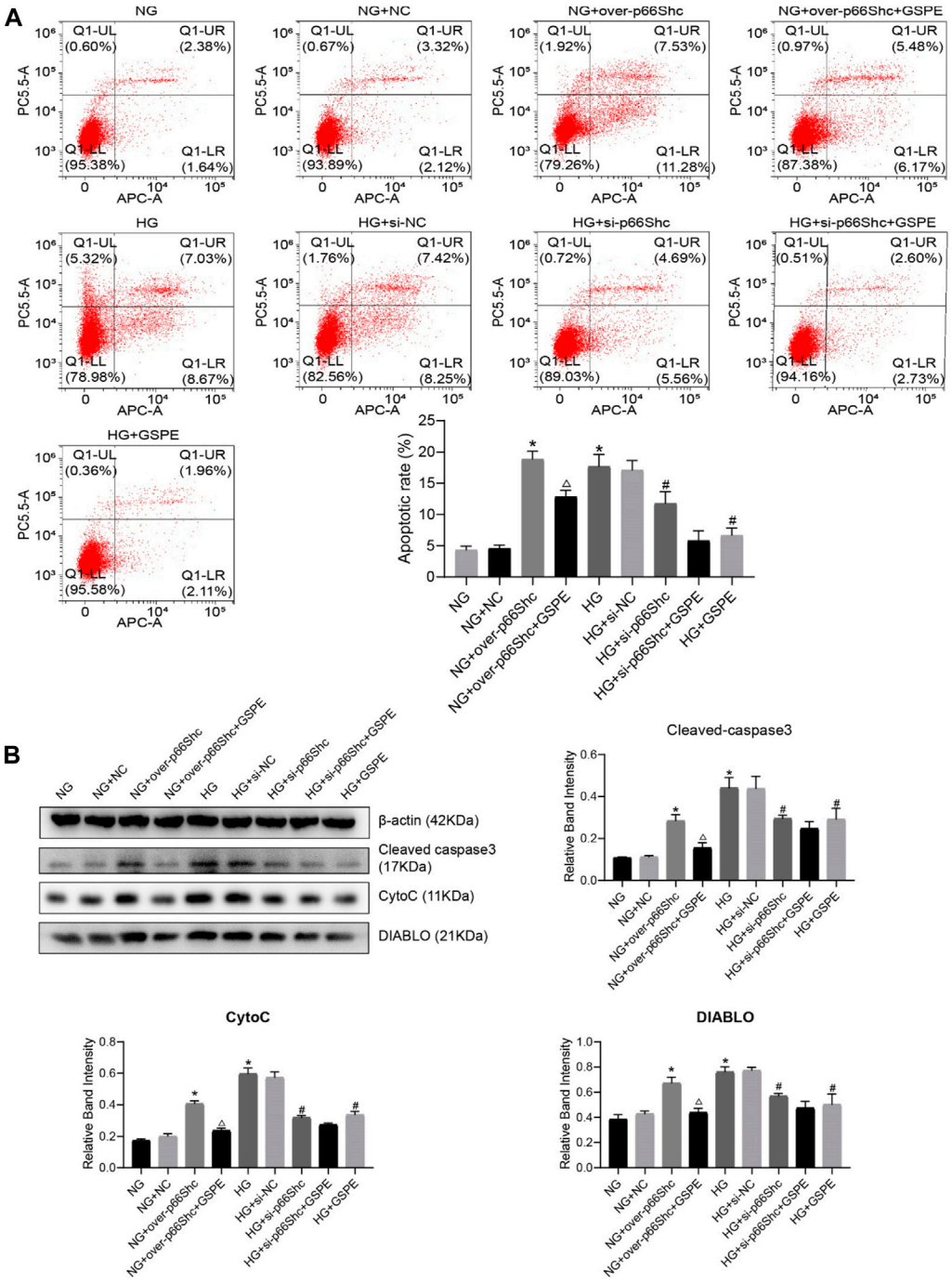

FIGURE 8
(A) Flow cytometry analysis of apoptosis in cultured HK-2 cells in different groups and quantitation of these results. Mean ± SD. n = 3. $*p <$ 0.05 vs. NG group; $\#p < 0.05$ vs. HG group; $\triangle p < 0.05$ vs. NG + over-p66Shc group. **(B)** Western blot for determining the protein levels of mitochondrial associated proteins (Cleaved caspase-3, CytoC, and DIABLO) in each group and quantification of bands. Mean ± SD. n = 3. $*p <$ 0.05 vs. NG group; $\#p < 0.05$ vs. HG group; $\triangle p < 0.05$ vs. NG + over-p66Shc group.

the interruption of mitochondrial fusion. In addition, we found that protein expression of mitochondrial biogenesis (SIRT1, PGC-1α, NRF1, TFAM) and fusion (MFN1) decreased *in vivo* and *in vitro*, while mitochondrial fission-related protein Drp1 increased. This suggested that disturbances in mitochondrial biogenesis and dynamics greatly promote

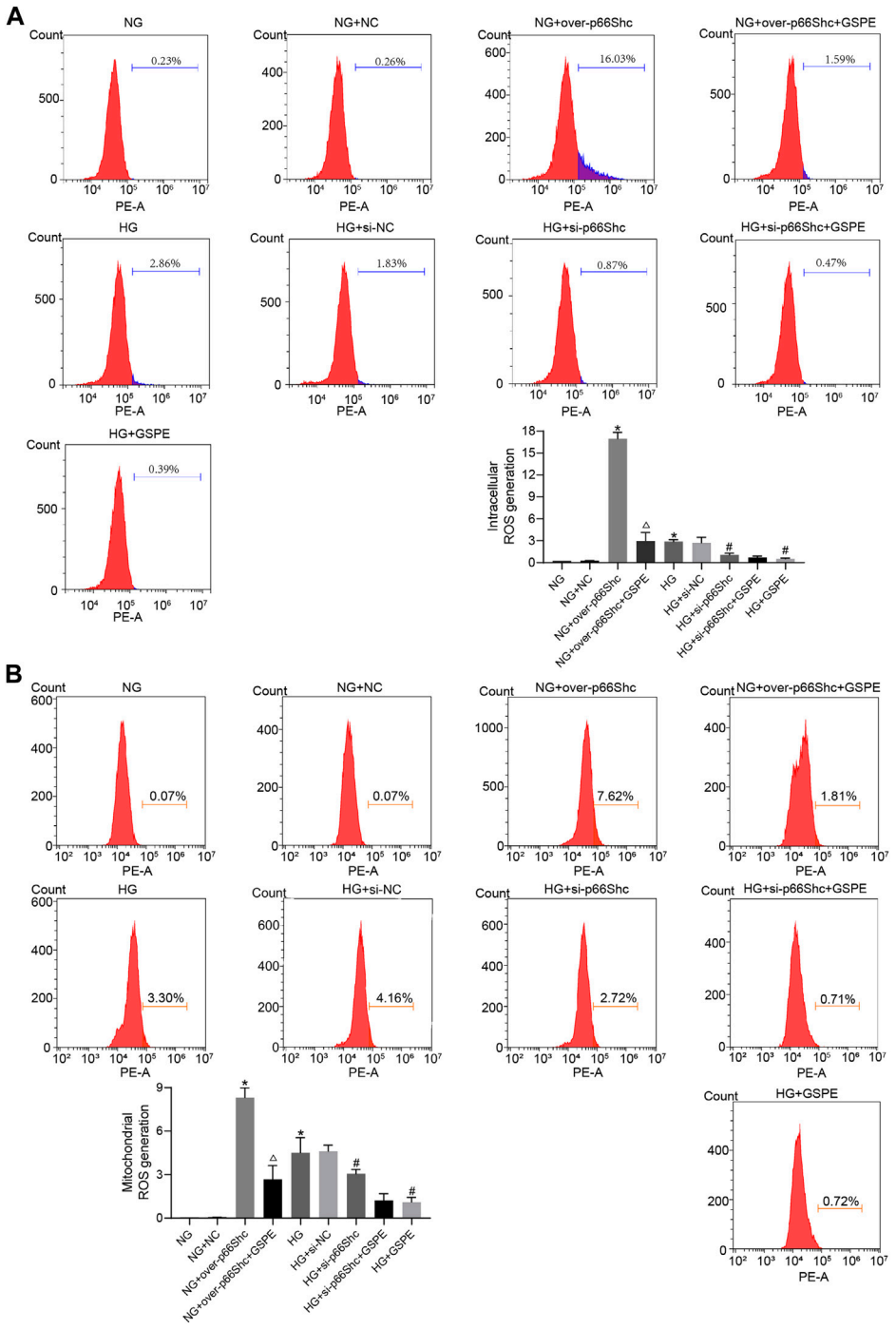

FIGURE 9
(A) Assessment of intracellular ROS generation in various treated groups by DCFH-DA staining. Mean ± SD. n = 3. $*p < 0.05$ vs. NG group; $\#p < 0.05$ vs. HG group; $\triangle p < 0.05$ vs. NG + over-p66Shc group. **(B)** Assessment of mitochondrial ROS generation in various treated groups by MitoSox staining. Mean ± SD. n = 3. $*p < 0.05$ vs. NG group; $\#p < 0.05$ vs. HG group; $\triangle p < 0.05$ vs. NG + over-p66Shc group.

mitochondrial dysfunction which eventually accelerates the progression of DKD. However, these changes were reversed after GSPE treatment. GSPE was demonstrated to affect physiological processes in renal tissues and HK-2 cells by enhancing mitochondrial biogenesis and weakening mitochondrial fission.

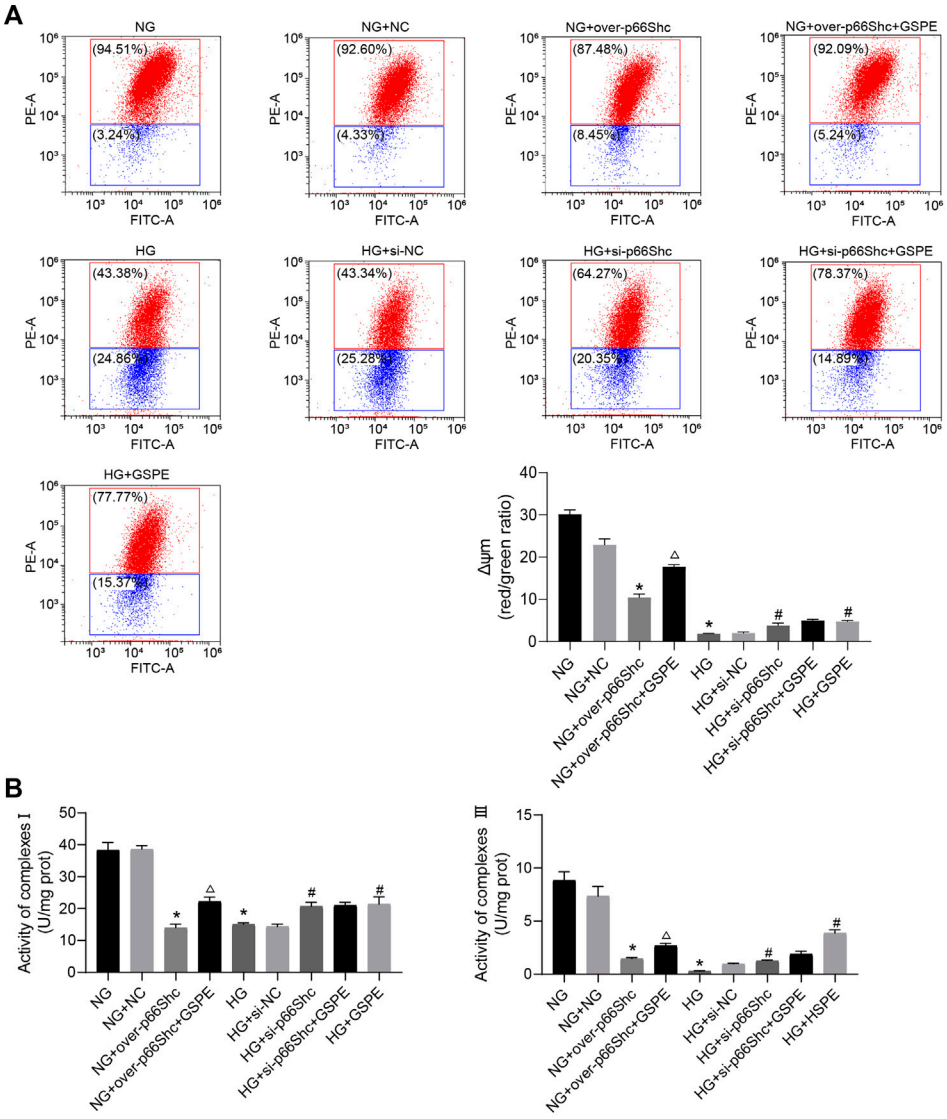

FIGURE 10
(A) Flow cytometry analysis of Δψm in cultured HK-2 cells in different groups and quantitation of these results. Mean ± SD. n = 3. $*p < 0.05$ vs. NG group; $\#p < 0.05$ vs. HG group; $\triangle p < 0.05$ vs. NG + over-p66Shc group. **(B)** Assessment of the activity of mitochondrial respiratory chain enzyme complexes **I** and **III**. Mean ± SD. n = 3. $*p < 0.05$ vs. NG group; $\#p < 0.05$ vs. HG group; $\triangle p < 0.05$ vs. NG + over-p66Shc group.

P66Shc is a member of the Shc protein family, which is an important regulatory protein involved in oxidative stress (Boengler et al., 2019). Recently, researchers discovered that the expression of p66Shc is significantly higher in diabetic patients than in non-diabetic patients (JZ et al., 2021). In the present study, we found that diabetic rats exhibited an increased level of p66Shc. The same phenomenon was observed in HK-2 cells cultured with high glucose, which were consistent with the results of previous literature. High glucose induces phosphorylation of p66shc, which enhances the translocation of p66Shc from the cytosol to the mitochondria. Once p66Shc has entered the mitochondria, the Cyto C release as well as hydrogen peroxide formation occurs (Miller et al., 2021). Subsequently, Δψm is down-regulated, which can trigger the opening of mitochondrial permeability pores, leading to mitochondrial swelling and promoting increased apoptosis (Giorgio et al., 2005). Meanwhile, excessive production of ROS reduced the activity of the mitochondrial respiratory chain and decreased ATP production, which would cause disturbances in mitochondrial structure and function (Spinazzi et al., 2012; Brand, 2016). Consistent with the above process, we demonstrated that inhibition of p66Shc was sufficient to raise mitochondrial function and reduce the incidence of apoptosis. However, GSPE abrogated the increase in p66Shc expression and reversed the above, suggesting p66Shc as a therapeutic target of GSPE.

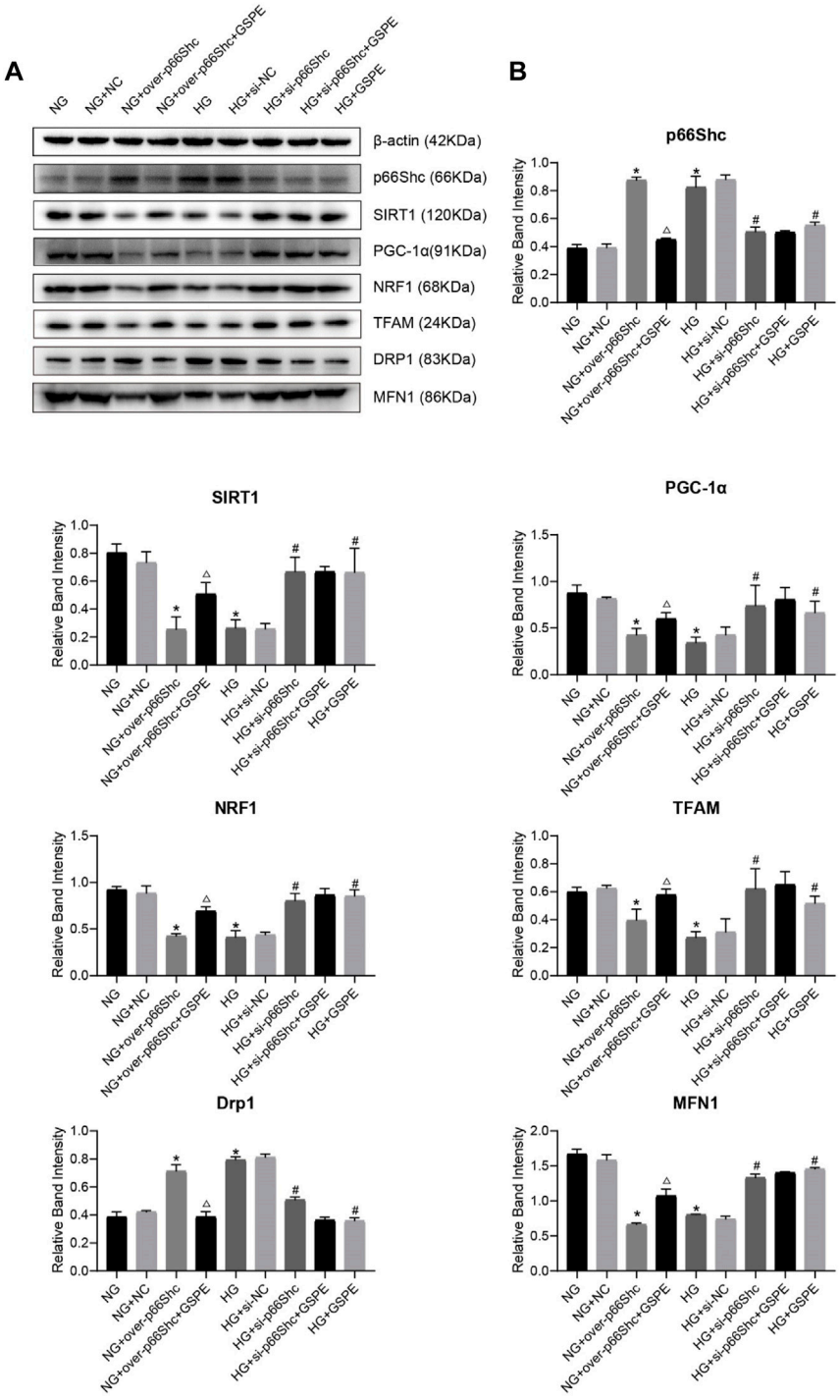

FIGURE 11
(A) Western blot for determining the protein levels of p66Shc, SIRT1, PGC-1α, NRF1, TFAM, MFN1, and DRP1 in each group. **(B)** Quantification of bands in Figure 9A. Mean ± SD. n = 3. $*p < 0.05$ vs. NG group; $\#p < 0.05$ vs. HG group; $\triangle p < 0.05$ vs. NG + over-p66Shc group.

It has been indicated that p66Shc can interfere with mitochondrial dynamics and biogenesis (Pérez et al., 2018) (Li et al., 2017) (Wu et al., 2019). Through transfection of si-p66Shc and over-p66Shc *in vitro*, our experiments confirmed that p66Shc regulated the efficiency of mitochondrial biogenesis by regulating the expression of SIRT1, PGC-1α, and its target genes

NRF1 and TFAM. There was a significant drop in the protein level of MFN1 while the protein level of Drp1 increased when cells were overexpressed with p66Shc or stimulated by HG conditions. The dynamic balance of mitochondrial fission/fusion was disrupted. These results indicated that p66Shc reduced mitochondrial biogenesis and fusion in HK-2 cells, thereby promoting cell damage and apoptosis. These changes could be reversed by GSPE intervention. Therefore, GSPE may affect mitochondrial dynamics and biogenesis by negatively regulating p66Shc, to improve mitochondrial function and alleviate diabetes-induced apoptosis. This discovery has not been reported before.

5 Conclusion

In conclusion, our data showed for the first time that the nephroprotective effect of GSPE in DKD is mediated by suppression of p66Shc expression, and subsequently activation of mitochondrial biogenesis and inhibition of mitochondrial fission. That suggested p66Shc may represent an attractive target for GSPE in the treatment of DKD. Our data provide further support for the therapeutic efficacy of GSPE to promote mitochondrial function and provide benefits for DKD. We are optimistic that GSPE has great potential for further research.

Data availability statement

The original contributions presented in the study are included in the article/Supplementary Material, further inquiries can be directed to the corresponding authors.

Ethics statement

The animal study was reviewed and approved by Institutional Animal Care and Use Committee of Shandong University.

Author contributions

XL, ZG, and YS conceived and designed the experiments; YS, and HY. performed the experiments; YS, QS, FP, and QX. analyzed the data; YS. wrote the original draft; XL. obtained funding, reviewed, and edited the draft. All authors have read and agreed to the published version of the manuscript.

Funding

This work was supported by Projects of the Natural Science Foundation of Shandong Province of China (Grant No. ZR2019MH072).

Conflict of interest

The authors declare that the research was conducted in the absence of any commercial or financial relationships that could be construed as a potential conflict of interest.

Publisher's note

Supplementary material

The Supplementary Material for this article can be found online at: https://www.frontiersin.org/articles/10.3389/fphar.2022.1035755/full#supplementary-material

References

Bhargava, P., and Schnellmann, R. G. (2017). Mitochondrial energetics in the kidney. *Nat. Rev. Nephrol.* 13 (10), 629–646. doi:10.1038/nrneph.2017.107

Boengler, K., Bornbaum, J., Schluter, K. D., and Schulz, R. (2019). P66shc and its role in ischemic cardiovascular diseases. *Basic Res. Cardiol.* 114 (4), 29. doi:10.1007/s00395-019-0738-x

Brand, M. D. (2016). Mitochondrial generation of superoxide and hydrogen peroxide as the source of mitochondrial redox signaling. *Free Radic. Biol. Med.* 100, 14–31. doi:10.1016/j.freeradbiomed.2016.04.001

Brownlee, M. (2005). The pathobiology of diabetic complications: A unifying mechanism. *Diabetes* 54 (6), 1615–1625. doi:10.2337/diabetes.54.6.1615

Cai, X., Bao, L., Ren, J., Li, Y., and Zhang, Z. (2016). Grape seed procyanidin B2 protects podocytes from high glucose-induced mitochondrial dysfunction and apoptosis via the AMPK-SIRT1-PGC-1α axis *in vitro*. *Food Funct.* 7 (2), 805–815. doi:10.1039/c5fo01062d

Diaz-Morales, N., Rovira-Llopis, S., Banuls, C., Escribano-Lopez, I., de Maranon, A. M., Lopez-Domenech, S., et al. (2016). Are mitochondrial fusion and fission impaired in leukocytes of type 2 diabetic patients? *Antioxid. Redox Signal* 25 (2), 108–115. doi:10.1089/ars.2016.6707

Forbes, J. M., and Thorburn, D. R. (2018). Mitochondrial dysfunction in diabetic kidney disease. *Nat. Rev. Nephrol.* 14 (5), 291–312. doi:10.1038/nrneph.2018.9

Galvan, D. L., Green, N. H., and Danesh, F. R. (2017). The hallmarks of mitochondrial dysfunction in chronic kidney disease. *Kidney Int.* 92 (5), 1051–1057. doi:10.1016/j.kint.2017.05.034

Gao, Z., Liu, G., Hu, Z., Shi, W., Chen, B., Zou, P., et al. (2018). Grape seed proanthocyanidins protect against streptozotocin-induced diabetic nephropathy by attenuating endoplasmic reticulum stress-induced apoptosis. *Mol. Med. Rep.* 18 (2), 1447–1454. doi:10.3892/mmr.2018.9140

Gilbert, R. E. (2017). Proximal tubulopathy: Prime mover and key therapeutic target in diabetic kidney disease. *Diabetes* 66 (4), 791–800. doi:10.2337/db16-0796

Giorgio, M., Migliaccio, E., Orsini, F., Paolucci, D., Moroni, M., Contursi, C., et al. (2005). Electron transfer between cytochrome c and p66Shc generates reactive oxygen species that trigger mitochondrial apoptosis. *Cell* 122 (2), 221–233. doi:10.1016/j.cell.2005.05.011

Global, regional (2020). Global, regional, and national burden of chronic kidney disease, 1990-2017: A systematic analysis for the global burden of disease study 2017. *Lancet* 395 (10225), 709–733. doi:10.1016/S0140-6736(20)30045-3

Grau-Bové, C., Gines, I., Beltran-Debon, R., Terra, X., Blay, M., Pinent, M., et al. (2021). Glucagon shows higher sensitivity than insulin to grapeseed proanthocyanidin extract (GSPE) treatment in cafeteria-fed rats. *Nutrients* 13 (4), 1084. doi:10.3390/nu13041084

Hao, J. P., Shi, H., Zhang, J., Zhang, C. M., Feng, Y. M., Qie, L. Y., et al. (2018). Role of GSPE in improving early cerebral vascular damage by inhibition of Profilin-1 expression in a ouabain-induced hypertension model. *Eur. Rev. Med. Pharmacol. Sci.* 22 (20), 6999–7012. doi:10.26355/eurrev_201810_16171

Hao, L., Zhong, W., Dong, H., Guo, W., Sun, X., Zhang, W., et al. (2021). ATF4 activation promotes hepatic mitochondrial dysfunction by repressing NRF1-TFAM signalling in alcoholic steatohepatitis. *Gut* 70 (10), 1933–1945. doi:10.1136/gutjnl-2020-321548

Jha, J. C., Banal, C., Chow, B. S. M., Cooper, M. E., and Jandeleit-Dahm, K. (2016). Diabetes and kidney disease: Role of oxidative stress. *Antioxid. Redox Signal* 25 (12), 657–684. doi:10.1089/ars.2016.6664

Jiang, H., Shao, X., Jia, S., Qu, L., Weng, C., Shen, X., et al. (2019). The mitochondria-targeted metabolic tubular injury in diabetic kidney disease. *Cell Physiol. Biochem.* 52 (2), 156–171. doi:10.33594/000000011

Jz, A. L., AlFaris, N. A., Al-Farga, A. M., Alshammari, G. M., BinMowyna, M. N., and Yahya, M. A. (2021). Curcumin reverses diabetic nephropathy in streptozotocin-induced diabetes in rats by inhibition of PKCβ/p(66)Shc axis and activation of FOXO-3a. *J. Nutr. Biochem.* 87, 108515. doi:10.1016/j.jnutbio.2020.108515

Lagouge, M., Argmann, C., Gerhart-Hines, Z., Meziane, H., Lerin, C., Daussin, F., et al. (2006). Resveratrol improves mitochondrial function and protects against metabolic disease by activating SIRT1 and PGC-1alpha. *Cell* 127 (6), 1109–1122. doi:10.1016/j.cell.2006.11.013

Lassen, E., and Daehn, I. S. (2020). Molecular mechanisms in early diabetic kidney disease: Glomerular endothelial cell dysfunction. *Int. J. Mol. Sci.* 21 (24), 9456. doi:10.3390/ijms21249456

Lenzen, S. (2008). The mechanisms of alloxan- and streptozotocin-induced diabetes. *Diabetologia* 51 (2), 216–226. doi:10.1007/s00125-007-0886-7

Li, X., Gao, Z., Gao, H., Li, B., Peng, T., Jiang, B., et al. (2017). Nephrin loss is reduced by grape seed proanthocyanidins in the experimental diabetic nephropathy rat model. *Mol. Med. Rep.* 16 (6), 9393–9400. doi:10.3892/mmr.2017.7837

Liu, M., Yun, P., Hu, Y., Yang, J., Khadka, R. B., and Peng, X. (2020). Effects of grape seed proanthocyanidin extract on obesity. *Obes. Facts* 13 (2), 279–291. doi:10.1159/000502235

Lu, M., Yin, N., Liu, W., Cui, X., Chen, S., and Wang, E. (2017). Curcumin ameliorates diabetic nephropathy by suppressing NLRP3 inflammasome signaling. *Biomed. Res. Int.* 2017, 1516985. doi:10.1155/2017/1516985

Lytvyn, Y., Bjornstad, P., van Raalte, D. H., Heerspink, H. L., and Cherney, D. Z. I. (2020). The new biology of diabetic kidney disease-mechanisms and therapeutic implications. *Endocr. Rev.* 41 (2), 202–231. doi:10.1210/endrev/bnz010

Menini, S., Amadio, L., Oddi, G., Ricci, C., Pesce, C., Pugliese, F., et al. (2006). Deletion of p66Shc longevity gene protects against experimental diabetic glomerulopathy by preventing diabetes-induced oxidative stress. *Diabetes* 55 (6), 1642–1650. doi:10.2337/db05-1477

Miller, B., Palygin, O., El-Meanawy, A., Mattson, D. L., Geurts, A. M., Staruschenko, A., et al. (2021). p66Shc-mediated hydrogen peroxide production impairs nephrogenesis causing reduction of number of glomeruli. *Life Sci.* 279, 119661. doi:10.1016/j.lfs.2021.119661

Mir, H. A., Ali, R., Mushtaq, U., and Khanday, F. A. (2020). Structure-functional implications of longevity protein p66Shc in health and disease. *Ageing Res. Rev.* 63, 101139. doi:10.1016/j.arr.2020.101139

Oshima, M., Shimizu, M., Yamanouchi, M., Toyama, T., Hara, A., Furuichi, K., et al. (2021). Trajectories of kidney function in diabetes: A clinicopathological update. *Nat. Rev. Nephrol.* 17 (11), 740–750. doi:10.1038/s41581-021-00462-y

Pérez, H., Finocchietto, P. V., Alippe, Y., Rebagliati, I., Elguero, M. E., and Villalba, N. (2018). p66(Shc) inactivation modifies RNS production, regulates Sirt3 activity, and improves mitochondrial homeostasis, delaying the aging process in mouse brain. *Oxid. Med. Cell Longev.* 2018, 8561892.

Popov, L. D. (2020). Mitochondrial biogenesis: An update. *J. Cell Mol. Med.* 24 (9), 4892–4899. doi:10.1111/jcmm.15194

Prasain, J. K., Peng, N., Dai, Y., Moore, R., Arabshahi, A., Wilson, L., et al. (2009). Liquid chromatography tandem mass spectrometry identification of proanthocyanidins in rat plasma after oral administration of grape seed extract. *Phytomedicine* 16 (2-3), 233–243. doi:10.1016/j.phymed.2008.08.006

Qin, X., Jiang, M., Zhao, Y., Gong, J., Su, H., Yuan, F., et al. (2020). Berberine protects against diabetic kidney disease via promoting PGC-1α-regulated mitochondrial energy homeostasis. *Br. J. Pharmacol.* 177 (16), 3646–3661. doi:10.1111/bph.14935

Qin, X., Zhao, Y., Gong, J., Huang, W., Su, H., Yuan, F., et al. (2019). Berberine protects glomerular podocytes via inhibiting drp1-mediated mitochondrial fission and dysfunction. *Theranostics* 9 (6), 1698–1713. doi:10.7150/thno.30640

Qu, B., Gong, K., Yang, H., Li, Y., Jiang, T., Zeng, Z., et al. (2018). SIRT1 suppresses high glucose and palmitate-induced osteoclast differentiation via deacetylating p66Shc. *Mol. Cell Endocrinol.* 474, 97–104. doi:10.1016/j.mce.2018.02.015

Reidy, K., Kang, H. M., Hostetter, T., and Susztak, K. (2014). Molecular mechanisms of diabetic kidney disease. *J. Clin. Invest.* 124 (6), 2333–2340. doi:10.1172/JCI72271

Rodgers, J. T., Lerin, C., Haas, W., Gygi, S. P., Spiegelman, B. M., and Puigserver, P. (2005). Nutrient control of glucose homeostasis through a complex of PGC-1alpha and SIRT1. *Nature* 434 (7029), 113–118. doi:10.1038/nature03354

Rovira-Llopis, S., Banuls, C., Diaz-Morales, N., Hernandez-Mijares, A., Rocha, M., and Victor, V. M. (2017). Mitochondrial dynamics in type 2 diabetes: Pathophysiological implications. *Redox Biol.* 11, 637–645. doi:10.1016/j.redox.2017.01.013

Scarpulla, R. C., Vega, R. B., and Kelly, D. P. (2012). Transcriptional integration of mitochondrial biogenesis. *Trends Endocrinol. Metab.* 23 (9), 459–466. doi:10.1016/j.tem.2012.06.006

Serrano, J., Casanova-Marti, A., Gual, A., Perez-Vendrell, A. M., Blay, M. T., Terra, X., et al. (2017). A specific dose of grape seed-derived proanthocyanidins to inhibit body weight gain limits food intake and increases energy expenditure in rats. *Eur. J. Nutr.* 56 (4), 1629–1636. doi:10.1007/s00394-016-1209-x

Spinazzi, M., Casarin, A., Pertegato, V., Salviati, L., and Angelini, C. (2012). Assessment of mitochondrial respiratory chain enzymatic activities on tissues and cultured cells. *Nat. Protoc.* 7 (6), 1235–1246. doi:10.1038/nprot.2012.058

Sun, L., Xiao, L., Nie, J., Liu, F. Y., Ling, G. H., Zhu, X. J., et al. (2010). p66Shc mediates high-glucose and angiotensin II-induced oxidative stress renal tubular injury via mitochondrial-dependent apoptotic pathway. *Am. J. Physiol. Ren. Physiol.* 299 (5), F1014–F1025. doi:10.1152/ajprenal.00414.2010

Wang, Z., Zhao, Y., Sun, R., Sun, Y., Liu, D., Lin, M., et al. (2020). circ-CBFB upregulates p66Shc to perturb mitochondrial dynamics in APAP-induced liver injury. *Cell Death Dis.* 11 (11), 953. doi:10.1038/s41419-020-03160-y

Wu, Y. Z., Zhang, L., Wu, Z. X., Shan, T. T., and Xiong, C. (2019). Berberine ameliorates doxorubicin-induced cardiotoxicity via a SIRT1/p66Shc-mediated pathway. *Oxid. Med. Cell Longev.* 2019, 2150394. doi:10.1155/2019/2150394

Xiao, L., Xu, X., Zhang, F., Wang, M., Xu, Y., Tang, D., et al. (2017). The mitochondria-targeted antioxidant MitoQ ameliorated tubular injury mediated by mitophagy in diabetic kidney disease via Nrf2/PINK1. *Redox Biol.* 11, 297–311. doi:10.1016/j.redox.2016.12.022

Xu, X., Zhu, X., Ma, M., Han, Y., Hu, C., Yuan, S., et al. (2016). p66Shc: A novel biomarker of tubular oxidative injury in patients with diabetic nephropathy. *Sci. Rep.* 6, 29302. doi:10.1038/srep29302

Xue, H., Li, P., Luo, Y., Wu, C., Liu, Y., Qin, X., et al. (2019). Salidroside stimulates the Sirt1/PGC-1α axis and ameliorates diabetic nephropathy in mice. *Phytomedicine* 54, 240–247. doi:10.1016/j.phymed.2018.10.031

Yacoub, R., Lee, K., and He, J. C. (2014). The role of SIRT1 in diabetic kidney disease. *Front. Endocrinol. (Lausanne)* 5, 166. doi:10.3389/fendo.2014.00166

Yang, D., Li, S., Gao, L., Lv, Z., Bing, Q., Lv, Q., et al. (2018). Dietary grape seed procyanidin extract protects against lead-induced heart injury in rats involving endoplasmic reticulum stress inhibition and AKT activation. *J. Nutr. Biochem.* 62, 43–49. doi:10.1016/j.jnutbio.2018.07.013

Youle, R. J., and van der Bliek, A. M. (2012). Mitochondrial fission, fusion, and stress. *Science* 337 (6098), 1062–1065. doi:10.1126/science.1219855

Zhan, J., Wang, K., Zhang, C., Zhang, C., Li, Y., Zhang, Y., et al. (2016). GSPE inhibits HMGB1 release, attenuating renal IR-induced acute renal injury and chronic renal fibrosis. *Int. J. Mol. Sci.* 17 (10), 1647. doi:10.3390/ijms17101647

Zheng, D., Tao, M., Liang, X., Li, Y., Jin, J., and He, Q. (2020). p66Shc regulates podocyte autophagy in high glucose environment through the Notch-PTEN-PI3K/Akt/mTOR pathway. *Histol. Histopathol.* 35 (4), 405–415. doi:10.14670/HH-18-178

frontiers | Frontiers in Pharmacology

TYPE Original Research
PUBLISHED 15 February 2023
DOI 10.3389/fphar.2023.1069348

OPEN ACCESS

EDITED BY
Swayam Prakash Srivastava,
Yale University, United States

REVIEWED BY
Yuta Takagaki,
Joslin Diabetes Center and Harvard Medical School, United States
Fatima Rizvi,
Boston University, United States

*CORRESPONDENCE
Qiu-Ling Fan,
cmufql@163.com

SPECIALTY SECTION
This article was submitted to Renal Pharmacology, a section of the journal Frontiers in Pharmacology

RECEIVED 13 October 2022
ACCEPTED 06 February 2023
PUBLISHED 15 February 2023

CITATION
Li X, Ma T-K, Wang M, Zhang X-D, Liu T-Y, Liu Y, Huang Z-H, Zhu Y-H, Zhang S, Yin L, Xu Y-Y, Ding H, Liu C, Shi H and Fan Q-L (2023), YY1-induced upregulation of LncRNA-ARAP1-AS2 and ARAP1 promotes diabetic kidney fibrosis *via* aberrant glycolysis associated with EGFR/PKM2/HIF-1α pathway. *Front. Pharmacol.* 14:1069348. doi: 10.3389/fphar.2023.1069348

YY1-induced upregulation of LncRNA-ARAP1-AS2 and ARAP1 promotes diabetic kidney fibrosis *via* aberrant glycolysis associated with EGFR/PKM2/HIF-1α pathway

Xin Li[1,2], Tian-Kui Ma[1], Min Wang[1], Xiao-Dan Zhang[1], Tian-Yan Liu[1], Yue Liu[1], Zhao-Hui Huang[1], Yong-Hong Zhu[1], Shuang Zhang[2], Li Yin[2], Yan-Yan Xu[2], Hong Ding[2], Cong Liu[3], Hang Shi[4] and Qiu-Ling Fan[1,5]*

[1]Department of Nephrology, First Hospital of China Medical University, Shenyang, China, [2]Department of Nephrology, Fourth Hospital of China Medical University, Shenyang, China, [3]Department of General Surgery, First Hospital of Harbin Medical University, Harbin, China, [4]Department of Intensive Care Unit, Sun Yat-sen Memorial Hospital of Sun Yat-sen University, Guangzhou, China, [5]Department of Nephrology, Shanghai General Hospital, Shanghai Jiao Tong University School of Medicine, Shanghai, China

Objectives: Dimeric pyruvate kinase (PK) M2 (PKM2) plays an important role in promoting the accumulation of hypoxia-inducible factor (HIF)-1α, mediating aberrant glycolysis and inducing fibrosis in diabetic kidney disease (DKD). The aim of this work was to dissect a novel regulatory mechanism of Yin and Yang 1 (YY1) on lncRNA-ARAP1-AS2/ARAP1 to regulate EGFR/PKM2/HIF-1α pathway and glycolysis in DKD.

Materials and methods: We used adeno-associated virus (AAV)-ARAP1 shRNA to knocked down ARAP1 in diabetic mice and overexpressed or knocked down YY1, ARAP1-AS2 and ARAP1 expression in human glomerular mesangial cells. Gene levels were assessed by Western blotting, RT-qPCR, immunofluorescence staining and immunohistochemistry. Molecular interactions were determined by RNA pull-down, co-immunoprecipitation, ubiquitination assay and dual-luciferase reporter analysis.

Results: YY1, ARAP1-AS2, ARAP1, HIF-1α, glycolysis and fibrosis genes expressions were upregulated and ARAP1 knockdown could inhibit dimeric PKM2 expression and partly restore tetrameric PKM2 formation, while downregulate HIF-1α accumulation and aberrant glycolysis and fibrosis in *in-vivo* and *in-vitro* DKD models. ARAP1 knockdown attenuates renal injury and renal dysfunction in diabetic mice. ARAP1 maintains EGFR overactivation *in-vivo* and *in-vitro* DKD models. Mechanistically, YY1 transcriptionally upregulates ARAP1-AS2 and indirectly regulates ARAP1 and subsequently promotes EGFR activation, HIF-1α accumulation and aberrant glycolysis and fibrosis.

Conclusion: Our results first highlight the role of the novel regulatory mechanism of YY1 on ARAP1-AS2 and ARAP1 in promoting aberrant glycolysis and fibrosis by EGFR/

PKM2/HIF-1α pathway in DKD and provide potential therapeutic strategies for DKD treatments.

KEYWORDS

LncRNA-ARAP1-AS2, ARAP1, diabetic kidney disease, HIF-1α, glycolysis, fibrosis, PKM2

1 Introduction

Diabetic kidney disease (DKD) is an important cause of end-stage renal disease. Current treatment strategies include 1) blood glucose control such as DPP-4 inhibitor linagliptin and SGLT-2 inhibitor empagliflozin (Srivastava et al., 2020a; Pugliese et al., 2020; Herrington et al., 2023), 2) blood pressure control such as Ang-II receptor blockers (ARBs) or angiotensin converting enzyme (ACE) inhibitors (Roett et al., 2012) and 3) blood lipid control (Srivastava et al., 2014), as well as new potential therapeutic strategies as 1) SIRT3 activation, 2) glycolysis inhibitors, 3) Rho kinase (ROCK) inhibitor Fasudil, 4) endogenous antifibrotic peptide N-acetyl-seryl-aspartyl-lysyl-proline (AcSDKP), which is associated with fibroblast growth factor receptor 1 (FGFR1) phosphorylation, 5) endothelial and podocyte glucocorticoid receptor (GR) delivery and so on (Kitada et al., 2013; Srivastava et al., 2016; Srivastava et al., 2018; Morita and Kanasaki, 2020; Srivastava et al., 2021a; Srivastava et al., 2021b; Wang et al., 2021). However, current treatments cannot completely stop or delay disease progression. Therefore, in-depth study of the pathogenesis of DKD and search for targets and biomarkers of accurate diagnosis and early individualized treatment have become urgent public health issues to be solved.

Glomerular mesangial cells (GMCs) are the main cell types responsible for the generation of extracellular matrix (ECM) (Qiao et al., 2019). The massive deposition of ECM is a critical indicator of diabetic renal fibrosis, closely associated with activated fibroblasts, which can be produced by epithelial cells *via* epithelial-to-mesenchymal transition (EMT), by bone marrow-derived M2 phenotype macrophages *via* macrophage-to-mesenchymal transition (MMT), by endothelial cells *via* endothelial-to-mesenchymal transition (EndMT). And TGF-β, BMP, Wnt and Sonic Hedgehog signaling play a crucial role in the activation of mesenchymal transition processes (Srivastava et al., 2020b). The fibrosis in kidney has been shown to be associated with aberrant glycolysis, known as the Warburg effect (Liu et al., 2021). Such aberrant glycolysis, which is characterized by the accumulation of hypoxia-inducible factor-1α (HIF-1α), promotes the expression of fibrotic genes and the expansion of mesangial matrix (Jia et al., 2022). However, in DKD, the molecular mechanism of aberrant glycolysis in GMCs has not been fully elucidated.

The epidermal growth factor receptor (EGFR) enhances the production of the key ECM components collagen I (COL I), collagen IV (COL IV), and fibronectin (FN) in GMCs, aggravating renal fibrosis and glomerulosclerosis in DKD (Uchiyama-Tanaka et al., 2002; Wu et al., 2009a; Wu et al., 2009b; Taniguchi et al., 2013). EGFR activation mediates HIF-1α activation and subsequent the induction of aberrant glycolysis, which finally promoting renal fibrosis in DKD (Yu et al., 2012; Li et al., 2015). Pyruvate kinase (PK) M2 (PKM2), the critical enzyme in glycolysis, can be aggregated into tetramer and dimer forms, and PKM2 in the dimer state can enter the nucleus to regulate gene expression (Azoitei et al., 2016; Zhang et al., 2019a). The transformation between PKM2 dimer and tetramer plays an important role in many diseases, such as DKD and breast cancer (Liu et al., 2021; Wu et al., 2022). EGFR activation can increase dimer PKM2 expression and induce translocation of dimer PKM2 into the nucleus, where PKM2 acts both as a protein kinase and a transcriptional coactivator for HIF-1α in tumor tissues (He et al., 2014; Azoitei et al., 2016). In the fibrotic kidney of diabetic mice, PKM2 tetramer formation is suppressed, while the PKM2 dimer expression is induced and enter the nucleus and directly interacts with HIF-1α, promoting HIF-1α transactivation as well as the expression of its downstream glycolytic genes. Activation of tetrameric PKM2 formation can reduce the entry of PKM2 dimer form into the nuclear and activation of HIF-1α, alleviate abnormal glycolysis and renal fibrosis, and play a role in renal protection (Luo et al., 2011; Qi et al., 2017; Sizemore et al., 2018; Liu et al., 2021). We have reported that natural antisense lncRNA-ARAP1-AS2 can interact with its sense target gene ARAP1, a type 2 diabetes susceptibility gene product, which finally contributing to the fibrosis process through maintaining the EGFR persistent transactivation in human proximal tubular cells (HK-2) exposed to the high glucose condition (Yang et al., 2019a; Li et al., 2020a; Li et al., 2020b). Nevertheless, the relationship between ARAP1-AS2/ARAP1, EGFR activation, PKM2 and HIF-1α activation as well as aberrant glycolysis in DKD is currently unknown.

Non-coding RNAs (ncRNAs) are a kind of functional RNA molecule, including microRNA (miRNA), circular RNA (circRNA) and long non-coding RNA (lncRNA), playing a pivotal in regulating MMT, EMT and EndMT progress in DKD (Srivastava et al., 2013; Srivastava et al., 2020b; Peng et al., 2021; Zhang et al., 2021). miRNA have been intensely investigated and miRNA crosstalk in the kidney is found to regulate various disease progresses, such as MMT, EMT and EndMT (Srivastava et al., 2013). However, the functional role of lncRNAs remains poorly understood. Evidence have demonstrated that lncRNAs are involved in the pathophysiology, such as pathologic processes in mesangial cells, podocytes, oxidative stress, EMT, EndMT and actions on miRNAs in DKD (Srivastava et al., 2021c). Yin and Yang 1 (YY1), a novel therapeutic target for early DKD-associated tubulointerstitial fibrosis (Yang et al., 2022), mainly distributed in the nucleus and directly or indirectly binds to gene promoters to activate or repress expression *via* chromatin remodeling or histone modification in DKD (Yang et al., 2019b). YY1 is also known to interact with lncRNA (An and Ding, 2021). To date, the regulatory mechanism of YY1 on ARAP1-AS2 is unclear in DKD.

Currently, the involvement of ARAP1-AS2/ARAP1 during the pathogenesis of DKD in diabetic mice and renal cell populations other than human proximal tubular cells remains unclear. In this study, we investigated the hypothesis that ARAP1 can aggravate ECM accumulation and renal dysfunction and glomerulosclerosis in diabetic db/db mice as well as in GMCs exposed to high glucose

through aberrant glycolysis, associated with HIF-1α accumulation led by increased PKM dimer formation as well as decreased PKM tetramer formation through maintaining the EGFR persistent activation. We also explored the prediction that YY1 targets the promoter of ARAP1-AS2 and positively regulates ARAP1-AS2 transcriptional activity in DKD. We provide the first evidence for YY1 regulate EGFR persistent activation, transformation between PKM2 dimer and tetramer, HIF-1α accumulation and aberrant glycolysis and fibrosis in DKD through the ARAP1-AS2/ARAP1 axis. These results further highlight the possibility of pursuing the YY1/ARAP1-AS2/ARAP1 axis as a promising therapeutic target for DKD treatment.

2 Materials and methods

2.1 Cell culture

Human renal mesangial cells (HRMCs) were purchased from ScienCell Research (San Diego, United States), and the mouse mesangial cell (MMC) line SV40 MES-13 was purchased from the American Type Culture Collection (ATCC). All cells were cultured in DMEM (Gibco, United States) containing 10% fetal bovine serum (Gibco, Australia), streptomycin (100 μg/mL) and penicillin (100 U/mL) at 37°C and 5% CO_2. Standard medium containing 5 mM D-glucose was used for the normal glucose (NG) condition. We added 20 mM glucose (yielding a final concentration of 25 mM) or mannitol for the high glucose (HG) condition or osmotic control (MA) and stimulated the cells for 48 h. The concentration was chosen based on our previous studies (Lu et al., 2015; Wang et al., 2018a; Ma et al., 2019).

2.2 Plasmids, siRNAs, the EGFR tyrosine kinase inhibitor AG1478 and transfection

We used the same methods as in our previous reports for synthesizing shRNA targeting human ARAP1 and siRNA targeting human ARAP1-AS2 (Li et al., 2020a; Li et al., 2020b). The siRNAs targeting mouse ARAP1, overexpression plasmids and siRNAs targeting human YY1 and overexpression plasmids targeting human ARAP1were purchased from Sangon Biotechnology (Shanghai, China). The specific EGFR tyrosine kinase inhibitor AG1478 (MedChemExpress LLC) was used to suppress the phosphorylation of EGFR in HRMCs. Powdered AG1478 was dissolved in DMSO, and the final concentration of AG1478 administered to HRMCs was 10 μmol/L. Cells were exposed to AG1478 for 48 h. Transfection methods, cell lines created by transfection and their names are described in the Supplementary Material and Methods.

2.3 RNA pulldown sequencing (pulldown-seq)

RNA pulldown-seq was performed as our group reported previously (Li et al., 2020b) and the details are provided in the Supplementary Material and Methods.

2.4 RNA pulldown assay

Biotin-labelled sense or antisense oligos of ARAP1-AS2 were incubated with HRMCs' lysates for 2 h. The complex was pulled down by streptavidin-coated magnetic beads (M-280 Dynabeads; Invitrogen). The amount of YY1 mRNA was measured by qRT-PCR.

2.5 Functional enrichment analysis

Genes enriched in the RNA pulldown-seq assay were evaluated by functional and enrichment analysis using GO (Gene Ontology 2004) (http://geneontology.org/) and KEGG (http://www.genome.jp/kegg/) databases ($p < 0.05$, fold enrichment>1.5). For GO analyses, enriched biological processes (BPs), molecular functions (MFs), and cellular components (CCs) were assessed.

2.6 Dual-luciferase reporter analysis

For gene promoter luciferase analysis, HRMCs were plated into 24-well plates. The possible YY1 binding sites in the ARAP1-AS2 promoter sequence were predicted by the JASPAR tool. ARAP1-AS2 WT/Mut plasmids were constructed by inserting ARAP1-AS2 promoter fragments containing wild-type (Wt) or mutant (Mut) YY1 binding sites into the pGL4.10 reporter vector (SyngenTech, Beijing, China, Supplementary Figure S1), and the plasmids were co-transfected into cells with siYY1 or siNC. A reporter gene assay was conducted after 48 h using a Dual Luciferase Assay System (Promega).

2.7 Animals

All animal procedures were approved by the Institutional Animal Care and Use Committee of China Medical University, and ethical approval was obtained from the Ethics Committee of China Medical University (number: CMU2019222). Ten-week-old diabetic male db/db mice (C57BLKS/J-leprdb/leprdb, $n = 30$) and normal control male db/m mice (C57BLKS/J-leprdb/+, $n = 10$) were purchased from the Model Animal Research Center of Nanjing University (Nanjing, China). Mice were housed at 22°C ± 2.0°C under a 12-h:12-h light/dark cycle under 50% ± 20% humidity at the Laboratory Animal Center of China Medical University and fed food and water *ad libitum*. We collected tail vein blood when the mice were 12 weeks of age and measured fasting blood glucose levels to confirm spontaneous hyperglycemia. Diabetes was defined as a blood glucose level greater than 16.7 mM.

2.8 Knockdown of ARAP1 in diabetic mice

Adeno-associated virus (AAV) 2/9-shARAP1 and AAV2/9-NC were purchased from Sangon Biotechnology (Shanghai, China). The viral vector construction framework for AAV2/9-shARAP1 is described in Supplementary Table S1, and the AAV vector backbone are provided in Supplementary Figure S2.

Experimental groups in animal studies and their designations are described in the Supplementary Material and Methods. The mice were fasted for more than 8 h before measuring blood glucose and urine. Body weight (BW) and fasting blood glucose levels were measured once every 2 weeks for 8 successive weeks. Individual metabolic cages were used to collect mouse urine samples every 2–3 weeks. All mice were euthanized at 20 weeks, and blood and kidney tissue samples were collected for subsequent analyses.

2.9 Serum and urine biochemistry

A VITROS 950 automatic biochemical analyzer (Johnson & Johnson, NJ) was used to measure serum creatinine and blood urea nitrogen (BUN). The ELISA for mouse urinary albumin and neutrophil gelatinase-associated lipocalin (NGAL) was performed as described previously by our team (Zhang et al., 2019b). Urinary creatinine concentrations were measured with a creatinine assay kit (NJJCBIO, C011-2, China). The UACR was calculated as the ratio of urinary albumin concentration and creatinine concentration (mg/g). Urine samples were collected when the mice were 12 weeks of age and were considered to have DKD when the UACR was greater than 3 mg/mmol.

2.10 Kidney pathology

Mouse kidney tissues were fixed in 4% paraformaldehyde and embedded in paraffin. Sections (3 μm) were obtained and stained with hematoxylin-eosin (H-E), Masson's trichrome, and periodic acid-Schiff (PAS) according to the manufacturer's instructions. The slides were examined under a Leica microscope for subsequent analysis. The glomerulosclerosis index (GSI) was calculated as described previously by our group, and the details are provided in the Supplementary Material and Methods (Ma et al., 2022). To obtain GSI, 3 experienced renal pathologists independently scored 30–50 glomeruli, and the average value was used as the final data (Ma et al., 2001).

2.11 Isolation of mouse glomeruli

Mouse glomeruli were isolated as previously described, and the details are provided in the Supplementary Material and Methods (Zhao et al., 2018).

2.12 Immunohistochemical (IHC) analysis

Detailed description of methods for IHC is provided in the Supplementary Material and Methods. The primary antibodies used in this study and the dilution ratio are provided in Supplementary Table S2.

2.13 Immunofluorescence staining

2.13.1 For HRMC

The process was provided in Supplementary Material and Methods. The primary antibodies used were anti-HIF-1α (1:200, NB100-123, Novus, United States).

2.13.2 For tissue sections

The process was provided in Supplementary Material and Methods. The primary antibodies used were anti-ARAP1 (1:50, sc-393138, Santa Cruz Biotechnology) and anti-HIF-1α (1:200, NB100-123, Novus, United States).

2.14 qRT-PCR

Detailed description of methods is provided in the Supplementary Material and Methods. Primer sequences are provided in Supplementary Table S3.

2.15 Western blot analysis

Detailed description of methods is provided in the Supplementary Material and Methods. The antibody dilution ratios are provided in Supplementary Table S4.

2.16 Cell counting Kit-8 (CCK-8) assay

Twenty-five hundred (2.5×10^3) cells per well were seeded in a 96-well plate. Ten microliters of CCK-8 reagent (Dojindo) were added to the medium in each well on Days 0, 1, 2 and 3, and the 96-well plate was maintained at 37°C for 2 h. Then, the absorbance was measured using a microplate reader (BioTek Instruments).

2.17 Coimmunoprecipitation (Co-IP)

2.17.1 For HRMC

Co-IP experiments for cell protein lysates were performed as previously described (Li et al., 2020b). The primary antibodies used were as follows: anti-ARAP1 (sc-393138, Santa Cruz Biotechnology), anti-CIN85 (#12304, Cell Signaling Technology) and corresponding control mouse IgG or rabbit IgG (B900620, B900610, Proteintech).

2.17.2 For mouse glomeruli

We performed Co-IP experiments using a Dynabeads Protein G Immunoprecipitation kit (Invitrogen, United States) according to the manufacturer's instructions, and detailed description of the methods is provided in the Supplementary Material and Methods.

2.18 Ubiquitination assay

2.18.1 For HRMC

Ubiquitination experiments for cell protein lysates were performed as previously described (Li et al., 2020b). The primary antibodies used for Western blotting were as follows: anti-EGFR antibody (ab52894, Abcam), anti-ubiquitin (#3933, Cell Signaling Technology) and corresponding control rabbit IgG (B900610, Proteintech).

2.18.2 For mouse glomeruli

For EGFR ubiquitination, detailed description of the methods is provided in the Supplementary Material and Methods.

2.19 Cross-linking assay

Mouse glomeruli or HRMCs were lysed with sodium phosphate buffer (pH 7.3) containing 0.5% Triton X-100 and protease inhibitor for 30 min at 4°C. The lysates were centrifuged at 20,000 rpm for 30 min at 4°C, and the supernatants were collected. The supernatants were then treated with 0.01% glutaraldehyde for 5 min at 37°C and were terminated by using 50 mM Tris-Cl (pH 8.0). These samples were separated by 10% SDS-PAGE and analyzed by Western blot with anti-PKM2 antibody (15822-1-AP, Proteintech).

2.20 Statistical analyses

Data are presented as the mean ± SD. Student's t-test and ANOVA with *post hoc* tests were used to analyze the significance of differences between groups. $p < 0.05$ was considered statistically significant. Statistical analysis of the results was performed with SPSS 26.0 software (IBM). Each experiment was done at least for repeated three times independently.

3 Results

3.1 Knockdown of ARAP1 reduces renal PKM2 dimer expression, HIF-1α accumulation, fibrogenesis and aberrant glycolysis accompanied by restoring tetrameric PKM2 formation in diabetic mice

The kidney fibrosis program in DKD is associated with an accumulation of HIF-1α and aberrant glycolysis (Li et al., 2020c; Liu et al., 2021). Previous reports have indicated that AAV2/9 can mediate robust ectopic gene expression in renal tissue (Dearborn et al., 2016; Liu et al., 2020). First, MMCs were used to validate the siRNA sequence with the best knockdown effect. ARAP1 mRNA and protein expression was significantly upregulated in high glucose-induced MMCs (Supplementary Figures S3A, B). Mouse siARAP1 (No. c) showed the best knockdown effect (Supplementary Figures S3C, D), and this sequence was chosen for constructing AAV2/9-shARAP1. The sequence is provided in Supplementary Table S5. qRT-PCR results showed that 1×10^{11}GC/animal of AAV2/9-shARAP1 had the best knockdown effect in db/db mice (Supplementary Figure S3E). The purity of the isolated glomeruli lysates was confirmed by the significant upregulation of Podocin expression, a marker of glomerular podocytes, and the almost complete absence of Cadherin-16 expression, a tubular marker (Supplementary Figure S4). AAV2/9-shARAP1 was injected by tail vein at 13th week (Figure 1). IHC staining results showed that the expressions of ARAP1, HIF-1α, COL I, COL IV and FN were significantly increased in the kidney tissues of db/db mice and were markedly reduced by AAV-shARAP1 (Figure 1B). Immunofluorescence staining validated increased ARAP1 and HIF-1α expression in the kidney tissues of diabetic db/db mice compared with that of db/m mice, and AAV-shARAP1 reduced the expression of ARAP1 and HIF-1α. Moreover, HIF-1α nucleus accumulation was significantly increased in the kidney tissues of db/db mice and were markedly reduced by AAV-shARAP1 (Figures 1C, D). To further confirm our data, the Western blot results showed that the protein expression levels of ARAP1, HIF-1α and glycolysis enzymes, such as PKM2, LDHA, HK2 and the key ECM components COL I, COL IV and FN were significantly increased in isolated glomeruli lysates from diabetic db/db mice compared with that of db/m mice and were markedly reduced by AAV-shARAP1 (Figure 2A). Our cross-linking analysis showed abundant monomeric and dimeric PKM2 expression were markedly reduced by AAV-shARAP1 in diabetic mice glomeruli, while the decreased tetrameric PKM2 expression were partly restored by AAV-shARAP1 (Figure 2B). The overall results indicated that ARAP1 inhibition was highly effective in limiting renal fibrosis and aberrant glycolysis by reducing the PKM2 dimer expression and subsequent HIF-1α nucleus accumulation and activation in diabetic mice.

3.2 Knockdown of ARAP1 attenuates renal injury and restores normal renal function in diabetic mice

The diabetic db/db mice presented with hyperglycemia, which was accompanied by a significant increase in body weight compared with db/m mice. Treatment with AAV-shARAP1 did not affect hyperglycemia or body weight change in diabetic db/db mice (Figures 3A, B). Compared with db/m mice, the UACR of db/db mice was considerably upregulated and was effectively reduced by AAV-shARAP1 treatment. The magnitude of UACR reduction increased as the treatment time extended (Figure 3C). Urinary NGAL, a marker of tubular injury, serum creatinine and BUN were reduced by AAV-shARAP1 treatment in db/db mice (Figures 3D–F). HE, PAS and Masson's staining showed mesangial matrix expansion and glomerulosclerosis progressed and kidney fibrosis in db/db mice, and AAV-shARAP1 treatment considerably reduced the morphological changes (Figure 3G). Moreover, the GSI score was reduced by AAV-shARAP1 in the kidneys of diabetic mice (PAS staining, Supplementary Figure S5). These data showed the reno-protective effects of ARAP1 gene knockdown in diabetic mice.

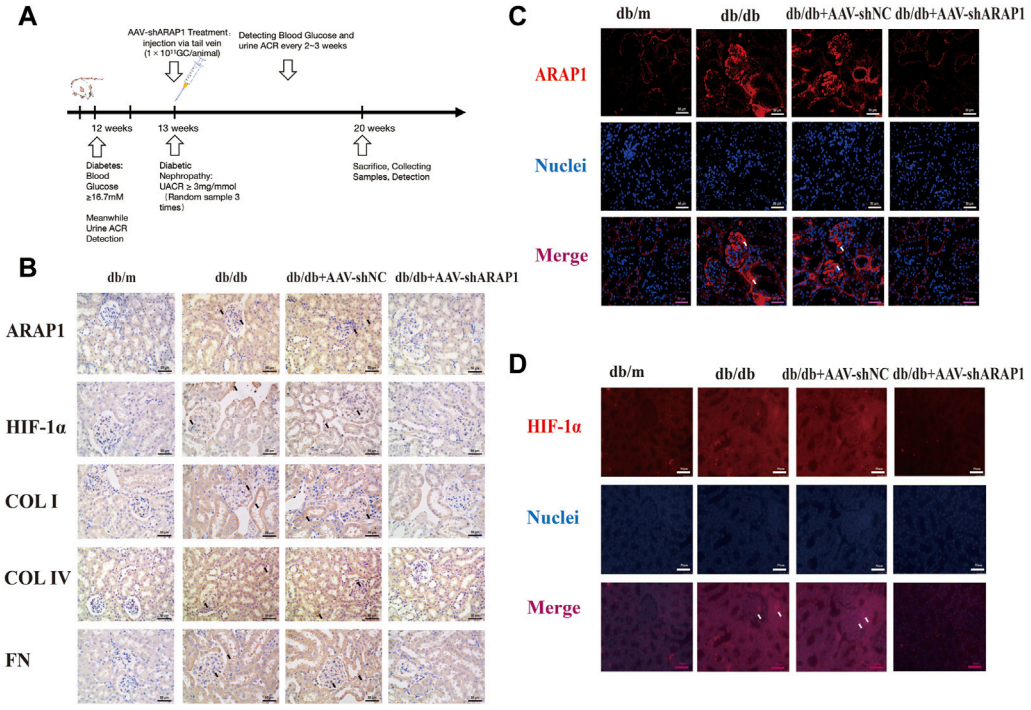

FIGURE 1
ARAP1 knockdown reduces renal HIF-1α accumulation, fibrogenesis and aberrant glycolysis in diabetic mouse **(A)** Experimental flow chart. **(B)** IHC detection of ARAP1, HIF-1α, COL I, COL IV and FN in kidney tissues from db/m, db/db, db/db + AAV-shNC and db/db + AAV-shARAP1 mice (×400). Bar = 50 μm. **(C,D)** The effect of AAV2/9-shARAP1 on the expression of ARAP1 and HIF-1α in the mouse kidney tissues was examined by immunofluorescent staining (×400). Bar = 50 μm. Arrows indicate positive staining.

3.3 Knockdown of ARAP1 inhibits dimeric PKM2 expression HIF-1α expression, pro-fibrotic responses and aberrant glycolysis accompanied by restoring tetrameric PKM2 formation in high glucose-induced human glomerular mesangial cells

The abnormal expression of ARAP1 in high glucose-induced HK-2 cells was reported in our previous study (Yang et al., 2019a; Li et al., 2020a; Li et al., 2020b). We further verified ARAP1 expression in HRMCs and found that ARAP1 was significantly upregulated in HRMCs exposed to the high glucose condition (Figures 4A, B). qRT-PCR and Western blot analysis showed that shARAP1 (No. 3) knocked down ARAP1 expression most effectively in high glucose-induced HRMCs (Figures 4C, D). The shRNA sequence targeting ARAP1 is provided in Supplementary Table S6. Immunofluorescence staining shows the location of increased HIF-1α in nuclei of high glucose-treated HRMCs, while the high glucose-induced HIF-1α nuclear accumulation was reduced by ARAP1 shRNA (Figure 4E). Similar with the observation *in vivo*, high glucose levels induced increased HIF-1α, PKM2, LDHA, HK2, COL I, COL IV and FN were effectively reduced by ARAP1 shRNA treatment (Figure 4F). Our cross-linking analysis showed abundant monomeric and dimeric PKM2 expression were markedly reduced by AAV-shARAP1 in high glucose-induced HRMCs, while the decreased tetrameric PKM2 expression were markedly increased by AAV-shARAP1 (Figure 4G). Overall, the findings indicated that ARAP1 may play a role in promoting dimeric PKM2 expression, HIF-1α accumulation and aberrant glycolysis and driving the pro-fibrotic responses in high glucose-induced HRMCs.

3.4 ARAP1 promotes dimeric PKM2 expression accompanied by inhibiting tetrameric PKM2 formation by maintaining persistent EGFR activation through regulating EGFR ubiquitination in DKD

We previously reported that ARAP1 interacted with CIN85 and regulates the ubiquitination of EGFR in high glucose-induced human proximal tubular cells (Li et al., 2020b). In the current study, we explored the interaction between ARAP1, CIN85 and EGFR in high glucose-induced HRMCs and diabetic db/db mice. The Western blot results showed that CIN85 was significantly increased in high glucose-induced HRMCs, while ARAP1 shRNA had no effect on CIN85 expression (Figure 5A). IHC staining showed that AAV-shARAP1 had no effect on CIN85 expression in db/db mice (Figure 5B). Likewise, we found that CIN85 protein expression in isolated glomeruli lysates from diabetic db/db mice was not affected by AAV-shARAP1 (Figure 5C). These results collectively suggested that ARAP1 did not regulate the expression of CIN85 in high glucose-induced HRMCs or diabetic db/db mouse glomeruli.

10.3389/fphar.2023.1069348

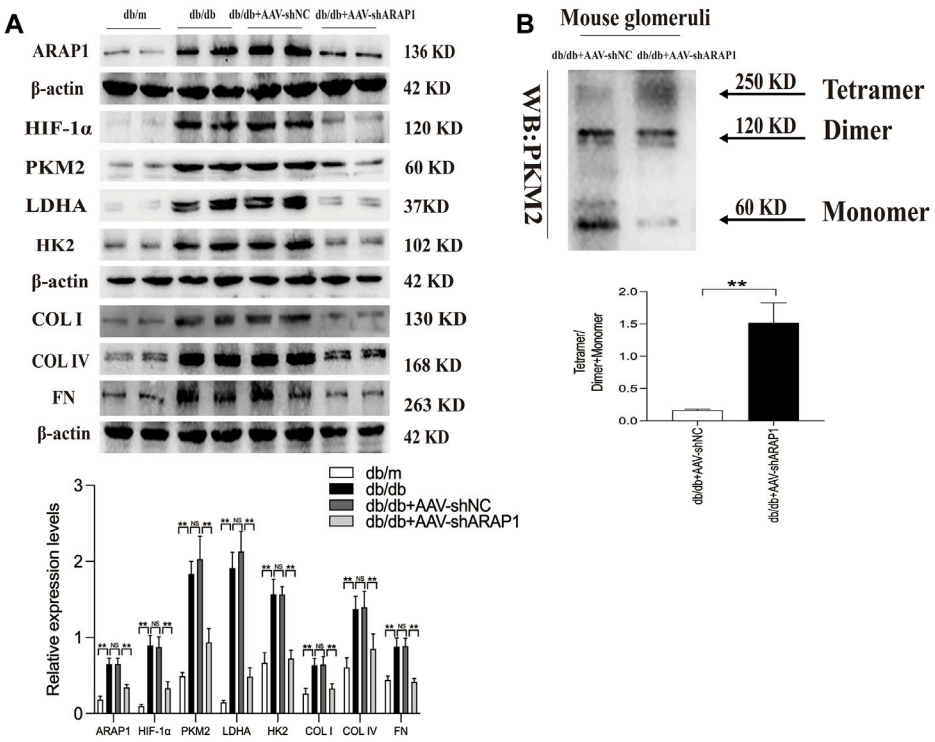

FIGURE 2
ARAP1 knockdown inhibits dimeric PKM2 expression, HIF-1α accumulation, fibrogenesis and aberrant glycolysis, while partly restore tetrameric PKM2 formation in diabetic mouse **(A)** The effect of AAV2/9-shARAP1 on ARAP1, HIF-1α, PKM2, LDHA, HK2, COL I, COL IV and FN protein expression in the isolated glomeruli lysates of mouse kidney tissues was examined by Western blot analysis. **(B)** Cross-linking detection of PKM2 in the isolated glomeruli lysates of mouse. In all panels, the data are representative of at least three independent experiments. Data are presented as the mean ± SD. $^{*}p < 0.05$, $^{**}p < 0.01$, NS, not significant.

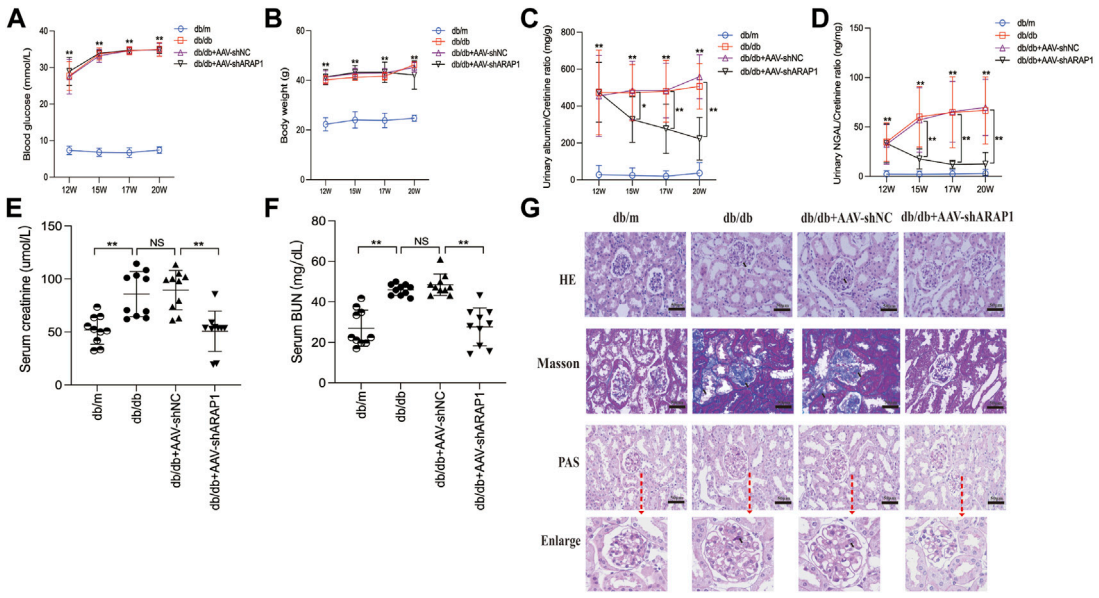

FIGURE 3
ARAP1 knockdown attenuates renal function and tissue injury in the kidneys of diabetic mouse **(A)** Blood glucose (mmol/L) and **(B)** body weight (g) was measured at the indicated weeks. **(C)** Urinary ACR at various time points (12, 15, 17 and 20 weeks of age). **(D)** Urinary Ngal at various time points (12, 15, 17 and 20 weeks of age). **(E)** Serum creatinine at 20 weeks of age. **(F)** Serum BUN at 20 weeks of age. **(G)** Representative images of HE, PAS and Masson staining (×400). Bar = 50 μm. Arrows indicate positive staining. In all panels, the data are representative of at least three independent experiments. Data are presented as the mean ± SD. $^{*}p < 0.05$, $^{**}p < 0.01$, NS, not significant.

10.3389/fphar.2023.1069348

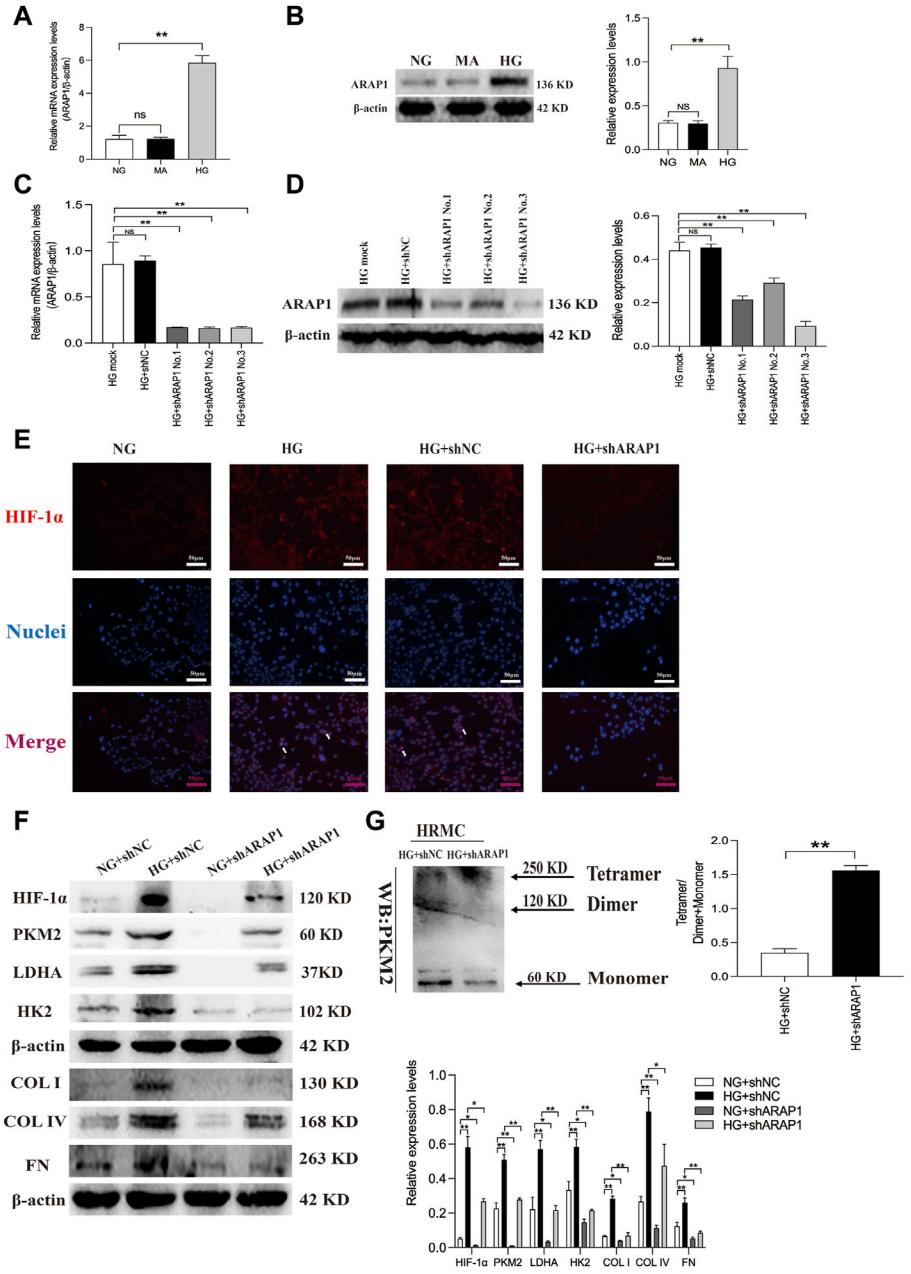

FIGURE 4
ARAP1 knockdown inhibits high glucose-induced dimeric PKM2 expression, HIF-1α nuclear accumulation, pro-fibrotic responses and aberrant glycolysis, while partly restore tetrameric PKM2 formation in human glomerular mesangial cells. **(A,B)** qRT-PCR and Western blot analysis showed that the mRNA and protein levels of ARAP1 were upregulated in HG group compared with NG group and MA group. **(C,D)** Forty-eight hours after transfection of ARAP1 shRNA (3,000 ng) in the HG group in 6-well plates, the ARAP1 knockdown efficiency was examined by qRT-PCR and Western blot analysis. **(E)** HIF-1α was assessed by immunofluorescence after treatment with high glucose or ARAP1 shRNA (×400). Bar = 50 μm. Arrows indicate positive staining. **(F)** Forty-eight hours after transfection of ARAP1 shRNA in the NG group and HG group, the protein expression of HIF-1α, PKM2, LDHA, HK2, COL I, COL IV and FN was examined by Western blot analysis. **(G)** Cross-linking detection of PKM2 in human glomerular mesangial cells. In all panels, the data are representative of at least three independent experiments. Data are presented as the mean ± SD. *$p < 0.05$, **$p < 0.01$, NS, not significant.

To further confirm that ARAP1 interacts with CIN85, we performed Co-IP assays using protein extracts from HRMCs. The proteins were immunoprecipitated using a mouse anti-ARAP1 antibody or anti-mouse IgG as a negative control, and the precipitates were analyzed by Western blot analysis with a rabbit anti-CIN85 antibody recognizing CIN85. The anti-ARAP1 antibody recognizing ARAP1 successfully precipitated CIN85, but the anti-mouse IgG failed to precipitate CIN85 in normal glucose and high glucose-induced HRMCs (Figure 5D). Consequently, we performed Co-IP assays using protein extracts from isolated glomeruli lysates. The proteins were immunoprecipitated using a rabbit anti-ARAP1 antibody or anti-rabbit IgG as a negative

control, and the precipitates were analyzed by Western blot analysis with a rabbit anti-CIN85 antibody recognizing CIN85. The anti-ARAP1 antibody recognizing ARAP1 successfully precipitated CIN85, but the anti-rabbit IgG failed to precipitate CIN85 (Figure 5E). Therefore, our data suggested that ARAP1 could interact with CIN85 in high glucose-induced HRMCs and diabetic db/db mouse glomeruli.

EGFR activation promotes dimer PKM2 expression and nuclear translocation to activate HIF-1α, contributing to abnormal glycolysis and tumor cell proliferation (Yang et al., 2011; Yang et al., 2018; Wang et al., 2020). EGFR activation promotes HIF-1α activation and ECM accumulation in mesangial cells in response to high glucose, which finally resulted in matrix upregulation and glomerular fibrosis (Uttarwar et al., 2011; Li et al., 2015), but the exact regulatory mechanism of ARAP1 on EGFR activation and PKM2/HIF-1α pathway in mesangial cells has not been reported. Therefore, we used HRMCs and glomeruli of diabetic mice to further dissect the regulatory mechanism of ARAP1 on persistent EGFR activation. The Western blot results showed that the expression levels of total EGFR and activation of EGFR as indicated by its phosphorylation at two phosphorylation sites (Y1068 and Y1173) were consistently inhibited after shARAP1 transfection in high glucose-induced HRMCs (Figure 6A). The protein expression levels of total EGFR and

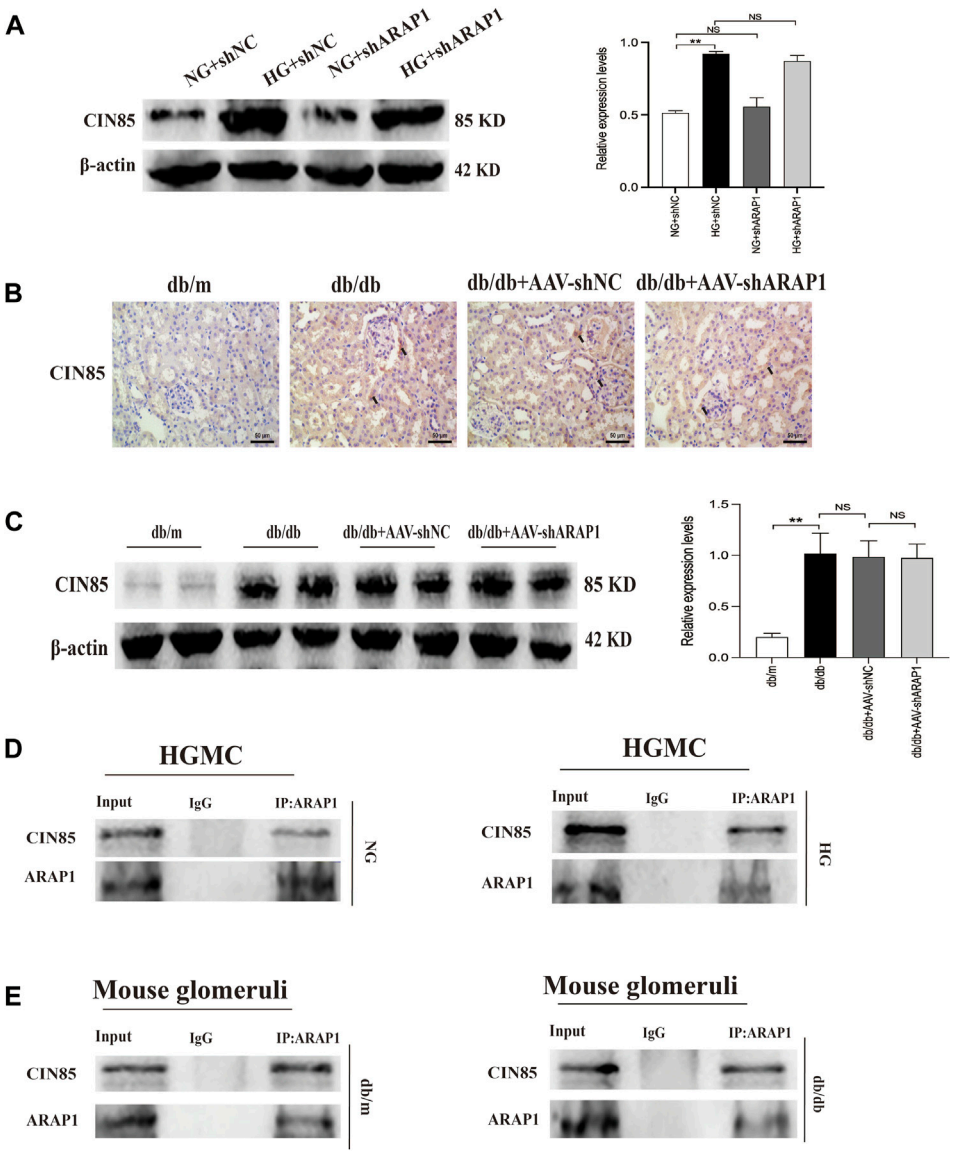

FIGURE 5
Interaction between ARAP1 and CIN85 **(A)** Forty-eight hours after transfection of ARAP1 shRNA in the NG group and HG group, the protein expression of CIN85 was examined by Western blot analysis. **(B)** IHC detection of CIN85 in kidney tissues from db/m, db/db, db/db + AAV-shNC and db/db + AAV-shARAP1 mice (×400). Bar = 50 μm. Arrows indicate positive staining. **(C)** The effect of AAV2/9-shARAP1 on the protein expression of CIN85 in the isolated glomeruli lysates of mouse kidney tissues was examined by Western blot analysis. **(D,E)** The physical interaction between ARAP1 and CIN85 in human glomerular mesangial cells and mouse glomeruli was detected by Co-IP analysis. IgG was used as a negative control. In all panels, the data are representative of at least three independent experiments. Data are presented as the mean ± SD. *$p < 0.05$, **$p < 0.01$, NS, not significant.

10.3389/fphar.2023.1069348

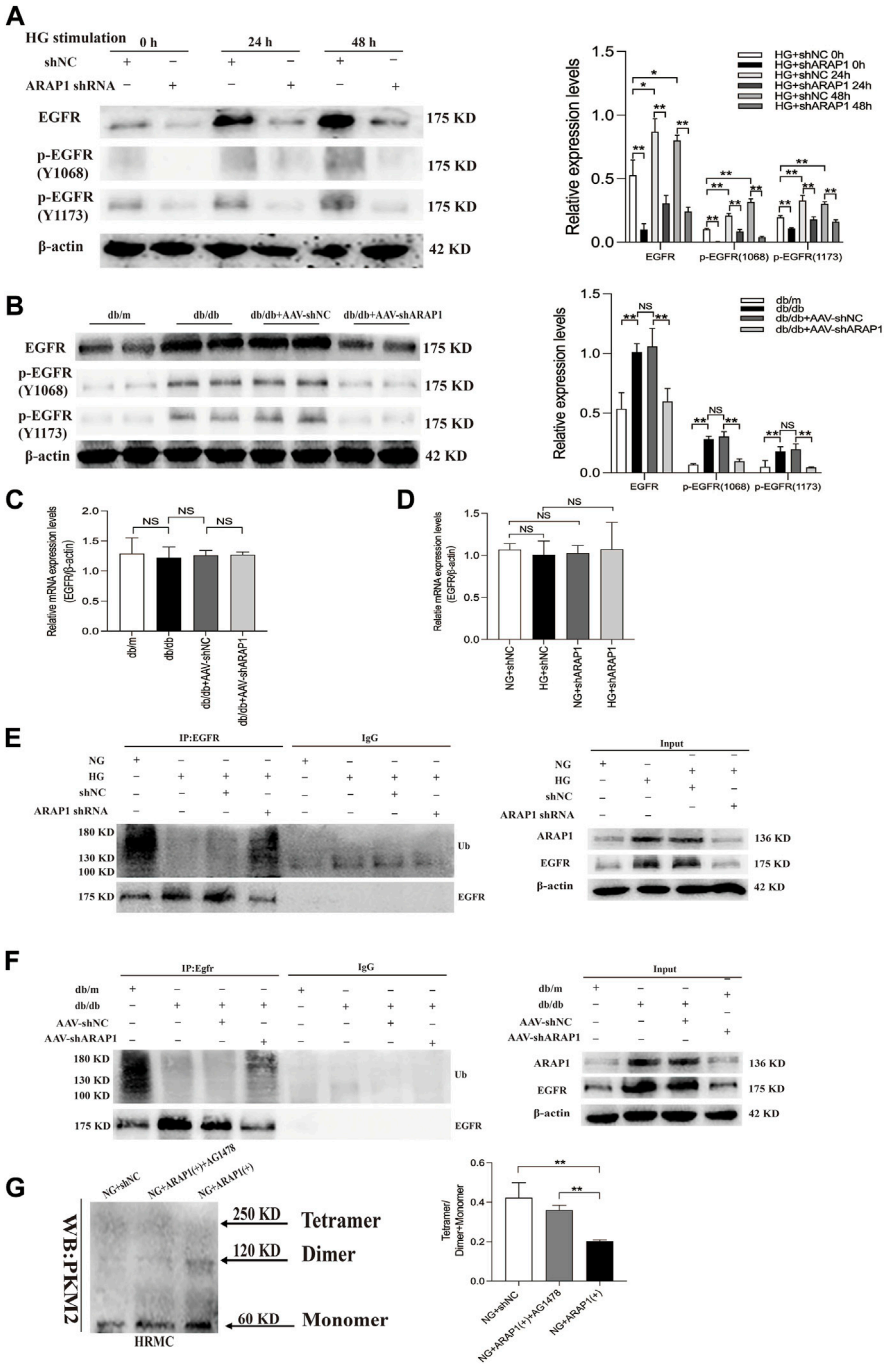

FIGURE 6
ARAP1 regulates dimeric and tetrameric PKM2 expression by reducing EGFR ubiquitination and maintaining persistent EGFR activation **(A)** Human glomerular mesangial cells were pre-treated with ARAP1 shRNA for 24 h and then divided into the NG group and HG group. The protein expression levels of total EGFR and EGFR phosphorylated at two phosphorylation sites (Y1068 and Y1173) were detected at 24 and 48 h after stimulation by high glucose. HRMCs were pre-treated with ARAP1 shRNA for 24 h and then divided into NG and HG groups. 0 h means that the HRMCs were only transfected with ARAP1 shRNA for 24 h under normal glucose and were not stimulated with high glucose. **(B)** Effect of AAV2/9-shARAP1 on the protein expression of total EGFR, and EGFR phosphorylated at two phosphorylation sites (Y1068 and Y1173) in the isolated glomeruli lysates of mouse kidney tissues was examined by Western blot analysis. **(C)** The mRNA expression of total EGFR in the isolated glomeruli lysates of kidney tissues from the db/m, db/db, db/db + AAV-shNC and db/db + AAV-shARAP1 mice was measured by qRT-PCR. **(D)** Forty-eight hours after transfection of ARAP1 shRNA in the NG group and HG group, the mRNA expression of total EGFR was measured by qRT-PCR. **(E)** ARAP1 knockdown with ARAP1 shRNA increased EGFR ubiquitination in human glomerular mesangial cells cultured with high glucose. **(F)** ARAP1 knockdown with AAV2/9-shARAP1 increased EGFR ubiquitination in the isolated glomeruli lysates of diabetic db/db mouse kidney tissues. **(G)** After transfection of ARAP1 overexpression plasmid accompanied by AG1478 treatment in the NG group, PKM2 monomer, dimer and tetramer in human glomerular mesangial cells were detected by cross-linking assay. In all panels, the data are representative of at least three independent experiments. Data are presented as the mean ± SD. *$p < 0.05$, **$p < 0.01$, NS, not significant.

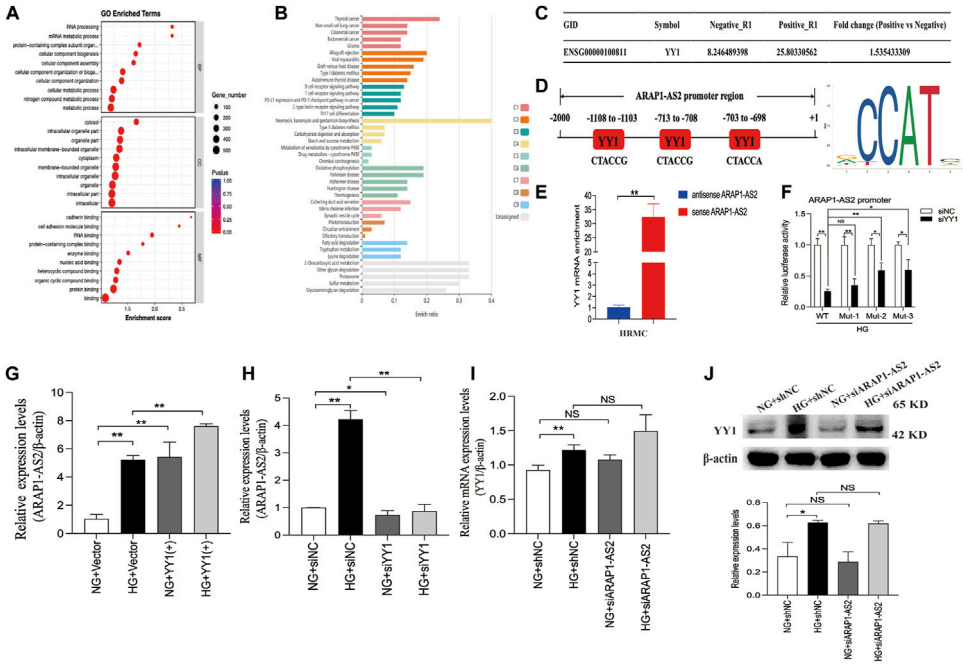

FIGURE 7
Regulatory mechanism of YY1 on ARAP1-AS2 **(A)** GO analysis of RNA pull-down seq. **(B)** KEGG enrichment analysis of RNA pull-down seq. **(C)** The enrichment of YY1 in the complexes pulled down by ARAP1-AS2. A higher fold change value indicates more enrichment. **(D)** Three YY1 binding sites in the promoter of ARAP1-AS2 were predicted by the JASPAR tool. **(E)** RNA pull-down assays were performed to examine whether ARAP1-AS2 could bind YY1 in HRMCs. YY1 was pulled down by ARAP1-AS2, and the level of YY1 was measured by qRT-PCR. **(F)** Luciferase reporter analysis demonstrated the effect of YY1 silencing on the luciferase activity of the ARAP1-AS2 promoter reporter in indicated experimental groups. **(G,H)** Forty-eight hours after transfection of the YY1 overexpression plasmid or YY1 siRNA in the NG group and HG group, the expression level of ARAP1-AS2 was measured by qRT-PCR. **(I)** Forty-eight hours after transfection of the ARAP1-AS2 siRNA in the NG group and HG group, the mRNA expression level of YY1were measured by qRT-PCR. **(J)** Forty-eight hours after transfection of the ARAP1-AS2 siRNA in the NG group and HG group, the protein expression level of YY1 was examined by Western blot analysis. In all panels, the data are representative of at least three independent experiments. Data are presented as the mean ± SD. *$p < 0.05$, **$p < 0.01$, NS, not significant.

EGFR phosphorylated at two phosphorylation sites (Y1068 and Y1173) were upregulated in isolated glomeruli lysates from diabetic db/db mice and were markedly reduced by AAV-shARAP1 (Figure 6B). There was no significant change in total EGFR mRNA expression in cells or mouse glomeruli (Figures 6C, D). Ubiquitination assays revealed that EGFR ubiquitination was significantly reduced in high glucose-induced HRMCs and the glomeruli of db/db mice and was markedly enhanced after ARAP1 knockdown (Figures 6E, F). To clarify the relationship between ARAP1, EGFR and PKM2, we performed a rescue experiment in HRMCs. The transfection efficacy of ARAP1 overexpressed plasmid was verified by Western blot (Supplementary Figure S6G). The results of cross-linking analysis showed that increased abundant monomeric and dimeric PKM2 expression by ARAP1 overexpression plasmids were markedly reduced by AG1478 in normal glucose-induced HRMCs, while the decreased tetrameric PKM2 expression induced by ARAP1 overexpression plasmids were partially restored by AG1478 (Figure 6G). Together, these data demonstrated that the ARAP1 interacts with CIN85 to reduce EGFR ubiquitination and thus stabilized the level of total EGFR proteins to maintain the persistent activation of EGFR and subsequent increased dimeric PKM2 expression as well as decreased tetrameric PKM2 formation in DKD.

3.5 YY1 directly promotes ARAP1-AS2 transcriptional activity *in vitro*

YY1 is known to interact with LncRNAs and regulate the transcriptional activity of LncRNAs (An and Ding, 2021). Results of the RNA pulldown-seq of ARAP1-AS2 in HK-2 cells were reported in our previous study (Li et al., 2020b). To explore the potential biological function of the genes enriched in ARAP1-AS2 pulldown, GO and KEGG pathway enrichment analyses were conducted. GO analyses revealed these genes to be mainly enriched in "metabolic process" (BP), "RNA and protein binding" (MF) and "membrane-bounded organelle" (CC) (Figure 7A). According to KEGG analysis, the enriched genes were closely related to diabetes mellitus and the ubiquitin-mediated proteolysis pathway (Figure 7B; Supplementary Table S7). The complexes pulled down were enriched in YY1 (Figure 7C). We identified 3 YY1 binding sites in the ARAP1-AS2 promoter using the JASPAR tool (Figure 7D). RNA pull-down assays showed that YY1 was pulled down only by sense ARAP1-AS2 in HRMCs (Figure 7E). Luciferase reporter analysis demonstrated that in HRMCs stimulated with high glucose, siYY1 reduced the activity of the ARAP1-AS2 promoter, and mutations at sites 2 and 3, but not site 1, partly restored the promoter activity (Figure 7F). These data proved that YY1 targeted the ARAP1 promoter at sites 2 and 3. We further verified that ARAP1-AS2 and YY1 were significantly upregulated in high glucose-induced

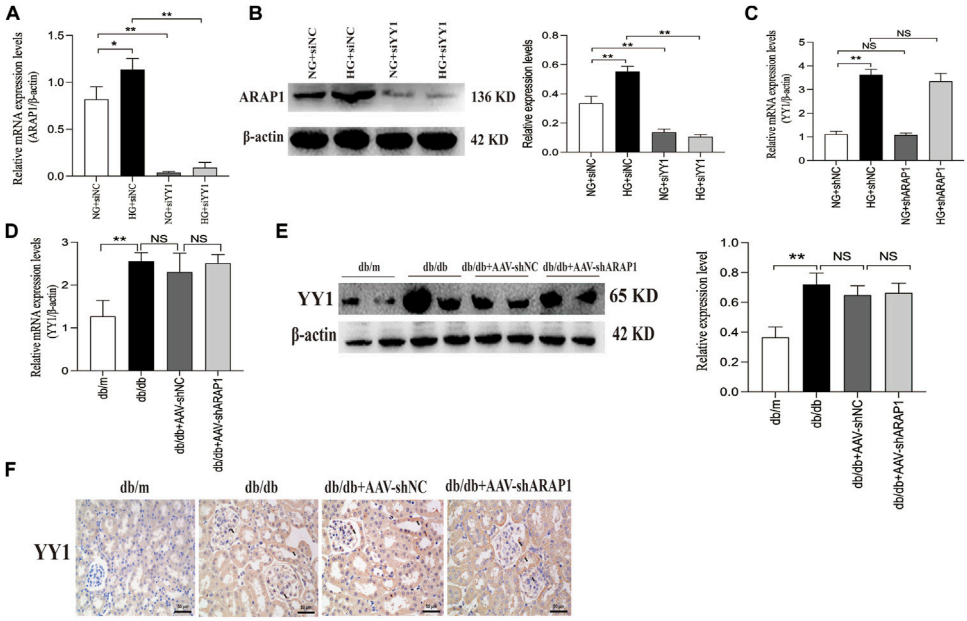

FIGURE 8
Effect of YY1 on ARAP1 **(A)** Forty-eight hours after transfection of the YY1 siRNA in the NG group and HG group, the mRNA expression level of ARAP1were measured by qRT-PCR. **(B)** Forty-eight hours after transfection of the YY1 siRNA in the NG group and HG group, the protein expression level of ARAP1 was examined by Western blot analysis. **(C)** Forty-eight hours after transfection of the ARAP1 shRNA in the NG group and HG group, the mRNA expression level of YY1 were measured by qRT-PCR. **(D)** The mRNA expression of YY1 in the isolated glomeruli lysates of kidney tissues from the db/m, db/db, db/db + AAV-shNC and db/db + AAV-shARAP1 mice was measured by qRT-PCR. **(E)** The protein expression of YY1 in the isolated glomeruli lysates of kidney tissues from the db/m, db/db, db/db + AAV-shNC and db/db + AAV-shARAP1 mice was measured by Western blot analysis. **(F)** IHC detection of YY1 in kidney tissues from db/m, db/db, db/db + AAV-shNC and db/db + AAV-shARAP1 mice (×400). Bar = 50 μm. Arrows indicate positive staining.

HRMCs (Supplementary Figures S6A, C, D). We transfected the siRNAs targeting ARAP1-AS2 and YY1, YY1 overexpression plasmids and verified their activity (Supplementary Figures S6B, E, F). The siRNA sequence targeting ARAP1-AS2 and YY1 is described in Supplementary Table S5. The results of qRT-PCR revealed that the levels of ARAP1-AS2 were significantly upregulated by YY1 overexpression plasmids, while the expression of ARAP1-AS2 was decreased by YY1 siRNAs (Figures 7G, H). There was no change in the mRNA and protein expression of YY1 after ARAP1-AS2 knockdown (Figures 7I, J). These results indicate that YY1 directly and positively regulates ARAP1-AS2 transcriptional activity in high glucose-induced HRMCs.

3.6 YY1 regulate EGFR activation, HIF-1α accumulation and aberrant glycolysis and ECM accumulation in human glomerular mesangial cells, possibly through the ARAP1-AS2/ARAP1 axis

We further verified that the mRNA and protein expression of ARAP1 were significantly downregulated after YY1 knockdown (Figures 8A, B). There was no change in the mRNA expression of YY1 after ARAP1 knockdown (Figure 8C). Similar with the *in-vitro* results, we found that the increased mRNA and protein expressions of YY1 in isolated glomeruli lysates from diabetic db/db mice was not affected by AAV-shARAP1 (Figures 8D, E). Likewise, IHC staining showed that AAV-shARAP1 had no effect on YY1expression in db/db mice (Figure 8F).

To clarify the relationship between YY1, ARAP1-AS2, ARAP1, EGFR activation, HIF-1α accumulation and ECM accumulation, we performed a rescue experiment in HRMCs. The results of qRT-PCR showed that the effect of YY1 overexpression on increasing the levels of ARAP1-AS2 in the NG group was inhibited by siARAP1-AS2 (Figure 9A). Western blot analysis showed that the effect of YY1 overexpression on increasing the levels of ARAP1, total EGFR and EGFR phosphorylated at two phosphorylation sites (Y1068 and Y1173), HIF-1α,PKM2, LDHA, HK2 and ECM components COL I, COL IV and FN in the NG group was inhibited by siARAP1-AS2 (Figures 9B, D, E). Ubiquitination assays revealed that the effect of YY1 overexpression on reducing EGFR ubiquitination was significantly restored by siARAP1-AS2 in high glucose-induced HRMCs (Figure 9C). Moreover, the CCK-8 assay revealed that the effect of YY1 overexpression on promoting cell proliferation in the NG group was blocked by siARAP1-AS2 (Figure 9F). These results demonstrate that YY1 may have regulated EGFR ubiquitination and activation, HIF-1α accumulation and aberrant glycolysis and ECM accumulation in human glomerular mesangial cells through the ARAP1-AS2/ARAP1 axis in human glomerular mesangial cells.

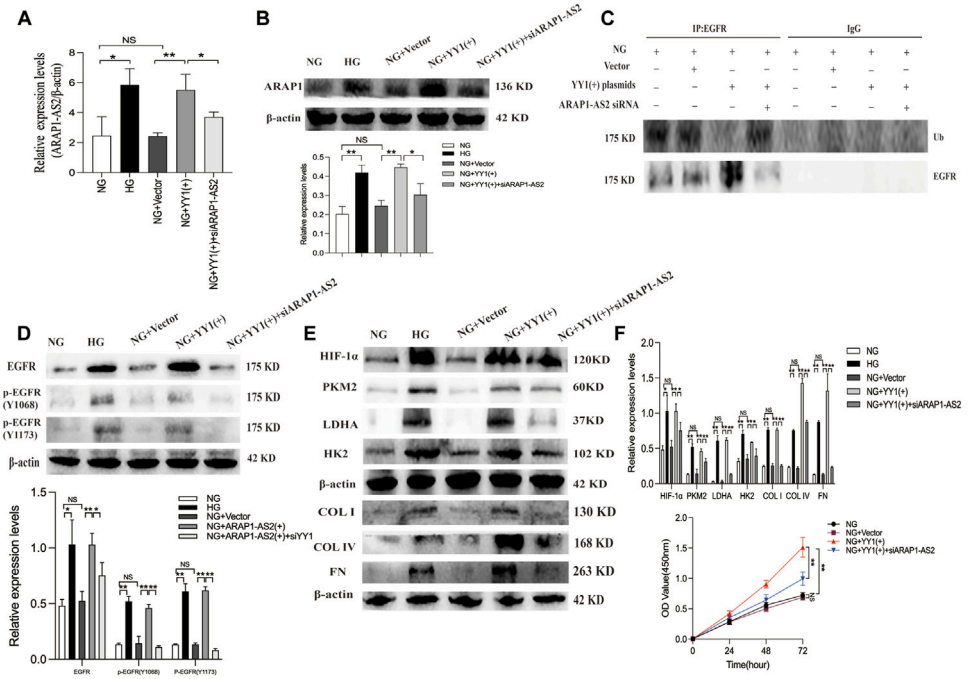

FIGURE 9
YY1 regulate EGFR ubiquitination and activation, HIF-1α accumulation and aberrant glycolysis and ECM accumulation in human glomerular mesangial cells through the ARAP1-AS2/ARAP1 axis. **(A)** Forty-eight hours after co-transfection of the YY1 overexpression plasmid and ARAP1-AS2 siRNA in the NG group, the expression level of ARAP1-AS2 was examined by qRT-PCR. **(B)** Forty-eight hours after co-transfection of the YY1 overexpression plasmid and ARAP1-AS2 siRNA in the NG group, the protein expression levels of ARAP1 were examined by Western blot analysis. **(C)** Forty-eight hours after co-transfection of the YY1 overexpression plasmid and ARAP1-AS2 siRNA in the NG group, EGFR ubiquitination were examined. **(D)** Forty-eight hours after co-transfection of the YY1 overexpression plasmid and ARAP1-AS2 siRNA in the NG group, the protein expression levels of total EGFR, and EGFR phosphorylated at two phosphorylation sites (Y1068 and Y1173) were examined by Western blot analysis. **(E)** Forty-eight hours after co-transfection of the YY1 overexpression plasmid and ARAP1-AS2 siRNA in the NG group, the protein expression levels of HIF-1α, PKM2, LDHA, HK2, COL I, COL IV and FN were examined by Western blot analysis. **(F)** After co-transfection of the YY1 overexpression plasmid and ARAP1-AS2 siRNA, cell proliferation was evaluated by CCK-8 assay at 0, 24, 48 and 72 h. In all panels, the data are representative of at least three independent experiments. Data are presented as the mean ± SD. *$p < 0.05$, **$p < 0.01$, NS, not significant.

4 Discussion

Recent studies have shown that HIF-1α is activated to induce aberrant transcription of genes encoding glycolytic enzymes in the pathogenesis of DKD (Isoe et al., 2010; Liu et al., 2021). PKM2 can be aggregated into tetramer and dimer forms. Dimeric PKM2 acts as a key protein kinase in aberrant glycolysis by promoting the accumulation of HIF-1α, while tetrameric PKM2 functions as a pyruvate kinase in oxidative phosphorylation (Luo et al., 2011; Sizemore et al., 2018). The transformation between them plays an important role in energy supply of tumor cells, epithelial-mesenchymal transition (EMT), invasion and metastasis and cell proliferation (Zhang et al., 2019a). It has been proved that the PKM2 tetramer form decreases, the dimer form increases and enters the nucleus to activate HIF-1α in DKD (Liu et al., 2021). In this study, we first verified that ARAP1 knockdown can alleviate ECM accumulation and renal dysfunction and glomerulosclerosis in diabetic db/db mice as well as in GMCs exposed to high glucose through reducing aberrant glycolysis *via* decreasing HIF-1α nuclear accumulation, possibly associated with reduced expression and nucleus translocation of dimer PKM2 accompanied by restoring tetramer formation led by breaking the EGFR persistent transactivation. We provide the first evidence for YY1 regulate EGFR activation, dimer PKM2 accumulation, HIF-1α activation and aberrant glycolysis and ECM accumulation in DKD through the ARAP1-AS2/ARAP1 axis.

One of the characteristics of DKD is ECM accumulation, which eventually leads to glomerular sclerosis and fibrosis (Doi et al., 2018). Studies have demonstrated that HIF-1α promotes aberrant glycolysis, which finally leading to ECM accumulation and renal fibrosis in mouse models of chronic/hypoxic renal injury models (Cai et al., 2020; Wei et al., 2022). Our diabetic db/db mice showed the pro-fibrotic activities in the kidney accompanied by kidney dysfunction and increased proteinuria and kidney injury in this study, indicating that our diabetic model presented with progressive DKD. Our group has reported excessive ECM accumulation and kidney fibrosis in diabetic db/db mice (Zhang et al., 2019b; Ma et al., 2022). Our cross-linking experiment first demonstrated that ARAP1 inhibition reduced PKM2 dimer expression and partially restored tetramer formation in high glucose-induced HRMCs and db/db mouse glomeruli. The HIF-1α activation, aberrant glycolytic genes expression and pro-fibrotic activities, such as the increased collagen accumulation in kidney glomeruli,

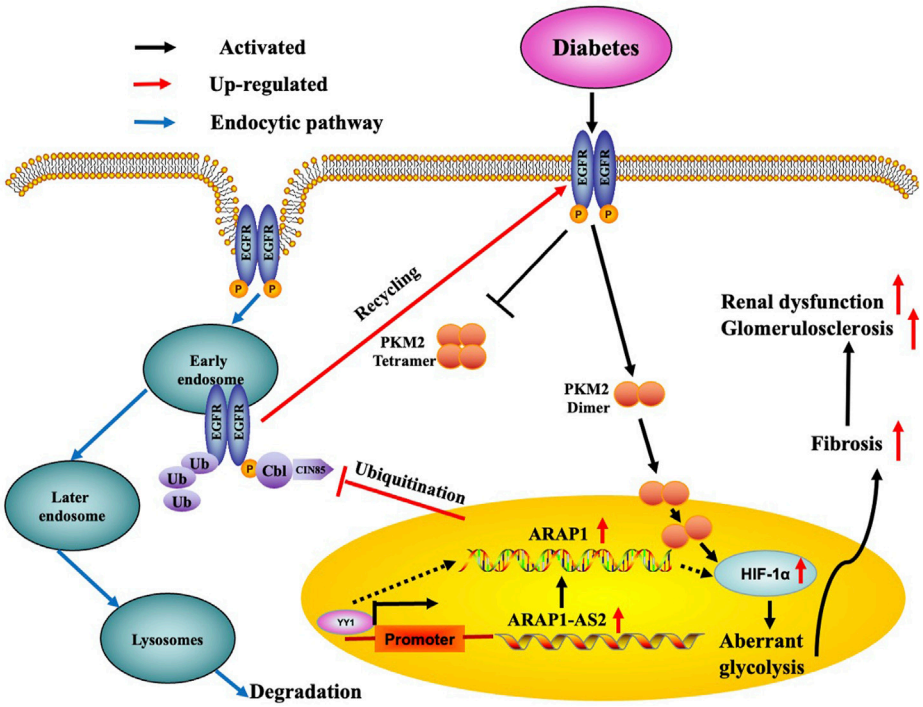

FIGURE 10
Schematic representation of the proposed model: possible regulatory mechanism of YY1, ARAP1-AS2, and ARAP1 on HIF-1α accumulation and aberrant glycolysis in DKD. Increased YY1 expression in a high-glucose environment can upregulate ARAP1-AS2 expression by targeting its promoter and then indirectly upregulate ARAP1 expression. Subsequently, ARAP1 binds to CIN85 and reduces the ubiquitination of EGFR, thus stabilizing total EGFR protein levels to support the persistent activation of EGFR in DKD. The persistent activation of EGFR then promotes PKM2 dimer expression and nucleus translocation to activate HIF-1α, accompanied by reducing tetramer formation, which finally leads to aberrant glycolysis and aggravates ECM accumulation and glomerulosclerosis and fibrosis in human glomerular mesangial cells exposed to high glucose and diabetic db/db mice.

kidney dysfunction and kidney injury, were significantly prevented after administration of AAV2/9-shARAP1in the diabetic mice.

Mesangial cells can cause glomerular injury through excessive cell proliferation and ECM accumulation (Wang et al., 2018b) and maintain the glomerular capillary structural architecture and mesangial matrix homeostasis (Abboud, 2012). Excessive accumulation of ECM in the glomerulus leads to glomerulosclerosis and contributes to the initiation and progression of DKD. In the present study, we found that ARAP1 was markedly increased in db/db mouse glomeruli and that ARAP1 and its natural antisense lncRNA, ARAP1-AS2, were significantly upregulated in high glucose stimulated-HRMCs, which increased the accumulation of PKM2 dimer accompanied by reducing tetramer formation, activation of HIF-1α and expression of aberrant glycolytic and ECM genes. To date, the regulatory mechanism of ARAP1-AS2 in DKD has been reported only in HK-2 cells by our study team (Li et al., 2020a; Li et al., 2020b), while the potential involvement of other renal cell populations and its effect in animal models remained unknown. This study also provides a new finding that ARAP1-AS2 is a novel target of YY1 and positively regulated by YY1 in DKD. Luciferase reporter analysis and rescue experiments demonstrated that YY1 targets ARAP1-AS2 promoter and promotes EGFR activation, HIF-1α accumulation and aberrant glycolysis and ECM accumulation through the ARAP1-AS2/ARAP1 axis in high glucose stimulated-HRMCs. All these findings further confirmed the important role of ARAP1-AS2/ARAP1 in the pathogenesis of DKD as reported by our group (Yang et al., 2019a; Li et al., 2020a; Li et al., 2020b), but there may also be limitations to this study, as our current data cannot exclude the role of lncRNA-ARAP1-AS2/ARAP1 in other cell types, such as podocytes, in DKD.

EGFR is widely expressed in the glomeruli (Chen et al., 2015) and HIF-1α has been clearly demonstrated to be a downstream target of EGFR (Wang et al., 2018c; Wang et al., 2022). EGFR activation has been reported to participate in the activation of HIF-1α by promoting dimer PKM2 expression and enter nucleus, eventually leading to ECM accumulation and renal fibrosis in DKD (Yang et al., 2011; Overstreet et al., 2017). We previously reported that ARAP1 could maintain persistent EGFR activation by reducing the ubiquitination of EGFR through interacting with CIN85 and that ARAP1-AS2 directly interacted with ARAP1 and promoted ARAP1 expression and then regulated CIN85 indirectly in HK-2 cells (Li et al., 2020b); however, the mechanism of persistent EGFR activation in other renal cell populations and animal models of DKD is still unknown. Currently, we focus on the mechanism of EGFR activation in HRMCs and diabetic mice. We found that the interaction between ARAP1 and CIN85 exist in high glucose-stimulated HRMCs and diabetic db/db mouse glomeruli, while

ARAP1 knockdown had no effect on CIN85 expression. Our results suggest that ARAP1 knockdown could maintain the decreased levels of total EGFR and the sustained inhibition of EGFR activation. The reduced ubiquitination level of EGFR was significantly reversed after ARAP1 knockdown in high glucose-stimulated HRMCs and db/db mouse glomeruli. However, qRT-PCR results showed that ARAP1 has no effect on the transcription of EGFR. Cross-linking rescue experiment results showed that increased dimeric PKM2 expression induced by ARAP1 overexpression plasmids were markedly reduced by AG1478 in normal glucose-induced HRMCs, while the decreased tetrameric PKM2 expression were partially restored by AG1478. All these findings confirmed ARAP1 can promote dimeric PKM2 expression as well as inhibit tetrameric PKM2 formation by maintaining persistent EGFR activation in high glucose-stimulated HRMCs and diabetic db/db mouse glomeruli. Based on the above results, we indicated that YY1 targets the promoter of ARAP1-AS2 and promotes ARAP1-AS2 and its sense target gene ARAP1 expression. YY1 promotes HIF-1α accumulation and aberrant glycolysis through the ARAP1-AS2/ARAP1 axis, associated with maintaining the EGFR persistent transactivation and increased PKM2 dimer expression and nucleus translocation accompanied by reducing tetramer formation, which finally leads to ECM accumulation and glomerulosclerosis and fibrosis in high glucose-induced human glomerular mesangial cells and diabetic db/db mice (Figure 10).

In summary, our results revealed that ARAP1-AS2/ARAP1 play a role in human glomerular mesangial cells and diabetic db/db mice glomeruli. YY1-induced upregulation of ARAP1-AS2 and ARAP1 promotes kidney fibrosis by HIF-1α accumulation and aberrant glycolysis through promoting EGFR persistent activation and PKM2 dimer expression and nucleus translocation accompanied by reducing tetramer formation. The novel mechanism of YY1, ARAP1-AS2, and ARAP1 in regulating aberrant glycolysis and fibrosis by EGFR/PKM2/HIF-1α pathway will further enhance our understanding of lncRNA functions in DKD and may suggest a potential therapeutic strategy for DKD.

Data availability statement

The original contributions presented in the study are included in the article/Supplementary Material, further inquiries can be directed to the corresponding author.

Ethics statement

The animal study was reviewed and approved by the Institutional Animal Care and Use Committee (IACUC) of China Medical University (approval number: CMU2019222).

Author contributions

XL, T-KM, and Q-LF have made substantial contributions to conception and design or acquisition of data, or analysis and interpretation of data and been involved in drafting the manuscript or revising it critically for important intellectual content. MW, X-DZ, T-YL, YL, Z-HH, Y-HZ, HD, SZ, LY, Y-YX, CL, and HS, have made substantial contributions to analysis and interpretation of data. Q-LF agreed to be accountable for all aspects of the work in ensuring that questions related to the accuracy or integrity of any part of the work are appropriately investigated and resolved. Q-LF given final approval of the version to be published. All authors listed have made a substantial, direct, and intellectual contribution to the work, and approved it for publication.

Funding

The work was supported by the National Natural Science Foundation of China (No. 82070754, 81770724), National Key Research and Development Plan Program-Precision Medicine Research" Special Project (No. 2017YFC0907600), Xing Liao Talents Program Science and Technology Innovation Leading Talent Fund (Distinguished Professor of Liaoning Province) (No. XLYC1902080), Liaoning Province Postdoctoral Science Fund (3110211225), Shanghai Pujiang Talent Plan (22PJD061).

Conflict of interest

The authors declare that the research was conducted in the absence of any commercial or financial relationships that could be construed as a potential conflict of interest.

Publisher's note

Supplementary material

The Supplementary Material for this article can be found online at: https://www.frontiersin.org/articles/10.3389/fphar.2023.1069348/full#supplementary-material

References

Abboud, H. E. (2012). Mesangial cell biology. *Exp. Cell Res.* 318 (9), 979–985. doi:10.1016/j.yexcr.2012.02.025

An, Z., and Ding, W. (2021). Acinetobacter baumannii up-regulates LncRNA-GAS5 and promotes the degradation of STX17 by blocking the activation of YY1. *Virulence* 12 (1), 1965–1979. doi:10.1080/21505594.2021.1953851

Azoitei, N., Becher, A., Steinestel, K., Rouhi, A., Diepold, K., Genze, F., et al. (2016). PKM2 promotes tumor angiogenesis by regulating HIF-1α through NF-κB activation. *Mol. Cancer* 15, 3. doi:10.1186/s12943-015-0490-2

Cai, T., Ke, Q., Fang, Y., Wen, P., Chen, H., Yuan, Q., et al. (2020). Sodium-glucose cotransporter 2 inhibition suppresses HIF-1α-mediated metabolic switch from lipid oxidation to glycolysis in kidney tubule cells of diabetic mice. *Cell death Dis.* 11 (5), 390. doi:10.1038/s41419-020-2544-7

Chen, J., Chen, J. K., and Harris, R. C. (2015). EGF receptor deletion in podocytes attenuates diabetic nephropathy. *J. Am. Soc. Nephrol. JASN* 26 (5), 1115–1125. doi:10.1681/ASN.2014020192

Dearborn, J. T., Ramachandran, S., Shyng, C., Lu, J. Y., Thornton, J., Hofmann, S. L., et al. (2016). Histochemical localization of palmitoyl protein thioesterase-1 activity. *Mol. Genet. metabolism* 117 (2), 210–216. doi:10.1016/j.ymgme.2015.11.004

Doi, T., Moriya, T., Fujita, Y., Minagawa, N., Usami, M., Sasaki, T., et al. (2018). Urinary IgG4 and Smad1 are specific biomarkers for renal structural and functional changes in early stages of diabetic nephropathy. *Diabetes* 67 (5), 986–993. doi:10.2337/db17-1043

Roett, M. A., Liegl, S., and Jabbarpour, Y. (2012). Diabetic nephropathy—The family physician's role. *Am. Fam. Physician* 85, 883–889.

He, J., Wang, M., Jiang, Y., Chen, Q., Xu, S., Xu, Q., et al. (2014). Chronic arsenic exposure and angiogenesis in human bronchial epithelial cells via the ROS/miR-199a-5p/HIF-1α/COX-2 pathway. *Environ. Health Perspect.* 122, 255–261. doi:10.1289/ehp.1307545

Herrington, W. G., Staplin, N., Wanner, C., Green, J. B., Hauske, S. J., Emberson, J. R., et al. (2023). Empagliflozin in patients with chronic kidney disease. *N. Engl. J. Med.* 388 (2), 117–127. doi:10.1056/NEJMoa2204233

Isoe, T., Makino, Y., Mizumoto, K., Sakagami, H., Fujita, Y., Honjo, J., et al. (2010). High glucose activates HIF-1-mediated signal transduction in glomerular mesangial cells through a carbohydrate response element binding protein. *Kidney Int.* 78 (1), 48–59. doi:10.1038/ki.2010.99

Jia, Y., Chen, J., Zheng, Z., Tao, Y., Zhang, S., Zou, M., et al. (2022). Tubular epithelial cell-derived extracellular vesicles induce macrophage glycolysis by stabilizing HIF-1α in diabetic kidney disease. *Mol. Med.* 28 (1), 95. doi:10.1186/s10020-022-00525-1

Kitada, M., Kume, S., Takeda-Watanabe, A., Kanasaki, K., and Koya, D. (2013). Sirtuins and renal diseases: Relationship with aging and diabetic nephropathy. *Clin. Sci. (Lond). Feb* 124 (3), 153–164. doi:10.1042/CS20120190

Li, R., Uttarwar, L., Gao, B., Charbonneau, M., Shi, Y., Chan, J. S., et al. (2015). High glucose up-regulates ADAM17 through HIF-1α in mesangial cells. *J. Biol. Chem.* 290 (35), 21603–21614. doi:10.1074/jbc.M115.651604

Li, L., Xu, L., Wen, S., Yang, Y., Li, X., and Fan, Q. (2020). The effect of lncRNA-ARAP1-AS2/ARAP1 on high glucose-induced cytoskeleton rearrangement and epithelial-mesenchymal transition in human renal tubular epithelial cells. *J. Cell. physiology* 235 (7-8), 5787–5795. doi:10.1002/jcp.29512

Li, X., Ma, T. K., Wen, S., Li, L. L., Xu, L., Zhu, X. W., et al. (2020). LncRNA ARAP1-AS2 promotes high glucose-induced human proximal tubular cell injury via persistent transactivation of the EGFR by interacting with ARAP1. *J. Cell. Mol. Med.* 24 (22), 12994–13009. doi:10.1111/jcmm.15897

Li, J., Liu, H., Takagi, S., Nitta, K., Kitada, M., Srivastava, S. P., et al. (2020). Renal protective effects of empagliflozin via inhibition of EMT and aberrant glycolysis in proximal tubules. *JCI insight* 5 (6), e129034. doi:10.1172/jci.insight.129034

Liu, L., Zhang, L., Zhao, J., Guo, X., Luo, Y., Hu, W., et al. (2020). Tumor necrosis factor receptor-associated protein 1 protects against mitochondrial injury by preventing high glucose-induced mPTP opening in diabetes. *Oxidative Med. Cell. Longev.* 2020, 6431517. doi:10.1155/2020/6431517

Liu, H., Takagaki, Y., Kumagai, A., Kanasaki, K., and Koya, D. (2021). The PKM2 activator TEPP-46 suppresses kidney fibrosis via inhibition of the EMT program and aberrant glycolysis associated with suppression of HIF-1α accumulation. *J. diabetes investigation* 12 (5), 697–709. doi:10.1111/jdi.13478

Lu, X., Fan, Q., Xu, L., Li, L., Yue, Y., Xu, Y., et al. (2015). Ursolic acid attenuates diabetic mesangial cell injury through the up-regulation of autophagy via miRNA-21/PTEN/Akt/mTOR suppression. *PloS one* 10 (2), e0117400. doi:10.1371/journal.pone.0117400

Luo, W., Hu, H., Chang, R., Zhong, J., Knabel, M., O'Meally, R., et al. (2011). Pyruvate kinase M2 is a PHD3-stimulated coactivator for hypoxia-inducible factor 1. *Cell* 145 (5), 732–744. doi:10.1016/j.cell.2011.03.054

Ma, L. J., Marcantoni, C., Linton, M. F., Fazio, S., and Fogo, A. B. (2001). Peroxisome proliferator-activated receptor-gamma agonist troglitazone protects against nondiabetic glomerulosclerosis in rats. *Kidney Int.* 59 (5), 1899–1910. doi:10.1046/j.1523-1755.2001.0590051899.x

Ma, T. K., Xu, L., Lu, L. X., Cao, X., Li, X., Li, L. L., et al. (2019). Ursolic acid treatment alleviates diabetic kidney injury by regulating the ARAP1/at1r signaling pathway. *Diabetes, metabolic syndrome Obes. targets Ther.* 12, 2597–2608. doi:10.2147/DMSO.S222323

Ma, T., Li, X., Zhu, Y., Yu, S., Liu, T., Zhang, X., et al. (2022). Excessive activation of notch signaling in macrophages promote kidney inflammation, fibrosis, and necroptosis. *Front. Immunol.* 13, 835879. doi:10.3389/fimmu.2022.835879

Morita, M., and Kanasaki, K. (2020). Sodium-glucose cotransporter-2 inhibitors for diabetic kidney disease: Targeting Warburg effects in proximal tubular cells. *Diabetes Metab.* 46 (5), 353–361. doi:10.1016/j.diabet.2020.06.005

Overstreet, J. M., Wang, Y., Wang, X., Niu, A., Gewin, L. S., Yao, B., et al. (2017). Selective activation of epidermal growth factor receptor in renal proximal tubule induces tubulointerstitial fibrosis. *FASEB J. official Publ. Fed. Am. Soc. Exp. Biol.* 31 (10), 4407–4421. doi:10.1096/fj.201601359RR

Peng, F., Gong, W., Li, S., Yin, B., Zhao, C., Liu, W., et al. (2021). circRNA_010383 acts as a sponge for miR-135a, and its downregulated expression contributes to renal fibrosis in diabetic nephropathy. *Diabetes* 70 (2), 603–615. doi:10.2337/db20-0203

Pugliese, G., Penno, P., Natali, A., Barutta, F., Di Paolo, S., Reboldi, G., et al. (2020). Diabetic kidney disease: New clinical and therapeutic issues. Joint position statement of the Italian diabetes society and the Italian society of Nephrology on "the natural history of diabetic kidney disease and treatment of hyperglycemia in patients with type 2 diabetes and impaired renal function". *J. Nephrol.* 33, 9–35. doi:10.1007/s40620-019-00650-x

Qi, W., Keenan, H. A., Li, Q., Ishikado, A., Kannt, A., Sadowski, T., et al. (2017). Pyruvate kinase M2 activation may protect against the progression of diabetic glomerular pathology and mitochondrial dysfunction. *Nat. Med. Jun* 23 (6), 753–762. doi:10.1038/nm.4328

Qiao, S., Liu, R., Lv, C., Miao, Y., Yue, M., Tao, Y., et al. (2019). Bergenin impedes the generation of extracellular matrix in glomerular mesangial cells and ameliorates diabetic nephropathy in mice by inhibiting oxidative stress via the mTOR/β-TrcP/Nrf2 pathway. *Free Radic. Biol. Med.* 145, 118–135. doi:10.1016/j.freeradbiomed.2019.09.003

Sizemore, S. T., Zhang, M., Cho, J. H., Sizemore, G. M., Hurwitz, B., Kaur, B., et al. (2018). Pyruvate kinase M2 regulates homologous recombination-mediated DNA double-strand break repair. *Cell Res. Nov.* 28 (11), 1090–1102. doi:10.1038/s41422-018-0086-7

Srivastava, S. P., Koya, D., and Kanasaki, K. (2013). MicroRNAs in kidney fibrosis and diabetic nephropathy: Roles on EMT and EndMT. *Biomed. Res. Int.* 2013, 125469. doi:10.1155/2013/125469

Srivastava, S. P., Shi, S., Koya, D., and Kanasaki, K. (2014). Lipid mediators in diabetic nephropathy. *Fibrogenes. Tissue Repair* 7, 12. doi:10.1186/1755-1536-7-12

Srivastava, S. P., Shi, S., Kanasaki, M., Nagai, T., Kitada, M., He, J., et al. (2016). Effect of antifibrotic microRNAs crosstalk on the action of N-acetyl-seryl-aspartyl-lysyl-proline in diabetes-related kidney fibrosis. *Sci. Rep.* 6, 29884. doi:10.1038/srep29884

Srivastava, S. P., Li, J., Kitada, M., Fujita, H., Yamada, Y., Goodwin, J. E., et al. (2018). SIRT3 deficiency leads to induction of abnormal glycolysis in diabetic kidney with fibrosis. *Cell. death. Dis.* 9, 997. doi:10.1038/s41419-018-1057-0

Srivastava, S. P., Goodwin, J. E., Kanasaki, K., and Koya, D. (2020). Inhibition of angiotensin-converting enzyme ameliorates renal fibrosis by mitigating DPP-4 level and restoring antifibrotic MicroRNAs. *Genes (Basel)* 11 (2), 211. doi:10.3390/genes11020211

Srivastava, S. P., Hedayat, A. F., Kanasaki, K., and Goodwin, J. E. (2020). Erratum: microRNA crosstalk influences epithelial-to-mesenchymal, endothelial-to-mesenchymal, and macrophage-to-mesenchymal transitions in the kidney. *Front. Pharmacol.* 11, 11. doi:10.3389/fphar.2020.00011

Srivastava, S. P., Zhou, H., Setia, O., Liu, B., Kanasaki, K., Koya, D., et al. (2021). Loss of endothelial glucocorticoid receptor accelerates diabetic nephropathy. *Nat. Commun.* 12 (1), 2368. doi:10.1038/s41467-021-22617-y

Srivastava, S. P., Zhou, H., Setia, O., Dardik, A., Fernandez-Hernando, C., and Goodwin, J. (2021). Podocyte glucocorticoid receptors are essential for glomerular endothelial cell homeostasis in diabetes mellitus. *J. Am. Heart Assoc.* 10 (15), e019437. doi:10.1161/JAHA.120.019437

Srivastava, S. P., Goodwin, J. E., Tripathi, P., Kanasaki, K., and Koya, D. (2021). Interactions among long non-coding RNAs and microRNAs influence disease phenotype in diabetes and diabetic kidney disease. *Int. J. Mol. Sci.* 22 (11), 6027. doi:10.3390/ijms22116027

Taniguchi, K., Xia, L., Goldberg, H. J., Lee, K. W., Shah, A., Stavar, L., et al. (2013). Inhibition of Src kinase blocks high glucose-induced EGFR transactivation and collagen synthesis in mesangial cells and prevents diabetic nephropathy in mice. *Diabetes* 62 (11), 3874–3886. doi:10.2337/db12-1010

Uchiyama-Tanaka, Y., Matsubara, H., Mori, Y., Kosaki, A., Kishimoto, N., Amano, K., et al. (2002). Involvement of HB-EGF and EGF receptor transactivation in TGF-beta-mediated fibronectin expression in mesangial cells. *Kidney Int.* 62 (3), 799–808. doi:10.1046/j.1523-1755.2002.00537.x

Uttarwar, L., Peng, F., Wu, D., Kumar, S., Gao, B., Ingram, A. J., et al. (2011). HB-EGF release mediates glucose-induced activation of the epidermal growth factor receptor in mesangial cells. *Am. J. physiology Ren. physiology* 300 (4), F921–F931. doi:10.1152/ajprenal.00436.2010

Wang, E. M., Fan, Q. L., Yue, Y., and Xu, L. (2018). Ursolic acid attenuates high glucose-mediated mesangial cell injury by inhibiting the phosphatidylinositol 3-kinase/akt/mammalian target of rapamycin (PI3K/Akt/mTOR) signaling pathway. *Med. Sci. Monit. Int. Med. J. Exp. Clin. Res.* 24, 846–854. doi:10.12659/msm.907814

Wang, S., Wen, X., Han, X. R., Wang, Y. J., Shen, M., Fan, S. H., et al. (2018). Repression of microRNA-382 inhibits glomerular mesangial cell proliferation and extracellular matrix accumulation via FoxO1 in mice with diabetic nephropathy. *Cell Prolif.* 51 (5), e12462. doi:10.1111/cpr.12462

Wang, G., Li, Y., Yang, Z., Xu, W., Yang, Y., and Tan, X. (2018). ROS mediated EGFR/MEK/ERK/HIF-1α Loop Regulates Glucose metabolism in pancreatic cancer. *Biochem. biophysical Res. Commun.* 500 (4), 873–878. doi:10.1016/j.bbrc.2018.04.177

Wang, L., Lu, Y. F., Wang, C. S., Xie, Y. X., Zhao, Y. Q., Qian, Y. C., et al. (2020). HB-EGF activates the EGFR/HIF-1α pathway to induce proliferation of arsenic-transformed cells and tumor growth. *Front. Oncol.* 10, 1019. doi:10.3389/fonc.2020.01019

Wang, J., Xiang, H., Lu, Y., Wu, T., and Ji, G. (2021). New progress in drugs treatment of diabetic kidney disease. *Biomed. Pharmacother. Sep.* 141, 111918. doi:10.1016/j.biopha.2021.111918

Wang, C. H., Lo, C. Y., Huang, H. Y., Wang, T. Y., Weng, C. M., Chen, C. J., et al. (2022). Oxygen desaturation is associated with fibrocyte activation via epidermal growth factor receptor/hypoxia-inducible factor-1α Axis in chronic obstructive pulmonary disease. *Front. Immunol.* 13, 852713. doi:10.3389/fimmu.2022.852713

Wei, X., Hou, Y., Long, M., Jiang, L., and Du, Y. (2022). Molecular mechanisms underlying the role of hypoxia-inducible factor-1 α in metabolic reprogramming in renal fibrosis. *Front. Endocrinol.* 13, 927329. doi:10.3389/fendo.2022.927329

Wu, D., Peng, F., Zhang, B., Ingram, A. J., Kelly, D. J., Gilbert, R. E., et al. (2009). PKC-beta1 mediates glucose-induced Akt activation and TGF-beta1 upregulation in mesangial cells. *J. Am. Soc. Nephrol.* 20 (3), 554–566. doi:10.1681/ASN.2008040445

Wu, D., Peng, F., Zhang, B., Ingram, A. J., Kelly, D. J., Gilbert, R. E., et al. (2009). EGFR-PLC gamma1 signaling mediates high glucose-induced PKC beta1-Akt activation and collagen I upregulation in mesangial cells. *Am. J. physiology Ren. physiology* 297 (3), F822–F834. doi:10.1152/ajprenal.00054.2009

Wu, H., Guo, X., Jiao, Y., Wu, Z., and Lv, Q. (2022). TRIM35 ubiquitination regulates the expression of PKM2 tetramer and dimer and affects the malignant behaviour of breast cancer by regulating the Warburg effect. *Int. J. Oncol. Dec* 61 (6), 144. doi:10.3892/ijo.2022.5434

Yang, W., Xia, Y., Ji, H., Zheng, Y., Liang, J., Huang, W., et al. (2011). Nuclear PKM2 regulates β-catenin transactivation upon EGFR activation. *Nature* 480 (7375), 118–122. doi:10.1038/nature10598

Yang, W., Xia, Y., Cao, Y., Zheng, Y., Bu, W., Zhang, L., et al. (2018). EGFR-induced and PKCε monoubiquitylation-dependent NF-κB activation upregulates PKM2 expression and promotes tumorigenesis. *Mol. Cell* 69 (2), 347. doi:10.1016/j.molcel.2017.12.034

Yang, Y., Lv, X., Fan, Q., Wang, X., Xu, L., Lu, X., et al. (2019). Analysis of circulating lncRNA expression profiles in patients with diabetes mellitus and diabetic nephropathy: Differential expression profile of circulating lncRNA. *Clin. Nephrol.* 92 (1), 25–35. doi:10.5414/CN109525

Yang, T., Shu, F., Yang, H., Heng, C., Zhou, Y., Chen, Y., et al. (2019). YY1: A novel therapeutic target for diabetic nephropathy orchestrated renal fibrosis. *Metabolism Clin. Exp.* 96, 33–45. doi:10.1016/j.metabol.2019.04.013

Yang, T., Hu, Y., Chen, S., Li, L., Cao, X., Yuan, J., et al. (2022). YY1 inactivated transcription co-regulator PGC-1α to promote mitochondrial dysfunction of early diabetic nephropathy-associated tubulointerstitial fibrosis. *Cell Biol. Toxicol.* doi:10.1007/s10565-022-09711-7

Yu, H., Li, Q., Kolosov, V. P., Perelman, J. M., and Zhou, X. (2012). Regulation of cigarette smoke-mediated mucin expression by hypoxia-inducible factor-1α via epidermal growth factor receptor-mediated signaling pathways. *J. Appl. Toxicol.* 32, 282–292. doi:10.1002/jat.1679

Zhang, Z., Deng, X., Liu, Y., Liu, Y., Sun, L., and Chen, F. (2019). PKM2, function and expression and regulation. *Cell Biosci.* 9 (9), 52. doi:10.1186/s13578-019-0317-8

Zhang, C., Zhu, X., Li, L., Ma, T., Shi, M., Yang, Y., et al. (2019). A small molecule inhibitor MCC950 ameliorates kidney injury in diabetic nephropathy by inhibiting NLRP3 inflammasome activation. *Diabetes, metabolic syndrome Obes. targets Ther.* 12, 1297–1309. doi:10.2147/DMSO.S199802

Zhang, H., Yan, Y., Hu, Q., and Zhang, X. (2021). LncRNA MALAT1/microRNA let-7f/KLF5 axis regulates podocyte injury in diabetic nephropathy. *Life Sci.* 266, 118794. doi:10.1016/j.lfs.2020.118794

Zhao, X., Chen, Y., Tan, X., Zhang, L., Zhang, H., Li, Z., et al. (2018). Advanced glycation end-products suppress autophagic flux in podocytes by activating mammalian target of rapamycin and inhibiting nuclear translocation of transcription factor EB. *J. pathology* 245 (2), 235–248. doi:10.1002/path.5077

frontiers | Frontiers in Pharmacology

TYPE Original Research
PUBLISHED 27 February 2023
DOI 10.3389/fphar.2023.1047184

OPEN ACCESS

EDITED BY
Swayam Prakash Srivastava,
Yale University, United States

REVIEWED BY
Shouzhu Xu,
Shaanxi University of Chinese Medicine, China
Marta Riera,
Hospital del Mar Medical Research Institute (IMIM), Spain

*CORRESPONDENCE
Xin Zhang,
walterzhangx@139.com

SPECIALTY SECTION
This article was submitted to Renal Pharmacology, a section of the journal Frontiers in Pharmacology

RECEIVED 17 September 2022
ACCEPTED 16 February 2023
PUBLISHED 27 February 2023

CITATION
Fang YP, Zhang YF, Jia CX, Ren CH, Zhao XT and Zhang X (2023), Niaoduqing alleviates podocyte injury in high glucose model *via* regulating multiple targets and AGE/RAGE pathway: Network pharmacology and experimental validation.
Front. Pharmacol. 14:1047184.
doi: 10.3389/fphar.2023.1047184

Niaoduqing alleviates podocyte injury in high glucose model *via* regulating multiple targets and AGE/RAGE pathway: Network pharmacology and experimental validation

Yipeng Fang[1,2,3], Yunfei Zhang[4], Chenxi Jia[3], Chunhong Ren[5], Xutao Zhao[6] and Xin Zhang[1,2,3]*

[1]Laboratory of Molecular Cardiology, The First Affiliated Hospital of Shantou University Medical College, Shantou, Guangdong, China, [2]Laboratory of Medical Molecular Imaging, The First Affiliated Hospital of Shantou University Medical College, Shantou, Guangdong, China, [3]Shantou University Medical College, Shantou, Guangdong, China, [4]Tianjin Hospital of Tianjin University, Tianjin, China, [5]International Medical Service Center, The First Affiliated Hospital of Shantou University Medical College, Shantou, Guangdong, China, [6]Jinan Municipal Hospital of Traditional Chinese Medicine, Jinan, Shandong, China

Purpose: The aim of present study was to explore the pharmacological mechanisms of Niaoduqing granules on the treatment of podocyte injury in diabetic nephropathy (DN) *via* network pharmacology and experimental validation.

Methods: Active ingredients and related targets of Niaoduqing, as well as related genes of podocyte injury, proteinuria and DN, were obtained from public databases. Gene ontology (GO), Kyoto Encyclopedia of Genes and Genomes (KEGG) and protein-protein interaction (PPI) network analysis were performed to investigate the potential mechanisms. High glucose (HG) -induced MPC5 cell injury model was treated with the major core active ingredients of Niaoduqing and used to validate the predicted targets and signaling pathways.

Results: Totally, 16 potential therapeutic targets were identified by intersecting the targets of Niaoduqing and disease, in which 7 of them were considered as the core targets *via* PPI network analysis. KEGG enrichment analysis showed that AGE-RAGE signaling pathway was identified as the most crucial signaling pathway. The results of *in vitro* experiments revealed that the treatment of Niaoduqing active ingredients significantly protected MPC5 cells from HG-induced apoptosis. Moreover, Niaoduqing could significantly attenuate the HG-induced activation of AGE-RAGE signaling pathway, whereas inhibited the over-expression of VEGF-A, ICAM-1, PTGS-2 and ACE in HG-induced MPC5 cells.

Conclusion: Niaoduqing might protect against podocyte injury in DN through regulating the activity of AGE/RAGE pathway and expression of multiple genes. Further clinical and animal experimental studies are necessary to confirm present findings.

KEYWORDS

Niaoduqing particles, uremic clearance granule, diabetic nephropathy, podocyte injury, proteinuria, network pharmacology, AGE/RAGE signaling

1 Introduction

Diabetic nephropathy (DN) is one of the most common complications of diabetes mellitus, which involves the entire kidneys (Anders et al., 2018). In China, the prevalence of total diabetes in adults was 11.2% (Li et al., 2020a). DN develops in approximately 20%–40% of patients with diabetes and consequently has become the leading cause of chronic kidney disease (CKD) and end-stage renal disease (ESRD) (Zhang et al., 2016; American Diabetes Association, 2020). Over the years, lifestyle change, risk factor control, proteinuria inhibition and interstitial fibrosis prevention are the primary modes of treatment for DN. However, current management approaches cannot stop the progression of renal failure (Yang et al., 2019a).

The pathogenesis of DN is complex and multifactorial, among which podocyte injury plays the key role. In diabetes, declining insulin sensitivity, oxidative stress and inflammatory reaction cause permanent functional and/or structural change of podocytes, that is regarded as one of the major causes of proteinuria. Podocyte damage, including dysfunction, shedding and apoptosis, is considered as the early pathological change underlying various glomerular diseases, including DN (Cao et al., 2014; Ni et al., 2018; Podgórski et al., 2019). Proteinuria is one of the early clinical manifestations of diabetic kidney disease, and persistent proteinuria accelerates the progression of renal disease (Brinkkoetter et al., 2019; Yang et al., 2019b). Thus, podocyte might be a potential therapeutic target for DN (Ni et al., 2018), and controlling proteinuria represents an effective method delaying the progression of diabetic kidney damage. Angiotensin converting enzyme inhibitors (ACEI) and angiotensin receptor blocker (ARB) are widely used in patients with proteinuria, in order to reduce albuminuria and decrease the risk of cardiovascular diseases through inhibiting the activity of renin-angiotensin system (RAS); however, whether ACEI or ARB can prevent the progression towards ESRD are still uncertain (Marre et al., 2004). According to the theory of traditional Chinese medicine (TCM), Chinese compound medicines treat diverse diseases through "multi-component, multi-targets and multi-pathways" method (Zhang et al., 2020). The complex mechanisms of DN suggest that a combination of medicines may play better therapeutic activities in DN. Niaoduqing granules, consisted of 9 herbal medicines, are commonly used in ESRD. As Li et al. (2022a) reported, Niaoduqing granules can effectively improve renal function, inhibit renal fibrosis and decrease the level of inflammatory responses through regulating MAPK/NF-κB signaling pathway in the ESRD model induced by 5/6 nephrectomy. TGF-β is considered as one of the crucial targets for the anti-fibrosis of Niaoduqing (Miao et al., 2010; Lu et al., 2013; Huang et al., 2014; Wu et al., 2016). As Huang YR et al. reported, Niaoduqing granules ameliorate tubule-interstitial fibrosis and renal dysfunction in the renal failure model induced by adenine and unilateral ureteral obstruction though promoting extracellular matrix degradation and maintaining MMP-2/TIMP-1 balance or regulating TGF-beta1/Smad signaling pathway in kidney tissue (Huang et al., 2014). In addition, Niaoduqing can also treat tubule-interstitial fibrosis *via* inhibiting tubular epithelial-to-mesenchymal transition (EMT) and regulating TGF-beta1/Smad pathway (Lu et al., 2013). The interaction between Niaoduqing and TGF-β1 may be related to the methylation/demethylation regulation of TGF-β1 promoter (Miao et al., 2010). What's more, Niaoduqing granules can ameliorate CKD-related anemia though erythropoietin (EPO) receptor signaling pathway (Wang et al., 2017). Except for ameliorating renal function and fibrosis, Niaoduqing also has good effects on managing uremic pruritus (Lu et al., 2021). Niaoduqing also regulate the amino acid, lipid and energy metabolisms in the chronic renal failure rat model (Zhu et al., 2018). The therapeutic effects of Niaoduqing on DN have been evaluated in some Chinese articles. As Wu et al. (2009) found in an intervention research including 76 DN patients without dialysis or kidney transplant, Niaoduqing exposure can effectively improve the clinical symptoms (92.10% vs. 65.78%, $p < 0.05$), and reduce the level of blood urea nitrogen (BUN, 15.9 ± 1.75 mmol/L vs. 16.9 ± 1.34 mmol/L, $p < 0.05$), blood creatinine (Scr, 383.2 ± 74.58 μmol/L vs. 425.74 ± 86.32 μmol/L, $p < 0.05$) and urine protein (0.81 ± 0.67 g/24 h vs. 1.38 ± 0.45 g/24 h, $p < 0.05$). Compared with using ACEI/ARB alone, the better renal function is observed in patients received combination therapy with Niaoduqing (Li et al., 2016; Wei and Ruan, 2018). What's more, a recent network meta-analysis reported that Niaoduqing has a better effect on controlling proteinuria in patients with early stage DN, compared with other six kinds of TCM (Zhao et al., 2022). Although some studies have proved the positive role of Niaoduqing in the treatment of diabetes nephropathy and proteinuria, the underline mechanisms of Niaoduqing for early stage DN are still unclear and need to be further explored.

Network pharmacology is an analytic tool for systematic pharmacology based on the "network target, multi-component" strategy, which has been widely applied to analyze the active ingredients and core potential therapeutic targets of drugs to disease, especially in Chinese compound medicines (Hopkins, 2007; Kibble et al., 2015). In the present study, we explored the core ingredients and potential mechanisms of Niaoduqing granules on the treatment of podocyte damage and proteinuria in DN through network pharmacology followed by experimental validation, so as to search for novel and effective therapeutic strategies for podocyte protection and proteinuria reduction in DN. The flow chart of our study was shown in Figure 1.

2 Materials and methods

2.1 Screen the active ingredients and targets of Niaoduqing granules

Niaoduqing granules consist of nine components, including Bai Shao, Bai Shu, Che Qian Cao, Da Huang, Dan Shen, Fu Ling, Huang Qi, Ku Shen and Sang Bai Ye. The active ingredients of the above night components were screened through the Traditional Chinese Medicine Systems Pharmacology Database and Analysis Platform (TCMSP, https://tcmsp-e.com/tcmsp.php) according to the condition of oral bioavailability (OB) ≥ 30% and drug-like properties (DL) ≥ 0.18 (Ru et al., 2014). Related targets of the active ingredients, defined as Niaoduqing-related targets, were selected through

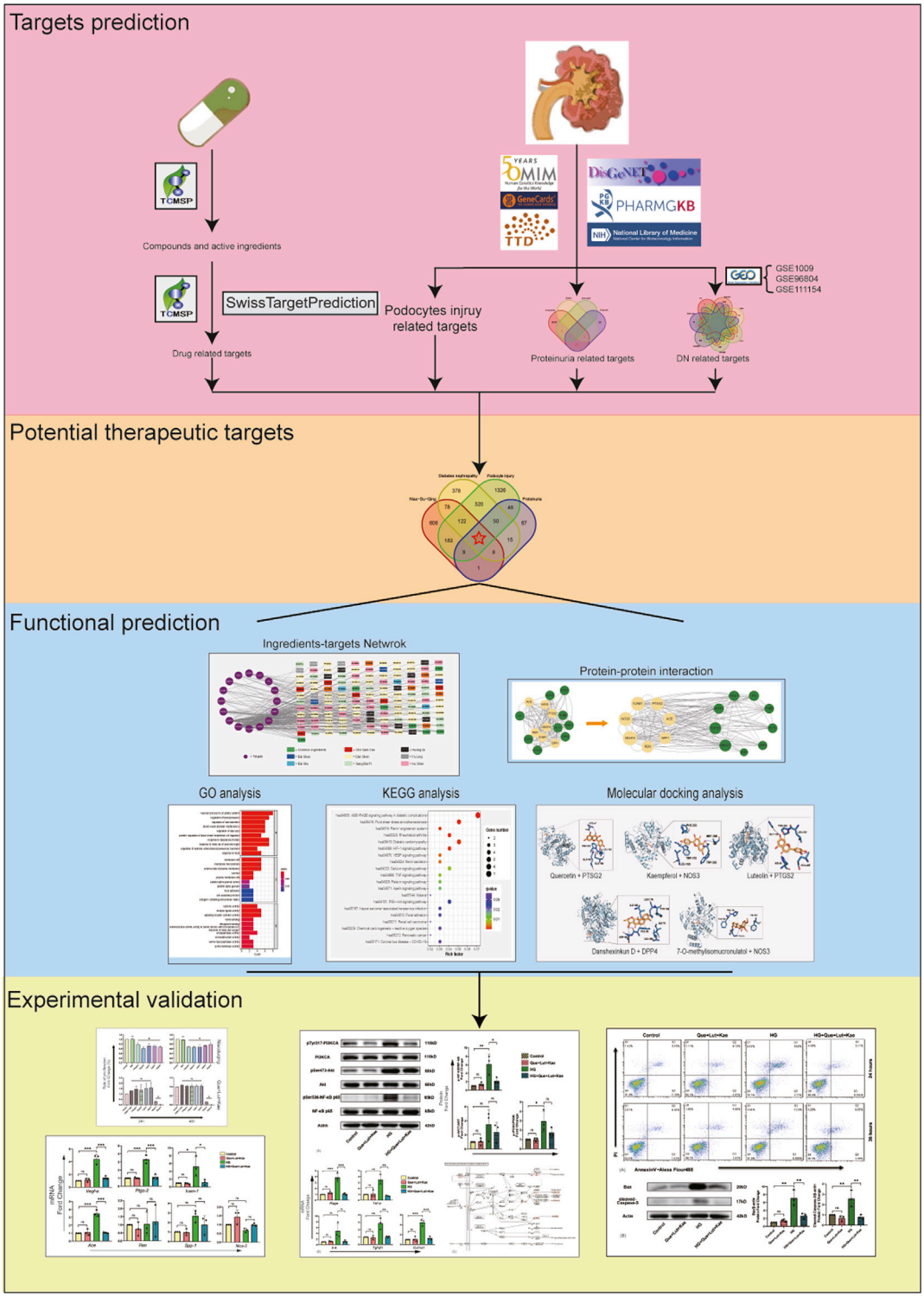

FIGURE 1
Flow chart of present study.

TCMSP database and Swiss Target Prediction website (http://www.swisstargetprediction.ch/) (Ru et al., 2014; Daina et al., 2019). In Swiss Target Prediction website, only the top 100 predicted targets with probability greater than 0 were included. SMILE strings, which should be used in the Swiss Target Prediction website, were obtained through Pubchem website (https://pubchem.ncbi.nlm.nih.gov/). The conversions from protein names to the unique entry gene IDs were

performed through the uniprot database (https://www.uniprot.org/).

2.2 Screen differentially expressed genes related to DN from GEO database

DN related databases (GSE1009, GSE96804 and GSE111154) were obtained from Gene Expression Omnibus (GEO) database. After removing duplicate and missing data, we screened the differentially expressed genes (DEGs) according to the following criteria: $|\log FC| \geq 1$ and p-value < 0.05. Volcano plots and heat maps were used to represent the DEGs.

2.3 Collect related targets and potential therapeutic targets

Disease targets of DN, proteinuria and podocyte injury were attained by searching GeneCards database (https://www.genecards.org/) (Stelzer et al., 2016), the Online Mendelian Inheritance in Man database (OMIM, https://omim.org/) (Amberger and Hamosh, 2017), Therapeutic target database (TTD, http://db.idrblab.net/ttd/) (Li et al., 2018), DisGeNET database (https://www.disgenet.org/home/) (Piñero et al., 2015), NCBI (https://www.ncbi.nlm.nih.gov/) and PharmgKB database (https://www.pharmgkb.org/) (Whirl-Carrillo et al., 2021) with "diabetes nephropathy," "proteinuria" and "podocyte injury" as keywords and "*Homo sapiens*" as the organism.

All disease targets obtained from the above databases and the DEGs of DN obtained from GSE1009, GSE96804 and GSE111154 datasets were pooled together, and those targets appearing in at least two databases and datasets were defined as DN-related targets in present study. Similar protocol was applied to screen the proteinuria-related genes: only the overlapping targets appearing in at least two databases were identified as proteinuria-related genes.

Niaoduqing-related targets were intersected with the DN-related targets, the proteinuria-related targets and the podocyte injury-related targets to identify the potential therapeutic targets of Niaoduqing on the treatment of podocyte injury and proteinuria in DN. "venn" and "VennDiagram" packages from R language were used to create the Venn diagram to depict the intersections between different databases and datasets. Cytoscape 3.6.1 software was used to construct the relationship network among night components, active ingredients and the potential therapeutic targets.

2.4 The analysis of PPI network, GO and KEGG

The protein-protein interactions (PPI) results among potential therapeutic targets were obtained from the SRTING database (https://cn.string-db.org/, Version: 11.5), with the minimum required interaction score set at "median confidence (0.400)" level. Cytoscape 3.6.1 and its CytoNCA plugin were used to further analyze the original PPI network. Three topological parameters, including betweenness centrality, closeness centrality and degree value, were calculated and considered as the evidence for the screen of core targets. The higher the values were, the more important the targets were (Azuaje et al., 2011). Nodes with all three parameters higher than the median were used to build the sub-network and considered as the core targets.

Gene Ontology (GO) and Kyoto Encyclopedia of Genes and Genomes (KEGG) pathway enrichment analysis were performed using "Cluster profiler" package from R language to investigate the probable molecular mechanisms of Niaoduqing on the treatment of podocyte injury and proteinuria in DN. The top 10 enriched enters of molecular function (MF), biological process (BP) and cellular components (CC) in GO analysis were presented in bar chart. The top 20 enriched pathways were shown in bubble chart.

2.5 Molecular docking

The core ingredients and core targets were used in the molecular docking analysis. Firstly, the three-dimensional structure of core active ingredients was obtained from Pubchem website and translated into PDB format files using PyMOL software. Secondly, the 3D structure of the core target was obtained through the protein docking bank database (PDB, https://www.rcsb.org/). The water molecules, metal ions and small molecule ligands were removed, and the active pockets were identified by PyMOL software. Thirdly, AutoDock Vina 1.1.2 (Trott and Olson, 2010) was used to convert the ingredients and targets into PDBQT format files and perform molecular docking simulation. This binding energy estimated the stability of the target and the ingredient complexes. The first representative binding pose, with the lowest binding energy in our docking result, was visualized by PyMOL software.

2.6 Experimental validation *in vitro*

2.6.1 Drugs and reagents

Niaoduqing Granules were obtained from KangCheng Pharmaceutical Industry, China (No. Z20073256). The lyophilized powder of quercetin (Que, Q4951) was acquired from Sigma (St. Louis, United States). The lyophilized powders of kaempferol (Kae, S2314) and luteolin (Lut, S2320) were obtained from Selleck (Shanghai, China). Anti-PI3K antibody (110kD, AF5112) was purchased from Affinity Biosciences (Ohio, United States). Anti-phospho-PI3KCA antibody (p-PI3K^{Tyr317}, 110kD, bs-5570R) was obtained from Bioss Biotech (Beijing, China). Anti-AKT antibody (60 kD, 4691S), anti-phospho-AKT antibody (p-AKT^{Ser473}, 60kD, 4060S), anti-caspase-3 antibody (17kD, 9662) and anti-Bax antibody (20kD, 2772S) was acquired from Cell Signaling Technology (CST, Danvers, MA, United States). Anti-NF-κB antibody (65kD, A2547) and anti-phosphor-NF-κB p65/RelA antibody (p-NF-κB^{Ser536}, 65kD, AP0124) was purchased from ABclonal Biotech (Wuhan, China). Goat anti-mouse IgG second antibody (C1308), goat anti-rabbit IgG second antibody (C1309) and anti-actin antibody (42kD, C1313) was acquired from Pulilai Biotech (Beijing, China). Annexin V—Alexa Flour 488/PI Apoptosis Kit (FXP022) was purchased from 4A Biotech (Suzhou, China). CCK-8 (CK04) was obtained from Dojindo Laboratorise (Shanghai, China). Fetal bovine serum (FBS) was purchased from Zeta Life (California, United States).

TABLE 1 Primer sequences of RT-PCR.

Gene name	Forward primer sequences (5′-3′)	Reverse primer sequences (5′-3′)
Ace	CCAACAAGATTGCCAAGCTCA	AGTGGCTGCAGCTCCTGGTA
β-*actin*	ACCAACTGGGACGACATGGAGAAG	TACGACCAGAGGCATACAGGGACA
Col1a1	TGGCCTTGGAGGAAACTTTG	CTTGGAAACCTTGTGGACCAG
Icam-1	GCCTTGGTAGAGGTGACTGAG	GACCGGAGCTGAAAAGTTGTA
Il-6	TTATATCCAGTTTGGTAGCATCCAT	AGGCTTAATTACACATGTTCTCTGG
Nos-3	ATTTCCTGTCCCCTGCCTTCCGC	GGTTGCCTTCACACGCTTCGCC
Ptgs-2	TTCAACACACTCTATCACTGGC	AGAAGCGTTTGCGGTACTCAT
Rage	CAGGGTCACAGAAACCGG	ATTCAGCTCTGCACGTTCCT
Ren	GAGGCCTTCCTTGACCAATC	TGTGAATCCCACAAGCAAGG
Spp-1	TGGGCTCTTAGCTTAGTCTGTTG	CAGAAGCAAAGTGCAGAAGC
Tgfβ1	CCACCTGCAAGACCATCGAC	CTGGCGAGCCTTAGTTTGGAC
Tnf-α	CCCTCACACTCAGATCATCTTCT	GCTACGACGTGGGCTACAG
Vegf-α	CTTTTCGTCCAACTTCTGGGCTCTT	CCTTCTCTTCCTCCCCTCTCTTCTC
Wt-1	TACAGATGCATAGCCGGAAGCACA	TCACACCTGTGTGTCTCCTTTGGT

2.6.2 Cell culture

The conditionally immortalized mouse podocyte cell line Mouse Podocyte Clone 5 (MPC5) cells were purchased from Jennio Biotech (Guangzhou, China). MPC5 cells were maintained in RPMI 1640 medium supplemented with 15% FBS, 2 mM L-Glutamin, 100 IU/mL penicillin-streptomycin, and 5 U/mL recombinant mouse interferon-γ (IFN-γ, Yeasen Biotech, Shanghai, China, 91212ES60) at 33°C in a humidified atmosphere with 5% CO_2. To induce differentiation, MPC5 cells were shifted from 33°C to 37°C and cultured without IFN-γ for 14 days. To establish high glucose (HG) model, extra glucose (Sigma, St. Louis, United States, G7021) was added to growth medium and differentiated MPC5 cells were cultured under high glucose condition (44 mM). Since the solution of Niaoduqing granules showed toxic effect on the survival and proliferation of MPC5 cells, the mixture of three major active ingredients of Niaoduqing (Que + Lut + Kae) were used as an alternative for the *in vitro* experiments. MPC5 cells were randomly divided into four groups: the control group, Que + Lut + Kae (1 μg/mL) group, HG group and HG + Que + Lut + Kae group.

2.6.3 CCK-8 assay for cell viability

MPC5 cells were re-plated in 96-well plates (5,000 cells per well) and cultured at 37°C overnight. Then, growth medium was removed and 100 μL of culture medium with different concentrations of Niaoduqing granules (0.0625, 0.25, 1, 4, 16 μg/mL) and Que + Lut + Kae mixture (0.0625, 0.25, 1, 4, 16, 64 μg/mL) was added. Twenty four and 48 h after treatment, 100 μL of basic medium and 10 μL CCK-8 solution were added to each well and incubated for another 2 h. The optical density (OD) value was measured at 490 nm. The cell viability was calculated using the following formula: Cell viability% = $[(OD_{\text{value of experimental group}}) - (OD_{\text{value of cell-free group}})]/[(OD_{\text{value of control group}})-(OD_{\text{value of cell-free group}})] \times 100\%$.

2.6.4 Real time quantitative PCR (RT-qPCR) analysis

Total RNA was extracted from each group of MPC5 cells 48 h after treatment using Trizol method (Accurate Biotechnology, Changsha, China). The cDNA was synthesized using Evo M-MLV RT kit (Accurate Biotechnology, AG11734). The mRNA was quantified using the 2× SYBR Green Pro Taq HS Premix II (Accurate Biotechnology, AG11736), with *β-actin* gene as the internal control. The differences of the gene expression were analyzed using the delta-delta Ct method ($2^{-\triangle\triangle CT}$). The primer sequences for RT-qPCR are shown in Table 1.

2.6.5 Western blot

Protein was extracted from different groups of MPC5 cells using RIPA lysis buffer (Beyotime Biotech, Beijing, China, P0013K) containing 1:100 protease inhibitors and 1:100 phosphatase inhibitors. The protein was quantified using bicinchoninic acid kit (BCA, Beyotime Biotech, Beijing, China, P0012) according to the manufacturer's instruction. After adding 5 × protein loading buffer, all samples were denatured by boiling at 100°C for 10 min and separated by Sodium dodecyl sulfate-polyacrylamide gel electrophoresis (SDS-PAGE). The electrophoresis was performed at a constant voltage of 60 V for 60 min initially and then switched to 120 V. The gel was further blotted to PVDF membrane for 120 min at a constant current of 200 mA. After blocking with 5% skimmed milk, membranes were incubated with primary antibody at a concentration of 1:1000 at 4°C overnight and further incubated with secondary antibody at a concentration of 1:5000 for 1 h at room temperature. The protein blots were visualized using enhanced chemiluminescence reagent (NCM Biotech, Suzhou, China, P10100). Quantitative analysis was completed using ImageJ.

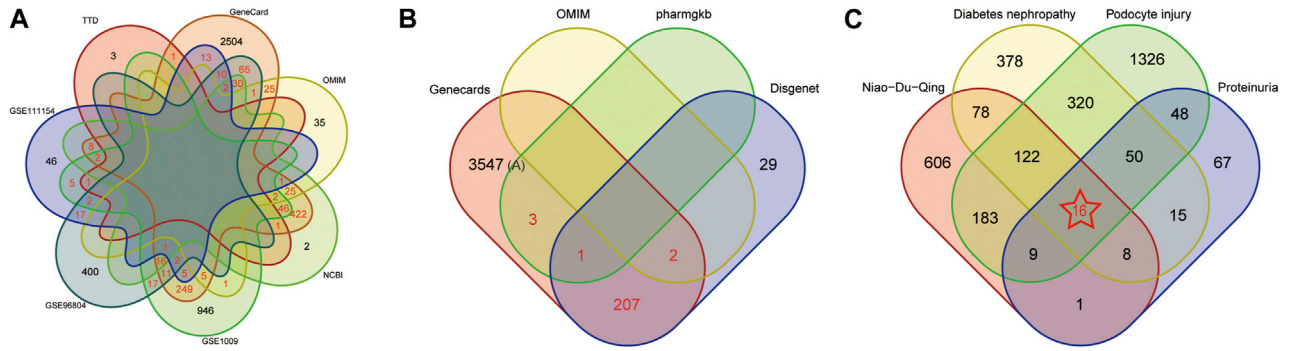

FIGURE 2
Screening Potential Therapeutic Targets of Niaoduqing on the treatment of podocyte injury and proteinuria in DN. **(A)** The Venn diagram of disease targets in 4 databases and 3 GEO datasets. Overlapping targets in at least two databases and dataset were considered as DN-related targets (marked in red color). **(B)** The Venn diagram of disease targets in 4 databases. Overlapping targets in at least two databases and dataset were considered as proteinuria-related targets (marked in red color). **(C)** The Venn diagram of potential therapeutic targets of Niaoduqing on the treatment of podocyte injury and proteinuria in DN. 16 overlapping targets was identified as the potential therapeutic targets (marked in red color with star).

2.6.6 Flow cytometric analysis

Apoptosis was determined using an Annexin V/Alexa Fluor 488/propidium iodide Apoptosis Detection Kit (FXP022-100, 4A Biotech Co., Ltd.) according to the manufacturers' instructions. Briefly, MPCs cells were washed twice with cold phosphate-buffered saline (PBS) and then re-suspended in 100 μL of 1 × binding buffer. The cell suspension was incubated with AnnexinV-Alexa Flour 488 (5 μL) for 5 min in dark at room temperature, then 10 μL of PI solution and 400 μL of PBS was added. Samples were measured on Accuri C6 flow cytometer (BD Biosciences) and data were analyzed by FlowJo 8.0 software (Tree Star, Ashland, OR).

2.7 Statistical analysis

Data shown in present study repeated at least three times. All data were showed as mean and standard deviation of the mean (SD) and analyzed by SPSS23.0 (SPSS, Armonk, New York, United States). Student's *t*-test and Bonferroni test in ANOVA were used to make comparisons between two and multiple groups. $p < 0.05$ was considered as a significant difference ($^{*}p < 0.05$, $^{**}p < 0.01$, $^{***}p < 0.001$, NS = non-statistically significant). GraphPad Prism 8 (GraphPad Software, United States) was used to visualize the results.

3 Results

3.1 Collection of active ingredients and predicted targets

A total of 206 active ingredients were identified, including 32 from Sang Bai Ye, 13 from Bai Shao, 8 from Bai Shu, 10 from Che Qian Cao, 16 from Da Huang, 67 from Dan Shen, 16 from Fu Ling, 20 from Huang Qi and 45 from Ku Shen (Supplementary Table S1). There were 11 common ingredients discovered in at least two herb compounds, in which 6 ingredients (hederagenin, sitosterol, formononetin, baicalin, gallic acid-3-O-(6′-O-galloyl)-glucoside, (24S)-24-Propylcholesta-5-Ene-3beta-Ol) were common to two herbs and 5 ingredients (quercetin, luteolin, kaempferol, beta-sitosterol, mairin) were common to three herbs (Supplementary Table S1). Among the active ingredients, 142 got predicted targets from TCMSP database and 133 obtained targets information from Swiss Targets Prediction website. 28 active ingredients had no target information (Supplementary Table S2). Finally, after eliminating the duplicates, we identified 1,022 predicted targets of Niaoduqing (Supplementary Table S3), and the relationship between active ingredients and predicted targets was shown in Supplementary Table S4.

3.2 Potential therapeutic targets of Niaoduqing on the treatment of podocyte injury and proteinuria in DN

1325, 574 and 115 DEGs were detected in the GSE1009 (Baelde et al., 2004), GSE96804 (Pan et al., 2018) and GSE111154 (Sircar et al., 2018), and the DEGs were further presented by volcano map and heat map, shown in Supplementary Figures S1–S3. The green and red nodes indicated downregulated and upregulated DEGs in the volcano map. In the heat map, red color nodes represented the high expression, while blue color nodes represented the down expression. We further obtained 3448, 95, 559 and 6 targets in "GeneCards," "OMIM," "NCBI" and "TTD" database using "diabetes nephropathy" as the keyword and "*homo sapiens*" as organism. After taking the intersection of targets appearing in at least two databases and datasets using Venn diagram, 986 overlapping targets was identified as DN-related targets (shown in Figure 2A). 3760, 239, 4 and 2 targets associated with proteinuria were found in "GeneCards," "DisGeNET," "OMIM" and "PharmgKB". 213 overlapping targets, which appeared in at least two databases, were considered as proteinuria related-targets shown in Figure 2B. 2072 and 3 targets were found using "podocyte injury" as the keyword and "*homo sapiens*" as organism in "GeneCards" and "OMIM" database. After removing 1 duplicating gene, 2074 unique targets were defined as the related targets of podocyte injury.

Further taking the intersection of targets of Niaoduqing, DN-related targets, proteinuria-related targets and podocyte injury-related targets, we obtained 16 potential therapeutic targets of

10.3389/fphar.2023.1047184

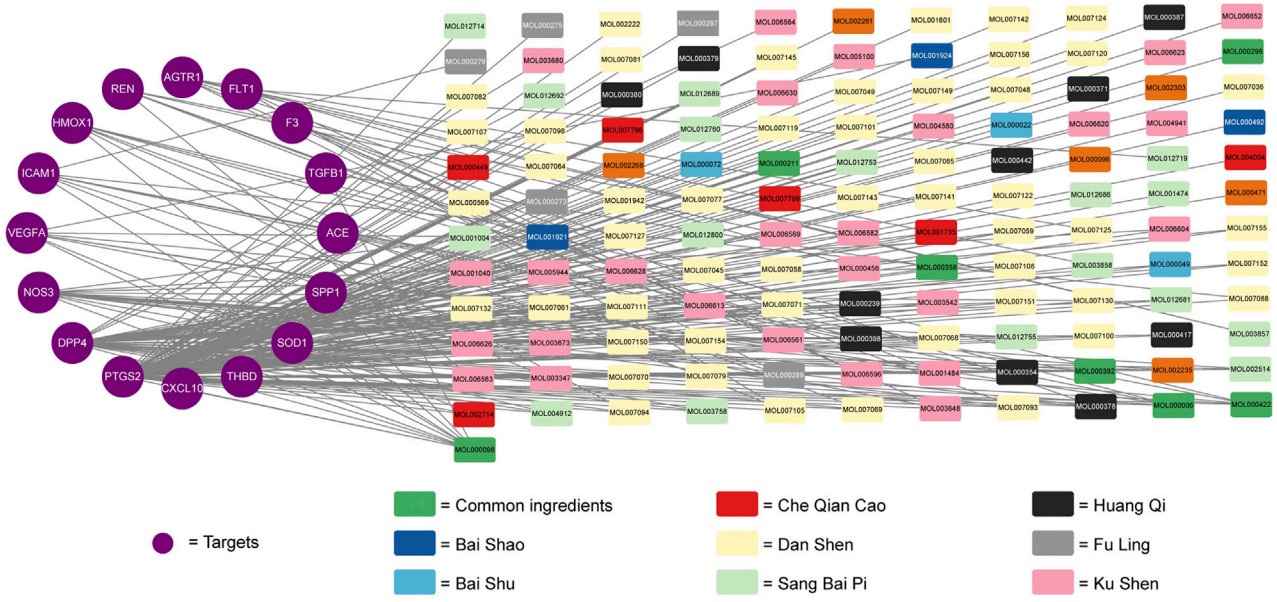

FIGURE 3
The compound-ingredients-therapeutic targets network of Niaoduqing on the treatment of podocyte injury and proteinuria in DN. The purple circle represented the potential therapeutic targets, while the colorful square represented the active ingredients from different compounds.

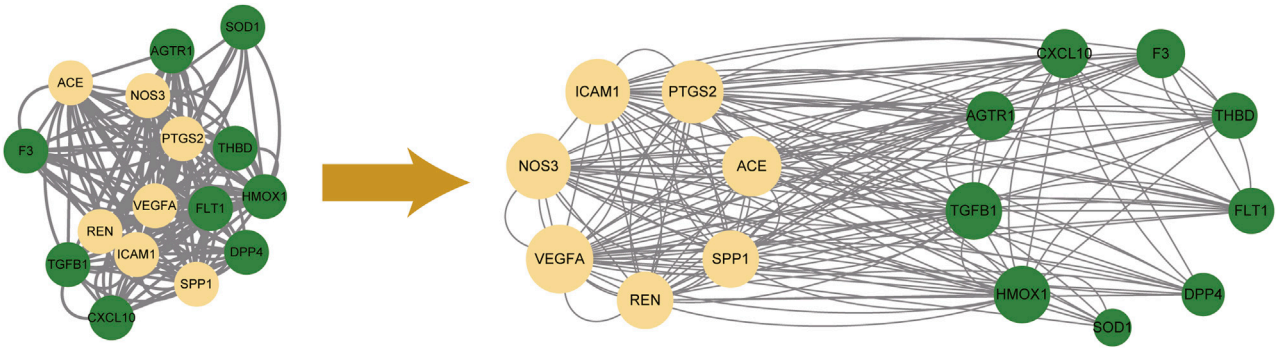

FIGURE 4
The protein-protein interaction network among 16 potential therapeutic targets. 7 core targets with the highest topological parameters were determined. Yellow nodes represented the selected targets (core targets), and green ones represented the remaining targets.

Niaoduqing on the treatment of podocyte injury and proteinuria in DN (shown in Figure 2C). The detail information about targets of DN, proteinuria, podocyte injury, and the overlapping potential therapeutic targets was shown in Supplementary Tables S5–S8.

3.3 Construction of the compound-ingredients-therapeutic targets network

Cytoscape 3.6.1 software was used to construct the compound-ingredients-therapeutic targets network. The network was constructed by 133 active ingredients and 16 potential therapeutic targets, with 149 nodes and 234 edges. Different color was used to represent different compounds of active ingredients (Shown in Figure 3). The higher the topological parameters were, the more nodes connected to it. The data about topological parameters of the nodes was shown in Supplementary Table S9. In all of the active ingredients, quercetin had the highest topological parameters, following by luteolin, kaempferol, 7-O-methylisomucronulatol and danshexinkun D, which were considered as the core ingredients of Niaoduqing on the treatment of podocyte injury and proteinuria in DN.

3.4 PPI network and core targets screening

Importing 16 potential therapeutic targets into STRING database, we established an active ingredients-disease co-expression targets PPI network, which contained 16 nodes and 160 edges. We further screened

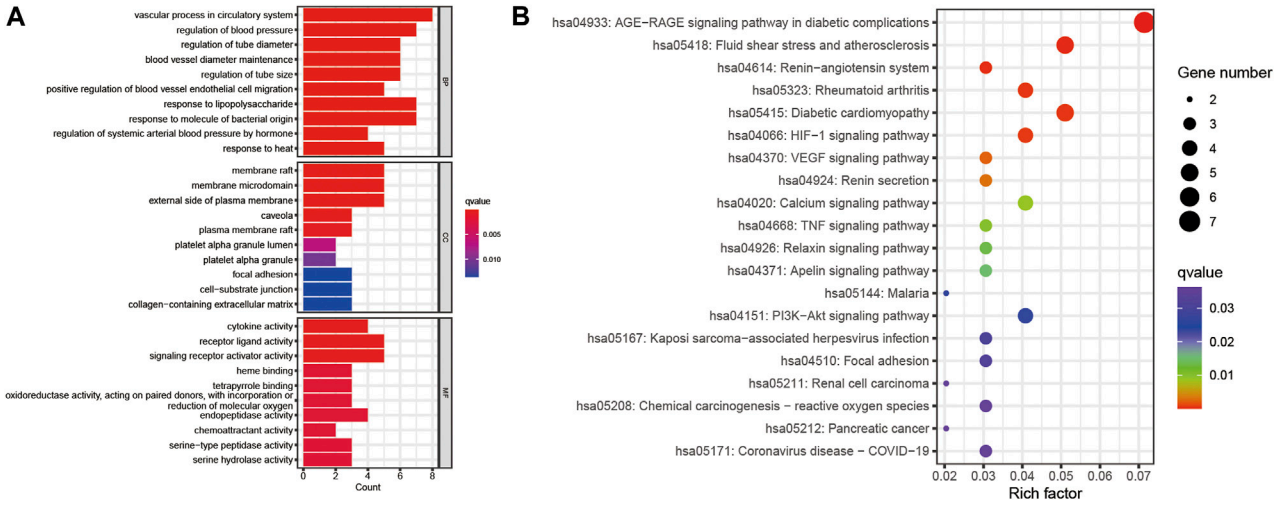

FIGURE 5
GO and KEGG enrichment of the 16 potential therapeutic targets. **(A)** The bar plot of top 10 GO enriched terms of BP, CC and MF function. **(B)** The bubble chart of top 20 KEGG enrichment pathways. The redder the bar, the smaller the *p*-value; the larger the bar, the greater the number of genes enriched in this processes and pathways.

targets with all three parameters higher than the median to construct the sub-network. We found that VEGFA, NOS3, ICAM1, PTGS2, ACE, SPP1 and REN were the core targets with the highest topological parameters (shown in Figure 4). The data about topological parameters of present network was shown in Supplementary Table S10.

3.5 GO and KEGG pathway analyses of potential therapeutic targets

GO analysis and KEGG enrichment analyses were performed based on the above 16 potential therapeutic targets of Niaoduqing on the treatment of podocyte injury and proteinuria in DN. The top 10 GO enrichment terms of MF, BP and CC were shown in Figure 5A. In addition, KEGG analysis was carried out to determine the key pathways of the overlapping genes (Supplementary Table S11), and the top 20 enriched signaling pathways were shown in Figure 5B. In all of them, AGE-RAGE signaling pathway in diabetic complications (hsa04933) exhibited the most significant enrichment, following by fluid shear stress and atherosclerosis (hsa05418), renin-angiotensin system (hsa04614), rheumatoid arthritis (hsa05323), diabetic cardiomyopathy (hsa05415) and HIF-1 signaling pathway (hsa04066). In addition to this, several inflammation signaling pathways and vascular barrier associated pathways were enriched, including VEGF signaling pathway (hsa04370), TNF signaling pathway (hsa04668), PI3K-Akt signaling pathway (hsa04151) and Focal adhesion (has 04510).

3.6 Molecular docking analysis

The potential therapeutic targets of Niaoduqing were further docked with the top five ingredients through molecule docking analysis. We acquired their docking methods and binding energies, and found that the binding energies of all molecular docking were less than −5.5 (Shown in Table 2). PTSG2 and DPP4 interacted with all five core ingredients, while NOS3 interacted with four of them. The most binding results with the lowest binding energy of each core ingredients were shown in Figure 6.

3.7 CCK-8 assay for cytotoxicity analysis

To determine the cytotoxicity and appropriate concentration of the crude Niaoduqing granules solution and its purified core active ingredients, differentiated MPC5 cells were exposed to drugs at different concentrations and CCK-8 assays were performed to detect the cell viability. As shown in Figure 7, the cell viability significantly decreased in Niaoduqing solution exposure group from the lowest to the highest concentration (1/16 to 64 μg/mL); therefore, the crude extract of Niaoduqing was not applicable for the *in vitro* experiment. In contrast, the mixture of three major purified Niaoduqing active ingredients (Que + Lut + Kae) did not show significant cytotoxicity up to 4 μg/mL ($p > 0.05$). Therefore, 1 μg/mL of Que + Lut + Kae was considered as a safe concentration and further used in our study.

3.8 *In vitro* validation of the predicted core targets

To validate the potential therapeutic targets of Niaoduqing in HG-induced podocytes injury model, RT-qPCR was performed to detect the relative expression levels of the above predicted targets. As shown in Figure 8, HG exposure significantly upregulated the expression levels of *Vegf-α* (***$p < 0.001$), *Ptgs-2* (***$p < 0.001$), *Icam-1* (*$p = 0.026$) and *Ace* (***$p < 0.001$) expression, but had no effect on *Ren* ($p = 1.000$), *Spp-1* ($p = 0.052$) and *Nos-3* ($p = 0.524$) expression. Compared with HG group, the upregulation of mRNA expression levels of *Vegf-α* (***$p < 0.001$), *Ptgs-2* (***$p < 0.001$),

TABLE 2 The binding energies results of molecular docking analysis.

Number	Ingredient	Symbol	PDB identifier	Binding energies (kcal/mol)
1	Quercetin	PTGS2	5ikv	−9.3
2	Kaempferol	NOS3	6pp1	−9.2
3	Luteolin	PTGS2	5ikv	−9.1
4	Danshexinkun d	DPP4	6b1o	−8.7
5	Danshexinkun d	NOS3	6pp1	−8.4
6	Danshexinkun d	REN	4s1g	−8.3
7	Quercetin	NOS3	6pp1	−8.1
8	Luteolin	HMOX1	1n45	−8.1
9	Quercetin	HMOX1	1n45	−8
10	Danshexinkun d	PTGS2	5ikv	−7.9
11	Luteolin	DPP4	6b1o	−7.8
12	Quercetin	DPP4	6b1o	−7.7
13	7-O-methylisomucronulatol	NOS3	6pp1	−7.6
14	Kaempferol	ICAM1	5mza	−7.6
15	Kaempferol	HMOX1	1n45	−7.5
16	Kaempferol	DPP4	6b1o	−7.5
17	7-O-methylisomucronulatol	PTGS2	5ikv	−7.2
18	Kaempferol	PTGS2	5ikv	−7
19	Quercetin	ICAM1	5mza	−7
20	Luteolin	ICAM1	5mza	−6.9
21	7-O-methylisomucronulatol	DPP4	6b1o	−6.8
22	Quercetin	CXCL10	1o7z	−6.8
23	Quercetin	SOD1	6fon	−6.7
24	Quercetin	TGFB1	4kv5	−6.2
25	Quercetin	SPP1	predicted	−6.2
26	Quercetin	THBD	1dx5	−6.1
27	Luteolin	VEGFA	1bj1	−5.9
28	7-O-methylisomucronulatol	F3	6r2w	−5.9
29	Quercetin	VEGFA	1bj1	−5.7

Icam-1 (*p = 0.034) and *Ace* (***p < 0.001) were significantly attenuated in HG + Que + Lut + Kae group. There was no statistical difference of expression levels for all target genes between control and Que + Lut + Kae group (all p > 0.05).

3.9 Niaoduqing ingredients attenuate high glucose induced activation of AGE/RAGE signaling pathway

To further investigate the potential mechanisms and evaluate the results of our network pharmacology analysis, the activity of AGE/RAGE signaling pathway in diabetic complications (hsa04933) was detected, which was the most enriched signaling pathway in KEGG analysis. As shown in Figures 9A, B, compared with the control group, the phosphorylation of PI3KCA (Tyr317, *p = 0.028) and NF-κB (Ser536, **p = 0.005), as well as the mRNA levels of target genes including *Rage* (***p < 0.001), *Tnf-α* (**p = 0.002), *Tgf-β1* (**p = 0.004), *Col1a1* (***p < 0.001) significantly increased in HG group. Strikingly, Niaoduqing ingredients treatment significantly reduced HG-induced the increase of phosphorylation of NF-κB (Ser536, *p = 0.024) and upregulation of the expression of *Rage* (***p < 0.001), *Tnf-α*

10.3389/fphar.2023.1047184

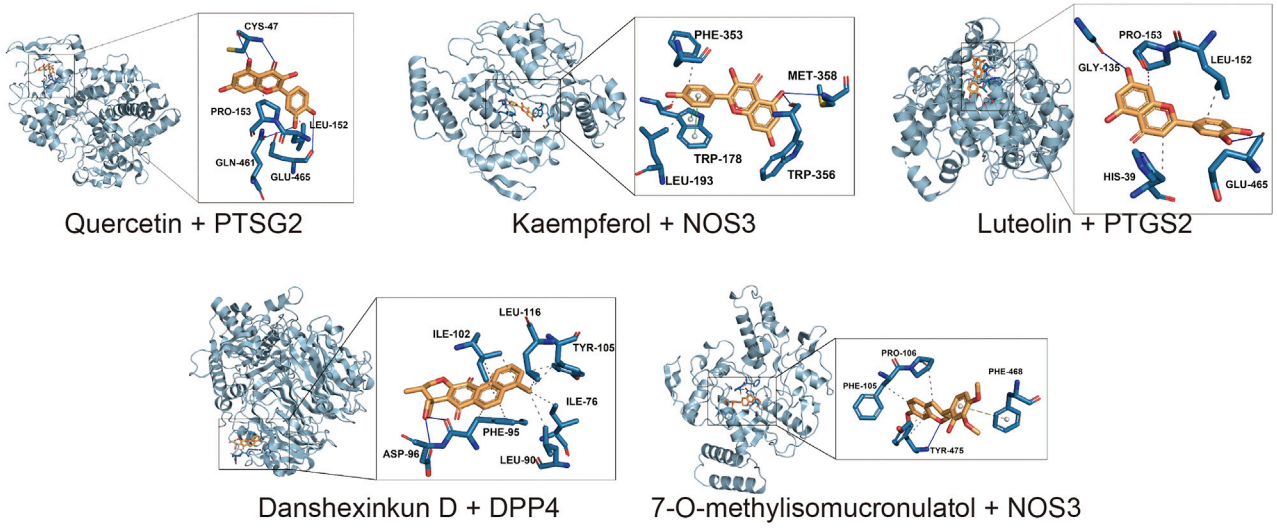

FIGURE 6
The result of molecular docking analysis between the core ingredients and the potential targets. The most binding results with the lowest binding energy of each core ingredients were shown.

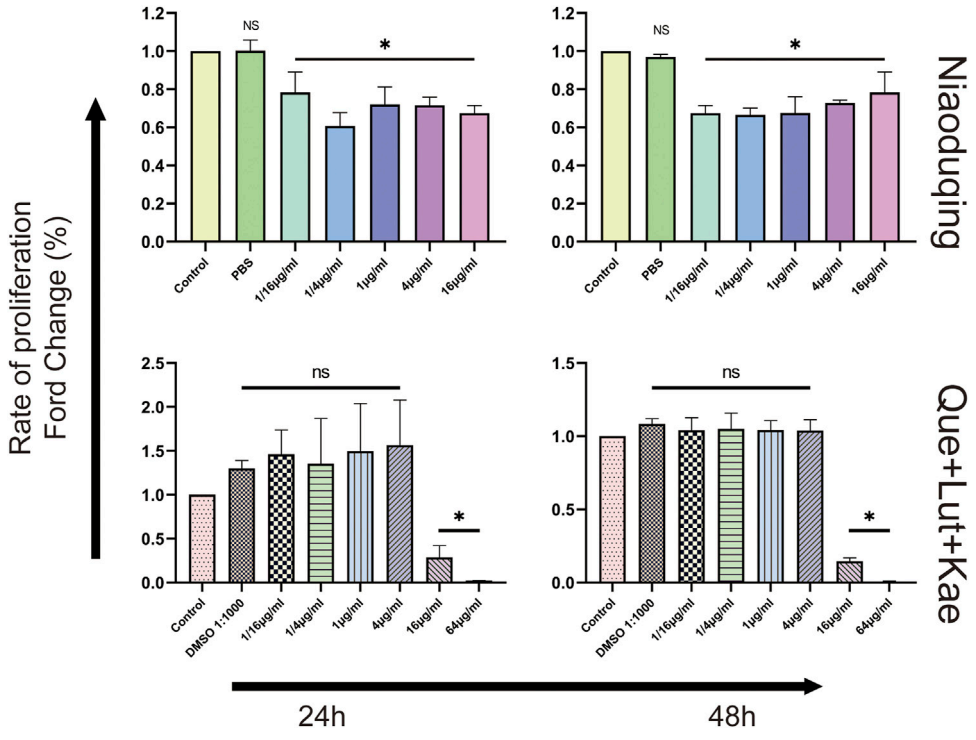

FIGURE 7
The cytotoxicity of the crude Niaoduqing granules solution and its purified core ingredients was detected by CCK-8 assay. The crude Niaoduqing solution showed obvious cytotoxic effect on MPC5 cells at all concentrations. No cytotoxicity of Que + Lut + Kae mixture was observed at the concentrations ranged from 1/16 μg/mL to 4 μg/mL. The data were represented visually with bar graphs. Data were presented as mean ± SD (n = 3 per group) of the representative data from three independent experiments. *$p < 0.05$, NS, non-statistically significant, compared with control group; analyzed by S-N-K test in ANOVA.

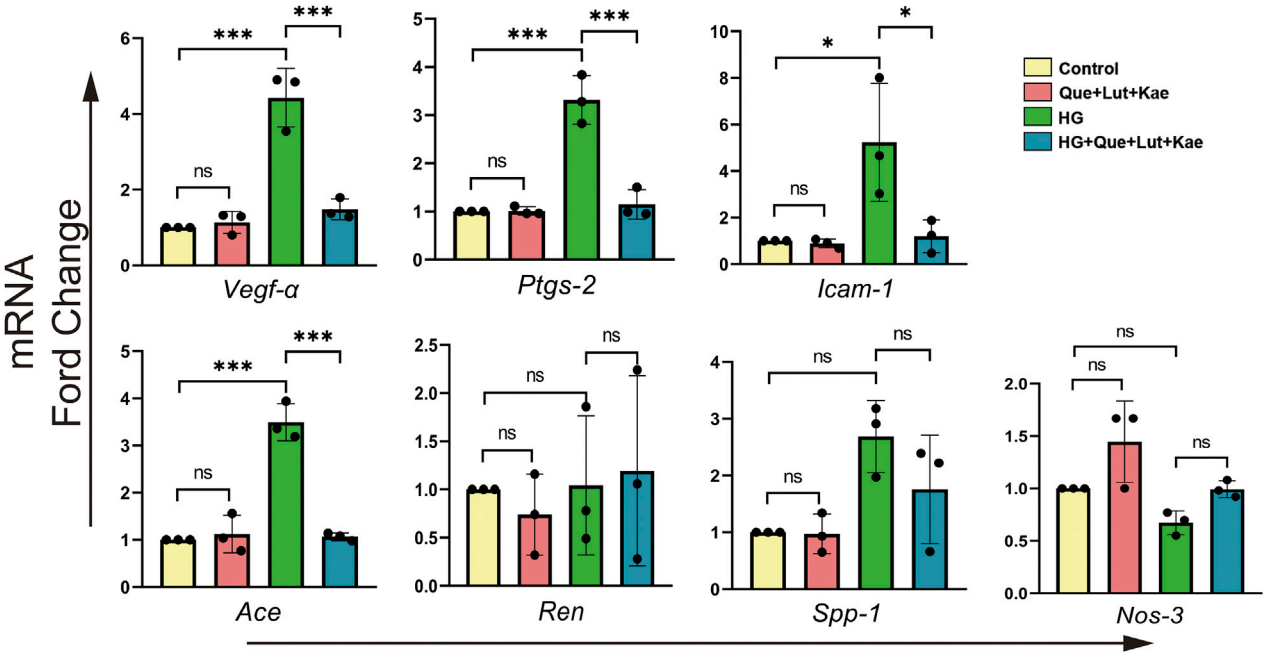

FIGURE 8
The effects of three major ingredients of Niaoduqing (Que + Lut + Kae) on predicted target genes. The treatment of Que + Lut + Kae mixture significantly attenuated the upregulation of the mRNA expression levels of *Vegf-α*, *Ptgs-2*, *Icam-1* and *Ace* in HG-induced MPC5 cells. The data were represented visually with bar graphs. Data were presented as mean ± SD (n = 3 per group) of the representative data from three independent experiments; *p < 0.05, **p < 0.01, ***p < 0.001, NS, non-statistically significant.

(**p = 0.001), *Tgf-β1* (**p = 0.004), and *Col1a1* (***p < 0.001). Although Que + Lut + Kae treatment also inhibited HG-induced phosphorylation of PI3KCA (Tyr317, p = 0.244) and AKT (Ser473, p = 1.000), but with no statistical significance. The details of AGE/RAGE signaling pathway were shown in Figure 9C. Our results indicated that the therapeutic effect of Niaoduqing might be through the regulation of ARG/RAGE signaling pathway.

3.10 Niaoduqing ingredients protect against HG-induced MPC5 cell apoptosis

Previous study showed that Niaoduqing had better effect on controlling proteinuria in patients with early stage DN (Zhao et al., 2022). Since podocyte damage is the major cause of proteinuria, Niaoduqing might be able to protect podocyte during early stage DN. Western blot and flow cytometry analysis were performed to further determine the protective effect of Niaoduqing against HG-induced MPC5 cell apoptosis. Flow cytometry data also showed that Que + Lut + Kae treatment significantly lowered the increase of HG-induced apoptosis rate of MPC5 cells (Figure 10A). As shown in Figure 10B, compared with the control group, Bax (**p = 0.001) and cleaved-Caspase-3 (**p = 0.012) protein levels significantly increased in HG-induced group, while Que + Lut + Kae treatment reduced HG-induced increase of protein levels of Bax (**p = 0.006) and cleaved-Caspase-3 (**p = 0.006). Our data suggested that Niaoduqing might reduce proteinuria through the protection of podocyte from high glucose induced apoptosis.

4 Discussions

Diabetic nephropathy poses a significant threat to the global public health and places enormous economic burden due to high morbidity, high mortality but poor control rate worldwide. To date, we still do not have effective treatment approach to stop or delay the progression of DN (Waanders et al., 2013). Podocyte is the major component of glomerular filtration barrier, and its injury would lead to the leakage of protein (proteinuria). Podocyte injury is considered as the major contributor to DN development, especially in the early stage. Several pathological processes, including persistent proteinuria inflammatory reaction, oxidative stress, vascular endothelial barrier injury and tissue fibrosis are all involved in the development of DN. Due to the complex mechanisms of DN development, treatment simply focusing on single target or pathway might be difficult to achieve satisfactory therapeutic results. Niaoduqing granule, a common clinically used TCM in CKD and ESKD, could treat diseases through a "multi-component, multi-targets and multi-pathways" way. However, the therapeutic effect and the underlying mechanisms of Niaoduqing on the treatment of DN and podocytes injury are still uncertain, especially of the early-stage DN.

In our network pharmacology analysis, 138 active components were considered as potential effective materials of Niaoduqing in podocytes protection and proteinuria reduction. Among the active components, various flavonoids were obtained, including quercetin, luteolin, kaempferol and so on. Flavonoids consisted of a large group of polyphenolic compounds of plant secondary metabolites that can be found widely in vegetables and fruits, and have numerous

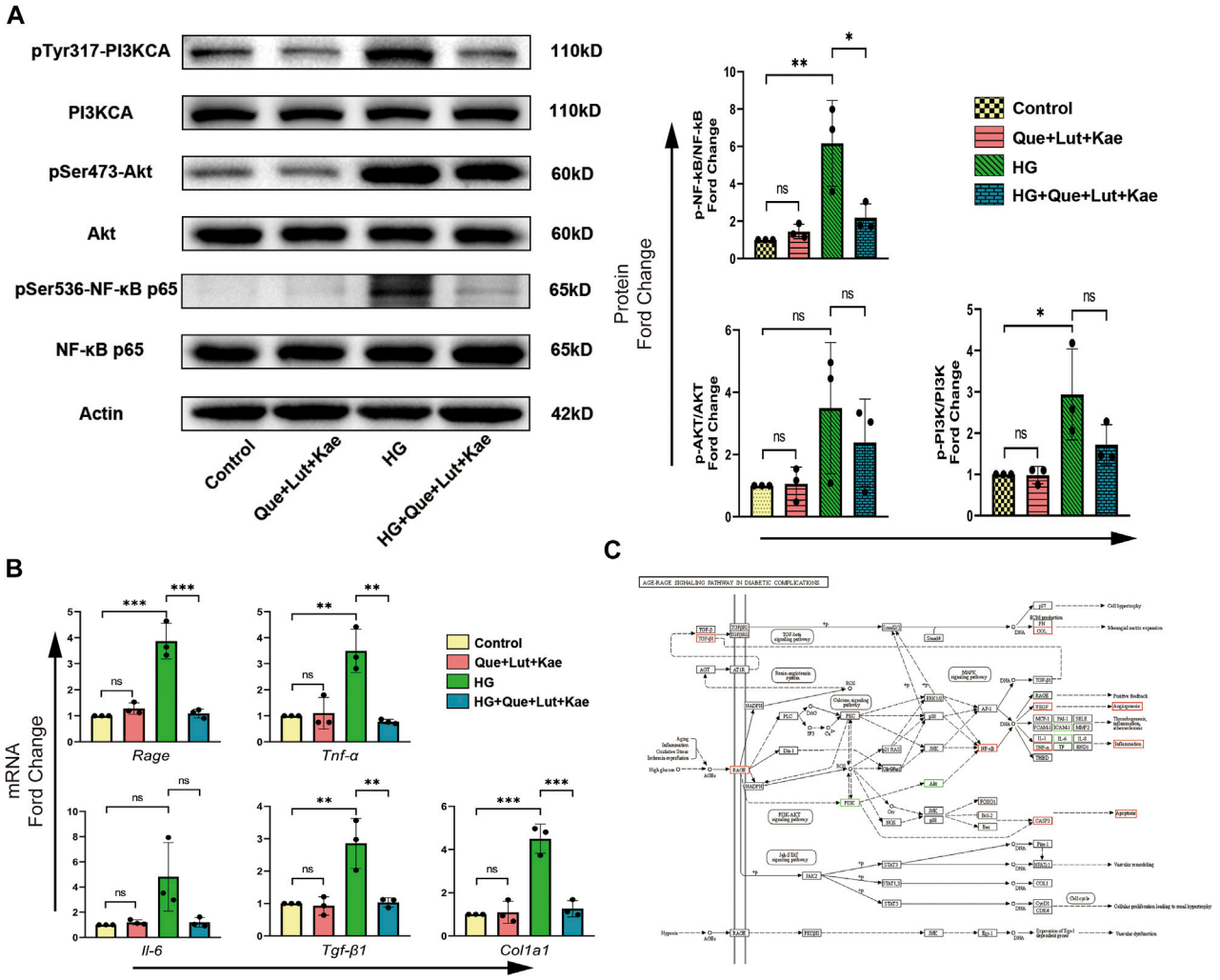

FIGURE 9
Three major ingredients of Niaoduqing (Que + Lut + Kae) participated in the regulation of AGE/RAGE signaling pathway in diabetic complications (hsa04933). **(A)** The protein expression and phosphorylation levels of PI3K, AKT and NF-κB in MPC5 cells were detected by Western blot. **(B)** The mRNA expression levels of *Rage, Tnf-α, Il-6, Tgf-β1* and *Col1a1* in MPC5 cells were determined by RT-qPCR. **(C)** The detail of AGE/RAGE signaling pathway in diabetic complications (hsa04933). Boxes represented the detected sites. Red boxes indicated the positive results, while green boxes indicated the inconclusive results. Data represented the mean ± SD of triplicate independent experiments; $^{*}p < 0.05$, $^{**}p < 0.01$, $^{***}p < 0.001$, NS, non-statistically significant.

biological functions in the treatment of various diseases (Seo et al., 2019). In this study, quercetin, luteolin and kaempferol were determined as the most three core ingredient due to its highest topological parameters and the most related overlapped targets. Additionally, with the good docking score, all of them could be considered for the subsequent analysis of Niaoduqing. Due to the cytotoxic injury of the crude extract of Niaoduqing to MPC5 cells, the mixture produced by mixing the purified quercetin, luteolin and kaempferol on a 1:1:1 scale was used in the *in vitro* experiment. Although only three core ingredients could not fully represent Niaoduqing compound, they might be considered as one of the best alternative methods for clarifying the therapeutic effect of Niaoduqing *in vitro* experiment. Quercetin is an effectively ingredient in alleviating diabetes and related complications (Yan et al., 2022). It inhibits inflammation, oxidative stress, fibrosis, hyperglycemia and dyslipidemia to stop the progression of DN in a time-dependent and dose-dependent manner (Li et al., 2022b). Luteolin is considered as a potential medicine for kidney intervention in DN, which has anti-inflammatory, anti-oxidative stress and anti-fibrosis properties (Zhang et al., 2021). It also delays apoptosis, deletion, fusion and mitochondrial membrane potential collapse of podocytes, and maintains the normal filtration function of basement membrane through regulating the Nphs2 and NLRP3 inflammasome (Yu et al., 2019; Xiong et al., 2020). Kaempferol also has various biological functions. Except for anti-inflammation and anti-oxidative stress, it can enhance the release of insulin and GLP-1 to inhibit fibrosis of kidney in DN model (Sharma et al., 2020; Luo et al., 2021). Except for them, some other ingredients have been reported to correlate with podocyte protection. Wang et al. (2022) found that paeoniflorin can restore autophagy and inhibit apoptosis to protect podocyte from injury *via* inhibiting VEGFR2-PI3K-AKT activity. As Ertürküner et al. (2014)

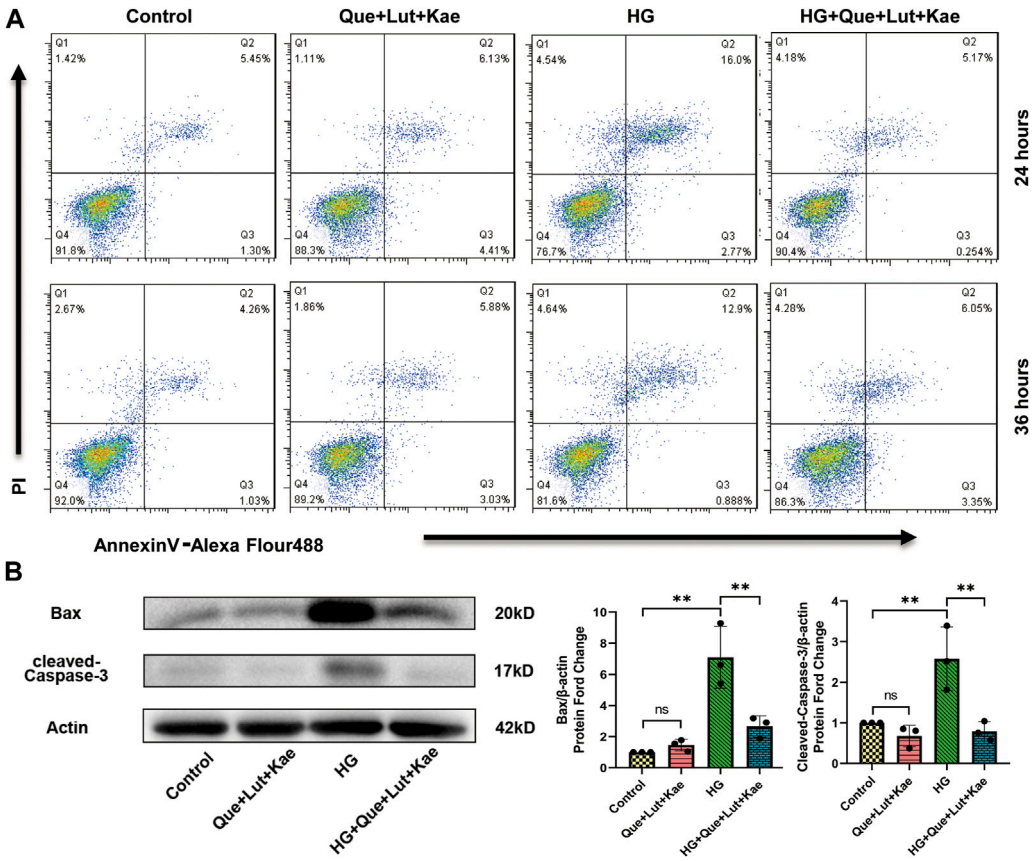

FIGURE 10
Three major ingredients of Niaoduqing (Que + Lut + Kae) reduced HG-induced MPC5 cells apoptosis rate. **(A)** Annexin V/propidium iodide staining and Flow cytometry were performed to determine the apoptosis rate of MPC5 cells. Q2 and Q3 indicated the early and late apoptosis, respectively. **(B)** The protein levels of Bax and cleaved-Caspase-3 in MPC5 cells were detected by Western blot. Data represented the mean ± SD of triplicate independent experiments; $*p < 0.05$, $**p < 0.01$, $***p < 0.001$, NS, non-statistically significant.

reported, mesangial matrix and podocyte has less damage and micro-albuminuria level decreased in the catechin-treated group compared with the untreated diabetic group, and catechin exposure even has the better protective effect on podocyte structure compared with ACEI. Xu et al. (2016) reported that matrine inhibits podocyte damage caused by adriamycin and improves renal function by maintaining the Th17/Treg balance. In addition, rhein and pachymic acid can ameliorate podocyte damage *via* regulating Wnt/β-catenin signaling pathway in DN mice (Duan et al., 2016; Chen et al., 2017). Multiple compounds and ingredients of Niaoduqing involved in the treatment of podocyte injury and proteinuria in DN, and flavonoids were considered as the most predominant effective constituents.

With the help of network pharmacology and experimental verification, we firstly identify some therapeutic targets of Niaoduqing in improving DN. Seven core potential targets with the higher topological parameters were screened out through PPI network construction and four of which were confirmed by *in vitro* cell experiment, including VEGF-A, ICAM1, PTGS2 and ACE. Our therapeutic targets mainly concentrate on the molecular process of vascular endothelial barrier, inflammatory reaction and RAS. All of those processes are involved in the pathogenesis of DN. Podocytes can produce VEGF-A, which is an important angiogenic factor and can induce vascular hyper-permeability and inflammation through interaction with endothelial VEGF receptor-2 (Tufro and Veron, 2012). The maintenance of normal VEGF-A levels is crucial for normal kidney structure and function, and either overexpression or insufficient of VEGF-A leads to kidney injury (Sivaskandarajah et al., 2012; Locatelli et al., 2022). ICAM-1 is one of the transmembrane glycoprotein of the immunoglobulin supergene family, which is widely expressed on endothelium, epithelium, macrophage, and so on. ICAM-1 expression would be upregulated under high glucose condition, which mediates the infiltration of inflammatory cells into renal glomeruli and results in kidney damage (Miyatake et al., 1998; Galkina and Ley, 2006). Inhibition of ICAM-1 expression effectively blocks inflammatory cell infiltration into the glomeruli and alleviates kidney injury (Miyatake et al., 1998; Chen et al., 2016). PTGS-2, also known as COX-2, is one of the key enzymes in catalyzing the conversion of arachidonic acid into prostaglandin and leukotriene, which exacerbates local inflammatory reaction. ACE is the core compounds of RAS. The activation of RAS has been recognized as one of the key potential mechanisms of kidney injury, including DN. The most commonly used antihypertensive drugs, ACEI and ARB, are recommended and widely used in DN patients to inhibit the RAS and improve outcomes (Liu et al., 2020). In the present study, the increased

mRNA expression levels of VEGF-A, ICAM-1, PTGS-2 and ACE in HG-induced group indicated that these genes may contribute to the development of DN and podocytes injury. The significant decrease of the expression levels after drug treatment suggested that the four hub targets may be the potential therapeutic targets of Niaoduqing in the management of DN and podocytes damage.

In KEGG pathway enrichment analysis, the potential molecular mechanism of Niaoduqing's treatment of podocytes injury and proteinuria in DN was most enriched in AGE-RAGE signaling pathways (has04933). Two of the four hub targets (VEGF-A and ICAM1) were involved in this pathway. AGE/RAGE pathway has been demonstrated to be involved in the development of DN (Pathomthongtaweechai and Chutipongtanate, 2020). In the present study, some representative indicators of AGE/RAGE pathway were detected to evaluate its activity, including Rage, PI3K/AKT, NF-κB, VEGF-A, ICAM-1, IL-6, TNF-A, Caspase-3, TGF-B1, COL-1A1. Binding to their receptors RAGE, AGEs can activate downstream signaling pathways a, including TGF-β, p21-RAS and MAPK, and lead to indirect kidney injury (Wautier et al., 2001; Yeh et al., 2001). The upregulation of RAGE expression could be considered as the evidence of pathway activation. The downstream signal molecules of AGE/RAGE pathway, including PI3K/AKT and NF-κB, were detected. Although we observed obvious differences in the phosphorylation level of $PI3K^{Tyr317}$ and AKT^{Ser473}, no statistical differences were obtained due to some fluctuating individual values and low number of replicates. NF-κB is a crucial transcription factor involved in the regulation of inflammation, immune response and stress responses. The upregulation and activation of NF-κB is observed in preclinical DN models and kidney tissues of patients with DN (Opazo-Ríos et al., 2020). Targeting NF-κB is confirmed to be an effective method for DN (Opazo-Ríos et al., 2020). In present study, Niaoduqing effectively inhibited the activation of NF-κB in HG-induced injury model. What's more, some phenotypes mediated by AGE/RAGE pathway were detected in our study. The increase of VEGF-A, ICAM-1, TNF-A and cleaved-Caspase-3 indicated the vascular barrier dysfunction, imbalance of inflammatory reaction and podocytes apoptosis in the HG-induced group. Niaoduqing alleviating those abnormal changes revealed its protective effect on podocytes in DN development. In sum, the administration of Niaoduqing effectively ameliorated podocytes damage caused by HG through partially regulating AGE/RAGE pathway.

Fibrosis of renal tissues is another crucial pathological feature of DN, especially in the end stage. The activation of myofibroblastic and inflammatory cells, extracellular matrix (ECM) expansion and collagens accumulation are identified as the key links of fibrosis development, in which EMT and endothelial to mesenchymal transition (EndMT) are the main sources of matrix-producing myofibroblasts (Srivastava et al., 2021). Inflammatory cytokines are the key profibrotic factors, including tumor necrosis factor-α (TNF-α) and interleukin-6 (IL-6) (Zheng et al., 2016). Many classical pathways have been reported to be closely related to kidney fibrosis, including Wnt signaling pathway and transforming growth factor β (TGF-β) signaling pathway. The loss of glucocorticoid receptor can promote fibrogenesis in kidney tissues *via* activating Wnt signaling pathway and interfering with metabolism of fatty acids (Srivastava et al., 2021). Fibroblast Growth Factor Receptor 1 (FGFR1), the endothelial receptor of fibroblast growth factor (FGF), is essential for combating EndMT, and the activation of FGFR1 signaling pathway has been reported to inhibit TGFβ signaling and TGFβ-induced EndMT (Woo et al., 2021). The deficiency of FGFR1 in endothelium can lead to serious fibrosis associated with EndMT (Li et al., 2020b), Compared with the control mice. Sirtuin-3 (SIRT3), one of the NAD-dependent mitochondrial deacetylases, also plays a crucial role in blocking tissues fibrosis *via* regulating TGF-β/Smad signaling pathway (Srivastava et al., 2018). The loss of SIRT3 can leads to induction of abnormal glycolysis and defective metabolism of kidney tissues, which is responsible for the progression of kidneys fibrosis in diabetes (Srivastava et al., 2018). In present study, we found that the expression of profibrotic factors (TNF-A) and fibrotic markers (TGF-β1 and COL-1A1) significantly increased after high glucose exposure, but the increase was inhibited by Niaoduqing ingredients treatment. These data suggested a therapeutic potential of Niaoduqing in alleviating podocytes fibrosis and inhibiting EndMT.

Recently, there are many potential drugs that have been proven to be effective against DN. As the commonly used anti-hypertension drugs, both ACEI and ARB show good effect on inhibiting kidney fibrosis, but their therapeutic effects are not completely consistent (Srivastava et al., 2020). The author found that DPP-4 and TGF-β signaling are identified as the downstream signals of ACEI in the treatment of kidney fibrosis, but both of them are not regulated by ARB. The anti-fibrotic effects of ACEI but no ARB, partly depend on N-acetyl-seryl-aspartyl-lysyl-proline (AcSDKP), which controls the metabolic switch between glucose and fatty acid metabolism. Another commonly used drug, sodium-dependent glucose transporters 2 inhibitor (SGLT-2i) is considered as a protector of kidney tissues in many kinds of kidney diseases. The application of SGLT-2i can reduce the progression of DN through promoting ketone body induced mechanistic target of rapamycin complex 1 (mTORC1) signaling inhibition (Tomita et al., 2020) The protective effect of SGLT-2i is also related to the inhibition of EMT and aberrant glycolysis (Li et al., 2020c). Compared with the individual application, the combination of SGLT-2i, ACEI and endothelin receptor antagonism can enhance their cardiac and renal protective effects in Type 2 diabetic model (Vergara et al., 2022). Tsuprykov O showed that dipeptidyl peptidase-4 (DPP-4) inhibitor, Linagliptin, has the comparable efficacy to ARB in preventing CKD progression in the 5/6 nephrectomy rats models. However, there may be differences in the underline mechanism of them (Tsuprykov et al., 2016). In addition, due to Warburg effect, which represents the abnormal shift of energy metabolism from mitochondrial oxidative phosphorylation to aerobic glycolysis, promotes fibrogenesis in kidney tissues, inhibiting glycolysis is considered as a potential anti-fibrotic method (Wei et al., 2019). As Wei et al. (2019) reported, both dichloroacetate and shikonin, two glycolysis inhibitors, effectively inhibited the process of renal interstitial fibrosis, and dichloroacetate was recommended because of its higher anti-fibrosis efficiency and lower toxicity. Those drugs are of concern and warrant further research, especially the comparison between Niaoduqing and those drugs.

There were some limitations in this current study. Firstly, whether the mixture of the purified quercetin, luteolin and kaempferol could fully substitutes for Niaoduqing granules is still unclear. Collecting animal serum containing Niaoduqing *via* serologic pharmacology method as previously described is an optional method to solve this problem (Lu et al., 2013). Secondly, missing data of animal experiment is another notable limitation. Further animal experimental validation using

Niaoduqing is warranted. Thirdly, some of the disease therapeutic targets and pathways may be missed, because we only pay attention to the top predicted targets and pathways. Other predicted targets and pathways need to be further confirmed by both *in vitro* and *in vivo* experiments in the future. Due to the above limitations of present study, our results should be interpreted with caution.

5 Conclusion

In present study, we found that the active ingredients of Niaoduqing, including quercetin, luteolin and kaempferol, could ameliorate the podocyte injury in DN through multi-ingredients, multi-targets and multi-pathways method using network pharmacology method and experimental verification. VEGFA, ICAM1, PTGS2, ACE may be the major targets, and AGE/RAGE signaling pathway in diabetic complications (hsa04933) might be one of the core signaling pathways. Further evidence of *in vivo* experiment and clinical data are necessary to confirm our findings.

Data availability statement

The datasets presented in this study can be found in online repositories. The names of the repository/repositories and accession number(s) can be found in the article/Supplementary Material.

Author contributions

YF designed the study, conducted experiments, interpreted the results and wrote the draft of the manuscript. YZ extracted the raw data from public databases, and arranged all figures and tables shown in the final manuscript. CJ contributed to article review. YF and XZ performed experimental validation. CR, XZ, and XZ interpreted the results, revised the manuscript and approved the final version. All of the authors gave final approval of the version to be published and agreed to be accountable for all aspects of the work.

Funding

Our present work was supported by National Nature Science Foundation of China, Grant/Award Numbers: 31371509; 2020 Li Ka Shing Foundation Cross-Disciplinary Research Grant, Grant/Award Number: 2020LKSFG20B; 2019 Traditional Chinese Medicine Science and Technology Fund of Jinan Municipal Health Commission, Grant/Award number: 2019-1-21; 2022 Characteristics and Innovation Grant for college of Guangdong Province, Grant/Award Number: 2022KTSCX040.

Conflict of interest

The authors declare that the research was conducted in the absence of any commercial or financial relationships that could be construed as a potential conflict of interest.

Publisher's note

All claims expressed in this article are solely those of the authors and do not necessarily represent those of their affiliated organizations, or those of the publisher, the editors and the reviewers. Any product that may be evaluated in this article, or claim that may be made by its manufacturer, is not guaranteed or endorsed by the publisher.

Supplementary material

The Supplementary Material for this article can be found online at: https://www.frontiersin.org/articles/10.3389/fphar.2023.1047184/full#supplementary-material

References

Amberger, J. S., and Hamosh, A. (2017). Searching online mendelian inheritance in man (OMIM): A knowledgebase of human genes and genetic phenotypes. *Curr. Protoc. Bioinforma.* 58, 1.2.1–1.2.12. doi:10.1002/cpbi.27

American Diabetes Association (2020). Microvascular complications and foot care: Standards of medical care in diabetes-2020. *Diabetes Care* 43 (1), S135–S151. doi:10.2337/dc20-S011

Anders, H. J., Huber, T. B., Isermann, B., and Schiffer, M. (2018). CKD in diabetes: Diabetic kidney disease versus nondiabetic kidney disease. *Nat. Rev. Nephrol.* 14 (6), 361–377. doi:10.1038/s41581-018-0001-y

Azuaje, F. J., Zhang, L., Devaux, Y., and Wagner, D. R. (2011). Drug-target network in myocardial infarction reveals multiple side effects of unrelated drugs. *Sci. Rep.* 1, 52. doi:10.1038/srep00052

Baelde, H. J., Eikmans, M., Doran, P. P., Lappin, D. W., de Heer, E., and Bruijn, J. A. (2004). Gene expression profiling in glomeruli from human kidneys with diabetic nephropathy. *Am. J. Kidney Dis.* 43 (4), 636–650. doi:10.1053/j.ajkd.2003.12.028

Brinkkoetter, P. T., Bork, T., Salou, S., Liang, W., Mizi, A., Ozel, C., et al. (2019). Anaerobic glycolysis maintains the glomerular filtration barrier independent of mitochondrial metabolism and dynamics. *Cell Rep.* 27 (5), 1551–1566.e5. doi:10.1016/j.celrep.2019.04.012

Cao, Y., Hao, Y., Li, H., Liu, Q., Gao, F., Liu, W., et al. (2014). Role of endoplasmic reticulum stress in apoptosis of differentiated mouse podocytes induced by high glucose. *Int. J. Mol. Med.* 33 (4), 809–816. doi:10.3892/ijmm.2014.1642

Chen, C., Huang, K., Hao, J., Huang, J., Yang, Z., Xiong, F., et al. (2016). Polydatin attenuates AGEs-induced upregulation of fibronectin and ICAM-1 in rat glomerular mesangial cells and db/db diabetic mice kidneys by inhibiting the activation of the SphK1-S1P signaling pathway. *Mol. Cell Endocrinol.* 427, 45–56. doi:10.1016/j.mce.2016.03.003

Chen, L., Chen, D. Q., Wang, M., Liu, D., Chen, H., Dou, F., et al. (2017). Role of RAS/Wnt/β-catenin axis activation in the pathogenesis of podocyte injury and tubulo-interstitial nephropathy. *Chem. Biol. Interact.* 273, 56–72. doi:10.1016/j.cbi.2017.05.025

Daina, A., Michielin, O., and Zoete, V. (2019). SwissTargetPrediction: Updated data and new features for efficient prediction of protein targets of small molecules. *Nucleic Acids Res.* 47 (1), W357–W364. doi:10.1093/nar/gkz382

Duan, S., Wu, Y., Zhao, C., Chen, M., Yuan, Y., Xing, C., et al. (2016). The wnt/β-catenin signaling pathway participates in rhein ameliorating kidney injury in DN mice. *Mol. Cell Biochem.* 411 (1-2), 73–82. doi:10.1007/s11010-015-2569-x

Ertürküner, S. P., Başar, M., Tunçdemir, M., and Seçkin, İ. (2014). The comparative effects of perindopril and catechin on mesangial matrix and podocytes in the streptozotocin induced diabetic rats. *Pharmacol. Rep.* 66 (2), 279–287. doi:10.1016/j.pharep.2013.09.010

Galkina, E., and Ley, K. (2006). Leukocyte recruitment and vascular injury in diabetic nephropathy. *J. Am. Soc. Nephrol.* 17 (2), 368–377. doi:10.1681/ASN.2005080859

Hopkins, A. L. (2007). Network pharmacology. *Nat. Biotechnol.* 25 (10), 1110–1111. doi:10.1038/nbt1007-1110

Huang, Y. R., Wei, Q. X., Wan, Y. G., Sun, W., Mao, Z. M., Chen, H. L., et al. (2014). Ureic clearance granule, alleviates renal dysfunction and tubulointerstitial fibrosis by promoting extracellular matrix degradation in renal failure rats, compared with enalapril. *J. Ethnopharmacol.* 155 (3), 1541–1552. doi:10.1016/j.jep.2014.07.048

Kibble, M., Saarinen, N., Tang, J., Wennerberg, K., Mäkelä, S., and Aittokallio, T. (2015). Network pharmacology applications to map the unexplored target space and therapeutic potential of natural products. *Nat. Prod. Rep.* 32 (8), 1249–1266. doi:10.1039/c5np00005j

Li, J., Teng, D., Shi, X., Qin, G., Qin, Y., Quan, H., et al. (2020a). Prevalence of diabetes recorded in mainland China using 2018 diagnostic criteria from the American diabetes association: National cross sectional study. *BMJ* 369, m997. doi:10.1136/bmj.m997

Li, J., Liu, H., Srivastava, S. P., Hu, Q., Gao, R., Li, S., et al. (2020b). Endothelial FGFR1 (fibroblast growth factor receptor 1) deficiency contributes differential fibrogenic effects in kidney and heart of diabetic mice. *Hypertension* 76, 1935–1944. doi:10.1161/HYPERTENSIONAHA.120.15587

Li, J., Liu, H., Takagi, S., Nitta, K., Kitada, M., Srivastava, S. P., et al. (2020c). Renal protective effects of empagliflozin via inhibition of EMT and aberrant glycolysis in proximal tubules. *JCI Insight* 5, e129034. doi:10.1172/jci.insight.129034

Li, R. N., Lu, Q., and Yang, X. L. (2016). Clinical observation of uremic clearance granule in the treatment of early diabetic nephropathy. *J Med Theory Pract* 29, 1406–1407.

Li, X., Deng, H., Guo, X., Yan, S., Lu, C., Zhao, Z., et al. (2022b). Effective dose/duration of natural flavonoid quercetin for treatment of diabetic nephropathy: A systematic review and meta-analysis of rodent data. *Phytomedicine* 105, 154348. doi:10.1016/j.phymed.2022.154348

Li, X., Zheng, J., Wang, J., Tang, X., Zhang, F., Liu, S., et al. (2022a). Effects of uremic clearance granules on p38 MAPK/NF-κB signaling pathway, microbial and metabolic profiles in end-stage renal disease rats receiving peritoneal dialysis. *Drug Des. Devel Ther.* 16, 2529–2544. doi:10.2147/DDDT.S364069

Li, Y. H., Yu, C. Y., Li, X. X., Zhang, P., Tang, J., Yang, Q., et al. (2018). Therapeutic target database update 2018: Enriched resource for facilitating bench-to-clinic research of targeted therapeutics. *Nucleic Acids Res.* 46 (D1), D1121–D1127. doi:10.1093/nar/gkx1076

Liu, X., Ma, L., and Li, Z. (2020). Effects of renin-angiotensin system blockers on renal and cardiovascular outcomes in patients with diabetic nephropathy: A meta-analysis of randomized controlled trials. *J. Endocrinol. Invest.* 43 (7), 959–972. doi:10.1007/s40618-020-01179-8

Locatelli, M., Zoja, C., Conti, S., Cerullo, D., Corna, D., Rottoli, D., et al. (2022). Empagliflozin protects glomerular endothelial cell architecture in experimental diabetes through the VEGF-A/caveolin-1/PV-1 signaling pathway. *J. Pathol.* 256 (4), 468–479. doi:10.1002/path.5862

Lu, P. H., Wang, J. Y., Chuo, H. E., and Lu, P. H. (2021). Effects of uremic clearance granules in uremic pruritus: A meta-analysis. *Toxins (Basel).* 13 (10), 702. doi:10.3390/toxins13100702

Lu, Z. Y., Liu, S. W., Xie, Y. S., Cui, S. y., Liu, X. s., Geng, W. j., et al. (2013). Inhibition of the tubular epithelial-to-mesenchymal transition *in vivo* and *in vitro* by the uremic clearance granule. *Chin. J. Integr. Med.* 19 (12), 918–926. doi:10.1007/s11655-013-1654-9

Luo, W., Chen, X., Ye, L., Jia, W., Zhao, Y., et al. (2021). Kaempferol attenuates streptozotocin-induced diabetic nephropathy by downregulating TRAF6 expression: The role of TRAF6 in diabetic nephropathy. *J. Ethnopharmacol.* 268, 113553. doi:10.1016/j.jep.2020.113553

Marre, M., Lievre, M., Chatellier, G., Mann, J. F. E., Passa, P., Menard, J., et al. (2004). Effects of low dose ramipril on cardiovascular and renal outcomes in patients with type 2 diabetes and raised excretion of urinary albumin: Randomised, double blind, placebo controlled trial (the DIABHYCAR study). *BMJ* 328 (7438), 495. doi:10.1136/bmj.37970.629537.0D

Miao, X. H., Wang, C. G., Hu, B. Q., Li, A., Chen, C. B., and Song, W. Q. (2010). TGF-beta1 immunohistochemistry and promoter methylation in chronic renal failure rats treated with Uremic Clearance Granules. *Folia Histochem Cytobiol.* 48 (2), 284–291. doi:10.2478/v10042-010-0001-7

Miyatake, N., Shikata, K., Sugimoto, H., Kushiro, M., Shikata, Y., Ogawa, S., et al. (1998). Intercellular adhesion molecule 1 mediates mononuclear cell infiltration into rat glomeruli after renal ablation. *Nephron* 79 (1), 91–98. doi:10.1159/000044997

Ni, Y., Wang, X., Yin, X., Li, Y., Liu, X., Wang, H., et al. (2018). Plectin protects podocytes from adriamycin-induced apoptosis and F-actin cytoskeletal disruption through the integrin α6β4/FAK/p38 MAPK pathway. *J. Cell Mol. Med.* 22 (11), 5450–5467. doi:10.1111/jcmm.13816

Opazo-Ríos, L., Plaza, A., Sánchez Matus, Y., Bernal, S., Lopez-Sanz, L., Jimenez-Castilla, L., et al. (2020). Targeting NF-κB by the cell-permeable NEMO-binding domain peptide improves albuminuria and renal lesions in an experimental model of type 2 diabetic nephropathy. *Int. J. Mol. Sci.* 21 (12), 4225. doi:10.3390/ijms21124225

Pan, Y., Jiang, S., Hou, Q., Qiu, D., Shi, J., Wang, L., et al. (2018). Dissection of glomerular transcriptional profile in patients with diabetic nephropathy: SRGAP2a protects podocyte structure and function. *Diabetes* 67 (4), 717–730. doi:10.2337/db17-0755

Pathomthongtaweechai, N., and Chutipongtanate, S. (2020). AGE/RAGE signaling-mediated endoplasmic reticulum stress and future prospects in non-coding RNA therapeutics for diabetic nephropathy. *Biomed. Pharmacother.* 131, 110655. doi:10.1016/j.biopha.2020.110655

Piñero, J., Queralt-Rosinach, N., Bravo, À., Deu-Pons, J., Bauer-Mehren, A., Baron, M., et al. (2015). DisGeNET: A discovery platform for the dynamical exploration of human diseases and their genes. *Database (Oxford)* 2015, bav028. doi:10.1093/database/bav028

Podgórski, P., Konieczny, A., Lis, Ł., Witkiewicz, W., and Hruby, Z. (2019). Glomerular podocytes in diabetic renal disease. *Adv. Clin. Exp. Med.* 28 (12), 1711–1715. doi:10.17219/acem/104534

Ru, J., Li, P., Wang, J., Zhou, W., Li, B., Huang, C., et al. (2014). Tcmsp: A database of systems pharmacology for drug discovery from herbal medicines. *J. Cheminform* 6, 13. doi:10.1186/1758-2946-6-13

Seo, M. Y., Kim, K. R., Lee, J. J., Ryu, G., Lee, S. H., Hong, S. D., et al. (2019). Therapeutic effect of topical administration of red onion extract in a murine model of allergic rhinitis. *Sci. Rep.* 9 (1), 2883. doi:10.1038/s41598-019-39379-9

Sharma, D., Kumar Tekade, R., and Kalia, K. (2020). Kaempferol in ameliorating diabetes-induced fibrosis and renal damage: An *in vitro* and *in vivo* study in diabetic nephropathy mice model. *Phytomedicine* 76, 153235. doi:10.1016/j.phymed.2020.153235

Sircar, M., Rosales, I. A., Selig, M. K., Xu, D., Zsengeller, Z. K., Stillman, I. E., et al. (2018). Complement 7 is up-regulated in human early diabetic kidney disease. *Am. J. Pathol.* 188 (10), 2147–2154. doi:10.1016/j.ajpath.2018.06.018

Sivaskandarajah, G. A., Jeansson, M., Maezawa, Y., Eremina, V., Baelde, H. J., and Quaggin, S. E. (2012). Vegfa protects the glomerular microvasculature in diabetes. *Diabetes* 61 (11), 2958–2966. doi:10.2337/db11-1655

Srivastava, S. P., Goodwin, J. E., Kanasaki, K., and Koya, D. (2020). Inhibition of angiotensin-converting enzyme ameliorates renal fibrosis by mitigating DPP-4 level and restoring antifibrotic MicroRNAs. *Genes (Basel)* 11, 211. doi:10.3390/genes11020211

Srivastava, S. P., Li, J., Kitada, M., Fujita, H., Yamada, Y., Goodwin, J. E., et al. (2018). SIRT3 deficiency leads to induction of abnormal glycolysis in diabetic kidney with fibrosis. *Cell Death Dis.* 9, 997. doi:10.1038/s41419-018-1057-0

Srivastava, S. P., Zhou, H., Setia, O., Liu, B., Kanasaki, K., Koya, D., et al. (2021). Loss of endothelial glucocorticoid receptor accelerates diabetic nephropathy. *Nat. Commun.* 12, 2368. doi:10.1038/s41467-021-22617-y

Stelzer, G., Rosen, N., Plaschkes, I., Zimmerman, S., Twik, M., Fishilevich, S., et al. (2016). The GeneCards suite: From gene data mining to disease genome sequence analyses. *Curr. Protoc. Bioinforma.* 54, 1.30.1–1.30.33. doi:10.1002/cpbi.5

Tomita, I., Kume, S., Sugahara, S., Osawa, N., Yamahara, K., Yasuda-Yamahara, M., et al. (2020). SGLT2 inhibition mediates protection from diabetic kidney disease by promoting ketone body-induced mTORC1 inhibition. *Cell Metab.* 32, 404–419.e6. doi:10.1016/j.cmet.2020.06.020

Trott, O., and Olson, A. J. (2010). AutoDock Vina: Improving the speed and accuracy of docking with a new scoring function, efficient optimization, and multithreading. *J. Comput. Chem.* 31 (2), 455–461. doi:10.1002/jcc.21334

Tsuprykov, O., Ando, R., Reichetzeder, C., von Websky, K., Antonenko, V., Sharkovska, Y., et al. (2016). The dipeptidyl peptidase inhibitor linagliptin and the angiotensin II receptor blocker telmisartan show renal benefit by different pathways in rats with 5/6 nephrectomy. *Kidney Int.* 89, 1049–1061. doi:10.1016/j.kint.2016.01.016

Tufro, A., and Veron, D. (2012). VEGF and podocytes in diabetic nephropathy. *Semin. Nephrol.* 32 (4), 385–393. doi:10.1016/j.semnephrol.2012.06.010

Vergara, A., Jacobs-Cacha, C., Llorens-Cebria, C., Ortiz, A., Martinez-Diaz, I., Martos, N., et al. (2022). Enhanced cardiorenal protective effects of combining SGLT2 inhibition, endothelin receptor antagonism and RAS blockade in type 2 diabetic mice. *Int. J. Mol. Sci.* 23, 12823. doi:10.3390/ijms232112823

Waanders, F., Visser, F. W., and Gans, R. O. (2013). Current concepts in the management of diabetic nephropathy. *Neth J. Med.* 71 (9), 448–458.

Wang, X., Jiang, L., Liu, X. Q., Huang, Y. B., Wang, A. L., Zeng, H. X., et al. (2022). Paeoniflorin binds to VEGFR2 to restore autophagy and inhibit apoptosis for podocyte protection in diabetic kidney disease through PI3K-AKT signaling pathway. *Phytomedicine* 106, 154400. doi:10.1016/j.phymed.2022.154400

Wang, X., Yu, S., Jia, Q., Chen, L., Zhong, J., Pan, Y., et al. (2017). NiaoDuQing granules relieve chronic kidney disease symptoms by decreasing renal fibrosis and anemia. *Oncotarget* 8 (34), 55920–55937. doi:10.18632/oncotarget.18473

Wautier, M. P., Chappey, O., Corda, S., Stern, D. M., Schmidt, A. M., and Wautier, J. L. (2001). Activation of NADPH oxidase by AGE links oxidant stress to altered gene expression via RAGE. *Am. J. Physiol. Endocrinol. Metab.* 280 (5), E685–E694. doi:10.1152/ajpendo.2001.280.5.E685

Wei, Q., Su, J., Dong, G., Zhang, M., Huo, Y., and Dong, Z. (2019). Glycolysis inhibitors suppress renal interstitial fibrosis via divergent effects on fibroblasts and tubular cells. *Am. J. Physiol. Ren. Physiol.* 316, F1162–F1172. doi:10.1152/ajprenal.00422.2018

Wei, X. F., and Ruan, S. L. (2018). Effect of Uremic Clearance Granule combined with olmesartan on early diabetic nephropathy and liver and kidney function. *Chin. J. Geront* 38, 874–876.

Whirl-Carrillo, M., Huddart, R., Gong, L., Sangkuhl, K., Thorn, C. F., Whaley, R., et al. (2021). An evidence-based framework for evaluating pharmacogenomics knowledge for personalized medicine. *Clin. Pharmacol. Ther.* 110 (3), 563–572. doi:10.1002/cpt.2350

Woo, K. V., Shen, I. Y., Weinheimer, C. J., Kovacs, A., Nigro, J., Lin, C. Y., et al. (2021). Endothelial FGF signaling is protective in hypoxia-induced pulmonary hypertension. *J. Clin. Invest.* 131, e141467. doi:10.1172/JCI141467

Wu, G., Zhang, Y., and Zhang, J. (2009). Oservation on therapeutic effects of Niaoduqing in treating diabetic renal insufficiency. *Shandong Med. J.* 49 (36), 89–90. doi:10.3969/j.issn.1002-266X.2009.36.047

Wu, W., Huang, Y. R., Wan, Y. G., Yang, H. M., Mao, Z. M., Yang, J. J., et al. (2016). Effects and mechanisms of UCG ameliorating renal interstitial fibrosis by regulating TGF-β1/SnoN/Smads signaling pathway in renal failure rats. *Zhongguo Zhong Yao Za Zhi* 41 (12), 2291–2297. doi:10.4268/cjcmm20161220

Xiong, C., Wu, Q., Fang, M., Li, H., Chen, B., and Chi, T. (2020). Protective effects of luteolin on nephrotoxicity induced by long-term hyperglycaemia in rats. *J. Int. Med. Res.* 48 (4), 300060520903642. doi:10.1177/0300060520903642

Xu, Y., Lin, H., Zheng, W., Ye, X., Yu, L., Zhuang, J., et al. (2016). Matrine ameliorates adriamycin-induced nephropathy in rats by enhancing renal function and modulating Th17/Treg balance. *Eur. J. Pharmacol.* 791, 491–501. doi:10.1016/j.ejphar.2016.09.022

Yan, L., Vaghari-Tabari, M., Malakoti, F., Moein, S., Qujeq, D., Yousefi, B., et al. (2022). Quercetin: An effective polyphenol in alleviating diabetes and diabetic complications. *Crit. Rev. Food Sci. Nutr.* 2022, 1–24. doi:10.1080/10408398.2022.2067825

Yang, H., Kan, L., Wu, L., Zhu, Y., and Wang, Q. (2019a). Effect of baicalin on renal function in patients with diabetic nephropathy and its therapeutic mechanism. *Exp. Ther. Med.* 17 (3), 2071–2076. doi:10.3892/etm.2019.7181

Yang, H., Xie, T., Li, D., Du, X., Wang, T., Li, C., et al. (2019b). Tim-3 aggravates podocyte injury in diabetic nephropathy by promoting macrophage activation via the NF-κB/TNF-α pathway. *Mol. Metab.* 23, 24–36. doi:10.1016/j.molmet.2019.02.007

Yeh, C. H., Sturgis, L., Haidacher, J., Zhang, X. N., Sherwood, S. J., Bjercke, R. J., et al. (2001). Requirement for p38 and p44/p42 mitogen-activated protein kinases in RAGE-mediated nuclear factor-kappaB transcriptional activation and cytokine secretion. *Diabetes* 50 (6), 1495–1504. doi:10.2337/diabetes.50.6.1495

Yu, Q., Zhang, M., Qian, L., Wen, D., and Wu, G. (2019). Luteolin attenuates high glucose-induced podocyte injury via suppressing NLRP3 inflammasome pathway. *Life Sci.* 225, 1–7. doi:10.1016/j.lfs.2019.03.073

Zhang, D., Zhang, Y., Gao, Y., Chai, X., Pi, R., Chan, G., et al. (2020). Translating traditional herbal formulas into modern drugs: A network-based analysis of xiaoyao decoction. *Chin. Med.* 15, 25. doi:10.1186/s13020-020-00302-4

Zhang, L., Long, J., Jiang, W., Shi, Y., He, X., Zhou, Z., et al. (2016). Trends in chronic kidney disease in China. *N. Engl. J. Med.* 375 (9), 905–906. doi:10.1056/NEJMc1602469

Zhang, M., He, L., Liu, J., and Zhou, L. (2021). Luteolin attenuates diabetic nephropathy through suppressing inflammatory response and oxidative stress by inhibiting STAT3 pathway. *Exp. Clin. Endocrinol. Diabetes* 129 (10), 729–739. doi:10.1055/a-0998-7985

Zhao, J., Ai, J., Mo, C., Shi, W., and Meng, L. (2022). Comparative efficacy of seven Chinese patent medicines for early diabetic kidney disease: A bayesian network meta-analysis. *Complement. Ther. Med.* 67, 102831. doi:10.1016/j.ctim.2022.102831

Zheng, S., Powell, D. W., Zheng, F., Kantharidis, P., and Gnudi, L. (2016). Diabetic nephropathy: Proteinuria, inflammation, and fibrosis. *J. Diabetes Res.* 2016, 5241549. doi:10.1155/2016/5241549

Zhu, M., Wu, Y., and Shou, Z. (2018). Effects of Niaoduqing granule on urine metabolic profile in chronic renal failure rats. *Zhejiang Da Xue Xue Bao Yi Xue Ban.* 47 (6), 628–635. doi:10.3785/j.issn.1008-9292.2018.12.11

Glossary

ACEI Angiotensin Converting Enzyme Inhibitors

AGE-RAGE Advanced Glycation End products—Receptor of Advanced Glycation End products

ARB Angiotensin Receptor Blocker

AcSDKP N-acetyl-seryl-aspartyl-lysyl-proline

BP Biological Process

CC Cellular Components

CKD Chronic Kidney Disease

DEGs Differentially Expressed Genes

DL Drug-like Properties

DN Diabetic Nephropathy

DPP-4 Dipeptidyl Peptidase-4

ECM Extracellular Matrix

EMT Epithelial to Mesenchymal Transition

EndMT Endothelial to Mesenchymal Transition

ESRD End-Stage Renal Disease

FGF(R) Fibroblast Growth Factor (Receptor)

GEO Gene Expression Omnibus

GO Gene Ontology

IL Interleukin

Kae Kaempferol

KEGG Kyoto Encyclopedia of Genes and Genomes

Lut Luteolin

MF Molecular Function

MMP Matrix Metalloproteinases

MPC5 Mouse Podocyte Clone 5 cells

OB Oral Bioavailability

OMIM Online Mendelian Inheritance in Man database

Que Quercetin

PDB Protein Docking Bank database

PPI Protein-Protein Interaction

RAS Renin-Angiotensin System

ROS Reactive Oxygen Species

SGLT-2i Sodium-Dependent Glucose Transporters 2 Inhibitor

SIRT3 Sirtuin-3

TCMSP Traditional Chinese Medicine Systems Pharmacology Database and Analysis Platform

TIMP Tissue Inhibitors of Metalloproteinases

TNF Tumor Necrosis Factor

TTD Therapeutic Target Database

Frontiers in Pharmacology

Explores the interactions between chemicals and living beings

The most cited journal in its field, which advances access to pharmacological discoveries to prevent and treat human disease.

Discover the latest Research Topics

See more →

Frontiers

Avenue du Tribunal-Fédéral 34
1005 Lausanne, Switzerland
frontiersin.org

Contact us

+41 (0)21 510 17 00
frontiersin.org/about/contact